Regional Carbonate Geochemistry and Biogeochemistry for Cu Exploration on the Yorke Peninsula, South Australia.

Keryn Dianne Wolff

B.Sc. Sustainable Environments; Deep Earth Resources, Honours Geology

A thesis submitted for the degree of

Doctor of Philosophy

School of Physical Sciences

Department of Geology

The University of Adelaide

South Australia

Deep Exploration Technologies, Cooperative Research Centre

(DET CRC)

April 2018

Contents

Abstract

This thesis describes the geochemistry from carbonate rocks and biogeochemistry from mallee across the Yorke Peninsula to better characterise and define mineral systems that may occur in IOCG prospective basement rocks masked by various overlying cover sequences. Presented here is geochemical data from three cliff escarpments (vertical geochemical profiles) which preserve cover sequences overlying basement rocks. Ca/Sr ratios were found to be a defining discriminator between marine and pedogenic carbonate rocks within the profiles; pedogenic carbonates have Ca/Sr ratios less than 650 and marine carbonates have Ca/Sr ratios greater than 1260. This simple discriminant can also be used to identify samples appropriate for carbonate sampling in mineral exploration, particularly in drill cuttings, as well as retrospective filtering of multi-element geochemical exploration data sets.

A regional sampling program was undertaken in the context of the regolith landform setting from a newly constructed map of Yorke Peninsula. The majority of carbonate material occurring at the surface across the Yorke Peninsula has Ca/Sr <650, with lesser occurrences of carbonate preserving Ca/Sr ratios between 650 and 1260 and one preserving marine Ca/Sr >1260. The majority of surface carbonates have Ca/Sr consistent with a mixture of rainfall sources and marine carbonate sources. With the dominant contributor of Ca and Sr from rainwater. Surface carbonates with Ca/Sr ratios >650 have a greater proportion of Ca and Sr sourced from marine carbonates, incorporated either from wind-blown dust or from in-situ marine carbonates. The systematically lower Ca/Sr of rainwater, compared to marine carbonates, translates into

systematically lower Ca/Sr in pedogenic compared to marine carbonates. This is an effective discriminator of carbonates formed by pedogenic processes and weathered marine carbonates. The dominantly pedogenic nature of the carbonate rocks sampled across the Yorke Peninsula means that they are appropriate for use in mineral exploration geochemistry for underlying iron oxide-copper-gold deposits. The range of the Cu values in the carbonate rocks is 1.4–36ppm. Elevated Cu concentrations (1.4–36ppm) occur more commonly within carbonate rocks within 3km of known Cu occurrences. .

Eucalyptus foliage was collected at a suitable time of year to maximise root absorption and minimise contamination from farming practices. The range of Cu concentrations within *Eucalyptus* with mallee-form was 1.6–10ppm. Mallee within 3km of known mineralisation has a concentration of 2–10ppm Cu. There was little statistical difference between the four mallee species sampled so that it is reasonable to use all data as a collective dataset. As mallee occur across a large portion of southern Australia, this method of sampling could prove to be a useful tool for frontiers in exploration where tenure occurs typically over large areas, with widespread cover and restricted access due to environmental and cultural sensitivities.

Declaration

I certify that this work contains no material which has been accepted for the award of any other degree or diploma in my name, in any university or other tertiary institution and, to the best of my knowledge and belief, contains no material previously published or written by another person, except where due reference has been made in the text. In addition, I certify that no part of this work will, in the future, be used in a submission in my name, for any other degree or diploma in any university or other tertiary institution without the prior approval of the University of Adelaide and where applicable, any partner institution responsible for the joint-award of this degree.

I acknowledge that copyright of published works contained within this thesis resides with the copyright holder(s) of those works.

I also give permission for the digital version of my thesis to be made available on the web, via the University's digital research repository, the Library Search and also through web search engines, unless permission has been granted by the University to restrict access for a period of time.

I acknowledge the support I have received for my research through the provision of an Australian Government Research Training Program Scholarship.

Keryn Dianne Wolff Date 15/04/2018

Acknowledgements

I wish to thank a number of people whom have supported me both personally and professionally throughout this project. Firstly, I would like to thank my God, in Heaven, whom created this beautiful world and gave us the intelligence that we use to investigate this world that we all live in. I would also like to thank my husband Randy Wolff , my son Bradley Versegi and my best friend Michelle Williams for their constant support and encouragement, in its many and varied forms. Thanks to Dr Steve Hill whom originally provided ideas for this PhD project and encouraged me to enrol with the University of Adelaide to undertake this research degree. I would like to thank my academic supervisors and in particular Dr Caroline Tiddy and Prof David Giles whom were extremely patient with me throughout all of the various challenges that I faced throughout the course of this PhD.

Many thanks are due to those whom contributed to this thesis in some way:

- David Bruce for assistance in the Clean Lab during isotope chemistry and the use of the Thermal Ionisation Mass Spectrometer (TIMS)
- Georgina Gordon for assistance with reflectance spectroscopy using HyLogger^{TM} 3-3, at the Department of Premiere and Cabinet's (DPC) Core Storage facility, previously located at Glenside, Adelaide.
- My co-authors- Georgina Gordon from the Geological Survey branch of the Department of the Premiere and Cabinet SA and Dr Ronald Smernik from the University of Adelaide.

- Dr David Gray and Dr Nathan Reid from CSIRO in WA, for their assistance with hydro-geochemistry.
- Field assistance from Randy Wolff, Bradley Versegi, Dr Nathan Reid (CSIRO Perth), Jim Safta (DPC) and Catherine Kelly from (DEWNR), was very much appreciated.
- Thanks to Roger Fidler from the Geological Survey branch of the Department of the Premiere and Cabinet SA, for assistance with carbonate rock preparation analysis.

I started this research because of my son Bradley and I finished it because of my Papa, Norm Aunger, whom turned 102 in January 2019.

This work has been supported by the Deep Exploration Technologies Cooperative Research Centre whose activities are funded by the Australian Government's Cooperative Research Centre Programme. The CRC funding agreement number is 20080065. This is DET CRC document number 2018/2003.

For more information see;

https://www.business.gov.au/assistance/cooperative-research-centres-programme/cooperative-research-centres-crcs-grants/customer-stories/deep-exploration-technologies, and also http://detcrc.com.au/.

Chapter 1: Introduction

1.1 Regolith carbonates and mineral exploration

World demand for metals is increasing at a rapid rate but the number of new world-class or tier-1 discoveries is declining (e.g. Giles et al., 2014; Hillis et al., 2014; Schodde, 2017b). In the last decade no new teir-1 deposits have been found at all in Australia (Schodde, 2017b). The rate of discovery is also hampered by ever increasing cost of exploration, particularly the expense of drilling (e.g. Giles et al., 2014; Schodde, 2014, 2017a; Schodde, 2017b). In Australia, exploration efforts are also hampered by depth of regolith cover which is often viewed as an impediment to exploration (e.g. Hillis et al., 2014; Lintern et al., 2013; Lintern et al., 2011; Reid and Hill, 2010; Reid et al., 2008; Sheard et al., 2008). There is a widespread view that most major mineral deposits occurring at, or near the surface, have mostly been discovered (e.g. Hillis et al., 2014), whilst any remaining deposits not yet discovered are concealed by deep and barren regolith cover (e.g. Guj and Schodde, 2013; Hillis et al., 2014; Lintern, 2007; Reid and Hill, 2010). To explore through this deep cover innovative exploration techniques need to be developed and tested (e.g. Giles et al., 2014; Hillis et al., 2014; Lintern et al., 2013; Smith, 1996).

A variety of sampling materials from the cover sequences have been identified as useful for geochemical exploration where potentially prospective basement is concealed (e.g. Anand and Pain, 2002). These materials may include glacial till and stream sediments (e.g. McClenaghan et al., 2017), groundwater (e.g. Gray et al., 2009), aeolian sand (e.g. Ghavami-Riabi et al., 2008), resistate mineral phases (e.g. monazite: Forbes et al., 2015), clay (e.g. Keeling and Hartley, 2005), soil (e.g. Brown and Hill, 2005; Lintern et al., 1997),

termitaria (Petts, 2009), radon gas (e.g. Fabris, 2010), surface carbonate rocks such as calcrete (e.g. Chen et al., 2002; Lintern, 2015; Lintern and Sheard, 1999; Reith et al., 2011; Sheard et al., 2008; Wolff et al., 2017), and vegetation (e.g. Hulme and Hill, 2003; Mitchell et al., 2015; Reid et al., 2008; van der Hoek et al., 2012; Wolff et al., 2018). These materials may provide geochemical information related to underlying buried mineralisation. To make use of these materials we need to understand the processes by which geochemical signatures develop in the cover sequences and how they might spatially relate to buried mineralisation (e.g. McQueen, 2008; Salama et al., 2016).

Landscape processes can both concentrate and dilute the geochemical and mineralogical signatures of underlying rocks (Anand, 2016b). These landscape processes include erosion and re-deposition through alluvial or colluvial means, aeolian transport of sediments from other locations near and far, dilution from rainwater chemistry or anthropogenic influence such as farming, land clearing, mining and infrastructure. This underlines the need to understand how geochemical signatures are expressed and the processes by which the signature developed in the cover sequence (Anand, 2016b). Mapping the regolith is a method suggested to provide context and insight on such processes that occur throughout the landscape under study, aiding the interpretation of the geochemical expression and determining beneficial sampling procedures (e.g. Anand, 2016a; McQueen et al., 1999; Pain et al., 2007).

Carbonate rocks are a cover sequence material that have been shown to be a useful sampling material for mineral exploration (e.g. Lintern and Sheard, 1999; Lintern et al., 2006; Reith et al., 2011; van der Hoek et al., 2012). Carbonate-dominant regolith occurs

globally around the mid latitudes ~30°N and 30°S (Fig. 1.1) and covers ~21% of the exposed Australian continent (Chen et al., 2002; Fig. 1.2). At this point it should be noted that the terms ‘cover sequence’, ‘cover material’ and ‘regolith’ are referring to the same thing, i.e. all highly weathered or sedimentary material, either transported or in situ, that occurs overlying fresh basement rock.

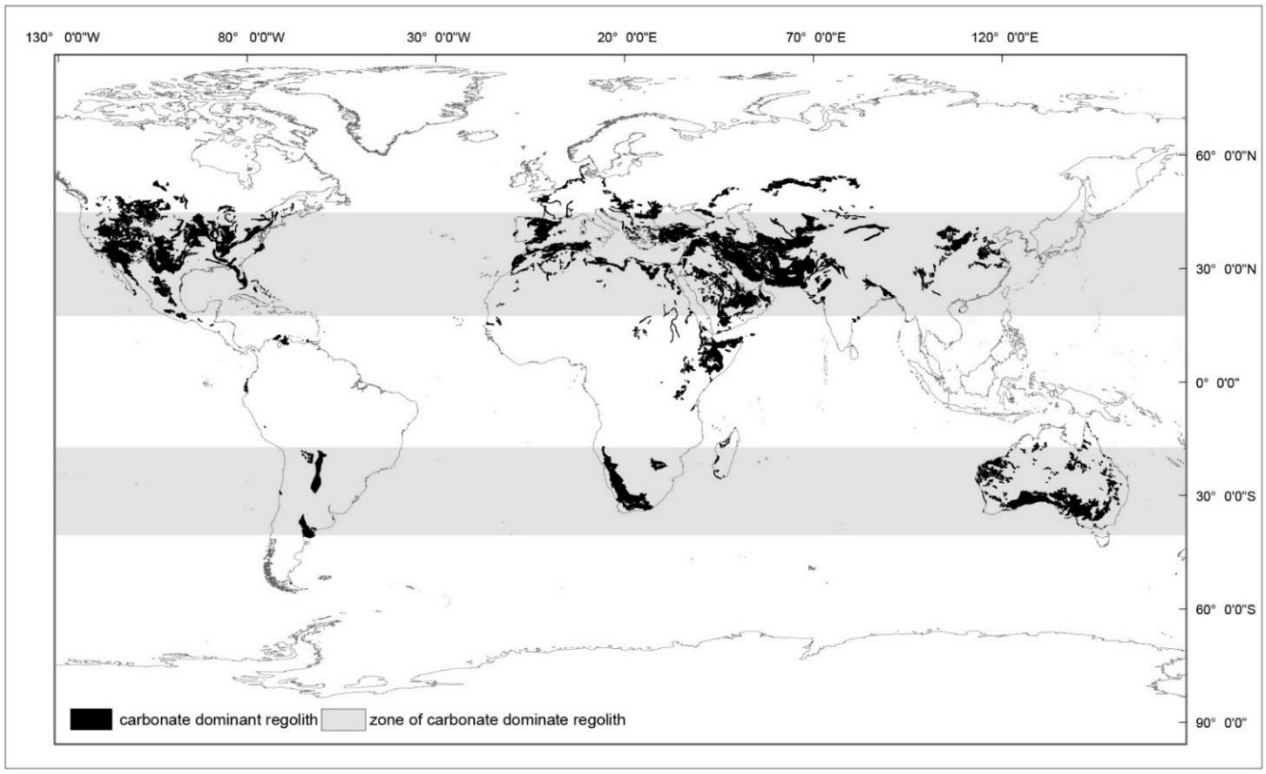

Figure 1-1 Worldwide distribution of carbonate dominant regolith including exposed limestone. Compiled from ISRIC (Batjes, 2012) and USGS datasets (USGS, 2016). Specific areas and general zones of carbonate dominated regolith are highlighted.

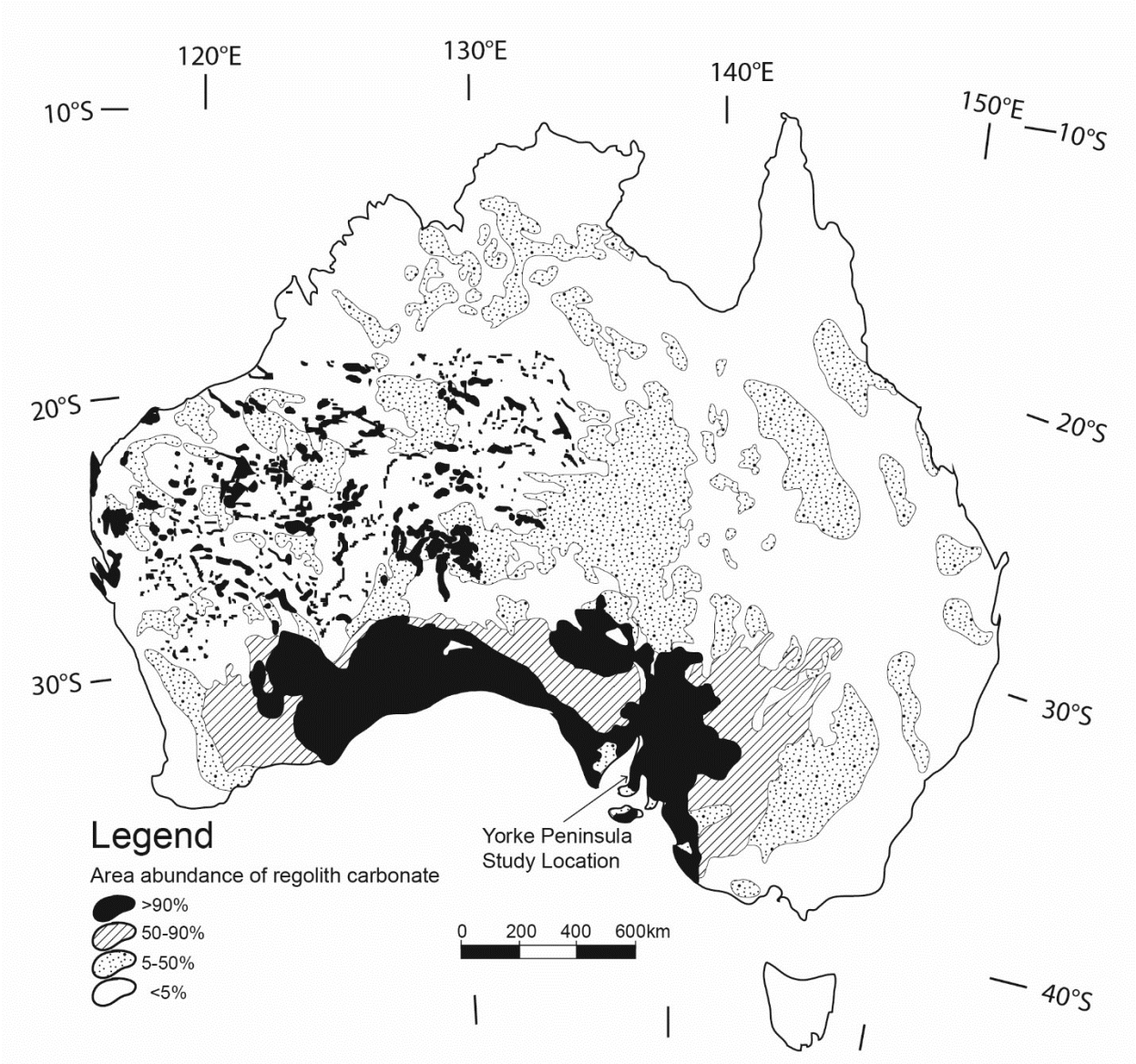

Figure 1-2 Distribution and abundance of regolith carbonate cover across Australia. Modified after Chen et al., (2002). The Yorke Peninsula study area of this thesis is indicated.

South Australia has extensive cover of carbonate rocks that are exposed at the surface (e.g. Lintern, 2015; McQueen et al., 1999) and have been a successful sample media for exploration with a focus on gold (e.g. Drown, 2003; Lintern, 2015; Lintern et al., 2012;

Lintern et al., 2011; Lintern et al., 2006; Reith et al., 2011; van der Hoek et al., 2012). The Challenger gold mine in the northern Gawler Craton (Fig. 1.3) was discovered using carbonate rock sampling methods (e.g. BonWick, 1997; Poustie and Abbot, 2006). Other studies also report concentrations of other elements in carbonate rocks (e.g. Cu: Keeling and Hartley, 2005).

In using surface samples such as carbonate rocks to identify potentially buried mineralisation, there is a need to understand how the geochemical signature is transferred from depth and upwards toward the surface. Various methods of element transfer include fluctuations in the water table through evaporation or capillary rise, movement facilitated by plant roots which can also be incorporated into the plant and then shed back to the surface as litter (Fig 1.4), and biomediation by bacteria (e.g. Lintern, 2007, 1989; Lintern et al., 2006; McQueen, 2006; McQueen et al., 1999; Reith et al., 2011; Schmidt Mumm and Reith, 2007).

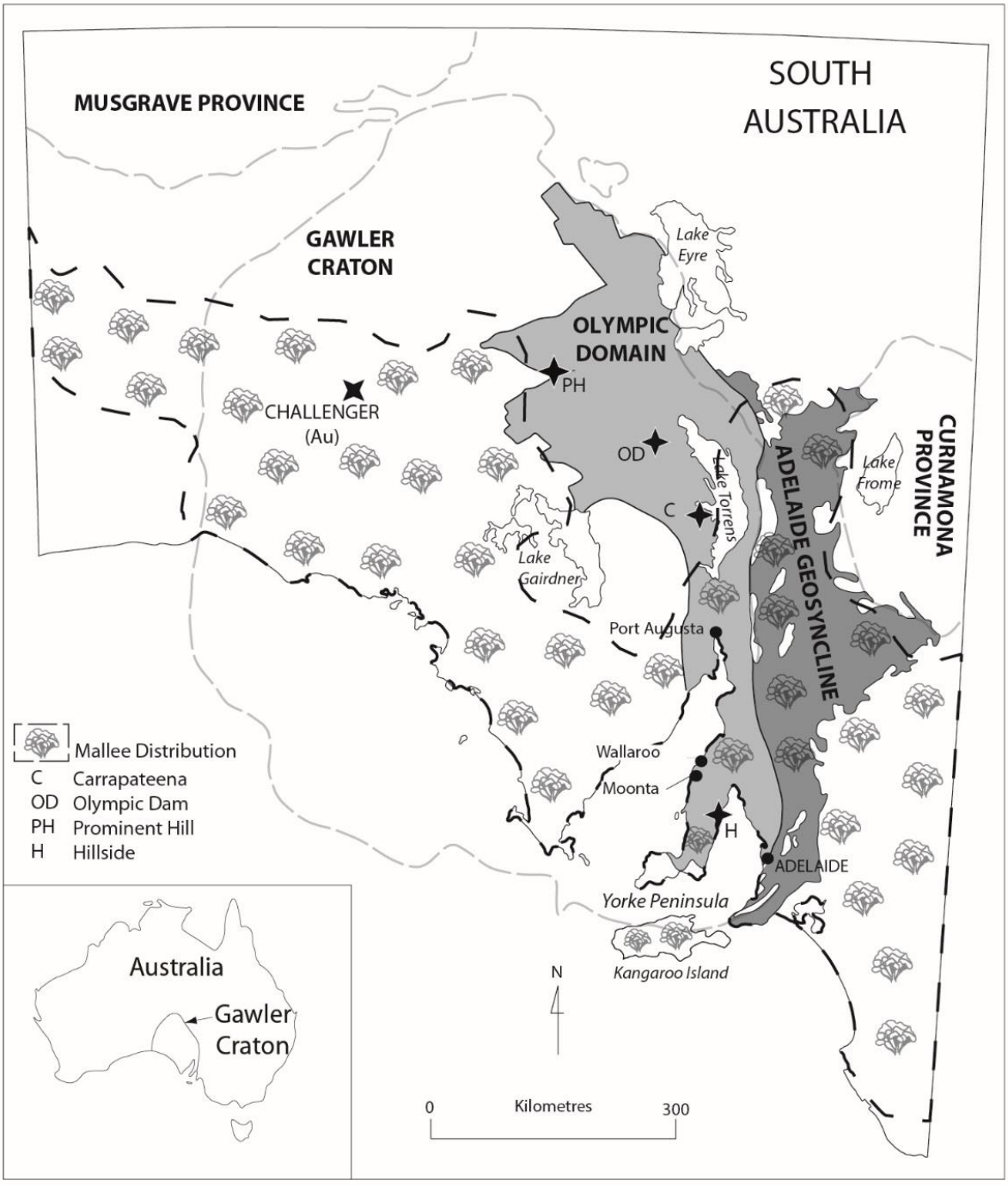

Figure 1-3 Simplified geological map of South Australia showing study location within the Olympic Domain of the Gawler Craton (modified after Conor et al., 2010). Also shown is mallee distribution across South Australia (modified after Australian Native Vegetation Assessment, 2001). Inset: Australia showing location of the Gawler Craton.

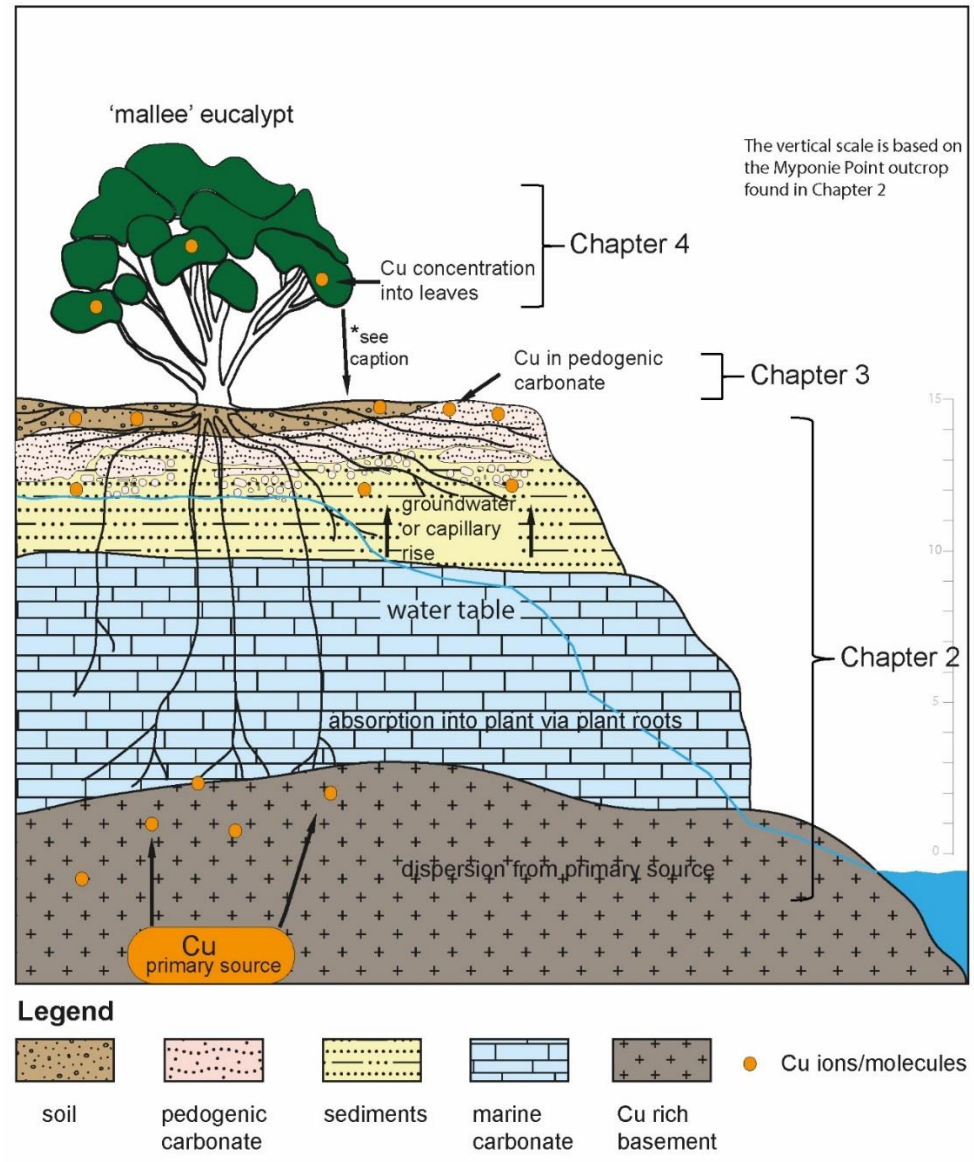

*Figure 1-4 Conceptual model demonstrating how Cu may occur in basement rocks and its movement into mallee eucalypts, groundwater and overlying sediments. * Leaf litter enriched in Cu may also concentrate Cu signatures from underlying substrate into the overlying soils (Lintern, 1989). Brackets shown depict the sections of this thesis where the subject matter is discussed further; Chapter 2: the basement rocks and overlying sediments; Chapter 3: the dispersion throughout surface occurring carbonate rocks; and Chapter 4: dispersion into mallee eucalypts.*

There is also a need to understand the origin of the carbonate rocks. Carbonate rocks can develop in a variety of locations within the regolith cover and in marine environments e.g. limestone (e.g. Chen et al., 2002). Carbonates occurring in the regolith may form in valleys and fluvial systems as groundwater carbonates or from soil forming processes and are referred to as pedogenic carbonate (e.g. Chen et al., 2002; Lintern, 2015; McQueen et al., 1999). Pedogenic carbonate can occur unconsolidated in powdery or nodular form or rock-like cemented material and sometimes referred to commonly as 'Calcrete' (Chen et al., 2002). The 'crete' part of the term 'calcrete' implies cementation which produces a hardened rock-like carbonate although calcrete can also be powdery (Chen et al., 2002). Pedogenic carbonate generally forms in the upper regolith (by interactions between Ca^{2+} and HCO_3^- and water (McQueen, 2006). These ions become saturated in the soil and when water is removed, such as during evaporation and evapotranspiration, pedogenic carbonate is formed (McQueen, 2006). A full description of carbonate rock formation, morphology and properties is comprehensively described in Chen, et al., (2002) This thesis uses the term carbonate and carbonate rock to describe material collected that is dominated by calcium carbonate by either; visual analysis in the event of being able to positively identify marine fossils, or by the presence of a high reaction when exposed to hydrochloric acid.

Pedogenic carbonate have potential to reflect subsurface chemistry as they are formed from processes such as fluctuations of the water table, capillary movement in pore fluids, evaporation of soil moisture in arid environments and through plants facilitating upward movement of groundwater (Chen et al., 2002; Lintern, 2007; Lintern et al., 1997; McQueen, 2006; McQueen et al., 1999). Conversely, marine carbonate rocks would be

expected to show the chemistry which reflects the chemistry at the time of deposition (e.g. Howarth and McArthur, 1997; Zhao et al., 2009). The distinction between these two types of carbonate rocks can be difficult when textural information is lost (e.g. Lintern, 2015). However, it is important to identify the different origins as the pedogenic carbonates have the potential to preserve detectable concentrations of pathfinder elements associated with potential underlying mineralisation (e.g. Lintern, 2007; Reith et al., 2011; Schmidt Mumm and Reith, 2007).

1.2 Biogeochemistry and mineral exploration

Plants are also an important part of the regolith environment and have been argued to be important for the development of geochemical signals in cover sediments (Brooks, 1973; Busche, 1989; Dunn, 2007; Lintern, 2007; Lintern et al., 1997). A variety of vegetation has been identified as useful sample media in exploration both globally and in Australia. Global examples include; creosote bush, burr bush and sagebrush in the Mojave Desert, (Busche, 1989); Dunn, (2007) summarises usage of many species; 118 various genera of herbaceous annuals, biennials and perennials in Iran, (Ghaderian and Ravandi, 2012); *Rumex acetosella* and *Minuartia verna* in northern Greece, (Kelepertsis and Andrulakis, 1983); and Common Juniper in Finland, (Närhi et al., 2014). Australian examples include; River Red Gums in northwest New South Wales and central east South Australia, (Hulme and Hill, 2003); *Eucalyptus* and *Melaleuca* across the Eyre Peninsula, South Australia, (Lintern, 2007); *Eucalyptus* at Kalgoorlie, Western Australia and at Wudinna, central South Australia, (Lintern et al., 2013); *Eucalyptus* at Broken Hill, New South Wales, (Mitchell et al., 2015); *Eucalyptus*, *Triodia* and *Acacia* in the Tanami Gold Province,

Northern Territory, (Reid and Hill, 2010); and *Eucalyptus* and *Casaurina* at the Tunkillia Au-prospect in central South Australia, (van der Hoek et al., 2012). Biogeochemistry has been shown to be successful in delineating buried extensions of Au mineralisation (e.g. Hulme, 2008). It is important to have an understanding of the species of vegetation that are present and their suitability for sampling, including the part of the plant that should be sampled, as well as knowledge of the abilities of the individual plant to be able to penetrate roots deeply into the cover, and the preferences, if any, for transfer of certain elements from depth (e.g. Butt et al., 2005b; Dunn, 2007; Lintern et al., 1997).

Various Eucalyptus species have been shown to be useful for detecting the near surface expression of buried mineralisation (Arne et al., 1999; Cohen et al., 1999; Dunn, 2007; Hulme and Hill, 2003; Lintern et al., 2013; Mitchell et al., 2015; Reid and Hill, 2010; van der Hoek et al., 2012) and at least 783 species are distributed throughout Australia (Slee et al., 2006). Mallee is the term used to describe a eucalypt form where multiple trunks may emerge from a lignotuber at, or just below ground level and serve the purpose to re-sprout from dormant buds following fire, drought or other disturbance (e.g. Brooker et al., 2002; Butt, 2005; Slee et al., 2006). At least 75 species are distributed throughout South Australia (Slee et al., 2006; Fig. 1.3). Eucalypt mallee have also been shown to be useful for defining surface expression of buried Au in Australia and South Australia (e.g. Lintern, 2007; Reid and Hill, 2010; van der Hoek et al., 2012; Fig. 1.4), however less is known regarding its usage as a sample medium (Dunn, 2007) on a regional scale or its usage to define subsurface Cu mineralisation (although see; Lintern, 2007). Using a combination of different sample media (e.g. Cohen et al., 1999; van der Hoek et al., 2012) can be an

effective way to undertake both fast and inexpensive, non-invasive reconnaissance for mineral exploration.

The Yorke Peninsula, South Australia, has been chosen as the location for this thesis as it is covered by large areas of both marine- and pedogenically-derived carbonate rocks (Zang et al., 2006) and an abundance of native eucalypt mallee (Brooker et al., 2002). This sampling media occurs in a region which comprises sparsely exposed Proterozoic basement rocks that are prospective for iron oxide, copper and gold mineralisation (Conor, 2016; Conor et al., 2010; Conor, 2002; Cowley, 2005; Cowley et al., 2003; Drexel et al., 1993; Ismail et al., 2014; Zang et al., 2006). This setting provides the ideal location to test the association of both marine- and pedogenically-derived carbonate rocks to each other and the carbonate rocks and mallee, with copper, sourced from the underlying basement.

In this thesis I have used carbonate rocks and vegetation on the Yorke Peninsula, South Australia to gain an understanding of the way Cu is dispersed from prospective basement throughout overlying regolith cover. The study also examines how this dispersion is expressed in carbonate rocks that occur at the surface and in vegetation, in particular mallee eucalypts, for the purpose of geochemical exploration.

Three exposed coastal profiles were vertically sampled for the purpose of identifying changes in chemistry associated with changes in lithology. Each profile contained marine and pedogenic carbonate rocks. Granitic basement rocks are preserved at the base of one profile. I then sampled carbonate rocks from the surface, along with leaves from *Eucalyptus* trees in a grid pattern from Stansbury and Hardwicke Bay in the south to

Wallaroo and Thomas Plains in the north, which covers all but the southernmost area of the Yorke Peninsula (Fig. 1.5). The results provide insight into the processes of developing geochemical signatures of underlying mineralisation and how to use them in exploration.

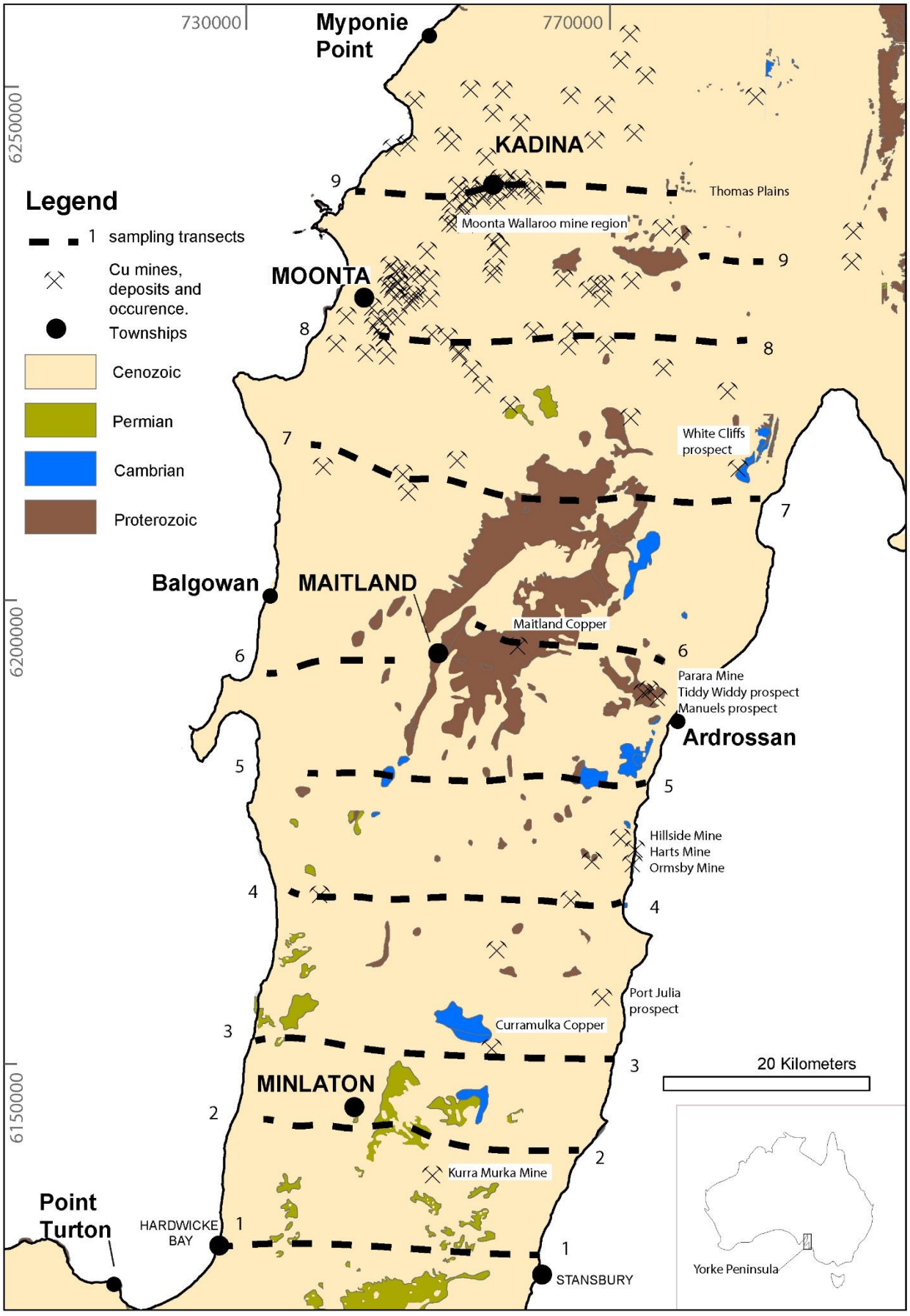
730000
770000
6250000
6200000
6150000
Myponie Point
KADINA
Thomas Plains
Moonta Wallaroo mine region
MOONTA
White Cliffs prospect
Balgowan
MAITLAND
Maitland Copper
Parara Mine
Tiddy Widdy prospect
Manuels prospect
Ardrossan
Hillside Mine
Harts Mine
Ormsby Mine
Port Julia prospect
Curramulka Copper
MINLATON
Kurra Murka Mine
Point Turton
HARDWICKE BAY
STANSBURY
20 Kilometers
Yorke Peninsula
Legend
1 sampling transects
Cu mines, deposits and occurence.
Townships
Cenozoic
Permian
Cambrian
Proterozoic

Figure 1-5 Simplified outcropping surface geology map of Yorke Peninsula (downloadable GIS data extracted from SARIG: https://map. sarig. sa.gov.au Last accessed 04/04/2017). All sample location sites presented in this thesis are shown. Chapter 1 locations include Myponie Point, Balgowan, Point Turton and Ardrossan. The dashed line represents the transect locations (numbered) where carbonate rocks and vegetation were sampled. The exact sample locations of the carbonate rocks and vegetation are given in Chapter 3 and 4 respectively. Inset map shows location of the Yorke Peninsula within Australia. Map projection/coordinate system: GDA 1994, MGA, zone 53.

1.3 Yorke Peninsula study area

1.3.1 Geology

The basement geology of the central Yorke Peninsula comprises Proterozoic rocks with minimal (<5%) exposure (Fig. 1.5) and is dominated by metasediments and volcanics of the ca.1750 Ma Wallaroo Group (Cowley et al., 2003). The Wallaroo group has undergone deformation, metamorphism and magmatic events (e.g. Ferris et al., 2002; Forbes et al., 2011; Hoek and Schaefer, 1998). The Wallaroo Group was intruded by the ca.1595-1575 Ma Hiltaba Suite granites (e.g. Conor et al., 2010; Skirrow et al., 2006) including the ca.1598-1575 Ma Tickera Granite, ca.1589 Ma Curramulka Gabbronorite and ca.1583 Ma Arthurton Granite (Binks et al., 2004; Cowley et al., 2003; Drexel et al., 1993; Wurst, 1994; Zang et al., 2006). Interactions between combinations of these geological events has led to mineralisation throughout the region (e.g. Conor et al., 2010; Morales-Ruano et al., 2002).

The Wallaroo Group in the central and northern Yorke Peninsula hosts IOCG+/-U mineralisation of varying concentration and depth, including the historic Moonta-Wallaroo district and the Hillside deposit (Conor et al., 2010; Zang et al., 2006). Copper occurs in shear zones as vein style mineralisation, within sulphides and oxidised in carbonates such as malachite and azurite (e.g. Conor, 1995; Conor et al., 2010; Department of the Premier and Cabinet, 2017; Zang et al., 2006). Depth of Cu mineralisation varies throughout the region from surface exposures, shallow, i.e. within 5–10m of cover, and up to 300m (e.g. Conor, 1995, Conor et al., 2010; Department of the Premier and Cabinet, 2017; Fabris, 2010; Zang et al., 2006). Grade of Cu mined throughout the region has varied from between 0.5% Cu concentrated in sulphidic ore, and up to as much as 44 wt% (e.g. Conor, 1995; Conor et al., 2010; Department of the Premier and Cabinet, 2017).

Basement rocks across the Yorke Peninsula rocks are concealed by a blanket of cover that can range from <1m and up to at least 1500m depth (e.g. Crawford, 1965; Drexel and Preiss, 1995; Zang et al., 2006; Zang and Hore, 2001) (Fig. 1.5). Basement rocks are unconformably overlain by sediments of the Cambrian Stansbury Basin and the Carboniferous to Permian Troubridge Basin (e.g. Drexel and Preiss, 1995; Zang et al., 2006; Fig. 1.6). Cenozoic sediments of the Yorke Peninsula include those of the St Vincent and Pirie Basins (e.g. Drexel and Preiss, 1995; Zang et al., 2006). Quaternary sediments such as sand, clay and calcareous soils and rocks have largely concealed the underlying geology (Crawford, 1965; Drexel and Preiss, 1995; Zang et al., 2006; Fig. 1.5).

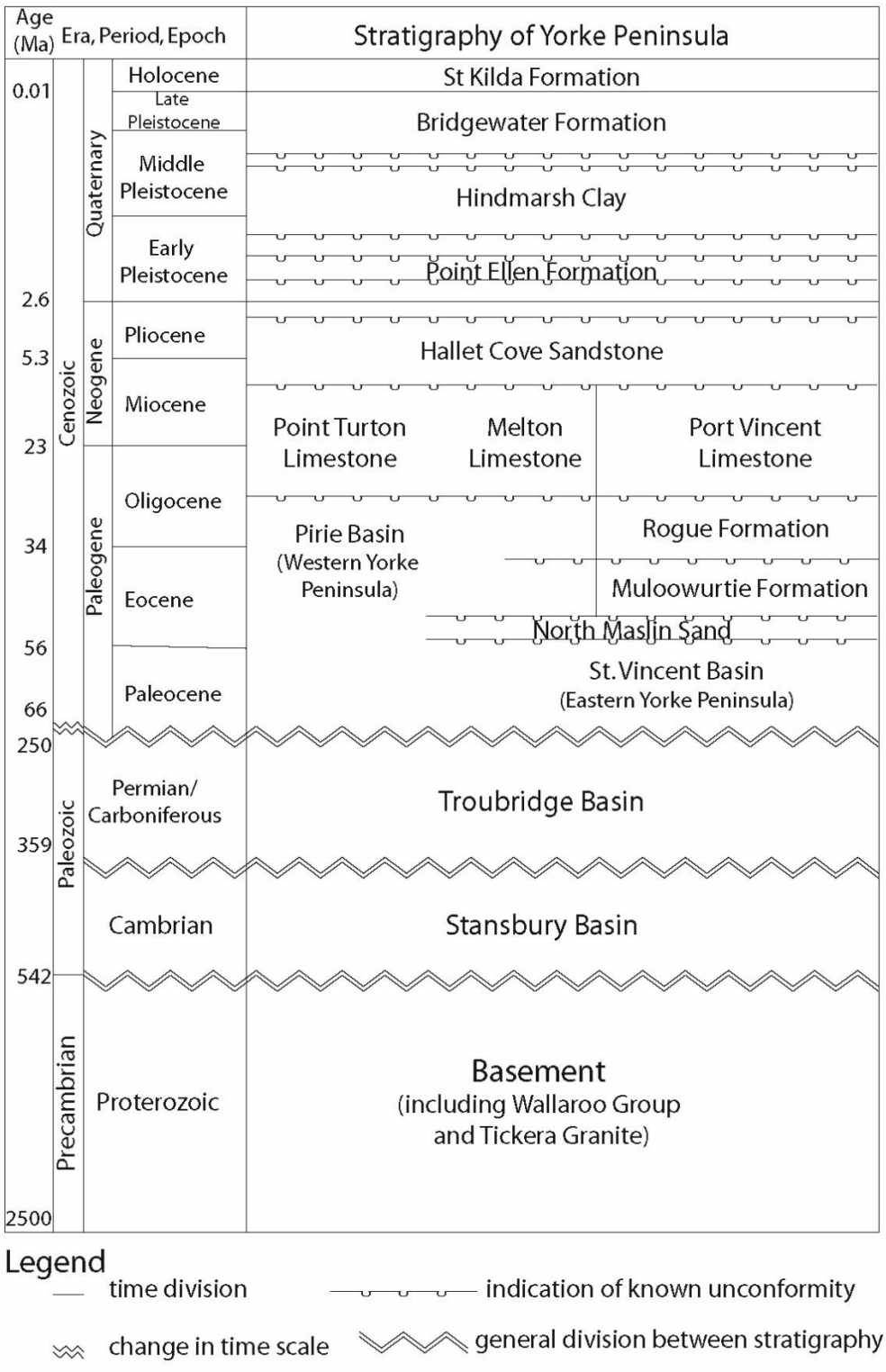

Figure 1-6 Simplified geological stratigraphy of the Yorke Peninsula. Modified after Drexel and Preiss (1995) and Zang et al (2006).

1.3.2 Landscape

The landscape throughout the Yorke Peninsula is mostly of low relief and comprises gentle undulating slopes and plains (Fig. 1.7). The average elevation is ~150m above sea level and the highest elevation (~250m ASL), occurs around Arthurton (Crawford, 1965; DEWNR, 2013; Roberts, 2007; Zang et al., 2006). The coastline varies from sandy or rocky beaches to cliffs and steeply eroded hills (Roberts, 2007; Fig. 1.7). Large areas of sand dunes and swales dominate portions of the north-west and central to south-east, whilst playa salt lakes and clay pans dominate the landscape to the south (Fig. 1.7). The water table generally occurs at ≥2m below the surface (DEWNR, 2017).

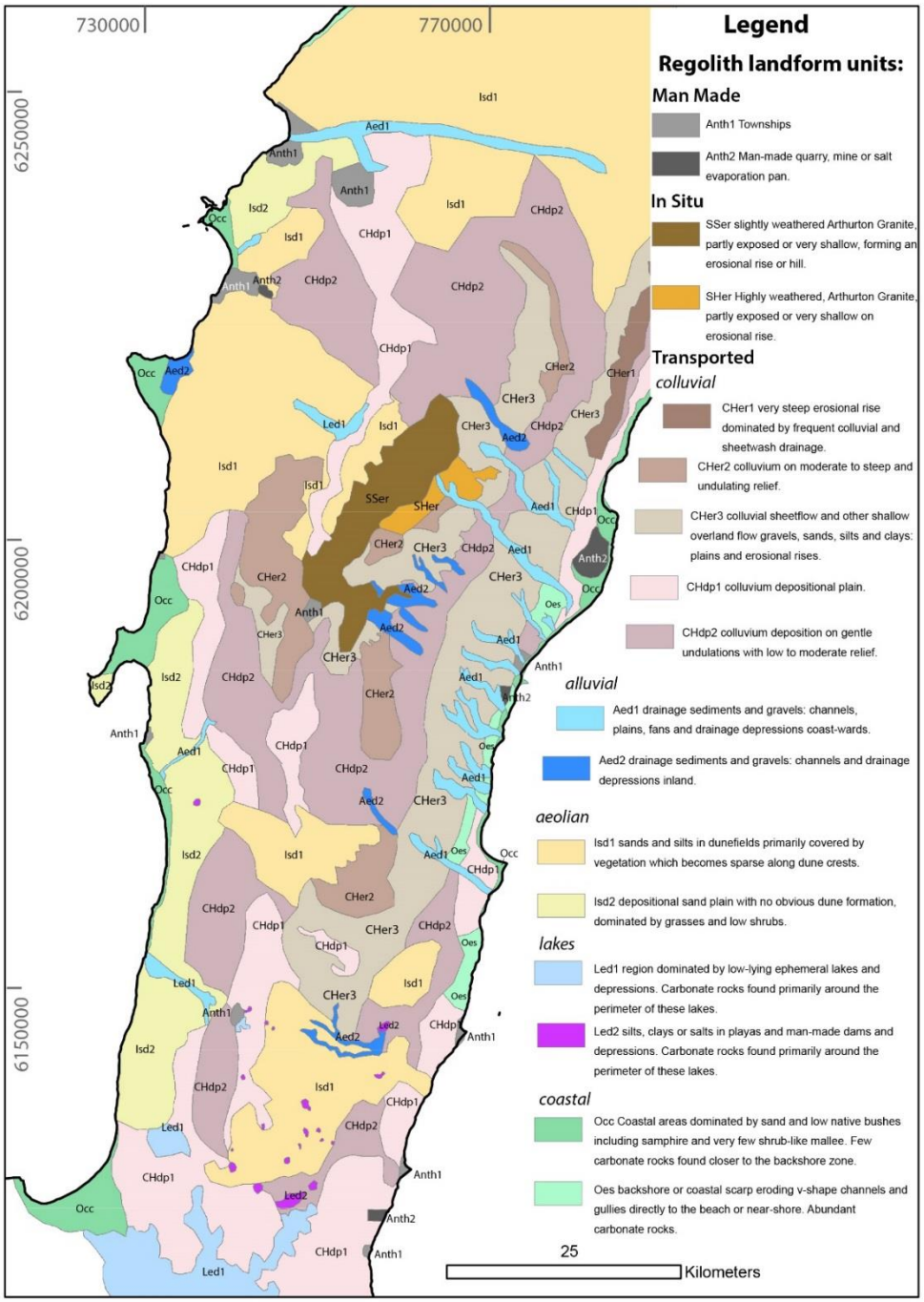

Figure 1-7 Regolith map (1:25,000) of the Yorke Peninsula. This map was produced using a combination of geophysical data and field observations which are detailed in Chapter 3, section '3.4 Methods'. Dominant features of the landscape are shown. Comprehensive descriptions of each landform are given in Chapter 3.

1.3.3 Climate

The climate is described as Mediterranean with hot dry summers and mild and wet winters (Neagle, 2008). The maximum average temperature ranges from 27 °C to 30 °C during summer and 15 °C to 16 °C during winter (Bureau of Meteorology, 2018). Rainfall across the Yorke Peninsula typically averages around 500 mm per year (average based on 116 years of recorded rainfall at Maitland, from 1879 to 2018; Bureau of Meteorology, 2018). Annual evaporation rate of rainfall is high. The general direction of the prevailing wind is from the west, being more from the north-west during the warmer months and the south-west during the cooler months.

1.3.4 Vegetation

Most of the natural vegetation, i.e. that which occurred prior to European settlement across the Yorke Peninsula, has been cleared for grazing and cropping (DEWNR, 2013; McDowell et al., 2012; Neagle, 2008; Zang et al., 2006). Widespread cropping includes cereal grains, oil grains and legumes as the majority of the region contains moderately fertile soils (DEWNR, 2017). Much of the remaining native vegetation is restricted to corridors along roadside verges and fence lines, which act as windbreaks. Patches of woodland typically remains on ground that is the least suitable for agriculture (Neagle, 2008). The majority of the native vegetation can be broadly characterized as open mallee woodland and shrubland (Neagle, 2008). There are thirteen species of mallee Eucalyptus (E.) that occur across the Yorke Peninsula (Brooker et al., 2002).

1.4 Objectives of the Study

The objective of this thesis is to:

1. Gain an understanding of how cover sequence materials exposed at the surface, of the Yorke Peninsula, can be used in exploring for underlying mineral deposits. This includes gaining an understanding of processes of element dispersion within cover sequence materials;

2. Gain an understanding of and evaluate the cover sequence sample media in exploration and how to recognise them using simple geochemical discrimination;

3. Understand how geochemical signatures related to mineralisation are expressed within pedogenic carbonates and mallee leaves;

4. Develop criteria for geochemical vectoring for mineralisation for iron-oxide-copper-gold (IOCG) deposits applicable for the exploration industry.

1.5 Methods

Methods used in this study are:

- field collection of carbonate rocks;
    - this was undertaken over a series of weekends
    - samples were identified visually as carbonate by noting a chalky white and sometimes crumbly texture and by the use of dilute HCL. More detailed information is given in Chapter 3

    - samples collected in the field were prepared for analysis by sorting and labelling as described in Chapter 3.
    - samples collected from profile outcrops (beach-front cliffs) were also sorted and labelled during collection. Sorting was also required to further separate samples for whole-rock analysis, isotope analysis, spectral analysis and microscopy. Further information for these methods are found in Chapter 2.
    - samples are currently stored at the University of Adelaide in the Mawson Building.
- field collection of *Eucalyptus* leaves;
    - sample collection of leaves was undertaken over a series of weekends at the same time as collection of carbonate rocks.
    - samples were collected and labelled in the field. Samples were later sorted, dried and species identified. Further details can be found in Chapter 4.
- field collection of water;
    - water samples were collected as described in Chapter 2 and again in Chapter 3. Water was collected to look at both isotopic and elemental content. Calcium and Sr concentrations were compared to those found in carbonate rock field samples which is detailed in Chapter 3.
- Carbonate rock analytical methods;
    - Whole-rock analysis is used to find the elemental make-up of each sample and detailed in Chapters 2 and 3. XRF is used for major element oxides and ICP-MS is used for trace elements. Geochemical data including all elements

analysed, their lab method and detection limits are found in Appendices 2, and 5.

- Isotopic analysis was undertaken on samples from escarpment profiles and thought to be useful for finding differences between marine and pedogenic carbonate rocks and is detailed in Chapter 2.
- Thin sections were prepared for microscopic analysis of samples and is detailed in Chapter 2. This was undertaken to provide a description of each sample in detail, and place into context with the profile escarpments where the samples were collected.
- Reflectance spectroscopy is used to identify minerals and mineral assemblages found in each sample collected from the escarpment profiles and detailed in Chapter 2. Further detail is found in Appendix 2.

- Vegetation analysis is much the same as whole-rock whereby dried samples are crushed and milled. This was undertaken to determine if the eucalypts are taking in elements in a way that can be used to define areas of interest with regard to mineral exploration. Other studies had proven successful by way of Au results (described in Chapter 4) where the results of this study proved more useful for using the concentrations of Cu. Elements (53) are analysed by ICP-MS after digestion of the milled samples in HNO_3 and then by Aqua Regia. This method is described in detail in Chapter 4. Full analytical results including Lab method and detection limits are presented in Appendix 8.
- Seawater was collected to analyse for Sr isotopes as a comparison to isotopes found in samples collected from the escarpment profiles (Chapter 2 and Appendix

2). Geochemical analysis of other elements including Ca, are presented in Chapter 3 and Appendix 6.

- Regolith Map has been constructed with the use of field observations along with various geophysical data. The detailed methods are described in Chapter 3.
- Software used throughout the preparation and writing of this thesis includes;
    - Microsoft Office Suite™
    - Esri- ArcGIS™
    - Reflex- Imdex ioGAS™
    - Adobe®- Illustrator™
    - Clarivate Analytics- EndNote X8™
    - CSIRO- The Spectral Geologist (TSG™)

1.6 Thesis structure

This thesis is presented as three research chapters that are each formatted as independent papers for publication in an international peer reviewed journal. There is some repetition in the Introduction sections of each of the chapters as a result. The major conclusions are presented in a final conclusions chapter.

Carbonate rocks are examined firstly as they are commonly found throughout the region and are a popular sample material as previously described in (1.1 Regolith carbonates and mineral exploration) The sequence of presentation firstly looks at how to differentiate pedogenic carbonates from marine carbonates presuming they are otherwise difficult to

identify apart (Chapter 2). The study of surface occurring carbonates across the entire region follows (Chapter 3). This regional study builds upon lessons learned from the first study presented in Chapter 2. To complement the study of pedogenic carbonate rocks, eucalypt trees, which are also found across the study area, are also included. *Eucalyptus* are known for being Au indicators as previously described (1.2 Biogeochemistry and mineral exploration). The intention with this thesis is to assess their usefulness in vectoring towards mineralisation but using mallee-form eucalypts instead of the larger *E. camaldulensis* (River Redgum) which occur less frequently across this location. My initial plan was to focus on Au and Cu, which occur in known mineral deposits on the Yorke Peninsula. Gold analyses in both carbonate rocks and mallee were largely below detection and were not useful for mineral exploration. Copper was the most useful element for identifying potential for underlying mineralisation. The following Chapters describe and discuss these results;

Chapter 2 focusses on how cover-sequence rocks exposed at the surface contain dispersion signatures from Cu rich basement. It uses samples collected from vertical coastal exposures of carbonate rocks overlying basement, where possible, and seawater. The samples collected were analysed by whole-rock geochemical methods, Sr isotopic analysis, petrographic analysis and spectral analysis using a HyLogger™ to define and differentiate between marine and pedogenic carbonate rocks. HyLogger™ was also used for mineral identification and to help discriminate materials, particularly pedogenic carbonate and marine carbonate from the presence of dolomite. The study found that Ca/Sr ratios were a simple method to differentiate between marine and pedogenic carbonate rocks as each rock type displayed unique and separate groupings of Ca/Sr

ratios. I found that Sr isotopic ratios ($^{87}Sr/^{86}Sr$) were not systematically different between marine and pedogenic carbonates which I interpreted to be due to the Sr and associated Ca being of a seawater origin. I found that marine carbonate rocks have Ca/Sr values >1260 and that pedogenic carbonate rocks have Ca/Sr ratios <650. I also found that Cu values in pedogenic carbonate rocks reflected Cu concentrations in the basement whereas marine carbonate did not. I concluded that potentially the quick and easy, field assessment of Ca/Sr ratios throughout a carbonate sampling exploration campaign will decrease the risk of collecting incorrect sample media and increase the risk of identifying potential pathfinder elements. This chapter has been published as a stand-alone paper in Journal of Geochemical Exploration; Vol. 181 (2017), pp 81-98.

Chapter 3 focuses on the source of Ca and Sr in carbonate rocks that are collected in a large-scale exploration-style sampling program, across the entire study region and tests the application of Ca/Sr ratios and any association the carbonate rocks may have to underlying IOCG +/- U basement rocks. It uses whole-rock geochemical results from 215 carbonate rocks sampled from alongside east-west road corridors and chemical composition of seawater collected from 2 locations; one location each on both the east and west coast. I developed a regolith map (Fig. 1.7) for the purposes of visually understanding the landscape and determine effects if any of surficial processes. Transects that locate where the samples were collected are in Figure 1.4. Ca/Sr ratios from Chapter 2 were applied to determine the types of carbonates that were sampled and to compare the chemistry of the rocks with the chemistry of the seawater. I found that the primary source of Ca and Sr throughout the region is sourced mainly from evaporative concentration of seawater derived components deposited in rain with some meteoric

fractionation. The majority of the carbonate rocks that were sampled, were found to contain a pedogenic range of Ca/Sr values which reflected the influence of variation in rainwater chemistry and that 1 sample reflected a marine carbonated Ca/Sr ratio. Statistical methods were used to determine if any empirical relationship of Cu concentration in the carbonate rocks related to Cu occurrence in the underlying basement rocks. I also compared Cu concentrations in carbonate rocks by proximity to known Cu occurrence. Copper concentrations in carbonate rocks were found to reflect Cu occurrence in basement rocks and that this was more likely to occur within a radius of 3km to a known Cu mine or deposit. I concluded that regolith carbonates are a potentially useful sampling media for Cu exploration on the Yorke Peninsula and that they can be easily differentiated from less useful marine carbonates on the basis of Ca/Sr ratios. This chapter has been published as a stand-alone paper, to the Journal of Geochemical Exploration: Vol. 194 (2018), pp 239–256.

Chapter 4 describes and discusses pioneering the usage of eucalypt trees for exploration sampling across the region to aid in characterising the IOCG +/- U prospectivity of the underlying sediments (Fig. 1.4). It uses biogeochemical results from 218 mallee eucalypts sampled from alongside east-west road corridors. I first needed to determine that the natural uptake of elements into the variety of eucalypts sampled, was similar and then rule out the possibility of contamination that may occur as a result of local farming e.g. fertiliser usage and dust. I found that timing of sample collection e.g. late summer, and method for obtaining the sample at each site e.g. away from the road, reduced the likelihood of contamination. I used statistical methods on the biogeochemical results from leaf samples collected from 4 different species of mallee eucalypt and found that there is

an empirical relationship between the Cu accumulation in the leaves and elevated Cu in the underlying basement rocks. I also compared populations of eucalypt with their proximity to known Cu mine or deposit and found that higher concentrations of Cu occur more commonly within 3 km of the known Cu occurrence. I concluded that mallee-eucalypt have the ability to transfer chemical signals from depth and as they are widespread throughout southern Australia, they could be used as an effective, rapid, cheap and non-invasive exploration method and can be applied at large scales. This chapter has been published as a stand-alone paper in Journal of Geochemical Exploration; Vol. 185 (2018), pp 139-152.

Chapter 5 summarizes the key conclusions from Chapters 2-4 and gives an overall picture of how this thesis has developed the use of carbonate rocks and mallee eucalypts as a mineral exploration sampling medium.

Chapter 2: Distinguishing pedogenic carbonates from weathered marine carbonates on the Yorke Peninsula, South Australia: Implications for mineral exploration

Foreword

This chapter presents whole-rock and strontium isotope geochemical data from geological profiles from the Yorke Peninsula in South Australia and provide a geochemical means of discriminating between Cenozoic marine carbonate-bearing rocks and Quaternary pedogenic carbonate-bearing rocks. The geochemistry from these profiles shows how cover-sequence rocks exposed at the surface contain dispersion signatures from Cu rich basement. Samples were collected by Dr Steve Hill during a field trip in 2012. Samples were photographed and logged by myself. Additional photographs were taken by Charlotte Mitchell. Isotopic analysis was undertaken at the University of Adelaide with assistance from Dr David Bruce. A Thermal Ionisation Mass Spectrometer (TIMS), was used to obtain Sr isotopes from whole-rock and seawater samples. Whole-rock geochemistry was undertaken by Acme Laboratories (now Bureau Veritas), Vancouver Canada. Reflectance spectroscopy was undertaken at the geological Survey core storage facility at Glenside, SA (now located at Tonsley, SA) by Georgina Gordon. Thin sections were prepared by Adelaide Petrographic Laboratories, Kensington, SA.

Statement of Authorship

Title of Paper	Distinguishing pedogenic carbonates from weathered marine carbonates on the Yorke Peninsula, South Australia: Implications for mineral exploration
Publication Status	☑ Published ☐ Accepted for Publication ☐ Submitted for Publication ☐ Unpublished and Unsubmitted work written in manuscript style
Publication Details	Journal of Geochemical Exploration Vol 181 (2017) pages 81–98 http://dx.doi.org/10.1016/j.gexplo.2017.06.019 Received 13 February 2017; Received in revised form 7 June 2017; Accepted 28 June 2017 Available online 08 July 2017 0375-6742/ © 2017 Elsevier B.V. All rights reserved.

Principal Author

Name of Principal Author (Candidate)	Keryn Wolff
Contribution to the Paper	Collection and preparation of all samples including seawater. Sorting packaging and labelling for delivery to laboratory for geochemical analysis. Preparing suitable samples for thin section creation. Petrographic analysis of thin sections. Preparation of all samples including seawater, for isotopic analysis. Undertaking the laboratory work for isotopic analysis of all samples. Using the mass spectrometer in the Mawson Building to gain isotopic information from each sample. Preparing samples for reflectance spectroscopy. Data entry and format of results suitable to use in relevant geochemical, statistical and GIS software programs. Compiling all illustrations used in the published article and making new ones where needed. Drafting initial document. Correcting to Co-authors and reviewers comments. Primary contact throughout the publications process.
Overall percentage (%)	90
Certification:	This paper reports on original research I conducted during the period of my Higher Degree by Research candidature and is not subject to any obligations or contractual agreements with a third party that would constrain its inclusion in this thesis. I am the primary author of this paper.
Signature	Date 12/04/2018

Co-Author Contributions

By signing the Statement of Authorship, each author certifies that:

i. the candidate's stated contribution to the publication is accurate (as detailed above);

ii. permission is granted for the candidate in include the publication in the thesis; and

iii. the sum of all co-author contributions is equal to 100% less the candidate's stated contribution.

Name of Co-Author	Caroline Tiddy
Contribution to the Paper	Review comments and editing suggestions
Signature	Date 12/04/2018

Name of Co-Author	David Giles
Contribution to the Paper	Review comments and editing suggestions
Signature	Date 12/04/2018

Please cut and paste additional co-author panels here as required.

Name of Co-Author	Steve Hill
Contribution to the Paper	Review comments and editing suggestions
Signature	Date 9/4/18

Name of Co-Author	Georgina Gordon
Contribution to the Paper	Assistance with reflectance spectroscopy and editing suggestions related specifically to reflectance spectroscopy.
Signature	Date 13/4/18

Distinguishing pedogenic carbonates from weathered marine carbonates on the Yorke Peninsula, South Australia: Implications for mineral exploration

Keryn Wolff, Caroline Tiddy, David Giles, Steven M. Hill, Georgina Gordon

As published in Journal of Geochemical Exploration, 2017

(Journal of Geochemical Exploration 181 (2017) 81–98)

(Appendix 1)

https://doi.org/10.1016/j.gexplo.2017.06.019

2.1 Abstract

We present whole-rock and strontium isotope geochemical data from geological profiles from the Yorke Peninsula in South Australia and provide a geochemical means of discriminating between Cenozoic marine carbonate-bearing rocks and Quaternary pedogenic carbonate-bearing rocks. Pedogenic carbonate-bearing rocks (commonly referred to as calcrete) are potentially useful mineral exploration sampling media whereas weathered marine carbonate-bearing rocks (limestone), are less useful. Distinguishing between the two in drill cuttings where textural information has been destroyed is difficult. Strontium isotope ratios are variable, strongly dependent on clastic sedimentary component and thus do not differentiate effectively between pedogenic and marine carbonate-bearing rocks. There is a systematic difference between Ca/Sr and Ca/Mg ratios in the pedogenic carbonate-bearing rocks compared to the weathered Cenozoic marine carbonate-bearing rocks. Pedogenic carbonate-bearing rocks have systematically lower Ca/Mg (< 28) and Ca/Sr (< 650) ratios than their marine counterparts Ca/Mg (> 35) and Ca/Sr (> 1260). This simple discriminant can be used to identify samples appropriate for carbonate sampling in mineral exploration, particularly in drill cuttings, as well as retrospective filtering of multi-element geochemical exploration data sets.

2.2 Introduction

Carbonate-dominated regolith has a widespread global distribution concentrated in the mid latitudes (Batjes, 2012; Chen et al., 2002) (Fig. 2.1). This material includes a range of weathered carbonate-bearing rocks, including limestone, as well as in situ, transported and reworked pedogenic carbonate-bearing rocks (sometimes referred to as calcrete but can also include dolomite), derived from atmospheric (e.g. dust and rain) accessions. The vast global extent of these lithologies has generated much interest in their origin, chemistry and paleo-environmental significance (Chen et al., 2002; Dart et al., 2012; Milnes, 1992; Milnes and Hutton, 1983; Poustie and Abbot, 2006; Quade et al., 1995).

Carbonate-bearing rocks have been widely studied for their strontium ($^{87}Sr/^{86}Sr$) isotopic composition to trace calcium source and mobility, soil carbonate origins and sedimentary environments (Dart et al., 2012; Liu et al., 2013; Quade et al., 1995; Zhao et al., 2009). This method has also been applied to trace sources of other elements such as using strontium (Sr) as a proxy for calcium (Ca) (Dart et al., 2007; Dart et al., 2012; Liu et al., 2013; Quade et al., 1995; Van der Hoven and Quade, 2002). Strontium isotopic studies using marine carbonate-bearing rocks typically relate to the chemistry of the water in

which they are formed and are commonly used for the purpose of dating (e.g. Burke et al., 1982; Howarth and McArthur, 1997; McArthur et al., 2001; McArthur et al., 2012).

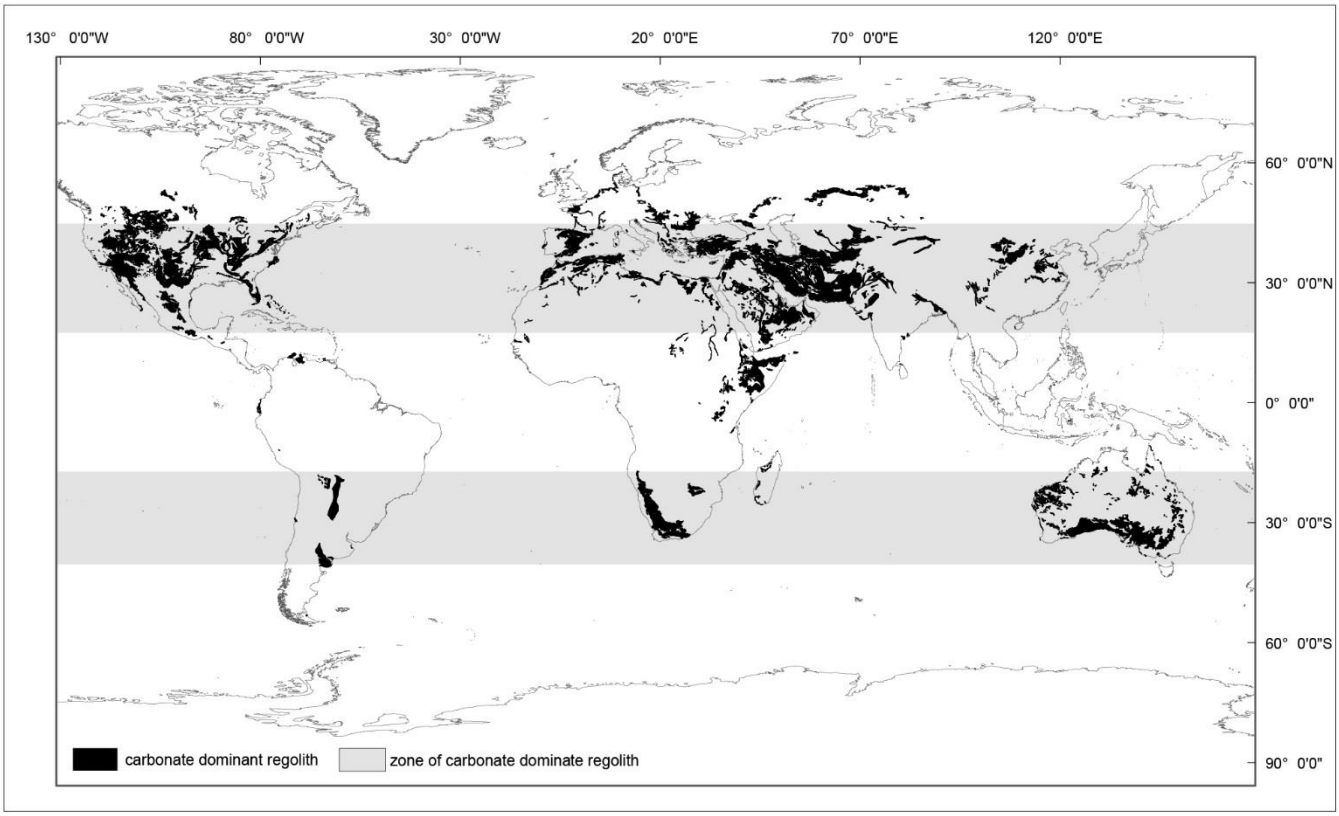

Figure 2.1. Worldwide distribution of carbonate dominant regolith including limestone. Compiled from ISRIC (Batjes, 2012) and USGS datasets (USGS, 2016). Specific areas and general zones of carbonate dominated regolith are highlighted.

Pedogenic carbonate-bearing rocks (such as calcrete) are widely used as a mineral exploration sampling medium (Chen et al., 2002; McQueen et al., 1999; Poustie and Abbot, 2006), and have been successfully utilised to discover and delineate various economic resource deposits around the world (Ghavami-Riabi et al., 2008; Lintern et al., 2005). The Challenger Gold Deposit within the Gawler Craton, South Australia (Fig. 2.2) was discovered following a regional carbonate rock sampling program (Poustie and

Abbot, 2006). A dramatic increase in interest in carbonate geochemistry followed (Chen et al., 2002; Lintern et al., 2012; Reith et al., 2011; van der Hoek et al., 2012). It is essential, although often very difficult, to distinguish marine carbonate-bearing rocks from pedogenic carbonate-bearing rocks when undertaking a carbonate sampling program. This difficulty in distinction arises due to weathering of marine carbonate rocks typically resulting in recrystallization and pedogenic overprinting rendering the resulting sample morphology indistinguishable. This can be problematic in mineral exploration sampling campaigns as those undertaking the sampling are not always geologically trained. Additionally, in cases where drilling is being undertaken (e.g. air core, reverse circulation, rotary air blast and coiled tubing drilling) the returned sample comprises rock flour and small chips. Fine-scale textural information can be extremely difficult to impossible to distinguish in such material (e.g. Hillis et al., 2014; Marjoribanks, 2010). Distinction is essential as pedogenic carbonate-bearing rocks have the potential to carry a geochemical signature transferred from underlying mineralisation (e.g. Chen et al., 2002) whereas marine carbonate-bearing rocks typically reflect the chemistry of the water in which they formed.

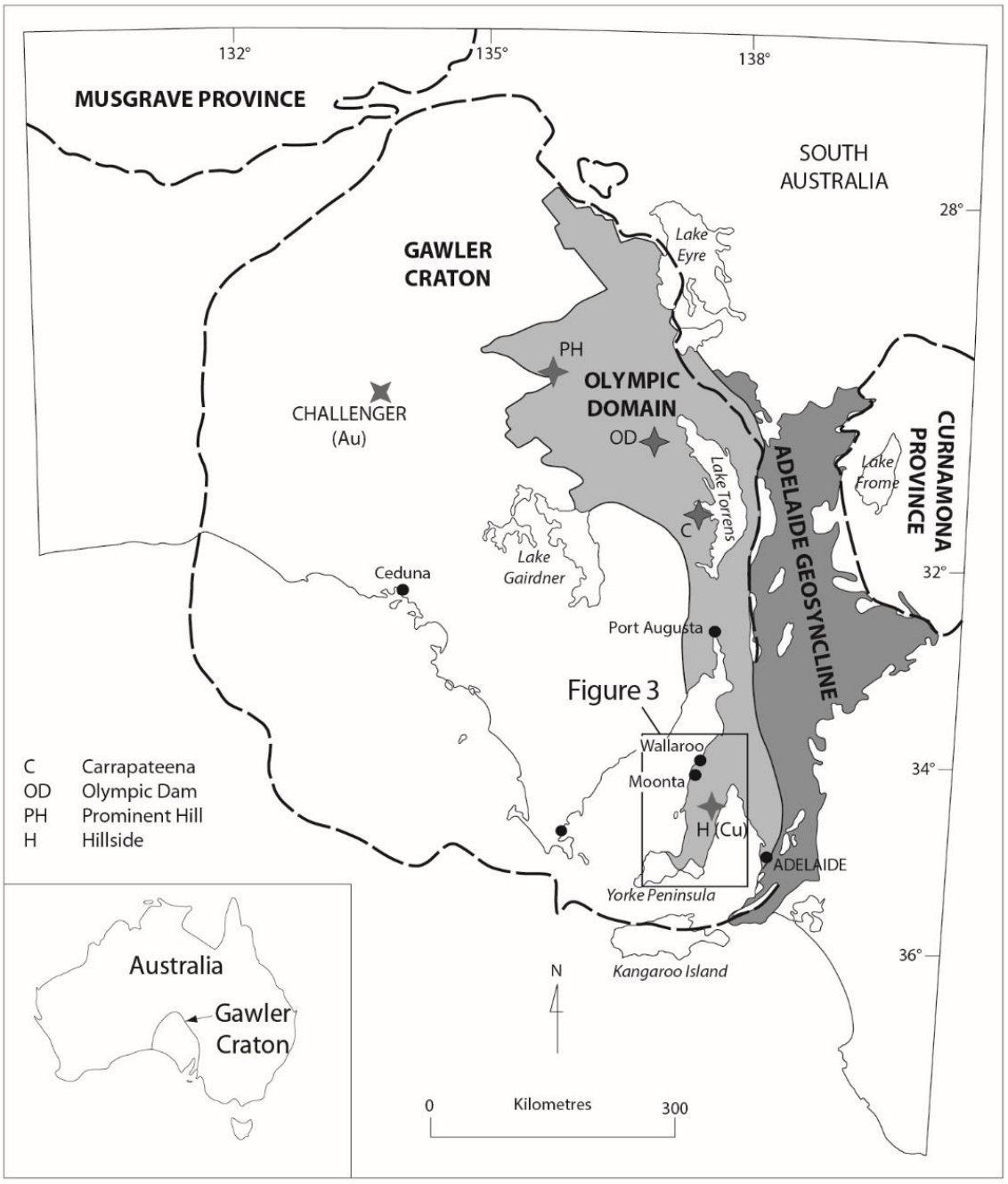

Figure 2.2. Simplified geological map showing the selected major geological provinces and the location of major IOCG deposits within the Olympic Domain. The rectangle indicates the location of Figure 2.3. Modified after Connor et al., (2010). Inset: Location within Australia.

The Yorke Peninsula in the southeastern Gawler Craton of South Australia (Fig. 2.2) is covered by large areas of both marine- and pedogenically-derived carbonate-bearing rocks. Additionally, the Yorke Peninsula region comprises sparsely exposed Proterozoic basement rocks that are prospective for iron oxide, copper and gold mineralisation (Conor, 2016; Conor et al., 2010; Conor, 2002; Cowley, 2005; Cowley et al., 2003; Drexel et al., 1993; Ismail et al., 2014; Zang et al., 2006). The ability to distinguish between weathered marine and pedogenic carbonate-bearing rocks in the cover sequence overlying a prospective region such as the Yorke Peninsula would therefore assist in exploration for mineral deposits under cover, as well as for reviewing and evaluating historical multi-element geochemical datasets.

This paper aims to set simple criteria that can be rapidly applied to distinguish between weathered marine and pedogenic carbonate-bearing rocks. This is done using hyperspectral analysis, microscopy and $^{87}Sr/^{86}Sr$ ratios to identify changes across three coastal carbonate-bearing profiles (Fig. 2.3), and combined with Ca/Sr ratios derived from whole-rock geochemical data. These results are then used to develop criteria to distinguish between marine and pedogenically derived carbonate-bearing rocks. The potential influence this may have on exploration practices using this sampling medium is then discussed.

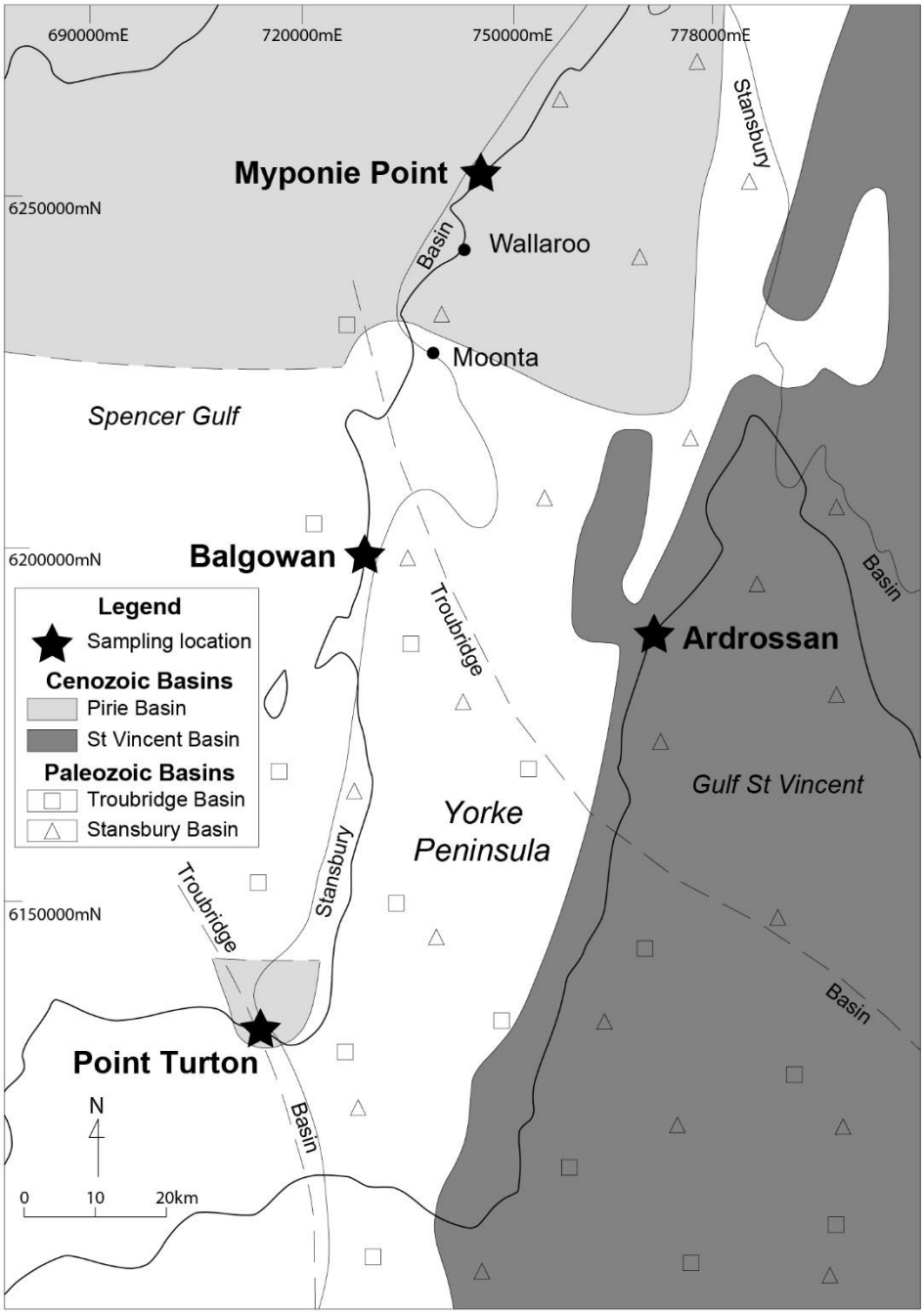

Figure 2.3. Map of Yorke Peninsula showing location of the Palaeozoic Stansbury and Troubridge Basins and Cenozoic Pirie and St Vincent Basins. Locations of logged and sampled profiles at Myponie Point, Balgowan and Point Turton as well as the sea water

sampling location of Ardrossan are shown. Basin outlines are modified from Drexel and Preiss (1995).

2.3 Strontium Chemistry of Marine Sediments and Regolith Carbonates

Strontium isotope ratios ($^{87}Sr/^{86}Sr$) can be used to analyse calcium-rich materials such as soil carbonates, marine limestone and seawater (e.g. Dart et al., 2012; Vasiliev et al., 2010; Veizer, 1989). Strontium is used as a surrogate for Ca, as chemical properties such as valence and ionic radius are similar for both elements, which allows for easy substitution of Ca by Sr. Strontium is typically found in trace amounts in minerals containing calcium (Bain and Bacon, 1994; Van der Hoven and Quade, 2002).

The methodology for dating seawater using marine carbonate $^{87}Sr/^{86}Sr$ ratios is well established (e.g. Burke et al., 1982; McArthur et al., 2001; McArthur et al., 2012). Marine organisms access Ca (and by association Sr) for growth from seawater, which preserves a unique $^{87}Sr//^{86}Sr$ ratio. The $^{87}Sr//^{86}Sr$ ratios can be reliably used because the ^{86}Sr isotope remains constant over time (Bain and Bacon, 1994; Van der Hoven and Quade, 2002). The stable ^{87}Sr isotope is derived from the radiogenic decay of the isotope ^{87}Rb (e.g. Bain and Bacon, 1994; Van der Hoven and Quade, 2002; Wickman, 1948). Diagenesis and re-precipitation of Sr in carbonate rocks therefore will preserve the initial $^{87}Sr//^{86}Sr$ ratio at the time of precipitation (Veizer, 1989).

Ratios for $^{87}Sr//^{86}Sr$ in seawater have varied gradually throughout time and have been used to develop a Sr isotope seawater curve (Burke et al., 1982; McArthur et al., 2001; McArthur et al., 2012) (Fig. 2.4). This seawater curve has been compiled from $^{87}Sr/^{86}Sr$

ratios of calcite-rich marine fossils (McArthur et al., 2012). Any deviation from this curve may be attributed to contaminating factors such as clastic sediment input or modern sea spray (Veizer, 1989). Formation and erosion of continental rocks during the Earth's tectonic history along with groundwater discharge, river discharge and mid ocean ridge interactions all affect the balance of ^{87}Rb, and the resulting ^{87}Sr, in the seawater (Veizer, 1989). The gradual increase in $^{87}Sr/^{86}Sr$ ratios during the Cenozoic and also notably between 0-40 Ma is attributed to continental erosion (by inference of Sr inputs to the modern oceans (Veizer, 1989).

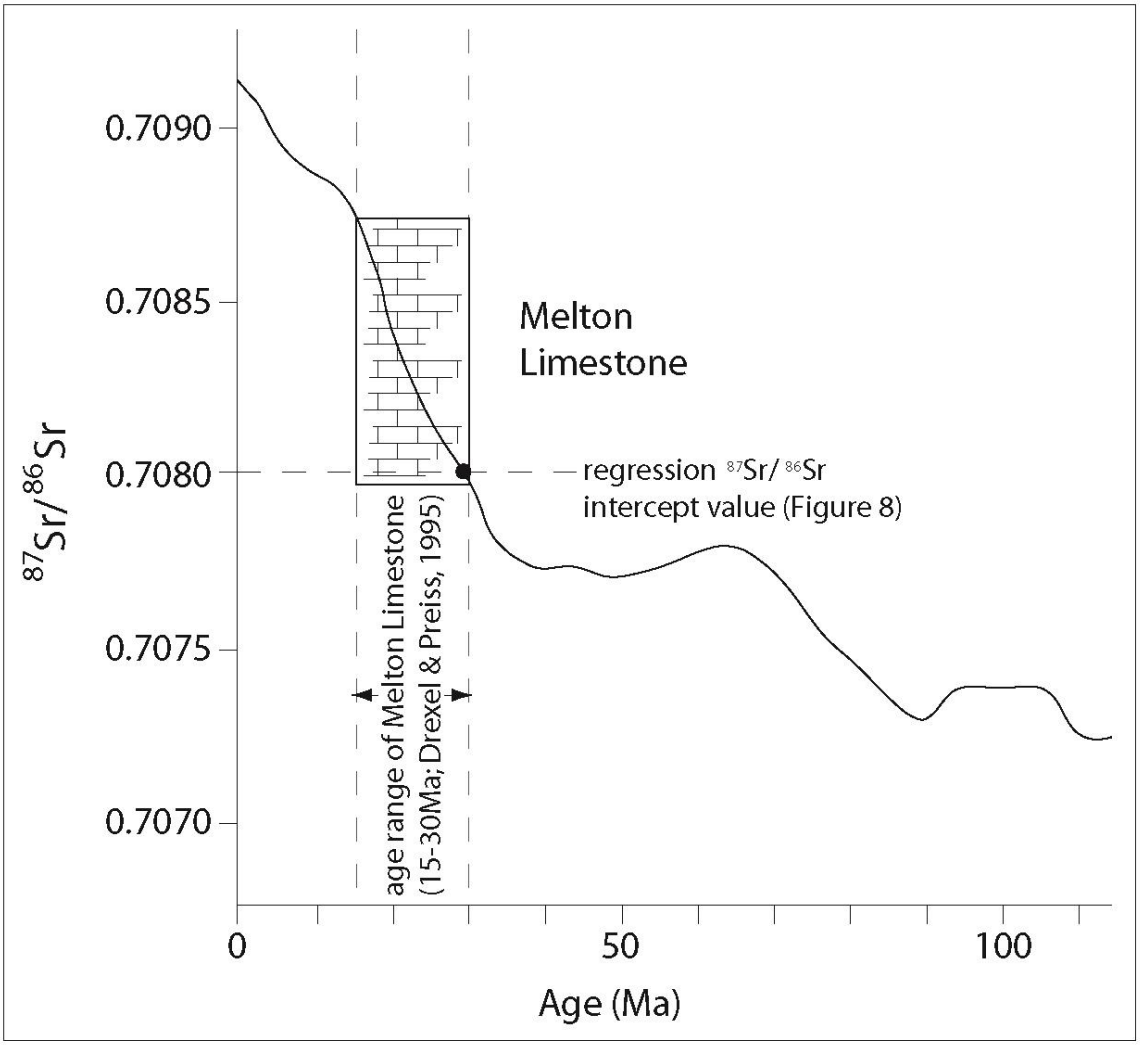

Figure 2.4. Seawater curve of strontium isotopes adapted from McArthur et al., (2012). The age range of Melton Limestone is highlighted. The black dot represents the $^{87}Sr/^{86}Sr$ regression intercept value derived in this study (also see Figure 2.12 and explanation in text).

2.4 Geological Setting

The geology of the Yorke Peninsula in the southeastern Gawler Craton (Fig. 2.2) has been well described by Crawford (1965), Drexel and Preiss (1995), Zang et al., (2006) and Conor et al., (2010). The basement geology of the central Yorke Peninsula comprises Proterozoic rocks with minimal (<5%) exposure, and is dominated by metasediments and volcanics of the ca.1750 Ma Wallaroo Group (Cowley et al., 2003), (Fig. 2.5). The Wallaroo group has been subject to deformation, metamorphism and magmatic events (e.g. Ferris et al., 2002; Forbes et al., 2011; Hoek and Schaefer, 1998).The Wallaroo Group was intruded by the ca.1595-1575 Ma Hiltaba Suite granites (e.g. Conor et al., 2010; Skirrow. et al., 2007) including the 1598-1575 Ma Tickera Granite, 1589 Ma Curramulka Gabbronorite and 1583 Ma Arthurton Granite (Binks et al., 2004; Cowley et al., 2003; Drexel et al., 1993; Wurst, 1994; Zang et al., 2006), (Fig. 2.5). Interactions between a combination of these geological events has led to mineralisation throughout the region (e.g. Conor et al., 2010; Morales-Ruano et al., 2002)

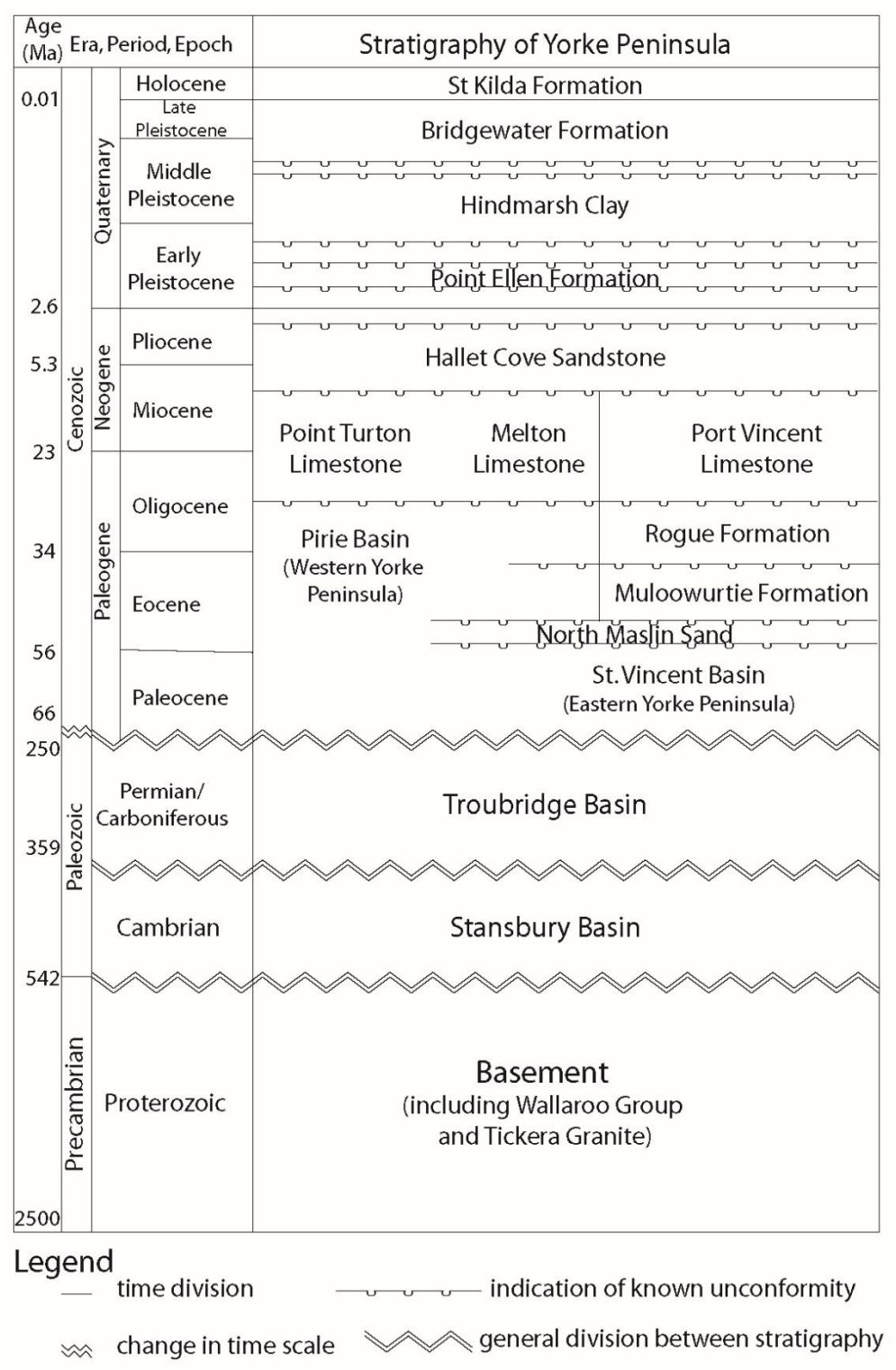

Figure 2.5. Simplified geological stratigraphy of the Yorke Peninsula. Modified after Drexel and Preiss (1995) and Zang et al (2006).

Mineralisation in the region is part of the southern extent of the Olympic Domain, which is also host to the giant Olympic Dam and smaller Prominent Hill and Carrapateena iron oxide-copper-gold deposits (Fig. 2.2). Mineralisation in the Olympic Domain is hosted within a range of rock types, including the Wallaroo Group and the Hiltaba Suite Granites (Conor et al., 2010; Cowley et al., 2003). The Yorke Peninsula also hosts Cu-Au mineralisation including the Hillside deposit and deposits in the historic Moonta-Wallaroo district (e.g. Conor et al., 2010; Ismail et al., 2014; Morales-Ruano et al., 2002) (Fig. 2.2).

These basement rocks are unconformably overlain by younger Cambrian to Quaternary sediments (Crawford, 1965; Drexel and Preiss, 1995; Zang et al., 2006). The Cambrian Stansbury Basin (Fig. 2.3) consists of alternating limestone and sand to mudstone formed during sea level fluctuations (Drexel and Preiss, 1995; Zang et al., 2006) (Fig. 2.5). The Carboniferous to Permian Troubridge Basin (Fig. 2.3) formed during periods of rapid temperature fluctuation and sea level change (Drexel and Preiss, 1995; Zang et al., 2006).

The Cenozoic (2.6-65 Ma) St. Vincent Basin, and contemporaneous Pirie Basin (Figs 2.3 & 2.5), overlies the aforementioned older, weathered sequences. The St. Vincent Basin covers a portion of the eastern side of the Yorke Peninsula (Fig. 2.3) and is outside of the study area. The Pirie Basin occurs across the western and central parts of the peninsula north of Moonta and extends south towards Point Turton (Fig 2.3). The Pirie and St Vincent Basins are reported to have been connected via a southwards flowing paleochannel that winds across the northern part of the Yorke Peninsula towards Ardrossan (Drexel and Preiss, 1995; Pain and Johnson, 2002).

The Pirie Basin includes three main stratigraphic units; Kanaka Beds, which is the earliest, overlain unconformably by the fossil-bearing, Late Oligocene to Middle Miocene (Drexel and Preiss, 1995) Melton Limestone and above this the Gibbon Beds (Drexel and Preiss, 1995; Zang et al., 2006). The Pirie Basin also includes the fossil-bearing, Oligocene to Miocene Point Turton Limestone restricted to the south, and is likely to be linked to the Melton Limestone further north (Drexel and Preiss, 1995; Zang et al., 2006). Melton Limestone is exposed in sinkholes, roadside cuttings, and coastal escarpments on the Yorke Peninsula.

During the Quaternary, sand, silt, clay and carbonate-bearing rock accumulations have largely concealed the underlying geology. Quaternary sediments include clays and quartz-rich sands and sandstone of the Hindmarsh Clay; carbonate-bearing rock such as aeolianite and calcarenite of the Bridgewater Formation; and modern beach deposits and dunes of the St Kilda formation (Crawford, 1965; Drexel and Preiss, 1995; Zang et al., 2006), (Fig 2.5). Sand-flat deposits, claypans and salt lakes have developed on areas with low relief (Crawford, 1965; Drexel and Preiss, 1995; Zang et al., 2006; James and Bone, 2015). Carbonate-bearing rock formation is ongoing with continuing accumulation of calcium carbonate and near-surface cementation (calcrete). Active erosion occurs along gullies, drainage lines and in coastal environments (Crawford, 1965; Drexel and Preiss, 1995; Zang et al., 2006).

2.5 Profile Description

Three sites, Myponie Point, Balgowan and Point Turton (Fig. 2.3) were selected for this investigation due to their excellent exposure of carbonate-bearing rock profiles extending

from fresh marine carbonate-bearing rocks to pedogenic carbonate-bearing rocks (Figures. 2.6, 2.7 and 2.8). Myponie Point also includes exposure of basement rocks.

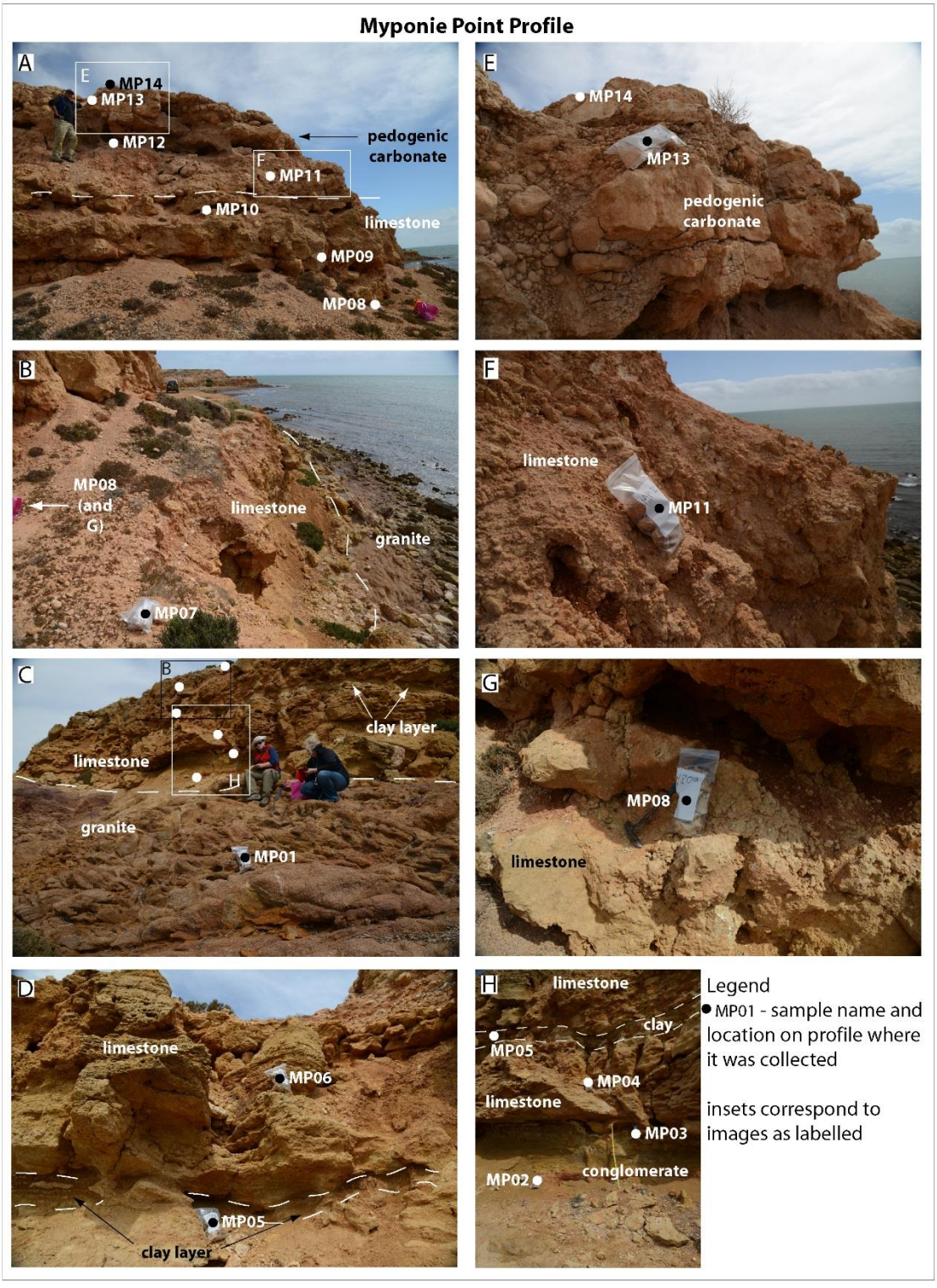

Figure 2.6. Field photos from Myponie Point showing exposure seen at profiles, location of samples and the nature of sampled materials. A) Top section of the profile showing pedogenic carbonate-bearing rocks overlying limestone, B) middle section of the profile showing limestone overlying basement granite, C) basement granite with view toward the overlying sediments and limestone, D) location of samples taken at the clay seam and overlying limestone, E) close up of the pedogenic carbonate rocks, F) upper portion of Melton Limestone, G) lower portion of Melton Limestone, H) shows the base of the Melton Limestone in relation to the underlying sediments and the clay seam . Location of profile is shown in Figure 2.3.

2.5.1 Myponie Point

Myponie Point is on the north-western coastline of the Yorke Peninsula (Fig. 2.3). Mesoproterozoic Tickera Granite of the Hiltaba Suite forms the basement at this location and is exposed approximately two meters above sea level and is subject to tidal influence. This granite comprises two phases; a light grey tonalite phase containing quartz and plagioclase; and, a red to brown monzonite phase containing microcline and quartz with minor plagioclase, biotite, muscovite and magnetite (Zang et al., 2006). The Tickera Granite has an emplacement age of 1586-1598 Ma (Cowley et al., 2003). The texture and fabric of these granites includes protomylonite structures (Cowley et al., 2003), suggesting they have undergone lower amphibolite facies metamorphism (Zang et al., 2006).

Melton Limestone, up to seven meters thick, unconformably overlies the Tickera Granite at this location (Fig. 2.5) (Lindsay, 1970). Fossils are common within the limestone (e.g. bryozoan (Zang et al., 2006) and Lepidocyclina (Crawford, 1965; Drexel and Preiss, 1995)). The limestone includes a fossil bearing sandstone unit. An unnamed basal unit containing thin lenses of glauconitic and gravelly sands is locally preserved (Drexel and Preiss, 1995). Pedogenic carbonate-bearing rock has developed on top of the limestone.

2.5.2 Balgowan

Balgowan is on the west coast of the Yorke Peninsula (Fig. 2.3). The Balgowan profile consists of middle Pleistocene Hindmarsh Clay, commonly one to five meters thick, overlain by the upper unit of the late Pleistocene Bridgewater Formation (Drexel and Preiss, 1995; Zang et al., 2006) (Fig. 2.5). The Hindmarsh Clay includes an arenaceous upper unit which contains a characteristic seam of alunite or kaolinite (Crawford, 1965; Zang et al., 2006). The presence of alunite and kaolinite in this Quaternary clay has been attributed to playa deposition (Drexel and Preiss, 1995; Zang et al., 2006). Crawford (1965) and Zang et al., (2006) suggest this is an effect of acidity and groundwater bleaching where acid soluble elements are leached away.

The upper unit of the Bridgewater Formation, less than ten meters thick, unconformably overlies the Hindmarsh Clay (Zang et al., 2006). It consists of calcareous aeolianite and bioclastic calcarenite and is commonly capped with cemented carbonate rock (calcrete) (Zang et al., 2006). Crawford (1965), describes this as ‘kunkarization’ (more commonly refers to calcrete formation), which is attributed to the calcium being leached and re-cemented as carbonate. The presence of shells in the middle section of the stratigraphy has been suggested to mark a break in time and change of sea level (Crawford, 1965).

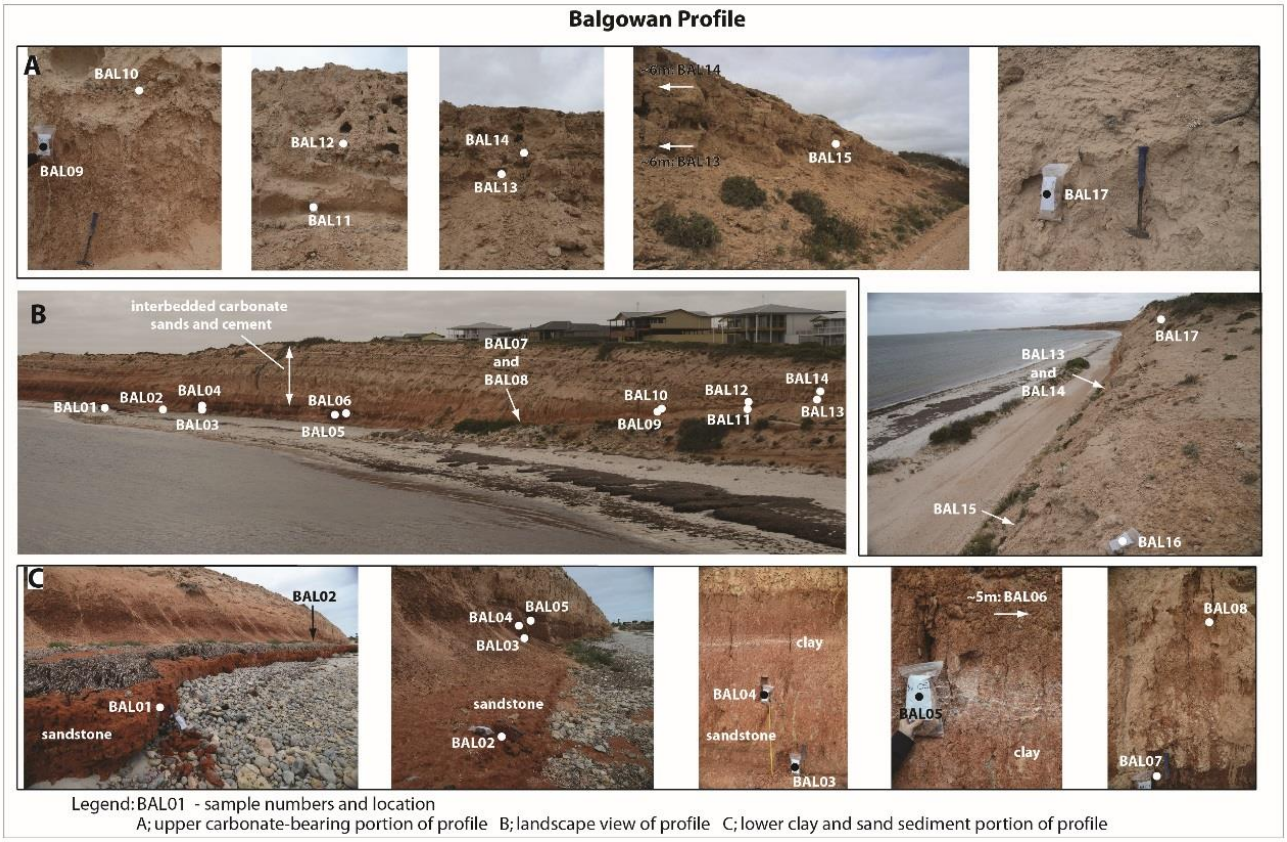

Figure 2.7. Field photos from Balgowan showing exposure seen at profiles, location of samples and the nature of sampled materials. Location of profile is shown in Figure 2.3.

2.5.3 Point Turton

Point Turton is in the south-western Yorke Peninsula (Fig. 2.3). Point Turton Limestone is the only exposed bedrock lithology at this location (Figures 2.8 and 2.9c). The limestone is up to sixteen meters thick and consists of a sandy section at the base with thin layered, tabular and trough cross-bedding. This is reportedly associated with a fluvial to shorefront environment (Zang et al., 2006). The upper section is dominated by fossiliferous limestone containing bryozoan and foraminifera (Zang et al., 2006). Point Turton Limestone has been deposited primarily at the southern extent of the Pirie Basin in a fault-

bound structure and on a high energy carbonate rock shelf (Zang et al., 2006). Point Turton Limestone correlates in age to the Melton Limestone at Myponie point (Zang et al., 2006). Dating undertaken on a diagnostic foraminifera in the Point Turton Limestone suggests an Oligocene to Miocene age (Drexel and Preiss, 1995; Zang et al., 2006). Cemented carbonated rock (calcrete) has formed on top of the limestone (Crawford, 1965).

Figure 2.8. Field photos from Point Turton showing exposure seen at profiles, location of samples and the nature of sampled materials. A) Shows an overview of the full profile at Point Turton with the Limestone and the overlying pedogenic carbonate indicated by a dashed line; B) shows individual sample lithology (samples PT07 to PT09 are not shown

as close ups due to the nature of the outcrop being very steep towards the top). Location of profile is shown in Figure 2.3.

2.6 Methodology

2.6.1 Sampling

2.6.1.1 Profile sampling

Samples of the exposed rocks at Myponie Point, Balgowan and Point Turton (Fig. 2.3) were taken for whole-rock geochemical and Sr isotopic analysis. The sampling locations are coastal escarpments chosen for their well-preserved carbonate-bearing rock profiles (Fig. 2.6, 2.7 and 2.8). As the marine and pedogenic carbonate-bearing rocks can be identified visually and texturally, at these locations, it avoids any ambiguity in investigation of chemical differences between the two carbonate-bearing rock types. By using profile sampling techniques, changes in chemical composition can be mapped across the face of the marine carbonate-bearing rocks to where it terminates at the boundary of the regolith counterpart directly overlying it. Profiles were mapped and sampled at a density sufficient to constrain variations in chemical composition relating to marine and regolith processes.

At each location, samples were collected by first removing the outermost surface to expose relatively fresh and uncontaminated material at intervals of half to one meter and working from the base to the top. Approximately two kg of material was taken for each sample. Where there were changes in lithology, this material was also sampled. Lithological logging was undertaken in conjunction with the sampling.

Sampling at Myponie Point was carried out in two stages through a vertical profile that was separated at a midway point by an ~three meter wide platform (Fig. 2.6). The Balgowan profile was sampled at half to one meter intervals each relevant interval by traversing an inclined boat ramp (Fig. 2.7). Sampling at Point Turton was carried out in a vertical profile (Fig. 2.8). The number of samples collected totalled; Myponie Point, n=14; Balgowan, n=17; and Point Turton, n=10.

2.6.1.2 Sea water sampling

Seawater was collected from a groin at Balgowan and from the Ardrossan jetty (n=2, Fig. 2.3). Seawater samples were collected in one litre sized, high-density polyethylene (HDPE) pre-rinsed bottles. The samples were used to provide a current $^{87}Sr/^{86}Sr$ ratios deemed to reflect the local region and identify any variations on each side of the Yorke Peninsula.

2.6.1.3 Sample preparation

Samples were separated into two portions. Samples were dried in an oven at 60° C. A portion of sample was crushed to a fine gravel size and then powdered using a tungsten carbide ring mill at the Mawson Laboratories, University of Adelaide. Approximately 100 g of the milled powder was set aside for whole-rock analysis. The remaining powder was retained for isotopic analysis. A small portion of each crushed and milled samples was retained for hyperspectral analysis. The remaining uncrushed portion was used for thin section preparation.

2.6.1.4 Whole-rock analysis

Sample powders were analysed for whole-rock geochemistry at Acme Laboratories, Vancouver, Canada. Major elements were analysed by X-ray fluorescence (XRF) following preparation of lithium borate fusion discs (ACME laboratory code 4X; see Appendix 2). Trace elements were analysed by ICP-MS following digestion in a solution of HCl and HNO_3 (ACME laboratory code 4B, see Appendix 2). Laboratory standards, laboratory and field duplicates and blanks were included for quality control. Two field samples from each profile location were duplicated prior to analyses. The laboratory duplicated analyses of 5 field samples and used the following standards; STD DS9 (n=3), STD GS311-1 (n=2), STD GS910-4 (n=2), STD OREAS45EA (n=3), STD OREAS72B (n=2), STD SO-18 (n=4), STD SY-4(D) (n=2), 9 Blanks and 2 G1 Prep wash, blanks.

2.6.1.5 $^{87}Sr/^{86}Sr$ isotopic analysis

Isotopic analyses for Sr from rock powder and seawater samples were undertaken at the University of Adelaide. Other authors including Quade et al., (1995) and Dart et al., (2012) separate the carbonate fraction from samples in their strontium isotopic studies to isolate and infer the source and input of Ca. As our aim was to replicate field conditions in exploration where the whole-rock is sampled and analysed rather than investigate the specific sources of Ca in the carbonate, the whole-rock digestion technique was adopted. This method will allow detection of subtle changes in the whole-rock across the sampling profile rather than identifying chemistry of the coatings on grains.

A nominal 0.2g of each sample powder was dissolved to completion using dilute HCl, HNO_3 and HF acids in turn. Reference material (NIST SRM987) was included for quality control. The seawater samples were evaporated to dryness and then treated in the same manner as the whole-rock samples. This was followed by separation in conventional cation exchange columns using 2mL AG50Wx8 (200-400 mesh) Bio-Rad cation exchange resin. $^{87}Sr/^{86}Sr$ ratios were determined using a Finnigan MAT 262 Thermal Ionisation Mass Spectrometer (TIMS) using single tantalum filaments.

2.6.1.6 Thin sections

Thin sections for each sample (i.e. Myponie Point, n=14; Balgowan, n=17; and Point Turton, n=10) were prepared by Adelaide Petrographic Laboratories, Adelaide. Samples were prepared following the standard procedure for incoherent and porous samples by first impregnating with an epoxy resin prior to the preparation of a polished and uncovered thin section. Thin sections were analysed using standard microscopy techniques.

2.6.1.7 Reflectance spectroscopy

Crushed gravel chips and milled powders were decanted into glass Petrie dishes, organised in depth order and analysed using HyLogger™ 3-3, at the Department of State Development (DSD) Core Storage facility at Glenside, Adelaide. HyLogger™ and HyChips™ modes were used in turn for both the Visible to shortwave (Vis–SWIR: 380nm–2500nm) and the thermal infra-red (TIR: 6000nm– 14,500nm; only available in HyLogging™ mode) wavelengths to obtain a representation of the mineral species (those identifiable using spectroscopic methods) in each powdered and gravel chip sample.

HyLogger™ instrumentation samples every 0.8cm producing approximately 125 spectra per meter of sample with overlapping pixels. Additionally a high resolution digital image is taken every 1mm along the sample (Huntington et al., 2006).

In HyLogger™ mode, samples were scanned four times across a sample, allowing for overlap, with the aim of maximising valid spectra. In HyChip™ mode samples were scanned three times using Vis–SWIR only and three readings were taken per sample.

Results were then processed in The Spectral Geologist (TSG), HotCore™ version 7, for viewing in free (TSG) Viewer™ software provided by AusSpec International Inc. The processing of samples included the removal of non-sample materials such as glass from the Petri dishes and wooden intervals between dishes. This method did not account for geological context and removal of mineral species that are not relevant to that geological environment. Routine calibrations were performed prior to analyses and celestine was scanned and used as a reference sample.

2.7 Results

A total of fourteen samples were collected at Myponie Point, seventeen samples were collected at Balgowan and nine samples collected at Point Turton. Locations are shown in Figures 2.3, 2.6, 2.7 and 2.8. Descriptions for grainsize follow that of the Wentworth classification where; very fine refers to very fine sand which is 62–125μm; fine sand is 125–250μm; medium sand is 250–500μm; coarse sand is 500–1000μm; very coarse sand is 1000–2000μm. Geochemical results for selected elements are presented in Table 2.1.

A complete table of elements analysed with the results is presented in Appendix 2. Reflectance spectroscopy results are presented in Appendix 3.

Table 2.1. Geochemical data for selected elements.

Sample location and name	height above sea level	$^{87}Sr/^{86}Sr$	CaO wt%	Sr ppm	MgO wt%	Ca/Sr	Ca/Mg	Al_2O_3 wt%	Cu ppm
Myponie Point									
MP01	2	1.1410	0.08	42.3	1.04	14	0.09	12.3	5.4
MP02	3	0.7598	0.13	42.0	0.51	22	0.30	3.3	3.4
MP03	3.2	0.8083	0.40	90.2	1.00	32	0.47	14.1	4.9
MP04	4	0.7272	36.98	102.1	0.68	2589	64	2.8	3.2
MP05	4.3	0.7679	0.50	65.3	1.28	55	0.46	7.1	4.6
MP06	5.3	0.7219	44.43	102.6	0.64	3095	82	1.8	2.4
MP07	6.3	0.7142	51.90	137.1	0.67	2706	92	0.9	2.0
MP08	7	0.7133	53.79	158.0	0.62	2433	103	0.6	1.6
MP09	8	0.7113	54.98	154.3	0.60	2547	109	0.3	2.3
MP10	9	0.7116	54.41	168.2	0.66	2312	98	0.5	1.9
MP11	10	0.7107	53.60	171.6	0.77	2233	83	0.6	1.5
MP12	11	0.7110	34.51	1341.2	6.36	184	6	2.4	4.7
MP13	12	0.7108	41.47	1260.5	3.50	235	14	2.0	6.0
MP14	13	0.7102	44.03	1429.7	2.74	220	19	1.5	4.5
Balgowan									
Bal01	0.5	0.7459	0.05	35.9	0.450	10	0.13	2.660	3.2
Bal02	1	0.7353	0.06	39.1	0.600	11	0.12	5.480	5.2
Bal03	2	0.7292	0.10	70.6	0.690	10	0.17	11.170	6.6
Bal04	3	0.7281	0.07	63.1	0.770	8	0.11	13.560	7.8
Bal05	4	0.7249	0.12	53.7	1.140	16	0.12	19.430	8.6
Bal06	4.5	0.7254	0.17	74.0	1.610	16	0.13	12.340	15.4
Bal07	4.8	0.7120	7.66	491.1	5.780	111	2	7.970	9.7
Bal08	5.3	0.7121	17.55	594.0	3.240	211	6	6.100	8.0
Bal09	5.8	0.7106	29.51	1078.6	3.740	196	9	4.720	8.1
Bal10	6.3	0.7103	40.06	957.1	1.730	299	27	2.410	4.3
Bal11	7	0.7100	36.44	1379.3	5.070	189	9	2.320	4.3
Bal12	8	0.7101	41.22	969.6	1.830	304	27	2.570	4.1
Bal13	8.5	0.7105	25.61	1194.8	6.590	153	5	2.020	6.6
Bal14	9	0.7104	34.92	1124.1	2.420	222	17	1.980	6.1
Bal15	9.5	0.7104	26.02	1234.6	5.680	151	5	2.350	5.0
Bal16	10	0.7104	34.42	942.6	1.920	261	21	2.700	7.0
Bal17	11	0.7107	22.91	831.3	2.650	197	10	2.440	4.3
Point Turton									
PT01	0	0.7096	51.82	176.1	1.50	2103	41	0.51	5.2
PT02	1	0.7097	52.73	154.5	0.77	2440	81	0.48	3.8
PT03	2	0.7097	52.74	203.5	1.09	1852	57	0.67	1.9
PT04	3	0.7094	52.18	239.6	1.80	1557	34	0.59	2.7
PT05a solution pipe externa surface	4	0.7102	51.08	290.1	1.27	1259	48	0.56	1.4
PT05b solution pipe internal surface	4.5	0.7109	38.04	441.5	1.94	616	23	2.17	2.4
PT06	5	0.7101	46.46	846.5	3.74	392	15	1.06	3.6
PT07	6	0.7102	45.63	725.2	2.59	450	21	1.47	3.5
PT08	7	0.7102	43.53	869.9	1.93	358	27	1.58	2.3
PT09	7.5	0.7101	43.02	1011.7	2.08	304	25	1.54	2.0
Seawater Samples									
BAL	0	0.70920							
ARD	0	0.70917							

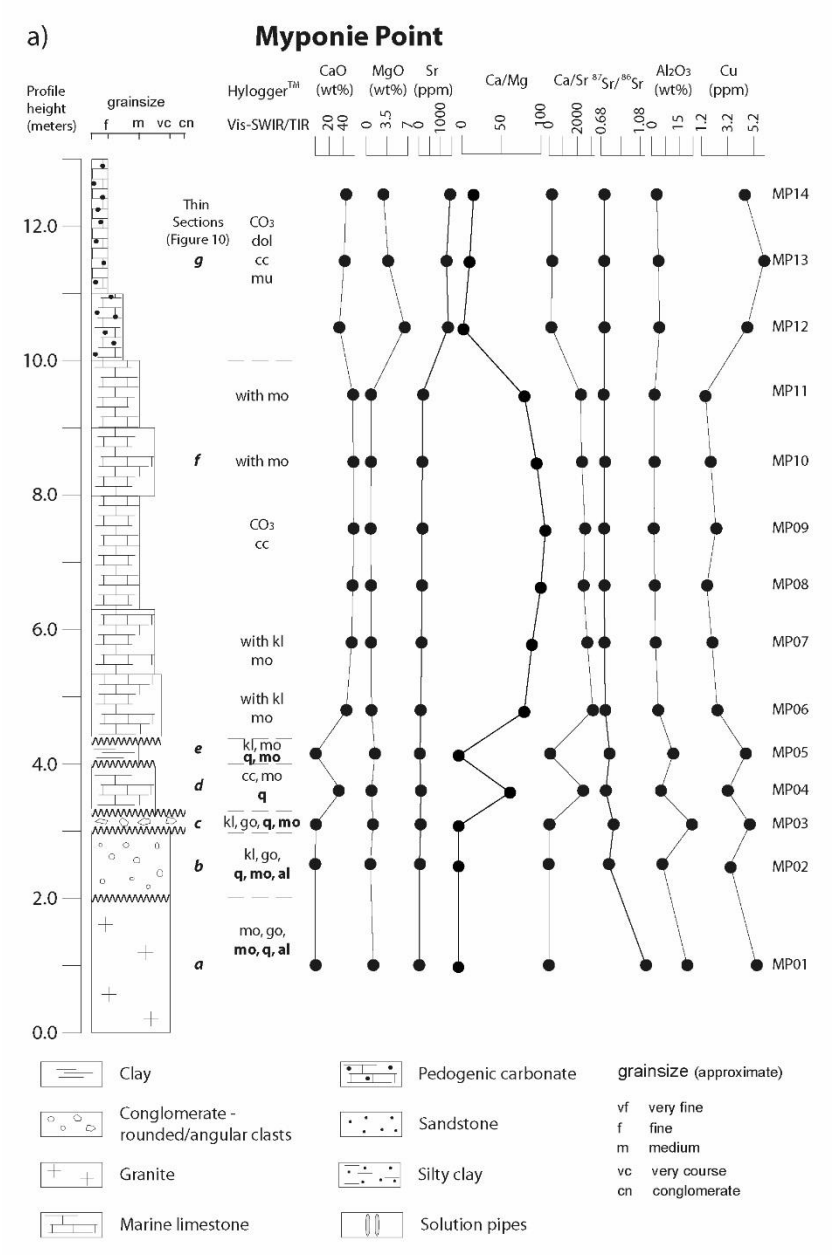

Figure 2.9. Simplified stratigraphy, selected geochemistry and hyperspectral analysis for a) Myponie Point, b) Balgowan and c) Point Turton profiles. Profile locations are shown in Figure 2.3. Abbreviations: al: albite; cc: calcite; CO_3: carbonate; dol: dolomite; go: goethite; hem: hematite; kl: kaolinite; mo: montmorillonite; mu: muscovite; q: quartz; sm: smectite. Regular text: Vis-SWIR; Bold text: TIR.

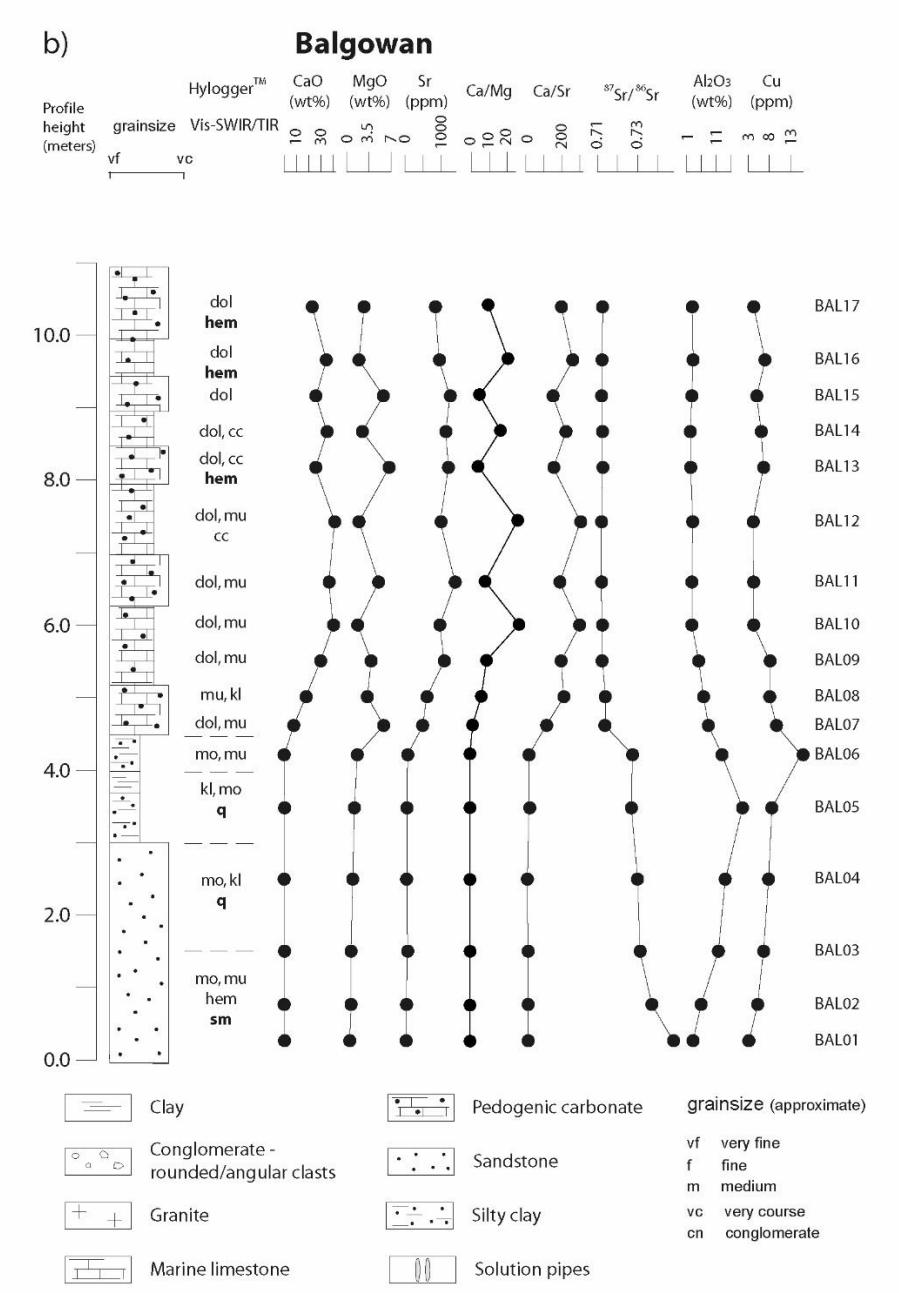

Figure 2.9. Simplified stratigraphy, selected geochemistry and hyperspectral analysis for a) Myponie Point, b) Balgowan and c) Point Turton profiles. Profile locations are shown in Figure 2.3. Abbreviations: al: albite; cc: calcite; CO_3: carbonate; dol: dolomite; go: goethite; hem: hematite; kl: kaolinite; mo: montmorillonite; mu: muscovite; q: quartz; sm: smectite. Regular text: Vis-SWIR; Bold text: TIR.

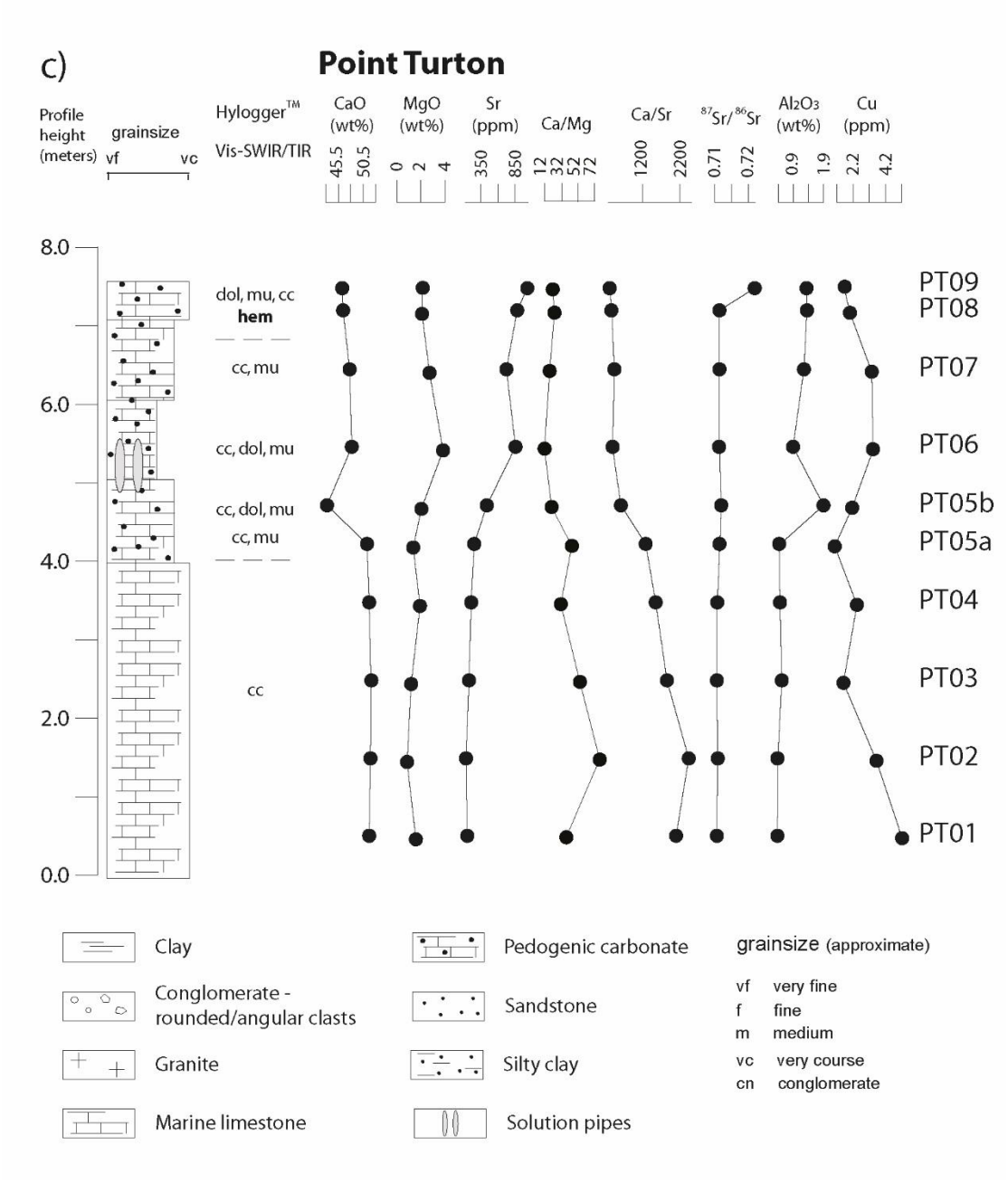

Figure 2.9. Simplified stratigraphy, selected geochemistry and hyperspectral analysis for a) Myponie Point, b) Balgowan and c) Point Turton profiles. Profile locations are shown in Figure 2.3. Abbreviations: al: albite; cc: calcite; CO_3: carbonate; dol: dolomite; go: goethite; hem: hematite; kl: kaolinite; mo: montmorillonite; mu: muscovite; q: quartz; sm: smectite. Regular text: Vis-SWIR; Bold text: TIR.

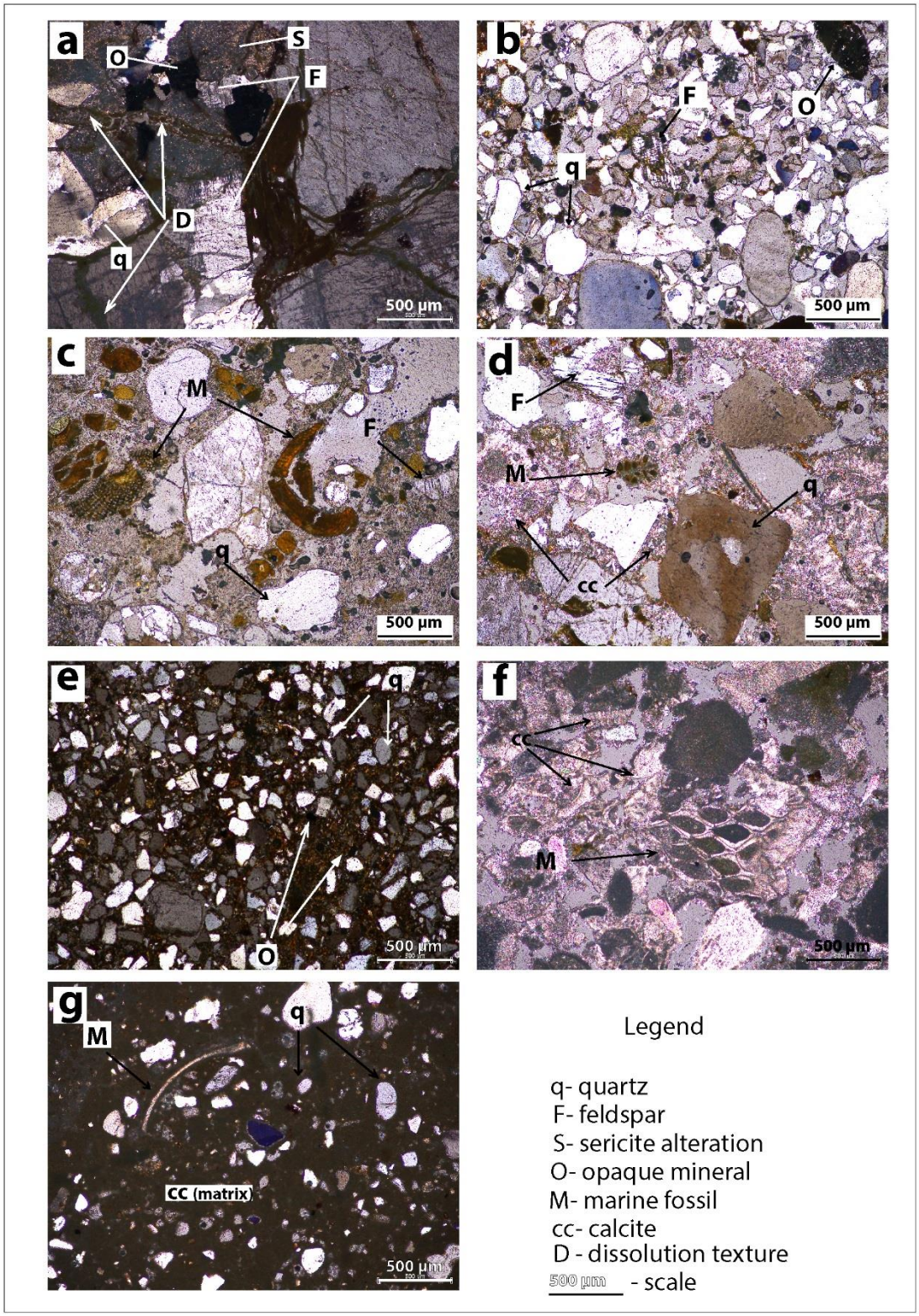

Figure 2.10. Caption is on following page.

Figure 2.10. Representative photomicrographs of lithologies at Myponie Point. a) chemical weathering textures in the Tickera Granite showing dissolution and replacement (such as sericite) at grain boundaries, along cracks and within mineral fractures, (0-2m, MP01); b) representative matrix from the conglomerate with fine to very coarse clasts dominated by quartz and feldspar with some opaque minerals (~3.1m, MP02); c) Base of the Melton Limestone sequence showing fossil marine fragments (bryozoa and mollusc) and rounded sub-angular quartz and feldspar in a clay and calcite matrix (~3.5m, MP03); d) Limestone containing marine fossil fragments (possibly bryozoa) in a calcite dominated cement, clastic component is less than 30% (~4m, MP04); e) sample from the clay bed showing fine, moderately to well-sorted sub-angular grains of quartz and opaque minerals in a clay-rich matrix (~4.3m, MP05); f) Representative sample of Melton Limestone containing abundant marine organisms (bryozoa in this field of view) in a calcite dominated cement (4.5- 10m, MP10); g) Micritic densely compact carbonate containing rounded fine- to coarse-grained quartz and small shell fragments (bivalve in this field of view) (10-14m, MP13). Numbers in parenthesis indicate the approximate height of the lithology represented in the photomicrograph from the Myponie Point profile (see also Figure 2.6 and log in Fig 2.9a) and their associated sample number.

2.7.1 Myponie Point

2.7.1.1 Profile description and petrography

The weathered granite is exposed up to three meters vertically (Fig. 2.6). The granite contains coarse-grained feldspar (albite) (Fig. 2.9a) and visible biotite and finer grains of

magnetite in hand specimen. In thin section, each mineral grain is broken or cracked with alteration along the grain boundaries (Fig. 2.10a).

Unconformably overlying the granite is a 1.5m thick conglomerate comprising poorly sorted coarse to very fine, well-rounded grains of quartz and feldspar (Fig. 2.10b) with minor amounts of biotite, opaque minerals and minor fine-grained zircon. The upper fifty centimetres of the conglomerate contains a mixture of angular blue-grey gravels set amongst medium to fine sub-rounded grains of quartz (Figures 2.6 & 2.9a). In thin section these polymict sediments preserve a very thin coating of clay (Fig. 2.10b).

Overlying these sediments is a 6.5m thick limestone sequence (Figures 2.6 and 2.9a). The base of the limestone contains broken fragments of shell mixed with rock fragments. In thin section these rock fragments are rounded and sub-angular pieces of quartz and feldspar (Fig. 2.10c, 2.10d). This mixture of fragments is cemented by a predominantly calcite-rich matrix with a minor clay component. A thin bed up to thirty centimetres thick containing moderately to well-sorted, very fine and sub-angular quartz sand supported by a clay-rich matrix (Fig. 2.10e) is preserved within the limestone sequence at 4.3m (Figures 2.6 and 2.9a). The clay bed preserves coloured horizontal banding of equal thickness (~two centimetres) that range from red at the base to alternating yellow and brown to yellow and white.

The limestone is five meters thick above the clay-rich bed (Fig. 2.9a). The limestone contains abundant, coarse to fine broken fragments of bryozoan, echinoid fragments and other shells up to one centimetre in diameter and is cemented by calcite (Fig. 2.10f). The shells have sharply defined, angular edges, which are either filled or edge-lined with

calcite crystals. Calcite cement accounts for up to twenty percent of the limestone whilst the fossils, also rich in calcite, dominate the composition (Fig. 2.10f).

The pedogenic carbonate-bearing rock at the top of the profile is approximately two meters thick (Figs 2.6 & 2.9a). The carbonate-bearing rock is dominated by dolomite (Fig. 2.9a) and is creamy white to light brown in colour. This pedogenic carbonate-bearing rock is generally fine grained, well-cemented, massive and contains nodules and pisolites. Many of the nodules and pisolites display concentric structures which are coloured varying shades of cream to brown. In thin section this rock appears largely homogenous with a tightly compacted calcite rich matrix (Fig. 2.10g). The nodules themselves contain the same homogenous calcite rich matrix, with the addition of sub-angular to well-rounded grains of quartz and other detrital fragments. The edges of these nodules are coated with calcite. Very few broken and sub-angular to sub-rounded fragments of shell are preserved in the upper parts of this profile (Fig. 2.10g).

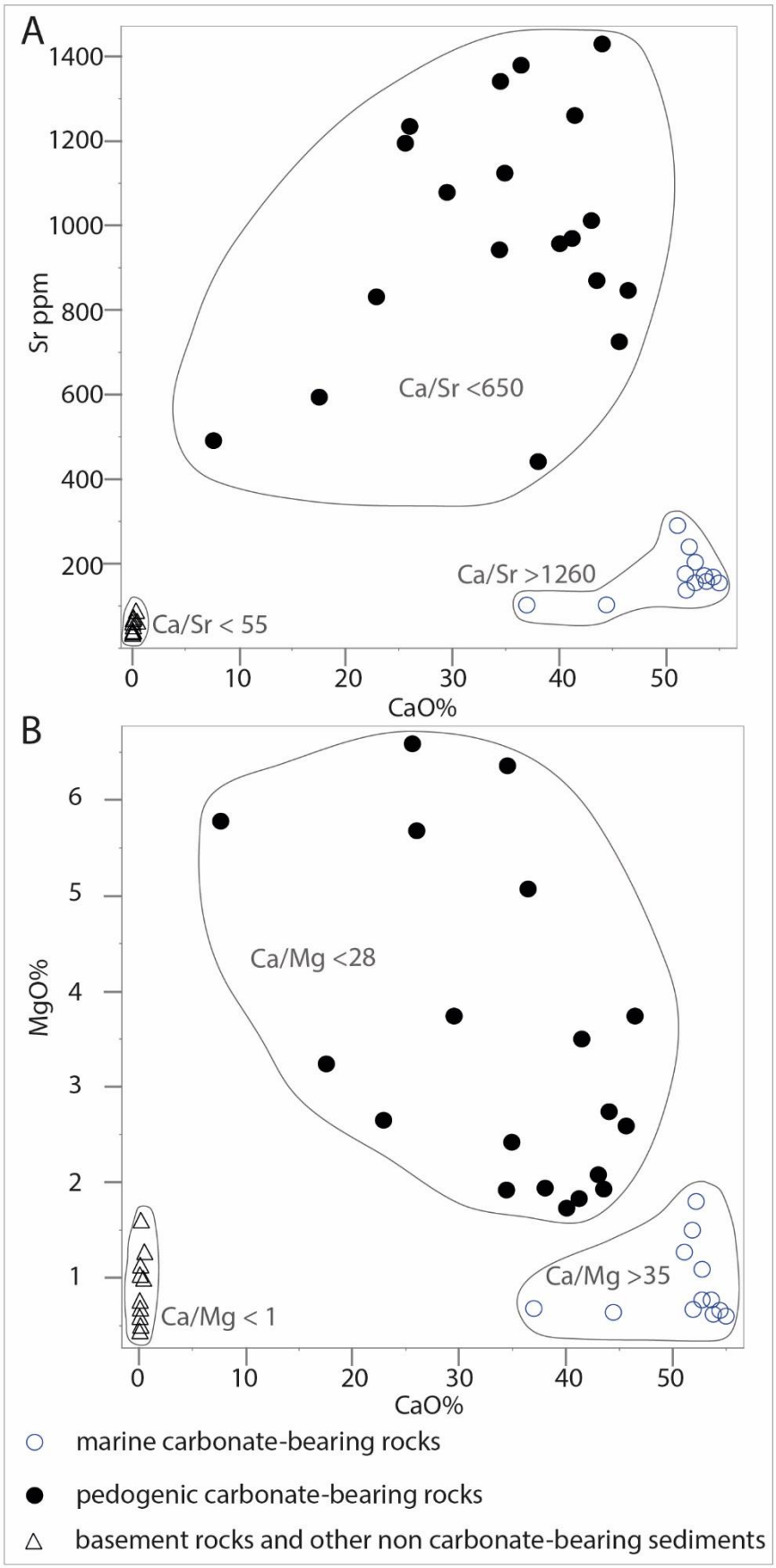
A
Sr ppm
1400
1200
1000
800
600
400
200
Ca/Sr <650
Ca/Sr >1260
Ca/Sr < 55
0
10
20
30
40
50
CaO%
B
MgO%
6
5
4
3
2
1
Ca/Mg <28
Ca/Mg >35
Ca/Mg < 1
0
10
20
30
40
50
CaO%
marine carbonate-bearing rocks
pedogenic carbonate-bearing rocks
basement rocks and other non carbonate-bearing sediments

Figure 2.11. XY plots showing a) Sr versus CaO wt% and labelled with corresponding Ca/Sr values and b) MgO wt% versus CaO wt% and labelled with corresponding Ca/Mg values.

2.7.1.2 Chemistry

CaO concentration ranges throughout the profile from 36 wt% in the basal limestone below the clay bed and up to 55 wt% in the limestone above the clay bed, and from 35-45 wt% in the surface samples (Fig. 2.9a and Table 2.1). CaO concentration in the basement granite is <0.1 wt%. Al_2O_3 content is included as a measure of clastic component. The basement granite contains 12.3 wt% Al_2O_3. Variable concentrations of Al_2O_3 occur in the sediments and clay above the granite (3–14 wt%), and lower concentrations occur in the limestone and the surface carbonate-bearing rock (<1 wt% and 2 wt% respectively) (Fig. 2.9a). Throughout the basement and limestone, MgO concentrations are <1 wt%, apart from the clay bed which has ~1.3 wt% MgO. The pedogenic carbonate-bearing rock has the highest MgO concentrations of ~2.7-6.4 wt% (Fig. 2.11).

Strontium has the lowest concentration in the granite (42.3ppm, Table 2.1), with ranges between 100-170ppm in the limestone and is highly elevated in concentration in the regolith carbonate at the surface (1260-1430ppm) (Fig. 2.9a). The $^{87}Sr/^{86}Sr$ ratio for the granite is 1.141. The $^{87}Sr/^{86}Sr$ ratio gradually decreases (from 0.722 to 0.711) throughout the marine limestone. The three pedogenic carbonate-bearing rock samples all have similar $^{87}Sr/^{86}Sr$ ratios around 0.711. The Ca/Mg ratio is lowest in the granite (0.09), ranges between 0.30–0.47 in the clastic sediments, is highest in the limestone (82– 109)

and drops to 6– 19 in the pedogenic carbonate-bearing rock (Fig. 2.9a, Table 2.1). The Ca/Sr ratio is lowest in the granite (14), ranges between 22–55 in the clastic sediments, is highest in the limestone (2233–3095) and drops to 184–235 in the pedogenic carbonate-bearing rock (Fig. 2.9a, Table 2.1).

The pedogenic carbonate-bearing rock contains the highest concentrations of Cu (4.5–6.0ppm, Table 1) (Fig. 2.9a). The Cu content is lowest within the limestone and ranges from 1.5–2.4ppm, and up to 3.2ppm in the lowermost limestone sample. The clay bed contains 4.6ppm Cu. The conglomerate and granite contain 3.4–5.4ppm Cu.

2.7.1.3 Hyperspectral analysis

The basal Tickera Granite has been highly weathered to dominantly montmorillonite with goethite response in the Vis-SWIR wavelengths (Fig. 2.9a). The TIR response confirms montmorillonite with quartz and plagioclase (albite). The overlying sandy gravels are dominated by kaolinite and goethite in the Vis-SWIR and quartz dominated with montmorillonite secondary, in the TIR (Fig. 2.9a). The basal limestone is dominated by carbonate (calcite) in the Vis-SWIR with quartz identified in the TIR (Fig. 2.9a). The clay bed is dominated by kaolinite and montmorillonite in Vis-SWIR and quartz with montmorillonite in the TIR wavelength (Fig. 2.9a).

The fossil-rich limestone is dominated by calcite with secondary kaolinite and montmorillonite identified in the Vis-SWIR wavelengths (Fig. 2.9a). The overlying pedogenic carbonate-bearing rock is also calcite dominant in Vis-SWIR wavelengths but identified as dolomite and also contains secondary calcite and muscovite (Fig. 2.9a).

2.7.2 Balgowan

2.7.2.1 Profile description and petrography

The coastline at Balgowan (Fig. 2.3) hosts a north to south trending escarpment between eleven to fifteen meters high (Fig. 2.7). The exposure provides an impressive contrast to the surrounding landscape with reddish brown sandstone and sediments at the base overlain by light cream coloured sands with interbedded fine-grained decimetre to metre thick cemented carbonate-bearing rock layers (Fig. 2.7). The sandstone outcrops one meter above sea level and contains up to 90% fine and well-sorted, rounded to sub-angular grains of quartz cemented by thin coatings of clay (Fig. 2.7).

Overlying the platform, at the extent of the high-tide mark, the escarpment rises from a clay-rich base around 2.5m thick (Figs 2.7 & 2.9b). Towards the top of this layer there is a mottled patchy seam of white powdery to crystalline clay around ten to twenty centimetres thick (Fig. 2.7). Above this seam the clays are hematite stained with an increasingly silty texture and carbonate nodules. Plant roots are preserved within this silty layer.

The silty clays are unconformably overlain by seven meters of interbedded carbonate-bearing sand and cement (Figs 2.7 and 2.9b). The lower-most carbonate-bearing rock contains an abundance of well-cemented carbonate nodules. Above this layer of nodular carbonate rocks are carbonate-rich sands interbedded with well-cemented carbonate-bearing rock layers, each up to two meters thick (Fig. 2.9b). Approximately halfway up the carbonate section, at 7.5 m, there are visible, broken and rounded fragments of shells

(BAL 12, Figure 2.9b). These shell fragments can also be identified in the cemented carbonate-bearing layers albeit only in thin section.

The uppermost sample collected (Fig. 2.7) comprises unconsolidated, very fine-grained nodular carbonate-bearing sand containing forty percent fine sub-angular quartz grains. Very fine rounded grains of zircon are also only identifiable in thin section.

2.7.2.2 Chemistry

The CaO concentrations range from <0.2 wt% in the clay layer and increase to 7 wt% at the unconformity (Fig. 2.9b, Table 2.1). The sandy interlayers of the carbonate-bearing rock section range from 17–35 wt% CaO while the cemented-carbonate rock platforms contain 35–41 wt% CaO (Fig. 2.9b). The Al_2O_3 content of the lowermost sandstone in the profile increases from ~2.7 wt% at the base to ~13.6 wt% to the top of the layer. The overlying silty clay contains ~12.3–19.4 wt% Al_2O_3. The lowermost 1.3m of the pedogenic carbonate-bearing rock contains 4.7–8.0 wt% Al_2O_3, and the remainder contains 2.0–2.7 wt% Al_2O_3 (Fig. 2.9b). MgO content is lowest within the sandstone and silty clay (0.5–1.6 wt%), and varies from ~1.7–5.8 wt% throughout the pedogenic carbonate-bearing rock (Figs. 2.9b and 2.11).

The Sr concentration is low in the basal sands and clay with values ranging 36–74ppm (Fig. 2.9b, Table 2.1). The carbonate-bearing sediment immediately above the unconformity contains 500–600ppm Sr. The Sr concentration is highest in the overlying carbonate-bearing rocks (830–1379ppm) (Fig. 2.9b). The basal quartz-rich and clay layers contain $^{87}Sr/^{86}Sr$ ratios ranging from 0.746 to 0.725. There is a distinct change in

values from the clays to the overlying carbonate-bearing rocks which have $^{87}Sr/^{86}Sr$ ratios limited to between 0.710 and 0.712 (Fig. 2.9b). There are no sharp distinctions between values for the well-cemented carbonate-bearing rock platforms, the sandy carbonate-bearing layers or the surface sample (Fig. 2.9b). The Ca/Mg ratios are lowest in the sands and clays at the base of the profile (0.11–0.17) and increase to a broad range between 2 and 27 in the overlying carbonate-bearing rocks (Fig. 2.9b, Table 2.1).The Ca/Sr ratios are lowest in the sands and clays at the base of the profile (8–16) and increase sharply to between 111 and 303 in the overlying carbonate-bearing rocks with an average of 208 (Fig. 2.9b, Table 2.1).

Copper content within the sandstone ranges from 3.2–7.8ppm (Fig. 2.9b, Table 2.1). The highest concentrations are preserved within the clay, which contains 8.6–15.4ppm Cu. The pedogenic carbonate-bearing rocks contains ~4.1 to ~9.7ppm Cu (Fig. 2.9b).

2.7.2.3 Hyperspectral analysis

The basal 0–1.5m of the Hindmarsh Clay is dominated by montmorillonite, muscovite and hematite in the Vis-SWIR wavelengths (Fig. 2.9b). Montmorillonite is also dominant in the TIR wavelength. The sediments above this (1.5–3m) are equally montmorillonite and kaolinite dominant in Vis-SWIR. Quartz dominates in the TIR wavelength at 1.5–3m. At three to four meters there is a distinct whitish seam which Vis-SWIR wavelengths identifies kaolinite and montmorillonite dominant and with quartz in the TIR wavelength. At 4– 4.5m the profile becomes montmorillonite and muscovite dominant again in the Vis-SWIR wavelength. The overlying carbonate-bearing rock sequences (4.5–11m) display an alternating trend of dolomite dominant to dolomite with calcite each alternating half to

one meter upwards in the Vis- SWIR wavelengths. Scattered occurrences of hematite detected in TIR wavelength (Fig. 2.9b).

2.7.3 Point Turton

2.7.3.1 Profile description and petrography

Exposed geology at Point Turton is limestone overlain by pedogenic carbonate-bearing rock (Fig. 2.8). The escarpment at this location is less than eight meters high and is fossil rich limestone with its base concealed by a pebbly shingle beach deposits (Fig. 2.9c). This limestone is porous and contains abundant fragments of shells including bryozoa, echinoids and bivalves cemented by calcite similar to that of the Melton Limestone (Zang et al., 2006).

At approximately four meters the fossiliferous limestone is overlain by 3.5–4m of well-cemented pedogenic carbonate-bearing rock (Fig. 2.8 & 2.9c). Dividing these two lithologies are faintly visible solution pipes containing fine pisolitic nodules (Fig. 2.8). The overlying pedogenic carbonate-bearing rocks have a fine micritic to massive texture with abundant nodules (up to two centimetres in size) (Fig. 2.8). These densely compacted, also micritic, carbonate nodules contain tiny grains of angular sand. Approximately five percent of the carbonate matrix contains grains of calcite that are identified only in thin section as broken shell fragments, similar to that of the pedogenic carbonate-bearing rocks from Myponie Point (Fig. 2.10g). An increase in sub-angular to well-rounded quartz content, also similar to Myponie Point, is in the top two meters of pedogenic carbonate at Point Turton.

2.7.3.2 Chemistry

The CaO concentration in the limestone ranges from 51–53 wt% (Fig. 2.9c, Table 2.1). The overlying pedogenic carbonate-bearing rocks contains 38–46 wt% CaO. The Al_2O_3 content of the limestone varies from ~0.5–0.6 wt%. Within the pedogenic carbonate-bearing rock, the Al_2O_3 content is generally ~1.1–1.6 wt%, and increases to ~2.2 and 8.5 wt% in the lower two samples of this lithology (Fig. 2.9c). The MgO concentration of the limestone is ~0.8–1.9 wt%. Within the pedogenic carbonate, the MgO concentration is ~1.9–3.7 wt%. One sample towards the base of the pedogenic carbonate-bearing rock contains only ~0.4 wt% MgO (Fig. 2.9c).

Strontium concentration in the limestone ranges between 155ppm and 290ppm (Table 2.1). The overlying pedogenic carbonate-bearing rocks contains 440ppm–870ppm Sr. The uppermost surface sample contains the highest Sr concentration of 1012ppm (Fig. 2.9c). The $^{87}Sr/^{86}Sr$ ratios are similar for all limestone samples (0.709) (Fig. 2.9c). The overlying pedogenic carbonate-bearing rock showed little variation in $^{87}Sr/^{86}Sr$ ratio compared to the limestone (0.710). The uppermost sample had the highest $^{87}Sr/^{86}Sr$ ratio of 0.721 (Fig. 2.9c). The Ca/Mg ratios range between 41–81 in the limestone and between 15–27 for the overlying carbonate-bearing rocks (Fig. 2.9c, Table 2.1). A sample of material taken from the inside surface of a solution pipe produced a Ca/Mg ratio of 23 (Fig. 2.9c, Table 2.1).The Ca/Sr ratios range between 1260– 2440 in the limestone and between 300– 450 for the overlying pedogenic carbonate-bearing rocks (Fig. 2.9c, Table 2.1). A sample of material taken from the inside surface of a solution pipe produced a slightly higher Ca/Sr ratio of 616 (Fig. 2.9c, Table 2.1).

The Cu content throughout the limestone and pedogenic carbonate-bearing rock is variable, and ranges from ~1.4-5.2ppm in the limestone and ~2.0–4.3ppm in the pedogenic carbonate-bearing rock (Fig. 2.9c, Table 2.1).

2.7.3.3 Hyperspectral analysis

Point Turton limestone is carbonate dominant in Vis-SWIR (Fig. 2.9c). The basal fossil-rich limestone portion shows as calcite dominant while the overlying pedogenic carbonate-bearing rock is dolomite and smectite dominant in Vis-SWIR wavelengths. Iron oxide (hematite) is detected within the upper ~0.5m in TIR wavelength.

2.7.4 Sea water analysis

The $^{87}Sr/^{86}Sr$ ratios for sea water samples from Balgowan and Ardrossan (Fig. 2.3) are 0.70920 and 0.70917 respectively (Table 2.1). During the course of the isotopic analyses, the average $^{87}Sr/^{86}Sr$ ratio of standard NIST SRM987 were 0.71024 ± 0.000009 (2SE, 20 runs). This compares to 0.71014 (Veizer, 1989) and 0.710248 (Howarth and McArthur, 1997).

2.8 Discussion

2.8.1 Stratigraphy of the Melton Limestone at Myponie Point

To identify carbonate origins it is important to understand the morphology of the exposed profile and the environmental processes affecting the geochemical content. The profile at Myponie Point will be discussed in detail here as it contains both marine carbonate-

bearing rocks (limestone) and pedogenic carbonate-bearing rocks (calcrete) as well as basement rock that also forms a large portion of the basement of the Yorke Peninsula.

The base of the Myponie Point profile comprises a highly weathered granite (Figures 2.5, 2.6 & 2.9a). The granite contains smectite dominant minerals identified with HyLogger^{TM} that are typical weathering products of alumino-silicate minerals (Anand, 2005). Continental materials can also be a source for siliciclastic contamination and higher $^{87}Sr/^{86}Sr$ ratios (Edmond, 1992; Veizer and Compston, 1976). The weathered granite is unconformably overlain by the Melton Limestone.

The stratigraphy of the Melton Limestone has been described in detail by Lindsay (1970). Five sequences of sedimentation are identified. From oldest to youngest these units are: 1. an unnamed fossiliferous gravel containing sub-rounded sands of granite fragments quartz and feldspar; 2. Melton Limestone, lower bryozoal member consisting of quartzose, bryozoal calcarenite, oxidised glauconite pellets and lithic pebbles (e.g. granite, feldspar, quartz and schist); 3. Melton Limestone, pink member which is documented as a pinkish coloured and densely recrystallized bryozoal limestone; 4. an unnamed unit that is only documented from an inland sinkhole and comprises densely recrystallized quartzose and calcarenitic composition containing specific fossil assemblage not observed in other units; and, 5. a yellow to cream brown, fossil-rich and densely recrystallized limestone that is the youngest and most widespread unit of the Melton Limestone (Lindsay, 1970). This young limestone unit weathers to a smooth, fine grained and bouldery limestone (Lindsay, 1970), which has much the same form as field exposures of the pedogenic carbonate that is frequently observed across the Yorke

Peninsula. Lindsay (1970) observes that this unit locally disconformably overlying unit 2 at Myponie Point.

The Melton Limestone at Myponie Point consists of a base of sandy gravels overlain by a coarse conglomerate containing fragments of shells, glauconite, quartz and lithic fragments in a clay-rich matrix (Figs 2.6a & 2.8). Lindsay (1970) identified this as units 1 and 2. These units are also described ~10km north of Myponie Point (Drexel and Preiss, 1995). The composition of the gravels includes feldspars (Figs 2.6 & 2.9a), which provide a source of radiogenic Sr and can therefore elevate the total $^{87}Sr/^{86}Sr$ ratio (e.g. Brantley et al., 1998). Weathering of these gravels to a clay fraction (e.g. montmorillonite) is expressed in HyLogger^{TM} results (Fig. 2.9a), and has produced a porous media suitable for dispersion of fluid (e.g. groundwater). These gravelly units also have elevated Al_2O_3 content relative to other units within the profile (Fig. 2.9a), which is used here as a proxy indicator for higher clastic component. The gravelly units are thus interpreted as a potential source of siliciclastic contamination of the limestone.

The sands and conglomerate are overlain by a thin (~30 cm) clay bed at 4.3 m, which is in turn overlain by limestone (Figs 2.6 and 2.9a). This clay bed is localised to the Myponie Point area and has not been described within the Melton Limestone elsewhere. The clay bed is overlain by limestone (Figures 2.5, 2.6 and 2.9a) that is equivalent to unit 5 of the Melton Limestone as described by Lindsay (1970). The contact between the clay bed and the overlying limestone is interpreted to represent the disconformity between units 2 and 5 and is described by Lindsay (1970). The uppermost pedogenic carbonate-bearing rock (Fig. 2.6) has a bouldery smooth appearance that is similar to the weathered

morphology of the limestone comprising unit 5 of the Melton Limestone. This visual similarity in appearance between the pedogenic carbonate-bearing rock and marine limestone is central to the main challenge being addressed in this paper.

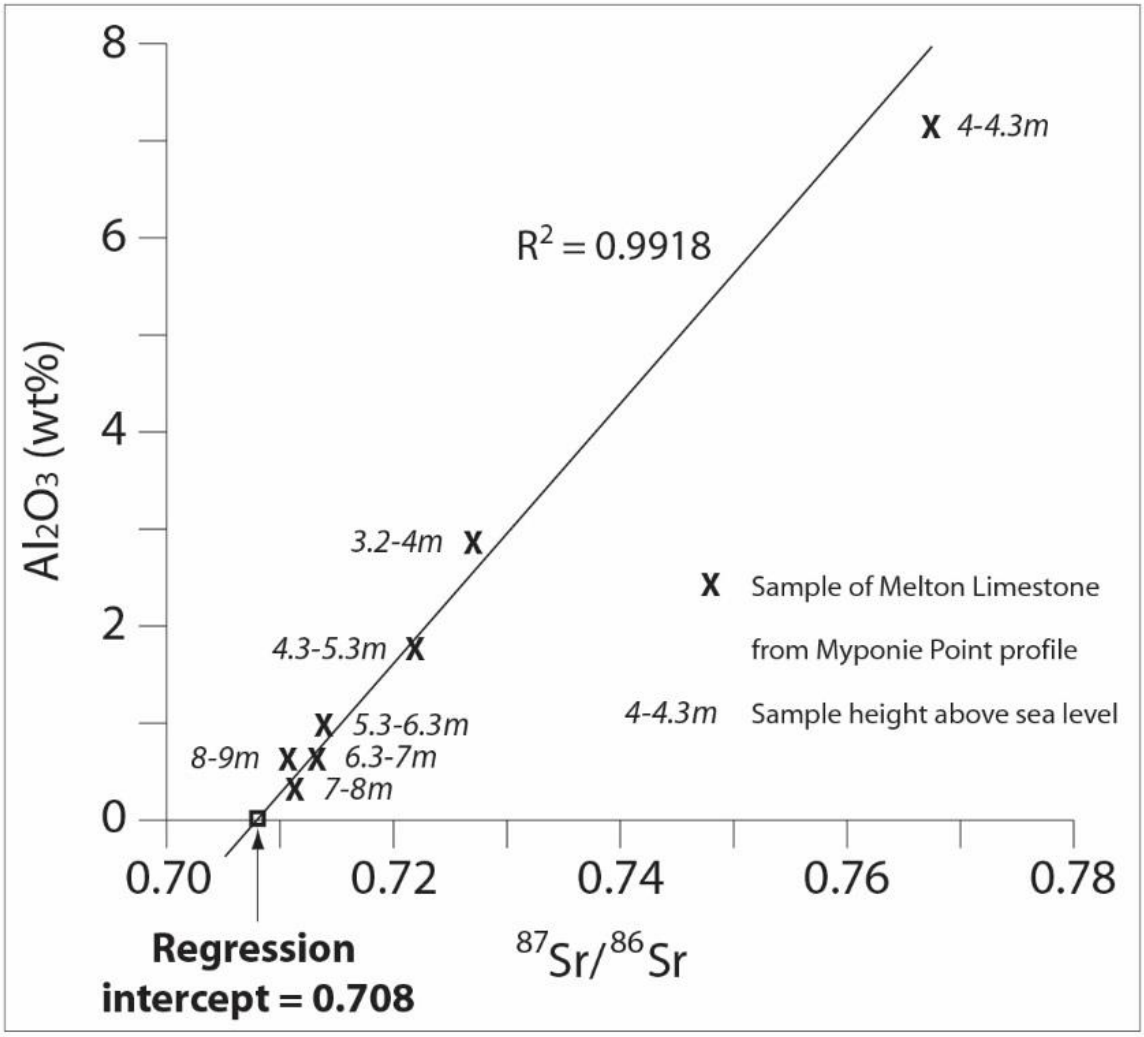

Figure 2.12. Plot of $^{87}Sr/^{86}Sr$ ratios versus Al_2O_3 wt% showing a regression trend-line for $^{87}Sr/^{86}Sr$ ratios of the Melton Limestone. Where this line intercepts (i.e. 0% Al_2O_3) represents a marine carbonate sample with the absence of clastic contamination.

2.8.2 Age of the Melton Limestone

The Melton Limestone has been suggested to be from the Oligocene to Miocene (33 Ma-15 Ma) (Drexel and Preiss, 1995; Zang et al., 2006); however, no specific age has been determined. The currently accepted age range has been based on principles of relative fossil ages in the Pirie Basin and neighbouring St. Vincent Basin (Lindsay, 1970). Here, we constrain the age of the Melton Limestone based on regression of $^{87}Sr/^{86}Sr$ ratios (Fig. 2.9). The regression intercept value of 0.708 for the Melton Limestone (Fig. 2.12) returns an age of 30 Ma when overlain onto the $^{87}Sr/^{86}Sr$ seawater curve (Fig. 2.4). Our estimate of 30 Ma for the Melton Limestone places the limestone in the Late Oligocene which coincidentally corresponds with the older limit of the currently published age range (Oligocene to Miocene; Drexel and Preiss, 1995; Zang et al., 2006). It is acknowledged that this age could be better defined with further isotopic analysis using the carbonate mineral fraction separated from other impurities in conjunction with multiple samples of the limestone, however this is not within the scope of this research. Additionally, this age determination only works for the Melton Limestone profile at Myponie Point due to it containing the least amount of siliciclastic contamination, as indicated by the low Al_2O_3 content (Figures 2.9a and 2.12). The Point Turton Limestone and limestone at Balgowan have slightly increased Al_2O_3 content, indicating these may be an argillic carbonate-bearing rock and are possibly contaminated by a siliciclastic component that may be enriched in radiogenic Sr (Fig. 2.9).

2.8.3 Differentiating between marine and pedogenic carbonate-bearing rocks

Distinguishing between marine and pedogenic carbonate-bearing rocks is critical in terms of sampling for mineral exploration programs as pedogenic carbonate-bearing rocks will preserve signatures of underlying mineralisation (Chen et al., 2002; Lintern et al., 2012; McQueen et al., 1999). Limestone formed in a marine environment does not typically contain pathfinder elements for ore deposition (e.g. Chen et al., 2002). For instance, the limestone in the Yorke Peninsula region has formed above basement rocks of the Olympic Domain that are prospective for IOCG deposits (Conor et al., 2010), but preserve no anomalous concentrations of ore pathfinder elements such as Cu (Fig. 2.9). Whether pedogenic carbonate-bearing rocks will preserve ore pathfinder elements is suggested to be due to the processes of carbonate rock formation (Lintern et al., 2012).

2.8.3.1 Textural and mineralogical differences

Distinguishing marine carbonate-bearing rocks from pedogenic carbonate-bearing rocks may be possible when there are visible fossils, however, this is not always the case (Lindsay, 1970). In an often costly exploration program, it is important to choose the right type of carbonate-bearing rock quickly and effectively in the field. Drill cuttings produced by various destructive drill methods can reduce the rock to a fine powder whereby destroying the original texture (Hillis et al., 2014; Marjoribanks, 2010). Whole-rock samples in the field environment are subject to weathering which also alters the texture.

Weathering alters the appearance of carbonate-bearing rocks through diagenetic alteration mechanisms such as dissolution, re-precipitation or recrystallization (Chen et

al., 2002; Crawford, 1965; Veizer, 1989). Dense recrystallization of these marine carbonate-bearing rocks has been described by a number of authors (e.g. Crawford, 1965; Lindsay, 1970; Drexel and Preiss, 1995). As an example, the effects of recrystallization can be observed within the Melton Limestone of this study, and is seen as calcite crystals along the edges of pore spaces and shells (Fig. 2.10). Chen et al., (2002) suggests that classifying a carbonate rock by its morphology is the recommended method, however the appearance and texture of a weathered exposure of Melton Limestone, for example bouldery and fine grained (Lindsay, 1970), could be easily mistaken for pedogenic carbonate-bearing rock (see also Milnes and Hutton, 1983; Hill et al., 1998).

Calcite is the dominant carbonate mineral in the marine limestone of this study (Fig. 2.9). However, calcite is also the main carbonate mineral found in pedogenic carbonate-bearing rock (calcrete) (e.g. Milnes and Hutton, 1983; Hill, et al., 1998). As an example, the marine and pedogenic carbonates in this study both contain calcite as a major component of the total carbonate rock profile (Fig. 2.9). Based on this study it would be difficult to place an individual sample of calcite into context unless there is a complete carbonate-bearing rock profile.

Additionally, the pedogenic carbonate-bearing rocks locally contain dolomite, as reflected by higher MgO content and spectral data (Fig. 2.9). The higher MgO content relating to increased dolomite content may be used to identify the pedogenic carbonate-bearing rocks, however the MgO concentrations are not consistent throughout the profiles (Fig. 2.9). For example, in the Myponie Point profile the base of the pedogenic carbonate

(sample MP11) has higher MgO concentration relative to the middle and top, implying higher dolomite content (Fig. 2.9a). At Balgowan and Point Turton, the MgO content within the pedogenic carbonate-bearing rocks inconsistent, and the mineralogy identified from spectral data varies between dolomite and calcite (Fig. 2.9b, c). Such variations in MgO concentrations and mineralogy imply that using mineralogy alone to discriminate between marine and pedogenic carbonate bearing rocks may not be reliable.

Recognising fossils in highly weathered, and finer grained carbonate-bearing rock samples (e.g. recrystallized) can be undertaken using thin sections (Fig. 2.10), however, this is not a technique that can be carried out quickly or in the field. Sample BAL12 from the Balgowan profile is described as being abundant is fossils fragments. Based on texture alone, this sample could easily be misidentified as a fossiliferous limestone. However, the spectral data shows dolomite and calcite (Fig. 2.9b), implying its mineralogy is similar to the surrounding pedogenic carbonate-bearing rocks. These observations imply that evidence other than mineralogy or texture may provide a more robust discrimination between marine and pedogenic carbonate-bearing lithologies.

2.8.3.2 Geochemical differences

Discrimination of marine and pedogenic carbonate-bearing rocks based on geochemical differences currently requires the rock samples to be analysed for a range of elements in a laboratory. Laboratory analysis is a routine procedure in mineral exploration and has the advantage of low detection limits over a wide element suite. The process, however, is time consuming and can take weeks to months before analytical data is available,

implying that discriminating between marine and pedogenic carbonate-bearing rocks as a sample media in the field is not possible.

2.8.4 Whole-rock geochemistry

Whole-rock geochemical data sets of carbonate-bearing rocks can provide a wide range of information. Aluminium and silica (Si) contents represent clay and siliciclastic components. When plotted against Ca, these elements will distinguish 'pure' versus impure carbonate-bearing rocks with siliciclastic input. The concentration of calcium alone is not enough to clearly distinguish a marine carbonate-bearing rocks from a pedogenic carbonate-bearing rock. As an example, a limestone sample from Myponie Point (4.8 m) contains the same amount of Ca (44 wt%) as an overlying pedogenic carbonate-bearing rock (12.5 m), which also contains 44 wt% (Fig. 2.9a, Table 2.1).

2.8.5 $^{87}Sr/^{86}Sr$ isotopic differences

$^{87}Sr/^{86}Sr$ ratios are widely used in carbonate studies for tracing the sources of calcium and for age dating of carbonate rocks (e.g. Burke et al., 1982; Chiquet et al., 1999; Hamidi et al., 1999; Howarth and McArthur, 1997; McArthur et al., 2001) . Our aim was to test whether the use of $^{87}Sr/^{86}Sr$ could also be used to distinguish between marine and pedogenic carbonate-bearing rocks by using the whole-rock. In the Myponie Point and Point Turton profiles, Sr isotope ratios for marine carbonate-bearing rocks are 0.722–0.711 and ~0.711 respectively, whilst ratios for pedogenic carbonate-bearing rocks are ~0.709 and ~0.710 respectively (Fig. 2.9, Table 2.1). This data shows that there are no systematic differences in $^{87}Sr/^{86}Sr$ ratios across the marine to pedogenic carbonate-

bearing rocks. Similarly, the change between well-cemented carbonate-bearing rock ($^{87}Sr/^{86}Sr = 0.710$) and sandy carbonate-bearing rock ($^{87}Sr/^{86}Sr = 0.710$), with or without detrital shells at Balgowan show no significant change in $^{87}Sr/^{86}Sr$ ratios (Fig. 2.9b).

The similarity of $^{87}Sr/^{86}Sr$ ratios is interpreted to be a relict signature of the original source of the Sr rather than the evolution of its deposition. Quade et al., (1995) demonstrated that carbonate-bearing soils from coastal South Australia and Victoria have $^{87}Sr/^{86}Sr$ ratios of 0.7094-0.7098, and that the Sr (and by inference the Ca) is of marine origin. The carbonate-bearing rocks studied here have comparable $^{87}Sr/^{86}Sr$ ratios (0.7101-0.7110) which may suggest also having significant marine input.

Partitioning of Sr into pore fluids during diagenesis will mobilise Sr to overlying or underlying sediments whilst still preserving the original $^{87}Sr/^{86}Sr$ ratio (e.g. Veizer, 1989; Van der Hoven and Quade, 2002). The pedogenic carbonate-bearing rocks at Myponie Point and Point Turton preserve $^{87}Sr/^{86}Sr$ ratios similar to the underlying marine carbonate-bearing rocks but contain a significant increase in Sr concentration (up to 1430ppm) (Fig. 2.9, Table 2.1), which may infer Sr mobilisation via pore fluid movement from the marine carbonate into the overlying pedogenic carbonate-bearing rocks, further atmospheric addition or relative accumulation (e.g. Quade et al., 1995; Van der Hoven and Quade, 2002).

The physical properties of Sr coupled with the $^{87}Sr/^{86}Sr$ values obtained from this study demonstrate that it is impossible to discriminate between marine and pedogenic carbonate-bearing rocks, at these locations, using Sr isotopes alone. The $^{87}Sr/^{86}Sr$ values are effective at giving clues as to the source of the Sr (and by association the calcium),

but do not clearly define any further differentiation resulting from pedogenic processes in the regolith. The Sr isotope therefore cannot be used on the whole-rock to distinguish marine and pedogenic carbonate-bearing rocks.

2.8.6 Making sense of multiple Sr isotope sources within marine and pedogenic carbonates

Veizer (1989) suggested that diagenetic alteration of marine carbonate-bearing rock will preserve the $^{87}Sr/^{86}Sr$ ratio of the original host/seawater where it formed. If there is a significant marine component of Sr, and as the $^{87}Sr/^{86}Sr$ composition of seawater changes with time (e.g. Burke et al., 1982; McArthur et al., 2001; 2012), it should theoretically be possible to distinguish between marine and pedogenic carbonates that formed at different times based on $^{87}Sr/^{86}Sr$ ratios. Radiogenic Sr, however, may be introduced via weathering of continental materials and will alter the initial $^{87}Sr/^{86}Sr$ ratios (e.g. Edmond, 1992; Peterman et al., 1970; Veizer and Compston, 1974, 1976). Additionally, there is such a wide range of contributing sources involved in pedogenic carbonate-bearing rock formation (e.g. groundwater, transported sediments, windblown dust; Chen et al., 2002), it becomes difficult to measure the Sr contribution from each source. Quade et al., (1995) concluded that the primary source of $^{87}Sr/^{86}Sr$ ratios in soil carbonates along coastal areas is dust and sea spray, but further inland the $^{87}Sr/^{86}Sr$ ratios increased as a function of increased continental dust input. Quade et al., (1995), also demonstrated that the increase in $^{87}Sr/^{86}Sr$ ratios further inland is a function of prevailing winds. Across the Yorke Peninsula, aeolian dust would be derived predominantly from the west to the east (marine source) but could also contain continental dust coming from the north (Anand,

2005). An example of these mixed sources of Sr can be seen in Figure 2.10g where the pedogenic carbonate-bearing rock contains rounded quartz grains and fragmented shells that have been interpreted as aeolian. As the Ca in the matrix of the pedogenic carbonate-bearing rock is likely to have a marine source (Quade et al., 1995), the overall $^{87}Sr/^{86}Sr$ ratio is closer to a marine value than a continental rock value (Fig. 2.9, Table 2.1).

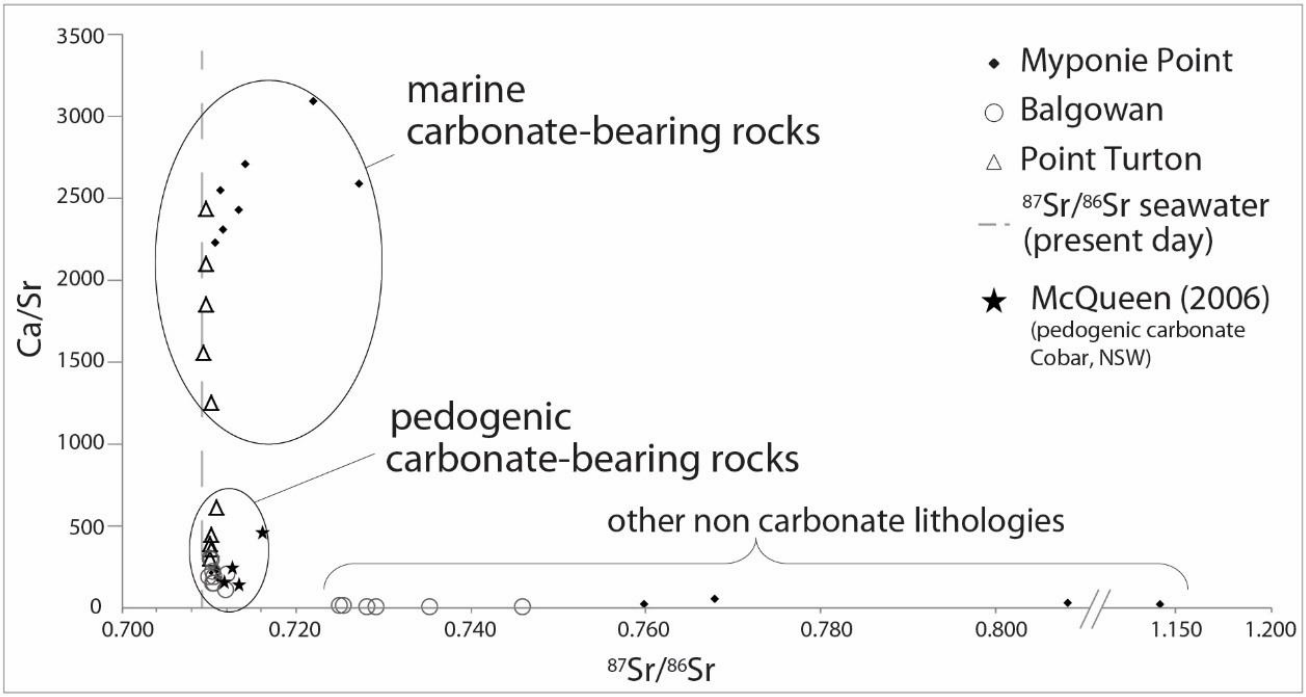

Figure 2.13. Ca/Sr values versus $^{87}Sr/^{86}Sr$ values for data from this study. Data groupings of marine carbonate-bearing rocks, pedogenic carbonate-bearing rocks and other lithologies (granite, sand or clay) are highlighted. Plot also includes data, for comparison, from McQueen (2006).

2.8.7 Ca/Sr and Ca/Mg element ratios

Quade et al., (1995) assessed the origin of soil carbonates in South Australia and Victoria using Ca/Sr ratios and evaluating the contributions of strontium, and by inference calcium, from bedrock (Ca/Sr = ~4-300), marine carbonates (Ca/Sr ~1100), sea spray or dust (Ca/Sr = 112) or local meteoric water (Ca/Sr = 680). The Ca/Sr ratio for rainwater was calculated from dissolution of carbonate dust derived from marine aeolianite in the region (Quade et al., 1995). The Ca/Sr ratios along with $^{87}Sr/^{86}Sr$ isotopes suggest the primary source of Ca within coastal soils was marine, and that soils further inland had higher contributions from inland dust (Quade et al., 1995).

This same technique for using the Ca/Sr ratio was used in this study to assess the usefulness as a discriminant between marine or pedogenic carbonate-bearing rock types (Fig. 2.11a). This was found to produce a highly effective means of separating the marine carbonate-bearing rocks from the pedogenic carbonate-bearing rocks regardless of the source of calcium defined by the $^{87}Sr/^{86}Sr$ ratios (Fig. 2.13).

Figure 2.13 demonstrates that the spread of $^{87}Sr/^{86}Sr$ ratios for all carbonate dominant lithologies is narrowly confined to 0.709– 0.711. The greatest range of $^{87}Sr/^{86}Sr$ ratios are only observed in the non-carbonate-bearing lithologies 0.725– 1.141. Conversely, three clear populations can be recognised in the Ca/Sr ratios (Fig. 2.11a, Fig. 2.13). Carbonate poor sediments and bedrock yield the lowest Ca/Sr ratios between 10 and 55. Ca/Sr values 1250– 3100 occur in the marine carbonate while the values in the pedogenic carbonate-bearing rocks are 100– 650 (Fig. 2.11a, Fig. 2.13, and Table 2.1).

The Ca/Sr data presented from our research demonstrates that marine and pedogenic carbonate-bearing rocks on the Yorke Peninsula preserve characteristic Ca/Sr ratios. Additionally, our Ca/Sr values fall within similar values presented by Quade et al., (1995), whereby the Ca/Sr ratio of marine carbonate-bearing rocks is significantly higher (> 1100) than pedogenic carbonate-bearing rocks (100– 650) and bedrock (< 300). Research undertaken by McQueen (2006), on pedogenic carbonate rocks, in the Cobar region of New South Wales, also display a similar pattern for Ca/Sr ratios (Fig. 2.13). This demonstrates that using Ca/Sr ratios to distinguish marine from pedogenic carbonate-bearing rocks is not a unique solution to the Yorke Peninsula and may be applied elsewhere.

In addition to Ca/Sr ratios, Ca/Mg ratios were investigated to assess their ability in differentiating between marine and pedogenic carbonate-bearing rocks due to the observation that the pedogenic carbonate-bearing rocks used in this study contain magnesium in the form of dolomite (Table 2.1, Fig. 2.9). Overall, the values for Ca/Mg have a comparatively limited range between 0.09 and 109 (Table 2.1). The pedogenic carbonate-bearing rocks have Ca/Mg ratios less than 28 whilst the marine carbonate-bearing rocks have Ca/Mg ratios greater than 35 (Fig. 2.11b). Therefore, the Ca/Mg ratios may be used to discriminate between the marine and pedogenic carbonate-bearing rocks.

Comparison between the results for using the Ca/Sr and Ca/Mg ratios to identify marine and pedogenic carbonate-bearing lithologies shows that the range of Ca/Sr ratios and gap between values for marine versus pedogenic carbonate-bearing rocks (range: 8-3095; gap: 643) is much larger than for the Ca/Mg ratios (range: 0.09-109; gap: 8).

Additionally, although the Mg concentration (reflecting the dolomite content) is locally elevated within the pedogenic carbonate-bearing rocks within the three profiles investigated in the Yorke Peninsula, it is unknown whether this applies across the whole Yorke Peninsula or elsewhere. Understanding the processes of MgO (and dolomite) concentration in the pedogenic carbonate-bearing rocks is beyond the scope of this study, and the extent to which Ca/Mg ratios may be used to distinguish between marine and pedogenic carbonate-bearing rocks is unclear. The use of Ca/Sr ratios is therefore favoured due to the larger range and gap in values that allow room for error in field analysis and data interpretation, as well as the knowledge that this ratio discrimination is applicable to areas beyond the Yorke Peninsula (McQueen 2006 data).

2.8.8 Mineral exploration sampling

The results of this study show that the Ca/Sr ratio using whole-rock geochemical data can be used to effectively discriminate between marine and pedogenic carbonate-bearing rocks. Calcium and often Sr data are routinely collected in laboratory whole-rock geochemical analysis, and generating this data is significantly less time consuming than analysis of Sr isotopes. Additionally, modern technologies such as portable XRF (pXRF) instruments allow immediate collection of whole-rock geochemical data in the field, and are capable of measuring Ca and Sr to detection limits of <50ppm and 5ppm respectively (e.g. Olympus). The Ca and Sr concentrations in marine carbonate-bearing rocks on the Yorke Peninsula range from 36–55 wt% and 100–290ppm respectively, and in the pedogenic carbonate-bearing rocks range from 35-46 wt% and 440–1430ppm respectively (Fig. 2.7). These values are significantly above the pXRF detection limit.

Portable XRF data collected in the field could therefore be used for immediate assessment of Ca/Sr ratios, and discrimination between marine versus pedogenic carbonate-bearing rocks.

The Myponie Point profile is proximal to the historic Cu mineralisation in the Moonta-Wallaroo district (Fig. 2.3). No mineralisation occurrences have been recognised proximal to the Balgowan or Point Turton profiles. The Cu content within samples taken from the Myponie Point profile shows noticeably higher concentrations within the pedogenic carbonate-bearing rock (4.5–6.0ppm Cu) accompanied by lower Ca/Sr ratios (<240), compared to the limestone (1.5–2.4ppm and Ca/Sr >2200) and corresponds to Cu concentrations in basement samples (3.4–5.4ppm Cu) with lower Ca/Sr ratios (< 55) (Fig. 2.9a, Table 2.1). This correlation supports the notion that pedogenic carbonate-bearing rocks are better recognisable using Ca/Sr ratios and may contain increased contents of economic and/or pathfinder elements proximal to mineralisation.

The ability to utilise Ca/Sr ratios in the field directly impacts the methodology of exploration campaigns that target carbonate rock sampling, due to the necessity to sample pedogenic carbonate-bearing rocks that will preserve pathfinder element signatures related to potentially buried mineralisation (compared to marine carbonate-bearing rocks that are unlikely to preserve such signatures) (e.g. Chen et al., 2002). Visual discrimination between marine and pedogenic carbonate-bearing rocks is often difficult, which implies there is a risk that the incorrect lithology will be sampled. Whole-rock geochemical analysis using pXRF technology in the field and immediate assessment of Ca/Sr ratios removes the potential for such sampling error.

2.9 Conclusion

Distinguishing between both marine and pedogenic carbonate-bearing rocks that have been highly weathered in the field is difficult and almost impossible in drill cuttings. The use of $^{87}Sr/^{86}Sr$ ratios does not clearly differentiate between marine and pedogenic carbonate-bearing rocks, and needs to be used with caution as contaminants from continental rocks introduce increased radiogenic Sr. The use of Ca/Sr ratios derived from a whole-rock geochemical data set is much easier to use to discriminate the difference between marine and pedogenic carbonate-bearing rock. The possibility exists for this type of calculation to be performed quickly in the field using existing portable whole-rock geochemical analyser technology. Field assessment of Ca/Sr ratios throughout a carbonate sampling exploration campaign will decrease the risk of collecting incorrect sample media, increase the risk of identifying potential pathfinder elements and is applicable to the Yorke Peninsula and possibly other similar carbonate regolith dominated terrains.

Chapter 3: Pedogenic carbonate sampling for Cu exploration on the Yorke Peninsula

Foreword

This chapter presents whole-rock geochemical data from surface occurring carbonate rocks across the Yorke Peninsula, South Australia in order to evaluate the potential of regolith carbonates as a geochemical sampling media for buried Cu mineralization. An understanding of the geochemistry has shown that the majority of carbonate material at the surface has a pedogenic origin (Ca/Sr ratios <650).The Ca and Sr concentration within the carbonate rocks is influenced by the chemical composition of rainwater and underlying marine carbonate. Samples were collected by Randall Wolff and Bradley Versegi during a series of field trips in 2012. Samples were photographed and logged by myself. All samples were crushed and milled by Amdel Laboratories (now Bureau Veritas) in Adelaide. Whole-rock geochemistry was undertaken by Acme Laboratories (now Bureau Veritas), Vancouver Canada. Seawater sampling was undertaken during 2013 with the assistance of Dr Nathan Reid from CSIRO, Perth. Water samples were analysed by Dr Nathan Reid.

Statement of Authorship

Title of Paper	Pedogenic carbonate sampling for Cu exploration on the Yorke Peninsula, South Australia
Publication Status	☐ Published ☐ Accepted for Publication ☑ Submitted for Publication ☐ Unpublished and Unsubmitted work written in manuscript style
Publication Details	Submitted to Journal of Geochemical Exploration

Principal Author

Name of Principal Author (Candidate)	Keryn Wolff
Contribution to the Paper	Collection and preparation of all carbonate samples. Collection of seawater samples. Sorting packaging and labelling all samples for delivery to the relevant laboratory for geochemical analysis. Data entry and format of all results suitable to use in relevant geochemical, statistical and GIS software programs. Compiling all illustrations used in the published article and making new ones where needed. Drafting the initial document. Correcting to co-authors and reviewers comments. Primary contact throughout the publications process.
Overall percentage (%)	90
Certification:	This paper reports on original research I conducted during the period of my Higher Degree by Research candidature and is not subject to any obligations or contractual agreements with a third party that would constrain its inclusion in this thesis. I am the primary author of this paper.
Signature	Date 12/04/2018

Co-Author Contributions

By signing the Statement of Authorship, each author certifies that:

i. the candidate's stated contribution to the publication is accurate (as detailed above);

ii. permission is granted for the candidate in include the publication in the thesis; and

iii. the sum of all co-author contributions is equal to 100% less the candidate's stated contribution.

Name of Co-Author	Caroline Tiddy
Contribution to the Paper	Review comments and editing suggestions
Signature	Date 12/04/2018

Name of Co-Author	David Giles
Contribution to the Paper	Review comments and editing suggestions
Signature	Date 12/04/2018

Please cut and paste additional co-author panels here as required.

Name of Co-Author	Steve Hill			
Contribution to the Paper	Review comments and editing suggestions			
Signature			Date	9/4/2018

Pedogenic carbonate sampling for Cu exploration on the Yorke Peninsula

Keryn Wolff, Steve Hill, Caroline Tiddy, Dave Giles,

As submitted to the Journal of Geochemical Exploration 2018

Accepted and published

(Journal of Geochemical Exploration 194 (2018) 239–256)

https://doi.org/10.1016/j.gexplo.2018.08.007

(Appendix 4)

3.1 Abstract

We report on the geochemistry of 215 regolith carbonate rocks collected across the Yorke Peninsula, South Australia in order to evaluate the potential of regolith carbonates as a geochemical sampling media for buried Cu mineralization. The Yorke Peninsula forms the southern part of the Olympic Domain iron-oxide-copper-gold (IOCG) mineral province and is host to a number of Cu-bearing mineral deposits and prospects including Hillside and the historic Moonta-Wallaroo mining district. The majority of the Yorke Peninsula is covered by a veneer of Cambrian to Quaternary sedimentary rocks and regolith, including marine limestones and regolith carbonates. We present a new regolith map of the Yorke Peninsula and use it to provide landscape context and regional characterization of the sampled regolith materials. The major element chemistry of the carbonate rocks is dominated by CaO (33 wt%–53 wt%), reflecting the calcite component. Other major components include SiO_2 and Al_2O_3, reflecting quartz (typically quartz sand in carbonate indurated quaternary sands) and clay minerals respectively. Ca/Sr ratios vary between <200 and >1200 with 86% of the samples < 650. The Ca/Sr < 650 group of samples forms a continuous array on a plot of Ca vs Sr which overlaps with the range of values expected from sea water derived Ca and Sr subjected to variable degrees of meteoric fractionation. These samples are interpreted to be regolith carbonates with little input of marine carbonate. A single sample has Ca/Sr >1260, consistent with a significant component of marine limestone. Twenty nine samples have Ca/Sr >650 and <940 which may indicate mixing of dominantly meteoric sources with a lesser component of marine carbonate. We recommend that geochemical results from samples with Ca/Sr >650 be treated with caution as the regolith carbonate trace element geochemical signal may be diluted by the

marine carbonate component. Copper concentrations found in the carbonate rocks with Ca/Sr <650 range from 1.4ppm to 36ppm and form a slightly right-skewed, near log normal population. Samples with elevated log_{10}Cu concentrations have a broad spatial coincidence with areas of known Cu enrichment in the basement and not related to dust or windblown contamination. Copper concentrations show no systematic relationship with common dust-born contaminants (Al_2O_3, Fe_2O_3, Zr) which would be expected if the Cu was derived from windblown spoil from the historic mining operations. We conclude that regolith carbonates are a potentially useful sampling media for Cu exploration on the Yorke Peninsula and that they can be easily differentiated from less useful marine carbonates on the basis of Ca/Sr ratios.

3.2 Introduction

Regolith carbonates are globally widespread and generally occur in semi-arid to dry environments (e.g. Chen et al., 2002; Dart et al., 2007; Khadkikar et al., 2000; Khadkikar et al., 1998; Reith et al., 2011; Wolff et al., 2017). Regolith carbonate covers at least 21% of Australia, and is more common in the southern, drier regions (e.g. Chen et al., 2002; Dart et al., 2007; Lintern, 2015; McQueen, 2006; Fig. 1). Regolith carbonate rocks are commonly referred to as calcrete (e.g. Chen et al., 2002; Lintern et al., 2012; McQueen et al., 1999), but can also include other carbonate dominant rocks such as dolomite or highly weathered and re-precipitated limestone (e.g. Chen et al., 2002; Wolff et al., 2017).

Regolith carbonates can form by a variety of processes (e.g. Chen et al., 2002; Prudencio et al., 2011). These include accumulations or deposition/precipitation of Ca during soil forming processes (pedogenesis) which commonly occurs in arid climates (e.g. McQueen, 2006; Prudencio et al., 2011; Reith et al., 2011). Detailed description of regolith carbonate formation and morphology is described in Chen et al., (2002). Previous studies suggest that the Ca component of pedogenic carbonate rock in southern Australia is primarily derived from rainwater, whilst the C component of pedogenic carbonate is sourced from C4 plants (e.g. Lintern et al., 2006; Quade et al., 1995). Calcium may also be derived from the weathering of underlying rocks (Dietrich et al., 2017) or carried in wind born dust, for example in dust derived from exposed marine carbonate rocks (Quade et al., 1995; Van der Hoven and Quade, 2002). Strontium is typically enriched in carbonate rocks, where it is a common ionic substitute for Ca (e.g. Dart et al., 2012; Lintern et al., 2006; Van der Hoven and Quade, 2002). Strontium isotopes have been

used by a number of authors in an attempt to constrain possible sources of Sr, and by inference Ca, in pedogenic carbonate rocks. Quade et al., (1995) concluded that the ocean is the primary source of Sr in pedogenic carbonates from coastal regions of southern Australia, whereas further inland Sr isotopes tend to reflect local dust composition. A local dust source, in this case derived from nearby exposed marine carbonates, was also favoured by Van der Hoven and Quade (2002) in their study of pedogenic carbonates from New Mexico. In contrast Dietrich et al., (2017) argued that Sr isotopes in carbonates from norther Cameroon are best explained by weathering of in-situ sources with a lesser component of wind born dust.

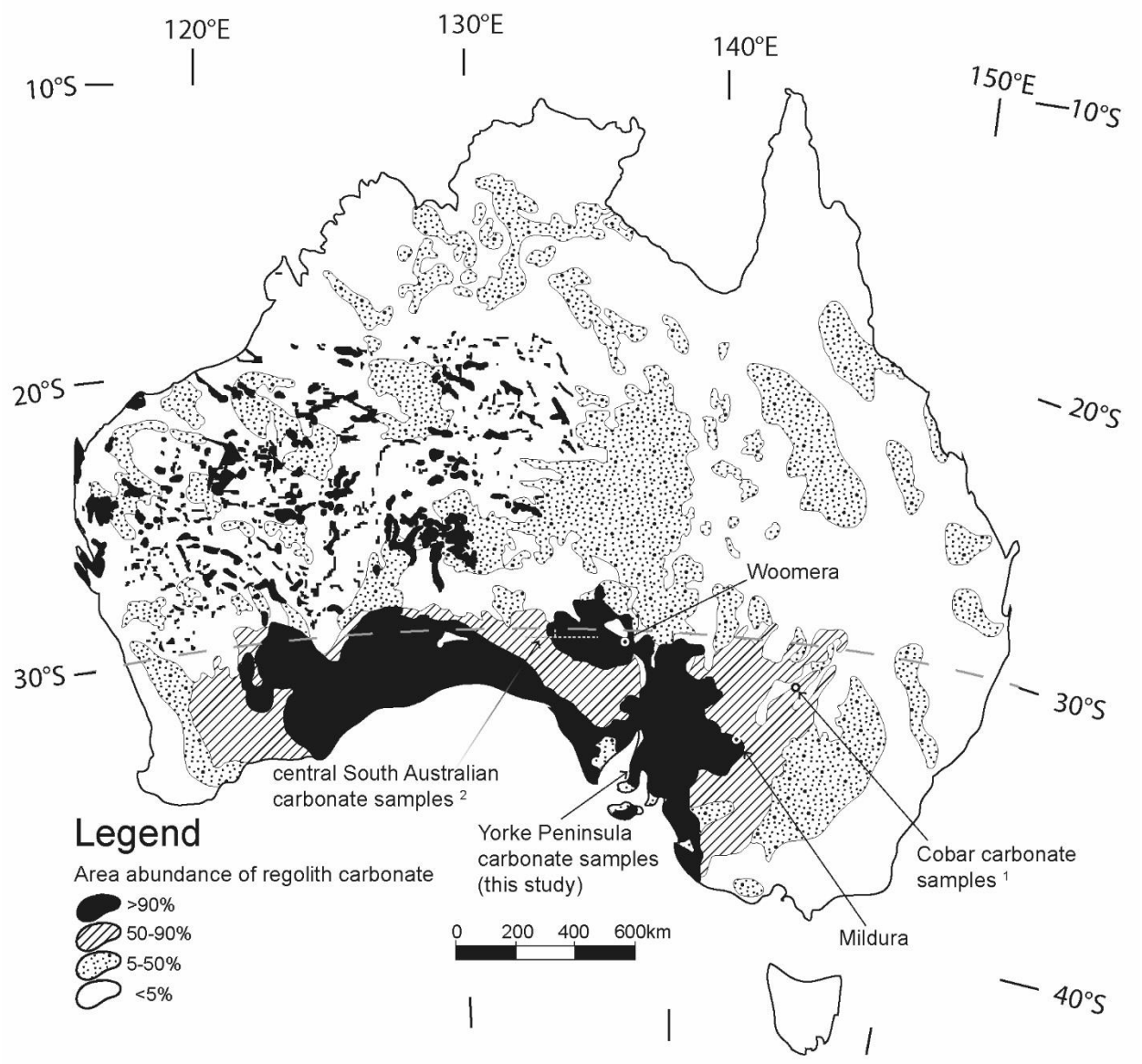

Figure 3.1. Carbonate distribution and abundance across Australia, modified after Chen et al., (2002). Carbonate sampling locations from other authors are shown and numbered: 1. McQueen (2006); 2. Lintern and Sheard (1999) and Lintern et al., (2006). Latitude 30°S is shown by the grey dashed line. Pedogenic carbonates tend to occur more frequently south and groundwater carbonates tend to occur more frequently north of this latitude (e.g. McQueen, 2006; McQueen et al., 1999).

Carbonate rocks formed during pedogenesis have the potential to incorporate geochemical signatures from the underlying substrate. (e.g. Chen et al., 2002; Lintern et

al., 2012; Lintern et al., 2011; McQueen, 2006; Salama et al., 2016; Wolff et al., 2017). Pedogenic carbonate has become popular and successful sampling medium for use in Au exploration in Australia (e.g. Chen et al., 2002; Lintern, 2015; Lintern et al., 2012; Reith et al., 2011) and may also be useful as an indicator of buried Cu mineralization (e.g. Lintern, 2015; Wolff et al., 2017). Regional geochemical exploration surveys using surface carbonates have been extensively carried out throughout southern Australia including in the Cobar region, New South Wales (McQueen, 2006; Fig. 1), the Challenger Gold Deposit region, South Australia (Lintern and Sheard, 1999; Lintern et al., 2006; Poustie and Abbot, 2006; Fig. 1), the ET Gold deposit, Gawler Craton, South Australia (Lintern et al., 2011) and a number of regions in Western Australia (e.g. Lintern, 1989; Lintern et al., 1997; Lintern et al., 2009).

The Yorke Peninsula, South Australia (Fig. 2), is covered by late Cenozoic to Quaternary transported sediments including pedogenic carbonate that has formed over weathered, early Cenozoic to Cambrian sedimentary rocks including marine limestone (e.g. Zang et al., 2006; Fabris, 2010; Fig. 3). Underlying Early to Middle Proterozoic basement rocks of the Yorke Peninsula region are part of the broader Olympic Domain (Fig. 2) and are prospective for iron-oxide-copper-gold (IOCG) mineralization (Conor et al., 2010). Basement rocks of the Olympic Domain host the super-giant Olympic Dam IOCG-U deposit as well as the Prominent Hill, Carrapateena, and Hillside IOCG deposits (e.g. Conor et al., 2010; Zang et al., 2006; Fig. 2). The potential for pedogenic carbonate rocks to be used as exploration sampling media requires that Cu, Au and other ‘pathfinder’ elements enriched in IOCG mineralization can be mobilized from the basement rocks

such as to form detectable dispersion halos in the overlying carbonates (Dietman, 2009; Ghavami-Riabi et al., 2008; Hartley, 2000; Keeling and Hartley, 2005).

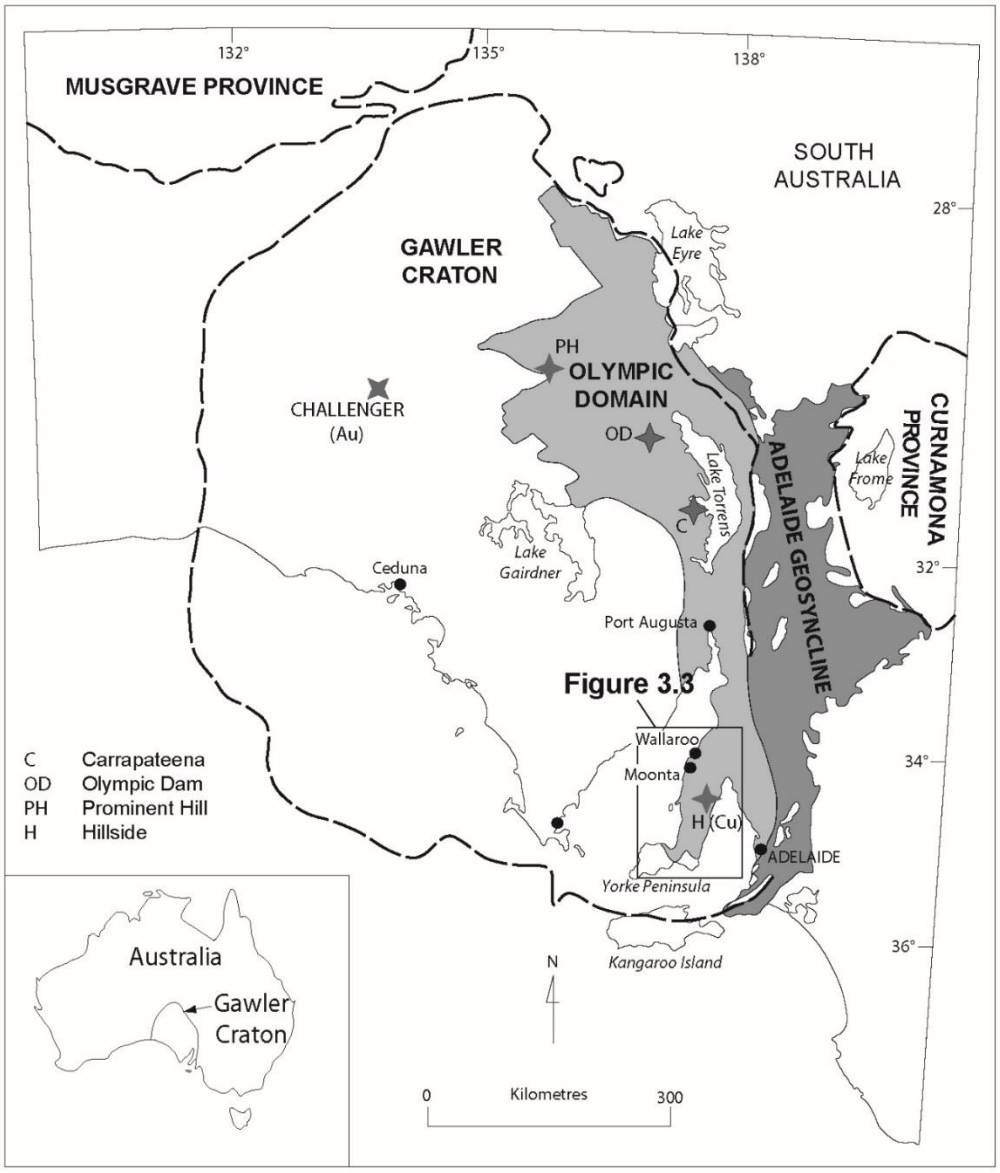

Figure 3.2. Simplified geological map of the Gawler Craton showing the location of IOCG mineralization throughout the Olympic Domain. The study area is outlined by the black rectangle. Inset: Location of the Gawler Craton within Australia. Modified after Conor et al., (2010).

In this paper we use a combination of regolith mapping, surface sampling of carbonate rocks and geochemistry to test the potential for this material as an exploration sampling medium for Cu on the Yorke Peninsula. We seek to constrain the possible sources of Ca and Sr in the carbonate rocks by comparison with Ca/Sr from seawater, rainwater and locally exposed marine carbonate rocks. We conclude that Ca/Sr ratios can be used to differentiate between carbonate rocks that were derived from pedogenic or marine processes (see also Wolff et al., (2017). We then focus on Cu concentrations in the pedogenic carbonate rocks and show that there is a spatial association between elevated Cu and known mineral occurrences in the basement rocks. The implications for using the carbonates from this region as a sample medium for Cu exploration are discussed.

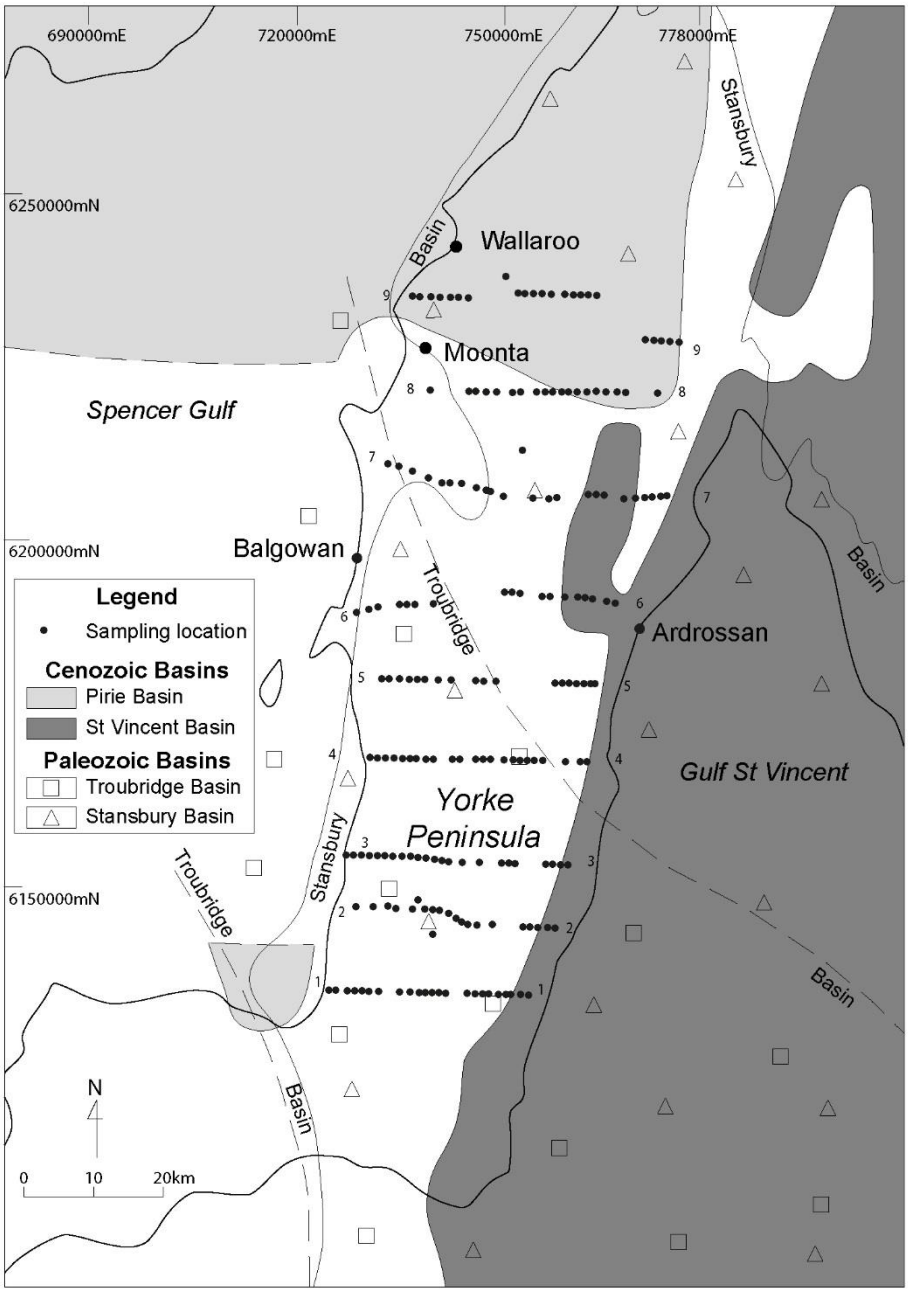

Figure 3.3. Map of Yorke Peninsula showing location of the Palaeozoic Stansbury and Troubridge Basins and Cenozoic Pirie and St Vincent Basins. Basin outlines are modified from Drexel and Preiss (1995). Locations of regional carbonate rock samples are shown by black dots. Transects are numbered 1 to 9.The Cu concentrations for samples from Hartley (2000) proximal to Moonta are shown. The location of Balgowan and Ardrossan

where seawater samples were taken are also shown. Map location is shown in Figure 3.2.

3.3 Background

3.3.1 Geology

The geology of the Yorke Peninsula has been described previously by Conor et al., (2010), Crawford (1965), Drexel and Preiss (1995), and Zang et al., (2006). The Yorke Peninsula is within the southern Olympic Domain of the Gawler Craton (Fig. 3.2). Proterozoic basement rocks within the Yorke Peninsula are poorly exposed, with less than 5% exposure (Cowley et al., 2003; Fig. 3.4). Basement packages are dominated by metasedimentary and volcanic rocks of the Late Paleoproterozoic Wallaroo Group (ca 1750 Ma; Conor et al., 2010). The Wallaroo Group was deformed during the ca 1730-1690 Ma Kimban Orogeny (Ferris et al., 2002; Hand et al., 2007; Hoek and Schaefer, 1998) and later intruded by ca 1595-1575 Ma Hiltaba Suite granites and minor mafic magmatic rocks (Cooper et al., 1985; Cowley et al., 2003; Creaser, 1996; Creaser and Cooper, 1993; Creaser and Fanning, 1993; Fanning et al., 1988).

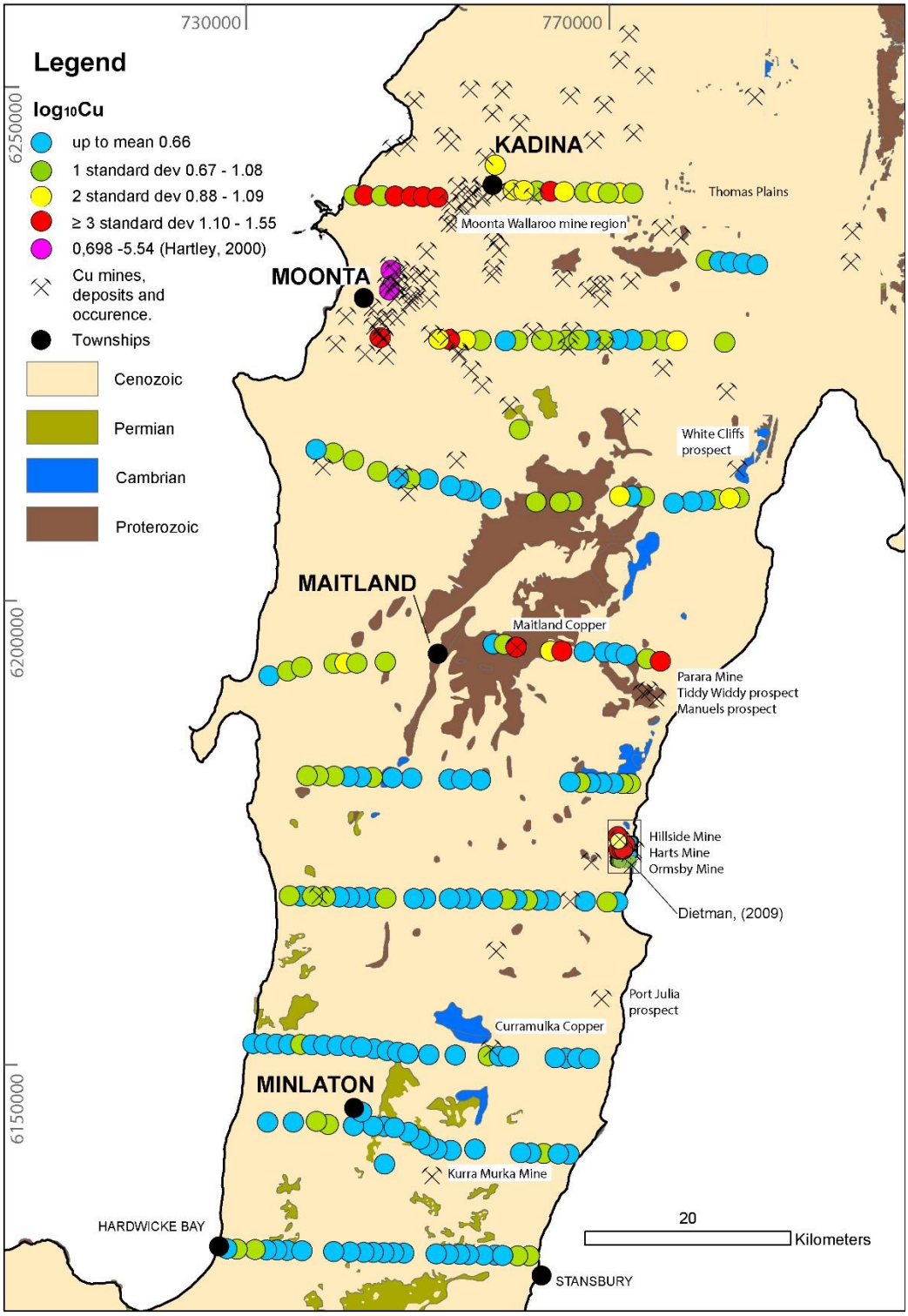

Figure 3.4. Simplified surface geology map of Yorke Peninsula (Extracted from SARIG: https://map.sarig.sa.gov.au). Cenozoic geology includes Miocene aged limestone found in the Pirie and St Vincent Basins (see also Fig. 3.3) and Quaternary limestone. Cambrian

geology includes limestone found in the Stansbury Basin (see also Fig. 3.3). Cu concentrations from this study are displayed as the log_{10} values and colored by standard deviation. Cu concentrations reported in Hartley (2000) (NE of Moonta) and Dietman, (2009) (Hillside and Harts Mines) are also shown.

IOCG mineralization in the Olympic Domain includes the super-giant Olympic Dam deposit, and the smaller Prominent Hill and Carrapateena deposits (Fig. 3.2). The Yorke Peninsula also hosts IOCG mineralization including the Hillside deposit and the historic Moonta-Wallaroo district (Figs 3.2 & 3.4). IOCG mineralization is interpreted to have been derived from hydrothermal fluids that were coeval with intrusion of the Hiltaba Suite granites (Conor et al., 2010; Morales-Ruano et al., 2002). Mineralization in the Yorke Peninsula is hosted within both the Wallaroo Group and the Hiltaba Suite granites (Conor et al., 2010; Cowley et al., 2003). Wallaroo-style IOCG mineralization tends to be dispersed within, or associated with, quartz vein-hosted Fe and Cu sulphides in altered biotite-magnetite alteration zones hosted by metasedimentary rocks (e.g. Conor, 1995; Skirrow. et al., 2007). Moonta-style mineralization is found within porphyritic felsic intrusions within the Wallaroo Group (Skirrow et al., 2007).

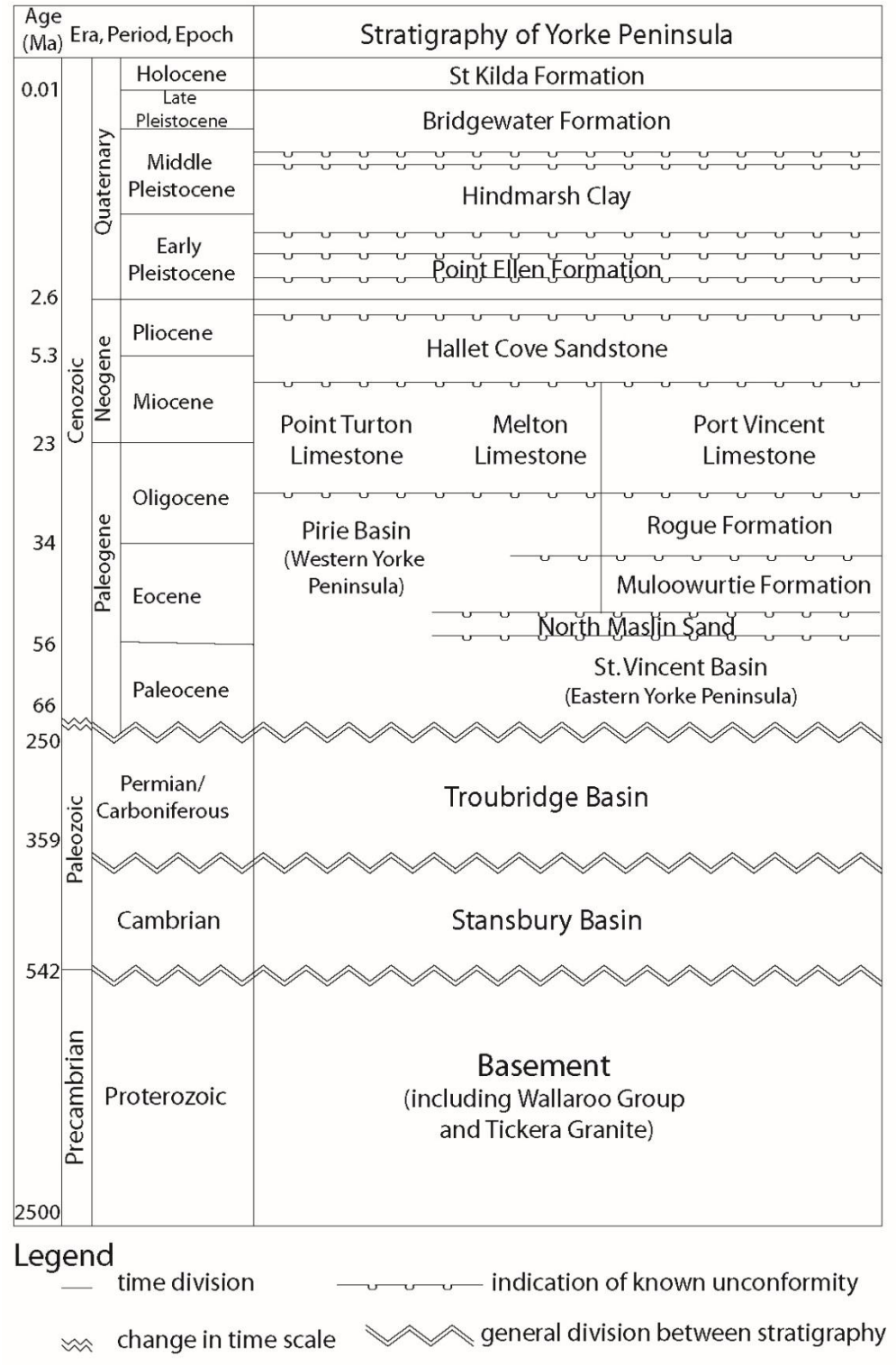

Figure 3.5. Simplified stratigraphic diagram of the Yorke Peninsula. Modified after Drexel and Preiss (1995) and Zang et al., (2006).

The basement rocks are unconformably overlain by sedimentary rocks of the Cambrian (540-500 Ma) Stansbury Basin, Carboniferous to Permian (350-260 Ma) Troubridge Basin and the Cenozoic (65-2.6 Ma) St Vincent and Pirie Basins (Drexel and Preiss, 1995; Zang et al., 2006; Figs 3.2 & 3.5). Cenozoic sedimentary rocks include limestone, siltstone, sandstone and mudstone deposited during fluctuating sea levels, uplift and rifting (e.g. Crawford, 1965; Drexel and Preiss, 1995; Zang et al., 2006).

Quaternary deposits (2.6 Ma to present) which include variably consolidated sands, silts, clays and regolith carbonates cover >90% of the Yorke Peninsula and conceal the underlying geology (e.g. Drexel and Preiss, 1995; Zang et al., 2006; Fig. 3.4). Sand dunes and beach deposits have formed along most shore and backshore environments along the coastline (e.g. the St Kilda Formation, Fig. 3.5; Zang et al., 2006). Extensive sand dunes have also formed across inland regions primarily in the north and along the eastern coastline (Fig. 3.6). Sand-flats, claypans and ephemeral lakes have developed in areas of low relief. Calcium carbonate-rich rocks with laminar, nodular or powdery textures have formed in the upper portion of the soil profile throughout most of the region (e.g. Drexel and Preiss, 1995; Zang et al., 2006). The western side of the Yorke Peninsula is dominated by calcareous sand dunes whilst the eastern margin is dominated by calcareous, loamy soils overlying pedogenic carbonate rock (e.g. McDowell et al., 2012; Neagle, 2008). Active erosion and re-deposition of colluvium occurs within gullies, drainage lines and along the coastline (Zang et al., 2006).

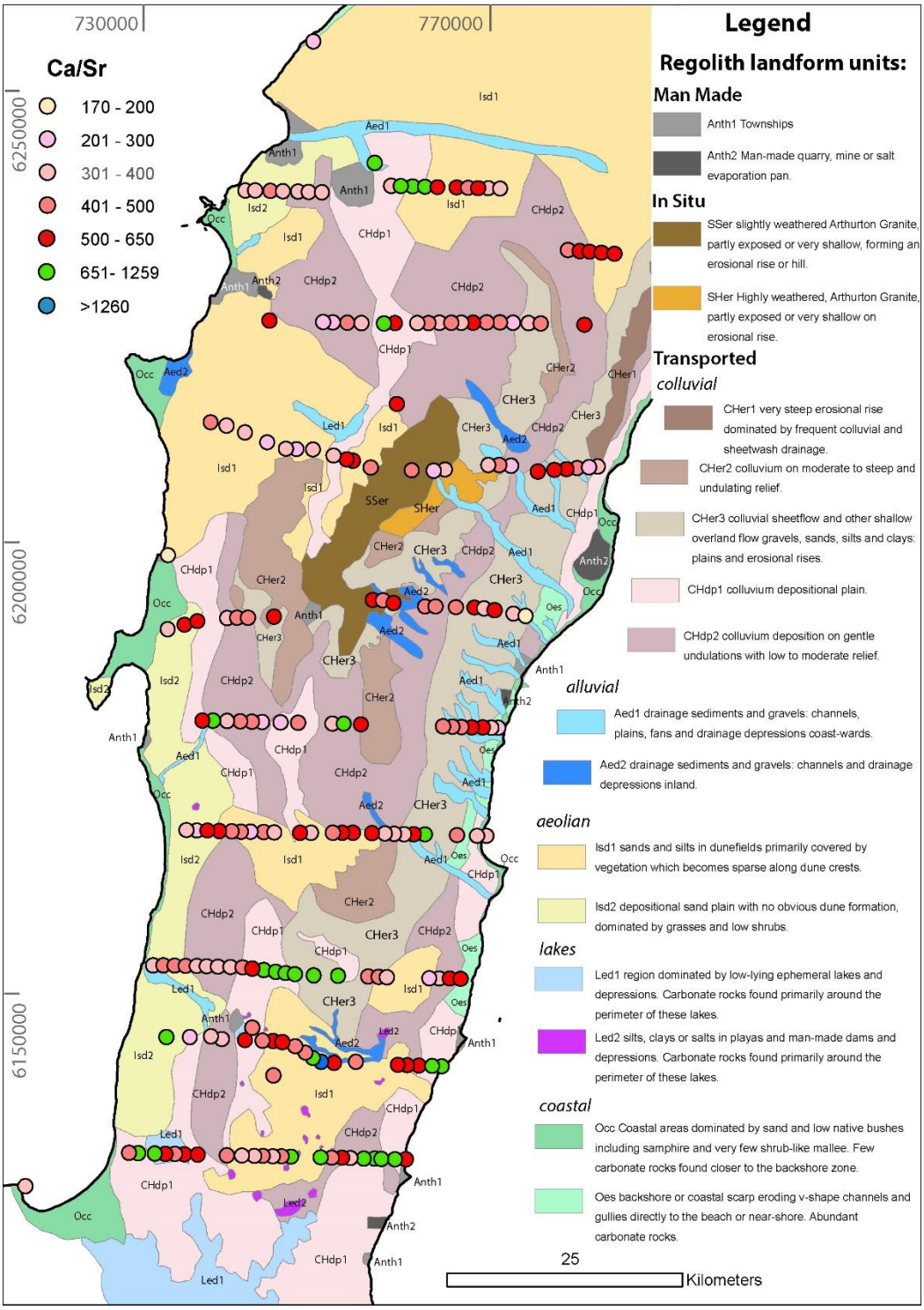

Figure 3.6. 1:25,000 scale regolith map of the Yorke Peninsula. Carbonate rock sample locations from this study are shown and coloured by Ca/Sr ratio values. Categories used

are based on Wolff et al., (2017) where Ca/Sr <650 are described as pedogenic carbonate and are coloured from pink to red; Ca/Sr >1260 are described as marine carbonate and coloured blue. Intermediate Ca/Sr values (651–1259) are coloured green. Detailed map methods are found in section 3.4.1 Regolith Landform Map.

3.3.2 Landscape, climate and vegetation.

The Yorke Peninsula is low relief, with gently undulating hills and valleys generally less than 100m above sea level and up to 230m above sea level north of Maitland (e.g. Neagle, 2008; Roberts, 2007; Zang et al., 2006). The region has been cleared of most naturally occurring vegetation for agriculture with approximately 13% native vegetation remaining (McDowell et al., 2012; Neagle, 2008). A variety of vegetation species including eucalypt mallee, tea trees and wattle trees tend to dominate the landscape whilst samphire, saltbush, mangroves and other coastal shrubs dominate coastal sandflats and backshore environments with low relief (e.g. McDowell et al., 2012; Neagle, 2008).

The region has a Mediterranean climate (McDowell et al., 2012) with average daytime temperatures ranging from 15°C in winter to 30°C during summer (Bureau of Meteorology, 2018). Rainfall averages approximately 470mm per year (Bureau of Meteorology, 2018). No major water catchments occur in the central Yorke Peninsula region (e.g. DEWNR, 2013) and any surface drainage is infrequent, with many watercourses terminating in ephemeral salt lakes and clay pans (e.g. DEWNR, 2013; Roberts, 2007). Wind across the study area is generally derived from the north-west during summer and from the south to south west during winter (e.g. Bureau of Meteorology, 2017; Hesse and McTainsh, 2003)

3.4 Methods

3.4.1 Regolith Landform Map

A 1:25,000 regolith map was produced using a combination of geophysical data including Google Earth™, United States Geological Survey (USGS) and Aster global-DEM (a product of METI and NASA) (Fig 3.6). Surface geology and elevation features were verified using South Australian Resource Information Gateway (SARIG, Department of the Premier and Cabinet, 2017). The present landscape has been significantly modified due to land use, therefore ground truthing and verification of the map was undertaken at each sampling site (Fig. 3.3). Correlations assuming a non-complex continuation of landform features within each area mapped were made between field sampling sites under areas of land cleared for cropping and using the various digital data previously described. Regolith landform unit codes (RLU) used are based on Pain et al., (2007).

3.4.2 Sampling Methods

3.4.2.1 Carbonate Sampling

A total of 215 surface carbonate rock samples were collected at approximately 1km intervals along ten east-west transects spaced approximately 10km apart (Fig. 3.3). Each transect numbered 1 to 9, followed a road corridor extending from one coastline of the Yorke Peninsula to the other (Fig.3.3). Where no carbonate rocks were present, the sample spacing was extended until a suitable sample could be located. The resulting sampling grid extends from Stansbury and Hardwicke Bay in the south, to Kadina and Thomas Plains in the north (Fig. 3.3).

Due to possible contamination factors such as increased dust and car emissions samples were collected as far from the side of the road as possible. Major intersections, townships, driveway entrances and quarried carbonate rocks (often incorporated in historic fence lines) were avoided. Gloves were used to collect all samples. Larger boulder sized samples were broken up with a geological hammer prior to collection. Smaller cobble sized samples were removed from the soil by hand or by levering out of the ground with a geological hammer. Where possible larger rocks were sampled so as to reduce the surface to volume ratio in an attempt to minimize concentration of any adhering surface contaminants. The samples were brushed lightly with a soft brush to remove surface contamination. The sample was placed into plastic zip-lock bag and labelled with a unique identifier and numbered according to the order it was collected. One in every 10 field samples were replicated. A small portion of each sample was reserved for reference. The average sample size was approximately 2kg.

3.4.2.2 Seawater sampling

Seawater was collected at Ardrossan and Balgowan (Fig. 3.3). At Balgowan water was collected off the end of a groin by reaching out and submerging a bucket firstly to pre-rinse and then again to collect the sample. At Ardrossan the water was collected from the end of the jetty by tying a rope to the bucket handle and lowering it into the water to firstly pre-rinse and then again to collect the sample. In both instances, seawater samples were decanted into 125ml, high density polyethylene (HDPE) bottles and labelled.

3.4.3 Sample preparation and analysis

3.4.3.1 Carbonate samples

The entirety of the carbonate rock samples were milled to a fine powder using a tungsten carbide ring mill at Amdel Laboratories Adelaide. Approximately 100g portions of this material was sent to Bureau Veritas (Acme Laboratories; www.acmelab.com) in Vancouver, Canada for whole-rock geochemical analysis. Major element oxides were analysed using X-ray fluorescence (XRF) on $LiBO_2$ fused glass beads (ACME laboratory code 4X; see Appendix 5). Trace elements were analysed using ICP-MS following two separate preparations. Rare earth and refractory elements were analysed following lithium borate fusion. Aqua regia digest was used for all remaining trace elements (Mo, Cu, Pb, Zn, Ni, As, Cd, Sb, Bi, Ag, Au, Hg, Tl and Se; ACME laboratory code 4X and 4B, see Appendix 5). Routine laboratory standards, duplicates and blanks were included for quality control. One in every 10 samples were duplicated (n = 23). Sixteen blanks were included with XRF and 10 blanks were included with ICP-MS.

3.4.3.2 Seawater samples

Seawater sample preparation involved the addition of concentrated nitric acid (69 %) to each sample in the laboratory. Approximately 0.25µL was added to each full 125ml bottle. Acidification is undertaken to ensure any Fe oxides were fully dissolved as described by (Gray et al., 2009). Samples were packed in a plastic storage container and sealed prior to sending to South Australia Department of Land and Water for analysis of major and trace elements by ICP-OES and ICP-MS. Concentrations for Ca, determined by ICP-

OES, were reported in mg/L. Concentrations for Sr, determined by ICP-MS, were reported in ug/L. Elements of interest were converted to ppm for the purpose of this paper.

3.5 Results

3.5.1 Regolith Landform Map

The Regolith Landform Map is presented in Figure 3.6. The majority of the region is dominated by transported sediments with few *in-situ* rocks observed around the central region. Rocks that are exposed and were observed *in-situ* are predominantly weathered granite. The western half of the Yorke Peninsula is dominated by sand and sand dunes (e.g. Isd1 and Isd2). Coastal environments include tide dominated sand flats with few steep backshore sand dunes or cliffs (e.g. Occ). The central region of the Yorke Peninsula (Fig. 3.6) is characterized by undulating hills and valleys with a range of *in-situ* erosional (SSer, Sher) and colluvial (Cher1, CHer2, CHer3, CHdp1, CHdp2) regolith environments. Outcropping rocks in the most central area of the peninsula are variably weathered and found primarily buried beneath a shallow cover of soil (SSer and Sher). The eastern portion of the mapped area (Fig. 3.6), is dominated by cliffs and steep hills with incised drainage channels (CHer1, Cher3, CHdp1, Aed1, Aed2). The southern portion of the mapped area is lower in elevation and dominated primarily by depositional plains including sand dunes, and sandy beach deposits along the coastline (CHdp1, CHdp2, Isd1 and Oes). The area with the lowest relief, the southernmost portion of the map (Fig. 3.6), features a region of salt lakes and clay pans that fill with water only after heavy rain (CHdp1, Led1 and Led2). Carbonate rocks occur across all regolith landform units, except the lake units (Led1, Led2) and the coastal units (Occ, Oes). The carbonate rocks have

a variety of forms: 1) soft or powdery carbonate-rich sands and soils forming a thin veneer at the surface (Fig. 3.7); 2) well-indurated, massive or laminated tabular forms from decimetre to meter thickness (e.g. Fig. 3.7a), and; 3) nodular forms with variable proportions and density of nodules from gravel to cobble size and with a thickness of approximately one meter (e.g. Fig. 3.7b, c). All three carbonate forms are often found at the same location with calcareous soils typically overlying tabular forms, which in turn overly nodular forms. These carbonate morphologies are typical of those found in regolith carbonate profiles (e.g. Chen et al., 2002; Lintern, 2015).

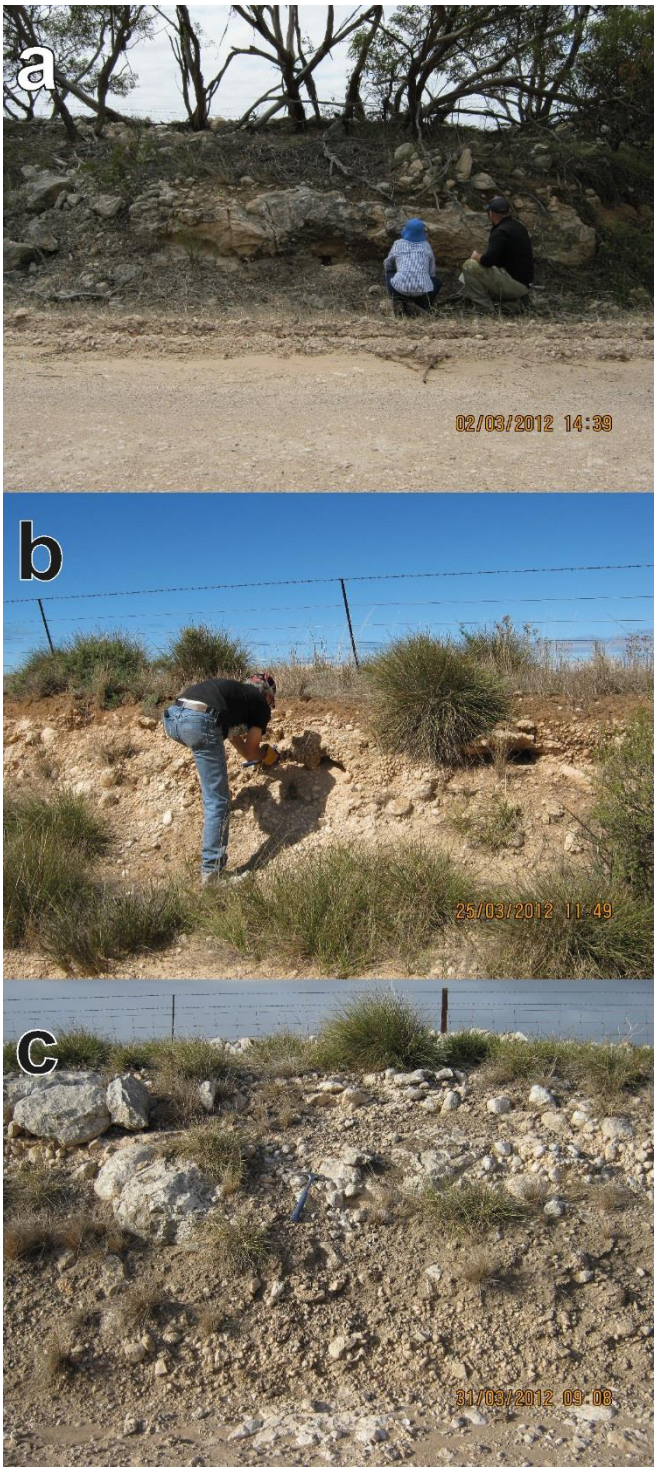

Figure 3.7. Field photographs of selected carbonate rock texture typically found across the Yorke Peninsula. a) Massive, well indurated, tabular carbonate with bouldery carbonate rocks both above and below. Thickness of hardpan carbonate shown is approximately 0.5m – 1 m. Observed along a roadside cutting; b) Laminar carbonate rock underlain by carbonate nodules and cobbles, exposed along a roadside cutting. This carbonate is found beneath a thin i.e. < 25cm layer of soil; c) Bouldery to cobble carbonate rock which is partly coalesced and forms a massive layer of carbonate. Below this carbonate are many nodules and cobbles of carbonate which occur in a calcareous silty matrix.

3.5.2 Whole-Rock Analysis

Geochemical data are shown in Figures 3.8, 3.9 and 3.10. Representative geochemical data are given in Table 3.1. Geochemical results for all samples and elements analysed are presented in Appendix 5.

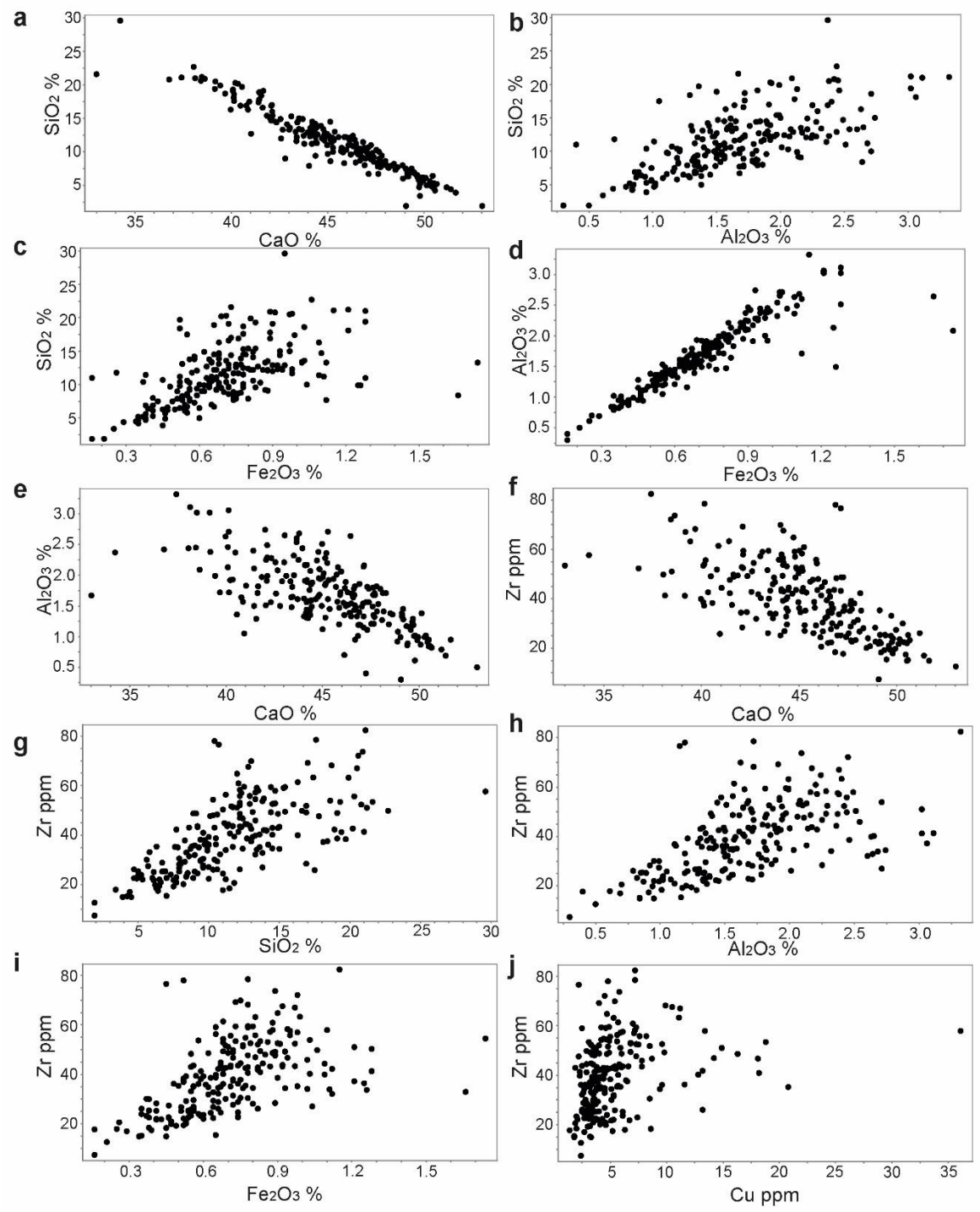

Figure 3.8. Whole-rock geochemical plots for selected major and trace elements for the regional Yorke Peninsula carbonate samples; a) SiO_2 versus CaO; b) SiO_2 versus Al_2O_3; c) SiO_2 versus Fe_2O_3; d) Al_2O_3 versus Fe_2O_3; e) Al_2O_3 versus CaO; f) Zr versus CaO; g) Zr versus SiO_2; h) Zr versus Al_2O_3; i) Zr versus Fe_2O_3 and j) Zr versus Cu.

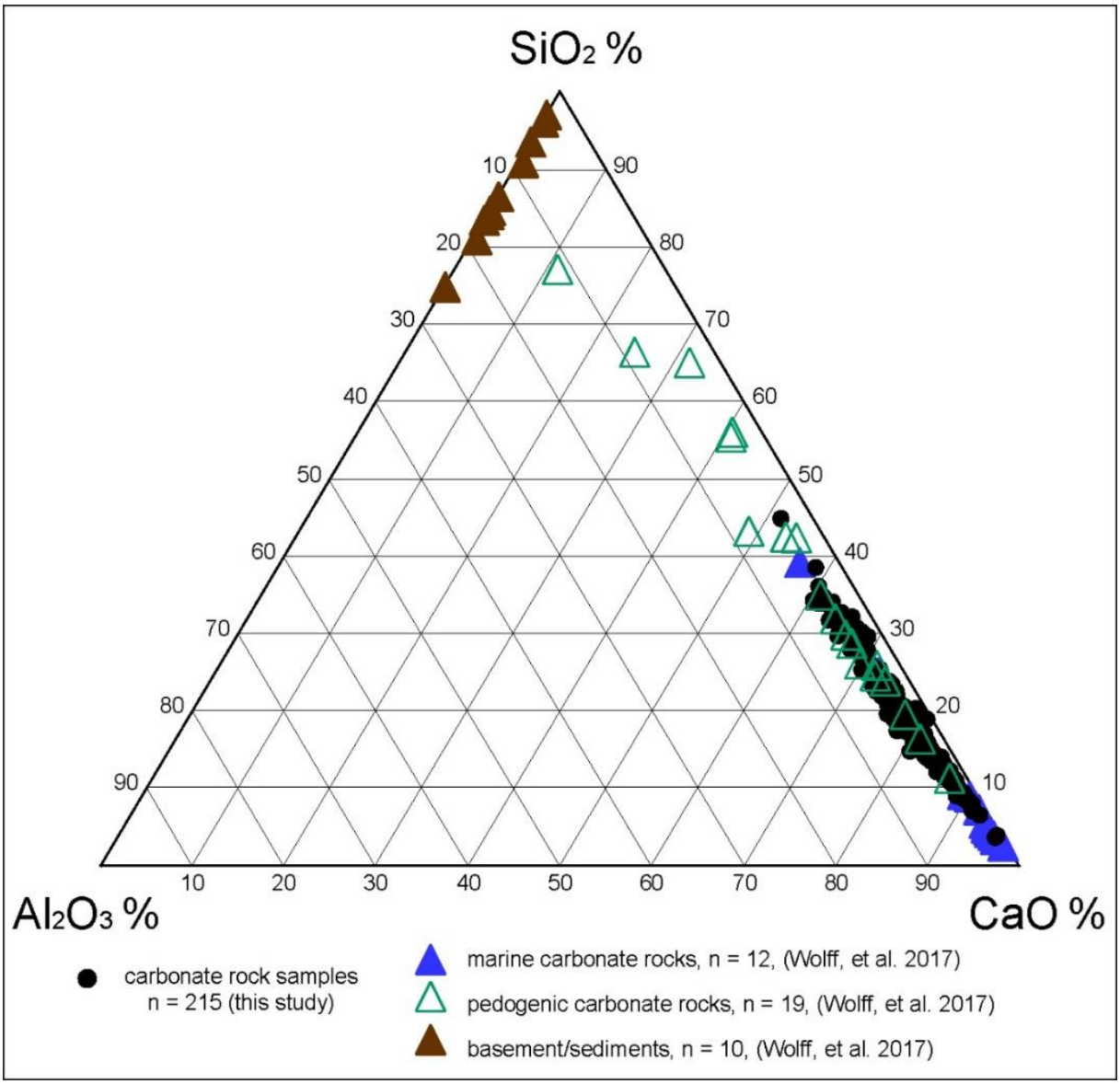

Figure 3.9. Ternary diagram showing composition of the carbonate rocks sampled from the Yorke Peninsula. We have used SiO_2 wt% to represent sand, CaO wt% to represent carbonate rocks and Al_2O_3 wt% to represent clay. For comparison, rocks from Wolff, et al., (2017), also from the Yorke Peninsula, are shown.

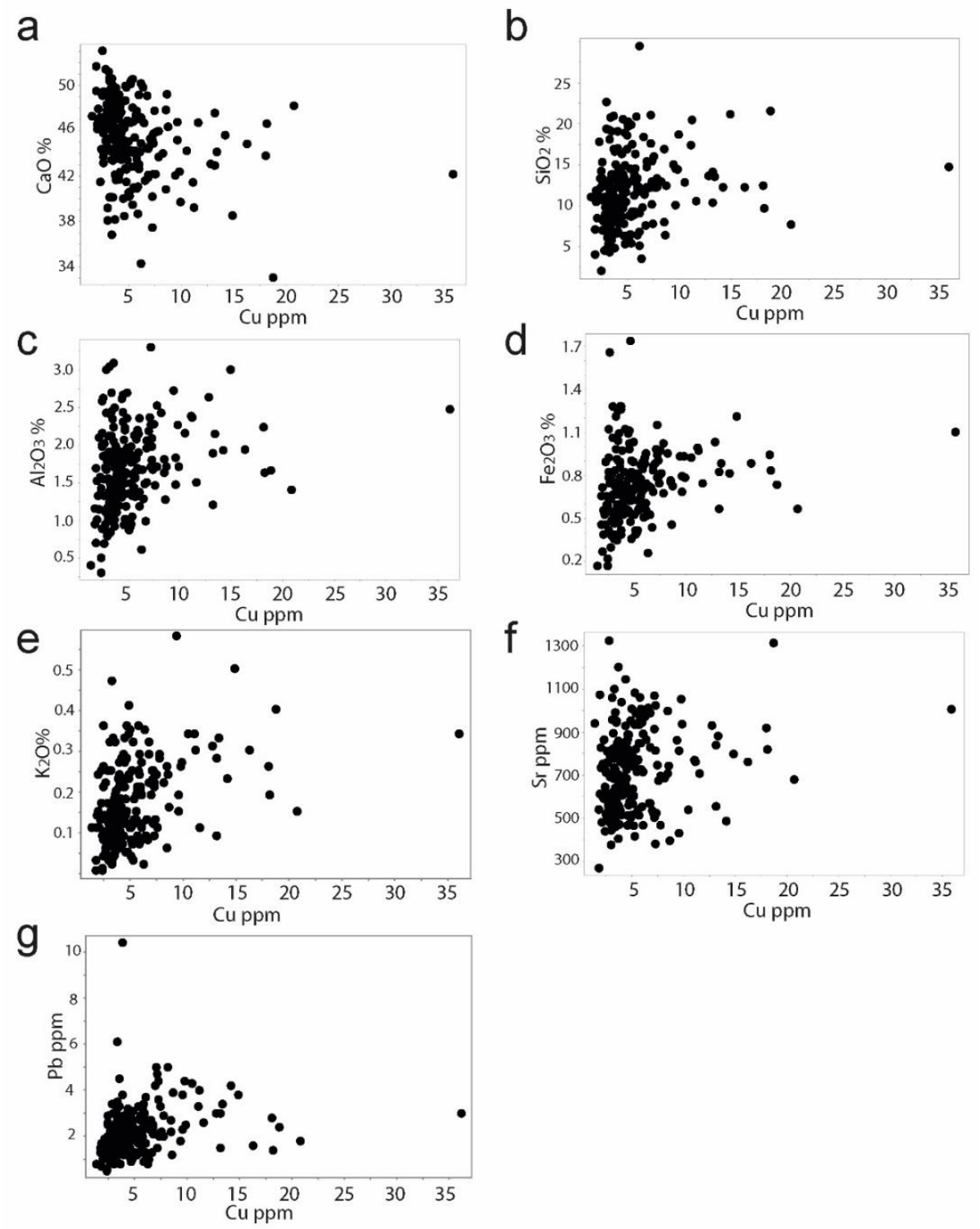

Figure 3.10. Whole-rock geochemical plots for Cu versus selected major and trace elements for the Yorke Peninsula carbonate samples. Cu ppm versus: a) CaO; b) SiO_2; c) Al_2O_3; d) Fe_2O_3; e) K_2O; f) Sr and g) Pb.

Table 3.1. Summary statistics of whole-rock geochemical data of the regional Yorke Peninsula carbonate samples for selected elements, calculated $CaCO_3$ content (from CaO concentration) and Ca/Sr ratios; and Ca and Sr seawater chemistry for the Ardrossan and Balgowan samples. All whole-rock data is presented in Appendix 4 5. Seawater chemistry is presented in Appendix 5 6.

whole rock chemistry	**Al_2O_3**	**SiO_2**	**Fe_2O_3**	**K_2O**	**MgO**	**CaO**	**$CaCO_3$**	**Sr**	**Ca/Sr**	**Zr**	**Pb**	**Cu**
Units	%	%	%	%	%	%	%	ppm	ratio	ppm	ppm	ppm
Detection limit	0.01	0.1	0.01	0.01	0.01	0.01		0.5		0.1	0.1	0.1
Analytical method	XRF	XRF	XRF	XRF	XRF	XRF	calculated from CaO %	ICP-MS	calculated ratio	ICP-MS	ICP-MS	ICP-MS
n	215	215	215	215	215	215	215	215	215	215	215	215
Minimum	0.30	1.90	0.20	0.01	0.67	33.01	55.12	267.00	179	7.40	0.50	1.40
Maximum	3.32	29.60	1.80	0.58	7.20	53.02	81.86	1331.60	1324	82.40	10.40	36.10
Mean	1.68	11.59	0.72	0.17	1.59	45.26	71.56	723.47	485	39.32	2.22	5.35
Standard deviation	0.54	4.50	0.24	0.10	0.84	3.40	4.53	191.92	156	14.76	1.09	3.82

seawater chemistry	**Ca**	**Sr**	**Ca/Sr**
Units	***mg/L***	***µg/L***	
Analytical method	ICP-OES	ICP-MS	calculated ratio
Ardrossan	459	9840	46
Balgowan	445	10090	44

3.5.2.1 Major element chemistry

Calcium oxide (CaO) concentration ranges from 33 wt% to 53 wt% (Fig. 3.8a). Assuming all calcium occurs as carbonate ($CaCO_3$), the concentration of calcium carbonate ranges from ~ 55 wt% to 80 wt% with an average of 72 wt% (Table 3.1). Silica (SiO_2) concentration ranges from 2 wt% to 30 wt% with the majority of samples containing ~ 20 wt% or less (Fig. 3.8a, and b). SiO_2, Al_2O_3 and Fe_2O_3 are positively correlated (Fig. 3.8b, c and d) and all three have negative correlations with CaO (Fig. 3.8a and e). Other major elements with concentrations at percent level include MgO which ranges from 0.6 wt% to 7 wt% (Table 3.1) and K_2O which ranges from 0.01 wt% to 0.6 wt% (Table 3.1). MgO and K_2O are negatively correlated to CaO, whilst K_2O and Al_2O_3 are positively correlated.

On a ternary diagram of SiO_2, Al_2O_3 and CaO the carbonate rocks sampled in this study form a linear trend between CaO and SiO_2 with minor Al_2O_3 (Fig. 3.9). Mineralogically, this is consistent with a mixture of materials dominated by carbonate (CaO) and quartz sand (SiO_2) with minor clay (Al_2O_3) content.

3.5.2.2 Trace element chemistry

Strontium (Sr) concentration ranges from 270ppm to 1330ppm (Fig. 3.10f). Lead (Pb) concentration ranges from 0.5ppm to 10.4ppm (Fig. 3.10g). Zirconium (Zr) concentration ranges from 7ppm to 83ppm (Fig. 3.8f, g, h, i, and j). Relationships of Zr to major elements are considered important to this study as they can be used to interpret potential sources of contamination and the origin of the Cu. Zirconium has a negative relationship to CaO (Fig. 3.8f) and a positive relationship with SiO_2, Al_2O_3 and Fe_2O_3 (Figs. 3.8g, h, and i, respectively).

Copper (Cu) concentration ranges from 1.4ppm to 36ppm, and has a mean concentration of 5.35ppm (Table 3.1; Figs 3.10 and 3.11). Copper concentrations are right skewed (Fig. 3.11a), with a log-normal distribution (Fig. 3.11b). The normal probability plot shows that there a number of samples that are significantly above the mean (Fig. 3.11c). Concentrations of Cu above the mean are spatially distributed around the Moonta mining region and east of Maitland (Fig 3.3). Relationships of Cu to major and trace elements are considered important to this study as they can be used to interpret potential sources of contamination and the origin of the Cu. Cu has no clear relationship with the major elements CaO, SiO_2, Al_2O_3, Fe_2O_3 or K_2O (Figs. 3.10a, b, c, d, and e, respectively) nor the trace elements Zr, Sr or Pb (Fig. 3.8j; Fig. 3.10f and g respectively).

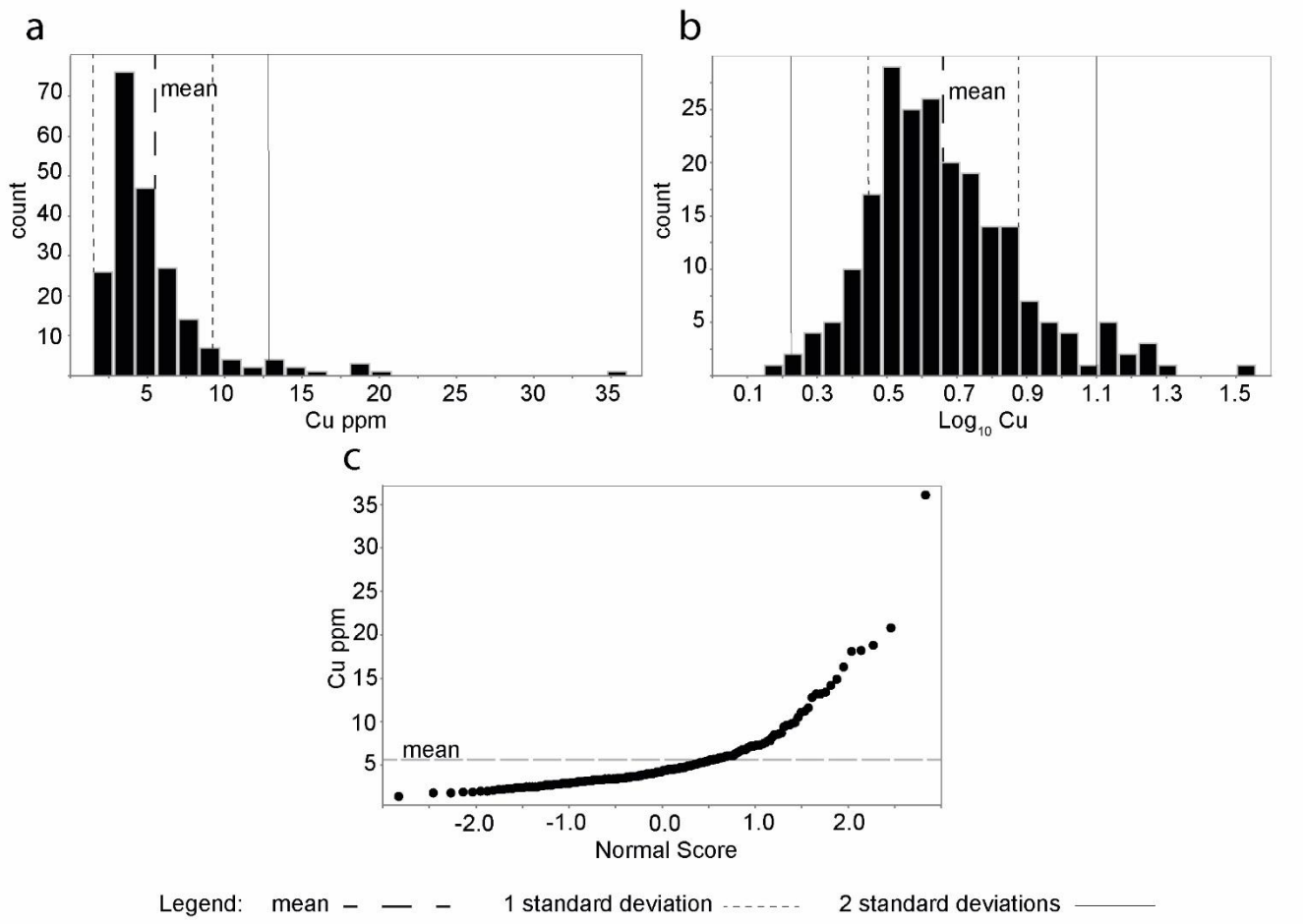

Figure 3.11. Histograms and probability plot for the regional Yorke Peninsula carbonate samples showing a) the concentration of Cu in all samples. The mean and 1 and 2 standard deviations above the mean are shown; b) the log_{10} Cu concentration of all samples. The mean and 1 and 2 standard deviations from the mean are shown; c) normal probability plot of Cu concentration for all samples. The mean is indicated by the dashed line.

3.5.2.3 Ca/Sr ratios

Ca/Sr ratios range from <200 to >1200 (Table 3.1). Eighty six percent (184 of 215) of the carbonate samples have Ca/Sr ratios <650 (Fig. 3.12), below the threshold value for pedogenic carbonates on the Yorke Peninsula proposed by Wolff et al., (2017). One

carbonate rock sample has a Ca/Sr ratio of >1260, above the threshold value for marine carbonates proposed by Wolff et al (2017) (Fig. 3.12). This sample is located east of Minlaton within 4 km of outcropping Cambrian limestones (Figs 3.4 & 3.6). Thirty samples have Ca/Sr ratios between 650 and 1260 (Fig. 3.12). Higher Cu concentrations (Cu > 10ppm) in carbonate rocks generally correlate to lower Ca/Sr ratios (Fig 3.13).

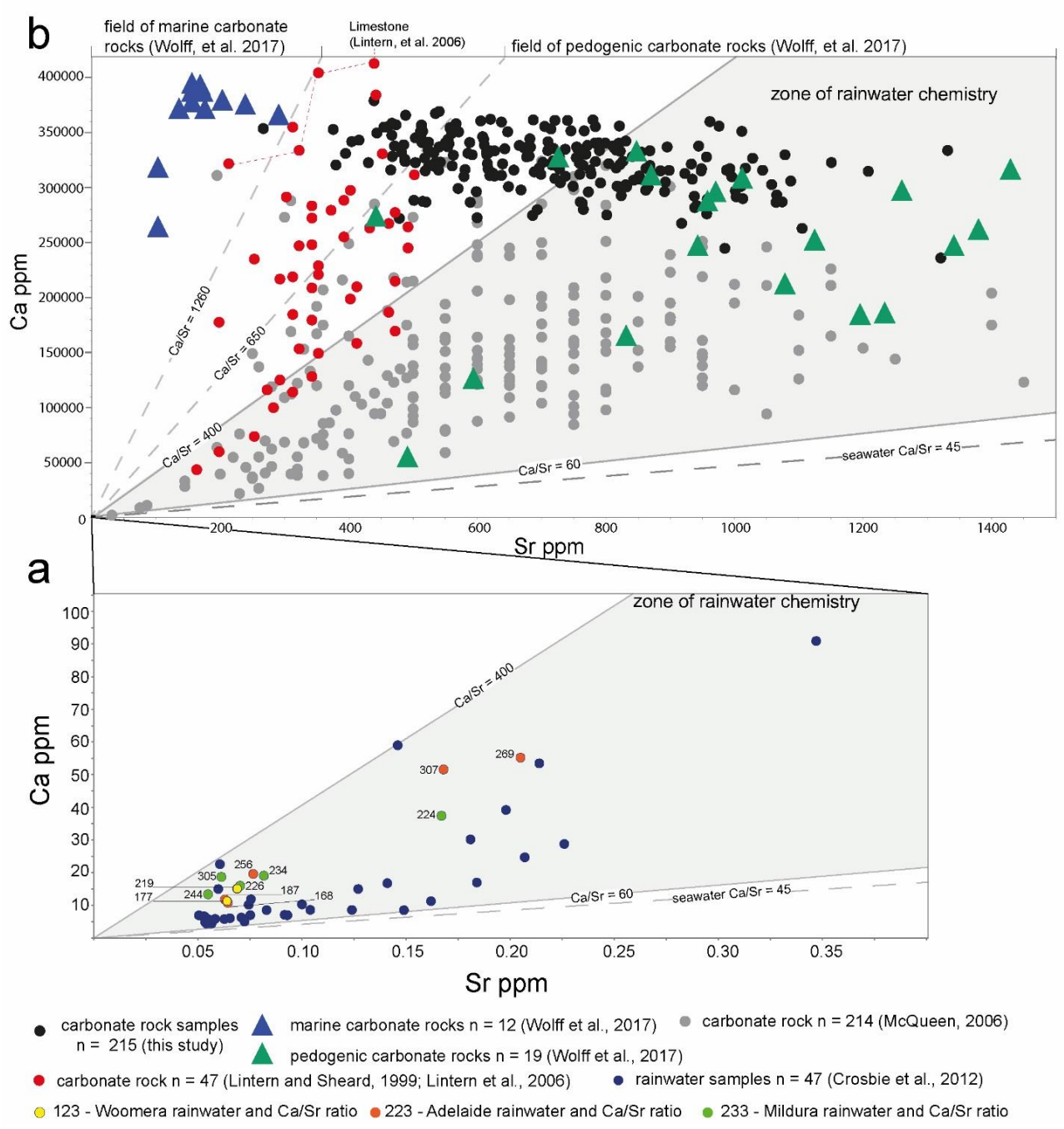

Figure 3.12. Plot of Ca versus Sr. a) Ca versus Sr concentrations for rainwater chemistry taken from Crosbie et al., (2012). Note difference in scale and placement into the larger Ca versus Sr diagram shown in (b). Rainwater samples for Woomera, Adelaide and Mildura are highlighted in yellow, orange and green respectively. Ca/Sr ratios calculated from rainwater chemistry reported in Crosbie et al., (2012) are labelled for highlighted

samples; b) Ca versus Sr diagram showing composition of carbonate samples from the regional Yorke Peninsula (black: this study), coastal Yorke Peninsula pedogenic carbonates (green: Wolff et al., 2017), coastal Yorke Peninsula marine carbonate rocks (blue: Wolff et al., 2017), the Cobar region (grey: McQueen, 2006) and central South Australia (red: Lintern and Sheard, 1999; Lintern et al., 2006). Samples described as limestone by Lintern et al., (2006) are also highlighted. Fields of Ca/Sr ratios defining pedogenic- and marine-derived carbonates (Wolff et al., 2017) are shown at the top of the diagram. The zone of rainwater chemistry (grey shade) is extrapolated from the seawater composition reported in Crosbie et al., (2012) and shown in (a). The seawater Ca/Sr ratio is calculated from the average of the two Yorke Peninsula samples collected in this study (Table 3.1).

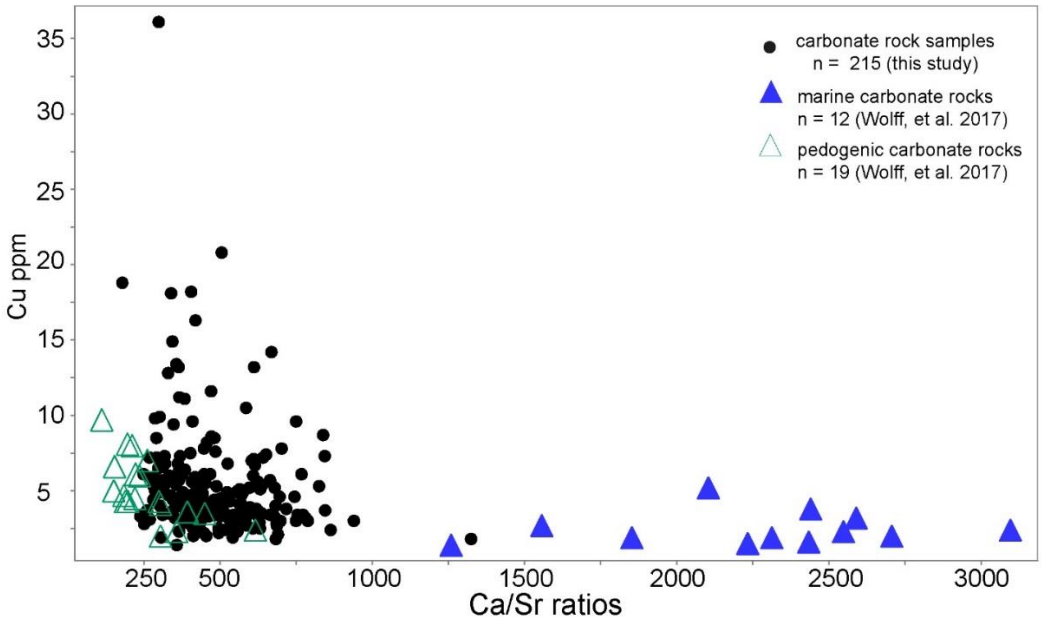

Figure 3.13. Plot of Ca/Sr ratios versus Cu for carbonate rock samples from this study. Coastal marine and pedogenic carbonates sampled by Wolff et al., (2017) are also shown.

3.5.2.4 Seawater Analysis

Results of seawater analysis are given in Table 3.1. The full dataset is given in Appendix 5. Seawater at Ardrossan contained Ca 459 mg/L and Sr 9840 µg/L. Seawater at Balgowan contained Ca 445 mg/L and Sr 10090 µg/L. The Ca/Sr ratio for seawater at the two locations is 46 and 44 respectively.

3.6 Discussion

3.6.1 Sources of Ca and Sr in pedogenic carbonate rocks on the Yorke Peninsula

Sources of Ca and Sr in pedogenic rocks on the Yorke Peninsula may include;1) in-situ weathering of underlying basement rocks or Cambrian to Cenozoic sedimentary rocks including marine limestone; 2) windblown dust from exposed basement rocks or marine limestones; 3) sea spray, and; 4) rainfall (e.g. Keeling and Hartley, 2005; Lintern, 2015; McQueen et al., 1999).

Hesse and McTainsh (2003) suggest that Ca-rich dust found across the Yorke Peninsula originates from Cenozoic continental shelf deposits along the western coastline of South Australia which have a Ca/Sr ratio of >1260 (e.g. Kyser et al., 1998; Quade et al., 1995, Wolff et al., 2017). This ratio is different to seawater Ca/Sr values (~45: Fig. 3.12) implying that the formation of the cold water Cenozoic carbonates of southern Australia involved significant fractionation of Ca and Sr from their seawater source. Rainwater has been proposed as a potential source of Ca and Sr in pedogenic carbonates in Australia (e.g. Hill et al., 1999; McQueen, 2006). Southern Australia receives its rainfall predominantly from evaporation from the Southern Ocean (e.g. Dart et al., 2007; Hill et al., 1999; Quade

et al., 1995; Van der Hoven and Quade, 2002). Calcium derived from the ocean is carried by aerosols and deposited by rainwater (Fantle and Tipper, 2014).

Airborne particles containing elements including Ca and Sr are preferentially removed from the atmosphere during rainfall and decrease relative to the volume of rain that falls (Shimamura et al., 2006). Oxygen isotope studies of rainwater have demonstrated that the removal of species from the atmosphere by rainwater is mass dependent, with heavier species being concentrated in the rain (e.g. Bowen and Wilkinson, 2002). As a result clouds tend to become more concentrated in lighter isotopes over time and as they move inland. Rainwater in coastal areas tends to contain higher concentrations of heavy isotopes. Whereas inland rain tends to be relatively enriched in lighter isotopes (Bowen and Wilkinson, 2002). This is known as the continental effect. Other fractionation effects may be related to altitude, latitude and seasonal variations (Cheng et al., 2010; Crosbie et al., 2012; Fantle and Tipper, 2014). Such mass dependent fractionation can be expected to effect the ratio of Ca to Sr in rainwater with the much heavier Sr being expected to be relatively enriched in coastal compared to inland rainwater. The sparse data available for Ca and Sr compositions of rainfall in Australia supports this (Crosbie et al., 2012).

Crosbie et al., (2012) measured rainwater chemistry from across Australia (Fig. 3.12a). Rainwater from high precipitation coastal regions have Ca/Sr ranging from ~60 to 100 (close to the seawater value of 45). Rainwater from Adelaide (the nearest rainwater collection site to the Yorke Peninsula; Fig. 3.2), Woomera and Mildura; Fig. 3.1) have Ca/Sr of approximately 150 to 300. The entire dataset collected by Crosbie et al., (2012)

forms an array that indicates the potential variation in Ca/Sr ratios, ranging from 60 to 400, within Australia (Fig. 3.12a).

The range of Ca/Sr ratios from the Yorke Peninsula carbonate dataset overlaps with the range of rainwater Ca/Sr reported by Crosbie et al., (2012). The whole dataset forms a roughly linear trend on the Ca versus Sr diagram that extends from the zone of 'rainwater' Ca/Sr (Fig. 3.12b) towards the composition of Cenozoic marine carbonate rocks from the Yorke Peninsula (>1260; Wolff et al., 2017). One data point from a carbonate sample from this study plots with the Yorke Peninsula marine carbonate rocks (Fig. 3.12b).

Cambrian to Pliocene-aged marine carbonates occur throughout the Yorke Peninsula and are exposed in the southern and eastern parts of the Peninsula (Fig. 3.4). Cenozoic marine carbonates are exposed over large areas of coastal southern Australia, including along the Great Australian Bight. It is possible that marine carbonates rocks could have contributed to the Ca and Sr budget of the pedogenic carbonates.

The trend from the zone of rainwater chemistry towards the composition of marine carbonate rocks suggests the Ca and Sr composition of the Yorke Peninsula regolith carbonates is a mixture of rainwater sources and marine carbonate sources, the latter either by the incorporation of wind-blown dust or from in-situ weathering of underlying marine carbonates. Simple two component mixing between a source with Ca/Sr consistent with Adelaide rainwater (~225) and a source consistent with Cenozoic Yorke Peninsula marine carbonates (~1400) suggests that the dominant source for most of the surface carbonates in this study was meteoric. Ca/Sr ratios of 650, at the higher Ca/Sr end of the array, correspond to a marine carbonate component of ~35%.The majority of

the regional Yorke Peninsula samples used in this study have Ca/Sr consistent with a dominant rainwater source. Eighty six percent (n=184; Fig. 3.12) of the samples have Ca/Sr < 650. A relatively small number of samples (n = 30) preserve Ca/Sr ratios between 650 and 1260 (Fig. 3.12) that are consistent with a marine component of >35%. Spatially, these intermediate composition samples are more frequent in the south of the study area, and are proximal to the exposures of marine carbonate (Figs 3.4 & 3.6). The Ca/Sr ratio > 1260 for one sample in the southern Yorke Peninsula (Fig. 3.6) suggests this sample is actually a marine carbonate, and may even be a weathered sample of the Cambrian limestone.

Based on the overlap in Ca/Sr ratios between the Yorke Peninsula samples and the zone of rainwater chemistry, the data are consistent with Ca and Sr from two sources:

1. A major component from rainwater, initially with seawater Ca/Sr and subjected to varying degrees of fractionation during precipitation which has produced Ca/Sr ratios ranging from <200 to ~400 (Fig. 3.12b).
2. A lesser component from marine carbonates, incorporated either from wind-blown dust or from in-situ marine carbonates.

The significant rainwater contribution to Ca and Sr in the Yorke Peninsula carbonates is consistent with the findings of Quade et al., (1995), who investigated sources of Ca in pedogenic carbonates from coastal South Australia and Victoria and concluded that the dominant source of Ca and Sr was from sea spray or rainwater. The systematically lower Ca/Sr of rainwater, compared to marine carbonates, translates into systematically lower Ca/Sr in pedogenic compared to marine carbonates. This is an effective discriminator of

carbonates formed by pedogenic processes and weathered marine carbonates, with the potential to be recognized in reconnaissance geochemical data (see also Wolff et al., 2017).

3.6.2 Influence on Ca and Sr concentrations in other carbonate rocks

The Ca and Sr concentrations within carbonate sample sets from Cobar, NSW (McQueen 2006) and proximal to the Challenger Au deposit and the transcontinental railway in central South Australia (Lintern and Sheard 1999, Lintern et al., 2006; Fig. 3.1) show similar influences of rainwater and/or marine carbonate chemistry. The spread in Ca concentrations in these datasets is indicative that the samples did not constitute pure carbonates, and it is likely there is some clastic input, however the Ca/Sr ratios show similar patterns to the data from the Yorke Peninsula (Fig 3.12b).

McQueen (2006) describes all samples from Cobar as regolith (pedogenic) carbonate, which is reflected in the low Ca/Sr ratios (< 650) preserved within most of the Cobar carbonate samples (Fig. 3.12b). Similar to the Yorke Peninsula samples, the Cobar carbonate samples show a spread in Ca/Sr ratios that range from within the zone of rainwater chemistry to chemistry similar to the Yorke Peninsula marine carbonates, with most samples plotting within the zone of rainwater chemistry (Fig. 3.12). This implies that the Ca and Sr concentrations for the majority of carbonate rocks in Cobar is influenced by rainwater composition. Crosbie et al., (2012) sampled rainwater from the township of Cobar, however Sr concentrations were below detection and could not be used. The nearest location with measurable amounts of both Ca and Sr was Mildura (Figs. 3.1 and 3.12a). The Ca/Sr ratios calculated for the Mildura rainwater are comparable to the Ca/Sr

ratios of the Cobar carbonate rocks, indicating the rainwater may have influenced the Ca and Sr concentrations of the majority of the Cobar carbonate rocks (Fig. 3.12). Almost all of the remaining samples that fall outside of the zone of rainwater chemistry plot within the intermediate region between rainwater chemistry and Yorke Peninsula marine carbonates, implying a mixed source. One samples plots with the Yorke Peninsula marine carbonates (Fig. 3.12b). Fossil-rich marine carbonates have been described in the Cobar area, and belong to the Ordovician to Devonian Girilambone Group (e.g. Burton, 2015; Glen, 1991; Iwata et al., 1995). The source of the high Ca/Sr ratio due to proximity to marine limestone can only be speculated due to having no context of the sample within the local geological stratigraphy. McQueen et al., (1999) suggested that Ca and Sr contributions to carbonate rocks in the region are primarily from aeolian dust and/or rain.

The carbonate rocks from central South Australia (Lintern and Sheard 1999, Lintern et al., 2006) display a much tighter range in Sr concentrations, with the majority of the samples preserving Ca/Sr ratios indicative of pedogenic (Ca/Sr <650) origin or being within the intermediate zone between pedogenic and marine origin (650 <Ca/Sr <1260) (Fig. 3.12b). A small number of samples (n=12) plot within the zone of rainwater chemistry (Fig. 3.12b). The closest rainwater sample point to the central South Australian carbonate samples is Woomera (Crosbie et al., 2012; Fig. 3.1). The Ca and Sr composition of the Woomera rainwater is in the middle of the range of rainwater chemistry determined by Crosbie et al., (2012), with Ca/Sr ratios being 177 and 219 (Fig. 3.12a). Some of the central South Australia carbonate samples(Lintern and Sheard 1999, Lintern et al., 2006) also have Ca and Sr compositions in the middle of the range of the zone of rainwater chemistry, suggesting rainwater may have influenced the concentrations of these

elements in some samples (Fig. 3.12b). However, the variation in Ca/Sr ratios between the rainwater and the central South Australian carbonates might be a function of the amount of precipitation (i.e. 4 mm for both data points) or the rainwater sample being taken from a geographically distant area to the central South Australia carbonate sampling location (Fig. 3.1). The majority of the central South Australian carbonate samples plot in the intermediate area between the zone of rainwater chemistry and the Yorke Peninsula marine carbonates (Fig. 3.12b). Lintern et al., (2006) describes three of the samples that fall within the mixed and marine carbonate zones as being limestone or preserving visible marine fossils (Fig. 3.12b). The central South Australian carbonate sample that plots within the field of marine carbonates (Fig. 3.12b) is also described as a limestone (Lintern et al., 2006). In general, the Ca and Sr content within the central South Australian carbonate samples shows a spread of Ca/Sr chemistry between that of rainwater chemistry and of local marine carbonates, indicating a potential mixed influence on Ca and Sr concentrations from both rainwater and the substrate.

Overall, the Ca and Sr concentrations in the Cobar and central South Australian carbonate samples shows variation similar to that observed in the Yorke Peninsula carbonate samples. It is acknowledged that other potential influences on Ca and Sr concentrations such as dust have not been considered in interpreting the potential influences on Ca and Sr concentrations in the Cobar or central South Australian carbonate samples. However, the data does indicate that a mixture of rainwater and/or marine carbonate rocks may have influenced the Ca and Sr chemistry of regolith carbonate rocks from a number of geographically disparate regions. This shows that influences on Ca and Sr concentrations within carbonates need to be considered when

using these elements to discriminate between pedogenic and marine origins for carbonate rocks using criteria such as that described in Wolff et al., (2017).

3.6.3 Sources of Cu in pedogenic carbonate rocks on Yorke Peninsula

The potential for pedogenic carbonate rocks to preserve detectable concentrations of pathfinder elements that may be indicative of buried mineralization has been recognized by a number of authors (e.g. Poustie & Abbot 2006; Chen et al., 2002; Lintern et al., 2012; van der Hoek et al., 2012). Of direct relevance to this study, Wolff et al., (2017) demonstrated that Cu concentrations are higher within pedogenic carbonates across the Yorke Peninsula. Comparison of Cu concentrations with Ca/Sr ratios for samples from this study (Fig. 3.13) shows that samples with higher Cu concentrations are mostly preserved in samples that have characteristically pedogenic Ca/Sr ratios (i.e. < 650) (Fig 3.13). Following Wolff et al., (2017) the pedogenic carbonates should be a suitable sample medium for mineral exploration. However, the potential sources of Cu still need to be considered and include windblown contamination and contributions from underlying (potentially mineralized) rocks.

3.6.3.1 Windblown contamination

Dust contaminants need to be considered as airborne particles may be enriched in Cu and blown onto the carbonate rocks from nearby mining. The influences of aeolian contaminants on the geochemistry of the Yorke Peninsula carbonate rocks data has previously been assessed here as a potential for Ca and Sr contribution. Positive relationships between Al_2O_3, SiO_2 and Fe_2O_3 that may suggest clay dust contamination

(Figs. 3.8b, c and d), and Zr versus SiO_2 and Al_2O_3 that may indicate windblown sand and soil (Fitzpatrick and Chittleborough, 2002; Kabata-Pendias and Pendias, 2001), (Fig. 3.8g and h) have been established. However, apart from a weak relationship of Cu to Al_2O_3, there is no relationship between Cu and any of the indicator elements of dust or other windblown contamination. Therefore, windblown contamination from clay dust, soil or sands is not considered as a source of Cu in the Yorke Peninsula carbonates.

Lead has also been suggested to be an indicator of dust contamination originating from Cu mining (e.g. Balabanova et al., 2014; Mighall et al., 2002). In this case, contamination would be manifest as a positive relationship between Pb and Cu. Comparison of Pb and Cu concentrations for the Yorke Peninsula samples shows no correlation (Fig. 3.10h), therefore contamination from dust originating from Cu mining is not considered to have influenced the Cu concentration within the samples used in this study.

3.6.3.2 Proximity to known Cu occurrence

Previous studies relating to geochemistry across the Yorke Peninsula demonstrate that Cu is mobile within the transported sediments and regolith materials overlying Cu-rich basement rocks (e.g. Dietman, 2009; Fabris, 2010; Keeling and Hartley, 2005). Dietman (2009) demonstrated that elevated Cu is preserved in carbonate rocks (e.g. 9–11ppm) and soils (e.g. 14–20ppm) as well as vegetation (e.g. 1.3–6.2ppm) around the Hillside Mine site (Fig. 3.4). Likewise, the Moonta mining region (Fig. 3.4) is known to contain elevated Cu in a variety of sample media e.g. clays and transported sediments (e.g. > 80ppm), carbonate rocks (e.g. < 25–30ppm) and vegetation (e.g. 6–10ppm), compared to regional background levels (e.g. Hartley, 2000; Keeling and Hartley, 2005; Wolff et al.,

2017; 2018). No regional survey had been undertaken that uses carbonate rocks to test its effectiveness as an exploration sampling medium across the entire Yorke Peninsula.

The carbonate rocks from this study that contain Cu at concentrations that are 2 and 3+ standard deviations above the mean value (12.99-16.80ppm Cu and >16.81ppm Cu respectively, Table 3.1) are spatially restricted to the Cu mining region of Moonta and Wallaroo and east of Maitland (Fig. 3.4). The relationship of elevated Cu and the spatial distribution with known Cu occurrences indicates that elevated Cu concentration within pedogenic carbonates can be used as an indicator towards Cu minerlisation on the Yorke Peninsula, and possibly elsewhere.

The relationship between elevated Cu in carbonate rocks and proximity to known mineralisation on a regional scale is illustrated by comparing the population statistics of samples within 3km of known Cu occurrences to those that are > 3km from known occurrences (Fig. 3.14). The carbonate samples within 3 km of a known Cu occurrence have a higher mean (e.g. Cu 7.02ppm) and a standard deviation of Cu 5.4ppm with a longer tail skewed to the right with a broader spread towards higher Cu concentrations (~13– 36ppm) compared with those that are further than 3km away (mean 4.8ppm indicated by black marker) and standard deviation (2.9ppm), (Fig. 3.14a). The higher mean and standard deviation in the group of samples ≤ 3km of known Cu occurrence could be influenced by two samples with higher Cu concentrations of ~20 and 36ppm. These two samples are located less than 500m, and are the closest of any sample collected in this study, to a known Cu occurrence (Fig. 3.4).

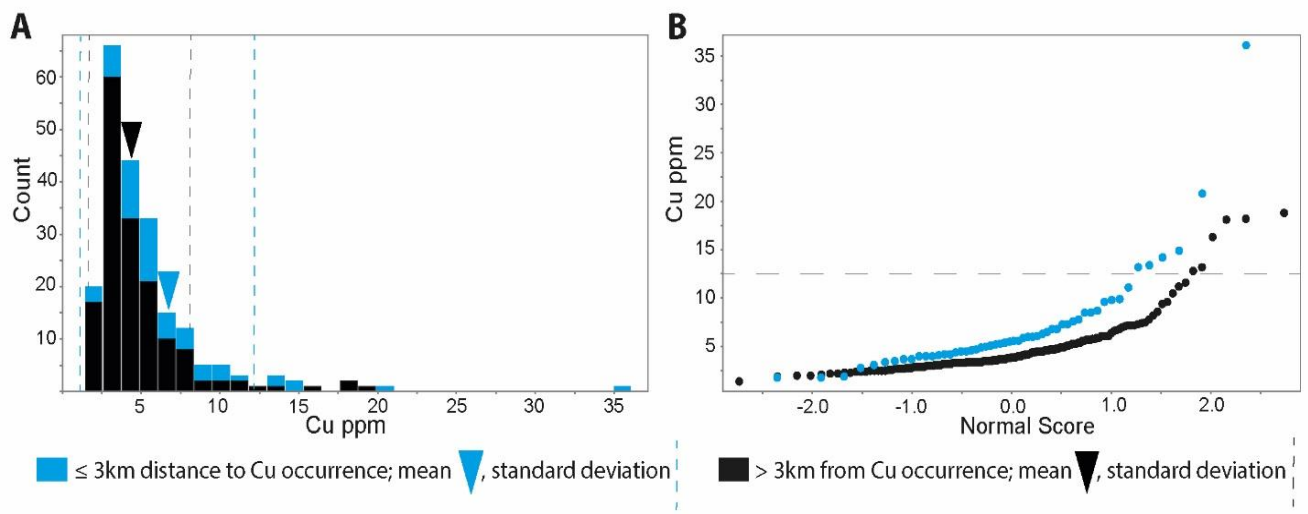

Figure 3.14. a) Histogram; and b) probability plot of Cu concentrations within the regional Yorke Peninsula samples coloured by proximity to known Cu occurrence. Samples within 3 km of a Cu occurrence are shown in blue, samples greater than 3 km from a known Cu occurrence are shown in black. The mean Cu concentrations for both groups are indicated by the triangles. The standard deviations for both groups are indicated by dashed lines of corresponding colour. The grey dashed line in b) identifies a breakpoint in both populations which coincides with 2 or more standard deviations from the mean.

It is noted that the Cu concentrations presented in this study are mostly less than those reported for carbonate Hartley (2000), which preserve > 30ppm Cu. This is due to the samples collected by Hartley (2000) being taken from vertical profile sampling of mine pit-walls directly adjacent or overlying mineralisation, at Moonta, whereas the samples in this study were taken as regional grab samples. Keeling and Hartley (2005), whom go on to further describe the regolith expression at Moonta, reported lateral dispersion of Cu within carbonate rocks approximately 100m distance from known Cu lodes within the mine pit. This implies that the potential for pedogenic carbonate rocks to concentrate Cu is considerably greater than what is reported from the regional samples used in this study,

and that higher Cu concentrations may be preserved proximal (e.g. within hundred(s) of meters) to mineralization.

The Yorke Peninsula is underlain by Cambrian and Cenozoic sediments of varying thickness (e.g. up to 70m or more; Fabris, 2010) that may form a barrier to Cu dispersion into the overlying pedogenic carbonates (e.g. Keeling and Hartley, 2005; Wolff et al., 2017). The preservation of elevated Cu concentrations in a number of samples indicates that the dispersion barriers may be laterally discontinuous (Fig. 3.4), or that high Cu concentrations may have formed in more than those carbonate rocks preserved if the barriers were less extensive. Overcoming the interaction between Cu dispersion and the potential for pedogenic carbonates to preserve elevated Cu concentrations could be achieved by collecting a greater number of samples (i.e. using a < 1 km spacing or < 10 km between traverses).

3.6.4 Implications for exploration

The widespread occurrence of carbonate rocks and their potential to incorporate elements such as Cu from the substrate makes them an ideal sampling tool for mineral exploration. However, a number of considerations should be taken into account when identifying and sampling pedogenic carbonate rocks for mineral exploration, including:

- Identification of potential sources of Ca and Sr such as local bedrock comprising Ca-rich lithology (e.g. marine carbonates), potential for inputs from dust and rain and proximity to the coastline to ensure that Ca/Sr ratios are truly reflective of the rock origin;

- Determination of whether the carbonate rocks contain a Ca/Sr ratio consistent with pedogenic carbonate rocks i.e. <650. Recognize also that there may be an intermediate of Ca/Sr values (650<Ca/Sr<1260) and investigate the geology of the region to understand the potential sample origin and whether other factors/contaminants have influenced the preserved Ca/Sr ratios;
- Identify potential sources that may contaminate the concentration of elements of interest (e.g. Cu in this study) within the carbonate rocks that occur throughout the region. This may include windblown mining dust or other dust from land use such as farming;
- Sample at a density that produces robust statistics to identify background levels versus higher concentrations, and that accounts for any potential barriers in element dispersion;
- Understand the regolith landscape processes in the region to determine whether Cu concentrations may reflect buried mineralization or are the effect of physical and/or chemical element transport.

3.7 Conclusion

A regional carbonate sampling survey across the Yorke Peninsula has shown that the majority of carbonate material at the surface has a pedogenic origin (Ca/Sr ratios < 650), with lesser occurrences of carbonate preserving Ca/Sr ratios intermediate between pedogenic- and marine-origin. One sample preserves a Ca/Sr ratio indicative of a marine-origin (Ca/Sr >1260). The Ca and Sr concentration within the carbonate rocks is influenced by the chemistry of rainwater and underlying marine carbonate. These

influences need to be considered when using Ca and Sr to discriminate between pedogenic and marine origins for carbonate rocks.

Pedogenic carbonate rocks throughout the Yorke Peninsula are shown to accumulate Cu in areas of known Cu mineralization. Pedogenic carbonate rocks from this study contain background Cu concentrations of ~5.3ppm and elevated Cu concentrations above 12.99ppm and up to 36ppm. Pedogenic carbonate rocks preserve high Cu in concentrations coincident with areas of current or historic Cu mining. Copper found in pedogenic carbonate rocks is determined to be related to dispersion from underlying Cu-rich basement and not from windblown contamination. This study has shown that pedogenic rocks from this region can be used for exploration purpose but some consideration needs to be taken as dilution by meteoric Ca and Sr can occur and may be more apparent when Ca/Sr ratios are >650.

Chapter 4: Biogeochemical expression of buried iron-oxide-copper-gold (IOCG) mineral systems in mallee eucalypts on the Yorke Peninsula, southern Olympic Domain; South Australia.

Foreword

This chapter presents biogeochemical data of foliage from locally occurring *Eucalyptus* across the Yorke Peninsula in South Australia in order to evaluate the potential of using this type of sampling medium in the exploration for buried Cu mineralisation. Samples were collected by during a series of field trips in 2012. Samples were identified using a software program called Eucalypts of Australia: Euclid (Slee et al., 2006). Samples were sorted labelled and dried with the assistance of Randall Wolff. Biogeochemistry of all samples was undertaken by Acme Laboratories (now Bureau Veritas), Vancouver Canada.

Statement of Authorship

Title of Paper	Biogeochemical expression of buried iron-oxide-copper-gold (IOCG) mineral systems in mallee eucalypts on the Yorke Peninsula, southern Olympic Domain; South Australia
Publication Status	☑ Published ☐ Accepted for Publication ☐ Submitted for Publication ☐ Unpublished and Unsubmitted work written in manuscript style
Publication Details	Journal of Geochemical Exploration Volume 185 (2018) pages 139–152 https://doi.org/10.1016/j.gexplo.2017.11.017 Received 20 April 2017; Received in revised form 30 October 2017; Accepted 21 November 2017 Available online 27 November 2017 0375-6742/ © 2017 Elsevier B.V. All rights reserved.

Principal Author

Name of Principal Author (Candidate)	Keryn Wolff
Contribution to the Paper	Collection and preparation of samples. Identifying individual species of sample collected. Sorting drying packaging and labelling for delivery to laboratory for geochemical analysis. Data entry and format of results suitable to use in relevant geochemical, statistical and GIS software programs. Compiling all illustrations used in the published article and making new ones where needed. Drafting the initial document. Correcting to Co-authors and reviewers comments. Primary contact throughout the publications process.
Overall percentage (%)	90
Certification:	This paper reports on original research I conducted during the period of my Higher Degree by Research candidature and is not subject to any obligations or contractual agreements with a third party that would constrain its inclusion in this thesis. I am the primary author of this paper.
Signature	Date 12/09/2018

Co-Author Contributions

By signing the Statement of Authorship, each author certifies that:

i. the candidate's stated contribution to the publication is accurate (as detailed above);

ii. permission is granted for the candidate in include the publication in the thesis; and

iii. the sum of all co-author contributions is equal to 100% less the candidate's stated contribution.

Name of Co-Author	Steve Hill
Contribution to the Paper	Review comments and editing suggestions
Signature	Date 9/4/2018

Name of Co-Author	Caroline Tiddy
Contribution to the Paper	Review comments and editing suggestions
Signature	Date 12/09/2018

Please cut and paste additional co-author panels here as required.

Name of Co-Author	David Giles
Contribution to the Paper	Review comments and editing suggestions
Signature	Date 12/04/2018

Name of Co-Author	Ronald Smernik
Contribution to the Paper	Review comments and editing suggestions
Signature	Date 7/4/2018

Biogeochemical expression of buried iron-oxide-copper-gold (IOCG) mineral systems in mallee eucalypts on the Yorke Peninsula, southern Olympic Domain; South Australia.

Keryn Wolff, Steve Hill, Caroline Tiddy, Dave Giles, Ron Smernik.

As published by Journal of Geochemical Exploration 2018

(Appendix 7)

(Journal of Geochemical Exploration 185 (2018) 139–152)

https://doi.org/10.1016/j.gexplo.2017.11.017

4.1 Abstract

We report on the results of a regional scale biogeochemical sampling program conducted on the Yorke Peninsula, South Australia, utilising four locally occurring *Eucalyptus* species with mallee-form. Our purpose is to determine if there is an empirical relationship between Cu accumulation in the mallee leaves and elevated Cu in the underlying basement rocks– such that the mallee species might be a useful biogeochemical exploration tool in this area. The basement rocks of the Yorke Peninsula are prospective for iron oxide-copper-gold (IOCG) mineralisation but are mantled by Cambrian to Quaternary sedimentary rocks of variable thickness that inhibit traditional surface geochemical exploration techniques. There is no evidence to link Cu concentrations to dust contamination or fertiliser usage. Leaves of the four mallee species have comparable log normal population distributions of Cu, with a range between 1.6ppm and 10ppm. Higher concentrations of Cu (>6ppm) occur more commonly within 3km of known Cu occurrences. These results suggest that all four mallee species have the ability to concentrate higher amounts of Cu in their leaves when the underlying/ local geology also contains elevated Cu. The results suggest that biogeochemical sampling of multiple mallee species over large regions could be a useful exploration technique in covered areas of southern Australia where mallee species are widespread and densely populated.

4.2 Introduction

Australia has vast areas of cover sediments ranging in depth from a few metres to a few hundred metres (Anand, 2005), which are an impediment to mineral exploration (e.g. Fabris, 2010; Hillis et al., 2014; Noble, 2012; Reid et al., 2008). Exploring these areas can be costly and time consuming when using traditional methods such as drilling (e.g. Hillis et al., 2014; Hulme and Hill, 2003; Reid and Hill, 2010). The use of biogeochemistry for identifying mineralisation through variable depths of cover is becoming well established and is a non-invasive, efficient and cost effective exploration method (e.g. Hulme and Hill, 2003; Lintern et al., 2013; Reid and Hill, 2010).

Globally, biogeochemistry has been used for detection of a wide range of mineral commodities including Au, Pt, Pd, base metals and rare earth elements (e.g. Cohen et al., 1987; Dunn, 1986, 2007; Kovalevsky, 1987; Lintern et al., 2013; Närhi et al., 2014; Rencz and Watson, 1989). In Australia, studies have also shown that various plant species have the ability to concentrate elements of interest (e.g. Au, Cu, Zn, As, Cr and Pb). These species include pine and native cypress (*Pinus radiata* and *Callitris sp.*: Arne et al., 1999; Ashley and Wolfenden, 2005; Cohen et al., 2005), gum trees (*Eucalyptus* including *camaldulensis*, *brevifolia*, *pruinosa* and *concinna*: Hulme and Hill, 2003; Lintern et al., 2013; Reid and Hill, 2010; van der Hoek et al., 2012), 'mulga' wattle (*Acacia aneura*: Lintern et al., 2013), saltbush (*Atriplex*: Brown and Hill, 2005), spinifex (*Triodia pungens*: Reid and Hill, 2010; Reid and Hill, 2013) and bluebush (*Maireana*: Lintern et al., 1997). Thus far, biogeochemistry in the Australian context has most commonly been restricted to local-scale 'orientation' sampling across areas of known mineralisation or less often,

laboratory experimentation (e.g. Lintern et al., 2013). Sampling programs of regional-scale are less common (although see Brown and Hill, 2005; Mitchell et al., 2015) but are an important component of the research agenda as they provide an unbiased, empirical measure of the entire sample population, which in turn provides the opportunity to differentiate ‘anomalous’ results from ‘background’.

The success of biogeochemistry as an indicator of mineralisation relies on the ability of the plant to transfer ore or pathfinder elements from depth through the roots upwards to the bark, twigs, fruit and leaves, which can then be sampled and analysed using similar methods as for rock or soils (e.g. Närhi et al., 2014; Reid and Hill, 2010). In order to penetrate thick cover and interact with a large volume of regolith and basement materials it is desirable that the target species for biogeochemical sampling have deep and/or laterally extensive root systems. Eucalypts are particularly suitable as they typically form extensive root systems that penetrate deeply into the cover sediments (e.g.Fensham and Fairfax, 2007; Handreck, 1997; Hulme and Hill, 2003; Lintern et al., 2013; Lintern et al., 1997; Wrigley and Fagg, 2010), (Figure 4.1). Hulme and Hill, (2003) reported that *Eucalyptus camaldulensis* has root systems that can occupy soil volumes > 4000 m^3. Other eucalypts such as *Eucalyptus marginata* have roots that may penetrate as deeply as 40m (Wrigley and Fagg, 2010).

Fig. 4.1. Photo image of Eucalyptus that grow throughout the Yorke Peninsula. This photo shows the deep rooted nature of these genera. This species is an E. gracilis which also clearly displays the mallee-form with a visible lignotuber at the base of the trunk. Person pictured for scale is approximately 1.5m tall.

Eucalyptus is the most widespread native genus throughout Australia (Brooker et al., 2002; Hulme and Hill, 2003). There are at least 783 *Eucalyptus* species of which 60% may have a ‘mallee’ growth habit under appropriate conditions (e.g. Slee et al., 2006). Mallee describes a growth habit where multiple trunks emerge from a lignotuber at, or just below ground level and serve the purpose to re-sprout from dormant buds following fire or other disturbance (e.g. Brooker et al., 2002; Butt, 2005; Slee et al., 2006). Eucalypts tend to adopt the mallee form in drier climates and are common across arid southern Australia (e.g. Australian Native Vegetation Assessment, 2001, Figure 4.2). Approximately 96 species of *Eucalyptus* are found in South Australia and 75 of those are considered mallee (Slee et al., 2006). Hybridisation can be characteristic of mallee species and this complicates identification (Brooker et al., 2002).

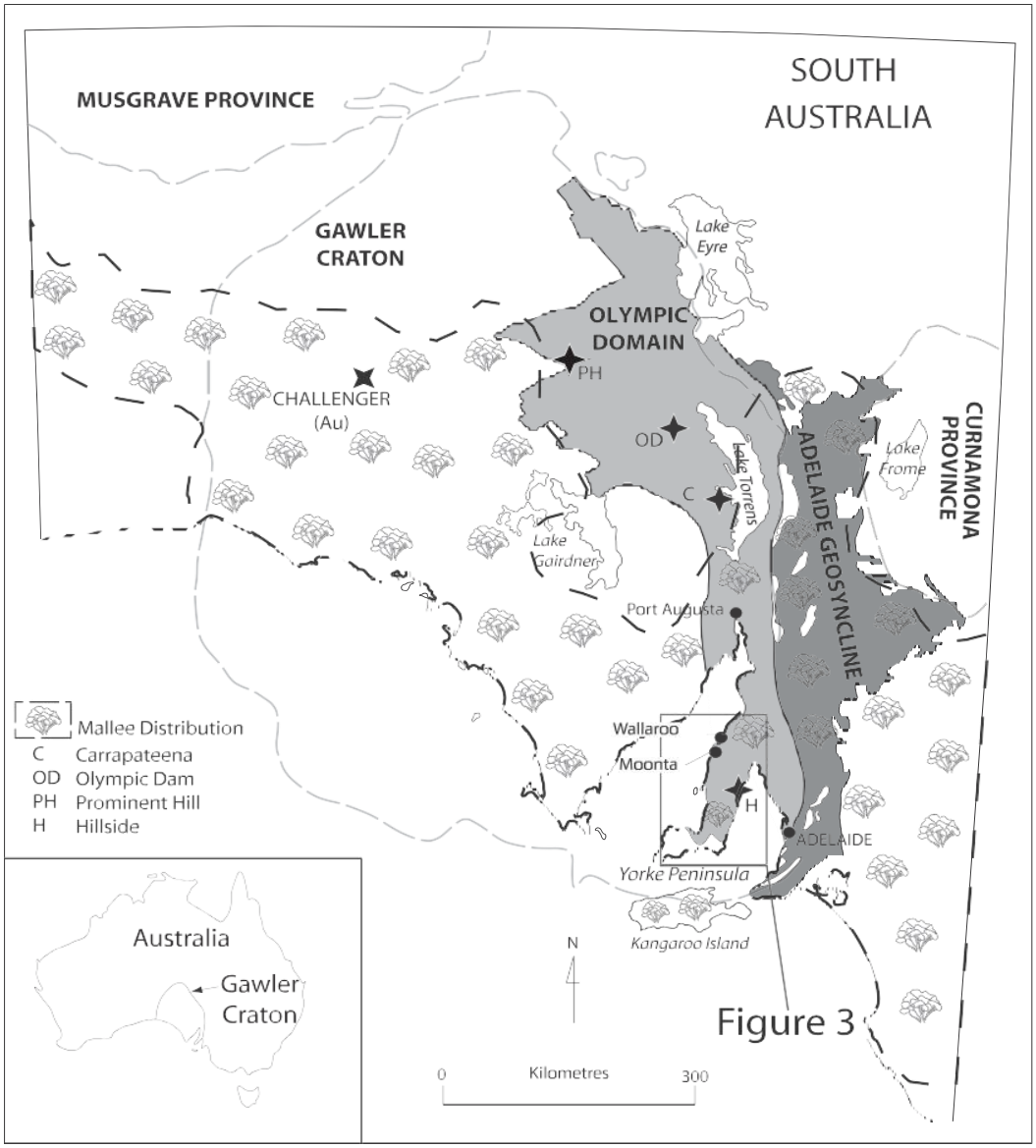

Fig. 4.2. Simplified geological map of South Australia showing study location within the Olympic Domain of the Gawler Craton (modified after Conor et al., 2010). Also shown is mallee distribution across South Australia (modified after Australian Native Vegetation Assessment, 2001). Inset: Australia showing location of the Gawler Craton.

The ability of eucalypts to concentrate trace metals within their organs (e.g. leaves, twigs, bark and fruit) has been established in several studies (e.g. Dunn, 2007; Butt et al., 2005a and references therein). Consequently *Eucalyptus* biogeochemistry has the potential to identify areas of anomalous trace metal concentrations within the regolith or underlying basement (e.g. Butt et al.,

2005a; Dunn, 2007; Hulme and Hill, 2003; Reid and Hill, 2010; van der Hoek et al., 2012). There are no published studies investigating the ability of mallee-eucalypts to incorporate Cu for the purpose of mineral exploration.

The basement rocks of the Yorke Peninsula region of South Australia are considered highly prospective for iron oxide-copper-gold mineralisation (IOCG) (e.g. Conor et al., 2010). The region has less than 5% exposed basement rocks, the remainder being covered by a diverse range of sediments (e.g. Cowley et al., 2003; Wolff et al., 2017; Zang et al., 2006). These cover sediments form a barrier to geochemical exploration (e.g. Fabris, 2010; Mokhtari et al., 2009; Salama et al., 2016). Thirteen mallee *Eucalyptus* species are distributed throughout this region (Brooker et al., 2002), and some trees are proximal to known Cu mineralisation (Figure 4.3).

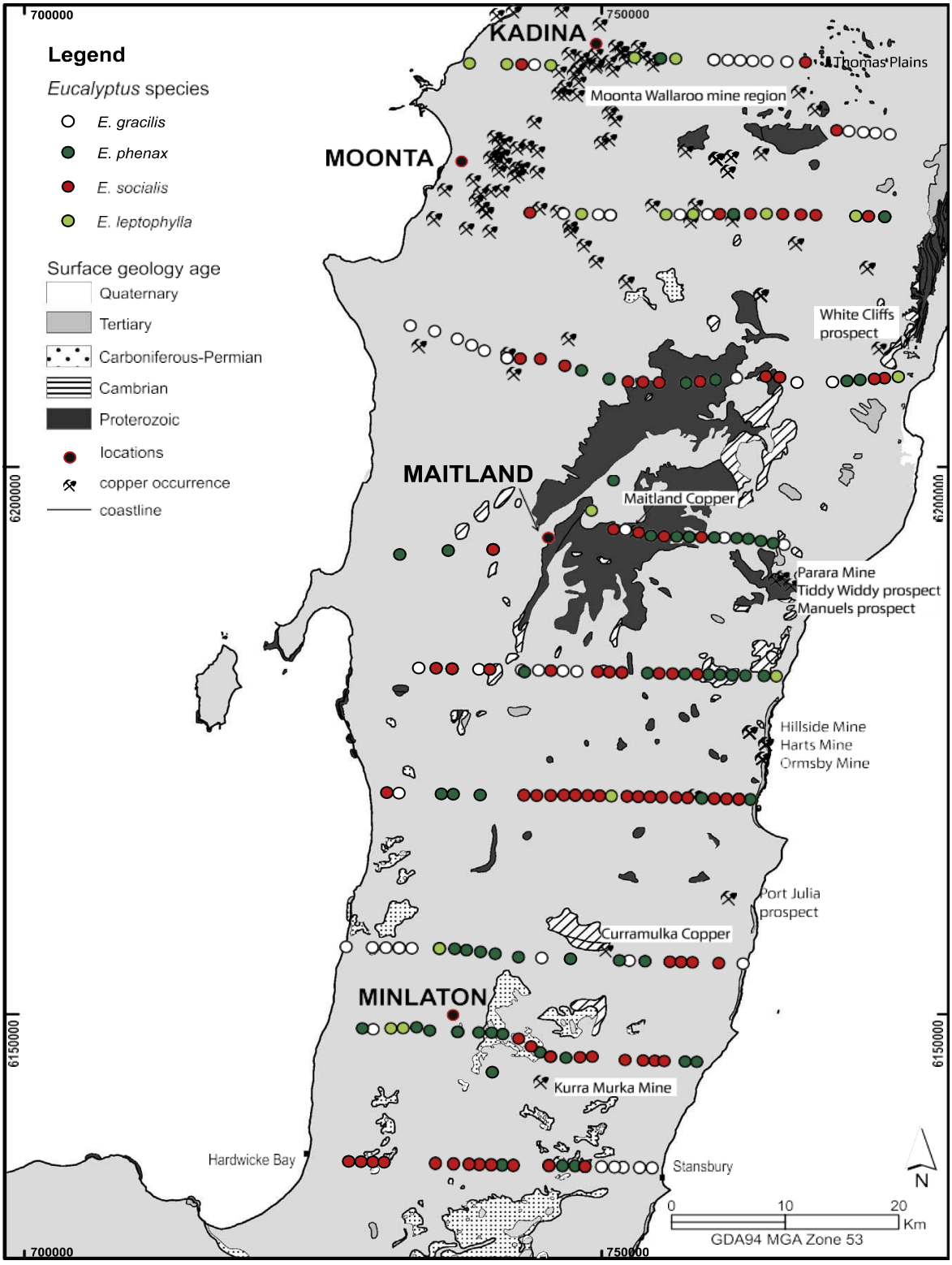

Fig. 4.3. Simplified surface geology map of Yorke Peninsula (downloadable GIS data extracted from SARIG: https://map. sarig. sa.gov.au Last accessed 04/04/2017). The location of the various Eucalyptus species sampled is shown. The location of this map, within South Australia, is shown in Fig. 4.2.

In this paper we present the results of a regional-scale sampling program (218 samples over an area of 4000 km^2), focussing on Cu concentration in the leaves of mallee-eucalypt species across the Yorke Peninsula. Our purpose is to characterise the sample population and determine if there is an empirical relationship between elevated Cu concentration in the mallee leaves and elevated Cu in the underlying basement rocks – such that the mallee leaves might be a useful biogeochemical exploration tool in this area. In order to achieve this purpose we first seek to rule out potential sources of contamination in the leaf chemistry (wind-blown dust and fertiliser), assess variations in the population statistics that might indicate inter-species differences in Cu accumulation and then apply some simple tests to determine if higher concentrations of Cu in the mallee leaves correlate with known Cu accumulations in the basement rock.

4.3 Study Area

4.3.1 Geological setting and mineralisation

The Yorke Peninsula is within the Olympic Domain on the southeastern margin of the Gawler Craton (Figure 4.2). Iron-oxide-copper-gold (IOCG) mineralisation hosted within the broader Olympic Domain includes the supergiant Olympic Dam as well as the Prominent Hill and Carrapateena deposits (Figure 4.2) (Conor et al., 2010). IOCG mineralisation in the Olympic Domain is hosted within variable rock types including the Proterozoic Wallaroo Group and Hiltaba Suite granites (Conor et al., 2010; Cowley et al., 2003). The Wallaroo Group in the central and northern Yorke Peninsula hosts IOCG mineralisation of varying concentration and depth, including the historic

Moonta-Wallaroo district and the Hillside deposit (Conor et al., 2010; Zang et al., 2006), (Figure 4.2).

The Moonta-Wallaroo Cu mining district on the western Yorke Peninsula (Figure 4.3) hosts vein style Cu mineralisation in shear zones that cross cut Paleo- to Mesoproterozoic rocks (Conor et al., 2010). The depth of Cu mineralisation, in the Moonta-Wallaroo district, ranges from 100m to 300m in mined locations and around 15m or less at some prospects (Department of the Premier and Cabinet, 2017). Historically, the average grade of Cu mined throughout the district was around 5% (Conor et al., 2010). At Hillside on the eastern Yorke Peninsula (Figure 4.3), Cu mineralisation is hosted by Proterozoic basement rocks within a shear zone beneath 5 to 10m of cover and sub-cropping in the vicinity of the historic Hillside mine shaft (Fabris, 2010). As at Moonta-Wallaroo, historic mining activity included a significant component of shallow, oxidised material (native Cu and Cu-carbonates) with grades up to 44% Cu, whereas current identified resources are dominated by sulphide material with typical concentrations of 0.5 to 2% Cu (Department of the Premier and Cabinet, 2017).

Copper has also historically been mined around Maitland and at scattered locations along the east-coast (Figure 4.3). Maitland Copper Mine (Figure 4.3) hosts high-grade Cu in surface carbonates (up to 25% Cu) whilst the primary Cu lodes (typically 0.3–11% Cu) are in quartz vein fractures within schist from the Wallaroo Group between 10m and 70m deep (Department of the Premier and Cabinet, 2017). Harts Mine (Figure 4.3), contained up to 40% Cu sulphides in quartz vein fractures, with lesser concentrations as Cu carbonate found in weathered Wallaroo Group rocks exposed at the surface (e.g. Conor, 1995;

Department of the Premier and Cabinet, 2017). Parara Mine (Figure 4.3) was mined for Cu sulphides to a depth of 60m (Zang et al., 2006) and produced 23.4t at 25 % Cu (Department of the Premier and Cabinet, 2017). Copper, as azurite and malachite also occurs in Cambrian carbonate rocks at Curramulka (Zang et al., 2006) and Kurra Murka, albeit in only minor concentrations (e.g. deposit no. 5122, Department of the Premier and Cabinet, 2017). Other Cu occurrences, prospects and abandoned mines are shown in Figure 4.3.

The Wallaroo Group forms the basement in the central and northern Yorke Peninsula and is unconformably overlain by younger Cambrian to Quaternary sediments of <1m and up to at least 1500m thickness (Crawford, 1965; Drexel and Preiss, 1995; Zang et al., 2006; Zang and Hore, 2001) (Figure 4.3). Cambrian sediments include alternating limestone, sandstone and mudstone of up to 1400m (Drexel and Preiss, 1995; Zang et al., 2006). Carboniferous to Permian sedimentation is dominated by glaciogenic sedimentary rocks including glacial diamictite, till, and shallow marine sedimentary rocks containing glacial erratics (Drexel and Preiss, 1995; Zang et al., 2006). Cenozoic sediments include fossiliferous and sandy limestone of the St Vincent Basin and Pirie Basin, clays and sands as well as aeolian dunes, beach and tidal sediments and soil (Zang et al., 2006). There has been extensive development of indurated pedogenic materials, particularly pedogenic carbonates which are typically located at, or within meters of, the current erosion surface within the sedimentary cover rocks (e.g. Cowley et al., 2003; Wolff et al., 2017; Zang et al 2006).

4.3.2 Landscape

The Yorke Peninsula is mostly of low relief and comprises gentle undulating slopes and plains with an average height of 150m above sea level (ASL) (DEWNR, 2013; Roberts, 2007). The highest elevations across the Yorke Peninsula occur in the central region surrounding Arthurton (250m ASL) (Crawford, 1965; DEWNR, 2013; Zang et al., 2006). The coastline varies from sandy or rocky beaches to cliffs and steeply eroded hills (Roberts, 2007). Large areas of sand dunes and swales dominate portions of the north-west and central to south-east areas of the Yorke Peninsula, whilst playa salt lakes and clay pans dominate the landscape to the south. The water table generally occurs at 2m or greater below the surface (DEWNR, 2017). There is a NNE-SSW trending escarpment extending along the eastern coastline northwards from Ardrossan (Crawford, 1965) forming rugged, eroded cliffs and steep-sloped hills.

4.3.3 Climate

The climate across the Yorke Peninsula is typically ‘Mediterranean’ with hot dry summers and mild and wetter winters (Neagle, 2008). The maximum average temperature ranges from 27°C to 30°C during summer and 15°C to 16°C during winter. Rainfall across the Yorke Peninsula typically averages around 500mm per year with June recording the greatest rainfalls (~70mm; Bureau of Meteorology, 2017). Annual evaporation rate of rainfall is high. The general direction of the prevailing wind is from the west, being more from the north-west during the warmer months and the south-west during the cooler months.

4.3.4 Vegetation

Most of the natural vegetation, i.e. that which occurred prior to European settlement across the Yorke Peninsula, has been cleared for grazing and cropping (DEWNR, 2013; McDowell et al., 2012; Neagle, 2008; Zang et al., 2006). Widespread cropping includes cereal grains, oil grains and legumes as the majority of the region contains moderately fertile soils (DEWNR, 2017). Much of the remaining native vegetation is restricted to corridors along roadside verges and fence lines, which act as windbreaks. Patches of woodland typically remains on ground that is the least suitable for agriculture (Neagle, 2008).

The majority of the native vegetation can be broadly characterized as open mallee woodland and shrubland (Neagle, 2008). The woodlands contain *Eucalyptus*, *Melaleuca* (Tea tree), *Acacia* (wattle), *Allocasaurina* (sheoak) and *Callitris* (cypress) with an understory of grasses or sedges such as *Triodia* (spinifex), *Gahnia* (sedge), *Lomandra* (a perennial herb), *Atriplex* (saltbush) and *Lepidosperma* (sedge). Coastal shrublands and lowlands contain *Eucalyptus*, *Avicennia marina* (mangrove), *Atriplex* (saltbush), *Maireana* (bluebush) and *Halosarcia* (samphire), while watercourse communities contain *Eucalyptus, Acacias and* various understory grasses (Neagle, 2008; Zang et al., 2006).

There are fourteen species of *Eucalyptus (E.)* that occur across the Yorke Peninsula of which thirteen are considered mallee (Brooker et al., 2002). With the exception of *E. diversifolia* (*Eucalyptus sub genera Eucalyptus*) all other eucalypts fall into various sections of the sub genera *Symphyomyrtus* as follows: *E*. angulosa, *E. rugosa*, *E. incrassata*, *E. dumosa*, *E. percostata*, *E. brachycalyx* and *E. phenax* subsp *phenax*, *E. calycogona* subsp *calycogona*,

E. gracilis, *E. leptophylla*, *E. socialis* subsp *socialis*, *E. socialis* subsp *glossy leaves* and *E. oleosa* subsp *oleosa*. *Eucalyptus* sub genera *Exsertaria*; *E. camaldulensis subsp camaldulensis* (River Red Gum) is the only native occurring eucalypt-tree (single trunk, tree form) found on the Yorke Peninsula. Hybridisation of species from sub genera can occur which makes identification difficult (Brooker et al., 2002). Natural integration between more closely related species found throughout the region such as *E.incrassata* and *E. angulosa* can also occur (Brooker et al., 2002).

4.4 Materials and Methods

4.4.1 Sampling strategy

This study differs from typical 'orientation' style biogeochemical surveys in that there are not specific positive or negative control points. Although there are areas of known mineralisation within the survey area we have not sought to establish key locations where it is possible to compare known Cu concentrations in the subsurface with Cu concentrations in the sampled leaves. Nor do we have access to data from which we can independently determine the bioavailability of key elements in the subsurface. Rather, our strategy has been to collect regional samples in a program that is subject to the same practical considerations as experienced by exploration companies operating in covered terrains – where there may be little or no prior knowledge of the subsurface metal distribution or speciation *but* where biogeochemistry offers the potential for cheap, rapid and environmentally sensitive first pass reconnaissance sampling. The most relevant question in this survey is; can the biogeochemistry be used as an empirical tool to highlight sub regions within the survey area

where there is a greater likelihood of discovering economic Cu mineralisation and where further exploration should be focussed?

In order to answer this question we first need to characterise the entire sample population (by systematic sampling avoiding the temptation to focus on known mineralisation) and then determine if there is a spatial relationship between elevated concentrations of ore and pathfinder elements and areas of known mineralisation.

The framework of our sampling program was provided by the grid-like distribution of remnant mallee forest along road corridors throughout the Yorke Peninsula. Samples of leaves from mallee-eucalypts were collected approximately every 1 km along ten, east-west road corridors with a north-south spacing of roughly 10 km (Figure 4.3). Samples from four different mallee-form sub-species of *Eucalyptus* were collected and include *E. gracilis*, *E. phenax, E. socialis* and *E. leptophylla* (Figure 4.3). Individual eucalypts were identified using EUCLID (Brooker et al., 2002). A variety of species were sampled as individual sub-species of *Eucalyptus* have preferred habitats e.g. inland, dunes and swales, or coastal cliff-tops (Neagle, 2008). Where no eucalypts were present at designated sample locations, the spacing was extended slightly until a suitable tree could be located. Overall, a grid pattern was formed that extended from Stansbury and Hardwicke Bay in the south to Kadina and Thomas Plains in the north (Figure 4.3).

Samples were collected at the end of summer (March through to April, 2012) prior to winter rainfall. In other studies from arid Australia (e.g. Hulme and Hill, 2003; Reid and Hill, 2010) this timing has been associated with maximum biogeochemical expression, with the inference that water and metal are

sourced from the deeper parts of root systems during times of scarce surface water. This timing is also prior to application of fertilisers used during and following crop sowing (Department of State Development, 2014), which may be a potential source of contamination.

4.4.2 Sampling methods

A total of 218 leaf samples were collected from trees that appeared healthy and mature (i.e. not a sapling). Hands were cleaned and dried between samples in order to minimise potential contamination transferred by hand. Approximately 200 g of leaves were collected at each site and where possible, were sampled from trees on the southern side of the road and at the farthest side of the tree from the road. This method was chosen to reduce contamination from road dust. All samples were placed in calico bags to allow air circulation and delay the onset of rotting as per Dunn (2007). Samples were later dried in their original calico bags in an oven at 60° C for 36-48 hours. Dried samples were sorted by separating the leaves from any twigs which may have remained attached and discarding any leaves that did not appear to be healthy. Approximately 60-80 g of the best leaves were reserved for analysis.

Dust contamination may result in analytical data that reflect the composition of the dust rather than the concentration of metals accumulated in the tissues of the plant (Lintern et al., 2013b; Mitchell et al., 2015). Such contamination may be minimized by sampling methodology, for example by ensuring hands are cleaned and dried between samples and choice of sample location (as above) and by post sampling treatment, for example washing with water prior to drying

(e.g. Arne et al., 1999; Hulme, 2008; Mitchell et al., 2015). Some studies (e.g. Dunn, 2007; Hulme and Hill, 2003) have shown that dust contamination on Eucalyptus leaves is negligible and not greatly improved by washing. This led Hulme and Hill (2003) and Dunn (2007) to infer that dust particles shed easily from the waxy surfaces of eucalyptus leaves and that washing is not a critical component of the sampling protocol for eucalypt species. Following this advice we did not wash the samples collected in this study. However we have analysed for a range of elements typically enriched in wind-born dust (Al, Fe, Zr) as a means of quantifying potential dust contamination.

As the application of fertiliser is widespread across the entire sampling area, and also represents a potential wind-born contaminant, the chemistry of a locally used fertiliser (urea and diammonium phosphate (DAP), Fabris, 2010) was used to determine any contamination and/or influence on the leaf chemistry.

Samples were sent to ACME Analytical Laboratories in Vancouver, Canada for analysis. Samples were first macerated to 100-mesh prior to aqua regia digestion of 5g aliquots. Inductively-coupled plasma-mass spectrometry (ICP-MS) was used to determine element concentrations. Included with these analyses were ACME Laboratories standards as well as additional duplicates. One in every 10 samples were replicated in the laboratory. Laboratory standards were included in the analytical batches at a rate of 1 standard for every ten unknowns. The standards included; STD CDV-1 (n=8), STD V14 (n= 2) and STD V16 (n= 10). Laboratory blanks were also included at a rate of one in every ten unknowns. All analyses of standards and blanks fell within acceptable range of the expected values, with expected and mean ± standard

deviation of the measured Cu concentrations (ppm) as follows: CDV-1 (8.61, 8.49±0.84), V14 (4.8, 4.85±0.23), V16 (6.69, 6.65± 0.67), and blank (<0.01, 0.003± 0.01).

4.4.3 Data Treatment and Statistics

The biogeochemical data were imported into ioGAS^{TM} software in order to characterise population statistics, determine the extent of dust and fertiliser contamination, compare between mallee species and assess spatial relationships with areas of known mineralisation.

Standard data treatment included constructing histograms and probability plots of both the raw concentration data and $\log_{10}$ concentration data of the mallee leaf analyses. As a general rule the trace metal concentrations, including Cu, tend to have log normal population distributions and as such it is appropriate to report key population statistics (mean, standard deviations, range) of the $\log_{10}$ data. We used such statistics as a means of comparing the concentrations of numerous elements in the leaves of the four main mallee species analysed in this study, in order to test if there were systematic, species-dependent differences in element uptake. X-Y plots were used to assess the potential for dust and fertiliser contamination, in particular seeking to identify linear trends in suspected contaminants (Al, Fe and Zr in dust; K, P and Zn in fertiliser) and determine any correlation between these elements and Cu.

Lastly, we have applied a simple test to determine if elevated concentrations of Cu in mallee leaves are likely to be spatially correlated with Cu mineralisation in the subsurface. Our options for geostatistical correlation are limited in this survey area because the distribution of Cu concentration in the subsurface is

largely unknown. We do not have access to a regional Cu-in-basement dataset of comparable spatial resolution to the mallee data and instead have used the distribution of historic Cu prospects as an imperfect first pass approximation. Our approach is to apply a 3km search radius around known Cu prospects and compare the populations of Cu in mallee leaves from inside and outside the search radius.

4.5 Results

4.5.1 Distribution of mallee

The distribution of mallee-eucalypt species sampled is shown in Figure 4.3. A total of 218 samples were taken from four species as follows; *E. gracilis* (53), *E. phenax* (60), *E. socialis* (87), and *E. leptophylla* (18). *E. gracilis* was found to be concentrated in the north and south of the study area. *E. phenax* was found to be broadly distributed across the central and southern regions of the study area, with only a few sampled in the northern area. *E. socialis* was the most commonly sampled and most widespread species. The northern-most transect had the least amount of *E. socialis* sampled. *E. leptophylla* was found to be concentrated in the northern portion of the study area, with only sparse distribution in the central and southern areas.

4.5.2 Chemistry

Of the 53 elements analysed, 28 were above analytical detection limits in the leaf samples. Results for these are included in Appendix 8. Representative data for selected elements are given in Table 4.1. The focus of this paper is on Cu as there is not enough Au above detection limits to be useful (Appendix 8). There are no particularly useful patterns in the other 21 elements.

Leaves from all mallee species contain Cu ranging from 1.59ppm to 10.04ppm (Table 4.1). The distribution of Cu in all species is shown in Figure 4.4. The average Cu for all species sampled is 3.80ppm (Table 4.1). Both the lowest and highest concentrations occur in *E. Phenax*. *E. phenax, E. socialis and E. gracilis* contain similar average Cu concentrations while *E. leptophylla* contains the highest average Cu (ppm) concentration (Table 4.1; Figure 4.4). The widest range in Cu concentration is found in *E. phenax* (Table 4.1; Figure 4.4).

Aluminium, Fe and Zr results are included as measures of dust contamination. Aluminium was measured at or slightly above analytical detection limit in 92 samples (Table 4.1, Appendix 8). Concentration of Al ranged from 0.01 wt% to 0.03 wt% which is barely above detection limit (Al, 0.01 wt%). Up to half of each species sampled contained Al concentrations above detection limits. Of these only half again were above detection limits by only 0.01 wt% or 0.02 wt%. Iron was measured in all leaf samples and concentrations ranged from 0.006 wt% to 0.028 wt% (Table 4.1). The range in Fe concentration was similar for all four species. Zirconium was measured in all samples and concentration ranged from 0.02ppm to 0.21ppm. There were minimal differences in Zr concentration among eucalypt species with *E. socialis* containing the highest average concentration (Table 4.1). Aluminium and Zr display a mutual linear relationship although the low detection values and fewer results affect how these appear (Figure 4.5a). Iron and Zr share a very close positive linear relationship (Figure 4.5a). Copper has a poorly correlated relationship with Zr (Figure 4.5a).

Potassium, P, and Zn results are included as potential measures of fertiliser contamination and to measure any potential preference for trace element uptake related to plant physiology and growth (Table 4.1, Figure 4.5b).

Phosphorus was measured in all samples and concentrations ranged from 0.04 wt% to 1.63 wt% (Table 4.1). There were minimal differences in average P concentrations across all four species with *E. phenax* containing the highest average concentration (Table 4.1, Figure 4.5b). Potassium was measured in all samples and concentrations ranged from 0.29 wt% to 0.90 wt% (Figure 4.5b). The range of K concentration was similar in all four species (Table 4.1). Zinc was detected in all samples and concentrations ranged from 4.7ppm to 26.7ppm (Table 4.1). Similar Zn average concentrations were found within all four species. There is no clear relationship between K and P. Potassium and P concentrations are clustered, with little scatter, above the fertilizer mixing line and below the average plant composition (Figure 4.5b). Zinc and P appear to have a very weak positive relationship with a slight clustering of data points and some scatter but also well above the fertilizer mixing line (Figure 4.5b). Copper and P do not show strong correlation of results (Figure 4.5b).

Table 4.1. Biogeochemistry summary statistics of Eucalyptus leaves representative of the Yorke Peninsula.

Eucalyptus species	*n*	element	units	detection	min	max	mean	median	std deviation
E. gracilis	53				1.95	8.35	4.09	3.89	1.41
E. phenax	60				1.59	10.04	3.86	3.46	1.53
E. socialis	87	Cu	ppm	0.01	1.67	7.77	3.29	3.01	1.16
E. leptophylla	18				2.15	8.83	5.21	5.02	1.75
all species	218				1.59	10.04	3.8	3.44	1.48
E. gracilis	53				0.29	0.92	0.59	0.59	0.15
E. phenax	60				0.20	1.00	0.56	0.54	0.16
E. socialis	87	Cu	$\log_{10}$	n/a	0.22	0.89	0.49	0.48	0.14
E. leptophylla	18				0.33	0.95	0.69	0.70	0.16
all species	218				0.20	1.00	0.55	0.54	0.16
E. gracilis	53				0.05	0.13	0.08	0.07	0.02
E. phenax	60				0.04	0.16	0.07	0.06	0.03
E. socialis	87	P	wt%	0.001	0.04	0.13	0.07	0.06	0.02
E. leptophylla	18				0.06	0.11	0.08	0.08	0.02
all species	218				0.04	0.16	0.07	0.07	0.02
E. gracilis	53				0.31	0.87	0.46	0.45	0.10
E. phenax	60				0.29	0.87	0.55	0.54	0.13
E. socialis	87	K	wt%	0.01	0.30	0.83	0.52	0.51	0.10
E. leptophylla	18				0.36	0.90	0.56	0.52	0.14
all species	218				0.29	0.90	0.52	0.50	0.12
E. gracilis	22				0.01	0.03	0.01	0.01	0.01
E. phenax	19				0.01	0.02	0.01	0.01	0.00
E. socialis	44	Al	wt%	0.01	0.01	0.03	0.02	0.02	0.01
E. leptophylla	7				0.01	0.02	0.02	0.02	0.00
all species	92				0.01	0.03	0.01	0.01	0.01
E. gracilis	53				0.01	0.03	0.01	0.01	0.00
E. phenax	60				0.01	0.02	0.01	0.01	0.00
E. socialis	87	Fe	wt%	0.001	0.01	0.03	0.01	0.01	0.00
E. leptophylla	18				0.01	0.02	0.01	0.01	0.00
all species	218				0.01	0.03	0.01	0.01	0.00
E. gracilis	53				4.7	22	12.35	12.10	3.28
E. phenax	60				5.4	24	12.22	11.45	4.46
E. socialis	87	Zn	ppm	0.1	7	26.7	13.65	13.40	3.37
E. leptophylla	18				7.5	23.4	14.57	14.95	4.24
all species	218				4.7	26.7	13.01	12.75	3.81
E. gracilis	53				0.02	0.18	0.06	0.06	0.03
E. phenax	60				0.03	0.14	0.06	0.06	0.02
E. socialis	87	Zr	ppm	0.01	0.02	0.21	0.08	0.07	0.04
E. leptophylla	18				0.03	0.13	0.07	0.06	0.03
all species	218				0.02	0.21	0.07	0.06	0.03

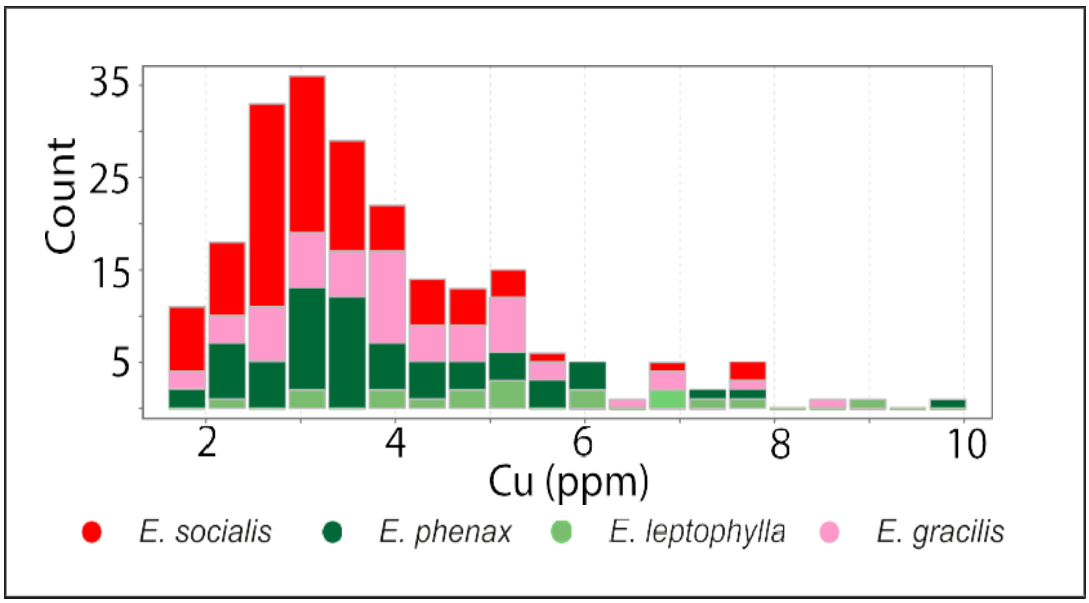

Fig. 4.4. Stacked histogram plot showing distribution of Cu in each species of mallee-eucalypt.

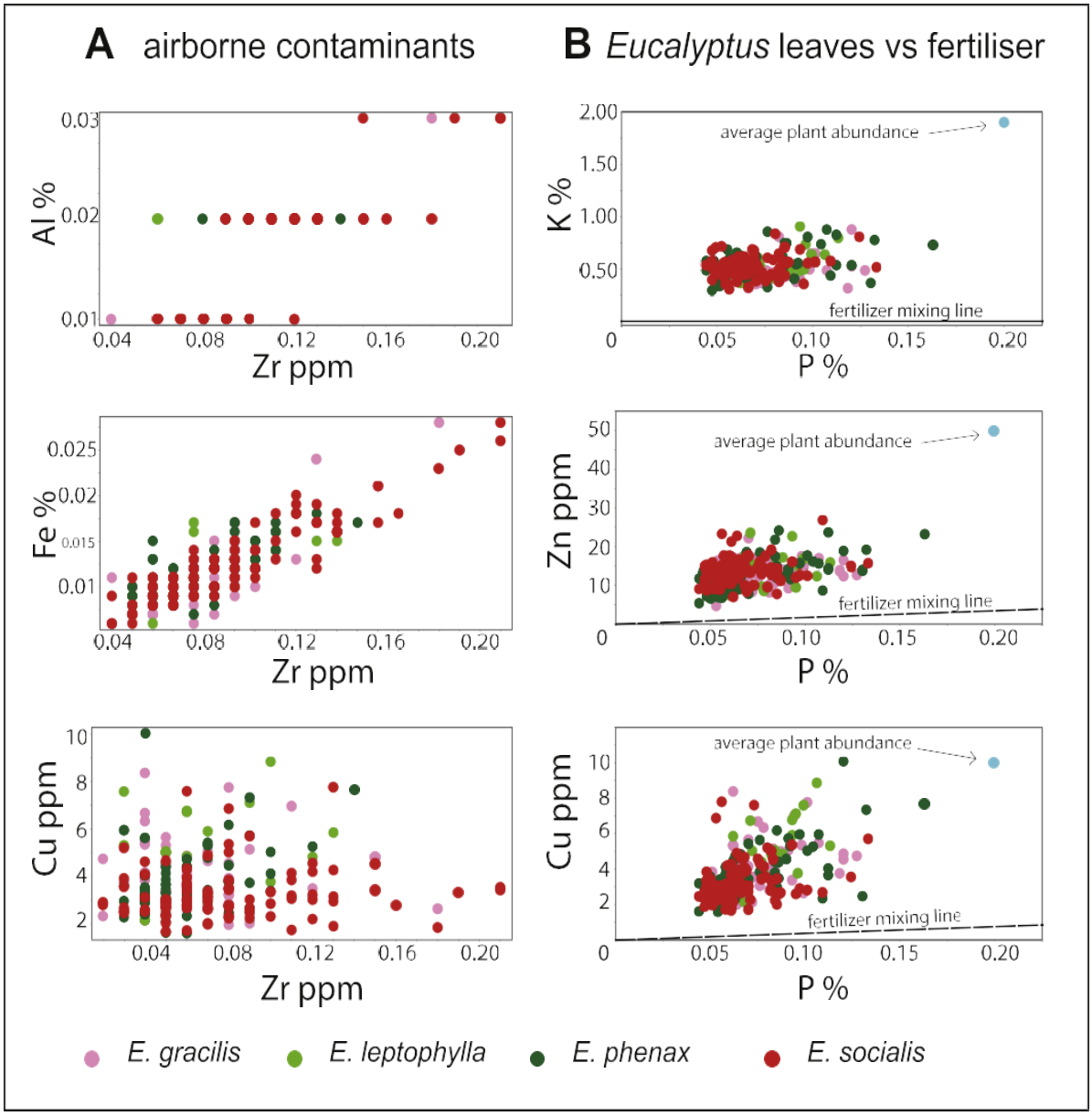

Fig. 4.5. Geochemical plots of various element concentrations found in mallee-eucalypt leaves from the Yorke Peninsula; A: concentrations of dust contaminants (Al, Fe and Zr) plotted against Cu; B: elements found in fertiliser (P, K and Zn) plotted against Cu concentration. A fertiliser mixing line based on di-ammonium phosphate (DAP) data from Fabris (2010) shows the expected trend in concentration based on fertiliser uptake. The blue dots indicate the average abundance of respective elements in all plants based on Dunn (2007).

4.6 Discussion

4.6.1 Potential sources of contamination

Dust and fertilisers are considered the two largest sources of potential contamination of the mallee leaves throughout the study area. Dust contamination needs to be considered as airborne particles may be enriched in Cu from nearby mining. Fertilisers used in cropping can contain Cu and therefore may influence the apparent Cu content of the mallee leaves. The influences of these contaminants on the geochemical data have been assessed by comparing the concentrations and associations of typical aeolian contaminants and various elements found in fertiliser samples.

4.6.2 Dust contamination

Airborne and/or roadside dust contamination can be assessed by comparing relationships between Al, Fe, Zr and Cu (e.g. Kabata-Pendias and Pendias, 2001). Within dust, Al and Fe are mostly found in fine grained clay (i.e. aluminosilicates) and iron-oxide particles. Both Al and Fe are major constituents in soils (Kabata-Pendias and Pendias, 2001). Zirconium is mostly found in sand (Fitzpatrick and Chittleborough, 2002), which occurs extensively throughout the region. Within plants, Al and Zr are not essential elements for growth and Fe is only required in trace amounts (e.g. Dunn, 2007) therefore small amounts of dust contamination would be expected to have a strong influence on the Al, Fe and Zr concentrations in the leaves.

Relationships between Al, Fe, Zr and Cu are shown in Figure 4.5a. A strong positive linear relationship is shown between Fe and Zr. A similar relationship is observed between Al and Zr, albeit not as distinctly linear due to Al

concentrations being so close to detection levels (Figure 4.5a). Although these elements are at very low concentrations, the linear relationships are consistent with dust contamination (e.g. from soil components, Kabata-Pendias and Pendias, 2001; Fitzpatrick and Chittleborough, 2002). There is no relationship between Cu and Zr (Figure 4.5a) as would be expected if dust contamination contributed substantially to the total Cu detected in leaf samples. This suggests that Cu is being incorporated into the eucalypts independently from the elements that comprise windblown dust and is sourced from elsewhere. The very low concentration levels of these elements (Al, Fe and Zr) also indicate that dust contamination has not impacted the overall chemical content of the leaves and that the improvement to data quality, by having pre-washed the samples, would be negligible.

4.6.3 Fertiliser contamination

Fertiliser application during the cropping season is widespread throughout the Yorke Peninsula (Department of State Development, 2014). Use of phosphate fertilisers have been shown to significantly increase the foliar content of P (e.g. Bennett et al., 1996; Crous et al., 2015) and could conceivably result in increased uptake of other essential nutrients or trace elements, either directly from the fertiliser or from the substrate as a result of more vigorous plant growth. Therefore, it is important to determine the impact, if any, of fertilisers on the Cu concentration in the eucalypt leaves. Whilst it is unknown exactly how much fertiliser the eucalypts have access to and are taking up, the concentrations of P, K, Zn and Cu in the leaves can be directly compared to actual fertiliser that is used throughout the region (Figure 4.5b).

Di-ammonium phosphate (DAP) fertiliser is commonly used throughout Yorke Peninsula (Fabris, 2010). This fertiliser contains relatively high concentrations of Cu (75ppm) which may be taken up by eucalypts dependant on root access, quantity applied and proximity to fertiliser application. This would therefore suggest that Cu concentrations in the eucalypts may merely be reflecting the fertiliser usage.

A fertilizer mixing line based on P, K, Zn and Cu concentrations in the DAP is shown in Figure 4.5b. Both K and Zn versus P concentrations sit well above the fertiliser mixing line (Figure 4.5b). Copper and P concentrations are also observed well above the fertiliser mixing line (Figure 4.5b).

The broad scatter of data points for Cu concentration versus P is different to the narrower range in concentrations for K and Zn versus P (Figure 4.5b) suggesting that there is no relationship of Cu to K, Zn or P and that these concentration patterns do not reflect contamination from fertiliser.

4.6.4 Natural uptake of elements

Essential elements for healthy plant growth such as P, K, Zn and Cu were not only included for fertiliser analysis but also used to assess whether the four species of mallee-eucalypts in this study are taking up elements in a similar manner. Phosphorus and K are considered major essential elements for plant growth while Zn and Cu are only required in trace amounts (Dunn, 2007). These elements were compared with ranges of plant concentrations reported by other authors (e.g. Attiwill and Adams, 1996; Barrow, 1977; Dunn, 2007; Gazola et al., 2015).

Phosphorus and K are both major essential elements that are taken up by eucalypts for growth but tend to have narrow concentration ranges in all species (e.g. Gazola et al., 2015; Grove et al., 1986; Judd et al., 1996). Similar narrow ranges in concentration of P and K are also observed in the eucalypts of this study (Figure 4.5b).

Zinc is required in trace amounts and tends to have an uptake synergistic with P (Kabata-Pendias and Pendias, 2001), implying that Zn, where available, will also be incorporated into the eucalypt along with P. A weak positive relationship between P and Zn was observed in the Yorke Peninsula data, (Figure 4.5b) suggesting the uptake of Zn reflects the natural uptake by the eucalypts in this region.

Copper is also required in trace amounts by eucalypts and similarly shares a synergistic partnership with P (Kabata-Pendias and Pendias, 2001). This also implies a natural uptake of Cu where P is available. The Yorke Peninsula data does not show any obvious relationship between Cu and P (Figure 4.5b); however, the broader range of Cu concentrations may mask any subtle relationships that may be present. The natural background levels of Cu taken up by the mallee in this region is suggested to be reflected by the dominant (average) population of Cu values (Figure 4.4; i.e. an average of Cu 3.8ppm). The Cu data also shows a population of samples with above average Cu concentrations (Figure 4.4), suggesting an active enrichment process other than natural uptake of elements.

Plants growing in a Cu-rich substrate will naturally take up higher concentrations of Cu (Dunn, 2007; Kabata-Pendias and Pendias, 2001). Kabata-Pendias and Pendias (2001) also suggest that when there are higher

concentrations of trace elements in soils, plants will take up more of that element even though it may not necessarily be a hyperaccumulator by definition (e.g. Kabata-Pendias and Pendias, 2001). The broad range of Cu concentrations within the Yorke Peninsula data and the observation of a population of samples with above average Cu concentrations (Figure 4.5b) suggests there are mallee-eucalypts that are taking up Cu in excess of biological requirements. Samples with higher Cu concentration are located in the north, east and southwest of the study area, and in most cases are coincident with regions of known Cu mineralisation (Figure 4.6). The spatial relationship between the higher Cu concentrations in the leaves to Cu occurrences suggests that there is elevated Cu in the substrate that the trees have access to.

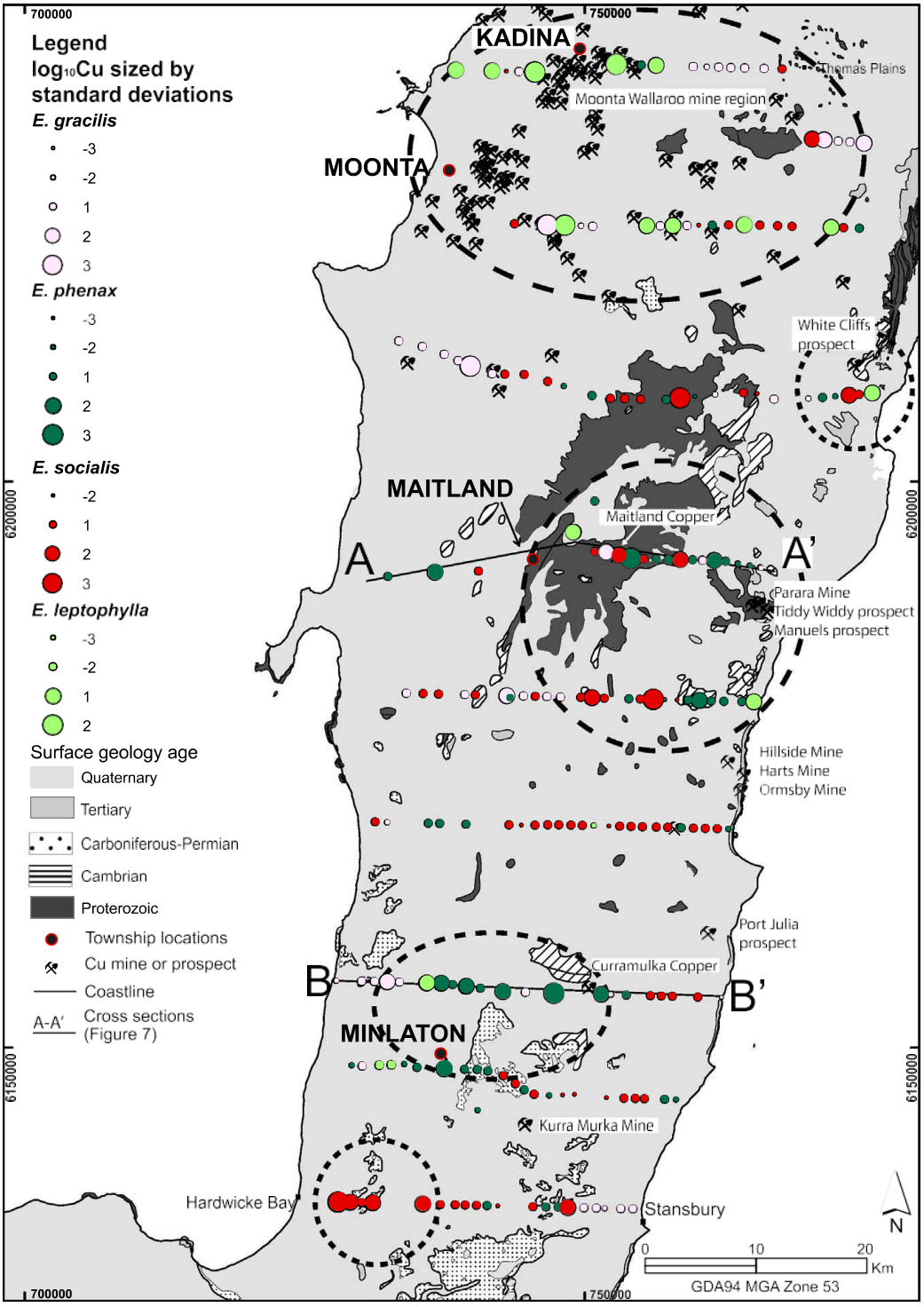

Fig. 4.6. Distribution of log$_{10}$Cu in mallee across Yorke Peninsula. The overall pattern of the various species of Eucalyptus display a trend for concentrating higher levels of Cu into their leaves nearby to regions where Cu is known to occur as indicated. Regions of elevated Cu concentration are indicated by dashed lines. Cross sections A-A' and B- B' are presented in Fig. 4.9.

4.6.5 Statistical considerations for Cu in Eucalypts

Previous authors (e.g. Butt et al., 2005b; Dunn, 2007) suggest that complications may arise if sampling a variety of different vegetation or by mixing species from the same genus, therefore there is a need to address any differences in the uptake of trace elements between *E. gracilis*, *E. phenax*, *E. socialis* and *E. leptophylla*. In this study, we are particularly interested in whether or not each species is taking up Cu in the same way. As there is limited existing data regarding trace element uptake in mallee eucalypts, we are limited in this study to comparing population statistics from each species (Table 4.1) in order to identify any systematic variations between them.

Comparison of data for all elements in the four species (Figure 4.7) shows they have very similar means and standard deviations, with each species overlapping in range within the first and third quartiles. We infer from these data that the four species have a very similar uptake of a wide range of nutrients and other trace elements which suggests that their biogeochemical response is comparable. Thus, we consider it reasonable to pool the data from the four species without performing any further normalisation.

E. leptophylla has slightly more Cu than the other three species, although still with overlapping populations at the first and third quartiles (Figure 4.7). Cu concentrations for *E. gracilis* (n=53), *E. phenax* (n=60) and *E. socialis* (n=87) have similar mean $\log_{10}$ Cu concentrations of between 0.49 and 0.59ppm. *E. leptophylla* (n=18) has a higher average $\log_{10}$ Cu concentration of 0.69ppm (Figure 4.8). The probability plots for *E. gracilis*, *E. phenax* and *E. socialis* are comparable, with relatively straight lines between -2 and +2 standard deviations (Figure 4.8). *E. leptophylla* also forms a straight line on the probability plot,

although displaced to higher values than the other species and with a higher mean (Figure 4.8). Although the Cu concentrations are slightly higher for *E*. leptophylla, the uptake of Cu displays a similar pattern for all four species (Figure 4.8) with the higher concentrations coinciding with nearby Cu occurrence (Figure 4.6).

E. leptophylla samples are more common in the Cu mining regions of Kadina and Moonta (Figure 4.3 and 4.6). As the biogeochemical uptake of trace elements (including Cu) is comparable for all four species, the possibility that higher concentrations of Cu in the plants are related to higher Cu concentration in the substrate and potentially proximity to buried Cu mineralisation needs to be considered.

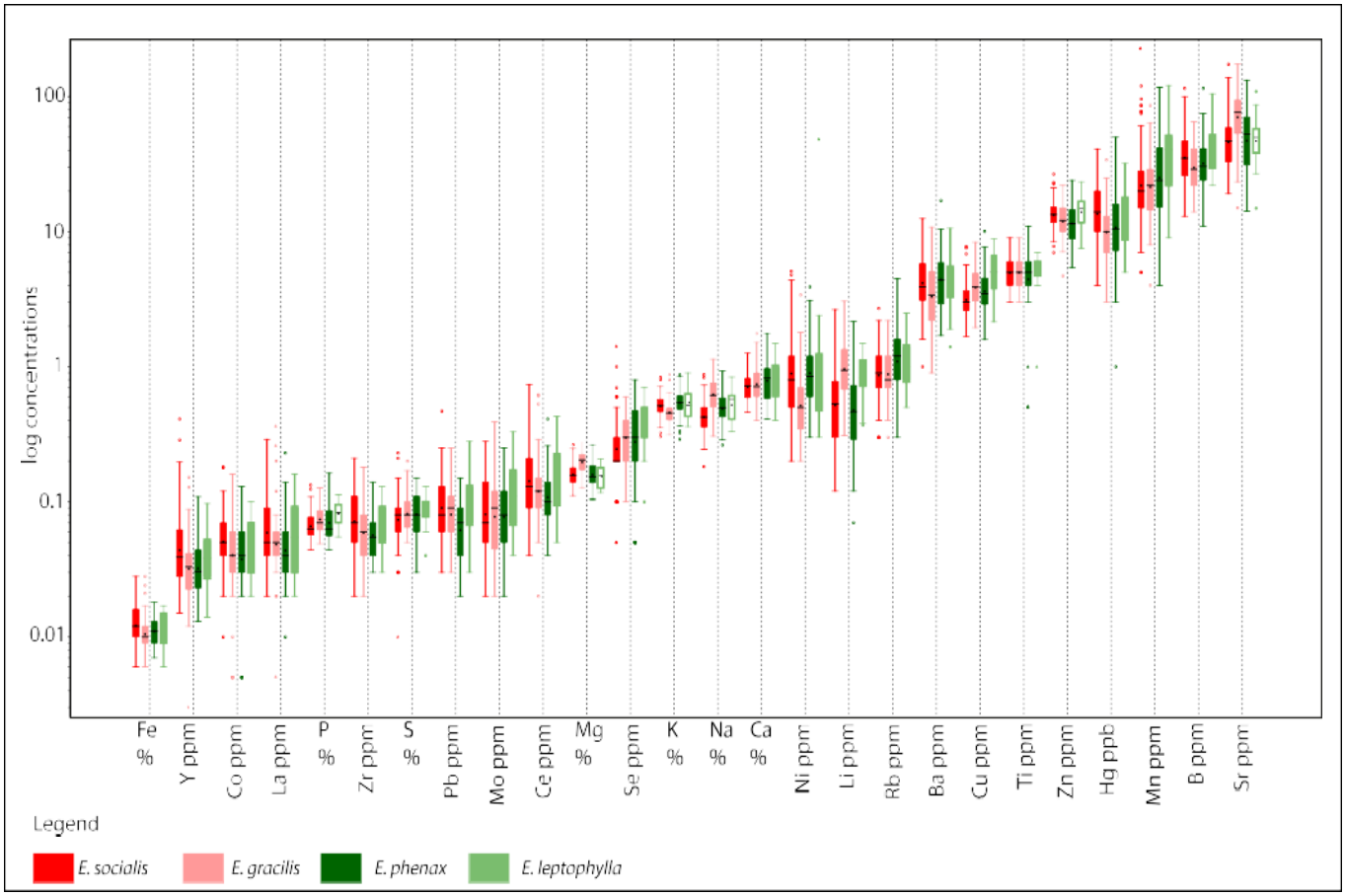

Fig. 4.7. Tukey box plots for all elements on a common Y axis and logged. Elements with >90% of their results above detection were used. Solid rectangles represent data that is within 1 standard deviation of the mean. Lines represent 2 standard deviations from the mean and outliers are represented by dots. Within the solid rectangles the black dash is the mean and the black dot is the median.

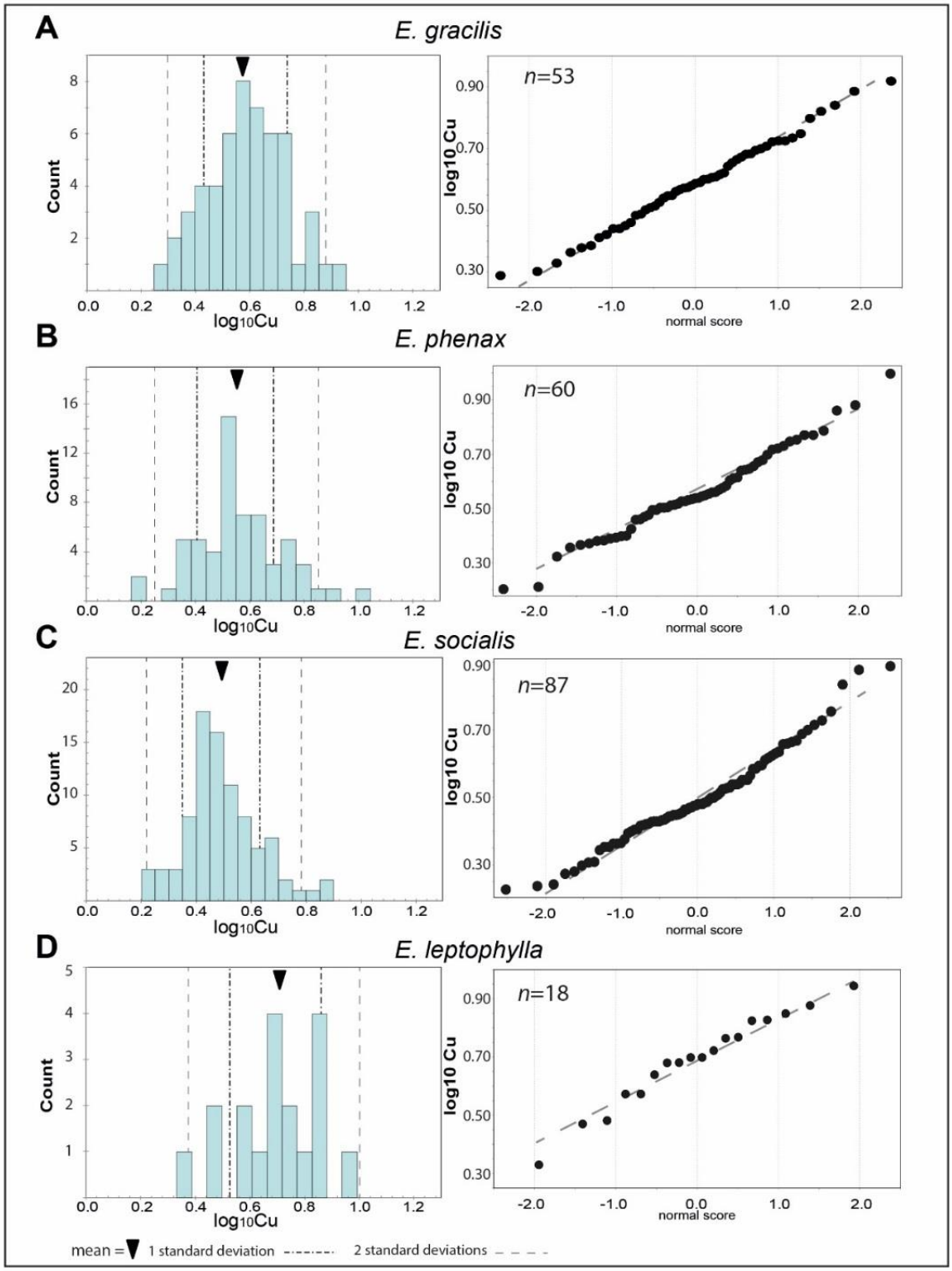

Fig. 4.8. Histograms (left) and normal probability plots (right) for A. E. gracilis; B. E. phenax; C. E. socialis; and D. E. leptophylla. Although E. leptophylla (D) has a higher overall concentration of Cu, the values remain within the ranges observed for the other species (A, B and C). Black arrow: (arithmetic) mean; dark dashed lines: 1 standard deviation; light dashed lines: 2 standard deviations.

4.6.6 Eucalypt expression of Cu nearby to Cu occurrence

Dietman (2009) demonstrated that the soils surrounding the Hillside Cu mine (Figure 4.3 and 4.6), are elevated in Cu. Likewise, clays, transported sediments and carbonate rocks that make up the soils surrounding the Moonta mining region contain elevated Cu compared to regional background levels (e.g. Keeling et al., 2005; Wolff et al.,2017). These studies suggest that Cu is mobile within the transported sediments and regolith materials overlying basement rocks enriched in Cu, and thus has the potential to be biologically available.

The tendency for the mallee eucalypt leaves to be slightly elevated in Cu in the vicinity of known mineral occurrences is supported by the results of this study (Figures 4.6 and 4.9). Mallee-eucalypts occurring nearby the Maitland and Curramulka Cu mines show elevated Cu in the leaves compared to the more distal eucalypts (Figure 4.9). Additionally, in the northern Yorke Peninsula, there is a complex pattern of elevated Cu concentration in *Eucalyptus* leaves throughout the Moonta-Wallaroo mine region and in the vicinity of White Cliffs prospect (Figure 4.9). This trend of Cu in *Eucalyptus* adjacent known Cu occurrence is observed independent of the species. This further supports the proposition that all four mallee-eucalypt species are taking up Cu similarly, and that they can collectively be used to identify regions of elevated Cu in soil and in the underlying basement.

The relationship between elevated Cu in mallee leaves and proximity to known mineralisation on a regional scale is illustrated by comparing the population statistics of trees within 3km of known Cu occurrences to those that are more than 3km from known occurrences (Figure 4.10). The trees closest to known Cu occurrences have a higher mean, greater standard deviation and are more

skewed to higher values (Figure 4.10a). The elevated concentrations in trees within 3km of a known Cu occurrence are also highlighted as being a separate data population with Cu concentrations > 4ppm and again at 6ppm (Figure 4.10b). This implies that trees within a relatively short distance of a Cu occurrence have a greater probability of taking up Cu in higher concentrations compared with those that are further away.

It is acknowledged that there are some trees that grow nearby to Cu occurrence that do not contain elevated Cu concentrations. There are various factors that may impact the trees ability to transfer Cu from the substrate to the leaves. For example, the depth of Cu-rich substrate may be beyond the depth of root penetration, the particular soil horizon that the roots reside in may not be elevated in Cu, or individual trees may have differing abilities to collect and store trace elements in their leaves (e.g. Dunn, 2007). As the trees were sampled 1km apart, subtle variations in depth of cover or the lithology of underlying basement rocks may hamper root access, which could also affect the ability for a tree to take in more Cu. Higher density sampling may resolve these issues.

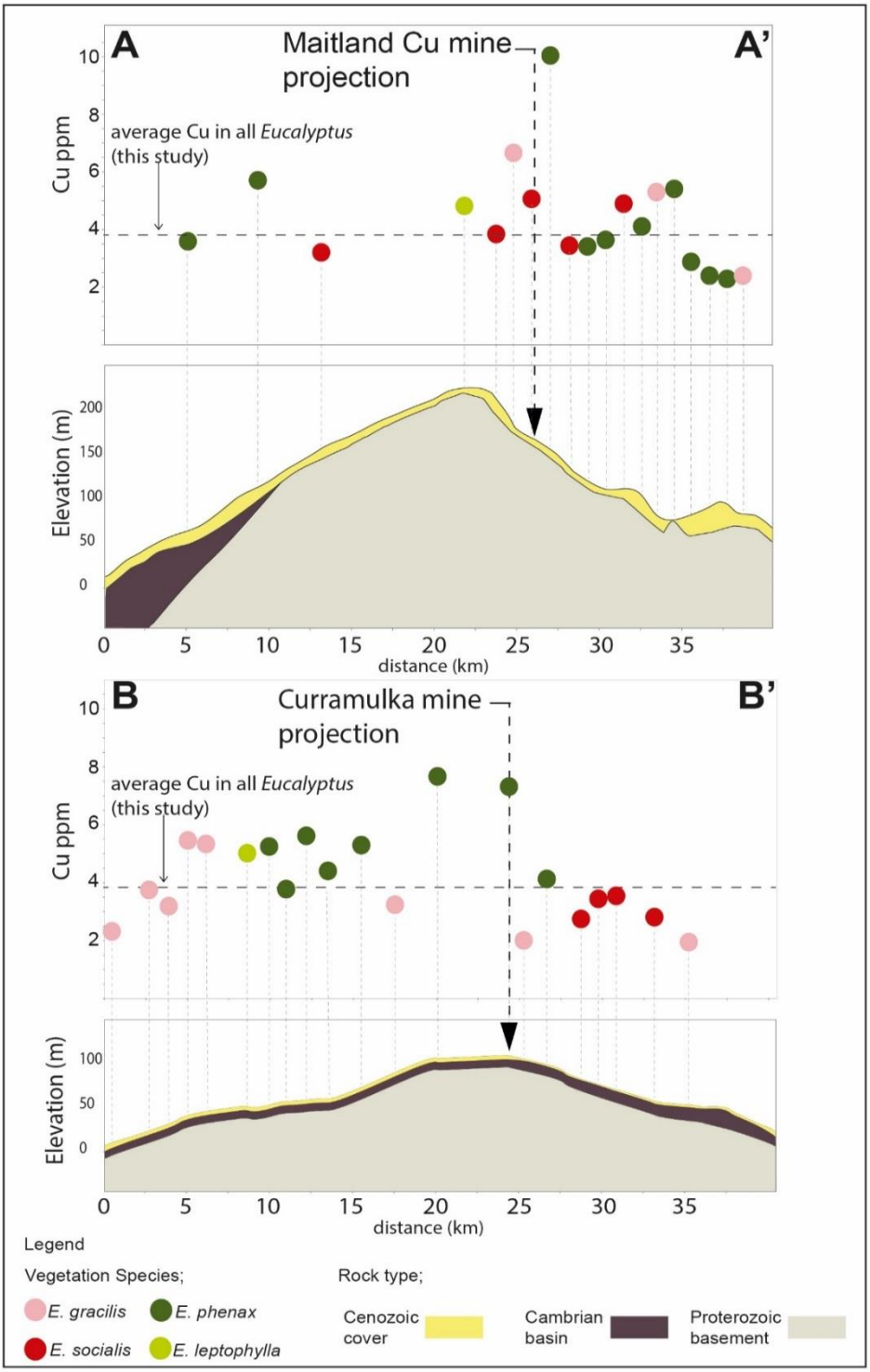

Fig. 4.9. Biogeochemical cross sections through transects containing Maitland Copper Mine (A to A' Fig. 4.6) and Curramulka Copper Mine (B to B' Fig. 4.6). The position of each mine is indicated within the respective transect. Both sections demonstrate a trend of decreasing Cu concentration in leaves of various Eucalyptus species with increasing distance from the mine.

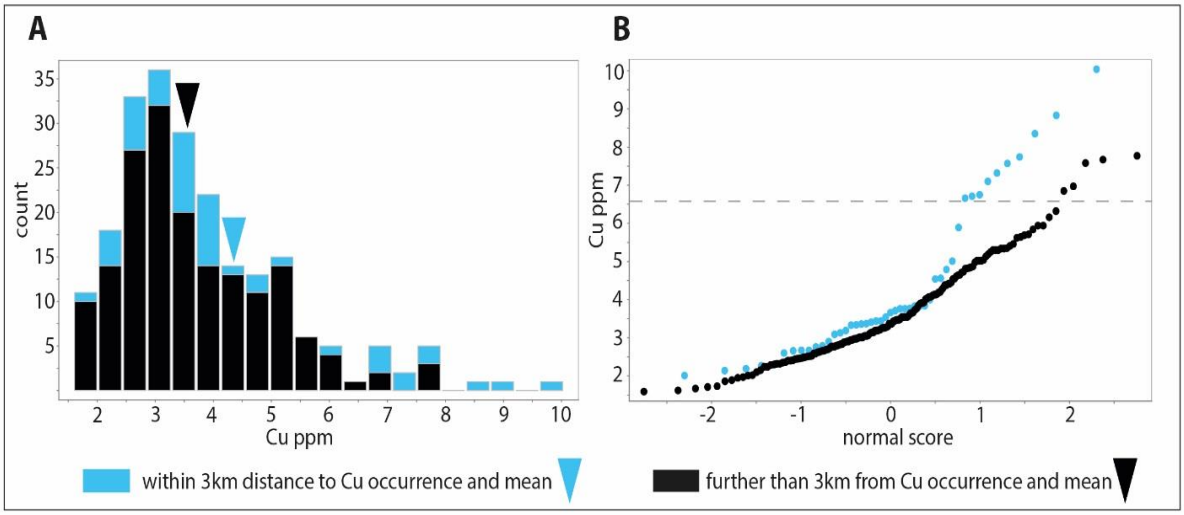

Fig. 4.10. A; histogram and B; probability plot showing relationship of Cu concentration in trees that are within 3km (blue) to known Cu occurrence compared to trees >3km away from Cu occurrence (black). Trees within 3km to known Cu occurrence have a higher mean Cu concentration (4.3ppm indicated by blue marker) and standard deviation (2ppm) with a longer tail skewed to the right with a broader spread towards higher Cu concentrations (2–10ppm) compared with those that are further than 3km away (mean 3.6ppm indicated by black marker) and standard deviation (1.2ppm). The dashed line in B identifies a breakpoint in both populations which we interpret as a threshold value of interest for this region.

4.6.7 Elevated Cu concentrations in trees that are not nearby to Cu occurrences

In comparing these two populations (i.e. trees within 3km from a Cu occurrence and trees more than 3km, Figure 4.10), the population within 3km of known Cu occurrences, has a higher proportion of samples above 4ppm Cu and a distinct sub population above 6ppm Cu. This Cu concentration (>6ppm) also corresponds to an apparent break on the Cu probability plot (Figure 4.10b) for the remaining samples that are not within 3km. This serves as a useful threshold for identifying interesting results worthy of follow up.

The Hardwicke Bay area has mallee-eucalypts that contain elevated concentrations of Cu yet are not directly adjacent to known Cu occurrences (Figure 4.6). The group of mallee-eucalypts at Hardwicke Bay (Figure 4.6) occur as a cluster of 3 samples that are spaced 1 km apart. It is possible that this cluster of trees with elevated Cu represents the surface expression of buried mineralisation. This area is underlain by thick Carboniferous-Permian sedimentary rocks (up to 500m e.g. Drexel and Preiss, 1995; Zang and Hore, 2001) that have not been reported to host mineralisation on Yorke Peninsula or elsewhere across South Australia (Drexel and Preiss, 1995). A possibility that cannot be ruled out is that the elevated Cu in mallee leaves at Hardwicke Bay is a transported signal, either via physical transport of Cu in Quaternary sediments or via groundwater.

4.6.8 Implications for biogeochemical exploration for Cu

The widespread occurrence of mallee-eucalypts and their ability to transfer elemental signals from deep in the substrate they grow in makes them a potential tool for exploration. There are limitations that should be considered in designing a mallee biogeochemical survey:

- Identify the species of vegetation and the extent of its occurrence within the region of interest.
- Identify potential sources of contamination that occur throughout the region. This may include land use such as farming or mining.
- Sample at a density that produces robust statistics to identify background levels versus concentrations that are above background.

- Understand the regolith landscape processes in the region to determine whether biogeochemical signatures may reflect buried mineralisation or are the effect of physical and/or chemical element transport.

4.7 Conclusions

A variety of mallee-eucalypt species are shown to accumulate Cu in their leaves in areas of known Cu mineralisation across the Yorke Peninsula. The mallee-eucalypts contain background Cu concentrations of ~3.8ppm with higher Cu concentrations above 6ppm and up to 10.04ppm. The higher concentrations of Cu are located nearby to Cu mines or prospects. The widespread distribution of mallee-eucalypt across southern Australia and their ability to access and transfer geochemical signals from deep within the substrate implies they are a readily available biogeochemical sample medium. This implies that sampling mallee-eucalypts in an environment such as Yorke Peninsula may be an effective, rapid, cheap and non-invasive exploration method that can be applied at large scales.

Chapter 5: Conclusion

This thesis presents the use of carbonate rocks and vegetation on the Yorke Peninsula, South Australia to gain:

1. an understanding of how surface cover sequence materials can be used as mineral exploration sampling media;
2. recognition of different types of sample media through simple geochemical discrimination that might also be undertaken in the field;
3. understanding how geochemical signatures related to mineralisation are expressed within different surface sample media, and;
4. Developing criteria for vectoring towards IOCG mineralisation.

Three exposed coastal profiles preserving basement rocks, intercalated marine carbonates and clastic lithologies, and pedogenic carbonates were sampled and used to identify lithogeochemical variations, to develop a geochemical discriminant between marine and pedogenic carbonates and assess their relevance as a sample medium for exploring for Cu. A regional carbonate sampling survey throughout the Yorke Peninsula was used to characterise the surface expression of known buried IOCG mineralisation (Fig 5.1). Locally occurring mallee eucalypts were sampled at the same sites as the regional carbonate survey and used to understand how underlying IOCG mineralisation is expressed as a geochemical signature within the mallee eucalyptus leaves (Fig 5.1).

In summary, using the results of this research, I have;

- Produced a comprehensive data set of geochemical, biogeochemical and hydrochemical data from the Yorke Peninsula, South Australia that previously was poorly known. This achieves the objectives for

understanding how geochemical signatures related to mineralisation are expressed within different surface sample media by having a comprehensive dataset available. My initial plan was to focus on Au and Cu, which occur in known mineral deposits on the Yorke Peninsula. Gold analyses in both carbonate rocks and mallee were largely below detection and were not useful for mineral exploration. Copper was the most useful element for identifying potential for underlying mineralisation and formed the basis of the following research;

- Produced a regolith landform map that displays clearly the dominant characteristics of the region, providing a means to visualise potential physical dispersion patterns of surface sediments through time. This achieves the objective of understanding how surface cover sequence materials can be used as mineral exploration sampling media that also has potential to benefit mineral explorers in the region;
- Developed criteria for discriminating pedogenic carbonate versus limestone, quickly, easily and in the field, without the need for costly methods to be used. This directly addresses the objective to recognise different types of sample media through simple geochemical discrimination that might also be undertaken in the field;
- Contributed substantially to the understanding of the use of mallee eucalypts as a complementary method of exploring for minerals. This addresses the objective to understand how geochemical signatures related to mineralisation are expressed within different surface sample media;
- Produced various maps that display geochemical data for Cu, which visually demonstrates that both carbonate rocks and mallee eucalypt

leaves that coincide with- or are very near to- areas of Cu mines and deposits contain higher amounts of Cu, relative to other such samples that are further away. This addresses the objective to develop criteria for vectoring towards IOCG mineralisation, in this case specifically, Cu;

- Produced detailed isotopic, petrographic and hyperspectral data for 3 vertical profiles providing comprehensive comparison data along with geochemical data whereby meeting the objective to understand how surface cover sequence materials can be used as mineral exploration sampling media as well as understanding how geochemical signatures related to mineralisation are expressed within different surface sample media.

The major conclusions of this research are:

- A regolith landform map of the area is essential to provide a visual guide to understanding of the source of sampling materials, in this case; carbonate rocks and mallee trees, in context with the surrounding landscape. This is especially important when conducting carbonate rock surveys in regions where limestone rocks also occur. A well-constructed map will be a good indicator of what to expect with regard to direction of erosion and dispersion and an indicator of transported versus in situ, sediments;
- Hyperspectral datasets were found to be useful for defining and differentiating mineral species where visual identification was difficult and where whole-rock chemistry had been undertaken rendering the sample to a homogenised powder. This was apparent when looking at composition of sediments that otherwise would had just been labelled

‘gravel’ or ‘weathered granite’ and ‘carbonate’ where carbonate also contained calcite and carbonate as expected, but also contained some or all of the following; dolomite, montmorillonite and sometimes even kaolinite;

- Isotopic data was initially thought to be the key to define differences between limestone and pedogenic carbonate as the limestone, theoretically should preserve isotopic signature of the seawater when it was originally formed and contain a heavier signature for pedogenically formed carbonates and heavier yet for basement rocks. Unfortunately due to various factors as described in Chapter 2, the isotopic differences were not significant enough for discriminating limestones from pedogenic carbonate rocks. However, the isotopes used ($^{87}Sr/^{86}Sr$) were suitable for determining an age approximation for the Melton Limestone which did agree with published dates and if undertaken again, could be refined so as to be more precise, although this was outside of the scope and purpose of the study. The usage of Sr isotopes was the lead in factor to looking at Sr as a whole element and its use in the ratio Ca/Sr which was found to be more useful;
- Ca/Sr ratios can be used to discriminate marine and pedogenic carbonate-bearing rocks across Yorke Peninsula. Pedogenic carbonate rocks have a Ca/Sr <650 and marine carbonate rocks have a Ca/Sr ratio >1260 (Fig. 5.1). This was based on the Ca/Sr ratio differences in the vertical profiles of Chapter 2 where it was able to be confirmed by visual analysis using field samples and thin sections. The Ca/Sr ratios were also found similarly in carbonate rocks throughout the Yorke Peninsula as well as other regions (Central South Australia and New South Wales;

Chapter 3) This has the potential to be assessed quickly in the field using existing portable whole-rock geochemical analyser technology or in retrospective filtering of older datasets;

- Pedogenic carbonate rocks throughout the Yorke Peninsula preserve geochemical signatures that can be related to known Cu occurrences within underlying basement rocks. Marine carbonates do not preserve the signature of Cu mineralisation across the Yorke Peninsula;
- Field assessment of Ca/Sr ratios during a carbonate sampling exploration campaign will decrease the risk of collecting incorrect sample media, and is applicable to the Yorke Peninsula and possibly other similar carbonate regolith dominated terrains such as southern Australia and other arid regions found around ~30°N and ~30°S (Chapter 2);
- The majority of carbonate material occurring at the surface across the Yorke Peninsula has a pedogenic origin (Ca/Sr ratios < 650), with lesser occurrences of carbonate preserving Ca/Sr ratios intermediate between pedogenic- and marine-origin and one preserving marine Ca/Sr ratios;
- The Ca and Sr concentration within the carbonate rocks across the Yorke Peninsula is influenced by the chemistry of both rainwater and underlying marine carbonate, may be more apparent in samples with a Ca/Sr >650 and needs to be considered when assessing a pedogenic or marine origin using Ca/Sr ratios;
- Pedogenic carbonate rocks contain background Cu concentrations of ~5.3ppm and elevated Cu concentrations above ~13ppm and up to 36ppm;

- Elevated Cu within the pedogenic carbonates is related to elemental dispersion from the underlying Cu-rich basement and not from other sources such as windblown contamination;
- Mallee eucalypt species have the ability to transfer elemental signals from deep in the substrate on which they grow (Fig. 5.1);
- Statistical analysis demonstrated the ability to combine the four sampled species;
- The sampled mallee eucalypts preserve background Cu concentrations of ~3.8ppm Cu, with higher concentrations between 6 and 10ppm;
- Elevated concentrations of Cu within the mallee eucalypt species are sourced from proximal areas of known Cu mineralisation and not from windblown contamination or farming practices (e.g. fertilizers) (Fig. 5.1).

This study has shown that pedogenic rocks and a variety of mallee eucalypt species from the Yorke Peninsula region are a suitable geochemical exploration sample media, and both sample types preserve elevated concentrations of Cu in areas proximal to known Cu occurrences. However, considerations are required when sampling both types of media. These include the influences of Ca and Sr sources (e.g. meteoric water, underlying substrate) that may affect Ca/Sr ratios used to discriminate pedogenic and marine carbonate rocks, and potential sources of contamination (e.g. windblown, fertilizer use). The widespread distribution of pedogenic carbonate rocks and mallee-eucalypt across southern Australia along with their ability to access and transfer geochemical signals from deep within the substrate implies they are a readily available sample medium that may be suitable for use throughout this region. The results provided insight into the processes of developing geochemical signatures of underlying mineralisation and their use in exploration.

Follow up future research in these areas of study could include, but is not limited to;

- Investigate what form the Cu is associated with or incorporated into the pedogenic carbonate;
- Investigating the depth that eucalypt trees roots are able to penetrate and still effectively transfer elemental signatures into their leaves;
- A detailed investigation into other areas around Australia or the rest of the world that may have a similar juxtaposition of pedogenic and marine carbonates and applying the methods used in this study.

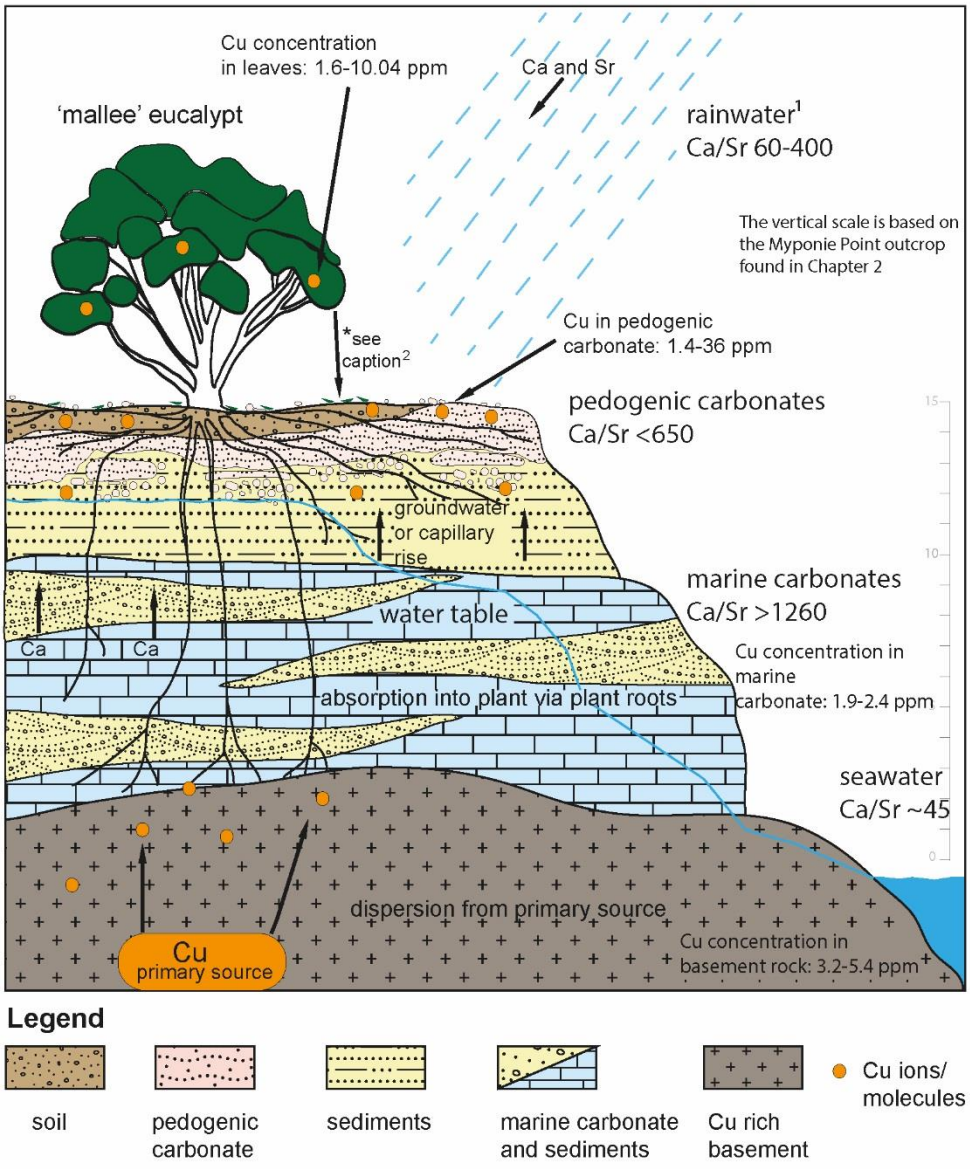

Figure 5.1 Conceptual model depicting key results of this research. Copper present in IOCG prospective basement rocks is dispersed throughout the overlying sediments and found lesser in marine carbonates and greater in both pedogenic carbonates and mallee-eucalypts. Chapter 2: Ca/Sr ratios results are presented along with the association of Cu in both the basement and the overlying pedogenic carbonate rocks; Chapter 3: Ca/Sr ratios are assessed on a regional dataset and sources of both Ca and Sr are discussed. Results of Cu dispersion throughout surface occurring carbonate rocks is presented; and Chapter 4: dispersion of Cu from underlying basement rocks into mallee-eucalypts is presented. [1] Rainwater Ca/ Sr ratios are extrapolated from Crosbie et al., (2012). [2] Leaf litter enriched in Cu may also concentrate Cu signatures from underlying substrate into the overlying soils (Lintern, 1989).

References

Australian Native Vegetation Assessment, 2001. Australian Natural Resources Atlas. National Land and Water Resources Audit, Land and Water Australia, Canberra.

Anand, R.R., 2005. Weathering history, landscape evolution and implications for exploration, in: Anand, R.R., Butt, C.R.M., Robertson, I.D.M., Scott, K.M., Cornelius, M. (Eds.). Cooperative Research Centre for Landscape Environments and Mineral Exploration (CRC LEME) CSIRO Exploration and Mining Bentley West. Aust. Australia.

Anand, R.R., 2016a. Importance of 3-D regolith-landform control in areas of transported cover: implications for geochemical exploration. Geochemistry: Exploration, Environment, Analysis: GEEA 16, 14–26.

Anand, R.R., 2016b. Regolith-landform processes and geochemical exploration for base metal deposits in regolith-dominated terrains of the Mt Isa region, northwest Queensland, Australia. Ore Geology Reviews 73, 451–474.

Anand, R.R., Pain, M., 2002. Regolith geology of the Yilgarn Craton, Western Australia: implications for exploration. Australian Journal of Earth Sciences 49, 3–162.

Arne, D.C., Stott, J.E., Waldron, H.M., 1999. Biogeochemistry of the Ballarat East goldfield, Victoria, Australia. Journal of Geochemical Exploration 67, 1–14.

Ashley, P.M., Wolfenden, B.J., 2005. Halls Peak massive sulphide deposits, New England, NSW, in: Butt, C.R.M., Robertson, I.D.M., Scott, K.M., Cornelius, M. (Eds.), Regolith expression of Australian ore systems; A compilation of exploration case histories with conceptual dispersion, process and exploration models. Cooperative Research Centre for Landscape Environments and Mineral Exploration (CRC LEME) CSIRO Exploration and Mining Bentley, Western Australia., pp 163–164

Attiwill, P.M., Adams, M.A., 1996. Nutrition of Eucalypts. CSIRO Publishing, Australia.

Bain, D.C., Bacon, J.R., 1994. Strontium isotopes as indicators of mineral weathering in catchments. Catena 22, 201–214.

Balabanova, B., T. Stafilov, T., R. Sˇajn, R., Bacˇeva, K., 2014. Comparison of response of moss, lichens and attic dust to geology and atmospheric pollution from copper mine. International Journal of Environmental Science and Technology 11, 517–528.

Batjes, N.H., 2012. ISRIC-WISE derived soil properties on a 5 by 5 arc-minutes global grid (ver. 1.2). Report 2012/01 (with data set, available at www.isric.org) ISRIC-World Soil Information, Wageningen, pp. 1–52.

Bennett, L.T., Weston, C.J., Judd, T.S., Attiwill, P.M., Whiteman, P.H., 1996. The effects of fertilizers on early growth and foliar nutrient concentrations of three plantation eucalypts on high quality sites in Gippsland, southeastern Australia. Forest Ecology and Management 89, 213–226.

Binks, P.J., Borner, J.E., Rau, G., Gunter, J., Busuttil, S., Little, G., McGeough, M., Fidler, R., Price, A., Hooper, B., 2004. MIM Exploration: Maitland. Annual and final reports to licence surrender for the period 7/9/1992 to 24/9/2004. Primary Industries and Resources South Australia Open File Envelope No 8725.

BonWick, C.M., 1997. Discovery of Challenger Gold Deposit Implications for further exploration on the Gawler Craton, New Generation Gold Mines ’97.

Case Histories of Discovery, Conference Proceedings, AMF, Glenside, Australia, pp. 7-1 – 7-15.

Bowen, G.J., Wilkinson, B., 2002. Spatial distribution of $\delta^{18}O$ in meteoric precipitation. Geology 30, 315–331.

Brantley, S.L., Chesley, J.T., Stillings, L.L., 1998. Isotopic ratios and release rates of strontium measured from weathering feldspars. Geochimica et Cosmochimica Acta 62, 1493–1500.

Brooker, M.I.H., Slee, A.V., Connors, J.R., Duffy, S.M., 2002. Eucalypts of Southern Australia; EUCLID Software CD, Second Edition. CSIRO Publishing, Australia.

Brooks, R.R., 1973. Geobotany and Biogeochemistry in Mineral Exploration. Harper and Row.

Brown, A.D., Hill, S.M., 2005. White Dam Au-Cu prospect, Curnamona Province, South Australia, in: Butt, C.R.M., Robertson, I.D.M., Scott, K.M., Cornelius, M. (Eds.), Regolith expression of Australian ore systems; a compilation of exploration case histories with conceptual dispersion, process

and exploration models. Cooperative Research Centre for Landscape Environments and Mineral Exploration (CRC LEME) CSIRO Exploration and Mining, Western Australia., pp 392–394.

Bureau of Meteorology, 2018. Climate statistics for Australian locations; Summary statistics Maitland SA. Commonwealth of Australia Bureau of Meteorology, Australia.

Bureau of Meteorology, 2017. Wind roses for selected locations in Australia. Commonwealth of Australia Bureau of Meteorology, Australia.

Burke, W.H., Denison, R.E., Hetherington, E.A., Koepnick, R.B., Nelson, H.F., Otto, J.B., 1982. Variation of seawater $^{87}Sr/^{86}Sr$ throughout Phanerozoic time. Geology 10, 516–519.

Burton, G.R., 2015. Petrological and geochemical evidence of metasomatism and the nature of the calcic progenitor rock at the Doradilla prospect, New South Wales. Report GS2015/1395, Geological Survey of New South Wales, Department of Primary Industries.

Busche, F.D., 1989. Using plants as an exploration tool for gold. Journal of Geochemical Exploration 32, 199–209.

Butt, C.R.M., 2005. Vegetation Communities, in: Butt, C.R.M., Robertson, I.D.M., Scott, K.M., Cornelius, M. (Eds.), Regolith expression of Australian ore systems; A compilation of exploration case histories with conceptual dispersion, process and exploration models. Cooperative Research Centre for Landscape Environments and Mineral Exploration (CRC LEME) CSIRO Exploration and Mining Bentley West. Aust. Australia., pp. 49–51.

Butt, C.R.M., Robertson, I.D.M., Scott, K.M., Cornelius, M., (Eds.). 2005a. Regolith expression of Australian ore systems; a compilation of exploration case histories with conceptual dispersion, process and exploration models. CRC LEME, Perth WA, 423 p.

Butt, C.R.M., Scott, K.M., Cornelius, M., Robertson, I.D.M., 2005b. Sample media, in: Butt, C.R.M., Robertson, I.D.M., Scott, K.M., Cornelius, M. (Eds.), Regolith expression of Australian ore systems; A compilation of exploration case histories with conceptual dispersion, process and exploration models. Cooperative Research Centre for Landscape Environments and Mineral Exploration (CRC LEME) CSIRO Exploration and Mining Bentley West. Aust. Australia., pp. 53–79.

Chatterjee, J., Singh, S.K., 2012. $^{87}Sr/^{86}Sr$ and major ion composition of rainwater of Ahmedabad, India: Sources of base cations. Atmospheric Environment 63, 60–67.

Chen, X.Y., Lintern, M.J., Roach, I.C., 2002. Calcrete: characteristics, distribution and use in mineral exploration, Cooperative Research Centre for Landscape Environments and Mineral Exploration., 170 p.

Cheng, M.-C., You, C.-F., Lin, F.-J., Chung, C.-H., Huang, K.-F., 2010. Seasonal variation in long-range transported dust to a subtropical islet offshore northern Taiwan: Chemical composition and Sr isotopic evidence in rainwater. Atmospheric Environment 44, 3386–3393.

Chiquet, A., Michard, A., Nahon, D., Hamelin, B., 1999. Atmospheric input vs in situ weathering in the genesis of calcretes: An Sr isotope study at Galvez (Central Spain). Geochimica et Cosmochimica Acta 63 (3–4), 311–323.

Cohen, D.R., Dunlop, A.C., Shen, X.C., Alipour, S., 2005. Mrangelli Pb-Zn-As prospect, Cobar District, New South Wales, in: Butt, C.R.M., Robertson, I.D.M., Scott, K.M., Cornelius, M. (Eds.), Regolith expression of Australian ore systems; a compilation of exploration case histories with conceptual dispersion, process and exploration models. Cooperative Research Centre for Landscape

Environments and Mineral Exploration (CRC LEME) CSIRO Exploration and Mining Bentley, Western Australia. pp 177–179.

Cohen, D.R., Hoffman, E.L., Nichol, I., 1987. Biogeochemistry: A geochemical method for gold exploration in the Canadian Shield. Journal of Geochemical Exploration 29, 49–73.

Cohen, D.R., Silva-Santisteban, C.M., Rutherford, N.F., Garnett, D.L., Waldron, H.M., 1999. Comparison of vegetation and stream sediment geochemical patterns in northeastern New South Wales. Journal of Geochemical Exploration 66, 469–489.

Conor, C., 1995. Moonta-Wallaroo region - An interpretation of the geology of the Maitland and Wallaroo 1:100,000 sheet areas. Primary Industries and Resources South Australia Open File Envelope No 8886.

Conor, C., 2016. Geological Field Excursion Guide - IOCGs - Where it all began: The Moonta-Wallaroo region of the eastern Gawler Craton. Department of State Development, South Australia. Report Book 2016/00009.

Conor, C., Raymond, O., Baker, T., Teale, G., Say, P., Lowe, G., 2010. Alteration and mineralisation in the Moonta-Wallaroo copper-gold mining field region, Olympic Domain, South Australia, in: Porter, T.M. (Ed.), Hydrothermal Iron Oxide Copper-Gold and Related Deposits: a Global Perspective. Advances in the Understanding of IOCG Deposits. PGC Publishing, Adelaide, pp. 147–170.

Conor, C.H.H., 2002. The Palaeo-Mesoproterozoic geology of northern Yorke Peninsula, South Australia: Hiltaba Suite-related alteration and mineralisation of the Moonta-Wallaroo Cu-Au District. Department of Primary Industries and Resources, South Australia. Report Book 2002/007.

Cooper, J.A., Mortimer, G.E., Rosier, C.M., Uppill, R.K., 1985. Gawler Range magmatism—further isotopic age data. Australian Journal of Earth Sciences 32, 115–123.

Cowley, W.M., 2005. Solid geology of South Australia. South Australia. Department of Primary Industries and Resources. Mineral Exploration Data Package, 15, in: Cowley, W.M. (Ed.). DMITRE, South Australia.

Cowley, W.M., Conor, C., Zang, W., 2003. New and revised Proterozoic stratigraphic units on northern Yorke Peninsula. In Primary Industries and Resources, MESA Journal 29, 46–58.

Crawford, A., 1965. The Geology of Yorke Peninsula: Bulletin No. 39. Geological Society of South Australia, 1–138.

Creaser, R.A., 1996. Petrogenesis of a Mesoproterozoic quartz latite-granitoid suite from the Roxby Downs area South Australia. Precambrian Research 79, 371–394.

Creaser, R.A., Cooper, J.A., 1993. U–Pb geochronology of Middle Proterozoic felsic magmatism surrounding the Olympic Dam Cu-U-Au-Ag and Moonta Cu-Au-Ag deposits, South Australia. Economic Geology 88, 186–197.

Creaser, R.A., Fanning, C.M., 1993. A U–Pb zircon study of the Mesoproterozoic Charleston Granite, Gawler Craton South Australia. Australian Journal of Earth Sciences 40, 519–526.

Crosbie, R., Morrow, D., Cresswell, R., Leaney, F., Lamontagne, S., Lefournour, M., 2012. New insights to the chemical and isotopic composition of

rainfall across Australia., CSIRO Water for a Healthy Country Flagship, Australia.

Crous, K.Y., Osvaldsson, A., Ellsworth, D.S., 2015. Is phosphorus limiting in a mature Eucalyptus woodland? Phosphorus fertilisation stimulates stem growth. Plant Soil 391, 293–305.

Dart, R.C., Barovich, K.M., Chittleborough, D.J., Hill, S.M., 2007. Calcium in regolith carbonates of central and southern Australia: Its source and implications for the global carbon cycle. Paleogeography, Palaeoclimatology, Palaeoecology 249, 322–334.

Dart, R.C., Barovich, K.M., Hill, S.M., Chittleborough, D.J., 2012. Sr-isotopes as a tracer of Ca sources and mobility in profiles hosting regolith carbonates from southern Australia. Australian Journal of Earth Sciences 59, 373–382.

Department of State Development, 2014. Understanding dryland farming: information for mineral explorers in South Australia. Report Book 2013/ 00017, Resources and Energy Group., V2.0, Department of State Development, Adelaide, South Australia.

Department of the Premier and Cabinet, 2017. South Australian Resources Information Gateway (SARIG), Map Theme- Geoscientific, Government of South Australia, https://map.sarig.sa.gov.au Last accessed 28/11/2017.

DEWNR, 2013. Non-prescribed surface water resources assessment - Northern and Yorke natural resources management region, Government of South Australia, through Department of Environment, Water and Natural Resources, Adelaide.

DEWNR, 2017. Nature Maps. Department of Environment, Water and Natural Resources, Government of South Australia. http://naturemaps.sa.gov.au/index.html Last accessed 04/04/2017.

Dietman, B.J., 2009. Regolith and associated geochemical and biogeochemical expression of buried copper-gold mineralisation at the Hillside Prospect, Yorke Peninsula. Honors Thesis, unpublished. University of Adelaide, p. 208.

Dietrich, F., Diaz, N., Deschamps, P., Ngatcha, B.N., Sebag, D., Verrecchia, E.P., 2017. Origin of calcium in pedogenic carbonate nodules from silicate watersheds in the Far North Region of Cameroon: Respective contribution of in situ weathering source and dust input. Chemical Geology 460, 54–69.

Drexel, J.F., Preiss, W.V., 1995. The geology of South Australia, Volume 2; The Phanerozoic. Geological Survey of South Australia, South Australia.

Drexel, J.F., Preiss, W.V., Parker, A.J., 1993. The geology of South Australia, Volume 1; the Precambrian. Geological Survey of South Australia, South Australia.

Drown, C., 2003. The Barns Gold Project: Discovery in an emerging district. MESA Journal 28, 4–9.

Dunn, C., 1986. Biogeochemistry as an aid to exploration for gold, platinum and palladium in the northern forests of Saskatchewan, Canada. Journal of Geochemical Exploration 25, 21–40.

Dunn, C., 2007. Biogeochemistry in Mineral Exploration, 2 ed. Elsevier, Amsterdam, The Netherlands.

Edmond, J.M., 1992. Himalayan tectonics, weathering processes, and the strontium isotope record in marine limestones. Science, New Series 258, 1594–1597.

Fabris, A.J., 2010. Investigation into the use of radon and soil sampling in exploration at the Hillside copper-gold deposit, South Australia. Primary Indusries and Resources SA, Government of South Australia.

Fanning, C.M., Flint, R.B., Parker, A.J., Ludwig, K.R., Blisset, A.H., 1988. Refined Proterozoic evolution of the Gawler Craton, South Australia, through U–Pb zircon geochronology. Precambrian Research 40/41, 363–386.

Fantle, M.S., Tipper, T., 2014. Calcium isotopes in the global biogeochemical Ca cycle: Implications for development of a Ca isotope proxy. Earth-Science Reviews 129, 148–177.

Fensham, R.J., Fairfax, R.J., 2007. Drought-related tree death of savanna eucalypts: species susceptibility, soil conditions and root architecture. Journal of Vegetation Science 18, 71–80.

Ferris, G.M., Schwarz, M.P., Heithersay, P., 2002. The geological framework, distribution and controls of Fe-oxide and related alteration, and Cu-Au mineralisation in the Gawler Craton, South Australia., in: Porter, T.M. (Ed.), Hydrothermal Iron Oxide Copper-Gold and Related Deposits: A Global Perspective, vol. 2. PGC Publishing, Adelaide, pp. 1–23.

Fitzpatrick, R.W., Chittleborough, D.J., 2002. Titanium and Zirconium Minerals, in: Dixon, J.B., Schulze, D.G. (Eds.), Soil Mineralogy with Environmental Applications (Soil Science Society of America Book Series, No. 7). Soil Science Society of America, Wisconsin, USA.

Forbes, C., Giles, D., Freeman, H., Sawyer, M., Normington, V., 2015. Glacial dispersion of hydrothermal monazite in the Prominent Hill deposit: An exploration tool. Journal of Geochemical Exploration 156, 10–33.

Forbes, C.J., Giles, D., Hand, M., Betts, P.G., Suzuki, K., Chalmers, N., Dutch, R., 2011. Using P–T paths to interpret the tectonothermal setting of prograde metamorphism: An example from the northeastern Gawler Craton, South Australia. Precambrian Research 185, 65–85.

Ghaderian, S.M., Ravandi, A.A.G., 2012. Accumulation of copper and other heavy metals by plants growing on Sarcheshmeh copper mining area, Iran. Journal of Geochemical Exploration 123, 25–32.

Ghavami-Riabi, R., Theart, H.F.J., De Jager, C., 2008. Detection of concealed Cu–Zn massive sulfide mineralization below eolian sand and a calcrete cover in the eastern part of the Namaqua Metamorphic Province, South Africa. Journal of Geochemical Exploration 97, 83–101.

Giles, D., Hillis, R., Cleverley, J., 2014. Deep Exploration Technologies Provide the Pathway to Deep Discovery, SEG Newsletter; Advancing Science and Discovery. Society of Economic Geologists, Inc., Colorado, pp. 1, 23 – 27.

Glen, R., 1991. The Geology of Cobar Country, Geological Survey of New South Wales. New South Wales Department of Minerals and Energy.

Gray, D.J., Noble, R.R.P., Reid, N., 2009. Hydrogeochemical mapping of northeast Yilgarn groundwater: Geological Survey of Western Australia, Record 2009/21, p. 78.

Guj, P., Schodde, R., 2013. Where are Australians Mines of Tomorrow? Australian Institute of Mining and Metallurgy Bulletin June 2013, 76 – 82.

Hamidi, E.M., Nahon, D., McKenzie, J.A., Michard, A., Colin, F., Kamel, S., 1999. Marine Sr (Ca) input in Quaternary volcanic rock weathering profiles from the Mediterranean coast of Morocco: Sr isotopic approach. Terra Nova 11, 157–161.

Hand, M., Reid, A., Jagodzinski, L., 2007. Tectonic framework and evolution of the Gawler Craton South Australia. Economic Geology 102, 1377–1395.

Hartley, K.L., 2000. Regolith studies of the Moonta copper mines, Yorke Peninsula, South Australia. B.Sc. Honours thesis, University of Melbourne, p. 66. Unpublished.

Hesse, P.P., McTainsh, G.H., 2003. Australian dust deposits: modern processes and the Quaternary record. Quaternary Science Reviews 22, 2007–2035.

Hill, S.M., McQueen, K.G., Foster, K.A., 1999. Regolith carbonate accumulations in Western and Central NSW: characteristics and potential as an exploration sampling medium., in: Taylor, G.M., Pain, C.F. (Eds.), State of the Regolith, Proceedings of Regolith. CRC LEME, Perth, 98, pp. 191–208.

Hillis, R., Giles, D., Van Der Wielen, S., Baensch, A., Cleverley, J., Fabris, A.J., Halley, S., Harris, M., Hill, S.M., Kanck, P.A., Kepic, A., Soe, S., Stewart, G., Uvarova, Y., 2014. Coiled Tubing Drilling and Real-Time Sensing-Enabling Prospecting Drilling in the 21st Century, in: Kelley, K.D., Golden, H.C. (Eds.), SEG Conference on Keystone- Building Exploration Capability for the 21st

Century. Society of Economic Geologists Special Publications Series, Issue 18, Keystone, Colorado pp 243–259,.

Hoek, J.D., Schaefer, B.F., 1998. Palaeoproterozoic Kimban mobile belt Eyre Peninsula: timing and significance of felsic and mafic magmatism and deformation. Australian Journal of Earth Sciences 45, 305–313.

Howarth, R.J., McArthur, J.M., 1997. Statistics for strontium isotope stratigraphy: a robust LOWESS fit to the marine Sr-isotope curve for 0 to 206 Ma, with look-up table for derivation of numeric age. Journal of Geology 105, 441–456.

Hulme, K.A., 2008. Eucalyptus camaldulensis (river red gum) Biogeochemistry; an Innovative Tool for Mineral Exploration in the Curnamona Province and Adjacent Regions. , PhD Thesis. University of Adelaide, South Australia. unpublished.

Hulme, K.A., Hill, S.M., 2003. River red gums as a biogeochemical sampling medium in mineral exploration and environmental chemistry programs in the Curnamona Craton and adjacent regions of NSW and SA., in: Roach, I.C. (Ed.), Advances in Regolith. CRC LEME.

Huntington, J.H., Mauger, A.J., Skirrow, R.G., Bastrakov, E.N., Connor, P., Mason, P., Keeling, J.K., Coward, D.A., Berman, M., Phillips, R., Whitbourn, L.B., Heithersay, P.S., 2006. Automated mineralogical core logging at the Emmie Bluff iron oxide copper-gold. . Primary Industries and Resources South Australia, MESA Journal 41, 38–44.

Ismail, R., Ciobanu, C.L., Cook, N.J., Teale, G.S., Giles, D., Schmidt Mumm, A., Wade, B., 2014. Rare earth sand other trace elements in minerals from skarn assemblages, Hillside iron oxide-copper-gold deposit, Yorke Peninsula, South Australia. Lithos, 184–187, 456–477.

Iwata, K., Schmidt, B.L., Leitch, E.C., Allan, A.D., Watanabe, T., 1995. Ordovidan microfossils from the Ballast Formation (Girilambone Group) of New South Wales. Australian Journal of Earth Sciences 42, 371–376.

James, N.P., Bone, Y., 2015. Pleistocene aeolianites at Cape Spencer, South Australia; record of a vanished inner neritic cool-water carbonate factory. . Sedimentology 62, 2038–2059.

Judd, T.S., Attiwill, P.M., Adams, M.A., 1996. Nutrient Concentration in Eucalyptus: A synthesis in relation to differences between taxa, sites and

components, in: Attiwill, P.M., Adams, M.A. (Eds.), Nutrition of Eucalypts. CSIRO Publishing, Australia, p. 448.

Kabata-Pendias, A., Pendias, H., 2001. Trace Elements in Soils and Plants. CRC Press LLC, Boca Raton, Florida.

Keeling, J.L., Hartley, K.L., 2005. Poona and Wheal Hughes Cu deposits, Moonta, South Australia, in: Butt, C.R.M., Robertson, I.D.M., Scott, K.M., Cornelius, M. (Eds.), Regolith Expression of Australian Ore Systems. Cooperative Research Centre for Landscape Environments and Mineral Exploration (CRC LEME) CSIRO Exploration and Mining Bentley Western Australia. pp 383–385.

Kelepertsis, A.E., Andrulakis, I., 1983. Geobotany -biogeochemistry for mineral exploration of sulphide deposits in northern Greece - heavy metal accumulation by Rumex acetosella L. and Minuartia verna (L.) hiern. Journal of Geochemical Exploration 18, 267–274.

Khadkikar, A.S., Chamyal, L.S., Ramesh, R., 2000. The character and genesis of calcrete in Late Quaternary alluvial deposits, Gujarat, western India, and its bearing on the interpretation of ancient climates. Paleogeography, Palaeoclimatology, Palaeoecology 162, 239–261.

Khadkikar, A.S., Merh, S.S., Malik, J.N., Chamyal, L.S., 1998. Calcretes in semi-arid alluvial systems: formative pathways and sinks. Sedimentary Geology 116, 251–260.

Kovalevsky, A.L., 1987. Biogeochemical Exploration for Mineral Deposits. VNU Science Press, The Netherlands.

Kyser, T.K., James, N.P., Bone, Y., 1998. Alteration of Cenozoic cool-water carbonates to low-Mg calcite in marine waters, Gambier Embayment, South Australia Journal of Sedimentary Research 68, 947–955.

Lindsay, J.M., 1970. Melton Limestone: multiple mid-Tertiary transgressions, south-eastern Gawler Platform. Geological Survey of South Australia, Quarterly Geological Notes 33, 2–10.

Lintern, M.J., 1989. Study of the distribution of gold in soils at Mt Hope, Western Australia. CSIRO Division of Exploration Geoscience. Restricted Report 24R, 40 pp. (Reissued as Open File Report 65, CRC LEME, Perth, 1999).

Lintern, M.J., 2005. Challenger gold prospect, Gawler Craton, South Australia, in: Butt, C.R.M., Robertson, I.D.M., Scott, K.M., Cornelius, M. (Eds.), Regolith Expression of Australian Ore Systems. Cooperative Research Centre for Landscape Environments and Mineral Exploration (CRC LEME) CSIRO Exploration and Mining Bentley West. Aust. Australia., pp. 236–238.

Lintern, M.J., 2007. Vegetation controls on the formation of gold anomalies in calcrete and other materials at the Barns Gold Prospect, Eyre Peninsula,South Australia. Geochemistry: Exploration, Environment, Analysis: GEEA 7, 249–266.

Lintern, M.J., 2015. The association of gold with calcrete. Ore Geology Reviews 66, 132–199.

Lintern, M.J., Anand, R.R., Ryan, C., Paterson, D., 2013. Natural gold particles in Eucalyptus leaves and their relevance to exploration for buried gold deposits. Nature Communications 4, 1.

Lintern, M.J., Butt, C.R.M., Scott, K.M., 1997. Gold in vegetation and soil - three case studies from the goldfields of southern Western Australia. Journal of Geochemical Exploration 58, 1–14.

Lintern, M.J., Hough, R., Ryan, C., 2012. Experimental studies on the gold-in-calcrete anomaly at Edoldeh Tank Gold Prospect, Gawler Craton, South Australia. Journal of Geochemical Exploration 112, 189–205.

Lintern, M.J., Hough, R., Ryan, C., Watling, J., Verrall, M., 2009. Ionic gold in calcrete revealed by LA-ICP-MS, SXRF and XANES. Geochimica et Cosmochimica Acta 73, 1666 –1683.

Lintern, M.J., Sheard, M., 1999. Geochemistry and stratigraphy of the Challenger Gold Deposit Volume 1: Text, Regolith studies related to the Challenger Gold Deposit, Gawler Craton, South Australia. CRC LEME open file report 78 / PIRSA report book 98/10.

Lintern, M.J., Sheard, M., Buller, N., 2011. The gold-in-calcrete anomaly at the ET gold prospect, Gawler Craton, South Australia. Applied Geochemistry 26, 2027–2043.

Lintern, M.J., Sheard, M., Chivas, A.R., 2006. The source of pedogenic carbonate associated with gold-calcrete anomalies in the western Gawler Craton, South Australia. Chemical Geology 235, 299–324.

Liu, W.-J., Liu, C.-Q., Zhao, Z.-Q., Xu, Z.-F., Liang, C.S., Li, L., Feng, J.-Y., 2013. Elemental and strontium isotopic geochemistry of the soil profiles developed on limestone and sandstone in karstic terrain on Yunnan-Guizhou Plateau, China: Implications for chemical weathering and parent materials. Journal of Asian Earth Sciences 67–68, 138–152.

Marjoribanks, R., 2010. Geological Methods in Mineral Exploration and Mining, 2 ed. Springer, Heidelberg.

McArthur, J.M., Howarth, R.J., Bailey, T.R., 2001. Strontium isotope stratigraphy: LOWESS Version 3: Best fit to the marine Sr-Isotope curve for 0–509 Ma and accompanying look-up table for deriving numerical age. Journal of Geology 109, 155–170.

McArthur, J.M., Howarth, R.J., Shields, G.A., 2012. Strontium Isotope Stratigraphy, The Geologic Time Scale. Elsevier.

McClenaghan, M.B., Parkhill, M.A., Pronk, A.G., Seaman, A.A., McCurdy, M.W., Leybourne, M.I., 2017. Indicator mineral and geochemical signatures associated with the Sisson W–Mo deposit, New Brunswick, Canada. Geochemistry: Exploration, Environment, Analysis: GEEA 17, 297–313.

McDowell, M.C., Baynes, A., Medlin, G.C., Prideaux, G.J., 2012. The impact of European colonization on the late-Holocene non-volant mammals of Yorke Peninsula, South Australia. The Holocene 22, 1441–1450.

McQueen, K.G., 2006. Calcrete geochemistry in the Cobar-Girilambone region, New South Wales; CRC LEME open file report 200, CRC LEME, Bentley, Western Australia.

McQueen, K.G., 2008. Identifying Geochemical Anomalies (appendix 7), in: Sheard, M.J., Keeling, J.L., Lintern, M.J., Hou, B., McQueen, K.G., Hill, S.M. (Eds.), A guide for mineral exploration through the regolith of the central Gawler Craton, South Australia CRC LEME, Perth.

McQueen, K.G., Hill, S.M., Foster, K.A., 1999. The nature and distribution of regolith carbonate accumulations in southeastern Australia and their potential as a sampling medium in geochemical exploration. Journal of Geochemical Exploration 67, 67–82.

Mighall, T.M., Abrahams, P.W., Grattan, J.P., Hayes, D., Timberlake, S., Forsyth, S., 2002. Geochemical evidence for atmospheric pollution derived from prehistoric copper mining at Copa Hill, Cwmystwyth, mid-Wales, UK. The Science of the Total Environment 292, 69–80.

Milnes, A.R., 1992. Calcretes. In: Martini, I. P., Chesworth, W. Developments in Earth Surface Processes. Weathering, Soils and Palaeosols. Elsevier, Amsterdam.

Milnes, A.R., Hutton, J.T., 1983. Calcretes in Australia. In: Soils: An Australian Viewpoint. CSIRO, Melbourne/Academic Press, London.

Mitchell, C., Hill, S.M., Giles, D., Hulme, K.A., 2015. El Niño–La Niña cycles and biogeochemical sampling: variability of element concentrations within E. camaldulensis leaves in semi-arid Australia. Geochemistry: Exploration, Environment, Analysis: GEEA 15, 350–360.

Mokhtari, A.R., Cohen, D.R., Gatehouse, S.G., 2009. Geochemical effects of deeply buried Cu–Au mineralization on transported regolith in an arid terrain. Geochemistry: Exploration, Environment, Analysis: GEEA 9, 227–236.

Morales-Ruano, S., Both, R.A., Golding, S.D., 2002. A fluid inclusion and stable isotope study of the Moonta copper–gold deposits, South Australia: evidence for fluid immiscibility in a magmatic hydrothermal system. Chemical Geology 192, 211–226.

Närhi, P., Middleton, M., Sutinen, R., 2014. Biogeochemical multi-element signatures in common juniper at Mäkärärova, Finnish Lapland: Implications for Au and REE exploration. Journal of Geochemical Exploration 138, 50–58.

Neagle, N., 2008. A Biological Survey of the Mid North and Yorke Peninsula, South Australia, 2003–2004: Assessment of Biodiversity Assets at Risk.

Noble, R.R.P., 2012. Transported cover in northwestern Victoria, Australia — An impediment to geochemical exploration for gold. Journal of Geochemical Exploration 112, 139–151.

Pain, C.F., Chan., R., Craig., M., Gibson., D., Kilgour., P., Wilford, J.R., 2007. RTMAP regolith database field book and users guide (Second Edition). CRC LEME open file report 231, CRC LEME, Bentley, Western Australia.

Pain, M., Johnson, P., 2002. Yorke Peninsula paleochannel: Adelaide's long-term sand source. In Primary Industries and Resources, MESA Journal 27, 10–14.

Peterman, Z.E., Hedge, C.E., Tourtelot, H.A., 1970. Isotopic composition of strontium in sea water throughout Phanerozoic time. Geochimica et Cosmochimica Acta 84, 105–120.

Petts, A., 2009. Termitaria as regolith landscape attributes and sampling media in northern Australia. PhD Thesis, University of Adelaide. Unpublished.

Poustie, T., Abbot, P., 2006. Challenger Gold Mine — looking at a long-term future. MESA Journal 40, 4–7.

Prudencio, M.I., Dias, M.I., Waerenborgh, J.C., Ruiz, F., Trindade, M.J., Abad, M., Marques, R., Gouveia, M.A., 2011. Rare earth and other trace and major elemental distribution in a pedogenic calcrete profile (Slimene, NE Tunisia). Catena 87, 147–156.

Quade, J., Chivas, A.R., McCulloch, M.T., 1995. Strontium and carbon isotope tracers and the origins of soil carbonate in South Australia and Victoria. Paleogeography, Palaeoclimatology, Palaeoecology 113, 103–117.

Reid, N., Hill, S.M., 2010. Biogeochemical sampling for mineral exploration in arid terrains: Tanami Gold Province, Australia. Journal of Geochemical Exploration 104, 105–117.

Reid, N., Hill, S.M., 2013. Spinifex biogeochemistry across arid Australia: Mineral exploration potential and chromium accumulation. Applied Geochemistry 29, 92–101.

Reid, N., Hill, S.M., Lewis, D.M., 2008. Spinifex biogeochemical expressions of buried gold mineralisation: The great mineral exploration penetrator of transported regolith. Applied Geochemistry 23, 76–84.

Reith, F., Etschmann, B., Dart, R.C., Brewe, D.L., Vogt, S., Schmidt-Mumm, A., Brugger, J., 2011. Distribution and speciation of gold in biogenic and abiogenic calcium carbonates - Implications for the formation of gold anomolus calcrete. Geochimica et Cosmochimica Acta 75, 1942–1956.

Rencz, A.N., Watson, G.P., 1989. Biogeochemistry and LANDSAT TM data: application to gold exploration in northern New Brunswick. Journal of Geochemical Exploration 34, 271–284.

Roberts, S., 2007. Northern and Yorke Natural Resources Management Region water monitoring review, DWLBC Report 2006/15, Department of Water, Land and Biodiversity Conservation, Adelaide.

Salama, W., Gonzalez-Alvarez, I., Anand, R.R., 2016. Significance of weathering and regolith/landscape evolution for mineral exploration in the NE Albany-Fraser Orogen, Western Australia. Ore Geology Reviews 73, 500–521.

Schmidt Mumm, A., Reith, F., 2007. Biomediation of calcrete at the gold anomaly of the Barns prospect, Gawler Craton, South Australia. Journal of Geochemical Exploration 92, 13–33.

Schodde, R., 2014. The Global Shift to Undercover Exploration - How fast? How effective?, Keynote paper for the Society of Economic Geologists 2014 Conference, Keystone, Colorado.

Schodde, R., 2017a. Challenges of Exploring Under Deep Cover, Presentation to the AMIRA International's Exploration Managers Conference, Healesville, Victoria.

Schodde, R., 2017b. Keynote address; The National State of Exploration Copper to the World Conference, 27th June, 2017, Adelaide, Australia.

Sheard, M.J., Keeling, J.L., Lintern, M.J., Hou, B., McQueen, K.G., Hill, S.M., 2008. A guide for mineral exploration through the regolith of the central Gawler Craton, South Australia. CRC LEME, Perth.

Shimamura, T., Wada, T., Iwashita, M., Takaku, Y., Ohashi, H., 2006. Scavenging properties of major and trace species in rainfall collected in urban and suburban Tokyo. Atmospheric Environment 40, 4220–4227.

Skirrow, R., Fairclough, M., Budd, A., Lyons, P., Raymond, O., Milligan, P., Bastrakov, E., Fraser, G., Highet, L., Holm, O., Williams, N., 2006. Iron-oxide Cu-Au (U) potential map of the Gawler Craton, South Australia (first edition) 1:500,000 scale. Geoscience Australia, Canberra.

Skirrow., R.G., Bastrakov., E.N., Barovich., K., Fraser., G.L., Creaser., R.A., Fanning., C.M., Raymond., O.L., Davidson., G.J., 2007. Timing of Iron Oxide Cu-Au-(U) Hydrothermal Activity and Nd Isotope Constraints on Metal Sources in the Gawler Craton, South Australia. Economic Geology 102, 1441–1470.

Slee, A.V., Brooker, M.I.H., Duffy, S.M., West, J.G., 2006. Eucalypts of Australia; EUCLID Software CD, Third Edition, CSIRO Publishing, Melbourne.

Smith, R.E., 1996. Regolith research in support of mineral exploration in Australia. Journal of Geochemical Exploration 57, 159–173.

USGS, 2016. USGS Science for a changing world. Mineral Resources On-Line Spatial Data. https://mrdata.usgs.gov/geology/ Last accessed Feb. 2017.

van der Hoek, B.G., Hill, S.M., Dart, R.C., 2012. Calcrete and plant inter-relationships for the expression of concealed mineralization at the Tunkillia gold prospect, central Gawler Craton, Australia. Geochemistry: Exploration, Environment, Analysis: GEEA 12, 361–372.

Van der Hoven, S.J., Quade, J., 2002. Tracing spatial and temporal variations in the sources of calcium in pedogenic carbonates in a semiarid environment. Geoderma 108, 259–276.

Vasiliev, I., Reichart, G., Davies, G., Krijgsman, W., Stoica, M., 2010. Strontium isotope ratios of the Eastern Paratethys during the Mio-Pliocene transition;

Implications for interbasinal connectivity. Earth and Planetary Science Letters 292, 123–131.

Veizer, J., 1989. Strontium isotopes in seawater through time. Annual Review of Earth and Planetary Sciences 17, 141–167.

Veizer, J., Compston, W., 1974. $^{87}Sr/^{86}Sr$ composition in seawater during the Phanerozoic. Geochimica et Cosmochimica Acta 38 1461–1484.

Veizer, J., Compston, W., 1976. $^{87}Sr/^{86}Sr$ in Precambrian carbonates as an index of crustal evolution. Geochimica et Cosmochimica Acta 40, 905–914.

Wickman, F.W., 1948. Isotope ratios—A clue to the age of certain marine sediments. Journal of Geology 56, 61–66.

Wolff, K., Hill, S.M., Tiddy, C., Giles, D., Smernik, R., 2018. Biogeochemical expression of buried iron-oxide-copper-gold (IOCG) mineral systems in mallee eucalypts on the Yorke Peninsula, southern Olympic Domain; South Australia. Journal of Geochemical Exploration 185, 139–152.

Wolff, K., Tiddy, C., Giles, D., Hill, S.M., Pedogenic carbonate sampling for Cu exploration on the Yorke Peninsula, South Australia. Journal of Geochemical Exploration 194, 239–256.

Wolff, K., Tiddy, C., Giles, D., Hill, S.M., Gordon, G., 2017. Distinguishing pedogenic carbonates from weathered marine carbonates on the Yorke Peninsula, South Australia: Implications for mineral exploration. Journal of Geochemical Exploration 181, 81–98.

Wrigley, J., Fagg, M., 2010. Eucalypts: a celebration / John Wrigley and Murray Fagg. Allen & Unwin, Crows Nest NSW.

Wurst, A.T., 1994. Analyses of late stage, Mesoproterozoic, syn and post tectonic, magmatic events in the Moonta Sub-Domain: Implications for Cu-Au mineralisation in the "Copper Triangle" of South Australia. Hons. Thesis. Unpublished. University of Adelaide.

Zang, W., Cowley, W.M., Fairclough, M., 2006. Maitland Special South Australia 1:250000 Geological Series Sheet S153-12 - Explanatory Notes PIRSA Publishing Services, South Australia.

Zang, W., Hore, S., 2001. TER 1 Yorke Peninsula: well completion report. Department of Primary Industry and Resources, South Australia.

Zhao, Y.-Y., Zheng, Y.-F., Chen, F., 2009. Trace element and strontium isotope constraints on sedimentary environment of Ediacaran carbonates in southern Anhui, South China. Chemical Geology, 345–362.

Appendix

Appendix 1 **Chapter 2 Published Article**

Appendix 2 **Chapter 2 Whole-rock and Seawater Analytical Results**

Appendix 3 **Chapter 2 Spectral Analysis (HyLogger^{TM})**

Appendix 4 **Chapter 3 Published Article**

Appendix 5 **Chapter 3 Whole-rock Analytical Results**

Appendix 6 **Chapter 3 Seawater Analytical Results**

Appendix 7 **Chapter 4 Published Article**

Appendix 8 **Chapter 4 Vegetation Analytical Results**

Appendix 1

Published Article

Chapter 2:

Distinguishing pedogenic carbonates from weathered marine carbonates on the Yorke Peninsula, South Australia: Implications for mineral exploration

Journal of Geochemical Exploration 181 (2017) 81–98

Contents lists available at ScienceDirect

Journal of Geochemical Exploration

journal homepage: www.elsevier.com/locate/gexplo

Distinguishing pedogenic carbonates from weathered marine carbonates on the Yorke Peninsula, South Australia: Implications for mineral exploration

Keryn Wolff[a,*], Caroline Tiddy[a,1], David Giles[a,1], Steven M. Hill[b], Georgina Gordon[b]

[a] Deep Exploration Technologies Cooperative Research Centre (DET CRC), Department of Earth Sciences, University of Adelaide, Australia
[b] Geological Survey of South Australia, Department of Premier and Cabinet, South Australia

ARTICLE INFO

Keywords:
Regolith
Calcrete
Carbonate
Limestone
Strontium isotopes
Ca/Sr ratios
Mineral exploration

ABSTRACT

We present whole rock and strontium isotope geochemistry from geological profiles from the Yorke Peninsula in South Australia and provide a geochemical means of discriminating between Cenozoic marine carbonate-bearing rocks and Quaternary pedogenic carbonate-bearing rocks. Pedogenic carbonate-bearing rocks (commonly referred to as calcrete) are potentially useful mineral exploration sampling media whereas weathered marine carbonate-bearing rocks (limestone), are less useful. Distinguishing between the two in drill cuttings where textural information has been destroyed is difficult. Strontium isotope ratios are variable, strongly dependent on clastic sedimentary component and thus do not differentiate effectively between pedogenic and marine carbonate-bearing rocks. There is a systematic difference between Ca/Sr and Ca/Mg ratios in the pedogenic carbonate-bearing rocks compared to the weathered Cenozoic marine carbonate-bearing rocks. Pedogenic carbonate-bearing rocks have systematically lower Ca/Mg (< 28) and Ca/Sr (< 650) ratios than their marine counterparts Ca/Mg (> 35) and Ca/Sr (> 1260). This simple discriminant can be used to identify samples appropriate for carbonate sampling in mineral exploration, particularly in drill cuttings, as well as retrospective filtering of multi-element geochemical exploration data sets.

1. Introduction

Carbonate-dominated regolith has a widespread global distribution concentrated in the mid latitudes (Batjes, 2012; Chen et al., 2002) (Fig. 1). This material includes a range of weathered carbonate-bearing rocks, including limestone, as well as in situ, transported and reworked pedogenic carbonate-bearing rocks (sometimes referred to as calcrete but can also include dolomite), derived from atmospheric (e.g. dust and rain) accessions. The vast global extent of these lithologies has generated much interest in their origin, chemistry and paleo-environmental significance (Chen et al., 2002; Dart et al., 2012; Milnes, 1992; Milnes and Hutton, 1983; Poustie and Abbot, 2006; Quade et al., 1995).

Carbonate-bearing rocks have been widely studied for their strontium ($^{87}Sr/^{86}Sr$) isotopic composition to trace calcium source and mobility, soil carbonate origins and sedimentary environments (Dart et al., 2012; Liu et al., 2013; Quade et al., 1995; Zhao et al., 2009). This method has also been applied to trace sources of other elements such as using strontium (Sr) as a proxy for calcium (Ca) (Dart et al., 2007; Dart et al., 2012; Liu et al., 2013; Quade et al., 1995; Van der Hoven and Quade, 2002). Strontium isotopic studies using marine carbonate-bearing rocks typically relate to the chemistry of the water in which they are formed and are commonly used for the purpose of dating (e.g. Burke et al., 1982; Howarth and McArthur, 1997; McArthur et al., 2001; McArthur et al., 2012).

Pedogenic carbonate-bearing rocks (such as calcrete) are widely used as a mineral exploration sampling medium (Chen et al., 2002; McQueen et al., 1999; Poustie and Abbot, 2006), and have been successfully utilised to discover and delineate various economic resource deposits around the world (Ghavami-Riabi et al., 2008; Lintern et al., 2005). The Challenger Gold Deposit within the Gawler Craton, South Australia (Fig. 2) was discovered following a regional carbonate rock sampling program (Poustie and Abbot, 2006). A dramatic increase in interest in carbonate geochemistry followed (Chen et al., 2002; Lintern et al., 2012; Reith et al., 2011; van der Hoek et al., 2012). It is essential, although often very difficult, to distinguish marine carbonate-bearing rocks from pedogenic carbonate-bearing rocks when undertaking a carbonate sampling program. This difficulty in distinction arises due to weathering of marine carbonate rocks typically resulting in recrystallization and pedogenic overprinting rendering the resulting sample morphology indistinguishable. This can be problematic in

* Corresponding author at: Department of Earth Sciences, Mawson Building, University of Adelaide, North Terrace Campus, Adelaide, SA 5005, Australia.
E-mail address: keryn.wolff@alumni.adelaide.edu.au (K. Wolff).
[1] Now at Future Industries Institute, University of South Australia

http://dx.doi.org/10.1016/j.gexplo.2017.06.019
Received 13 February 2017; Received in revised form 7 June 2017; Accepted 28 June 2017
Available online 08 July 2017
0375-6742/

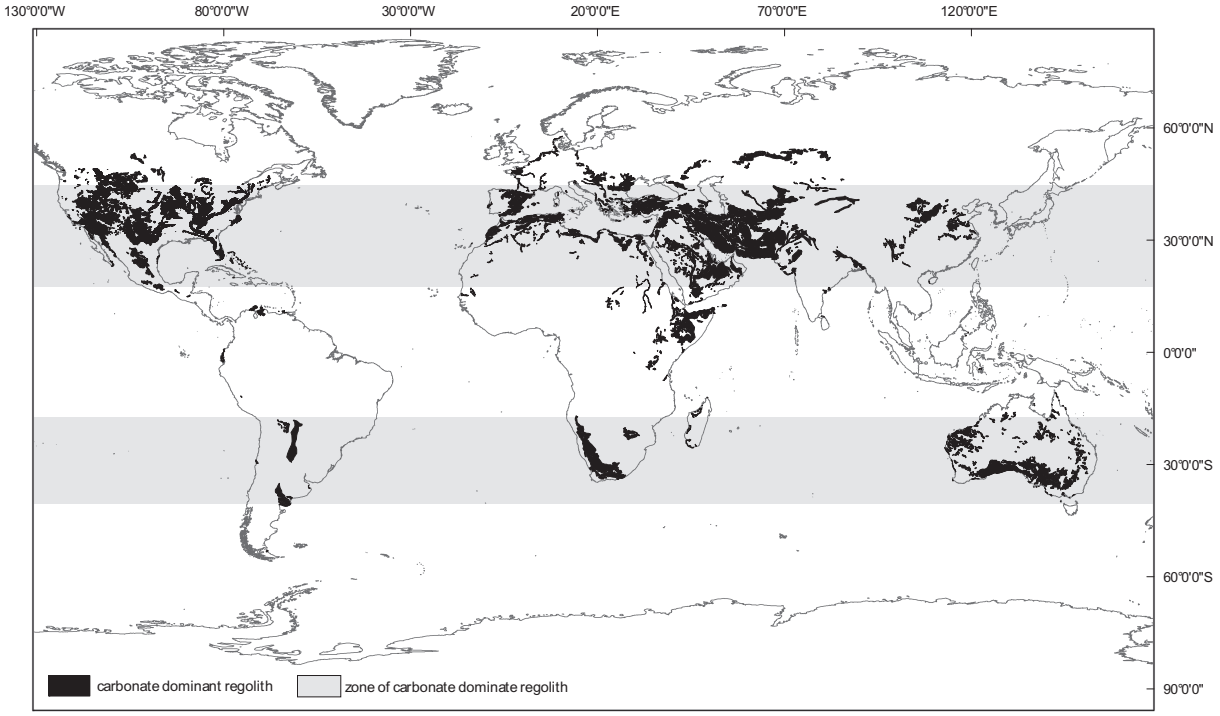

Fig. 1. Worldwide distribution of carbonate dominant regolith including limestone. Compiled from ISRIC (Batjes, 2012) and USGS datasets (USGS, 2016). Specific areas and general zones of carbonate dominated regolith are highlighted.

mineral exploration sampling campaigns as those undertaking the sampling are not always geologically trained. Additionally, in cases where drilling is being undertaken (e.g. air core, reverse circulation, rotary air blast and coiled tubing drilling) the returned sample comprises rock flour and small chips. Fine-scale textural information can be extremely difficult to impossible to distinguish in such material (e.g. Hillis et al., 2014; Marjoribanks, 2010). Distinction is essential as pedogenic carbonate-bearing rocks have the potential to carry a geochemical signature transferred from underlying mineralisation (e.g. Chen et al., 2002) whereas marine carbonate-bearing rocks typically reflect the chemistry of the water in which they formed.

The Yorke Peninsula in the southeastern Gawler Craton of South Australia (Fig. 2) is covered by large areas of both marine- and pedogenically-derived carbonate-bearing rocks. Additionally, the Yorke Peninsula region comprises sparsely exposed Proterozoic basement rocks that are prospective for iron oxide, copper and gold mineralisation (Conor, 2016; Conor et al., 2010; Conor, 2002; Cowley, 2005; Cowley et al., 2003; Drexel et al., 1993; Ismail et al., 2014; Zang et al., 2006). The ability to distinguish between weathered marine and pedogenic carbonate-bearing rocks in the cover sequence overlying a prospective region such as the Yorke Peninsula would therefore assist in exploration for mineral deposits under cover, as well as for reviewing and evaluating historical multi-element geochemical datasets.

This paper aims to set simple criteria that can be rapidly applied to distinguish between weathered marine and pedogenic carbonate-bearing rocks. This is done using hyperspectral analysis, microscopy and $^{87}Sr/^{86}Sr$ ratios to identify changes across three coastal carbonate-bearing profiles (Fig. 3), and combined with Ca/Sr ratios derived from whole rock geochemical data. These results are then used to develop criteria to distinguish between marine and pedogenically derived carbonate-bearing rocks. The potential influence this may have on exploration practices using this sampling medium is then discussed.

2. Strontium chemistry of marine sediments and regolith carbonates

Strontium isotope ratios ($^{87}Sr/^{86}Sr$) can be used to analyse calcium-rich materials such as soil carbonates, marine limestone and seawater (e.g. Dart et al., 2012; Vasiliev et al., 2010; Veizer, 1989). Strontium is used as a surrogate for Ca, as chemical properties such as valence and ionic radius are similar for both elements, which allows for easy substitution of Ca by Sr. Strontium is typically found in trace amounts in minerals containing calcium (Bain and Bacon, 1994; Van der Hoven and Quade, 2002).

The methodology for dating seawater using marine carbonate $^{87}Sr/^{86}Sr$ ratios is well established (e.g. Burke et al., 1982; McArthur et al., 2001; McArthur et al., 2012). Marine organisms access Ca (and by association Sr) for growth from seawater, which preserves a unique $^{87}Sr/^{86}Sr$ ratio. The $^{87}Sr/^{86}Sr$ ratios can be reliably used because the ^{86}Sr isotope remains constant over time (Bain and Bacon, 1994; Van der Hoven and Quade, 2002). The stable ^{87}Sr isotope is derived from the radiogenic decay of the isotope ^{87}Rb (e.g. Bain and Bacon, 1994; Van der Hoven and Quade, 2002; Wickman, 1948). Diagenesis and re-precipitation of Sr in carbonate rocks therefore will preserve the initial $^{87}Sr/^{86}Sr$ ratio at the time of precipitation (Veizer, 1989).

Ratios for $^{87}Sr/^{86}Sr$ in seawater have varied gradually throughout time and have been used to develop a Sr isotope seawater curve (Burke et al., 1982; McArthur et al., 2001; McArthur et al., 2012) (Fig. 4). This seawater curve has been compiled from $^{87}Sr/^{86}Sr$ ratios of calcite-rich marine fossils (McArthur et al., 2012). Any deviation from this curve may be attributed to contaminating factors such as clastic sediment input or modern sea spray (Veizer, 1989). Formation and erosion of continental rocks during the Earth's tectonic history along with groundwater discharge, river discharge and mid ocean ridge interactions all affect the balance of ^{87}Rb, and the resulting ^{87}Sr, in the seawater (Veizer, 1989). The gradual increase in $^{87}Sr/^{86}Sr$ ratios during the Cenozoic and also notably between 0 and 40 Ma is attributed to continental erosion (by inference of Sr inputs to the modern oceans (Veizer, 1989).

3. Geological setting

The geology of the Yorke Peninsula in the southeastern Gawler Craton (Fig. 2) has been well described by Crawford (1965), Drexel and

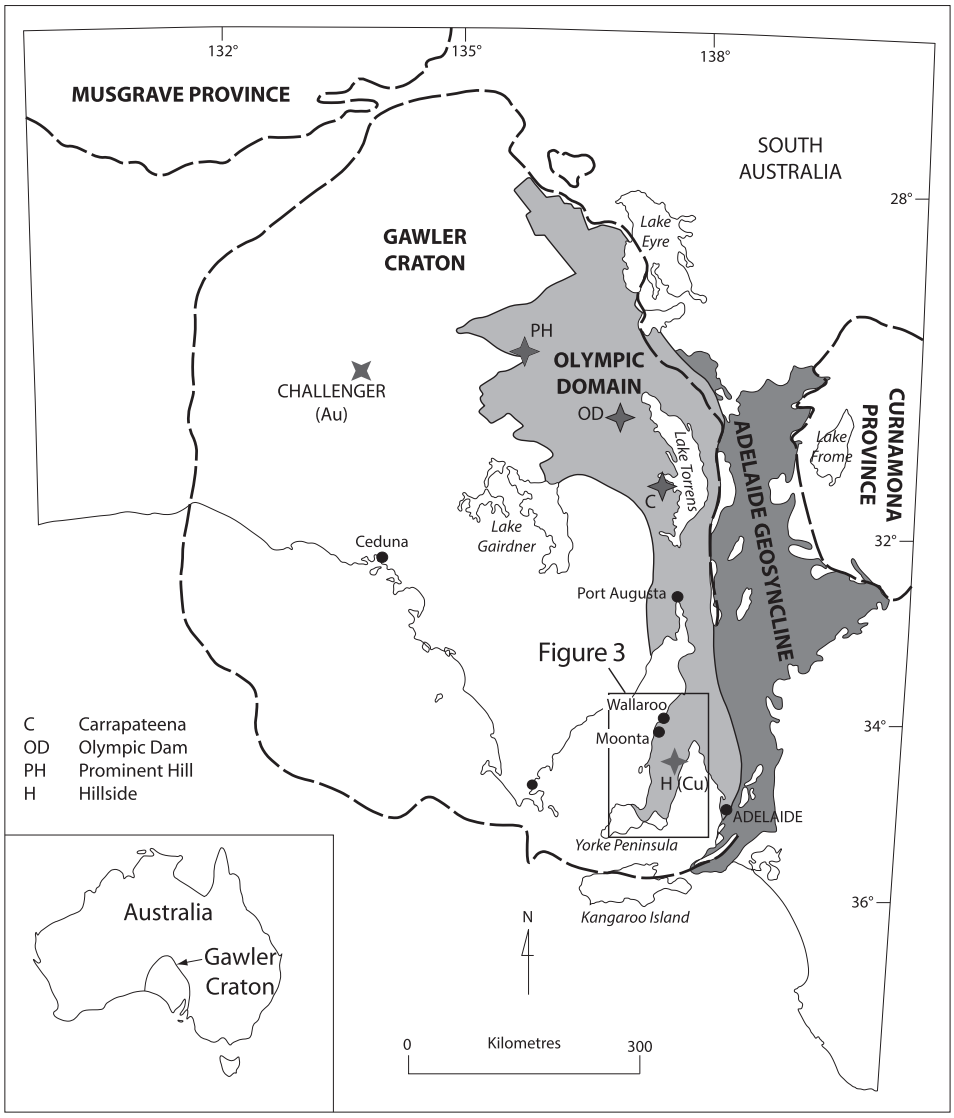

Fig. 2. Simplified geological map showing the selected major geological provinces and the location of major IOCG deposits within the Olympic Domain. The rectangle indicates the location of Fig. 3. Modified after Conor et al. (2010). Inset: Location within Australia.

Preiss (1995), Zang et al. (2006) and Conor et al. (2010). The basement geology of the central Yorke Peninsula comprises Proterozoic rocks with minimal (< 5%) exposure, and is dominated by metasediments and volcanics of the ca. 1750 Ma Wallaroo Group (Cowley et al., 2003), (Fig. 5). The Wallaroo group has been subject to deformation, metamorphism and magmatic events (e.g. Ferris et al., 2002; Forbes et al., 2011; Hoek and Schaefer, 1998). The Wallaroo Group was intruded by the ca. 1595–1575 Ma Hiltaba Suite granites (e.g. Conor et al., 2010; Skirrow et al., 2007) including the 1598–1575 Ma Tickera Granite, 1589 Ma Curramulka Gabbronorite and 1583 Ma Arthurton Granite (Binks et al., 2004; Cowley et al., 2003; Drexel et al., 1993; Wurst, 1994; Zang et al., 2006), (Fig. 5). Interactions between a combination of these geological events has led to mineralisation throughout the region (e.g. Conor et al., 2010; Morales-Ruano et al., 2002).

Mineralisation in the region is part of the southern extent of the Olympic Domain, which is also host to the giant Olympic Dam and smaller Prominent Hill and Carrapateena iron oxide-copper-gold deposits (Fig. 2). Mineralisation in the Olympic Domain is hosted within a range of rock types, including the Wallaroo Group and the Hiltaba Suite Granites (Conor et al., 2010; Cowley et al., 2003). The Yorke Peninsula also hosts Cu-Au mineralisation including the Hillside deposit and deposits in the historic Moonta-Wallaroo district (e.g. Conor et al., 2010; Ismail et al., 2014; Morales-Ruano et al., 2002) (Fig. 2).

These basement rocks are unconformably overlain by younger Cambrian to Quaternary sediments (Crawford, 1965; Drexel and Preiss, 1995; Zang et al., 2006). The Cambrian Stansbury Basin (Fig. 3) consists of alternating limestone and sand to mudstone formed during sea level fluctuations (Drexel and Preiss, 1995; Zang et al., 2006) (Fig. 5). The Carboniferous to Permian Troubridge Basin (Fig. 3) formed during periods of rapid temperature fluctuation and sea level change (Drexel and Preiss, 1995; Zang et al., 2006).

The Cenozoic (2.6–65 Ma) St. Vincent Basin, and contemporaneous Pirie Basin (Figs. 3 & 5), overlies the aforementioned older, weathered sequences. The St. Vincent Basin covers a portion of the eastern side of the Yorke Peninsula (Fig. 3) and is outside of the study area. The Pirie Basin occurs across the western and central parts of the peninsula north of Moonta and extends south towards Point Turton (Fig. 3). The Pirie and St Vincent Basins are reported to have been connected via a southwards flowing paleochannel that winds across the northern part of the Yorke Peninsula towards Ardrossan (Drexel and Preiss, 1995; Pain and Johnson, 2002).

The Pirie Basin includes three main stratigraphic units; Kanaka Beds, which is the earliest, overlain unconformably by the fossil-bearing, Late Oligocene to Middle Miocene (Drexel and Preiss, 1995) Melton Limestone and above this the Gibbon Beds (Drexel and Preiss, 1995; Zang et al., 2006). The Pirie Basin also includes the fossil-bearing, Oligocene to Miocene Point Turton Limestone restricted to the south, and is likely to be linked to the Melton Limestone further north

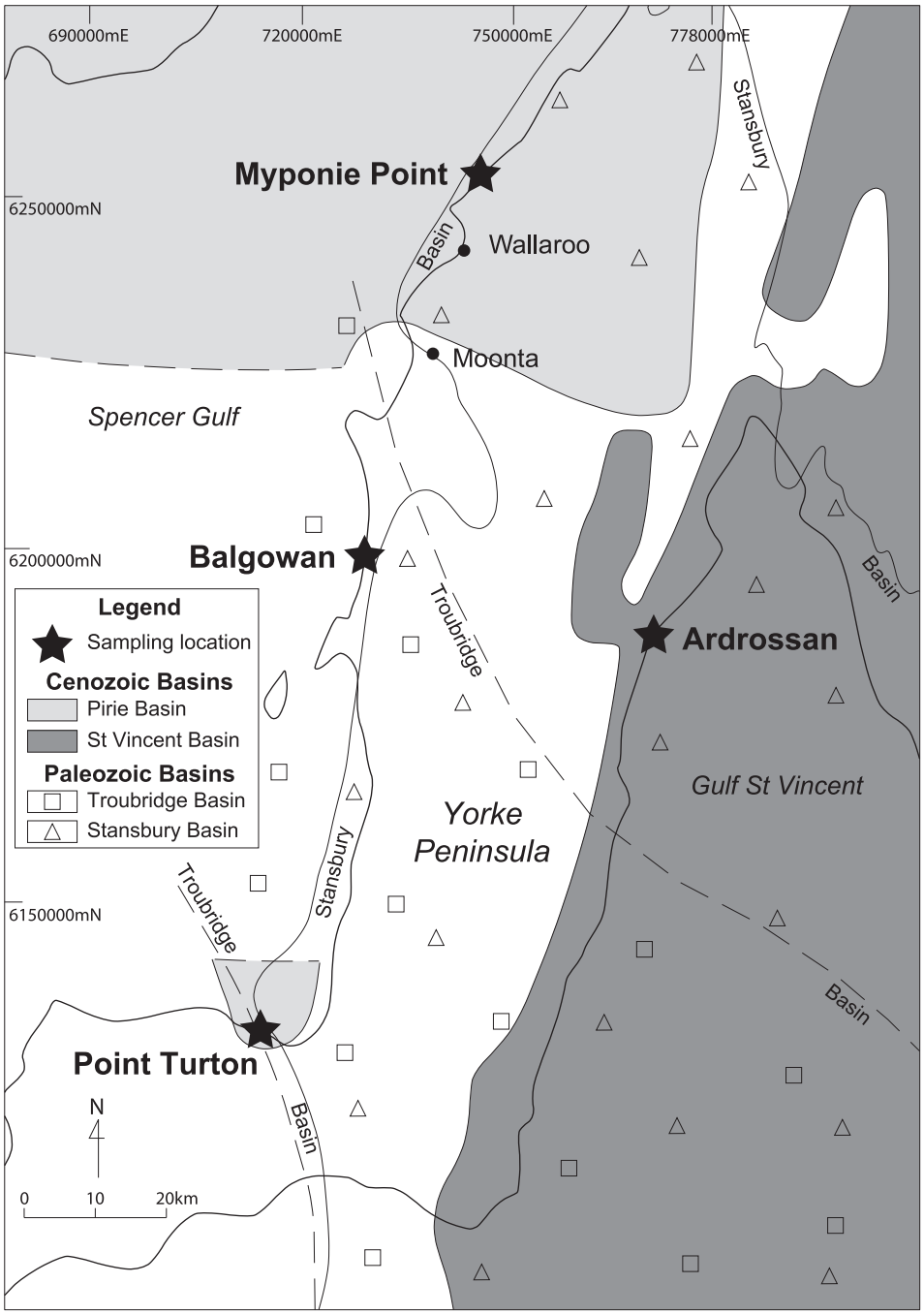

Fig. 3. Map of Yorke Peninsula showing location of the Palaeozoic Stansbury and Troubridge Basins and Cenozoic Pirie and St Vincent Basins. Locations of logged and sampled profiles at Myponie Point, Balgowan and Point Turton as well as the sea water sampling location of Ardrossan are shown. Basin outlines are modified from Drexel and Preiss (1995).

(Drexel and Preiss, 1995; Zang et al., 2006). Melton Limestone is exposed in sinkholes, roadside cuttings, and coastal escarpments on the Yorke Peninsula.

During the Quaternary, sand, silt, clay and carbonate-bearing rock accumulations have largely concealed the underlying geology. Quaternary sediments include clays and quartz-rich sands and sandstone of the Hindmarsh Clay; carbonate-bearing rock such as aeolianite and calcarenite of the Bridgewater Formation; and modern beach deposits and dunes of the St Kilda formation (Crawford, 1965; Drexel and Preiss, 1995; Zang et al., 2006), (Fig. 5). Sand-flat deposits, claypans and salt lakes have developed on areas with low relief (Crawford, 1965; Drexel and Preiss, 1995; Zang et al., 2006; James and Bone, 2015). Carbonate-bearing rock formation is ongoing with continuing accumulation of calcium carbonate and near-surface cementation (calcrete). Active erosion occurs along gullies, drainage lines and in coastal environments (Crawford, 1965; Drexel and Preiss, 1995; Zang et al., 2006).

4. Profile description

Three sites, Myponie Point, Balgowan and Point Turton (Fig. 3) were selected for this investigation due to their excellent exposure of carbonate-bearing rock profiles extending from fresh marine carbonate-bearing rocks to pedogenic carbonate-bearing rocks (Figs. 6, 7 and 8). Myponie Point also includes exposure of basement rocks.

4.1. Myponie Point

Myponie Point is on the north-western coastline of the Yorke Peninsula (Fig. 3). Mesoproterozoic Tickera Granite of the Hiltaba Suite forms the basement at this location and is exposed approximately two meters above sea level and is subject to tidal influence. This granite comprises two phases; a light grey tonalite phase

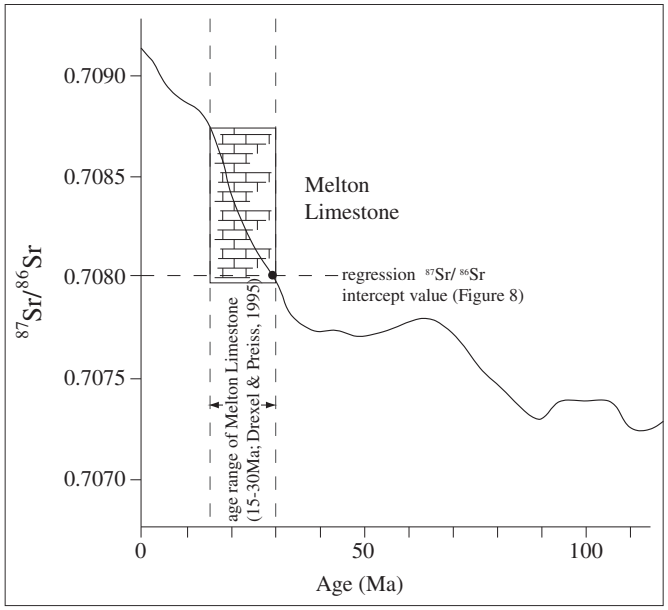

Fig. 4. Seawater curve of strontium isotopes adapted from McArthur et al. (2012). The age range of Melton Limestone is highlighted. The black dot represents the $^{87}Sr/^{86}Sr$ regression intercept value derived in this study (also see Fig. 12 and explanation in text).

containing quartz and plagioclase; and, a red to brown monzonite phase containing microcline and quartz with minor plagioclase, biotite, muscovite and magnetite (Zang et al., 2006). The Tickera Granite has an emplacement age of 1586–1598 Ma (Cowley et al., 2003). The texture and fabric of these granites includes proto-mylonite structures (Cowley et al., 2003), suggesting they have undergone lower amphibolite facies metamorphism (Zang et al., 2006).

Melton Limestone, up to seven meters thick, unconformably overlies the Tickera Granite at this location (Fig. 5) (Lindsay, 1970). Fossils are common within the limestone (e.g. bryozoan (Zang et al., 2006) and *Lepidocyclina* (Crawford, 1965; Drexel and Preiss, 1995)). The limestone includes a fossil bearing sandstone unit. An unnamed basal unit containing thin lenses of glauconitic and gravelly sands is locally preserved (Drexel and Preiss, 1995). Pedogenic carbonate-bearing rock has developed on top of the limestone.

4.2. Balgowan

Balgowan is on the west coast of the Yorke Peninsula (Fig. 3). The Balgowan profile consists of middle Pleistocene Hindmarsh Clay, commonly one to five meters thick, overlain by the upper unit of the late Pleistocene Bridgewater Formation (Drexel and Preiss, 1995; Zang et al., 2006) (Fig. 5). The Hindmarsh Clay includes an arenaceous upper unit which contains a characteristic seam of alunite or kaolinite (Crawford, 1965; Zang et al., 2006). The presence of alunite and kaolinite in this Quaternary clay has been attributed to playa deposition (Drexel and Preiss, 1995; Zang et al., 2006). Crawford (1965) and Zang et al. (2006) suggest this is an effect of acidity and groundwater bleaching where acid soluble elements are leached away.

The upper unit of the Bridgewater Formation, less than ten meters thick, unconformably overlies the Hindmarsh Clay (Zang et al., 2006). It consists of calcareous aeolianite and bioclastic calcarenite and is commonly capped with cemented carbonate rock (calcrete) (Zang et al., 2006). Crawford (1965), describes this as 'kunkarization' (more commonly refers to calcrete formation), which is attributed to the calcium being leached and re-cemented as carbonate. The presence of shells in the middle section of the stratigraphy has been suggested to mark a break in time and change of sea level (Crawford, 1965).

4.3. Point Turton

Point Turton is in the south-western Yorke Peninsula (Fig. 3). Point Turton Limestone is the only exposed bedrock lithology at this location (Figs. 8 and 9c). The limestone is up to sixteen meters thick and consists of a sandy section at the base with thin layered, tabular and trough cross-bedding. This is reportedly associated with a fluvial to shorefront environment (Zang et al., 2006). The upper section is dominated by fossiliferous limestone containing bryozoan and foraminifera (Zang et al., 2006). Point Turton Limestone has been deposited primarily at the southern extent of the Pirie Basin in a fault-bound structure and on a high energy carbonate rock shelf (Zang et al., 2006). Point Turton Limestone correlates in age to the Melton Limestone at Myponie point (Zang et al., 2006). Dating undertaken on a diagnostic foraminifera in the Point Turton Limestone suggests an Oligocene to Miocene age (Drexel and Preiss, 1995; Zang et al., 2006). Cemented carbonated rock (calcrete) has formed on top of the limestone (Crawford, 1965).

5. Methodology

5.1. Sampling

5.1.1. Profile sampling

Samples of the exposed rocks at Myponie Point, Balgowan and Point Turton (Fig. 3) were taken for whole rock geochemical and Sr isotopic analysis. The sampling locations are coastal escarpments chosen for their well-preserved carbonate-bearing rock profiles (Figs. 6, 7 and 8). As the marine and pedogenic carbonate-bearing rocks can be identified visually and texturally, at these locations, it avoids any ambiguity in investigation of chemical differences between the two carbonate-bearing rock types. By using profile sampling techniques, changes in chemical composition can be mapped across the face of the marine carbonate-bearing rocks to where it terminates at the boundary of the regolith counterpart directly overlying it. Profiles were mapped and sampled at a density sufficient to constrain variations in chemical composition relating to marine and regolith processes.

At each location, samples were collected by first removing the outermost surface to expose relatively fresh and uncontaminated material at intervals of half to one meter and working from the base to the top. Approximately two kg of material was taken for each sample. Where there were changes in lithology, this material was also sampled. Lithological logging was undertaken in conjunction with the sampling.

Sampling at Myponie Point was carried out in two stages through a vertical profile that was separated at a midway point by an ~three meter wide platform (Fig. 6). The Balgowan profile was sampled at half to one meter intervals each relevant interval by traversing an inclined boat ramp (Fig. 7). Sampling at Point Turton was carried out in a vertical profile (Fig. 8).

5.1.2. Sea water sampling

Seawater was collected from a groin at Balgowan and from the Ardrossan jetty (Fig. 3). Seawater samples were collected in one litre sized, high-density polyethylene (HDPE) pre-rinsed bottles. The samples were used to provide a current $^{87}Sr/^{86}Sr$ ratios deemed to reflect the local region and identify any variations on each side of the Yorke Peninsula.

5.2. Sample preparation

Samples were separated into two portions. Samples were dried in an oven at 60 °C. A portion of sample was crushed to a fine gravel size and then powdered using a tungsten carbide ring mill at the Mawson Laboratories, University of Adelaide. Approximately 100 g of the milled powder was set aside for whole rock analysis. The remaining powder was retained for isotopic analysis. A small portion of each crushed and milled samples was retained for hyperspectral analysis. The remaining

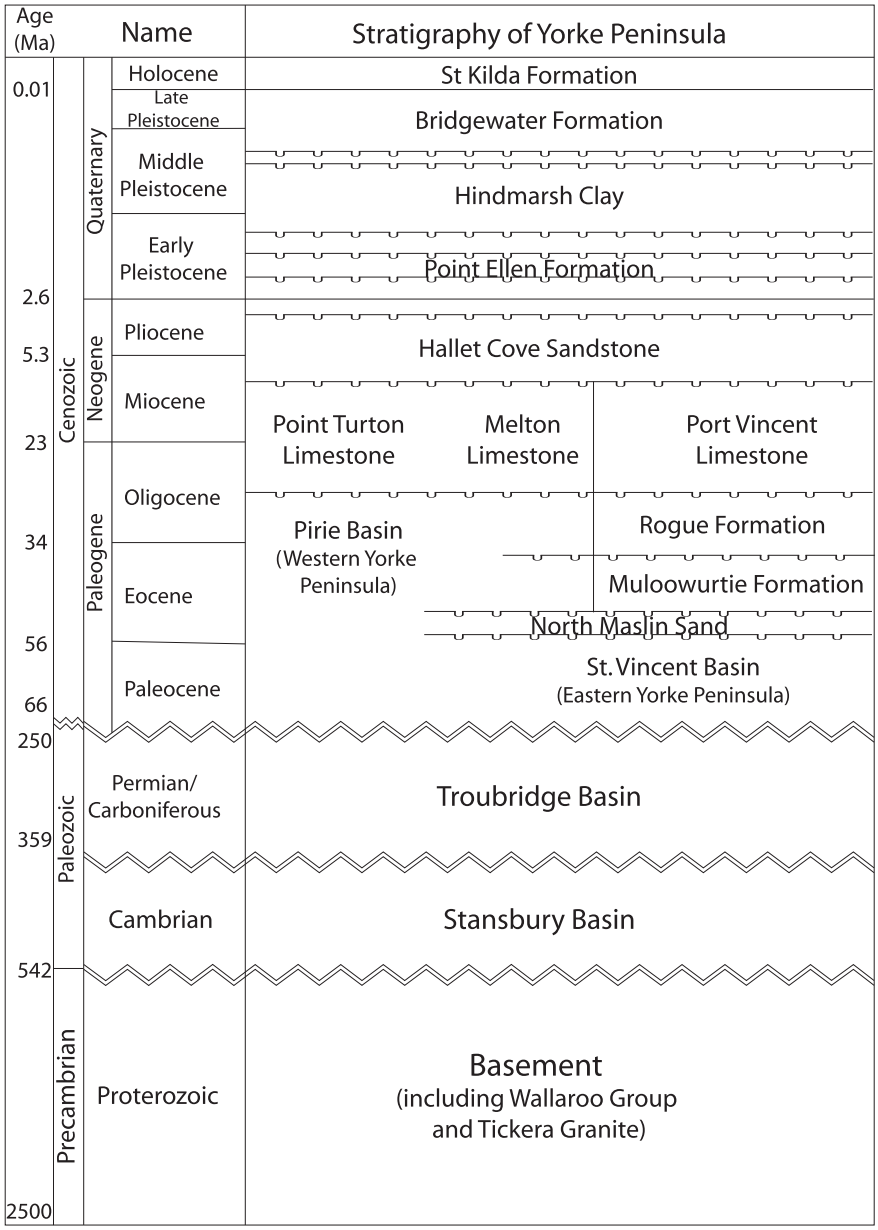

Fig. 5. Simplified geological stratigraphy of the Yorke Peninsula. Modified after Drexel and Preiss (1995) and Zang et al. (2006).

uncrushed portion was used for thin section preparation.

5.3. Whole-rock analysis

Sample powders were analysed for whole rock geochemistry at Acme Laboratories, Vancouver, Canada. Major elements were analysed by X-ray fluorescence (XRF) following preparation of lithium borate fusion discs. Trace elements were analysed by ICP-MS following digestion in a solution of HCl and HNO_3 (aqua-regia). Laboratory standards, laboratory and field duplicates and blanks were included for quality control.

5.4. $^{87}Sr/^{86}Sr$ isotopic analysis

Isotopic analyses for Sr from rock powder and seawater samples were undertaken at the University of Adelaide. Other authors including Quade et al. (1995) and Dart et al. (2012) separate the carbonate fraction from samples in their strontium isotopic studies to isolate and infer the source and input of Ca. As our aim was to replicate field conditions in exploration where the whole rock is sampled and analysed rather than investigate the specific sources of Ca in the carbonate, the whole rock digestion technique was adopted. This method will allow detection of subtle changes in the whole rock across the sampling profile rather than identifying chemistry of the coatings on grains.

A nominal 0.2 g of each sample powder was dissolved to completion using dilute HCl, HNO_3 and HF acids in turn. Reference material (NIST SRM987) was included for quality control. The seawater samples were evaporated to dryness and then treated in the same manner as the whole rock samples. This was followed by separation in conventional cation exchange columns using 2 mL AG50Wx8 (200–400 mesh) Bio-Rad cation exchange resin. $^{87}Sr/^{86}Sr$ ratios were determined using a Finnigan MAT 262 Thermal Ionisation Mass Spectrometer (TIMS) using single tantalum filaments.

5.5. Thin sections

Thin sections were prepared by Adelaide Petrographic Laboratories, Adelaide. Samples were prepared following the standard procedure for incoherent and porous samples by first impregnating with an epoxy resin prior to the preparation of a polished and uncovered thin section.

Fig. 6. Field photos from Myponie Point showing exposure seen at profiles, location of samples and the nature of sampled materials. A) Top section of the profile showing pedogenic carbonate-bearing rocks overlying limestone, B) middle section of the profile showing limestone overlying basement granite, C) basement granite with view towards the overlying sediments and limestone, D) location of samples taken at the clay seam and overlying limestone, E) close up of the pedogenic carbonate rocks, F) upper portion of Melton Limestone, G) lower portion of Melton Limestone, H) shows the base of the Melton Limestone in relation to the underlying sediments and the clay seam. Location of profile is shown in Fig. 3. (For interpretation of the references to colour in this figure, the reader is referred to the web version of this article.)

Thin sections were analysed using standard microscopy techniques.

5.6. Reflectance spectroscopy

Crushed gravel chips and milled powders were decanted into glass Petrie dishes, organised in depth order and analysed using HyLogger™ 3-3, at the Department of State Development (DSD) Core Storage facility at Glenside, Adelaide. HyLogger™ and HyChips™ modes were used in turn for both the Visible to shortwave (Vis–SWIR: 380 nm–2500 nm) and the thermal infra-red (TIR: 6000 nm–14,500 nm; only available in HyLogging™ mode) wavelengths to obtain a representation of the mineral species (those identifiable using spectroscopic methods) in each powdered and gravel chip sample. HyLogger™ instrumentation samples every 0.8 cm producing approximately 125 spectra per meter of sample with overlapping pixels.

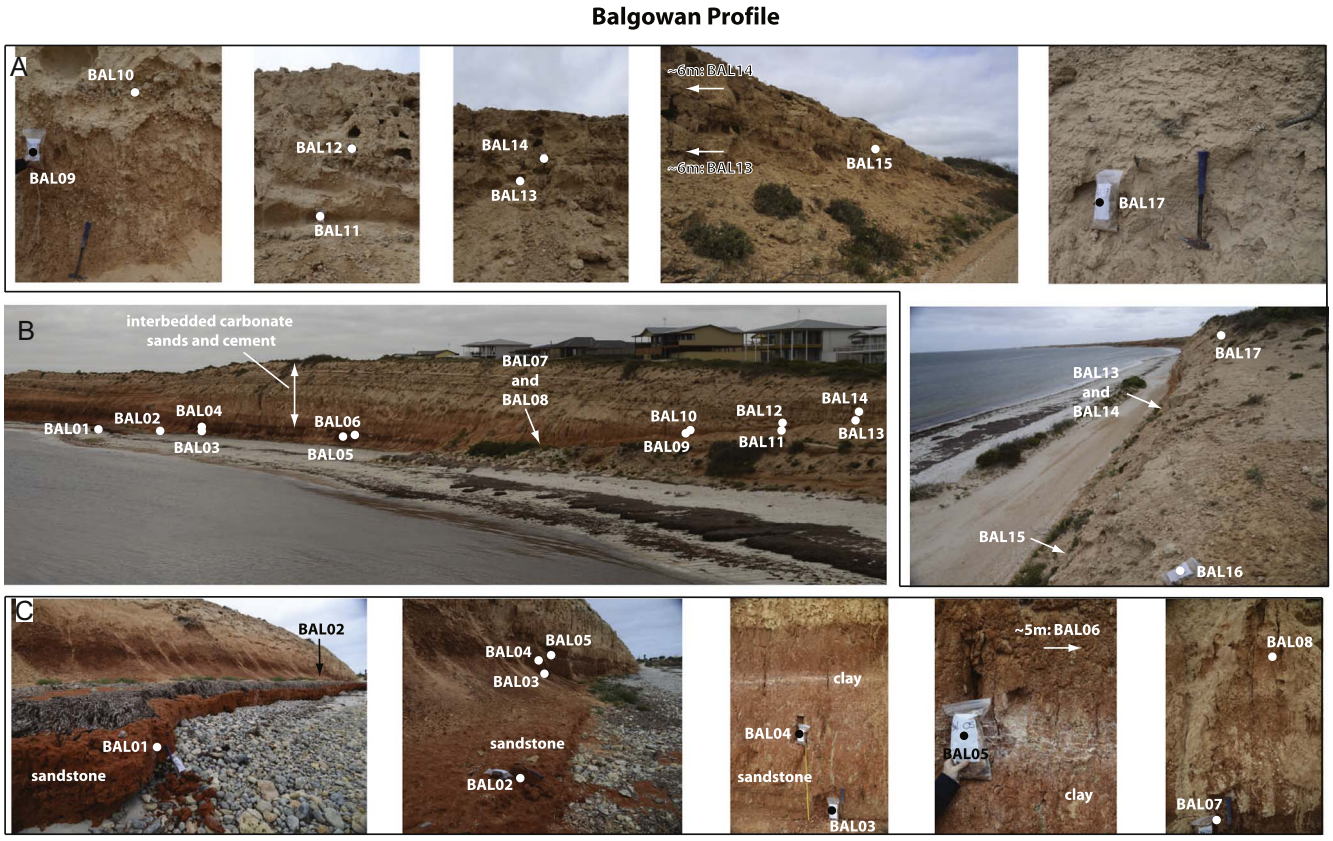

Fig. 7. Field photos from Balgowan showing exposure seen at profiles, location of samples and the nature of sampled materials. Location of profile is shown in Fig. 3. (For interpretation of the references to colour in this figure, the reader is referred to the web version of this article.)

Additionally a high resolution digital image is taken every 1 mm along the sample (Huntington et al., 2006).

In HyLogger™ mode, samples were scanned four times across a sample, allowing for overlap, with the aim of maximising valid spectra. In HyChip™ mode samples were scanned three times using Vis–SWIR only and three readings were taken per sample.

Results were then processed in The Spectral Geologist (TSG), HotCore™ version 7, for viewing in free (TSG) Viewer™ software provided by AusSpec International Inc. The processing of samples included the removal of non-sample materials such as glass from the Petri dishes and wooden intervals between dishes. This method did not account for geological context and removal of mineral species that are not relevant to that geological environment. Routine calibrations were performed prior to analyses and celestine was scanned and used as a reference sample.

6. Results

A total of fourteen samples were collected at Myponie Point, seventeen samples were collected at Balgowan and nine samples collected at Point Turton. Locations are shown in Figs. 3, 6, 7 and 8. Geochemical results for selected elements are presented in Table 1. A complete table of elements analysed with the results is presented in Supplementary Data Table.

6.1. Myponie Point

6.1.1. Profile description and petrography

The weathered granite is exposed up to three meters vertically (Fig. 6). The granite contains coarse-grained feldspar (albite) (Fig. 9a) and visible biotite and finer grains of magnetite in hand specimen. In thin section, each mineral grain is broken or cracked with alteration along the grain boundaries (Fig. 10a).

Unconformably overlying the granite is a 1.5 m thick conglomerate comprising poorly sorted coarse to very fine, well-rounded grains of quartz and feldspar (Fig. 10b) with minor amounts of biotite, opaque minerals and minor fine-grained zircon. The upper fifty centimetres of the conglomerate contains a mixture of angular blue-grey gravels set amongst medium to fine sub-rounded grains of quartz (Figs. 6 & 9a). In thin section these polymict sediments preserve a very thin coating of clay (Fig. 10b).

Overlying these sediments is a 6.5 m thick limestone sequence (Figs. 6 and 9a). The base of the limestone contains broken fragments of shell mixed with rock fragments. In thin section these rock fragments are rounded and sub-angular pieces of quartz and feldspar (Fig. 10c, d). This mixture of fragments is cemented by a predominantly calcite-rich matrix with a minor clay component. A thin bed up to thirty centimetres thick containing moderately to well-sorted, very fine and sub-angular quartz sand supported by a clay-rich matrix (Fig. 10e) is preserved within the limestone sequence at 4.3 m (Figs. 6 and 9a). The clay bed preserves coloured horizontal banding of equal thickness (~two centimetres) that range from red at the base to alternating yellow and brown to yellow and white.

The limestone is five meters thick above the clay-rich bed (Fig. 9a). The limestone contains abundant, coarse to fine broken fragments of bryozoan, echinoid fragments and other shells up to one centimetre in diameter and is cemented by calcite (Fig. 10f). The shells have sharply defined, angular edges, which are either filled or edge-lined with calcite crystals. Calcite cement accounts for up to 20% of the limestone whilst the fossils, also rich in calcite, dominate the composition (Fig. 10f).

The pedogenic carbonate-bearing rock at the top of the profile is

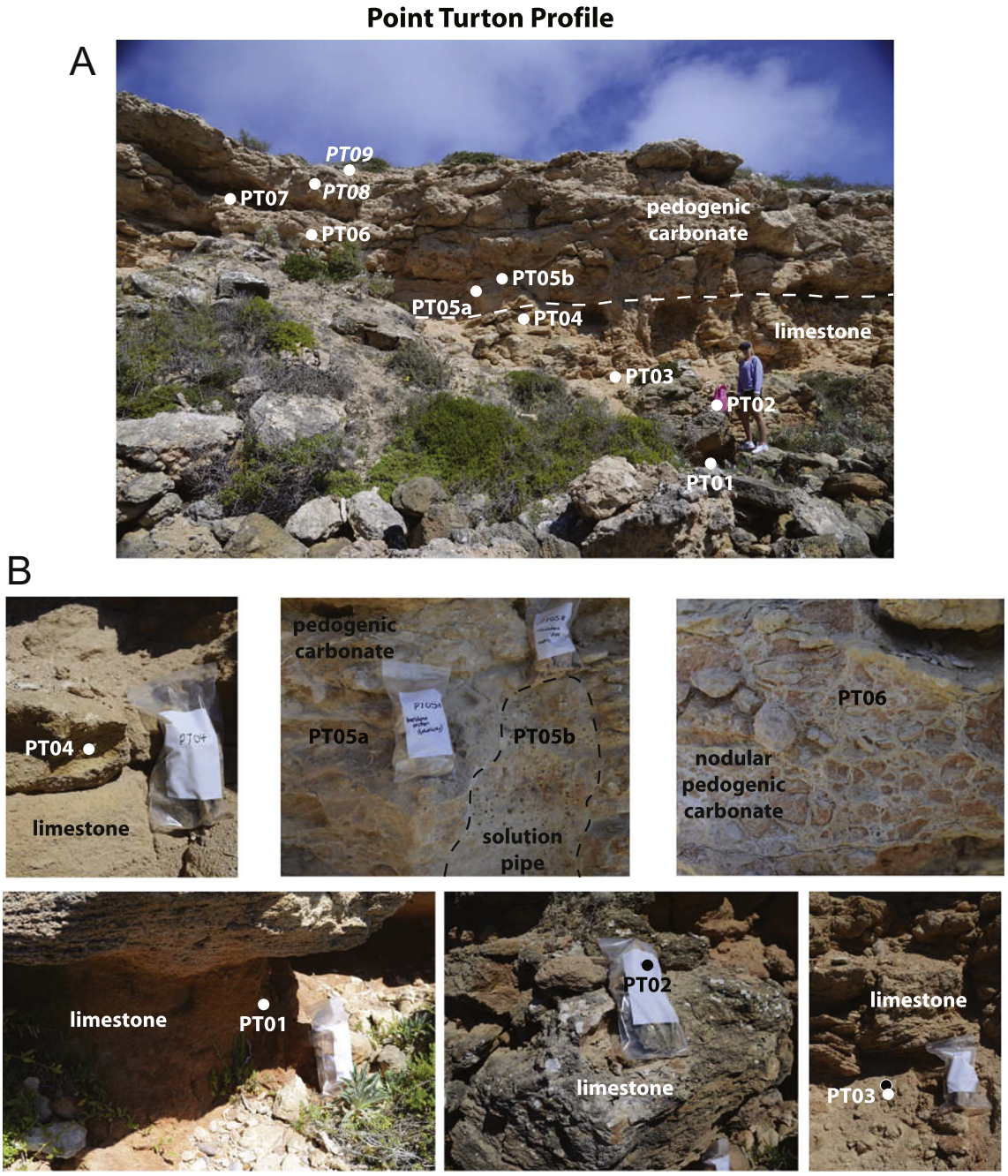

Fig. 8. Field photos from Point Turton showing exposure seen at profiles, location of samples and the nature of sampled materials. A) shows an overview of the full profile at Point Turton; B) shows individual sample lithology (samples PT07 to PT09 are not shown as close ups due to the nature of the outcrop being very steep towards the top). Location of profile is shown in Fig. 3.

approximately two meters thick (Figs. 6 & 9a). The carbonate-bearing rock is dominated by dolomite (Fig. 9a) and is creamy white to light brown in colour. This pedogenic carbonate-bearing rock is generally fine grained, well-cemented, massive and contains nodules and pisolites. Many of the nodules and pisolites display concentric structures which are coloured varying shades of cream to brown. In thin section this rock appears largely homogenous with a tightly compacted calcite rich matrix (Fig. 10g). The nodules themselves contain the same homogenous calcite rich matrix, with the addition of sub-angular to well-rounded grains of quartz and other detrital fragments. The edges of these nodules are coated with calcite. Very few broken and sub-angular to sub-rounded fragments of shell are preserved in the upper parts of this profile (Fig. 10g).

6.1.2. Chemistry

CaO concentration ranges throughout the profile from 36 wt% in the basal limestone below the clay bed and up to 55 wt% in the limestone above the clay bed, and from 35 to 45 wt% in the surface samples (Fig. 9a and Table 1). CaO concentration in the basement granite is < 0.1 wt%. Al_2O_3 content is included as a measure of clastic component. The basement granite contains 12.3 wt% Al_2O_3. Variable concentrations of Al_2O_3 occur in the sediments and clay above the granite (3–14 wt%), and lower concentrations occur in the limestone and the surface carbonate-bearing rock (< 1 wt% and 2 wt% respectively) (Fig. 9a). Throughout the basement and limestone, MgO concentrations are < 1 wt%, apart from the clay bed which has ~1.3 wt% MgO. The pedogenic carbonate-bearing rock has the highest MgO concentrations of ~2.7–6.4 wt%.

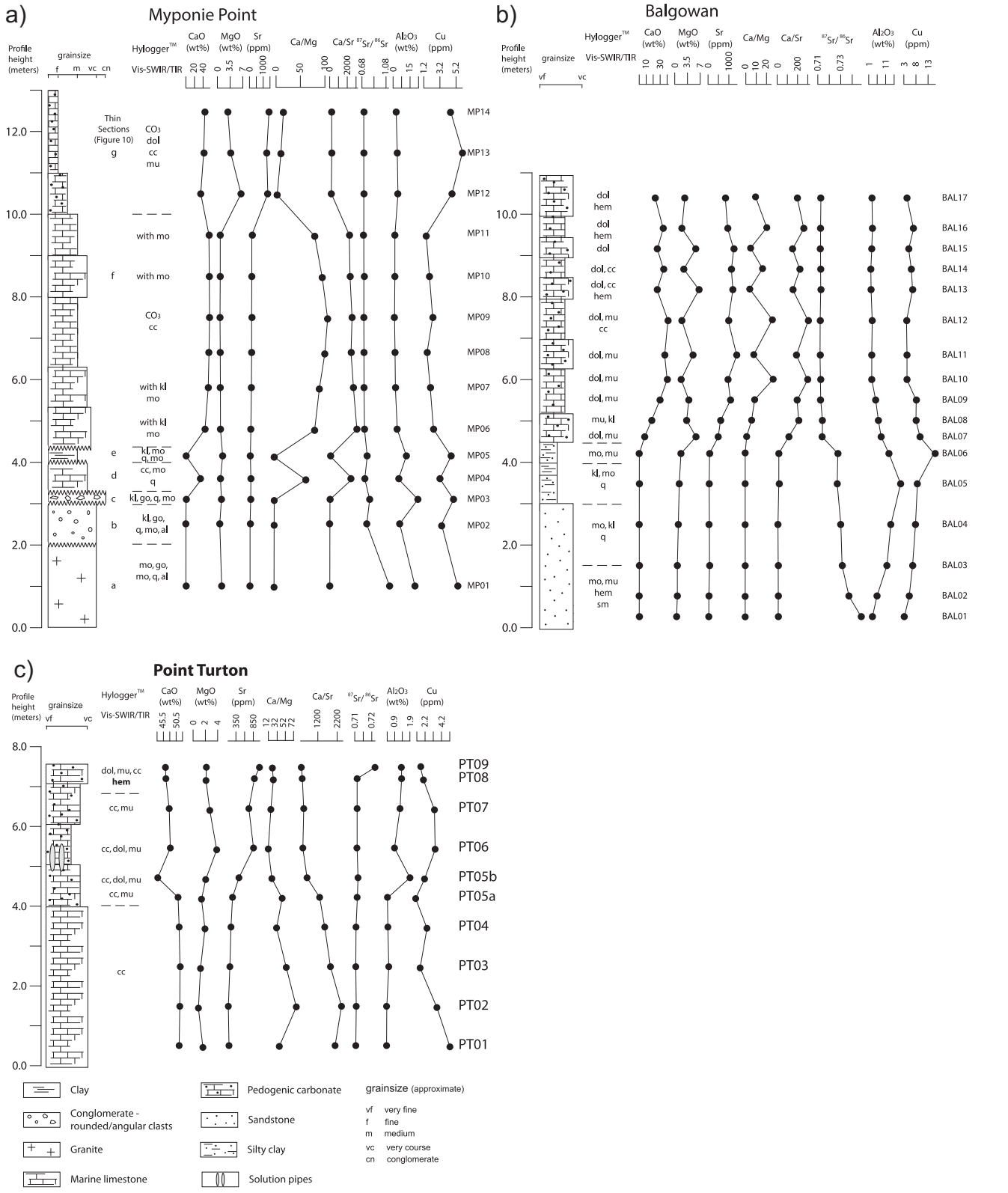

Fig. 9. Simplified stratigraphy, selected geochemistry and hyperspectral analysis for a) Myponie Point, b) Balgowan and c) Point Turton profiles. Profile locations are shown in Fig. 3. Abbreviations: al: albite; cc: calcite; CO_3: carbonate; dol: dolomite; go: goethite; hem: hematite; kl: kaolinite; mo: montmorillonite; mu: muscovite; q: quartz; sm: smectite. Regular text: Vis-SWIR; Bold text: TIR.

Strontium has the lowest concentration in the granite (42.3 ppm, Table 1), with ranges between 100 and 170 ppm in the limestone and is highly elevated in concentration in the regolith carbonate at the surface (1260–1430 ppm) (Fig. 9a). The $^{87}Sr/^{86}Sr$ ratio for the granite is 1.141. The $^{87}Sr/^{86}Sr$ ratio gradually decreases (from 0.722 to 0.711) throughout the marine limestone. The three pedogenic carbonate-bearing rock samples all have similar $^{87}Sr/^{86}Sr$ ratios around 0.711. The Ca/Mg ratio is lowest in the granite (0.09), ranges between 0.30 and 0.47 in the clastic sediments, is highest in the limestone (82–109) and drops to 6–19 in the pedogenic carbonate-bearing rock (Fig. 9a,

Table 1
Geochemical data for selected elements.

Sample location and name	height above sea level	$^{87}Sr/^{86}Sr$	CaO %	Sr ppm	MgO %	Ca/Sr	Ca/Mg	Al_2O_3%	Cu ppm
Myponie Point									
MP01	2	1.1410	0.08	42.3	1.04	14	0.09	12.3	5.4
MP02	3	0.7598	0.13	42.0	0.51	22	0.30	3.3	3.4
MP03	3.2	0.8083	0.40	90.2	1.00	32	0.47	14.1	4.9
MP04	4	0.7272	36.98	102.1	0.68	2589	64	2.8	3.2
MP05	4.3	0.7679	0.50	65.3	1.28	55	0.46	7.1	4.6
MP06	5.3	0.7219	44.43	102.6	0.64	3095	82	1.8	2.4
MP07	6.3	0.7142	51.90	137.1	0.67	2706	92	0.9	2.0
MP08	7	0.7133	53.79	158.0	0.62	2433	103	0.6	1.6
MP09	8	0.7113	54.98	154.3	0.60	2547	109	0.3	2.3
MP10	9	0.7116	54.41	168.2	0.66	2312	98	0.5	1.9
MP11	10	0.7107	53.60	171.6	0.77	2233	83	0.6	1.5
MP12	11	0.7110	34.51	1341.2	6.36	184	6	2.4	4.7
MP13	12	0.7108	41.47	1260.5	3.50	235	14	2.0	6.0
MP14	13	0.7102	44.03	1429.7	2.74	220	19	1.5	4.5
Balgowan									
Bal01	0.5	0.7459	0.05	35.9	0.450	10	0.13	2.660	3.2
Bal02	1	0.7353	0.06	39.1	0.600	11	0.12	5.480	5.2
Bal03	2	0.7292	0.10	70.6	0.690	10	0.17	11.170	6.6
Bal04	3	0.7281	0.07	63.1	0.770	8	0.11	13.560	7.8
Bal05	4	0.7249	0.12	53.7	1.140	16	0.12	19.430	8.6
Bal06	4.5	0.7254	0.17	74.0	1.610	16	0.13	12.340	15.4
Bal07	4.8	0.7120	7.66	491.1	5.780	111	2	7.970	9.7
Bal08	5.3	0.7121	17.55	594.0	3.240	211	6	6.100	8.0
Bal09	5.8	0.7106	29.51	1078.6	3.740	196	9	4.720	8.1
Bal10	6.3	0.7103	40.06	957.1	1.730	299	27	2.410	4.3
Bal11	7	0.7100	36.44	1379.3	5.070	189	9	2.320	4.3
Bal12	8	0.7101	41.22	969.6	1.830	304	27	2.570	4.1
Bal13	8.5	0.7105	25.61	1194.8	6.590	153	5	2.020	6.6
Bal14	9	0.7104	34.92	1124.1	2.420	222	17	1.980	6.1
Bal15	9.5	0.7104	26.02	1234.6	5.680	151	5	2.350	5.0
Bal16	10	0.7104	34.42	942.6	1.920	261	21	2.700	7.0
Bal17	11	0.7107	22.91	831.3	2.650	197	10	2.440	4.3
Point Turton									
PT01	0	0.7096	51.82	176.1	1.50	2103	41	0.51	5.2
PT02	1	0.7097	52.73	154.5	0.77	2440	81	0.48	3.8
PT03	2	0.7097	52.74	203.5	1.09	1852	57	0.67	1.9
PT04	3	0.7094	52.18	239.6	1.80	1557	34	0.59	2.7
PT05a solution pipe externa surface	4	0.7102	51.08	290.1	1.27	1259	48	0.56	1.4
PT05b solution pipe internal surface	4.5	0.7109	38.04	441.5	1.94	616	23	2.17	2.4
PT06	5	0.7101	46.46	846.5	3.74	392	15	1.06	3.6
PT07	6	0.7102	45.63	725.2	2.59	450	21	1.47	3.5
PT08	7	0.7102	43.53	869.9	1.93	358	27	1.58	2.3
PT09	7.5	0.7101	43.02	1011.7	2.08	304	25	1.54	2.0
Seawater samples									
BAL (Balgowan)	0	0.70920							
ARD (Ardrossan)	0	0.70917							

Table 1). The Ca/Sr ratio is lowest in the granite (14), ranges between 22 and 55 in the clastic sediments, is highest in the limestone (2233–3095) and drops to 184–235 in the pedogenic carbonate-bearing rock (Fig. 9a, Table 1).

The pedogenic carbonate-bearing rock contains the highest concentrations of Cu (4.5–6.0 ppm, Table 1) (Fig. 9a). The Cu content is lowest within the limestone and ranges from 1.5–2.4 ppm, and up to 3.2 ppm in the lowermost limestone sample. The clay bed contains 4.6 ppm Cu. The conglomerate and granite contain 3.4–5.4 ppm Cu.

6.1.3. Hyperspectral analysis

The basal Tickera Granite has been highly weathered to dominantly montmorillonite with goethite response in the Vis-SWIR wavelengths (Fig. 9a). The TIR response confirms montmorillonite with quartz and plagioclase (albite). The overlying sandy gravels are dominated by kaolinite and goethite in the Vis-SWIR and quartz dominated with montmorillonite secondary, in the TIR (Fig. 9a). The basal limestone is dominated by carbonate (calcite) in the Vis-SWIR with quartz identified in the TIR (Fig. 9a). The clay bed is dominated by kaolinite and montmorillonite in Vis-SWIR and quartz with montmorillonite in the TIR wavelength (Fig. 9a).

The fossil-rich limestone is dominated by calcite with secondary kaolinite and montmorillonite identified in the Vis-SWIR wavelengths (Fig. 9a). The overlying pedogenic carbonate-bearing rock is also calcite dominant in Vis-SWIR wavelengths but identified as dolomite and also contains secondary calcite and muscovite (Fig. 9a).

6.2. Balgowan

6.2.1. Profile description and petrography

The coastline at Balgowan (Fig. 3) hosts a north to south trending escarpment between eleven to fifteen meters high (Fig. 7). The exposure provides an impressive contrast to the surrounding landscape with reddish brown sandstone and sediments at the base overlain by light cream coloured sands with interbedded fine-grained decimetre to metre thick cemented carbonate-bearing rock layers (Fig. 7). The sandstone outcrops one meter above sea level and contains up to 90% fine and well-sorted, rounded to sub-angular grains of quartz cemented by thin coatings of clay (Fig. 7).

Overlying the platform, at the extent of the high-tide mark, the escarpment rises from a clay-rich base around 2.5 m thick (Figs. 7 & 9b). Towards the top of this layer there is a mottled patchy

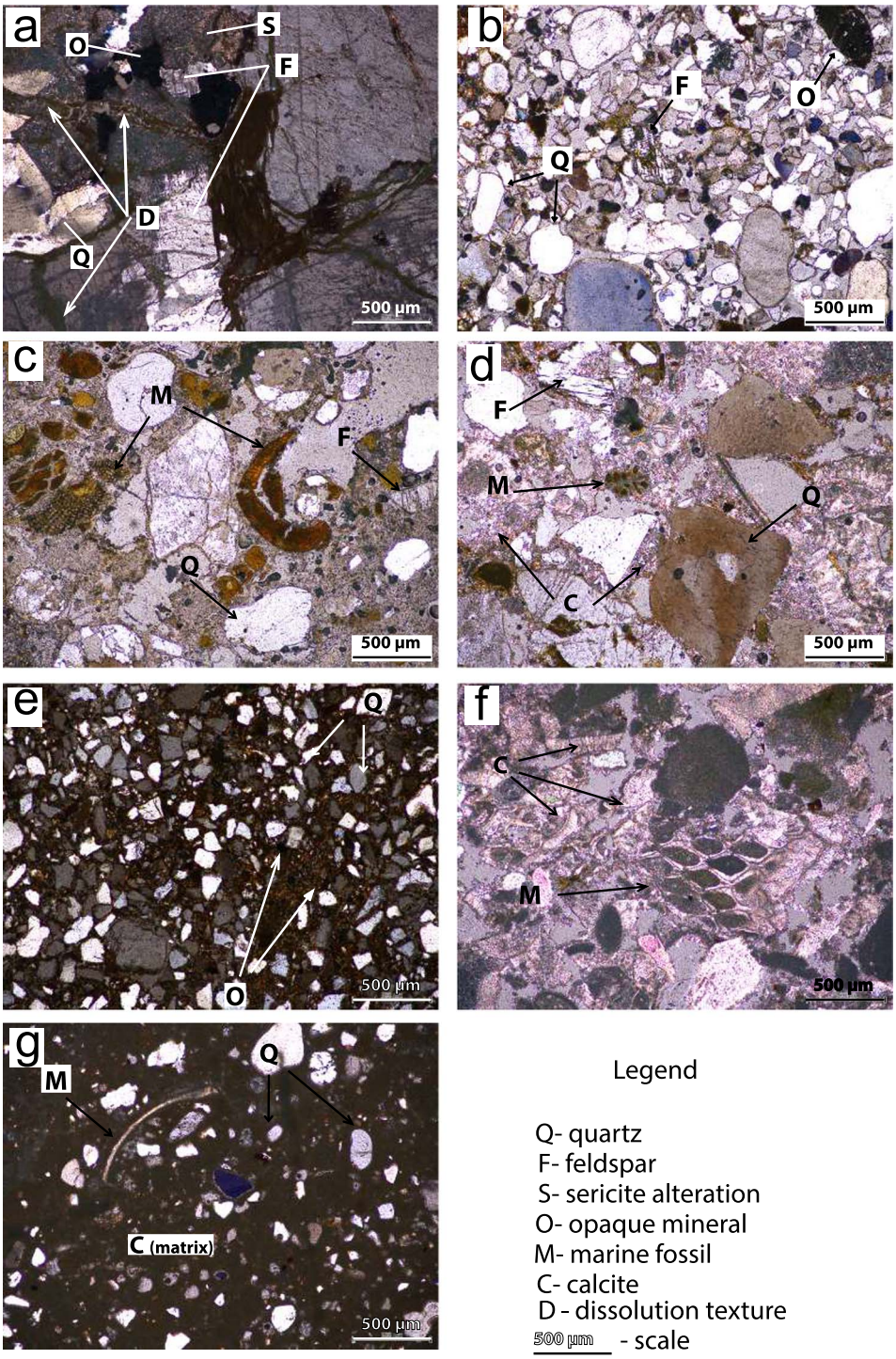

Fig. 10. Representative photomicrographs of lithologies at Myponie Point. a) chemical weathering textures in the Tickera Granite showing dissolution and replacement (such as sericite) at grain boundaries, along cracks and within mineral fractures, (0–2 m, MP01); b) representative matrix from the conglomerate with fine to very coarse clasts dominated by quartz and feldspar with some opaque minerals (~3.1 m, MP02); c) base of the Melton Limestone sequence showing fossil marine fragments (bryozoa and mollusc) and rounded sub-angular quartz and feldspar in a clay and calcite matrix (~3.5 m, MP03); d) limestone containing marine fossil fragments (possibly bryozoa) in a calcite dominated cement, clastic component is < 30% (~4 m, MP04); e) sample from the clay bed showing fine, moderately to well-sorted sub-angular grains of quartz and opaque minerals in a clay-rich matrix (~4.3 m, MP05); f) representative sample of Melton Limestone containing abundant marine organisms (bryozoa in this field of view) in a calcite dominated cement (4.5–10 m, MP10); g) micritic densely compact carbonate containing rounded fine- to coarse-grained quartz and small shell fragments (bivalve in this field of view) (10–14 m, MP13). Numbers in parenthesis indicate the approximate height of the lithology represented in the photomicrograph from the Myponie Point profile (see also Fig. 6 and log in Fig. 9a) and their associated sample number.

seam of white powdery to crystalline clay around ten to twenty centimetres thick (Fig. 7). Above this seam the clays are hematite stained with an increasingly silty texture and carbonate nodules. Plant roots are preserved within this silty layer.

The silty clays are unconformably overlain by seven meters of interbedded carbonate-bearing sand and cement (Figs. 7 and 9b). The lower-most carbonate-bearing rock contains an abundance of well-cemented carbonate nodules. Above this layer of nodular carbonate rocks are carbonate-rich sands interbedded with well-cemented carbonate-bearing rock layers, each up to two meters thick (Fig. 9b). Approximately halfway up the carbonate section, at 7.5 m, there are visible, broken and rounded fragments of shells (BAL 12, Fig. 9b). These shell fragments can also be identified in the cemented carbonate-bearing layers albeit only in thin section.

The uppermost sample collected (Fig. 7) comprises unconsolidated, very fine-grained nodular carbonate-bearing sand containing 40% fine sub-angular quartz grains. Very fine rounded grains of zircon are also only identifiable in thin section.

6.2.2. Chemistry

The CaO concentrations range from < 0.2 wt% in the clay layer and increase to 7 wt% at the unconformity (Fig. 9b, Table 1). The sandy interlayers of the carbonate-bearing rock section range from 17 to 35 wt % CaO whilst the cemented-carbonate rock platforms contain 35–41 wt

% CaO (Fig. 9b). The Al_2O_3 content of the lowermost sandstone in the profile increases from ~2.7 wt% at the base to ~13.6 wt% to the top of the layer. The overlying silty clay contains ~12.3–19.4 wt% Al_2O_3. The lowermost 1.3 m of the pedogenic carbonate-bearing rock contains 4.7–8.0 wt% Al_2O_3, and the remainder contains 2.0–2.7 wt% Al_2O_3 (Fig. 9b). MgO content is lowest within the sandstone and silty clay (0.5–1.6 wt%), and varies from ~1.7–5.8 wt% throughout the pedogenic carbonate-bearing rock (Fig. 9b).

The Sr concentration is low in the basal sands and clay with values ranging 36–74 ppm (Fig. 9b, Table 1). The carbonate-bearing sediment immediately above the unconformity contains 500–600 ppm Sr. The Sr concentration is highest in the overlying carbonate-bearing rocks (830–1379 ppm) (Fig. 9b). The basal quartz-rich and clay layers contain $^{87}Sr/^{86}Sr$ ratios ranging from 0.746 to 0.725. There is a distinct change in values from the clays to the overlying carbonate-bearing rocks which have $^{87}Sr/^{86}Sr$ ratios limited to between 0.710 and 0.712 (Fig. 9b). There are no sharp distinctions between values for the well-cemented carbonate-bearing rock platforms, the sandy carbonate-bearing layers or the surface sample (Fig. 9b). The Ca/Mg ratios are lowest in the sands and clays at the base of the profile (0.11–0.17) and increase to a broad range between 2 and 27 in the overlying carbonate-bearing rocks (Fig. 9b, Table 1).The Ca/Sr ratios are lowest in the sands and clays at the base of the profile (8–16) and increase sharply to between 111 and 303 in the overlying carbonate-bearing rocks with an average of 208 (Fig. 9b, Table 1).

Copper content within the sandstone ranges from 3.2–7.8 ppm (Fig. 9b, Table 1). The highest concentrations are preserved within the clay, which contains 8.6–15.4 ppm Cu. The pedogenic carbonate-bearing rocks contains ~4.1 to ~9.7 ppm Cu (Fig. 9b).

6.2.3. Hyperspectral analysis

The basal 0–1.5 m of the Hindmarsh Clay is dominated by montmorillonite, muscovite and hematite in the Vis-SWIR wavelengths (Fig. 9b). Montmorillonite is also dominant in the TIR wavelength. The sediments above this (1.5–3 m) are equally montmorillonite and kaolinite dominant in Vis-SWIR. Quartz dominates in the TIR wavelength at 1.5–3 m. At three to four meters there is a distinct whitish seam which Vis-SWIR wavelengths identifies kaolinite and montmorillonite dominant and with quartz in the TIR wavelength. At 4–4.5 m the profile becomes montmorillonite and muscovite dominant again in the Vis-SWIR wavelength. The overlying carbonate-bearing rock sequences (4.5–11 m) display an alternating trend of dolomite dominant to dolomite with calcite each alternating half to one meter upwards in the Vis- SWIR wavelengths. Scattered occurrences of hematite detected in TIR wavelength (Fig. 9b).

6.3. Point Turton

6.3.1. Profile description and petrography

Exposed geology at Point Turton is limestone overlain by pedogenic carbonate-bearing rock (Fig. 8). The escarpment at this location is less than eight meters high and is fossil rich limestone with its base concealed by a pebbly shingle beach deposits (Fig. 9c). This limestone is porous and contains abundant fragments of shells including bryozoa, echinoids and bivalves cemented by calcite similar to that of the Melton Limestone (Zang et al., 2006).

At approximately four meters the fossiliferous limestone is overlain by 3.5–4 m of well-cemented pedogenic carbonate-bearing rock (Figs. 8 & 9c). Dividing these two lithologies are faintly visible solution pipes containing fine pisolitic nodules (Fig. 8). The overlying pedogenic carbonate-bearing rocks have a fine micritic to massive texture with abundant nodules (up to two centimetres in size) (Fig. 8). These densely compacted, also micritic, carbonate nodules contain tiny grains of angular sand. Approximately 5% of the carbonate matrix contains grains of calcite that are identified only in thin section as broken shell fragments, similar to that of the pedogenic carbonate-bearing rocks from Myponie Point (Fig. 10g). An increase in sub-angular to well-rounded quartz content, also similar to Myponie Point, is in the top two meters of pedogenic carbonate at Point Turton.

6.3.2. Chemistry

The CaO concentration in the limestone ranges from 51 to 53 wt% (Fig. 9c, Table 1). The overlying pedogenic carbonate-bearing rocks contains 38–46 wt% CaO. The Al_2O_3 content of the limestone varies from ~0.5–0.6 wt%. Within the pedogenic carbonate-bearing rock, the Al_2O_3 content is generally ~1.1–1.6 wt%, and increases to ~2.2 and 8.5 wt% in the lower two samples of this lithology (Fig. 9c). The MgO concentration of the limestone is ~0.8–1.9 wt%. Within the pedogenic carbonate, the MgO concentration is ~1.9–3.7 wt%. One sample towards the base of the pedogenic carbonate-bearing rock contains only ~0.4 wt% MgO (Fig. 9c).

Strontium concentration in the limestone ranges between 155 ppm and 290 ppm (Table 1). The overlying pedogenic carbonate-bearing rocks contains 440 ppm – 870 ppm Sr. The uppermost surface sample contains the highest Sr concentration of 1012 ppm (Fig. 9c). The $^{87}Sr/^{86}Sr$ ratios are similar for all limestone samples (0.709) (Fig. 9c). The overlying pedogenic carbonate-bearing rock showed little variation in $^{87}Sr/^{86}Sr$ ratio compared to the limestone (0.710). The uppermost sample had the highest $^{87}Sr/^{86}Sr$ ratio of 0.721 (Fig. 9c). The Ca/Mg ratios range between 41 and 81 in the limestone and between 15 and 27 for the overlying carbonate-bearing rocks (Fig. 9c, Table 1). A sample of material taken from the inside surface of a solution pipe produced a Ca/Mg ratio of 23 (Fig. 9c, Table 1).The Ca/Sr ratios range between 1260 and 2440 in the limestone and between 300 and 450 for the overlying pedogenic carbonate-bearing rocks (Fig. 9c, Table 1). A sample of material taken from the inside surface of a solution pipe produced a slightly higher Ca/Sr ratio of 616 (Fig. 9c, Table 1).

The Cu content throughout the limestone and pedogenic carbonate-bearing rock is variable, and ranges from ~1.4–5.2 ppm in the limestone and ~2.0–4.3 ppm in the pedogenic carbonate-bearing rock (Fig. 9c, Table 1).

6.3.3. Hyperspectral analysis

Point Turton limestone is carbonate dominant in Vis-SWIR (Fig. 9c). The basal fossil-rich limestone portion shows as calcite dominant whilst the overlying pedogenic carbonate-bearing rock is dolomite and smectite dominant in Vis-SWIR wavelengths. Iron oxide (hematite) is detected within the upper ~0.5 m in TIR wavelength.

6.4. Sea water analysis

The $^{87}Sr/^{86}Sr$ ratios for sea water samples from Balgowan and Ardrossan (Fig. 3) are 0.70920 and 0.70917 respectively (Table 1). During the course of the isotopic analyses, the average $^{87}Sr/^{86}Sr$ ratio of standard NIST SRM987 were 0.71024 ± 0.000009 (2SE, 20 runs). This compares to 0.71014 (Veizer, 1989) and 0.710248 (Howarth and McArthur, 1997).

7. Discussion

7.1. Stratigraphy of the Melton Limestone at Myponie Point

To identify carbonate origins it is important to understand the morphology of the exposed profile and the environmental processes affecting the geochemical content. The profile at Myponie Point will be discussed in detail here as it contains both marine carbonate-bearing rocks (limestone) and pedogenic carbonate-bearing rocks (calcrete) as well as basement rock that also forms a large portion of the basement of the Yorke Peninsula.

The base of the Myponie Point profile comprises a highly weathered granite (Figs. 5, 6 & 9a). The granite contains smectite dominant minerals identified with HyLogger™ that are typical weathering products

of alumino-silicate minerals (Anand, 2005). Continental materials can also be a source for siliciclastic contamination and higher $^{87}Sr/^{86}Sr$ ratios (Edmond, 1992; Veizer and Compston, 1976). The weathered granite is unconformably overlain by the Melton Limestone.

The stratigraphy of the Melton Limestone has been described in detail by Lindsay (1970). Five sequences of sedimentation are identified. From oldest to youngest these units are: 1. an unnamed fossiliferous gravel containing sub-rounded sands of granite fragments quartz and feldspar; 2. Melton Limestone, lower bryozoal member consisting of quartzose, bryozoal calcarenite, oxidised glauconite pellets and lithic pebbles (e.g. granite, feldspar, quartz and schist); 3. Melton Limestone, pink member which is documented as a pinkish coloured and densely recrystallized bryozoal limestone; 4. an unnamed unit that is only documented from an inland sinkhole and comprises densely recrystallized quartzose and calcarenitic composition containing specific fossil assemblage not observed in other units; and, 5. a yellow to cream brown, fossil-rich and densely recrystallized limestone that is the youngest and most widespread unit of the Melton Limestone (Lindsay, 1970). This young limestone unit weathers to a smooth, fine grained and bouldery limestone (Lindsay, 1970), which has much the same form as field exposures of the pedogenic carbonate that is frequently observed across the Yorke Peninsula. Lindsay (1970) observes that this unit locally disconformably overlying unit 2 at Myponie Point.

The Melton Limestone at Myponie Point consists of a base of sandy gravels overlain by a coarse conglomerate containing fragments of shells, glauconite, quartz and lithic fragments in a clay-rich matrix (Figs. 6a & 8). Lindsay (1970) identified this as units 1 and 2. These units are also described ~10 km north of Myponie Point (Drexel and Preiss, 1995). The composition of the gravels includes feldspars (Figs. 6 & 9a), which provide a source of radiogenic Sr and can therefore elevate the total $^{87}Sr/^{86}Sr$ ratio (e.g. Brantley et al., 1998). Weathering of these gravels to a clay fraction (e.g. montmorillonite) is expressed in HyLogger™ results (Fig. 9a), and has produced a porous media suitable for dispersion of fluid (e.g. groundwater). These gravelly units also have elevated Al_2O_3 content relative to other units within the profile (Fig. 9a), which is used here as a proxy indicator for higher clastic component. The gravelly units are thus interpreted as a potential source of siliciclastic contamination of the limestone.

The sands and conglomerate are overlain by a thin (~30 cm) clay bed at 4.3 m, which is in turn overlain by limestone (Figs. 6 and 9a). This clay bed is localised to the Myponie Point area and has not been described within the Melton Limestone elsewhere. The clay bed is overlain by limestone (Figs. 5, 6 and 9a) that is equivalent to unit 5 of the Melton Limestone as described by Lindsay (1970). The contact between the clay bed and the overlying limestone is interpreted to represent the disconformity between units 2 and 5 and is described by Lindsay (1970). The uppermost pedogenic carbonate-bearing rock (Fig. 6) has a bouldery smooth appearance that is similar to the weathered morphology of the limestone comprising unit 5 of the Melton Limestone. This visual similarity in appearance between the pedogenic carbonate-bearing rock and marine limestone is central to the main challenge being addressed in this paper.

7.2. Age of the Melton Limestone

The Melton Limestone has been suggested to be from the Oligocene to Miocene (33 Ma–15 Ma) (Drexel and Preiss, 1995; Zang et al., 2006); however, no specific age has been determined. The currently accepted age range has been based on principles of relative fossil ages in the Pirie Basin and neighbouring St. Vincent Basin (Lindsay, 1970). Here, we constrain the age of the Melton Limestone based on regression of $^{87}Sr/^{86}Sr$ ratios (Fig. 9). The regression intercept value of 0.708 for the Melton Limestone (Fig. 12) returns an age of 30 Ma when overlain onto the $^{87}Sr/^{86}Sr$ seawater curve (Fig. 4). Our estimate of 30 Ma for the Melton Limestone places the limestone in the Late Oligocene which coincidentally corresponds with the older limit of the currently published age range (Oligocene to Miocene; Drexel and Preiss, 1995; Zang et al., 2006). It is acknowledged that this age could be better defined with further isotopic analysis using the carbonate mineral fraction separated from other impurities in conjunction with multiple samples of the limestone, however this is not within the scope of this research. Additionally, this age determination only works for the Melton Limestone profile at Myponie Point due to it containing the least amount of siliciclastic contamination, as indicated by the low Al_2O_3 content (Figs. 9a and 12). The Point Turton Limestone and limestone at Balgowan have slightly increased Al_2O_3 content, indicating these may be an argillic carbonate-bearing rock and are possibly contaminated by a siliciclastic component that may be enriched in radiogenic Sr (Fig. 9).

7.3. Differentiating between marine and pedogenic carbonate-bearing rocks

Distinguishing between marine and pedogenic carbonate-bearing rocks is critical in terms of sampling for mineral exploration programs as pedogenic carbonate-bearing rocks will preserve signatures of underlying mineralisation (Chen et al., 2002; Lintern et al., 2012; McQueen et al., 1999). Limestone formed in a marine environment does not typically contain pathfinder elements for ore deposition (e.g. Chen et al., 2002). For instance, the limestone in the Yorke Peninsula region has formed above basement rocks of the Olympic Domain that are prospective for IOCG deposits (Conor et al., 2010), but preserve no anomalous concentrations of ore pathfinder elements such as Cu (Fig. 9). Whether pedogenic carbonate-bearing rocks will preserve ore pathfinder elements is suggested to be due to the processes of carbonate rock formation (Lintern et al., 2012).

7.3.1. Textural and mineralogical differences

Distinguishing marine carbonate-bearing rocks from pedogenic carbonate-bearing rocks may be possible when there are visible fossils, however, this is not always the case (Lindsay, 1970). In an often costly exploration program, it is important to choose the right type of carbonate-bearing rock quickly and effectively in the field. Drill cuttings produced by various destructive drill methods can reduce the rock to a fine powder whereby destroying the original texture (Hillis et al., 2014; Marjoribanks, 2010). Whole rock samples in the field environment are subject to weathering which also alters the texture.

Weathering alters the appearance of carbonate-bearing rocks through diagenetic alteration mechanisms such as dissolution, re-precipitation or recrystallization (Chen et al., 2002; Crawford, 1965; Veizer, 1989). Dense recrystallization of these marine carbonate-bearing rocks has been described by a number of authors (e.g. Crawford, 1965; Lindsay, 1970; Drexel and Preiss, 1995). As an example, the effects of recrystallization can be observed within the Melton Limestone of this study, and is seen as calcite crystals along the edges of pore spaces and shells (Fig. 10). Chen et al. (2002) suggests that classifying a carbonate rock by its morphology is the recommended method, however the appearance and texture of a weathered exposure of Melton Limestone, for example bouldery and fine grained (Lindsay, 1970), could be easily mistaken for pedogenic carbonate-bearing rock (see also Milnes and Hutton, 1983; Hill et al., 1998).

Calcite is the dominant carbonate mineral in the marine limestone of this study (Fig. 9). However, calcite is also the main carbonate mineral found in pedogenic carbonate-bearing rock (calcrete) (e.g. Milnes and Hutton, 1983; Hill et al., 1998). As an example, the marine and pedogenic carbonates in this study both contain calcite as a major component of the total carbonate rock profile (Fig. 9). Based on this study it would be difficult to place an individual sample of calcite into context unless there is a complete carbonate-bearing rock profile.

Additionally, the pedogenic carbonate-bearing rocks locally contain dolomite, as reflected by higher MgO content and spectral data (Fig. 9). The higher MgO content relating to increased dolomite content may be used to identify the pedogenic carbonate-bearing rocks, however the MgO concentrations are not consistent throughout the profiles (Fig. 9).

For example, in the Myponie Point profile the base of the pedogenic carbonate (sample MP11) has higher MgO concentration relative to the middle and top, implying higher dolomite content (Fig. 9a). At Balgowan and Point Turton, the MgO content within the pedogenic carbonate-bearing rocks inconsistent, and the mineralogy identified from spectral data varies between dolomite and calcite (Fig. 9b, c). Such variations in MgO concentrations and mineralogy imply that using mineralogy alone to discriminate between marine and pedogenic carbonate bearing rocks may not be reliable.

Recognising fossils in highly weathered, and finer grained carbonate-bearing rock samples (e.g. recrystallized) can be undertaken using thin sections (Fig. 10), however, this is not a technique that can be carried out quickly or in the field. Sample BAL12 from the Balgowan profile is described as being abundant is fossils fragments. Based on texture alone, this sample could easily be misidentified as a fossiliferous limestone. However, the spectral data shows dolomite and calcite (Fig. 9b), implying its mineralogy is similar to the surrounding pedogenic carbonate-bearing rocks. These observations imply that evidence other than mineralogy or texture may provide a more robust discrimination between marine and pedogenic carbonate-bearing lithologies.

7.3.2. Geochemical differences

Discrimination of marine and pedogenic carbonate-bearing rocks based on geochemical differences currently requires the rock samples to be analysed for a range of elements in a laboratory. Laboratory analysis is a routine procedure in mineral exploration and has the advantage of low detection limits over a wide element suite. The process, however, is time consuming and can take weeks to months before analytical data is available, implying that discriminating between marine and pedogenic carbonate-bearing rocks as a sample media in the field is not possible.

7.4. Whole rock geochemistry

Whole rock geochemical data sets of carbonate-bearing rocks can provide a wide range of information. Aluminium and silica (Si) contents represent clay and siliciclastic components. When plotted against Ca, these elements will distinguish ‘pure’ versus impure carbonate-bearing rocks with siliciclastic input. The concentration of calcium alone is not enough to clearly distinguish a marine carbonate-bearing rocks from a pedogenic carbonate-bearing rock. As an example, a limestone sample from Myponie Point (4.8 m) contains the same amount of Ca (44%) as an overlying pedogenic carbonate-bearing rock (12.5 m), which also contains 44% (Fig. 9a, Table 1).

7.5. $^{87}Sr/^{86}Sr$ isotopic differences

$^{87}Sr/^{86}Sr$ ratios are widely used in carbonate studies for tracing the sources of calcium and for age dating of carbonate rocks (e.g. Burke et al., 1982; Chiquet et al., 1999; Hamidi et al., 1999; Howarth and McArthur, 1997; McArthur et al., 2001). Our aim was to test whether the use of $^{87}Sr/^{86}Sr$ could also be used to distinguish between marine and pedogenic carbonate-bearing rocks by using the whole rock. In the Myponie Point and Point Turton profiles, Sr isotope ratios for marine carbonate-bearing rocks are 0.722–0.711 and ~0.711 respectively, whilst ratios for pedogenic carbonate-bearing rocks are ~0.709 and ~0.710 respectively (Fig. 9, Table 1). This data shows that there are no systematic differences in $^{87}Sr/^{86}Sr$ ratios across the marine to pedogenic carbonate-bearing rocks. Similarly, the change between well-cemented carbonate-bearing rock ($^{87}Sr/^{86}Sr$ = 0.710) and sandy carbonate-bearing rock ($^{87}Sr/^{86}Sr$ = 0.710), with or without detrital shells at Balgowan show no significant change in $^{87}Sr/^{86}Sr$ ratios (Fig. 9b).

The similarity of $^{87}Sr/^{86}Sr$ ratios is interpreted to be a relict signature of the original source of the Sr rather than the evolution of its deposition. Quade et al. (1995) demonstrated that carbonate-bearing soils from coastal South Australia and Victoria have $^{87}Sr/^{86}Sr$ ratios of 0.7094–0.7098, and that the Sr (and by inference the Ca) is of marine origin. The carbonate-bearing rocks studied here have comparable $^{87}Sr/^{86}Sr$ ratios (0.7101–0.7110) which may suggest also having significant marine input.

Partitioning of Sr into pore fluids during diagenesis will mobilise Sr to overlying or underlying sediments whilst still preserving the original $^{87}Sr/^{86}Sr$ ratio (e.g. Veizer, 1989; Van der Hoven and Quade, 2002). The pedogenic carbonate-bearing rocks at Myponie Point and Point Turton preserve $^{87}Sr/^{86}Sr$ ratios similar to the underlying marine carbonate-bearing rocks but contain a significant increase in Sr concentration (up to 1430 ppm) (Fig. 9, Table 1), which may infer Sr mobilisation via pore fluid movement from the marine carbonate into the overlying pedogenic carbonate-bearing rocks, further atmospheric addition or relative accumulation (e.g. Quade et al., 1995; Van der Hoven and Quade, 2002).

The physical properties of Sr coupled with the $^{87}Sr/^{86}Sr$ values obtained from this study demonstrate that it is impossible to discriminate between marine and pedogenic carbonate-bearing rocks, at these locations, using Sr isotopes alone. The $^{87}Sr/^{86}Sr$ values are effective at giving clues as to the source of the Sr (and by association the calcium), but do not clearly define any further differentiation resulting from pedogenic processes in the regolith. The Sr isotope therefore cannot be used on the whole rock to distinguish marine and pedogenic carbonate-bearing rocks.

7.6. Making sense of multiple Sr isotope sources within marine and pedogenic carbonates.

Veizer (1989) suggested that diagenetic alteration of marine carbonate-bearing rock will preserve the $^{87}Sr/^{86}Sr$ ratio of the original host/seawater where it formed. If there is a significant marine component of Sr, and as the $^{87}Sr/^{86}Sr$ composition of seawater changes with time (e.g. Burke et al., 1982; McArthur et al., 2001, 2012), it should theoretically be possible to distinguish between marine and pedogenic carbonates that formed at different times based on $^{87}Sr/^{86}Sr$ ratios. Radiogenic Sr, however, may be introduced via weathering of continental materials and will alter the initial $^{87}Sr/^{86}Sr$ ratios (e.g. Edmond, 1992; Peterman et al., 1970; Veizer and Compston, 1974, 1976). Additionally, there is such a wide range of contributing sources involved in pedogenic carbonate-bearing rock formation (e.g. groundwater, transported sediments, windblown dust; Chen et al., 2002), it becomes difficult to measure the Sr contribution from each source. Quade et al. (1995) concluded that the primary source of $^{87}Sr/^{86}Sr$ ratios in soil carbonates along coastal areas is dust and sea spray, but further inland the $^{87}Sr/^{86}Sr$ ratios increased as a function of increased continental dust input. Quade et al. (1995), also demonstrated that the increase in $^{87}Sr/^{86}Sr$ ratios further inland is a function of prevailing winds. Across the Yorke Peninsula, aeolian dust would be derived predominantly from the west to the east (marine source) but could also contain continental dust coming from the north (Anand, 2005). An example of these mixed sources of Sr can be seen in Fig. 10g where the pedogenic carbonate-bearing rock contains rounded quartz grains and fragmented shells that have been interpreted as aeolian. As the Ca in the matrix of the pedogenic carbonate-bearing rock is likely to have a marine source (Quade et al., 1995), the overall $^{87}Sr/^{86}Sr$ ratio is closer to a marine value than a continental rock value (Fig. 9, Table 1).

7.7. Ca/Sr and Ca/Mg element ratios

Quade et al. (1995) assessed the origin of soil carbonates in South Australia and Victoria using Ca/Sr ratios and evaluating the contributions of strontium, and by inference calcium, from bedrock (Ca/Sr = ~4–300), marine carbonates (Ca/Sr ~1100), sea spray or dust (Ca/Sr = 112) or local meteoric water (Ca/Sr = 680). The Ca/Sr ratio for rainwater was calculated from dissolution of carbonate dust derived from marine aeolianite in the region (Quade et al., 1995). The Ca/Sr

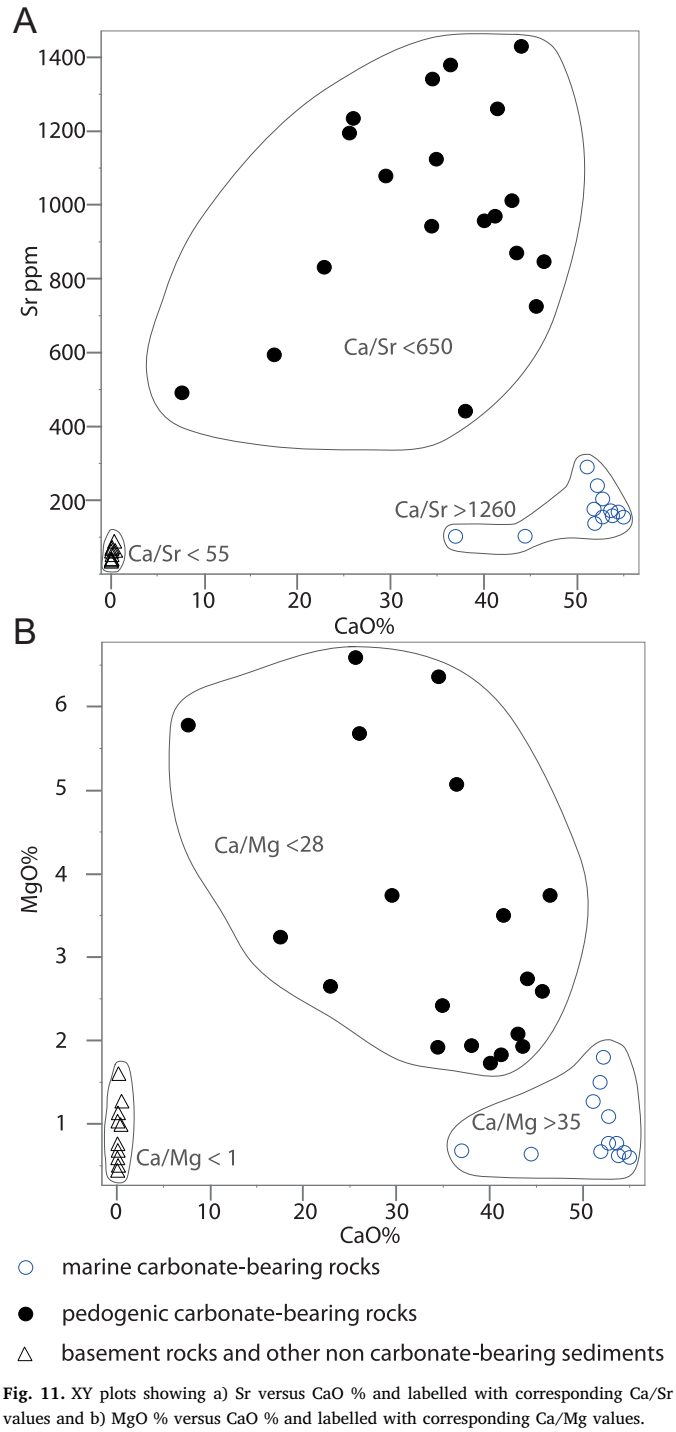

Fig. 11. XY plots showing a) Sr versus CaO % and labelled with corresponding Ca/Sr values and b) MgO % versus CaO % and labelled with corresponding Ca/Mg values.

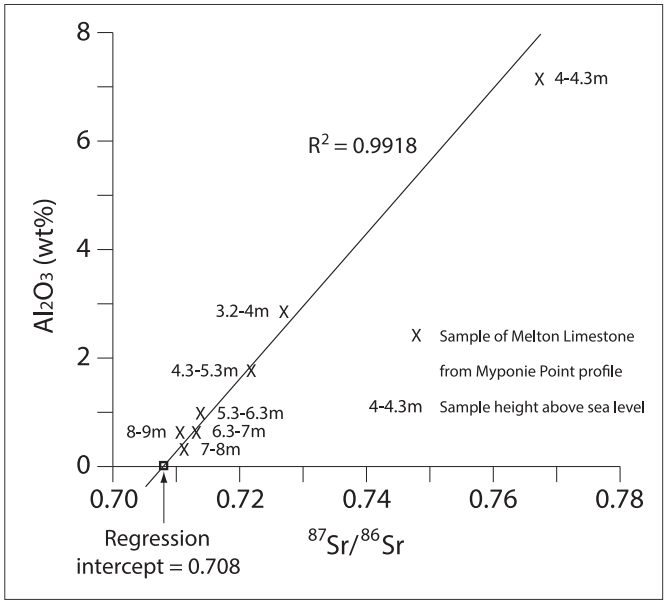

Fig. 12. Plot of $^{87}Sr/^{86}Sr$ ratios versus Al_2O_3 wt% showing a regression trend-line for $^{87}Sr/^{86}Sr$ ratios of the Melton Limestone. Where this line intercepts (i.e. 0% Al_2O_3) represents a marine carbonate sample with the absence of clastic contamination.

ratios along with $^{87}Sr/^{86}Sr$ isotopes suggest the primary source of Ca within coastal soils was marine, and that soils further inland had higher contributions from inland dust (Quade et al., 1995).

This same technique for using the Ca/Sr ratio was used in this study to assess the usefulness as a discriminant between marine or pedogenic carbonate-bearing rock types (Fig. 11a). This was found to produce a highly effective means of separating the marine carbonate-bearing rocks from the pedogenic carbonate-bearing rocks regardless of the source of calcium defined by the $^{87}Sr/^{86}Sr$ ratios (Fig. 13).

Fig. 13 demonstrates that the spread of $^{87}Sr/^{86}Sr$ ratios for all carbonate dominant lithologies is narrowly confined to 0.709–0.711. The greatest range of $^{87}Sr/^{86}Sr$ ratios are only observed in the non-carbonate-bearing lithologies 0.725–1.141. Conversely, three clear populations can be recognised in the Ca/Sr ratios (Fig. 11a, Fig. 13). Carbonate poor sediments and bedrock yield the lowest Ca/Sr ratios between 10 and 55. Ca/Sr values 1250–3100 occur in the marine carbonate whilst the values in the pedogenic carbonate-bearing rocks are 100–650 (Fig. 11a, Fig. 13, Table 1).

The Ca/Sr data presented from our research demonstrates that marine and pedogenic carbonate-bearing rocks on the Yorke Peninsula preserve characteristic Ca/Sr ratios. Additionally, our Ca/Sr values fall within similar values presented by Quade et al. (1995), whereby the Ca/Sr ratio of marine carbonate-bearing rocks is significantly higher (> 1100) than pedogenic carbonate-bearing rocks (100–650) and bedrock (< 300). Research undertaken by McQueen (2006), on pedogenic carbonate rocks, in the Cobar region of New South Wales, also display a similar pattern for Ca/Sr ratios (Fig. 13). This demonstrates that using Ca/Sr ratios to distinguish marine from pedogenic carbonate-bearing rocks is not a unique solution to the Yorke Peninsula and may be applied elsewhere.

In addition to Ca/Sr ratios, Ca/Mg ratios were investigated to assess their ability in differentiating between marine and pedogenic carbonate-bearing rocks due to the observation that the pedogenic carbonate-bearing rocks used in this study contain magnesium in the form of dolomite (Table 1, Fig. 9). Overall, the values for Ca/Mg have a comparatively limited range between 0.09 and 109 (Table 1). The pedogenic carbonate-bearing rocks have Ca/Mg ratios < 28 whilst the marine carbonate-bearing rocks have Ca/Mg ratios > 35 (Fig. 11b). Therefore, the Ca/Mg ratios may be used to discriminate between the marine and pedogenic carbonate-bearing rocks.

Comparison between the results for using the Ca/Sr and Ca/Mg ratios to identify marine and pedogenic carbonate-bearing lithologies shows that the range of Ca/Sr ratios and gap between values for marine versus pedogenic carbonate-bearing rocks (range: 8–3095; gap: 643) is much larger than for the Ca/Mg ratios (range: 0.09–109; gap: 8). Additionally, although the Mg concentration (reflecting the dolomite content) is locally elevated within the pedogenic carbonate-bearing rocks within the three profiles investigated in the Yorke Peninsula, it is unknown whether this applies across the whole Yorke Peninsula or elsewhere. Understanding the processes of MgO (and dolomite) concentration in the pedogenic carbonate-bearing rocks is beyond the scope of this study, and the extent to which Ca/Mg ratios may be used to distinguish between marine and pedogenic carbonate-bearing rocks

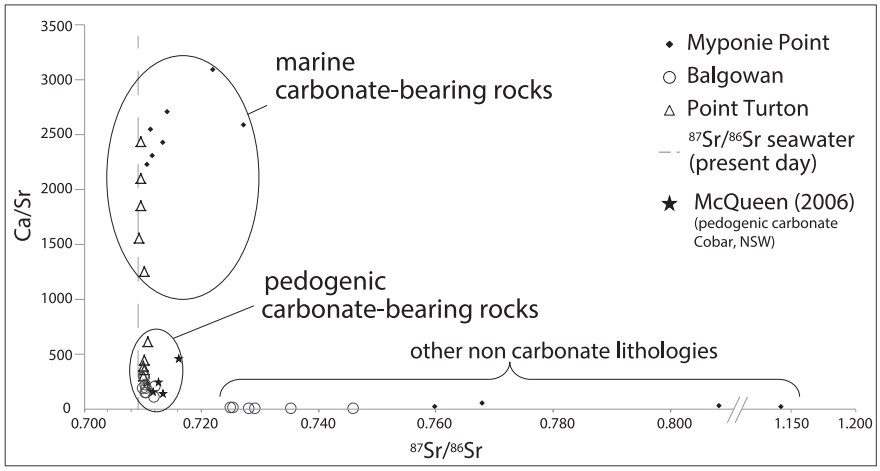

Fig. 13. Ca/Sr values versus $^{87}Sr/^{86}Sr$ values for data from this study. Data groupings of marine carbonate-bearing rocks, pedogenic carbonate-bearing rocks and other lithologies (granite, sand or clay) are highlighted. Plot also includes data, for comparison, from McQueen (2006).

is unclear. The use of Ca/Sr ratios is therefore favoured due to the larger range and gap in values that allow room for error in field analysis and data interpretation, as well as the knowledge that this ratio discrimination is applicable to areas beyond the Yorke Peninsula (McQueen, 2006 data).

7.8. Mineral exploration sampling

The results of this study show that the Ca/Sr ratio using whole rock geochemical data can be used to effectively discriminate between marine and pedogenic carbonate-bearing rocks. Calcium and often Sr data are routinely collected in laboratory whole rock geochemical analysis, and generating this data is significantly less time consuming than analysis of Sr isotopes. Additionally, modern technologies such as portable XRF (pXRF) instruments allow immediate collection of whole rock geochemical data in the field, and are capable of measuring Ca and Sr to detection limits of < 50 ppm and 5 ppm respectively (e.g. Olympus). The Ca and Sr concentrations in marine carbonate-bearing rocks on the Yorke Peninsula range from 36 to 55 wt% and 100–290 ppm respectively, and in the pedogenic carbonate-bearing rocks range from 35 to 46 wt% and 440–1430 ppm respectively (Fig. 7). These values are significantly above the pXRF detection limit. Portable XRF data collected in the field could therefore be used for immediate assessment of Ca/Sr ratios, and discrimination between marine versus pedogenic carbonate-bearing rocks.

The Myponie Point profile is proximal to the historic Cu mineralisation in the Moonta-Wallaroo district (Fig. 3). No mineralisation occurrences have been recognised proximal to the Balgowan or Point Turton profiles. The Cu content within samples taken from the Myponie Point profile shows noticeably higher concentrations within the pedogenic carbonate-bearing rock (4.5–6.0 ppm Cu) accompanied by lower Ca/Sr ratios (< 240), compared to the limestone (1.5–2.4 ppm and Ca/Sr > 2200) and corresponds to Cu concentrations in basement samples (3.4–5.4 ppm Cu) with lower Ca/Sr ratios (< 55) (Fig. 9a, Table 1). This correlation supports the notion that pedogenic carbonate-bearing rocks are better recognisable using Ca/Sr ratios and may contain increased contents of economic and/or pathfinder elements proximal to mineralisation.

The ability to utilise Ca/Sr ratios in the field directly impacts the methodology of exploration campaigns that target carbonate rock sampling, due to the necessity to sample pedogenic carbonate-bearing rocks that will preserve pathfinder element signatures related to potentially buried mineralisation (compared to marine carbonate-bearing rocks that are unlikely to preserve such signatures) (e.g. Chen et al., 2002). Visual discrimination between marine and pedogenic carbonate-bearing rocks is often difficult, which implies there is a risk that the incorrect lithology will be sampled. Whole rock geochemical analysis using pXRF technology in the field and immediate assessment of Ca/Sr ratios removes the potential for such sampling error.

8. Conclusion

Distinguishing between both marine and pedogenic carbonate-bearing rocks that have been highly weathered in the field is difficult and almost impossible in drill cuttings. The use of $^{87}Sr/^{86}Sr$ ratios does not clearly differentiate between marine and pedogenic carbonate-bearing rocks, and needs to be used with caution as contaminants from continental rocks introduce increased radiogenic Sr. The use of Ca/Sr ratios derived from a whole rock geochemical data set is much easier to use to discriminate the difference between marine and pedogenic carbonate-bearing rock. The possibility exists for this type of calculation to be performed quickly in the field using existing portable whole rock geochemical analyser technology. Field assessment of Ca/Sr ratios throughout a carbonate sampling exploration campaign will decrease the risk of collecting incorrect sample media, increase the risk of identifying potential pathfinder elements and is applicable to the Yorke Peninsula and possibly other similar carbonate regolith dominated terrains.

Supplementary data to this article can be found online at http://dx.doi.org/10.1016/j.gexplo.2017.06.019.

Acknowledgements

This work has been supported by the Deep Exploration Technologies Cooperative Research Centre whose activities are funded by the Australian Government's Cooperative Research Centre Programme (20080065). This is DET CRC Document **2017/949** and TRaX paper **374**. The comments received by Dr. K.G. McQueen and an anonymous reviewer, are greatly appreciated, and has improved this manuscript.

References

Anand, R.R., Cornelius, M., 2005. Weathering history, landscape evolution and implications for exploration. In: Anand, R.R., Butt, C.R.M., Robertson, I.D.M., Scott, K.M. (Eds.), Cooperative Research Centre for Landscape Environments and Mineral Exploration (CRC LEME) CSIRO Exploration and Mining Bentley West, (Aust. Australia).

Bain, D.C., Bacon, J.R., 1994. Strontium isotopes as indicators of mineral weathering in catchments. Catena 22, 201–214.

Batjes, N.H., 2012. ISRIC-WISE Derived Soil Properties on a 5 by 5 Arc-minutes Global Grid (Ver. 1.2). Report 2012/01 (with data set, available at www.isric.org) ISRIC-World Soil Information, Wageningen, pp. 0–52.

Binks, P.J., Borner, J.E., Rau, G., Gunter, J., Busuttil, S., Little, G., McGeough, M., Fidler, R., Price, A., Hooper, B., 2004. MIM Exploration: Maitland. (Annual and final reports to licence surrender for the period 7/9/1992 to 24/9/2004. Primary Industries and Resources South Australia Open File Envelope No 8725).

Brantley, S.L., Chesley, J.T., Stillings, L.L., 1998. Isotopic ratios and release rates of strontium measured from weathering feldspars. Geochim. Cosmochim. Acta 62,

1493–1500.
Burke, W.H., Denison, R.E., Hetherington, E.A., Koepnick, R.B., Nelson, H.F., Otto, J.B., 1982. Variation of seawater $^{87}Sr/^{86}Sr$ throughout Phanerozoic time. Geology 10, 516–519.
Chen, X.Y., Lintern, M.J., Roach, I.C., 2002. Calcrete: Characteristics, Distribution and Use in Mineral Exploration. Cooperative Research Centre for Landscape Environments and Mineral Exploration.
Chiquet, A., Michard, A., Nahon, D., Hamelin, B., 1999. Atmospheric input vs in situ weathering in the genesis of calcretes: an Sr isotope study at Galvez (Central Spain). Geochim. Cosmochim. Acta 63 (3–4), 311–323.
Conor, C.H.H., 2002. The Palaeo-Mesoproterozoic Geology of Northern Yorke Peninsula, South Australia: Hiltaba Suite-related Alteration and Mineralisation of the Moonta-Wallaroo Cu-Au District. Department of Primary Industries and Resources, South Australia (Report Book 2002/007).
Conor, C., 2016. Geological Field Excursion Guide - IOCGs - Where It All Began: The Moonta-Wallaroo Region of the Eastern Gawler Craton. Department of State Development, South Australia (Report Book 2016/00009).
Conor, C., Raymond, O., Baker, T., Teale, G., Say, P., Lowe, G., 2010. Alteration and mineralisation in the Moonta-Wallaroo copper-gold mining field region, Olympic Domain, South Australia. In: Porter, T.M. (Ed.), Hydrothermal Iron Oxide Copper-Gold and Related Deposits: A Global Perspective. Advances in the Understanding of IOCG Deposits PGC Publishing, Adelaide, pp. 147–170.
Cowley, W.M., 2005. In: Cowley, W.M. (Ed.), Solid Geology of South Australia. South Australia. Department of Primary Industries and Resources. Mineral Exploration Data Package. 15 DMITRE, South Australia.
Cowley, W.M., Conor, C., Zang, W., 2003. New and revised Proterozoic stratigraphic units on northern Yorke Peninsula. In primary industries and resources. MESA Journal 29, 46–58.
Crawford, A., 1965. The Geology of Yorke Peninsula: Bulletin No. 39. 1–138 Geological Society of South Australia.
Dart, R.C., Barovich, K.M., Chittleborough, D.J., Hill, S.M., 2007. Calcium in regolith carbonates of central and southern Australia: its source and implications for the global carbon cycle. Paleogeography, Palaeoclimatology, Palaeoecology 249, 322–334.
Dart, R.C., Barovich, K.M., Hill, S.M., Chittleborough, D.J., 2012. Sr-isotopes as a tracer of Ca sources and mobility in profiles hosting regolith carbonates from southern Australia. Aust. J. Earth Sci. 59, 373–382.
Drexel, J.F., Preiss, W.V., 1995. The Geology of South Australia, Volume 2; The Phanerozoic. Geological Survey of South Australia, South Australia.
Drexel, J.F., Preiss, W.V., Parker, A.J., 1993. The Geology of South Australia, Volume 1; The Precambrian. Geological Survey of South Australia, South Australia.
Edmond, J.M., 1992. Himalayan tectonics, weathering processes, and the strontium isotope record in marine limestones. Science, New Series 258, 1594–1597.
Ferris, G.M., Schwarz, M.P., Heithersay, P., 2002. The geological framework, distribution and controls of Fe-oxide and related alteration, and Cu-Au mineralisation in the Gawler Craton, South Australia. In: Porter, T.M. (Ed.), Hydrothermal Iron Oxide Copper-Gold and Related Deposits: A Global Perspective. vol. 2. PGC Publishing, Adelaide, pp. 1–23.
Forbes, C.J., Giles, D., Hand, M., Betts, P.G., Suzuki, K., Chalmers, N., Dutch, R., 2011. Using P–T paths to interpret the tectonothermal setting of prograde metamorphism: an example from the northeastern Gawler Craton, South Australia. Precambrian Res. 185, 65–85.
Ghavami-Riabi, R., Theart, H.F.J., De Jager, C., 2008. Detection of concealed Cu–Zn massive sulfide mineralization below eolian sand and a calcrete cover in the eastern part of the Namaqua Metamorphic Province, South Africa. J. Geochem. Explor. 97, 83–101.
Hamidi, E.M., Nahon, D., McKenzie, J.A., Michard, A., Colin, F., Kamel, S., 1999. Marine Sr (Ca) input in Quaternary volcanic rock weathering profiles from the Mediterranean coast of Morocco: Sr isotopic approach. Terra Nova 11, 157–161.
Hill, S.M., Taylor, G., McQueen, K.G., 1998. Discussion "Genesis of some calcretes in the southern Yilgarn Craton, Western Australia: implications for Mineral exploration. Aust. J. Earth Sci. 45, 177–182.
Hillis, R., Giles, D., Van Der Wielen, S., Baensch, A., Cleverley, J., Fabris, A.J., Halley, S., Harris, M., Hill, S.M., Kanck, P.A., Kepic, A., Soe, S., Stewart, G., Uvarova, Y., 2014. Coiled Tubing Drilling and Real-Time Sensing-Enabling Prospecting Drilling in the 21st Century. In: Kelley, K.D., Golden, H.C. (Eds.), SEG Conference on Keystone-Building Exploration Capability for the 21st Century. Society of Economic Geologists Special Publications Seriespp. 243–259 Issue 18. (Keystone, Colorado).
Hoek, J.D., Schaefer, B.F., 1998. Palaeoproterozoic Kimban mobile belt Eyre Peninsula: timing and significance of felsic and mafic magmatism and deformation. Aust. J. Earth Sci. 45, 305–313.
van der Hoek, B.G., Hill, S.M., Dart, R.C., 2012. Calcrete and plant inter-relationships for the expression of concealed mineralization at the Tunkillia gold prospect, central Gawler Craton, Australia. Geochemistry: Exploration, Environment, Analysis: GEEA 12, 361–372.
Howarth, R.J., McArthur, J.M., 1997. Statistics for strontium isotope stratigraph: a robust LOWESS fit to the marine Sr-isotope curve for 0 to 206 Ma, with look-up table for derivation of numeric age. J. Geol. 105, 441–456.
Huntington, J.H., Mauger, A.J., Skirrow, R.G., Bastrakov, E.N., Connor, P., Mason, P., Keeling, J.K., Coward, D.A., Berman, M., Phillips, R., Whitbourn, L.B., Heithersay, P.S., 2006. Automated mineralogical core logging at the Emmie Bluff iron oxide copper-gold. Primary Industries and Resources South Australia. MESA Journal 41, 38–44.
Ismail, R., Ciobanu, C.L., Cook, N.J., Teale, G.S., Giles, D., Schmidt Mumm, A., Wade, B., 2014. Rare earth sand other trace elements in minerals from skarn assemblages, Hillside iron oxide-copper-gold deposit, Yorke Peninsula, South Australia. Lithos 184–187, 456–477.
James, N.P., Bone, Y., 2015. Pleistocene aeolianites at Cape Spencer, South Australia; record of a vanished inner neritic cool-water carbonate factory. Sedimentology 62, 2038–2059.
Lindsay, J.M., 1970. Melton Limestone: multiple mid-Tertiary transgressions, south-eastern Gawler Platform. Geological Survey of South Australia, Quarterly Geological Notes 33, 2–10.
Lintern, M.J., Butt, C.R.M., Robertson, I.D.M., Scott, K.M., Cornelius, M., 2005. Challenger Gold Prospect, Gawler Craton, South Australia. Cooperative Research Centre for Landscape Environments and Mineral Exploration (CRC LEME) CSIRO Exploration and Mining Bentley West. Aust., Australia.
Lintern, M.J., Hough, R., Ryan, C., 2012. Experimental studies on the gold-in-calcrete anomaly at Edoldeh Tank Gold Prospect, Gawler Craton, South Australia. J. Geochem. Explor. 112, 189–205.
Liu, W.-J., Liu, C.-Q., Zhao, Z.-Q., Xu, Z.-F., Liang, C.S., Li, L., Feng, J.-Y., 2013. Elemental and strontium isotopic geochemistry of the soil profiles developed on limestone and sandstone in karstic terrain on Yunnan-Guizhou Plateau, China: implications for chemical weathering and parent materials. J. Asian Earth Sci. 67–68, 138–152.
Marjoribanks, R., 2010. Geological Methods in Mineral Exploration and Mining, 2 ed. Springer, Heidelberg.
McArthur, J.M., Howarth, R.J., Bailey, T.R., 2001. Strontium isotope stratigraphy: LOWESS version 3: best fit to the marine Sr-isotope curve for 0–509 Ma and accompanying look-up table for deriving numerical age. J. Geol. 109, 155–170.
McArthur, J.M., Howarth, R.J., Shields, G.A., 2012. Strontium Isotope Stratigraphy, The Geologic Time Scale. Elsevier.
McQueen, K.G., 2006. Calcrete Geochemistry in the Cobar-Girilambone Region, New South Wales; CRC LEME Open File Report 200. CRC LEME, Bentley, Western Australia.
McQueen, K.G., Hill, S.M., Foster, K.A., 1999. The nature and distribution of regolith carbonate accumulations in southeastern Australia and their potential as a sampling medium in geochemical exploration. J. Geochem. Explor. 67, 67–82.
Milnes, A.R., 1992. Calcretes. In: Martini, I.P., Chesworth, W. (Eds.), Developments in Earth Surface Processes. Weathering, Soils and Palaeosols. Elsevier, Amsterdam.
Milnes, A.R., Hutton, J.T., 1983. Calcretes in Australia. In: Soils: An Australian Viewpoint. CSIRO, Melbourne/Academic Press, London.
Morales-Ruano, S., Both, R.A., Golding, S.D., 2002. A fluid inclusion and stable isotope study of the Moonta copper–gold deposits, South Australia: evidence for fluid immiscibility in a magmatic hydrothermal system. Chem. Geol. 192, 211–226.
Pain, M., Johnson, P., 2002. Yorke Peninsula paleochannel: Adelaide's long-term sand source. In Primary Industries and Resources. MESA Journal 27, 10–14.
Peterman, Z.E., Hedge, C.E., Tourtelot, H.A., 1970. Isotopic composition of strontium in sea water throughout Phanerozoic time. Geochim. Cosmochim. Acta 84, 105–120.
Poustie, T., Abbot, P., 2006. Challenger gold mine — looking at a long-term future. MESA Journal 40, 4–7.
Quade, J., Chivas, A.R., McCulloch, M.T., 1995. Strontium and carbon isotope tracers and the origins of soil carbonate in South Australia and Victoria. Paleogeography, Palaeoclimatology, Palaeoecology 113, 103–117.
Reith, F., Etschmann, B., Dart, R.C., Brewe, D.L., Vogt, S., Schmidt-Mumm, A., Brugger, J., 2011. Distribution and speciation of gold in biogenic and abiogenic calcium carbonates – implications for the formation of gold anomolus calcrete. Geochim. Cosmochim. Acta 75, 1942–1956.
Skirrow, R.G., Bastrakov, E.N., Barovich, K., Fraser, G.L., Creaser, R.A., Fanning, C.M., Raymond, O.L., Davidson, G.J., 2007. Timing of iron oxide Cu-Au-(U) hydrothermal activity and Nd isotope constraints on metal sources in the Gawler Craton, South Australia. Econ. Geol. 102, 1441–1470.
USGS, 2016. USGS Science for a Changing World. Mineral Resources On-Line Spatial Data. https://mrdata.usgs.gov/geology/ (Last accessed Feb. 2017).
Van der Hoven, S.J., Quade, J., 2002. Tracing spatial and temporal variations in the sources of calcium in pedogenic carbonates in a semiarid environment. Geoderma 108, 259–276.
Vasiliev, I., Reichart, G., Davies, G., Krijgsman, W., Stoica, M., 2010. Strontium isotope ratios of the Eastern Paratethys during the Mio-Pliocene transition; implications for interbasinal connectivity. Earth Planet. Sci. Lett. 292, 123–131.
Veizer, J., 1989. Strontium isotopes in seawater through time. Annu. Rev. Earth Planet. Sci. 17, 141–167.
Veizer, J., Compston, W., 1974. $^{87}Sr/^{86}Sr$ composition in seawater during the Phanerozoic. Geochim. Cosmochim. Acta 38, 1461–1484.
Veizer, J., Compston, W., 1976. $^{87}Sr/^{86}Sr$ in Precambrian carbonates as an index of crustal evolution. Geochim. Cosmochim. Acta 40, 905–914.
Wickman, F.W., 1948. Isotope ratios—a clue to the age of certain marine sediments. J. Geol. 56, 61–66.
Wurst, A.T., 1994. Analyses of Late Stage, Mesoproterozoic, Syn and Post Tectonic, Magmatic Events in the Moonta Sub-Domain: Implications for Cu-Au Mineralisation in the "Copper Triangle" of South Australia. Hons thesis (Unpub.) University of Adelaide.
Zang, W.-L., Cowley, W.M., Fairclough, M., 2006. Maitland Special South Australia 1:250000 Geological Series Sheet S153-12 - Explanatory Notes. PIRSA Publishing Services, South Australia.
Zhao, Y.-Y., Zheng, Y.-F., Chen, F., 2009. Trace element and strontium isotope constraints on sedimentary environment of Ediacaran carbonates in southern Anhui, South China. Chem. Geol. 345–362.

Appendix 2

Chapter 2:

Geochemical Tables

Vertical lithogeochemical profiles:

Myponie Point

Balgowan

Point Turton

And

Seawater from Balgowan and Ardrossan

		Duplicate ID	DepthFrom ASL	DepthTo ASL	Sample Depth Top Down	Location	Orig_Grid_ID	Orig_East
Lab analytical method code	Lab analytical method code							
Unit	Unit							
Detection Limit	Detection Limit							
DataSet	**SampleID**							
Yorke Peninsula	PT01	PT10	0.00	1.00	7.50	Point Turton	GDA94 53H	714324
Yorke Peninsula	PT02	PT11	1.00	2.00	7.00	Point Turton	GDA94 53H	714324
Yorke Peninsula	PT03	NR	2.00	3.00	6.00	Point Turton	GDA94 53H	714324
Yorke Peninsula	PT04	NR	3.00	4.00	5.00	Point Turton	GDA94 53H	714324
Yorke Peninsula	PT05a	NR	4.00	4.50	4.00	Point Turton	GDA94_53H	714324
Yorke Peninsula	PT05b	NR	4.50	5.00	4.00	Point Turton	GDA94_53H	714324
Yorke Peninsula	PT06	NR	5.00	6.00	3.00	Point Turton	GDA94_53H	714324
Yorke Peninsula	PT07	NR	6.00	7.00	2.00	Point Turton	GDA94_53H	714324
Yorke Peninsula	PT08	NR	7.00	7.50	1.00	Point Turton	GDA94_53H	714324
Yorke Peninsula	PT09	NR	7.50	7.60	0.00	Point Turton	GDA94_53H	714324
Yorke Peninsula	PT05bFe+	NR	4.50	5.00	4.00	Point Turton	GDA94_53H	714324
Yorke Peninsula	PT10	PT01	0.00	1.00	7.50	Point Turton	GDA94_53H	714324
Yorke Peninsula	PT11	PT02	1.00	2.00	7.00	Point Turton	GDA94_53H	714324
Yorke Peninsula	BAL01	BAL18	0.00	0.50	11.00	Balgowan	GDA94_53H	729511
Yorke Peninsula	BAL02	BAL19	0.50	1.00	10.50	Balgowan	GDA94_53H	729511
Yorke Peninsula	BAL03	NR	1.00	2.00	9.50	Balgowan	GDA94_53H	729511
Yorke Peninsula	BAL04	NR	2.00	3.00	8.50	Balgowan	GDA94_53H	729511
Yorke Peninsula	BAL05	NR	3.00	4.00	7.50	Balgowan	GDA94_53H	729511
Yorke Peninsula	BAL06	NR	4.00	4.50	7.00	Balgowan	GDA94_53H	729511
Yorke Peninsula	BAL07	NR	4.50	4.80	6.60	Balgowan	GDA94_53H	729511
Yorke Peninsula	BAL08	NR	4.80	5.30	6.10	Balgowan	GDA94_53H	729511
Yorke Peninsula	BAL09	NR	5.30	5.80	5.20	Balgowan	GDA94_53H	729511
Yorke Peninsula	BAL10	NR	5.80	6.30	4.70	Balgowan	GDA94_53H	729511
Yorke Peninsula	BAL11	NR	6.30	7.00	4.00	Balgowan	GDA94_53H	729511
Yorke Peninsula	BAL12	NR	7.00	8.00	3.00	Balgowan	GDA94_53H	729511
Yorke Peninsula	BAL13	NR	8.00	8.50	2.50	Balgowan	GDA94_53H	729511
Yorke Peninsula	BAL14	NR	8.50	9.00	2.00	Balgowan	GDA94_53H	729511
Yorke Peninsula	BAL15	NR	9.00	9.50	1.50	Balgowan	GDA94_53H	729511
Yorke Peninsula	BAL16	NR	9.50	10.00	1.00	Balgowan	GDA94_53H	729511
Yorke Peninsula	BAL17	NR	10.00	11.00	0.00	Balgowan	GDA94_53H	729511
Yorke Peninsula	BAL18	BAL01	0.00	0.50	11.00	Balgowan	GDA94_53H	729511
Yorke Peninsula	BAL19	BAL02	0.50	1.00	10.50	Balgowan	GDA94_53H	729511
Yorke Peninsula	MP01	MP15	0.00	2.00	12.00	Myponie Point	GDA94_53H	744935
Yorke Peninsula	MP02	MP16	2.00	3.00	10.00	Myponie Point	GDA94_53H	744935
Yorke Peninsula	MP03	NR	3.00	3.20	9.80	Myponie Point	GDA94_53H	744935
Yorke Peninsula	MP04	NR	3.20	4.00	9.00	Myponie Point	GDA94_53H	744935
Yorke Peninsula	MP05	NR	4.00	4.30	8.70	Myponie Point	GDA94_53H	744935
Yorke Peninsula	MP06	NR	4.30	5.30	7.70	Myponie Point	GDA94_53H	744935
Yorke Peninsula	MP07	NR	5.30	6.30	6.70	Myponie Point	GDA94_53H	744935
Yorke Peninsula	MP08	NR	6.30	7.00	6.00	Myponie Point	GDA94_53H	744935
Yorke Peninsula	MP09	NR	7.00	8.00	5.00	Myponie Point	GDA94_53H	744935
Yorke Peninsula	MP10	NR	8.00	9.00	4.00	Myponie Point	GDA94_53H	744935
Yorke Peninsula	MP11	NR	9.00	10.00	3.00	Myponie Point	GDA94_53H	744935
Yorke Peninsula	MP12	NR	10.00	11.00	2.00	Myponie Point	GDA94_53H	744935
Yorke Peninsula	MP13	NR	11.00	12.00	1.00	Myponie Point	GDA94_53H	744935
Yorke Peninsula	MP14	NR	12.00	13.00	0.00	Myponie Point	GDA94_53H	744935
Yorke Peninsula	MP15	MP01	0.00	2.00	12.00	Myponie Point	GDA94_53H	744935
Yorke Peninsula	MP16	MP02	2.00	3.00	10.00	Myponie Point	GDA94_53H	744935
Seawater	Ardrosaan Seawater		0.00	0.00		Ardrossan		768561
Seawater	Balgowan Seawater		0.00	0.00		Balgowan		729320

	Orig_North	Sample Weight_kg	Sample_Description	SiO2_pct	Al2O3_pct	Fe2O3_pct
Lab analytical method code				4X	4X	4X
Unit				wt%	wt%	wt%
Detection Limit				0.1	0.01	0.01
SampleID						
PT01	6132167	2	fossiliferous, bedded limestone, shell fragments	1.80	0.51	1.04
PT02	6132167	2	fossiliferous, bedded limestone, shell fragments and visible bryozoa	4.10	0.48	0.71
PT03	6132167	2	fossiliferous, bedded limestone, shell fragments	2.70	0.67	0.63
PT04	6132167	2	fossiliferous, bedded limestone, shell fragments	2.50	0.59	0.82
PT05a	6132167	2	transition to a more blocky heterogeneous limestone	5.00	0.56	0.42
PT05b	6132167	2	dissolution pipe, nodules and some ferruginous gravels	16.20	2.17	1.01
PT06	6132167	2	calcrete, nodular 5cm with limestone nuclei. Cemented	6.00	1.06	0.44
PT07	6132167	2	calcrete, nodular 1cm with limestone nuclei. Cemented	9.20	1.47	0.60
PT08	6132167	2	nodules of calcrete, bouldery from 5cm in size. Cemented	14.10	1.58	0.62
PT09	6132167	2	nodules of calcrete, bouldery from 5cm in size, well cemented and containing angular gravels.	15.50	1.54	0.54
PT05bFe+	6132167	2	ferruginous gravels from the dissolution pipe	66.20	8.48	8.83
PT10	6132167	2	fossiliferous, bedded limestone, shell fragments duplicate of PT01	1.70	0.50	1.00
PT11	6132167	2	fossiliferous, bedded limestone, shell fragments and visible bryozoa duplicate of PT02	4.10	0.48	0.69
BAL01	6199118	2	very fine sand in red brown clay and silt	88.80	2.66	3.08
BAL02	6199118	2	very fine sand in red brown clay and silt	80.30	5.48	4.09
BAL03	6199118	2	very fine sand in red brown clay and silt, becoming more clay rich and less sand	72.10	11.17	4.90
BAL04	6199118	2	very fine sand in red brown clay and silt, becoming more clay rich and less sand with veining of greyish clay	68.60	13.56	4.72
BAL05	6199118	2	red brown clay with veining of whitish powdery material to flaky sheets throughout, possibly alunite	58.00	19.43	3.51
BAL06	6199118	2	red brown clay with fine grains and steining of hematitic composition. Roots are found to be present in this layer indicating a paleosol.	66.40	12.34	4.84
BAL07	6199118	2	this is the base of the carbonate sequence at this location. There is a paler watered down appearance to the redbrown earth along with the presence of creamy nodules. Has a very fine sandy texture.	52.60	7.97	3.16
BAL08	6199118	2	fine sandy texture with visible quartz grains (fine) pale creamy brown with fine to medium carbonate grains throughout. Appears generally sandy	46.60	6.10	2.38
BAL09	6199118	2	very fine to silty carbonate rich sandy layer light brown to cream in colour. No visible fossils	26.00	4.72	1.93
BAL10	6199118	2	carbonate nodules, pebbly to bouldery in size, forms a platform or band in the outcrop, the first and lowest band in a series. No fossils observed	18.00	2.41	1.00
BAL11	6199118	2	calcareous silty sand	18.10	2.32	0.97
BAL12	6199118	2	fossiliferous limestone layer, is bouldery, hard and well compacted and at 20-30cm thick, forms the second platform of limestone at this locale.	15.40	2.57	1.10
BAL13	6199118	2	calcareous sandy layer between platforms	35.20	2.02	0.73
BAL14	6199118	2	limestone band, 3rd platform up, blocky, around 40cm thick and relatively brittle. No fossils apparent	27.10	1.98	0.78
BAL15	6199118	2	calcareous silty interlayer, around a meter thick in total	35.20	2.35	0.85
BAL16	6199118	2	limestone platform, 4th one, sampled from uppermost surface	27.40	2.70	1.06
BAL17	6199118	2	calcareous dunes, aeolian?	47.10	2.44	0.85
BAL18	6199118	2	very fine sand in red brown clay and silt	88.80	2.69	3.22
BAL19	6199118	2	very fine sand in red brown clay and silt	80.90	5.48	4.07
MP01	6253622	2	weathered granite saprock with visible quartz mica feldspar less than 30% weathered, very yellowed in colour	68.80	12.34	5.30
MP02	6253622	2	weathered granite saprolith containing medium to find sands of quartz and coarse to sub angular fragments of granite grains; quartz, and feldspars. Is sandy shelly and gritty	87.00	3.33	2.76
MP03	6253622	2	pebbly layer just below a 'fluidised ' layer, subangular to subrounded pebbles and angular clasts. Grainsize coarse to very coarse and pebbly	61.60	14.11	4.93
MP04	6253622	2	fossiliferous limestone containing Bryozoa, echinoderm spines.. "Melton Limestone?" coarse to very coarse texture	25.60	2.82	1.79
MP05	6253622	2	limestone? A 30cm thick layer of clay rich, almost mud like texture, has a greyish red to yellow alteration banding. Is gritty with visible coarse subrounded grains of quartz	76.10	7.14	3.42
MP06	6253622	2	fossiliferous limestone, shell fragments with coarse quartz grit at the base	15.30	1.77	1.53
MP07	6253622	2	limestone, shelly, fossiliferous and very well cemented/competant, forms the first of a series of 'platforms'	5.30	0.93	1.01
MP08	6253622	2	hard competant limestone. Blocky and cemented in appearance and has rings of concretions	3.10	0.64	0.80
MP09	6253622	2	hard competant limestone. Blocky and cemented in appearance,has rings of concretions and fossils of echinoids and other fragments of shells present	1.40	0.31	0.63
MP10	6253622	2	limestone, fossiliferous containing bryozoa and echinoids and other broken shell fragments, gritty coarse to medium grainsize texture	2.20	0.54	0.44
MP11	6253622	2	rubbly calcareous with some fossil shell visible on broken surfaces	2.40	0.63	0.79
MP12	6253622	2	nodular weathered looking calcrete, gritty and easily broken, no apparent fossils	19.80	2.35	0.93
MP13	6253622	2	nodular and well cemented finer grained 'hardpan' calcrete, no fossils	14.10	1.97	0.80
MP14	6253622	2	chalky gritty calcrete containing nodules of calcrete with pisolitic growth ring textures	11.00	1.53	0.64
MP15	6253622	NR	Duplicate	68.70	12.27	5.47
MP16	6253622	NR	Duplicate	86.20	3.24	2.74
Ardrosaan Seawater	6187062		Ardrossan Jetty from first steps coming down into the water, calm conditions			
Balgowan Seawater	6199207		taken off the groin/rocks			

	CaO_pct	Ca/Sr	MgO_pct	Mg/Sr	Na2O_pct	K2O_pct	MnO_pct	TiO2_pct
Lab analytical method code	4X	user calculated	4X	user calculated	4X	4X	4X	4X
Unit	wt%	ratio	wt%	ratio	wt%	wt%	wt%	wt%
Detection Limit	0.01		0.01		0.01	0.01	0.01	0.01
SampleID								
PT01	51.82	2103	1.50	51	0.02	0.01	0.07	0.02
PT02	52.73	2440	0.77	30	0.01	0.05	0.03	0.04
PT03	52.74	1852	1.09	32	0.01	0.01	0.02	0.03
PT04	52.18	1557	1.80	45	0.02	0.04	0.04	0.03
PT05a	51.08	1259	1.27	26	0.03	0.01	0.01	0.02
PT05b	38.04	616	1.94	27	0.66	0.12	0.01	0.11
PT06	46.46	392	3.74	27	0.03	0.03	0.01	0.04
PT07	45.63	450	2.59	22	0.03	0.04	0.01	0.07
PT08	43.53	358	1.93	13	0.10	0.21	0.03	0.06
PT09	43.02	304	2.08	12	0.14	0.39	0.02	0.06
PT05bFe+	2.98	55	0.43	7	1.04	2.35	0.01	0.81
PT10	51.98	2070	1.59	53	0.02	0.01	0.07	0.02
PT11	52.44	2347	0.77	29	0.01	0.06	0.02	0.06
BAL01	0.05	10	0.45	1	0.96	0.01	0.38	0.02
BAL02	0.06	11	0.60	1	1.22	0.01	0.50	0.01
BAL03	0.10	10	0.69	1	1.24	0.01	0.61	0.02
BAL04	0.07	8	0.77	1	1.44	0.01	0.58	0.02
BAL05	0.12	16	1.14	2	1.53	0.02	0.43	0.01
BAL06	0.17	16	1.61	2	2.29	0.04	0.60	0.01
BAL07	7.66	111	5.78	2	0.81	0.03	0.42	0.01
BAL08	17.55	211	3.24	1	0.53	0.02	0.33	0.01
BAL09	29.51	196	3.74	1	0.28	0.02	0.25	0.02
BAL10	40.06	299	1.73	0	0.11	0.02	0.12	0.01
BAL11	36.44	189	5.07	0	0.12	0.01	0.12	0.02
BAL12	41.22	304	1.83	0	0.10	0.02	0.13	0.02
BAL13	25.61	153	6.59	0	0.32	0.01	0.10	0.01
BAL14	34.92	222	2.42	0	0.25	0.02	0.10	0.01
BAL15	26.02	151	5.68	0	0.26	0.02	0.11	0.01
BAL16	34.42	261	1.92	0	0.28	0.02	0.15	0.02
BAL17	22.91	197	2.65	0	0.53	0.01	0.12	0.03
BAL18	0.05	11	0.45	1	0.74	0.01	0.39	0.01
BAL19	0.07	12	0.60	1	1.03	0.01	0.51	0.01
MP01	0.08	14	1.04	148	1.60	6.32	0.01	0.68
MP02	0.13	22	0.51	73	0.95	1.04	0.01	0.15
MP03	0.40	32	1.00	67	2.71	2.41	0.02	0.12
MP04	36.98	2589	0.68	40	0.16	0.39	0.02	0.08
MP05	0.50	55	1.28	118	2.05	2.23	0.02	0.51
MP06	44.43	3095	0.64	38	0.12	0.35	0.08	0.05
MP07	51.90	2706	0.67	29	0.04	0.08	0.06	0.03
MP08	53.79	2433	0.62	24	0.01	0.07	0.03	0.02
MP09	54.98	2547	0.60	23	0.01	0.03	0.03	0.01
MP10	54.41	2312	0.66	24	0.01	0.02	0.02	0.02
MP11	53.60	2233	0.77	27	0.01	0.01	0.03	0.02
MP12	34.51	184	6.36	29	0.13	0.16	0.01	0.14
MP13	41.47	235	3.50	17	0.11	0.18	0.01	0.11
MP14	44.03	220	2.74	12	0.08	0.08	0.01	0.09
MP15	0.10	17	1.10		1.60	6.28	0.01	0.77
MP16	0.16	25	0.51		0.92	1.03	0.01	0.12
Ardrosaan Seawater								
Balgowan Seawater								

	P2O5_pct	Cr2O3_pct	Ba_pct	LOI_pct	SUM_pct	TOT/C_pct	TOT/S_pct	Ba_ppm	Be_ppm	Co_ppm	Cs_ppm	Ga_ppm	Hf_ppm
Lab analytical method code	4X	4X	4X	4X	4X	2A Leco	2A Leco	4B	4B	4B	4B	4B	4B
Unit	wt%	wt%	wt%	%	%	%	%	PPM	PPM	PPM	PPM	PPM	PPM
Detection Limit	0.01	0.001	0.01	-5.11	0.01	0.02	0.02	1	1	0.2	0.1	0.5	0.1
SampleID													
PT01	0.02	0.00	0.01	43.49	100.31	12.33	0.07	60.00	0.50	3.00	0.20	0.25	0.60
PT02	0.02	0.00	0.01	42.01	100.90	12.50	0.02	36.00	0.50	1.50	0.20	0.25	1.10
PT03	0.02	0.00	0.01	42.72	100.60	12.26	0.09	33.00	0.50	1.20	0.10	0.25	0.60
PT04	0.03	0.00	0.01	42.93	100.97	12.36	0.06	48.00	0.50	3.30	0.20	0.25	0.90
PT05a	0.01	0.00	0.01	42.34	100.77	12.35	0.07	99.00	0.50	2.00	0.20	0.25	0.40
PT05b	0.01	0.00	0.01	38.01	98.27	9.48	0.09	112.00	2.00	7.20	0.50	1.90	0.60
PT06	0.01	0.00	0.01	42.60	100.39	12.24	0.13	103.00	0.50	3.20	0.30	0.70	0.60
PT07	0.01	0.00	0.01	40.63	100.31	11.25	0.10	94.00	0.50	3.40	0.30	1.40	0.70
PT08	0.02	0.00	0.01	38.12	100.28	10.84	0.09	105.00	0.50	8.30	0.40	1.70	1.80
PT09	0.02	0.00	0.01	37.15	100.42	10.64	0.06	113.00	2.00	3.20	0.40	1.20	2.10
PT05bFe+	0.01	0.01	0.39	7.98	99.55	0.72	0.10	3756.00	0.50	42.40	1.50	10.60	7.90
PT10	0.02	0.00	0.01	43.61	100.57	12.24	0.07	58.00	0.50	3.10	0.20	0.25	0.50
PT11	0.03	0.00	0.01	41.97	100.57	12.40	0.01	41.00	0.50	1.20	0.20	0.25	1.20
BAL01	0.00	0.02	2.41	99.58	0.08	0.03	197.00	0.50	1.80	1.30	6.50	4.80	6.40
BAL02	0.01	0.02	5.65	99.36	0.12	0.03	257.00	0.50	2.60	2.40	10.20	4.40	8.10
BAL03	0.01	0.05	7.29	99.09	0.15	0.06	561.00	0.50	4.80	3.30	14.00	6.30	8.50
BAL04	0.01	0.03	8.46	99.26	0.14	0.07	331.00	2.00	3.70	3.50	13.30	5.80	8.50
BAL05	0.01	0.04	12.75	99.18	0.11	0.06	106.00	1.00	8.50	2.60	9.80	3.50	5.70
BAL06	0.02	0.02	9.19	99.11	0.11	0.05	203.00	2.00	20.70	4.60	14.90	5.60	10.10
BAL07	0.01	0.01	19.66	99.64	2.84	0.06	169.00	0.50	9.50	2.70	9.80	4.60	6.70
BAL08	0.01	0.02	22.49	100.23	4.48	0.05	182.00	0.50	7.50	1.90	7.50	2.90	5.20
BAL09	0.00	0.02	32.23	99.22	7.45	0.12	155.00	0.50	5.70	1.60	5.40	2.40	3.60
BAL10	0.00	0.01	36.20	99.77	9.40	0.11	102.00	1.00	6.60	0.70	2.20	1.30	1.40
BAL11	0.00	0.01	36.64	99.97	9.67	0.12	92.00	0.50	2.80	0.70	2.20	1.30	1.80
BAL12	0.00	0.01	37.36	99.91	9.77	0.11	124.00	0.50	5.50	1.00	2.60	1.40	1.50
BAL13	0.00	0.01	28.97	99.67	7.66	0.04	98.00	0.50	2.60	0.60	2.00	1.10	1.50
BAL14	0.00	0.01	31.96	99.63	8.65	0.07	86.00	0.50	5.70	0.70	2.00	1.10	1.20
BAL15	0.00	0.01	28.93	99.65	7.39	0.07	104.00	0.50	3.30	0.70	2.10	1.40	1.40
BAL16	0.00	0.01	31.38	99.59	8.29	0.06	114.00	0.50	5.00	0.90	2.70	1.90	1.70
BAL17	0.00	0.01	22.66	99.45	6.01	0.04	112.00	0.50	2.80	0.70	2.70	2.60	1.90
BAL18	0.00	0.02	2.77	99.73	0.06	0.03	164.00	0.50	1.70	1.30	7.10	5.90	5.80
BAL19	0.01	0.02	6.03	100.03	0.08	0.04	265.00	0.50	3.50	2.40	12.00	5.30	7.10
MP01	0.05	0.00	0.09	2.76	99.04	0.05	0.01	688.00	2.00	6.70	2.50	20.60	13.50
MP02	0.01	0.01	0.01	4.12	100.00	0.01	0.01	131.00	0.50	3.00	0.60	2.20	2.80
MP03	0.04	0.01	0.03	12.25	99.64	0.04	0.05	257.00	0.50	9.80	0.90	4.30	3.70
MP04	0.01	0.00	0.01	31.08	99.68	8.36	0.02	101.00	0.50	5.10	0.40	1.70	1.70
MP05	0.01	0.01	0.03	6.71	100.00	0.11	0.01	252.00	0.50	6.50	4.40	7.40	7.30
MP06	0.01	0.00	0.01	36.07	100.42	9.68	0.01	150.00	0.50	2.80	0.70	1.60	0.90
MP07	0.01	0.00	0.01	41.09	101.10	11.78	0.02	79.00	1.00	2.20	0.30	0.25	1.00
MP08	0.01	0.01	0.01	42.11	101.23	12.50	0.06	102.00	3.00	0.50	0.20	0.25	0.50
MP09	0.01	0.01	0.01	43.02	101.00	12.77	0.01	40.00	0.50	0.70	0.05	0.25	0.20
MP10	0.01	0.00	0.01	42.76	101.04	12.63	0.01	56.00	0.50	1.00	0.05	0.25	0.10
MP11	0.01	0.01	0.01	42.54	100.81	12.44	0.02	117.00	1.00	1.50	0.10	0.60	0.30
MP12	0.01	0.00	0.01	35.81	100.19	9.91	0.05	121.00	1.00	6.80	0.60	2.30	1.80
MP13	0.02	0.00	0.01	37.74	100.03	10.69	0.08	125.00	0.50	3.90	0.50	1.80	2.00
MP14	0.03	0.00	0.01	39.75	100.01	11.30	0.11	103.00	2.00	3.90	0.50	1.40	1.40
MP15	0.05	0.00	0.08	2.60	99.05	0.03	0.01	653.00	2.00	7.20	2.60	20.40	13.30
MP16	0.01	0.01	0.01	4.27	99.23	0.02	0.01	132.00	0.50	2.80	0.70	2.00	2.60
Ardrosaan Seawater													
Balgowan Seawater													

	Nb_ppm	Rb_ppm	Sn_ppm	Sr_ppm	Ta_ppm	Th_ppm	U_ppm	V_ppm	W_ppm	Zr_ppm	Y_ppm	La_ppm	Ce_ppm
Lab analytical method code	4B	4B	4B	4B	4B	4B	4B	4B	4B	4B	4B	4B	4B
Unit	PPM	PPM	PPM	PPM	PPM	PPM	PPM	PPM	PPM	PPM	PPM	PPM	PPM
Detection Limit	0.1	0.1	1	0.5	0.1	0.2	0.1	8	0.5	0.1	0.1	0.1	0.1
SampleID													
PT01	0.80	4.40	0.50	176.10	0.05	2.10	0.30	51.00	1.10	20.30	9.70	14.70	9.80
PT02	1.00	5.80	0.50	154.50	0.05	1.60	0.30	21.00	0.25	53.90	2.90	5.20	8.60
PT03	0.40	4.60	0.50	203.50	0.05	1.60	0.20	18.00	0.25	19.70	4.00	5.70	8.20
PT04	0.30	5.30	0.50	239.60	0.05	2.00	0.30	23.00	0.25	32.20	2.60	5.70	7.80
PT05a	0.20	3.40	0.50	290.10	0.05	1.10	0.30	12.00	0.25	11.60	4.80	6.60	7.30
PT05b	1.30	10.80	0.50	441.50	0.05	3.00	0.60	24.00	0.25	25.30	7.20	14.10	19.50
PT06	0.50	6.10	0.50	846.50	0.05	0.90	0.60	13.00	0.25	15.20	2.70	3.00	6.00
PT07	1.20	9.20	0.50	725.20	0.05	1.60	0.70	12.00	0.25	28.60	3.40	3.80	6.80
PT08	1.10	15.70	0.50	869.90	0.05	3.10	1.00	10.00	0.25	60.00	10.50	9.80	13.30
PT09	0.90	16.80	0.50	1011.70	0.05	2.30	0.80	9.00	0.25	73.00	7.70	8.30	10.30
PT05bFe+	14.30	70.10	1.00	386.20	1.20	8.30	1.70	232.00	217.20	318.70	14.30	14.50	28.90
PT10	0.80	4.00	0.50	179.50	0.05	2.10	0.20	47.00	1.10	14.80	10.80	17.30	10.00
PT11	0.80	6.30	0.50	159.70	0.05	1.60	0.30	22.00	0.25	38.10	2.60	4.80	7.90
BAL01	31.00	1.00	35.90	0.36	0.50	5.20	1.30	55.00	1.10	208.00	5.20	8.20	11.80
BAL02	44.60	2.00	39.10	0.39	0.50	8.10	1.10	77.00	1.30	174.30	6.30	10.00	14.90
BAL03	60.30	2.00	70.60	0.71	0.70	10.30	2.00	107.00	1.30	225.40	9.00	12.80	18.60
BAL04	62.10	2.00	63.10	0.63	0.60	12.00	2.90	241.00	1.40	184.60	8.10	14.80	19.00
BAL05	52.20	2.00	53.70	0.54	0.40	11.90	13.80	140.00	1.00	114.80	8.40	12.90	376.50
BAL06	83.60	3.00	74.00	0.74	0.60	13.70	2.70	150.00	1.40	209.50	26.40	33.60	63.10
BAL07	53.70	2.00	491.10	4.91	0.50	8.50	1.70	96.00	0.90	180.00	34.80	38.00	40.40
BAL08	42.90	1.00	594.00	5.94	0.30	6.10	1.30	80.00	0.70	125.70	15.50	16.70	30.70
BAL09	31.90	0.50	1078.60	10.79	0.20	4.60	2.00	53.00	0.25	93.50	11.10	12.40	24.00
BAL10	17.90	0.50	957.10	9.57	0.05	2.90	2.50	35.00	0.25	55.80	7.90	8.40	16.20
BAL11	17.20	1.00	1379.30	13.79	0.20	4.40	1.80	33.00	0.25	47.20	6.40	6.90	14.30
BAL12	18.20	0.50	969.60	9.70	0.20	2.60	1.80	38.00	0.25	48.90	8.30	8.40	16.70
BAL13	19.70	0.50	1194.80	11.95	0.20	2.30	1.20	23.00	0.25	48.10	6.20	5.80	12.60
BAL14	18.50	0.50	1124.10	11.24	0.05	2.00	1.50	20.00	0.25	42.80	5.00	4.80	10.50
BAL15	21.60	0.50	1234.60	12.35	0.10	2.50	1.00	27.00	0.25	54.10	7.00	6.00	12.20
BAL16	22.90	0.50	942.60	9.43	0.10	2.90	1.00	27.00	0.25	56.00	7.20	7.40	15.60
BAL17	23.80	2.00	831.30	8.31	0.20	2.50	0.60	18.00	0.25	98.80	6.50	6.60	13.30
BAL18	33.00	0.50	32.60	0.33	0.50	5.40	1.30	53.00	0.90	234.90	5.20	7.50	12.20
BAL19	50.10	2.00	40.30	0.40	0.80	8.10	1.20	78.00	0.80	197.70	6.50	9.20	13.60
MP01	49.00	452.40	6.00	42.30	4.40	48.30	6.70	56.00	0.60	498.00	50.50	133.00	235.80
MP02	4.40	42.80	0.50	42.00	0.30	7.80	1.00	136.00	1.00	103.20	3.40	3.90	5.80
MP03	5.00	102.00	1.00	90.20	0.50	8.40	22.20	127.00	2.30	135.10	34.20	36.10	86.90
MP04	2.40	38.50	0.50	102.10	0.20	4.60	3.40	66.00	0.60	65.40	16.80	46.90	102.60
MP05	10.60	107.30	2.00	65.30	1.00	15.90	2.10	144.00	1.50	281.30	14.40	16.70	74.50
MP06	1.90	30.70	0.50	102.60	0.20	4.10	1.40	62.00	0.70	29.00	12.30	23.40	17.40
MP07	1.40	8.50	0.50	137.10	0.05	2.70	1.70	58.00	0.25	34.60	7.90	17.50	11.10
MP08	1.10	7.30	0.50	158.00	0.05	2.00	2.20	64.00	0.25	16.70	7.30	7.70	9.10
MP09	0.40	3.00	0.50	154.30	0.05	1.60	2.50	52.00	0.25	4.80	13.10	19.70	5.60
MP10	0.30	4.10	0.50	168.20	0.05	1.50	0.60	36.00	0.25	6.50	16.80	16.50	5.80
MP11	0.40	4.90	0.50	171.60	0.10	2.50	0.70	48.00	0.25	9.90	9.10	10.20	9.10
MP12	1.90	15.80	0.50	1341.20	0.40	2.70	1.20	42.00	0.25	58.90	4.90	6.50	12.70
MP13	1.10	13.00	0.50	1260.50	0.20	2.40	1.20	37.00	0.25	61.00	6.50	7.40	13.00
MP14	1.10	10.10	0.50	1429.70	0.10	2.30	1.00	30.00	0.25	45.80	5.10	5.70	11.30
MP15	56.10	445.90	5.00	42.60	4.90	51.90	7.00	53.00	0.25	507.50	39.60	114.20	200.80
MP16 Ardrosaan Seawater	4.10	42.80	0.50	45.30	0.40	8.10	0.90	120.00	1.10	92.50	3.30	4.80	7.60
Balgowan Seawater													

	Pr_ppm	Nd_ppm	Sm_ppm	Eu_ppm	Gd_ppm	Tb_ppm	Dy_ppm	Ho_ppm	Er_ppm	Tm_ppm	Yb_ppm	Lu_ppm	Mo_ppm	Cu_ppm
Lab analytical method code	4B	4B	4B	4B	4B	4B	4B	4B	4B	4B	4B	4B	1DX	1DX
Unit	PPM	PPM	PPM	PPM	PPM	PPM	PPM	PPM	PPM	PPM	PPM	PPM	PPM	PPM
Detection Limit	0.02	0.3	0.05	0.02	0.05	0.01	0.05	0.02	0.03	0.01	0.05	0.01	0.1	0.1
SampleID														
PT01	2.39	9.40	1.45	0.32	1.54	0.17	1.24	0.22	0.59	0.07	0.49	0.04	0.30	5.20
PT02	1.13	4.50	0.67	0.10	0.66	0.07	0.46	0.10	0.21	0.03	0.17	0.03	0.05	3.80
PT03	1.24	4.00	0.80	0.18	0.81	0.10	0.72	0.16	0.35	0.04	0.26	0.03	0.05	1.90
PT04	1.17	3.90	0.87	0.11	0.68	0.08	0.57	0.09	0.25	0.03	0.14	0.01	0.10	2.70
PT05a	1.53	5.90	1.16	0.21	0.98	0.12	0.68	0.16	0.34	0.04	0.34	0.05	0.05	1.40
PT05b	3.30	11.90	2.20	0.45	1.96	0.23	1.47	0.24	0.63	0.09	0.50	0.07	0.10	2.40
PT06	0.79	3.40	0.62	0.14	0.60	0.07	0.54	0.09	0.29	0.04	0.24	0.02	0.05	3.60
PT07	0.88	3.20	0.70	0.16	0.57	0.08	0.59	0.11	0.28	0.04	0.29	0.04	0.05	3.50
PT08	2.32	8.50	1.88	0.41	1.93	0.26	1.67	0.31	0.81	0.12	1.02	0.10	0.10	2.30
PT09	1.91	7.70	1.54	0.34	1.42	0.19	1.13	0.21	0.64	0.10	0.62	0.08	0.05	2.00
PT05bFe+	3.06	10.90	2.16	0.47	2.19	0.36	2.45	0.54	1.73	0.24	1.87	0.24	2.30	4.30
PT10	2.62	9.80	1.56	0.31	1.76	0.20	1.32	0.24	0.57	0.06	0.56	0.06	0.30	4.90
PT11	0.95	4.60	0.60	0.10	0.52	0.07	0.35	0.08	0.26	0.03	0.11	0.02	0.05	2.90
BAL01	1.32	5.20	0.67	0.13	0.58	0.10	0.77	0.15	0.54	0.08	0.78	0.09	0.90	3.20
BAL02	1.65	5.60	0.98	0.21	0.99	0.13	1.01	0.18	0.71	0.12	0.69	0.11	0.40	5.20
BAL03	2.12	5.80	1.31	0.24	1.23	0.19	1.44	0.31	1.08	0.15	1.30	0.17	0.70	6.60
BAL04	2.21	7.30	1.26	0.25	1.20	0.17	1.46	0.26	0.90	0.15	1.09	0.15	3.30	7.80
BAL05	3.00	9.10	2.18	0.42	1.39	0.26	1.99	0.29	1.08	0.18	1.40	0.14	0.30	8.60
BAL06	8.77	32.30	5.95	1.34	5.53	0.97	5.70	1.14	3.27	0.53	4.10	0.53	0.10	15.40
BAL07	8.97	33.20	7.34	1.64	7.26	1.05	5.91	1.17	3.17	0.44	2.99	0.42	0.10	9.70
BAL08	4.22	16.50	3.21	0.76	3.02	0.45	2.50	0.52	1.53	0.23	1.59	0.23	0.05	8.00
BAL09	3.14	12.10	2.43	0.54	2.25	0.36	2.10	0.44	1.17	0.17	1.29	0.15	0.05	8.10
BAL10	2.09	8.90	1.48	0.35	1.53	0.23	1.43	0.29	0.90	0.11	0.85	0.09	0.10	4.30
BAL11	1.93	7.30	1.54	0.35	1.50	0.20	1.30	0.24	0.63	0.09	0.58	0.08	0.05	4.30
BAL12	2.24	7.80	1.82	0.38	1.60	0.25	1.57	0.28	0.79	0.11	0.80	0.10	0.05	4.10
BAL13	1.57	5.70	1.29	0.29	1.12	0.17	1.09	0.23	0.59	0.08	0.73	0.07	0.05	6.60
BAL14	1.28	5.70	1.08	0.22	0.93	0.14	0.94	0.18	0.44	0.07	0.42	0.05	0.05	6.10
BAL15	1.60	5.60	1.27	0.28	1.16	0.17	1.06	0.24	0.64	0.09	0.63	0.07	0.05	5.00
BAL16	1.99	7.00	1.61	0.31	1.38	0.21	1.11	0.23	0.68	0.09	0.78	0.08	0.30	7.00
BAL17	1.76	6.10	1.33	0.34	1.21	0.18	1.07	0.21	0.52	0.08	0.65	0.07	0.05	4.30
BAL18	1.40	5.00	0.77	0.15	0.68	0.10	0.83	0.14	0.54	0.08	0.58	0.11	0.80	3.40
BAL19	1.64	6.10	1.01	0.18	0.92	0.14	1.10	0.23	0.66	0.12	0.97	0.11	0.40	5.60
MP01	25.85	91.60	13.55	1.48	10.04	1.38	9.21	1.69	5.22	0.82	6.08	0.86	0.40	5.40
MP02	0.68	2.00	0.41	0.07	0.41	0.06	0.56	0.08	0.34	0.05	0.42	0.07	1.20	3.40
MP03	10.41	41.90	9.82	1.48	9.81	1.45	8.48	1.40	3.80	0.58	3.67	0.55	1.70	4.90
MP04	12.77	50.10	9.55	1.37	7.34	0.92	5.03	0.61	1.63	0.24	1.46	0.19	0.40	3.20
MP05	3.85	14.90	2.56	0.48	2.28	0.36	2.48	0.49	1.52	0.22	1.80	0.22	0.30	4.60
MP06	5.16	20.90	3.40	0.58	3.02	0.39	2.53	0.41	1.20	0.15	1.11	0.12	0.80	2.40
MP07	3.91	13.80	2.30	0.42	1.80	0.24	1.32	0.30	0.70	0.09	0.64	0.08	0.40	2.00
MP08	1.46	6.80	1.09	0.22	1.17	0.14	1.13	0.16	0.52	0.07	0.46	0.04	1.10	1.60
MP09	3.90	14.50	2.50	0.50	2.51	0.31	1.82	0.38	1.02	0.14	0.69	0.09	0.40	2.30
MP10	2.87	12.20	2.16	0.45	2.74	0.33	2.32	0.41	1.31	0.15	1.06	0.12	0.40	1.90
MP11	2.37	9.30	1.67	0.29	1.51	0.23	1.40	0.24	0.59	0.08	0.67	0.07	0.20	1.50
MP12	1.66	5.60	1.35	0.26	1.17	0.14	0.89	0.19	0.61	0.07	0.56	0.06	0.05	4.70
MP13	1.68	6.00	1.25	0.27	1.26	0.16	0.89	0.21	0.46	0.07	0.60	0.08	0.10	6.00
MP14	1.35	4.90	1.01	0.24	1.17	0.14	0.98	0.16	0.52	0.07	0.42	0.05	0.05	4.50
MP15	22.24	70.70	11.66	1.29	8.22	1.15	7.61	1.41	4.34	0.71	5.10	0.73	0.40	3.80
MP16	0.86	3.80	0.57	0.08	0.53	0.06	0.39	0.09	0.32	0.03	0.38	0.04	1.40	2.00
Ardrosaan Seawater														
Balgowan Seawater														

	Pb_ppm	Zn_ppm	Ni_ppm	As_ppm	Cd_ppm	Sb_ppm	Bi_ppm	Ag_ppm	Au_ppb	Hg_ppm	Tl_ppm	Se_ppm	$^{87}Sr/^{86}Sr$
Lab analytical method code	1DX	1DX	1DX	1DX	1DX	1DX	1DX	1DX	1DX	1DX	1DX	1DX	calculated described in text
Unit	PPM	PPM	PPM	PPM	PPM	PPM	PPM	PPM	PPB	PPM	PPM	PPM	ratio
Detection Limit	0.1	1	0.1	0.5	0.1	0.1	0.1	0.1	0.5	0.01	0.1	0.5	
SampleID													
PT01	7.00	4.00	15.30	42.00	0.30	1.20	0.05	0.05	0.25	0.01	0.05	0.25	0.709624
PT02	3.50	5.00	5.40	12.30	0.40	0.40	0.05	0.05	0.25	0.02	0.05	0.25	0.709687
PT03	2.90	3.00	4.30	11.80	0.20	0.30	0.05	0.05	0.25	0.02	0.05	0.25	0.709670
PT04	3.70	4.00	8.50	16.10	0.30	0.40	0.05	0.05	0.25	0.01	0.05	0.25	0.709404
PT05a	2.30	3.00	3.20	6.30	0.20	0.10	0.05	0.05	0.25	0.01	0.05	0.25	0.710188
PT05b	4.00	1.00	3.60	3.90	0.05	0.10	0.05	0.05	0.25	0.01	0.10	0.25	0.710875
PT06	1.60	2.00	5.80	2.30	0.05	0.05	0.05	0.05	0.80	0.02	0.05	0.25	0.710116
PT07	2.20	2.00	11.30	3.10	0.05	0.20	0.05	0.05	0.25	0.02	0.10	0.60	0.710208
PT08	3.30	2.00	8.80	4.10	0.05	0.05	0.05	0.05	0.25	0.02	0.05	0.60	0.710244
PT09	2.00	2.00	5.30	3.20	0.05	0.05	0.05	0.05	0.25	0.06	0.05	0.25	0.710128
PT05bFe+	22.60	2.00	12.20	47.90	0.05	0.20	0.20	0.05	0.25	0.01	0.05	0.50	0.720594
PT10	6.90	4.00	14.20	39.30	0.30	1.10	0.05	0.05	0.25	0.01	0.05	0.25	
PT11	3.50	4.00	4.90	12.70	0.30	0.40	0.05	0.05	0.25	0.03	0.05	0.25	
BAL01	2.80	4.00	2.40	2.60	0.05	0.05	0.05	0.05	0.25	0.01	0.05	0.25	0.745901
BAL02	5.00	7.00	3.50	2.90	0.05	0.05	0.10	0.05	0.25	0.01	0.05	1.20	0.735263
BAL03	8.00	10.00	4.70	5.00	0.05	0.05	0.20	0.05	0.25	0.01	0.10	2.40	0.729171
BAL04	8.70	11.00	4.90	6.90	0.05	0.05	0.20	0.05	0.25	0.01	0.10	1.40	0.728110
BAL05	33.30	10.00	6.30	12.30	0.05	0.05	0.10	0.05	0.25	0.01	0.10	0.25	0.724942
BAL06	16.00	22.00	12.60	9.30	0.05	0.05	0.20	0.05	3.10	0.01	0.20	0.25	0.725424
BAL07	10.30	17.00	8.80	6.20	0.05	0.05	0.10	0.05	2.20	0.01	0.20	0.25	0.711955
BAL08	7.20	14.00	6.30	5.30	0.05	0.05	0.10	0.05	0.80	0.01	0.10	0.25	0.712056
BAL09	4.90	11.00	5.30	4.40	0.05	0.05	0.05	0.05	1.70	0.01	0.10	0.25	0.710554
BAL10	3.10	7.00	5.50	3.50	0.05	0.05	0.05	0.05	1.40	0.01	0.10	0.25	0.710275
BAL11	2.60	6.00	4.00	3.60	0.05	0.05	0.05	0.05	1.50	0.01	0.05	0.25	0.709965
BAL12	2.90	5.00	6.40	3.60	0.05	0.05	0.05	0.05	1.40	0.01	0.05	0.25	0.710059
BAL13	2.00	4.00	6.60	2.10	0.05	0.05	0.05	0.05	1.70	0.01	0.20	0.25	0.710537
BAL14	2.10	5.00	10.10	2.10	0.05	0.05	0.05	0.05	1.10	0.01	0.20	0.50	0.710450
BAL15	2.40	5.00	8.10	2.80	0.05	0.05	0.05	0.05	2.30	0.01	0.20	0.25	0.710401
BAL16	2.90	7.00	10.40	2.00	0.05	0.05	0.05	0.05	0.70	0.01	0.10	0.50	0.710412
BAL17	2.50	7.00	5.80	1.70	0.05	0.05	0.05	0.05	1.30	0.01	0.10	0.25	0.710715
BAL18	2.60	3.00	2.60	2.70	0.05	0.05	0.05	0.05	0.25	0.01	0.05	0.80	
BAL19	4.80	7.00	3.90	3.20	0.05	0.05	0.10	0.05	0.25	0.01	0.05	1.00	
MP01	5.70	17.00	5.30	4.60	0.05	0.05	0.05	0.05	0.25	0.01	0.40	0.25	1.140986
MP02	1.80	10.00	7.00	30.30	0.05	0.40	0.05	0.05	0.60	0.01	0.05	0.25	0.759840
MP03	6.10	18.00	32.20	136.10	0.05	0.70	0.05	0.05	0.25	0.01	0.05	0.25	0.808264
MP04	4.10	8.00	13.70	36.50	0.10	0.40	0.05	0.05	0.25	0.01	0.05	0.25	0.727164
MP05	11.10	13.00	12.60	35.40	0.05	0.60	0.10	0.05	0.25	0.01	0.05	0.25	0.767907
MP06	3.40	6.00	11.40	42.30	0.20	0.60	0.05	0.05	0.25	0.01	0.05	0.25	0.721884
MP07	4.00	5.00	7.40	34.10	0.20	0.50	0.05	0.05	0.25	0.01	0.05	0.25	0.714168
MP08	2.40	3.00	4.90	32.70	0.05	1.00	0.05	0.05	0.25	0.01	0.05	0.25	0.713324
MP09	1.90	2.00	2.80	24.20	0.05	0.80	0.05	0.05	0.25	0.01	0.05	0.25	0.711263
MP10	1.30	2.00	1.70	15.60	0.05	0.30	0.05	0.05	0.25	0.01	0.05	0.25	0.711566
MP11	1.80	1.00	2.70	12.20	0.05	0.80	0.05	0.05	0.25	0.01	0.05	0.25	0.710700
MP12	2.60	7.00	8.90	4.90	0.05	0.20	0.05	0.05	1.70	0.01	0.05	0.25	0.711048
MP13	2.90	6.00	6.20	5.80	0.05	0.20	0.05	0.05	1.30	0.02	0.05	0.25	0.710825
MP14	2.30	11.00	6.50	4.30	0.05	0.10	0.05	0.05	0.70	0.01	0.05	0.25	0.710172
MP15	6.30	17.00	6.00	4.20	0.05	0.05	0.05	0.05	0.70	0.01	0.40	0.25	
MP16	1.80	9.00	7.90	29.30	0.05	0.50	0.05	0.05	0.25	0.01	0.05	0.25	
Ardrosaan Seawater													0.709166
Balgowan Seawater													0.709209

Appendix 3

Chapter 2:

Hyperspectral Analytical Results

Hylogger^{TM} 3-3 Image data for samples collected from vertical profiles described in Chapter 2. Scale shown is not to scale of the individual outcrop locations but of the length of the sample trays used in the Hylogger^{TM}.

Images copied from TSG viewer: downloadable from https://research.csiro.au/thespectralgeologist/support/installation-guide/

Point Turton

Table 1 summary HyLogger^{TM} mineral percent for Point Turton

Point Turton	
TIR Mineral	**System %**
Aspectral	62.25
Hematite	1.83
SWIR Mineral	**System %**
Calcite	48.32
Ankerite	9.53
Muscovite	5.11
Montmorillonite	3.01
Siderite	1.41
VNIR Mineral	**System %**
Goethite	26.06

Point Turton

HyLogger^{TM} mode: Thermal Infrared (TIR)

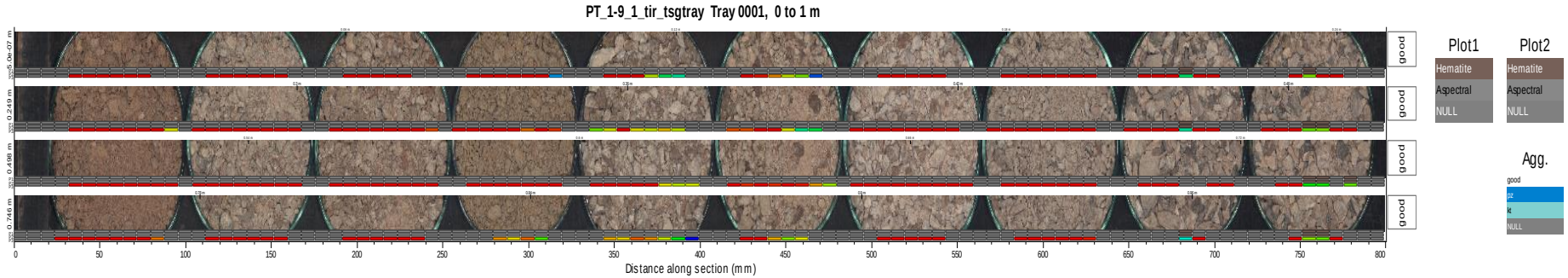

Figure 1 TIR image log of Point Turton samples shown left to right are; PT01, PT02, PT03, PT04, PT05a, PT05b, PT06, PT07, PT08 and PT09.

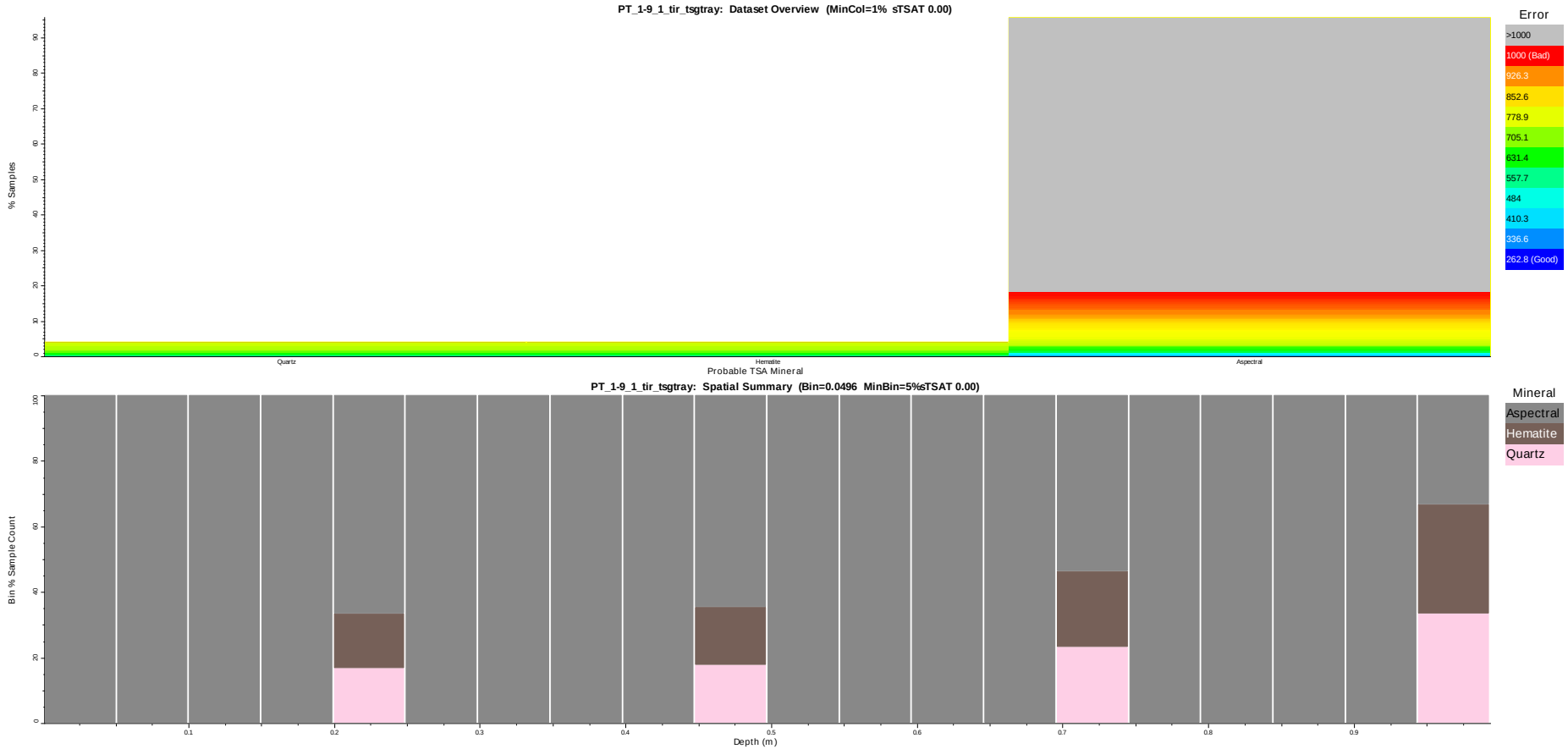

Figure 2 TIR spatial overview (above) and summary mineral content (below) of Point Turton samples. For scale: see Figure 1.

Point Turton

HyLogger^{TM} mode: Shortwave Infra-Red (SWIR)

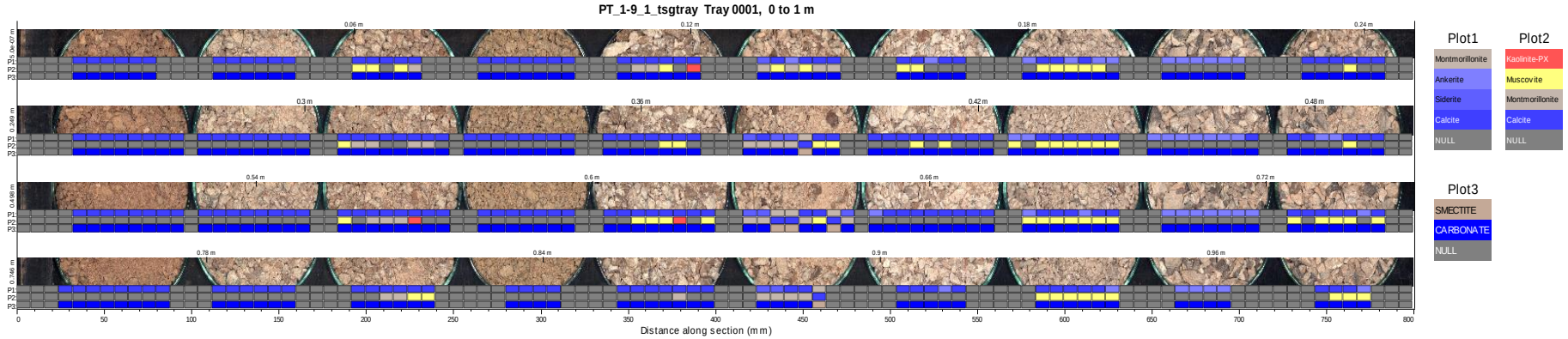

Figure 3 SWIR image log of Point Turton samples shown left to right are; PT01, PT02, PT03, PT04, PT05a, PT05b, PT06, PT07, PT08 and PT09.

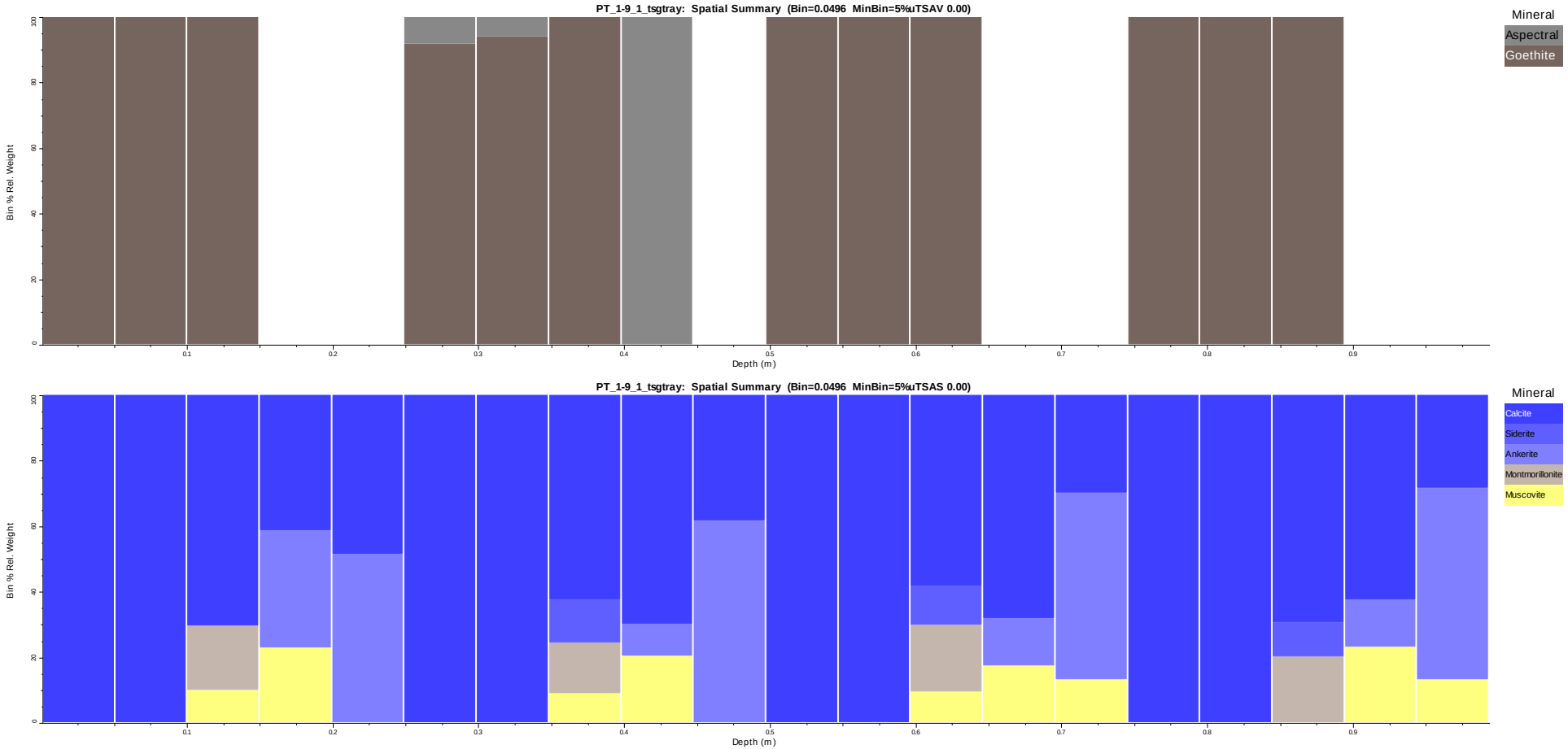

Figure 4 Very near infrared (VNIR) mineral content summary (above) and SWIR summary mineral content (below) of Point Turton samples. For scale: see Figure 3.

Balgowan

Table 2 summary HyLogger™ mineral percent for Balgowan

Balgowan	
TIR Mineral	**System %**
Aspectral	26.9
Quartz	7.04
Montmorillonite	6.59
Hematite	5.66
Kaolinite	1.24
Albite	1.11
SWIR Mineral	**System %**
Muscovite	18.26
Ankerite	15.62
Kaolinite-PX	6.25
Phengite	5.34
Montmorillonite	5.07
Kaolinite-WX	3.1
Siderite	2.61
Aspectral	1.74
Calcite	1.06
VNIR Mineral	**System %**
Goethite	2.12
Hematite	1.21

Balgowan

HyLogger^{TM} mode: TIR

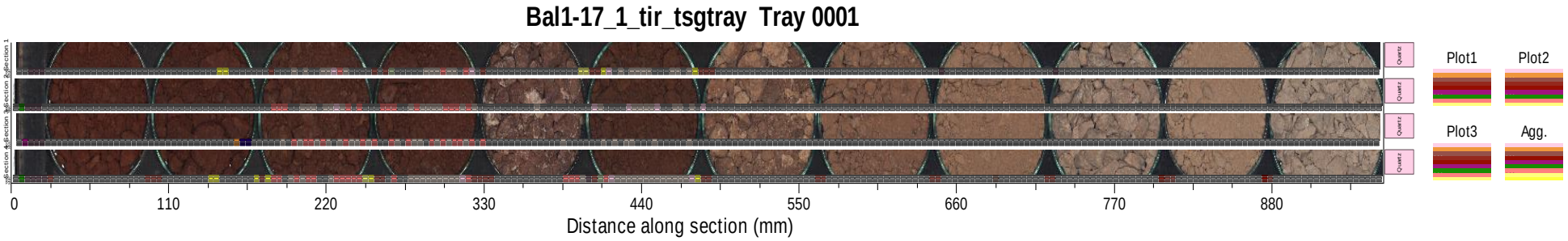

Figure 5 TIR image log of Balgowan Samples shown left to right are Bal01, Bal02, Bal03, Bal04, Bal05, Bal06, Bal07, Bal08, Bal09, Bal10, Bal11, Bal12.

Balgowan

HyLogger^{TM} mode: TIR

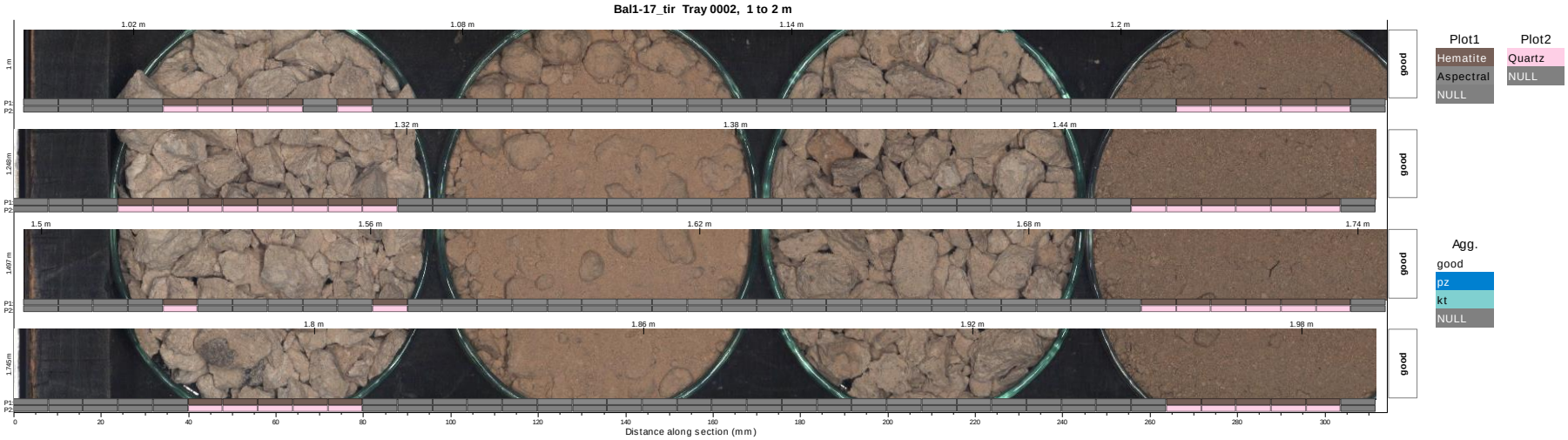

Figure 6 TIR image log of Balgowan Samples shown left to right are Bal13, Bal14, Bal15 and Bal16.

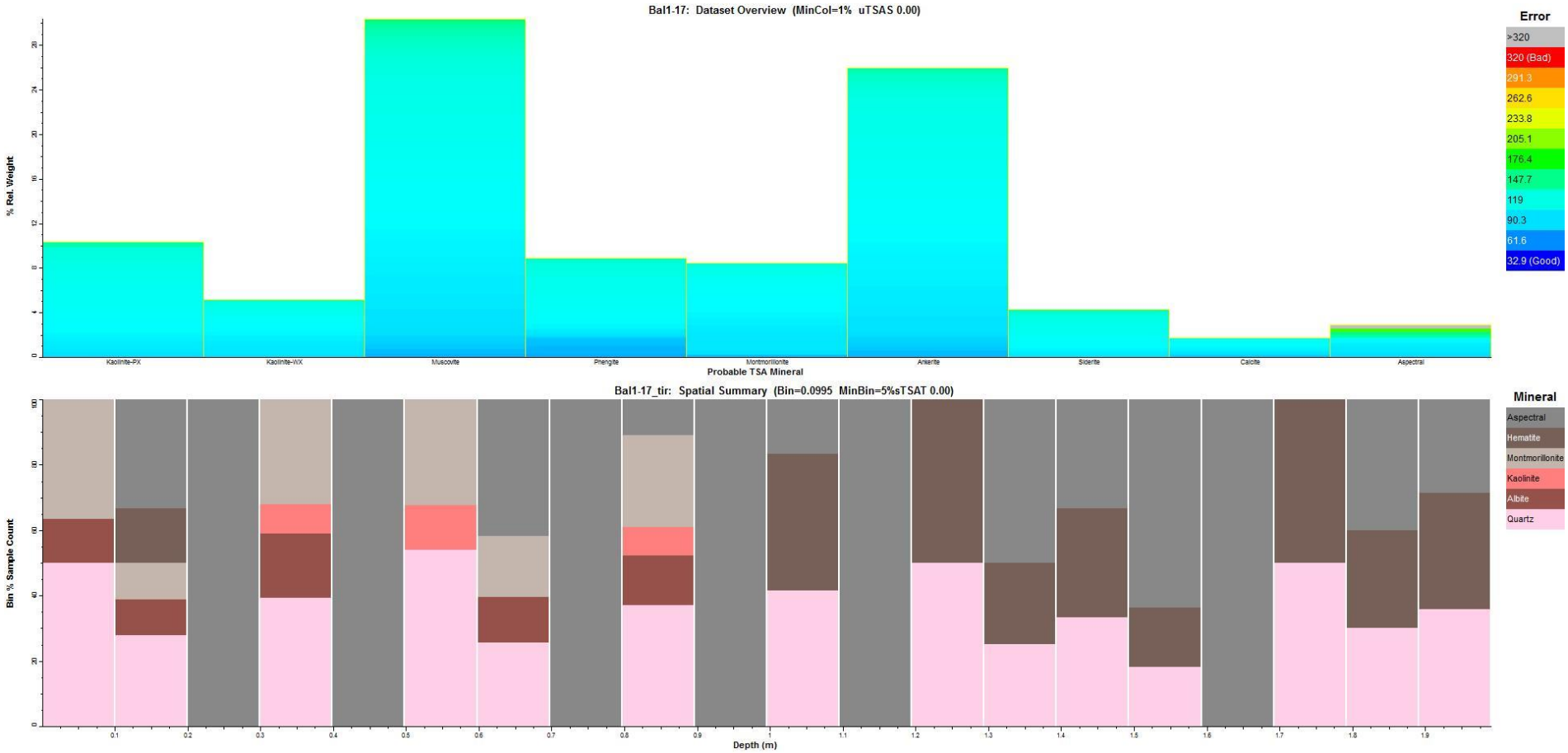

Figure 7 TIR spatial overview (above) and summary mineral content (below) of Balgowan samples. For scale: see Figure 5 and 6.

Balgowan

HyLogger^{TM} mode: SWIR

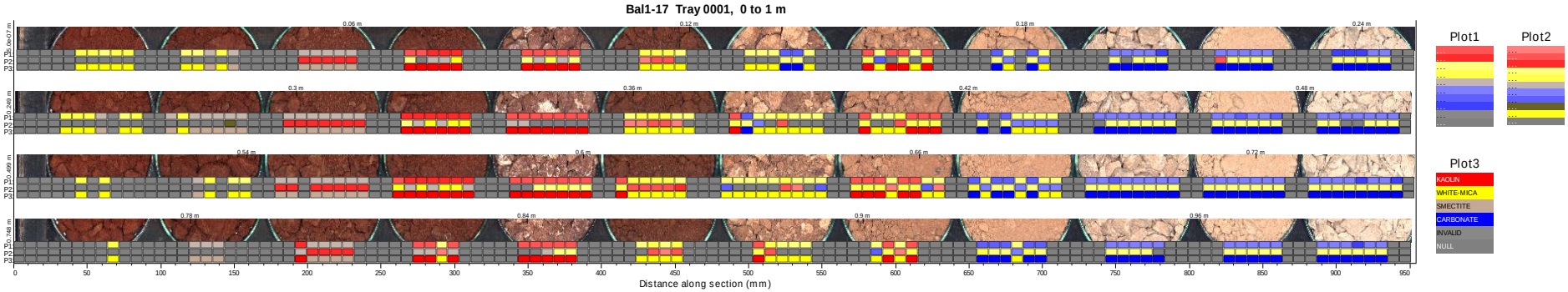

Figure 8 SWIR image log of Balgowan samples shown left to right are Bal01, Bal02, Bal03, Bal04, Bal05, Bal06, Bal07, Bal08, Bal09, Bal10, Bal11and Bal12.

Balgowan

HyLogger^{TM} mode: SWIR

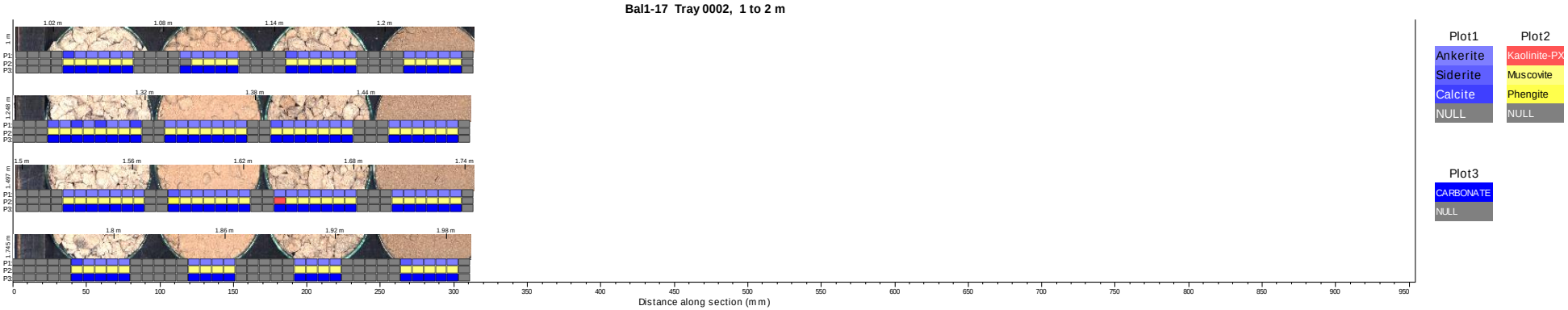

Figure 9 SWIR image log of Balgowan samples. Samples shown left to right are Bal13, Bal14, Bal15 and Bal16.

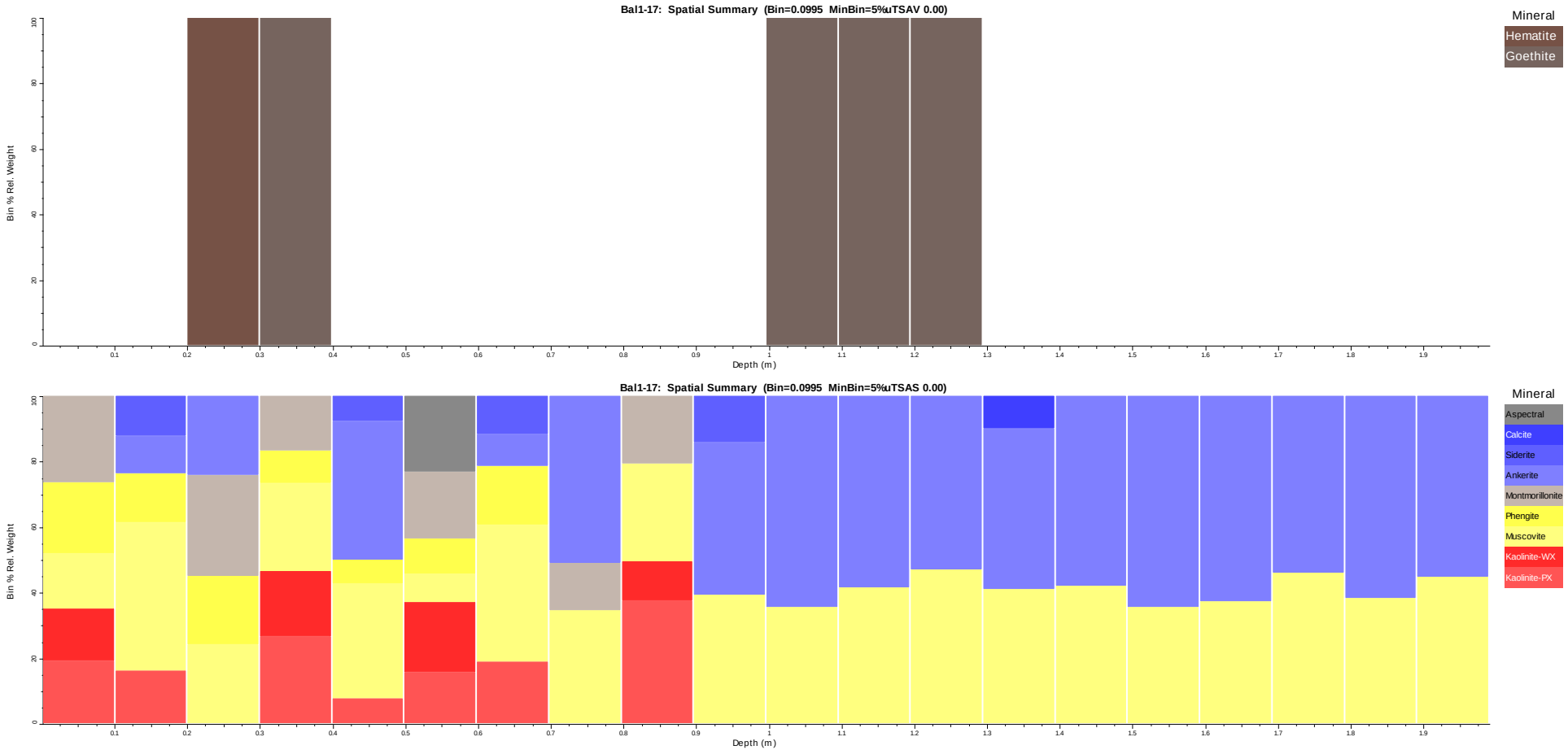

Figure 10 Very near infrared (VNIR) mineral content summary (above) and SWIR summary mineral content (below) of Balgowan samples. For scale: see Figure 8 and 9.

Myponie Point

Table 3 summary HyLogger™ mineral percent for Myponie Point

Myponie Point	
TIR Mineral	**System %**
Aspectral	38.85
Quartz	6.92
Albite	2.35
SWIR Mineral	**System %**
Calcite	27.61
Montmorillonite	8.99
Ankerite	6.8
Kaolinite-PX	5.99
Muscovite	3.61
Gibbsite	3.18
Kaolinite-WX	1.69
VNIR Mineral	**System %**
Goethite	49.28

Myponie Point

HyLogger^{TM} mode: TIR.

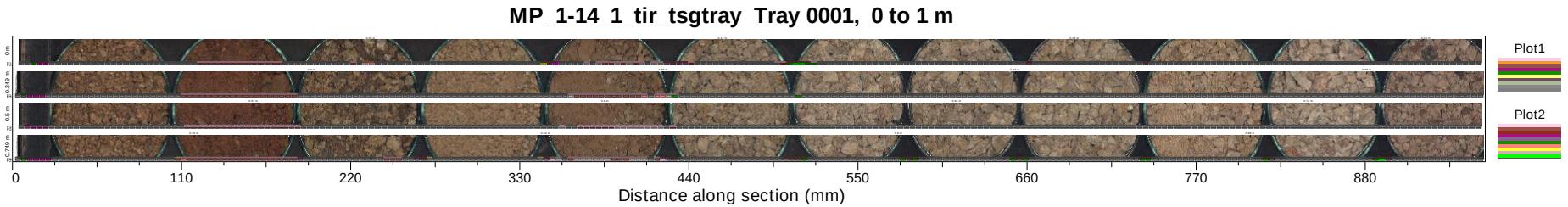

Figure 11 TIR image log of Myponie Point samples. Samples from left to right are MP01, MP02, MP03, MP04, MP05, MP06, MP07, MP08, MP09, MP10, MP11 and MP12.

Myponie Point

HyLogger^{TM} mode: TIR

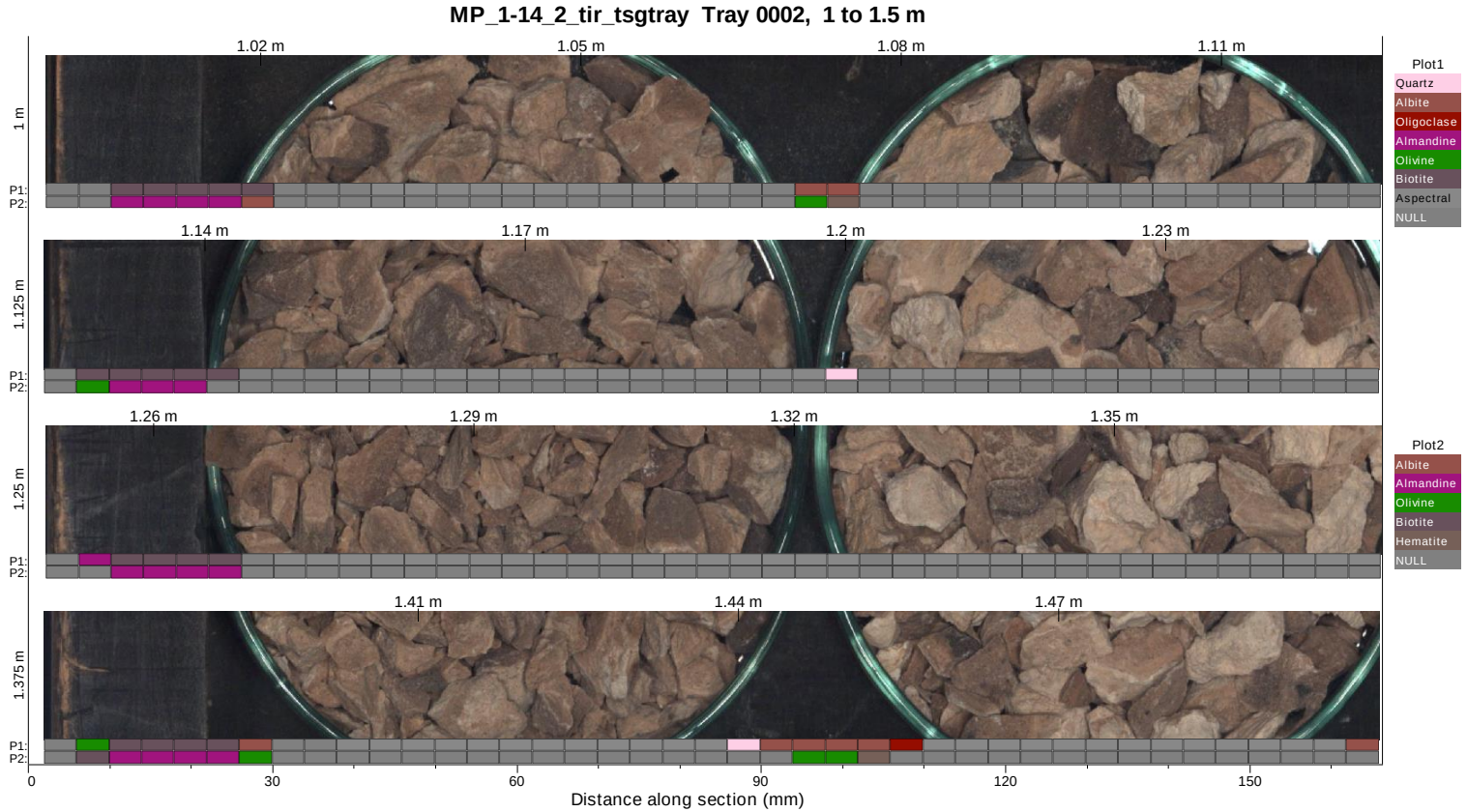

Figure 12 TIR image log of Myponie Point samples. Samples shown from left to right are MP13 and MP14.

Myponie Point

HyLogger^{TM} mode: TIR

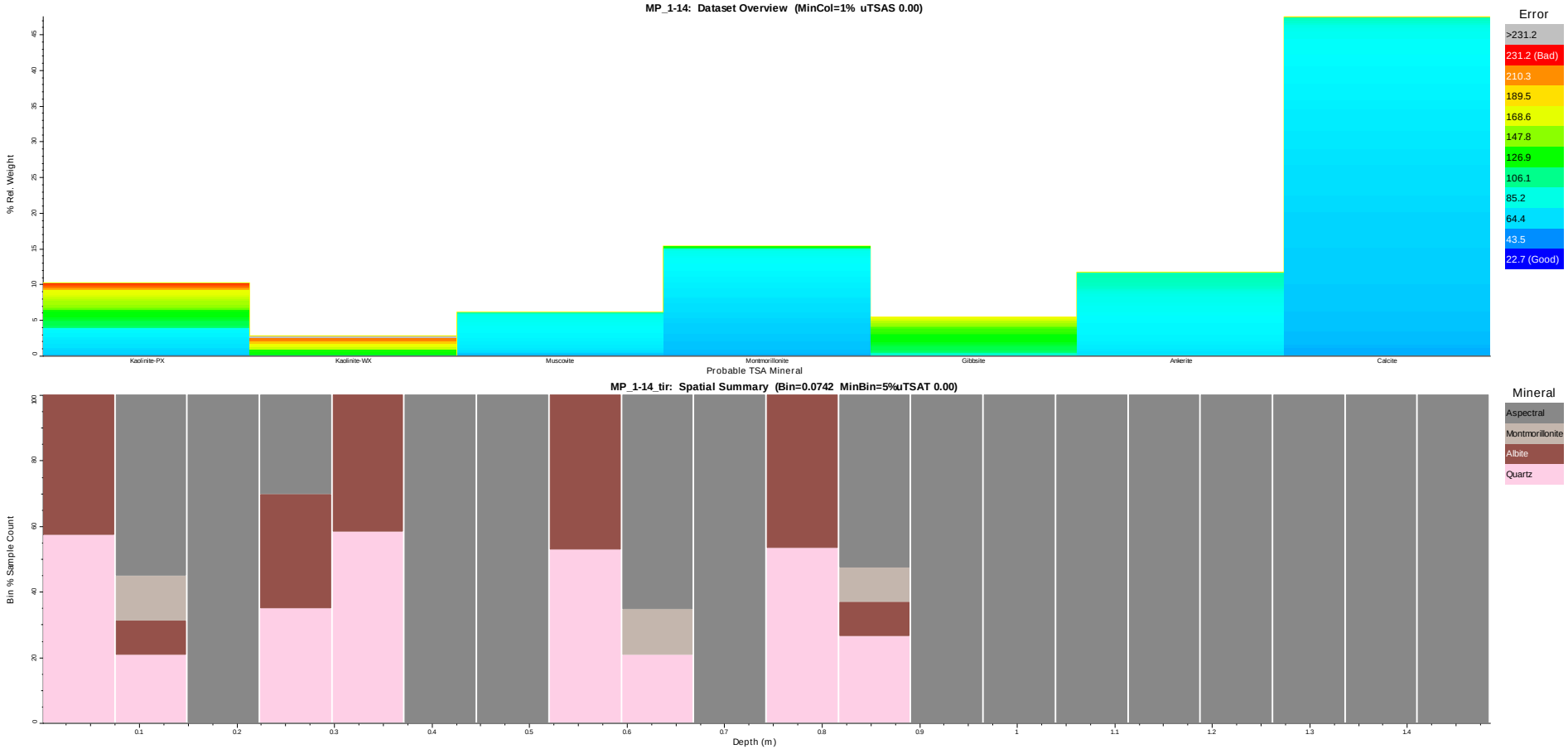

Figure 13 TIR spatial overview (above) and summary mineral content (below) of Myponie Point samples. For scale: see Figure 11 and 12.

Myponie Point

HyLogger^{TM} mode: SWIR

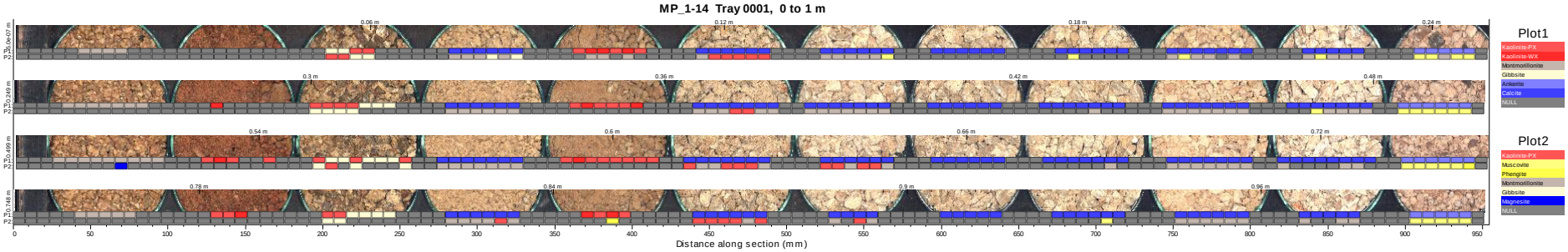

Figure 14 SWIR image log of Myponie Point samples. Samples shown from left to right are MP01, MP02, MP03, MP04, MP05, MP06, MP07, MP08, MP09, MP10, MP11, MP12.

Myponie Point

HyLogger^{TM} mode: SWIR

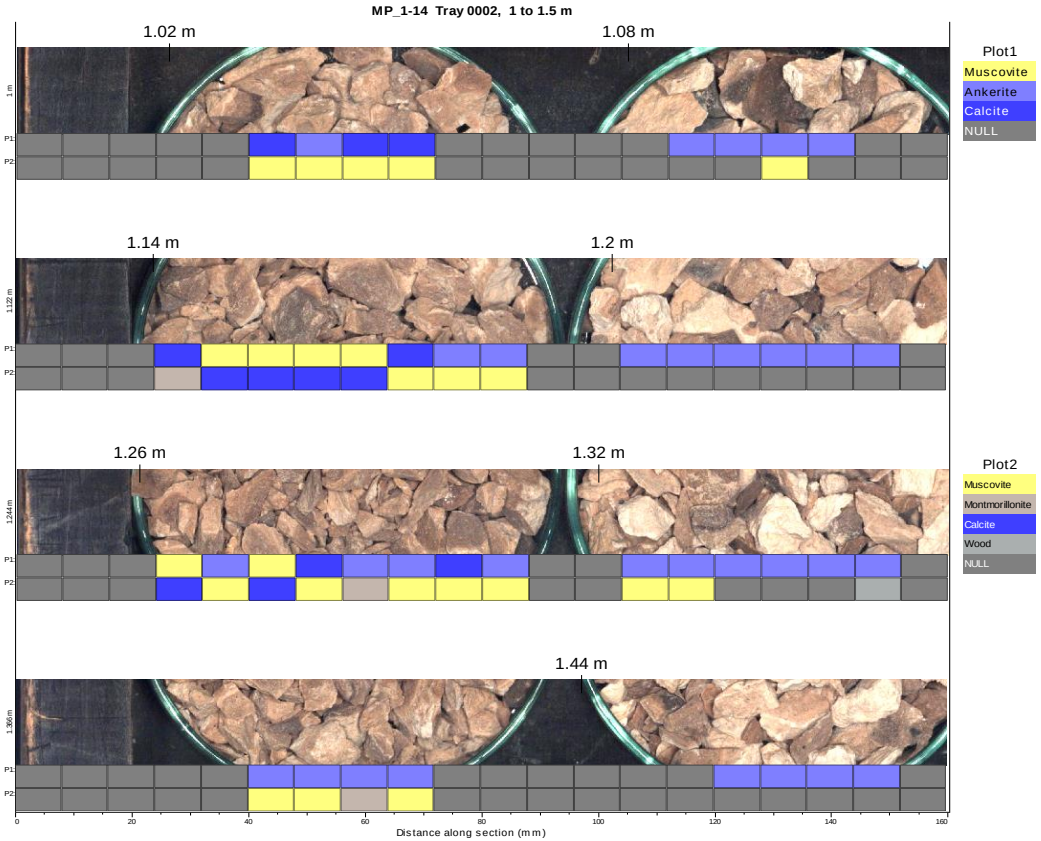

Figure 15 SWIR image log of Myponie Point samples. Samples shown from left to right are MP13 and MP14.

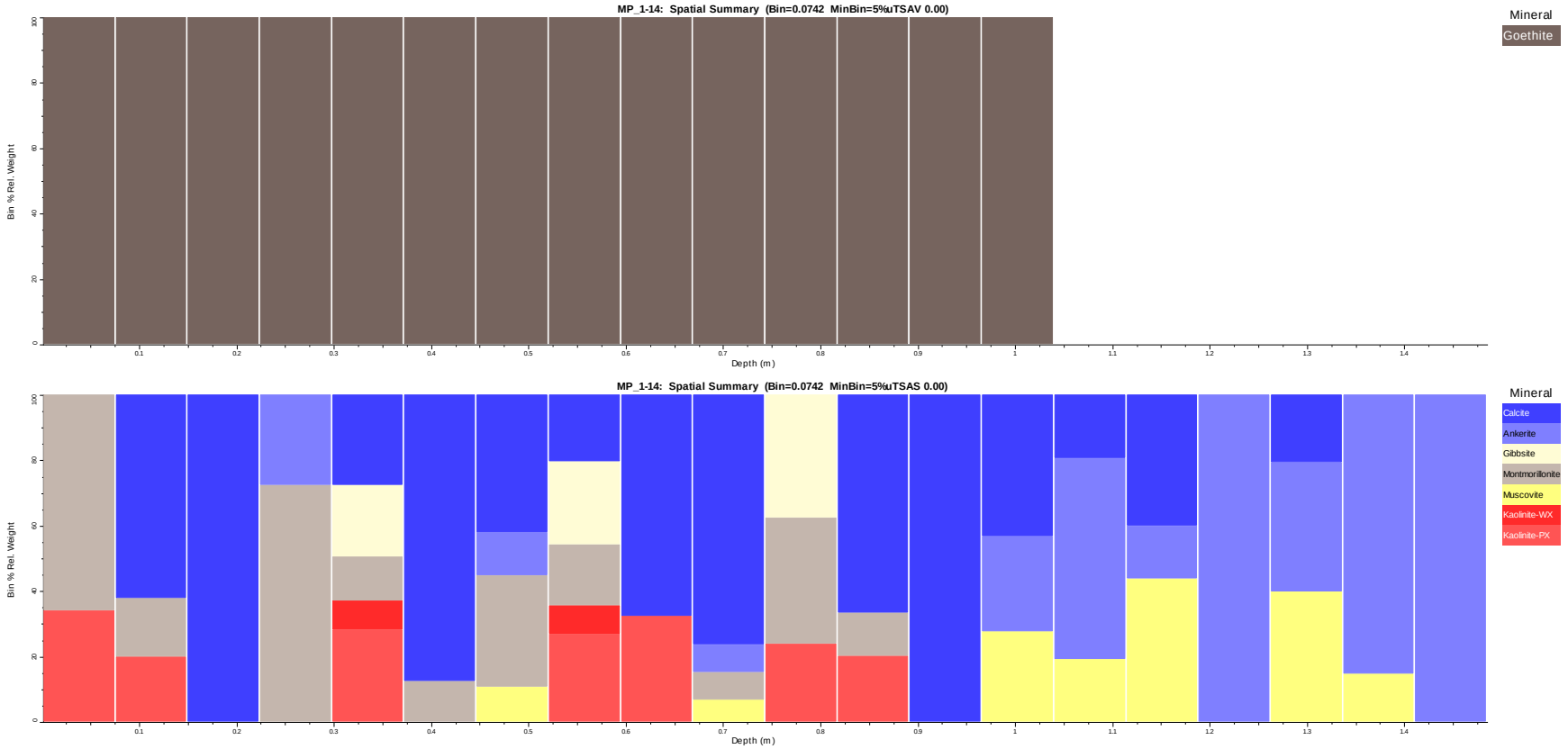

Figure 16 Very near infrared (VNIR) mineral content summary (above) and SWIR summary mineral content (below) of Myponie Point samples. For scale: see Figure 14 and 15.

Appendix 4

Published article

Chapter 3:

Pedogenic carbonate sampling for Cu exploration on the Yorke Peninsula, South Australia

Journal of Geochemical Exploration 194 (2018) 239–256

Journal of Geochemical Exploration 194 (2018) 239–256

Contents lists available at ScienceDirect

Journal of Geochemical Exploration

journal homepage: www.elsevier.com/locate/gexplo

Pedogenic carbonate sampling for Cu exploration on the Yorke Peninsula, South Australia

Keryn Wolff[a,*], Caroline Tiddy[a,1], Dave Giles[a,1], Steve M. Hill[b]

[a] Deep Exploration Technologies Cooperative Research Centre (DET CRC), Department of Earth Sciences, University of Adelaide, Australia
[b] Geological Survey of South Australia, Department of the Premier and Cabinet, Government of South Australia, Australia

ABSTRACT

We report on the geochemistry of 215 regolith carbonate rocks collected across the Yorke Peninsula, South Australia in order to evaluate the potential of regolith carbonates as a geochemical sampling media for buried Cu mineralization. The Yorke Peninsula forms the southern part of the Olympic Domain iron-oxide-copper-gold (IOCG) mineral province and is host to a number of Cu-bearing mineral deposits and prospects including Hillside and the historic Moonta-Wallaroo mining district. The majority of the Yorke Peninsula is covered by a veneer of Cambrian to Quaternary sedimentary rocks and regolith, including marine limestones and regolith carbonates. We present a new regolith map of the Yorke Peninsula derived from geophysical data and field observations and use it to provide landscape context and regional characterization of the sampled regolith materials. Whole rock geochemistry of the sampled carbonates is used to demonstrate that major element chemistry is dominated by CaO (33%–53%), reflecting the calcite component. Other major components include SiO_2 and Al_2O_3, reflecting quartz (typically quartz sand in carbonate indurated quaternary sands) and clay minerals respectively. Ca/Sr ratios vary between 179 and 1324 with 86% of the samples < 650. The Ca/Sr < 650 group of samples forms a continuous array on a plot of Ca vs Sr which overlaps with the range of values expected from sea water derived Ca and Sr subjected to variable degrees of meteoric fractionation. These samples are interpreted to be regolith carbonates with little input of marine carbonate. A single sample has Ca/Sr 1324, consistent with a significant component of marine limestone. Twenty nine samples have Ca/Sr > 650 and < 940 which may indicate mixing of dominantly meteoric sources with a lesser component of marine carbonate. We recommend that geochemical results from samples with Ca/Sr > 650 be treated with caution as the regolith carbonate trace element geochemical signal may be diluted by the marine carbonate component. Copper concentrations found in the carbonate rocks with Ca/Sr < 650 range from 1.4 ppm to 36 ppm and form a slightly right-skewed, near log normal population. Samples with elevated $\log_{10}$Cu concentrations have a broad spatial coincidence with areas of known Cu enrichment in the basement and not related to dust or windblown contamination. Copper concentrations show no systematic relationship with common dust-born contaminants (Al_2O_3, Fe_2O_3, Zr) which would be expected if the Cu was derived from windblown spoil from the historic mining operations. We conclude that regolith carbonates are a potentially useful sampling media for Cu exploration on the Yorke Peninsula and that they can be easily differentiated from less useful marine carbonates on the basis of Ca/Sr ratios.

1. Introduction

Regolith carbonates are globally widespread and generally occur in semi-arid to dry environments (e.g. Chen et al., 2002; Dart et al., 2007; Khadkikar et al., 2000; Khadkikar et al., 1998; Reith et al., 2011; Wolff et al., 2017). Regolith carbonate covers at least 21% of Australia, and is more common in the southern, drier regions (e.g. Chen et al., 2002; Dart et al., 2007; Lintern, 2015; McQueen, 2006; Fig. 1). Regolith carbonate rocks are commonly referred to as calcrete (e.g. Chen et al., 2002; Lintern et al., 2012; McQueen et al., 1999), but can also include other carbonate dominant rocks such as dolomite or highly weathered and re-precipitated limestone (e.g. Chen et al., 2002; Wolff et al., 2017).

Regolith carbonates can form by a variety of processes (e.g. Chen et al., 2002; Prudencio et al., 2011). These include accumulations or deposition/precipitation of Ca during soil forming processes (pedogenesis) which commonly occurs in arid climates (e.g. McQueen, 2006; Prudencio et al., 2011; Reith et al., 2011). Pedogenic carbonate tends to form in the soil moisture- or vadose zone of the regolith (e.g. Chen et al., 2002; Lintern et al., 2006) such as occurs throughout large regions of southern Australia (e.g. Zang et al., 2006; Drexel and Preiss, 1995). Calcium carbonate formed by groundwater enriched in Ca and is referred to as 'groundwater' or 'valley' carbonate (Chen et al., 2002). The primary difference between pedogenic and groundwater carbonate is that groundwater carbonate forms in the phreatic zone (Chen et al., 2002; Lintern et al., 2006). Detailed description of regolith carbonate formation and morphology is described in Chen et al. (2002).

Previous studies suggest that the Ca component of pedogenic carbonate rock in southern Australia is primarily derived from rainwater, whilst the C component of pedogenic carbonate is sourced from C4 plants (e.g. Lintern et al., 2006; Quade et al., 1995). Calcium may also

* Corresponding author at: Department of Earth Sciences, Mawson Building, University of Adelaide, North Terrace Campus, Adelaide, SA 5005, Australia.
E-mail address: keryn.wolff@yahoo.com (K. Wolff).
[1] Now at Future Industries Institute, University of South Australia.

https://doi.org/10.1016/j.gexplo.2018.08.007
Received 23 April 2018; Received in revised form 2 August 2018; Accepted 22 August 2018
Available online 29 August 2018
0375-6742/

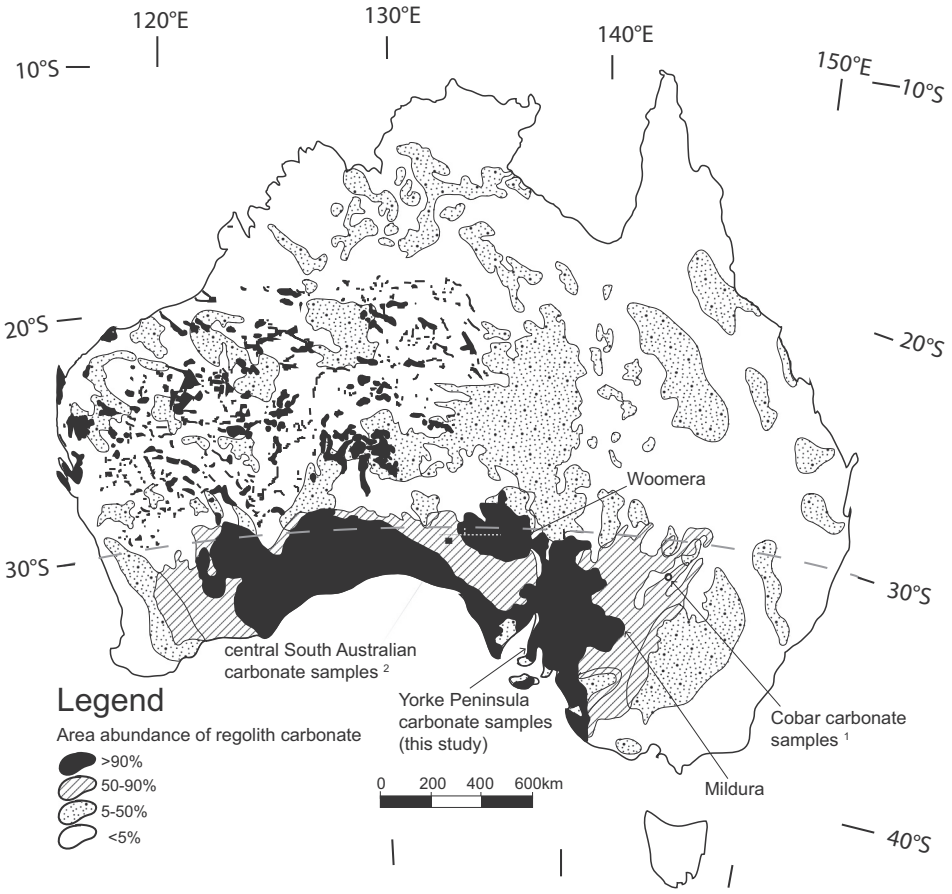

Fig. 1. Carbonate distribution and abundance across Australia, modified after Chen et al. (2002). Carbonate sampling locations from other authors are shown and numbered: 1. McQueen (2006); 2. Lintern and Sheard (1999) and Lintern et al. (2006). Latitude 30°S is shown by the grey dashed line. Pedogenic carbonates tend to occur more frequently south and groundwater carbonates tend to occur more frequently north of this latitude (e.g. McQueen, 2006; McQueen et al., 1999).

be derived from the weathering of underlying rocks (Dietrich et al., 2017) or carried in wind born dust, for example in dust derived from exposed marine carbonate rocks (Quade et al., 1995; Van der Hoven and Quade, 2002). Strontium is typically enriched in carbonate rocks, where it is a common ionic substitute for Ca (e.g. Dart et al., 2012; Lintern et al., 2006; Van der Hoven and Quade, 2002). Strontium isotopes have been used by a number of authors in an attempt to constrain possible sources of Sr, and by inference Ca, in pedogenic carbonate rocks. Quade et al. (1995) concluded that the ocean is the primary source of Sr in pedogenic carbonates from coastal regions of southern Australia, whereas further inland Sr isotopes tend to reflect local dust composition. A local dust source, in this case derived from nearby exposed marine carbonates, was also favored by Van der Hoven and Quade (2002) in their study of pedogenic carbonates from New Mexico. In contrast Dietrich et al. (2017) argued that Sr isotopes in carbonates from northern Cameroon are best explained by weathering of in-situ sources with a lesser component of wind born dust.

Carbonate rocks formed during pedogenesis have the potential to incorporate geochemical signatures from the underlying substrate. (e.g. Chen et al., 2002; Lintern et al., 2012; Lintern et al., 2011; McQueen, 2006; Salama et al., 2016; Wolff et al., 2017). Pedogenic carbonate has become popular and successful sampling medium for use in Au exploration in Australia (e.g. Chen et al., 2002; Lintern, 2015; Lintern et al., 2012; Reith et al., 2011) and may also be useful as an indicator of buried Cu mineralization (e.g. Lintern, 2015; Wolff et al., 2017). Regional geochemical exploration surveys using surface carbonates have been extensively carried out throughout southern Australia including in the Cobar region, New South Wales (McQueen, 2006; Fig. 1), the Challenger Gold Deposit region, South Australia (Lintern and Sheard, 1999; Lintern et al., 2006; Poustie and Abbot, 2006; Fig. 1), the ET Gold deposit, Gawler Craton, South Australia (Lintern et al., 2011) and a number of regions in Western Australia (e.g. Lintern, 1989; Lintern et al., 1997; Lintern et al., 2009).

The Yorke Peninsula, South Australia (Fig. 2), is covered by late Cenozoic to Quaternary transported sediments including pedogenic carbonate that has formed over weathered, early Cenozoic to Cambrian sedimentary rocks including marine limestone (e.g. Zang et al., 2006; Fabris, 2010; Fig. 3). Underlying Early to Middle Proterozoic basement rocks of the Yorke Peninsula region are part of the broader Olympic Domain (Fig. 2) and are prospective for iron-oxide-copper-gold (IOCG) mineralization (Conor et al., 2010). Basement rocks of the Olympic Domain host the super-giant Olympic Dam IOCG-U deposit as well as the Prominent Hill, Carrapateena, and Hillside IOCG deposits (e.g. Conor et al., 2010; Zang et al., 2006; Fig. 2). The potential for pedogenic carbonate rocks to be used as exploration sampling media requires that Cu, Au and other 'pathfinder' elements enriched in IOCG mineralization can be mobilized from the basement rocks such as to form detectable dispersion halos in the overlying carbonates (Dietman, 2009; Ghavami-Riabi et al., 2008; Hartley, 2000; Keeling and Hartley, 2005).

In this paper we use a combination of regolith mapping, surface sampling of carbonate rocks and geochemistry to test the potential for this material as an exploration sampling medium for Cu on the Yorke Peninsula. We seek to constrain the possible sources of Ca and Sr in the carbonate rocks by comparison with Ca/Sr from seawater, rainwater and locally exposed marine carbonate rocks. We conclude that Ca/Sr ratios can be used to differentiate between carbonate rocks that were derived from pedogenic or marine processes (see also Wolff et al. (2017)). We then focus on Cu concentrations in the pedogenic carbonate rocks and show that there is a spatial association between elevated Cu and known mineral occurrences in the basement rocks. The implications for using the carbonates from this region as a sample medium for Cu exploration are discussed.

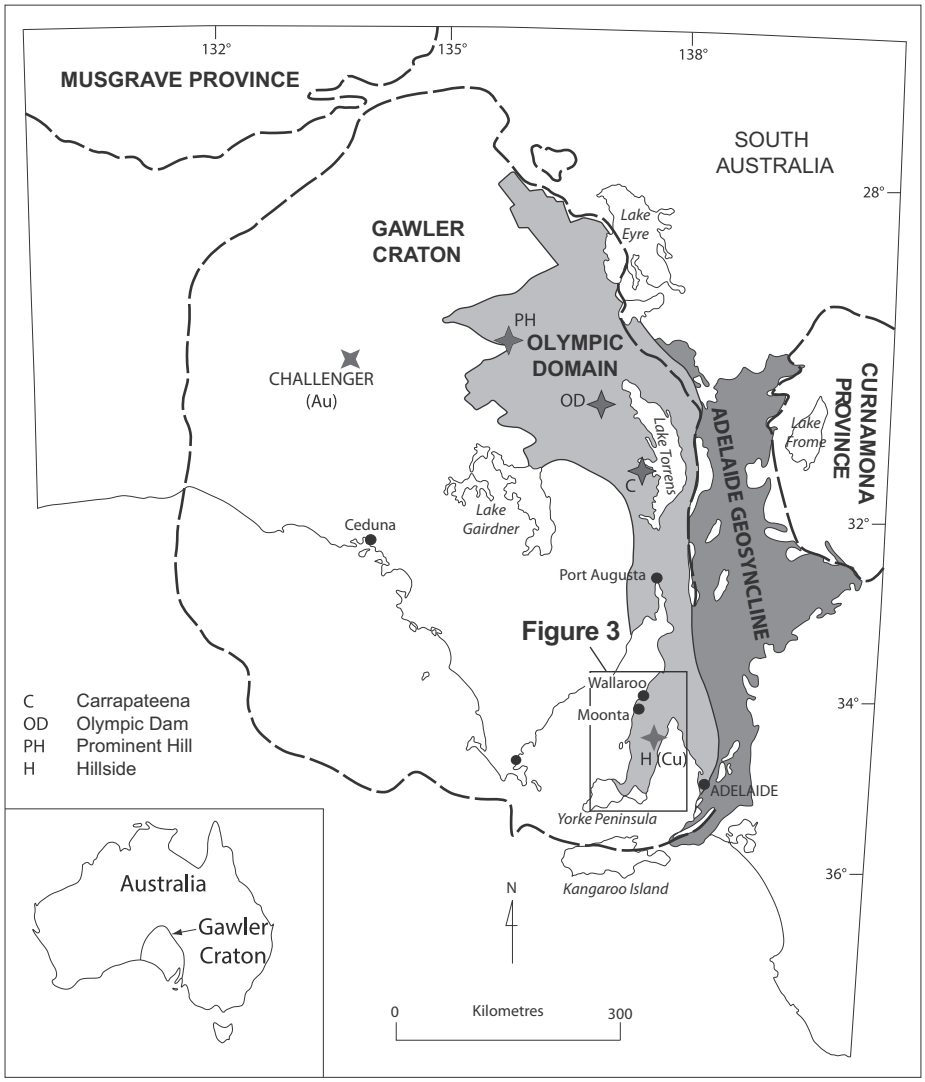

Fig. 2. Simplified geological map of the Gawler Craton showing the location of IOCG mineralization throughout the Olympic Domain. The study area is outlined by the black rectangle. Inset: Location of the Gawler Craton within Australia. Modified after Conor et al. (2010).

2. Geological setting

2.1. Geology

The geology of the Yorke Peninsula has been described previously by Conor et al. (2010), Crawford (1965), Drexel and Preiss (1995), and Zang et al. (2006). The Yorke Peninsula is within the southern Olympic Domain of the Gawler Craton (Fig. 2). Proterozoic basement rocks within the Yorke Peninsula are poorly exposed, with < 5% exposure (Cowley et al., 2003; Fig. 4). Basement packages are dominated by metasedimentary and volcanic rocks of the Late Paleoproterozoic Wallaroo Group (ca 1750 Ma; Conor et al., 2010). The Wallaroo Group was deformed during the ca 1730–1690 Ma Kimban Orogeny (Ferris et al., 2002; Hand et al., 2007; Hoek and Schaefer, 1998) and later intruded by ca 1595–1575 Ma Hiltaba Suite granites and minor mafic magmatic rocks (Cooper et al., 1985; Cowley et al., 2003; Creaser, 1996; Creaser and Cooper, 1993; Creaser and Fanning, 1993; Fanning et al., 1988).

IOCG mineralization in the Olympic Domain includes the supergiant Olympic Dam deposit, and the smaller Prominent Hill and Carrapateena deposits (Fig. 2). The Yorke Peninsula also hosts IOCG mineralization including the Hillside deposit and the historic Moonta-Wallaroo district (Figs. 2 & 4). IOCG mineralization is interpreted to have been derived from hydrothermal fluids that were coeval with intrusion of the Hiltaba Suite granites (Conor et al., 2010; Morales-Ruano et al., 2002). Mineralization in the Yorke Peninsula is hosted within both the Wallaroo Group and the Hiltaba Suite granites (Conor et al., 2010; Cowley et al., 2003). Wallaroo-style IOCG mineralization tends to be dispersed within, or associated with, quartz vein-hosted Fe and Cu sulfides in altered biotite-magnetite alteration zones hosted by metasedimentary rocks (e.g. Conor, 1995; Skirrow et al., 2007). Moonta-style mineralization is found within porphyritic felsic intrusions within the Wallaroo Group (Skirrow et al., 2007).

The basement rocks are unconformably overlain by sedimentary rocks of the Cambrian (540–500 Ma) Stansbury Basin, Carboniferous to Permian (350–260 Ma) Troubridge Basin and the Cenozoic (65–2.6 Ma) St Vincent and Pirie Basins (Drexel and Preiss, 1995; Zang et al., 2006; Figs. 2 & 5). Cenozoic sedimentary rocks include limestone, siltstone, sandstone and mudstone deposited during fluctuating sea levels, uplift and rifting (e.g. Crawford, 1965; Drexel and Preiss, 1995; Zang et al., 2006).

Quaternary deposits (2.6 Ma to present) which include variably consolidated sands, silts, clays and regolith carbonates cover > 90% of the Yorke Peninsula and conceal the underlying geology (e.g. Drexel and Preiss, 1995; Zang et al., 2006; Fig. 4). Sand dunes and beach deposits have formed along most shore and backshore environments along

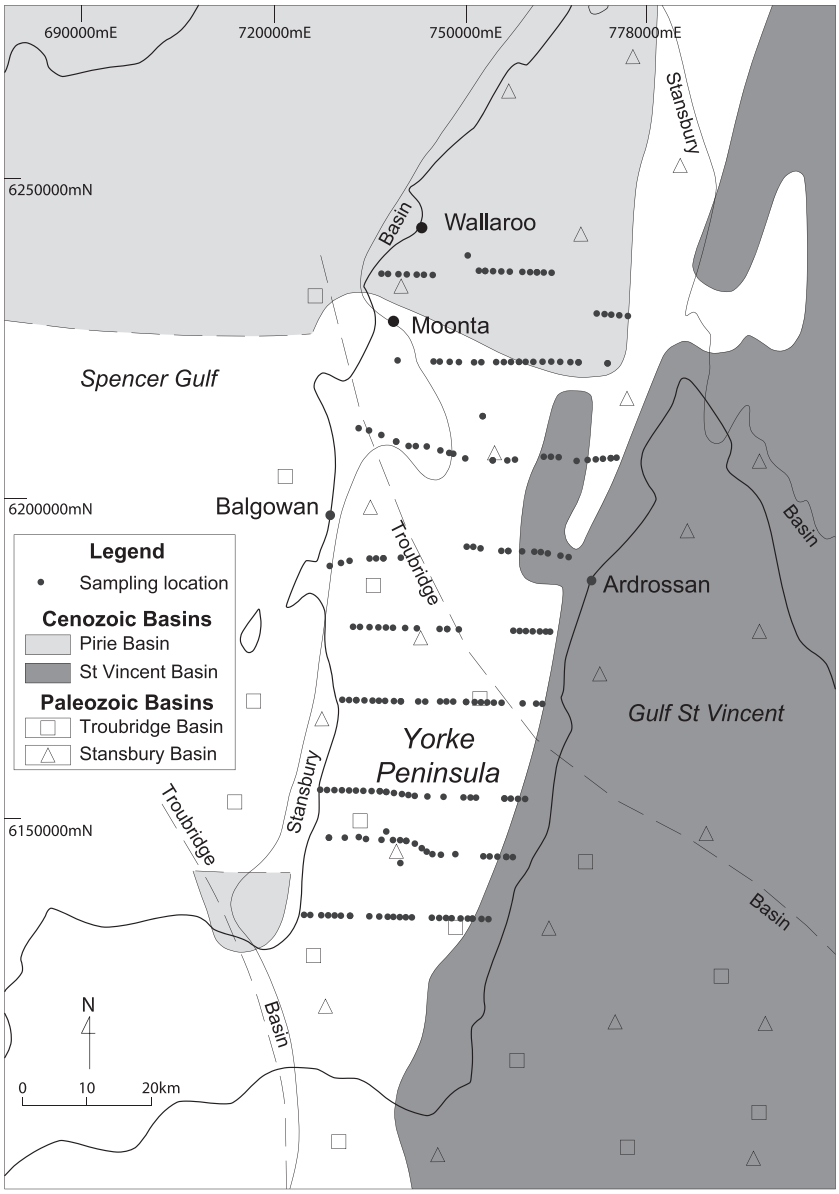

Fig. 3. Map of Yorke Peninsula showing location of the Palaeozoic Stansbury and Troubridge Basins and Cenozoic Pirie and St Vincent Basins. Basin outlines are modified from Drexel and Preiss (1995). Locations of regional carbonate rock samples are shown by black dots. The Cu concentrations for samples from Hartley (2000) proximal to Moonta are shown. The location of Balgowan and Ardrossan where seawater samples were taken are also shown. Map location is shown in Fig. 2.

the coastline (e.g. the St Kilda Formation, Fig. 5; Zang et al., 2006). Extensive sand dunes have also formed across inland regions primarily in the north and along the eastern coastline (Fig. 6). Sand-flats, clay-pans and ephemeral lakes have developed in areas of low relief. Calcium carbonate-rich rocks with laminar, nodular or powdery textures have formed in the upper portion of the soil profile throughout most of the region (e.g. Drexel and Preiss, 1995; Zang et al., 2006). The western side of the Yorke Peninsula is dominated by calcareous sand dunes whilst the eastern margin is dominated by calcareous, loamy soils overlying pedogenic carbonate rock (e.g. McDowell et al., 2012; Neagle, 2008). Active erosion and re-deposition of colluvium occurs within gullies, drainage lines and along the coastline (Zang et al., 2006).

2.2. Landscape, climate and vegetation

The Yorke Peninsula is low relief, with gently undulating hills and valleys generally < 100 m above sea level and up to 230 m above sea level north of Maitland (e.g. Neagle, 2008; Roberts, 2007; Zang et al., 2006). The region has been cleared of most naturally occurring vegetation for agriculture with approximately 13% native vegetation remaining (McDowell et al., 2012; Neagle, 2008). A variety of vegetation species including eucalypt mallee, tea trees and wattle trees tend to dominate the landscape whilst samphire, saltbush, mangroves and other coastal shrubs dominate coastal sandflats and backshore environments with low relief (e.g. McDowell et al., 2012; Neagle, 2008).

The region has a Mediterranean climate (McDowell et al., 2012) with average daytime temperatures ranging from 15 °C in winter to 30 °C during summer (Bureau of Meteorology, 2018). Rainfall averages approximately 470 mm per year (Bureau of Meteorology, 2018). No major water catchments occur in the central Yorke Peninsula region (e.g. DEWNR, 2013) and any surface drainage is infrequent, with many watercourses terminating in ephemeral salt lakes and clay pans (e.g. DEWNR, 2013; Roberts, 2007). Wind across the study area is generally derived from the north-west during summer and from the south to south west during winter (e.g. Bureau of Meteorology, 2017; Hesse and

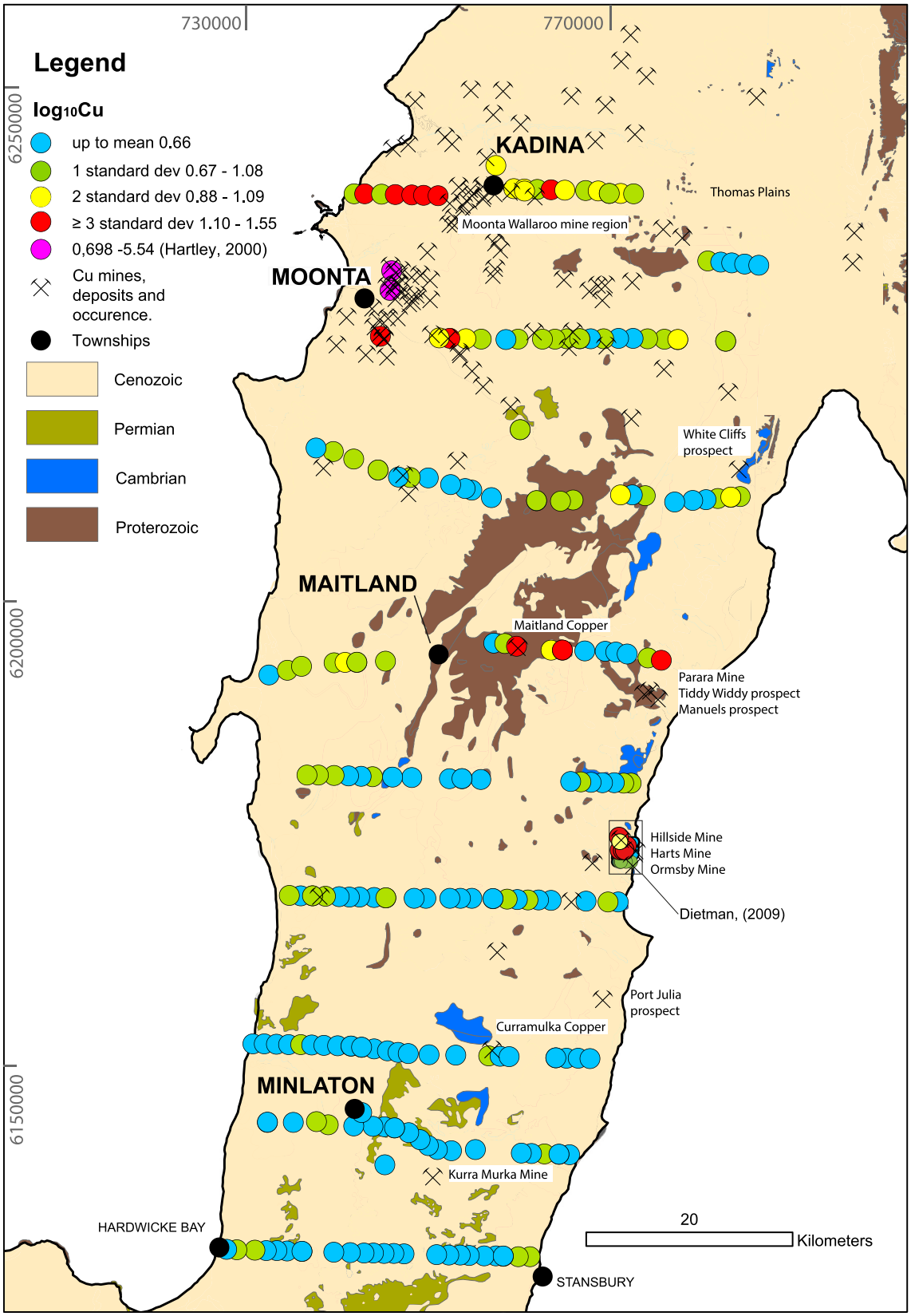

Fig. 4. Simplified surface geology map of Yorke Peninsula (Extracted from SARIG: https://map.sarig.sa.gov.au). Cenozoic geology includes Miocene aged limestone found in the Pirie and St Vincent Basins (see also Fig. 3) and Quaternary limestone. Cambrian geology includes limestone found in the Stansbury Basin (see also Fig. 3). Cu concentrations from this study are displayed as the $\log_{10}$ values and colored by standard deviation. Cu concentrations reported in Hartley (2000) (NE of Moonta) and Dietman (2009) (Hillside and Harts Mines) are also shown.

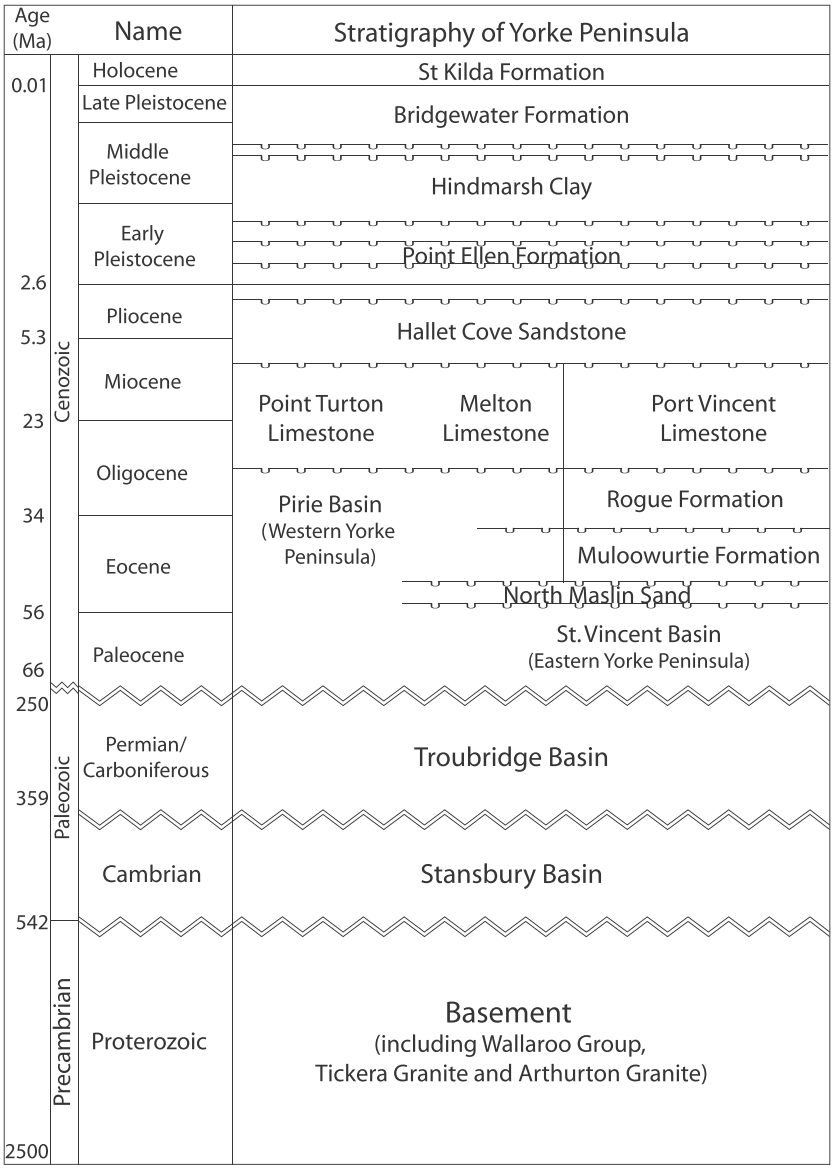

Fig. 5. Simplified stratigraphic diagram of the Yorke Peninsula. Modified after Drexel and Preiss (1995) and Zang et al. (2006).

McTainsh, 2003).

3. Methods

3.1. Regolith landform map

A 1:25000regolith map was produced using a combination of geophysical data including Google Earth™, United States Geological Survey (USGS) and Aster global-DEM (a product of METI and NASA) (Fig. 6). Surface geology and elevation features were verified using South Australian Resource Information Gateway (SARIG, Department of the Premier and Cabinet, 2017). The present landscape has been significantly modified due to land use, therefore ground truthing and verification of the map was undertaken at each sampling site (Fig. 3). Correlations assuming a non-complex continuation of landform features within each area mapped were made between field sampling sites under areas of land cleared for cropping and using the various digital data previously described. Regolith landform unit codes (RLU) used are based on Pain et al. (2007).

3.2. Sampling methods

3.2.1. Carbonate sampling

A total of 215 surface carbonate rock samples were collected at approximately 1 km intervals along ten east-west transects spaced approximately 10 km apart (Fig. 3). Each transect followed a road corridor extending from one coastline of the Yorke Peninsula to the other. Where no carbonate rocks were present, the sample spacing was extended until a suitable sample could be located. The resulting sampling grid extends from Stansbury and Hardwicke Bay in the south, to Kadina and Thomas Plains in the north (Fig. 3).

Due to possible contamination factors such as increased dust and car emissions samples were collected as far from the side of the road as possible. Major intersections, townships, driveway entrances and quarried carbonate rocks (often incorporated in historic fence lines) were avoided. Gloves were used to collect all samples. Larger boulder sized samples were broken up with a geological hammer prior to collection. Smaller cobble sized samples were removed from the soil by hand or by levering out of the ground with a geological hammer. Where possible larger rocks were sampled so as to reduce the surface to volume ratio in an attempt to minimize concentration of any adhering

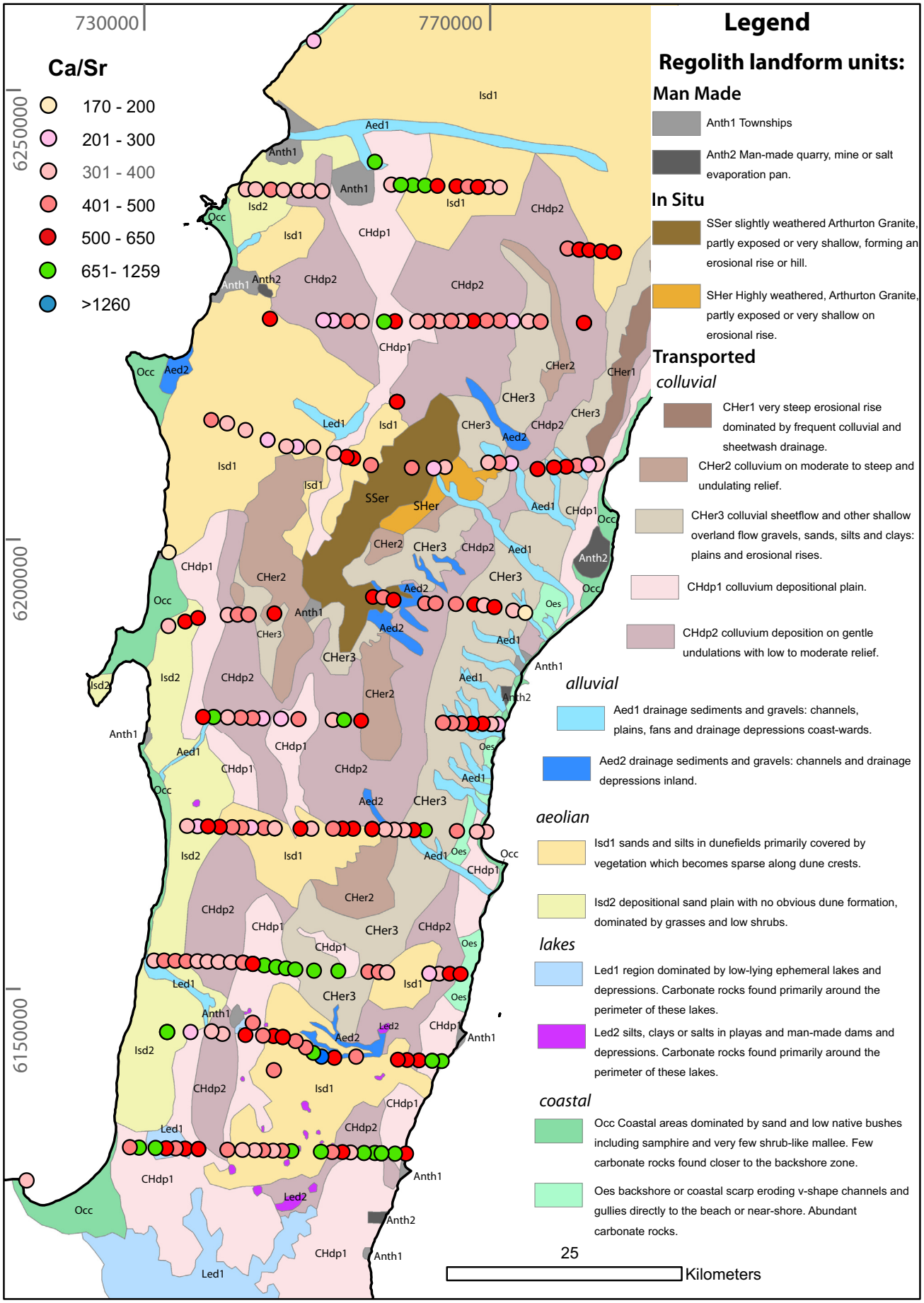

(caption on next page)

Fig. 6. 1:25000 scale regolith map of the Yorke Peninsula. Carbonate rock sample locations from this study are shown and colored by Ca/Sr ratio values. Categories used are based on Wolff et al. (2017) where Ca/Sr < 650 are described as pedogenic carbonate and are colored from pink to red; Ca/Sr > 1260 are described as marine carbonate and colored blue. Intermediate Ca/Sr values (651–1259) are colored green. (For interpretation of the references to color in this figure legend, the reader is referred to the web version of this article.)

surface contaminants. The samples were brushed lightly with a soft brush to remove surface contamination. The sample was placed into plastic zip-lock bag and labelled with a unique identifier and numbered according to the order it was collected. One in every 10 field samples were replicated. A small portion of each sample was reserved for reference. The average sample size was approximately 2 kg.

3.2.2. Seawater sampling

Seawater was collected at Ardrossan and Balgowan (Fig. 3) to define a Ca/Sr seawater line for samples taken as close as possible to the pedogenic carbonate rocks investigated in this study and to determine its impact, if any, on the Ca and Sr concentrations of the carbonate rocks across the Peninsula. The present-day Ca/Sr ratio of seawater is used to represent the Ca/Sr ratio of seawater through formation of the pedogenic carbonates as they have been interpreted to be have formed 22,000 years ago (Zang et al., 2006), and Coggon et al. (2010) report that Ca/Sr ratios of sea water have been close to what they are now since ~1.6 Ma (Ca/Sr ~50).

At Balgowan water was collected off the end of a groin by reaching out and submerging a bucket firstly to pre-rinse and then again to collect the sample. At Ardrossan the water was collected from the end of the jetty by tying a rope to the bucket handle and lowering it into the water to firstly pre-rinse and then again to collect the sample. In both instances, seawater samples were decanted into 125 ml, high density polyethylene (HDPE) bottles and labelled.

3.3. Sample preparation and analysis

3.3.1. Carbonate samples

The entirety of the carbonate rock samples were milled to a fine powder using a tungsten carbide ring mill at Amdel Laboratories Adelaide. Approximately 100 g portions of this material was sent to Bureau Veritas (Acme Laboratories) in Vancouver, Canada for whole-rock geochemical analysis. Major element oxides were analyzed using X-ray fluorescence (XRF) on $LiBO_2$ fused glass beads. Trace elements were analyzed using ICP-MS following two separate preparations. Rare earth and refractory elements were analyzed following lithium borate fusion. Aqua regia digest was used for all remaining trace elements (Mo, Cu, Pb, Zn, Ni, As, Cd, Sb, Bi, Ag, Au, Hg, Tl and Se). Routine laboratory standards, duplicates and blanks were included for quality control. One in every 10 samples were duplicated (n = 23). Sixteen blanks were included with XRF and 10 blanks were included with ICP-MS.

3.3.2. Seawater samples

Seawater sample preparation involved the addition of concentrated nitric acid (69%) to each sample in the laboratory. Approximately 0.25 µL was added to each full 125 ml bottle. Acidification is undertaken to ensure any Fe oxides were fully dissolved as described by (Gray et al., 2009). Samples were packed in a plastic storage container and sealed prior to sending to South Australia Department of Land and Water for analysis of major and trace elements by ICP-OES and ICP-MS. Concentrations for Ca, determined by ICP-OES, were reported in mg/L. Concentrations for Sr, determined by ICP-MS, were reported in ug/L. Elements of interest were converted to ppm for the purpose of this paper.

4. Results

4.1. Regolith landform map

The Regolith Landform Map is presented in Fig. 6. The majority of the region is dominated by transported sediments with few in-situ rocks observed around the central region. Rocks that are exposed and were observed in-situ are predominantly weathered granite. The western half of the Yorke Peninsula is dominated by sand and sand dunes (e.g. Isd1 and Isd2). Coastal environments include tide dominated sand flats with few steep backshore sand dunes or cliffs (e.g. Occ). The central region of the Yorke Peninsula (Fig. 6) is characterized by undulating hills and valleys with a range of in-situ erosional (SSer, Sher) and colluvial (Cher1, CHer2, CHer3, CHdp1, CHdp2) regolith environments. Outcropping rocks in the most central area of the peninsula are variably weathered and found primarily buried beneath a shallow cover of soil (SSer and Sher). The eastern portion of the mapped area (Fig. 6), is dominated by cliffs and steep hills with incised drainage channels (CHer1, Cher3, CHdp1, Aed1, Aed2). The southern portion of the mapped area is lower in elevation and dominated primarily by depositional plains including sand dunes, and sandy beach deposits along the coastline (CHdp1, CHdp2, Isd1 and Oes). The area with the lowest relief, the southernmost portion of the map (Fig. 6), features a region of salt lakes and clay pans that fill with water only after heavy rain (CHdp1, Led1 and Led2). Carbonate rocks occur across all regolith landform units, except the lake units (Led1, Led2) and the coastal units (Occ, Oes). The carbonate rocks have a variety of forms: 1) soft or powdery carbonate-rich sands and soils forming a thin veneer at the surface (Fig. 7); 2) well-indurated, massive or laminated tabular forms from decimeter to meter thickness (e.g. Fig. 7a), and; 3) nodular forms with variable proportions and density of nodules from gravel to cobble size and with a thickness of approximately one meter (e.g. Fig. 7b, c). All three carbonate forms are often found at the same location with calcareous soils typically overlying tabular forms, which in turn overly nodular forms. These carbonate morphologies are typical of those found in regolith carbonate profiles (e.g. Chen et al., 2002; Lintern, 2015).

4.2. Whole-rock analysis

Geochemical data are shown in Figs. 8, 9 and 10. Representative geochemical data are given in Table 1. Geochemical results for all samples and elements analyzed are presented in Supplementary Data Appendix 1.

4.2.1. Major element chemistry

Calcium oxide (CaO) concentration ranges from 33% to 53% (Fig. 8a). Assuming all calcium occurs as carbonate ($CaCO_3$), the concentration of calcium carbonate ranges from ~ 55% to 80% with an average of 72% (Table 1). Silica (SiO_2) concentration ranges from 2% to 30% with the majority of samples containing ~ 20% or less (Fig. 8a, and b). SiO_2, Al_2O_3 and Fe_2O_3 are positively correlated (Fig. 8b, c and d) and all three have negative correlations with CaO (Fig. 8a and e). Other major elements with concentrations at percent level include MgO which ranges from 0.6% to 7% (Table 1) and K_2O which ranges from 0.01% to 0.6% (Table 1). MgO and K_2O are negatively correlated to CaO, whilst K_2O and Al_2O_3 are positively correlated.

On a ternary diagram of SiO_2, Al_2O_3 and CaO the carbonate rocks sampled in this study form a linear trend between CaO and SiO_2 with minor Al_2O_3 (Fig. 9). Mineralogically, this is consistent with a mixture of materials dominated by carbonate (CaO) and quartz sand (SiO_2) with

Fig. 7. Field photographs of selected carbonate rock texture typically found across the Yorke Peninsula. a) Massive, well indurated, tabular carbonate with bouldery carbonate rocks both above and below. Thickness of hardpan carbonate shown is approximately 0.5 m–1 m. Observed along a roadside cutting; b) Laminar carbonate rock underlain by carbonate nodules and cobbles, exposed along a roadside cutting. This carbonate is found beneath a thin i.e. < 25 cm layer of soil; c) Bouldery to cobble carbonate rock which is partly coalesced and forms a massive layer of carbonate. Below this carbonate are many nodules and cobbles of carbonate which occur in a calcareous silty matrix.

minor clay (Al_2O_3) content.

4.2.2. Trace element chemistry

Strontium concentration ranges from 270 ppm to 1330 ppm (Fig. 10f). Lead (Pb) concentration ranges from 0.5 ppm to 10.4 ppm (Fig. 10g). Zirconium (Zr) concentration ranges from 7 ppm to 83 ppm (Fig. 8f, g, h, i, and j). Relationships of Zr to major elements are considered important to this study as they can be used to interpret potential sources of contamination and the origin of the Cu. Zirconium has a negative relationship to CaO (Fig. 8f) and a positive relationship with SiO_2, Al_2O_3 and Fe_2O_3 (Figs. 8g, h, and i, respectively).

Copper (Cu) concentration ranges from 1.4 ppm to 36 ppm, and has a mean concentration of 5.35 ppm (Table 1; Figs. 10 and 11). Copper concentrations are right skewed (Fig. 11a), with a log-normal distribution (Fig. 11b). Concentrations of Cu above the mean are spatially distributed around the Moonta mining region and east of Maitland (Fig. 3). Relationships of Cu to major and trace elements are considered important to this study as they can be used to interpret potential sources of contamination and the origin of the Cu. Cu has no clear relationship with the major elements CaO, SiO_2, Al_2O_3, Fe_2O_3 or K_2O (Figs. 10a, b, c, d, and e, respectively) nor the trace elements Zr, Sr or Pb (Fig. 8j; Fig. 10f and g respectively).

4.2.3. Ca/Sr ratios

Ca/Sr ratios range from 179 to 1324 (Table 1). Eighty six percent (184 of 215) of the carbonate samples have Ca/Sr ratios < 650 (Fig. 12), below the threshold value for pedogenic carbonates on the Yorke Peninsula proposed by Wolff et al. (2017). One carbonate rock sample has a Ca/Sr ratio of > 1260, above the threshold value for marine carbonates proposed by Wolff et al. (2017) (Fig. 12). This sample is located east of Minlaton within 4 km of outcropping Cambrian limestones (Figs. 4 & 6). Thirty samples have Ca/Sr ratios between 650 and 1260 (Fig. 12). Higher Cu concentrations (Cu > 10 ppm) in carbonate rocks generally correlate to lower Ca/Sr ratios (Fig. 13).

4.2.4. Seawater analysis

Results of seawater analysis are given in Table 1. The full dataset is given in Supplementary Data Appendix 2. Seawater at Ardrossan contained Ca 459 mg/L and Sr 9840 µg/L. Seawater at Balgowan contained Ca 445 mg/L and Sr 10,090 µg/L. The Ca/Sr ratio for seawater at the two locations is 46 and 44 respectively.

5. Discussion

5.1. Sources of Ca and Sr in pedogenic carbonate rocks on the Yorke Peninsula

Sources of Ca and Sr in pedogenic rocks on the Yorke Peninsula may include; 1) in-situ weathering of underlying basement rocks or Cambrian to Cenozoic sedimentary rocks including marine limestone; 2) windblown dust from exposed basement rocks or marine limestones; 3) sea spray, and; 4) rainfall (e.g. Keeling and Hartley, 2005; Lintern, 2015; McQueen et al., 1999).

Hesse and McTainsh (2003) suggest that Ca-rich dust found across the Yorke Peninsula originates from Cenozoic continental shelf deposits along the western coastline of South Australia which have a Ca/Sr ratio of > 1260 (e.g. Kyser et al., 1998; Quade et al., 1995; Wolff et al., 2017). This ratio is different to seawater Ca/Sr values (~45: Fig. 12) implying that the formation of the cold water Cenozoic carbonates of southern Australia involved significant fractionation of Ca and Sr from their seawater source. Rainwater has been proposed as a potential source of Ca and Sr in pedogenic carbonates in Australia (e.g. Hill et al., 1999; McQueen, 2006). Southern Australia receives its rainfall predominantly from evaporation from the Southern Ocean (e.g. Dart et al., 2007; Hill et al., 1999; Quade et al., 1995; Van der Hoven and Quade, 2002). Calcium derived from the ocean is carried by aerosols and deposited by rainwater (Fantle and Tipper, 2014).

Airborne particles containing elements including Ca and Sr are preferentially removed from the atmosphere during rainfall and decrease relative to the volume of rain that falls (Shimamura et al., 2006). Oxygen isotope studies of rainwater have demonstrated that the removal of species from the atmosphere by rainwater is mass dependent, with heavier species being concentrated in the rain (e.g. Bowen and Wilkinson, 2002). As a result clouds tend to become more concentrated in lighter isotopes over time and as they move inland. Rainwater in coastal areas tends to contain higher concentrations of heavy isotopes, whereas inland rain tends to be relatively enriched in lighter isotopes

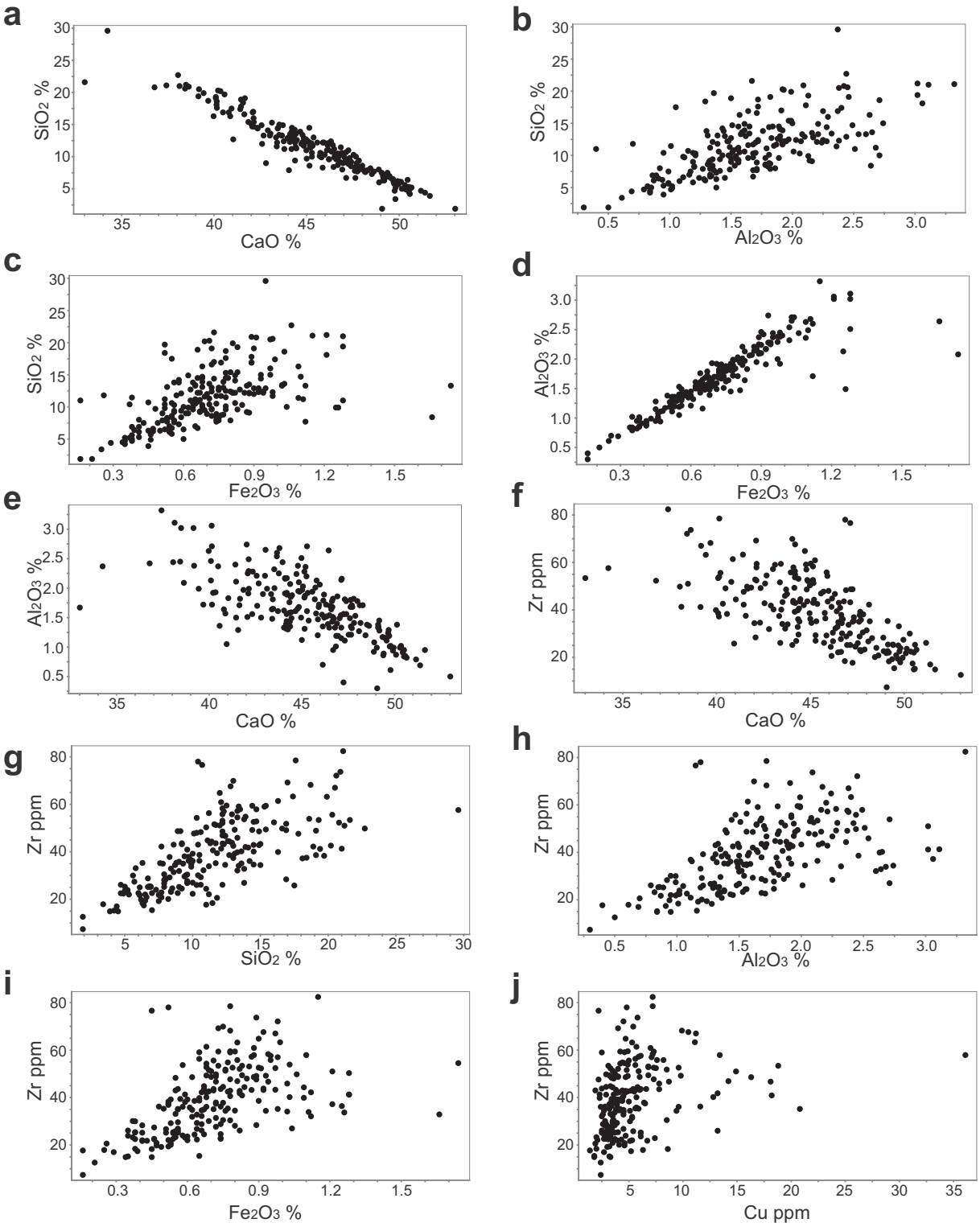

Fig. 8. Whole rock geochemical plots for selected major and trace elements for the regional Yorke Peninsula carbonate samples; a) SiO_2 versus CaO; b) SiO_2 versus Al_2O_3; c) SiO_2 versus Fe_2O_3; d) Al_2O_3 versus Fe_2O_3; e) Al_2O_3 versus CaO; f) Zr versus CaO; g) Zr versus SiO_2; h) Zr versus Al_2O_3; i) Zr versus Fe_2O_3 and j) Zr versus Cu.

(e.g. Bowen and Wilkinson, 2002). This is known as the continental effect. Other fractionation effects may be related to altitude, latitude and seasonal variations (Cheng et al., 2010; Crosbie et al., 2012; Fantle and Tipper, 2014). Such mass dependent fractionation can be expected to effect the ratio of Ca to Sr in rainwater with the much heavier Sr being expected to be relatively enriched in coastal compared to inland rainwater. The sparse data available for Ca and Sr compositions of rainfall in Australia supports this (Crosbie et al., 2012).

Crosbie et al. (2012) measured rainwater chemistry from across Australia (Fig. 12a). Rainwater from high precipitation coastal regions have Ca/Sr ranging from ~60 to 100 (close to the seawater value of 45). Rainwater from Adelaide (the nearest rainwater collection site to the Yorke Peninsula; Fig. 2), Woomera and Mildura; (Fig. 1) have Ca/Sr of approximately 150 to 300. The entire dataset collected by Crosbie

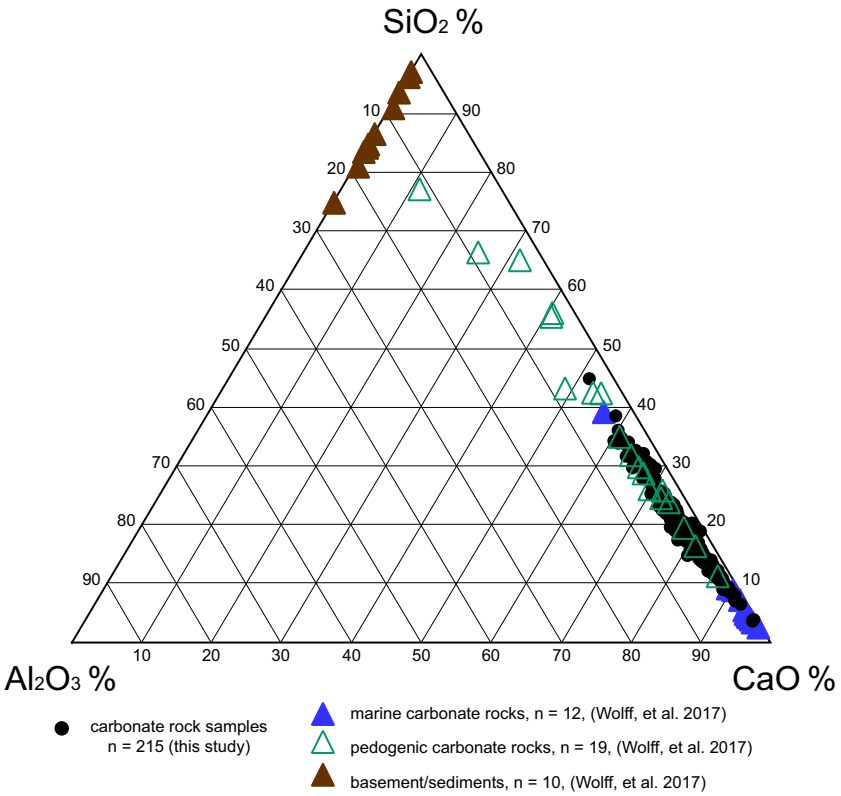

Fig. 9. Ternary diagram showing composition of the carbonate rocks sampled from the Yorke Peninsula. Sand is represented by SiO_2%, carbonate by CaO % and clay by Al_2O_3%.

et al. (2012) forms an array that indicates the potential variation in Ca/Sr ratios, ranging from 60 to 400, within Australia (Fig. 12a).

The range of Ca/Sr ratios from the Yorke Peninsula carbonate dataset overlaps with the range of rainwater Ca/Sr reported by Crosbie et al. (2012). The whole dataset forms a roughly linear trend on the Ca versus Sr diagram that extends from the zone of 'rainwater' Ca/Sr (Fig. 12b) towards the composition of Cenozoic marine carbonate rocks from the Yorke Peninsula (> 1260; Wolff et al., 2017). One data point from a carbonate sample from this study plots with the Yorke Peninsula marine carbonate rocks (Fig. 12b).

Cambrian to Pliocene-aged marine carbonates occur throughout the Yorke Peninsula and are exposed in the southern and eastern parts of the Peninsula (Fig. 4). Cenozoic marine carbonates are exposed over large areas of coastal southern Australia, including along the Great Australian Bight. It is possible that marine carbonates rocks could have contributed to the Ca and Sr budget of the pedogenic carbonates.

The trend from the zone of rainwater chemistry towards the composition of marine carbonate rocks suggests the Ca and Sr composition of the Yorke Peninsula regolith carbonates is a mixture of rainwater sources and marine carbonate sources, the latter either by the incorporation of wind-blown dust or from in-situ weathering of underlying marine carbonates. Simple two component mixing between a source with Ca/Sr consistent with Adelaide rainwater (~225) and a source consistent with Cenozoic Yorke Peninsula marine carbonates (~1400) suggests that the dominant source for most of the surface carbonates in this study was meteoric. Ca/Sr ratios of 650, at the higher Ca/Sr end of the array, correspond to a marine carbonate component of ~35%.The majority of the regional Yorke Peninsula samples used in this study have Ca/Sr consistent with a dominant rainwater source. Eighty six percent (n = 184; Fig. 12) of the samples have Ca/Sr < 650. A relatively small number of samples (n = 30) preserve Ca/Sr ratios between 650 and 1260 (Fig. 12) that are consistent with a marine component of > 35%. Spatially, these intermediate composition samples are more frequent in the south of the study area, and are proximal to the exposures of marine carbonate (Figs. 4 & 6). The Ca/Sr ratio > 1260 for one sample in the southern Yorke Peninsula (Fig. 6) suggests this sample is actually a marine carbonate, and may even be a weathered sample of the Cambrian limestone.

Based on the overlap in Ca/Sr ratios between the Yorke Peninsula samples and the zone of rainwater chemistry, the data are consistent with Ca and Sr from two sources:

1. A major component from rainwater, initially with seawater Ca/Sr and subjected to varying degrees of fractionation during precipitation which has produced Ca/Sr ratios ranging from < 200 to ~400 (Fig. 12b).
2. A lesser component from marine carbonates, incorporated either from wind-blown dust or from in-situ marine carbonates.

The significant rainwater contribution to Ca and Sr in the Yorke Peninsula carbonates is consistent with the findings of Quade et al. (1995), who investigated sources of Ca in pedogenic carbonates from coastal South Australia and Victoria and concluded that the dominant source of Ca and Sr was from sea spray or rainwater. The systematically lower Ca/Sr of rainwater, compared to marine carbonates, translates into systematically lower Ca/Sr in pedogenic compared to marine carbonates. This is an effective discriminator of carbonates formed by pedogenic processes and weathered marine carbonates, with the potential to be recognized in reconnaissance geochemical data (see also Wolff et al., 2017).

5.2. Influence on Ca and Sr concentrations in other carbonate rocks

The Ca and Sr concentrations within carbonate sample sets from Cobar, NSW (McQueen, 2006) and proximal to the Challenger Au deposit and the transcontinental railway in central South Australia

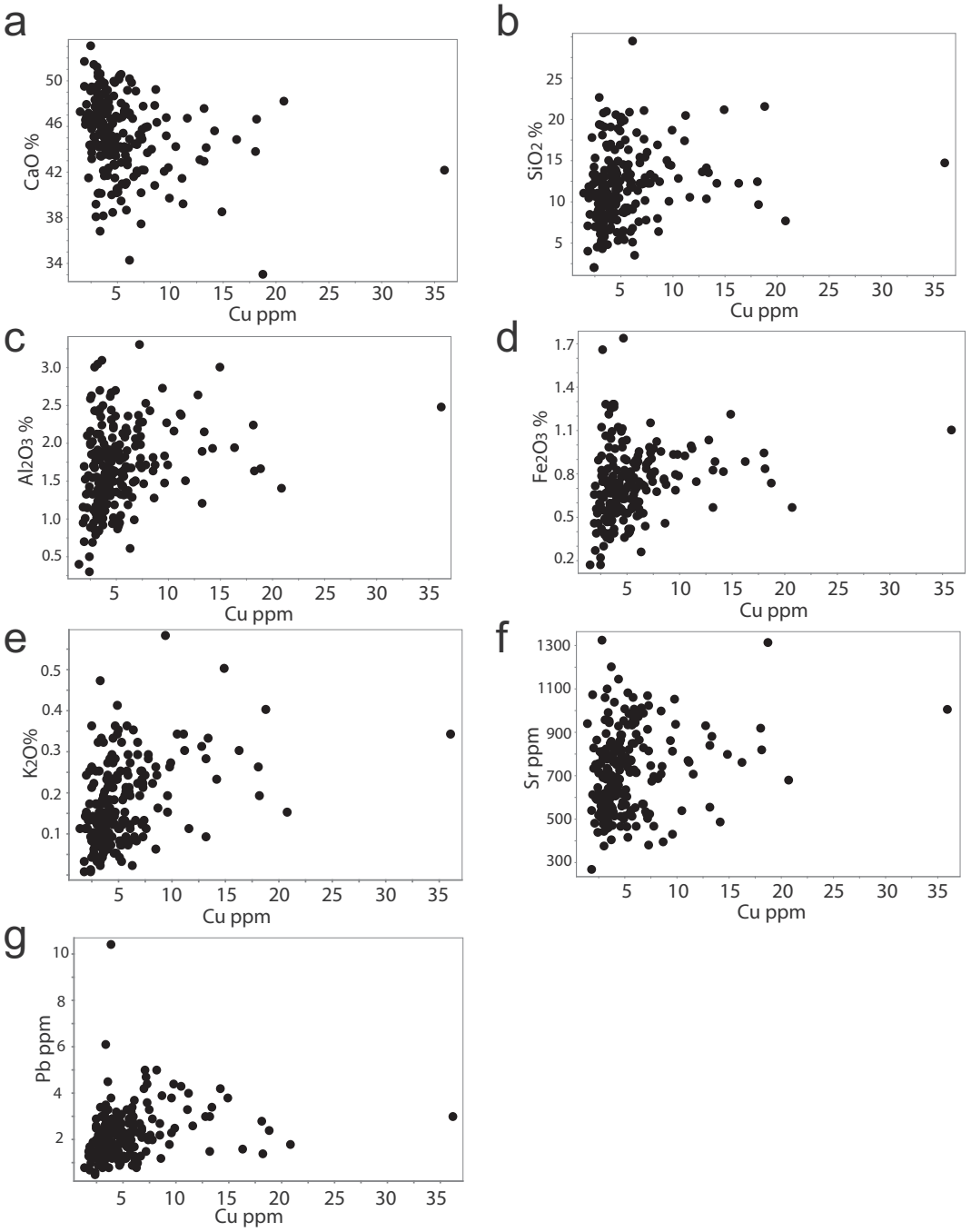

Fig. 10. Whole rock geochemical plots for Cu versus selected major and trace elements for the Yorke Peninsula carbonate samples. Cu ppm versus: a) CaO; b) SiO_2; c) Al_2O_3; d) Fe_2O_3; e) K_2O; f) Sr and g) Pb.

(Lintern and Sheard, 1999; Lintern et al., 2006) (Fig. 1) show similar influences of rainwater and/or marine carbonate chemistry. The spread in Ca concentrations in these datasets is indicative that the samples did not constitute pure carbonates, and it is likely there is some clastic input, however the Ca/Sr ratios show similar patterns to the data from the Yorke Peninsula (Fig. 12b).

McQueen (2006) describes all samples from Cobar as regolith (pedogenic) carbonate, which is reflected in the low Ca/Sr ratios (< 650) preserved within most of the Cobar carbonate samples (Fig. 12b). Similar to the Yorke Peninsula samples, the Cobar carbonate samples show a spread in Ca/Sr ratios that range from within the zone of rainwater chemistry to chemistry similar to the Yorke Peninsula marine carbonates, with most samples plotting within the zone of rainwater chemistry (Fig. 12b). This implies that the Ca and Sr concentrations for the majority of carbonate rocks in Cobar is influenced by rainwater composition. Crosbie et al. (2012) sampled rainwater from the township of Cobar, however Sr concentrations were below detection and could not be used. The nearest location with measurable amounts of both Ca and Sr was Mildura (Figs. 1 and 12). The Ca/Sr ratios calculated for the Mildura rainwater are comparable to the Ca/Sr ratios of the Cobar carbonate rocks, indicating the rainwater may have influenced the Ca and Sr concentrations of the majority of the Cobar carbonate rocks (Fig. 12). Almost all of the remaining samples that fall outside of the zone of rainwater chemistry plot within the intermediate region between rainwater chemistry and Yorke Peninsula marine carbonates, implying a mixed source. One sample plots with the Yorke

Table 1
Summary statistics of whole rock geochemical data of the regional Yorke Peninsula carbonate samples for selected elements, calculated $CaCO_3$ content (from CaO concentration) and Ca/Sr ratios; and Ca and Sr seawater chemistry for the Ardrossan and Balgowan samples. All data is presented in Appendix 1.

Whole rock geochemistry	Al_2O_3	SiO_2	Fe_2O_3	K_2O	MgO	CaO	$CaCO_3$	Sr	Ca/Sr	Zr	Pb	Cu
Units	%	%	%	%	%	%	%	ppm	Ratio	ppm	ppm	ppm
Detection limit	0.01	0.1	0.01	0.01	0.01	0.01		0.5		0.1	0.1	0.1
Analytical method	XRF	XRF	XRF	XRF	XRF	XRF	Calculated from CaO %	ICP-MS	Calculated ratio	ICP-MS	ICP-MS	ICP-MS
n	215	215	215	215	215	215	215	215	215	215	215	215
Minimum	0.30	1.90	0.20	0.01	0.67	33.01	55.12	267.00	179	7.40	0.50	1.40
Maximum	3.32	29.60	1.80	0.58	7.20	53.02	81.86	1331.60	1324	82.40	10.40	36.10
Mean	1.68	11.59	0.72	0.17	1.59	45.26	71.56	723.47	485	39.32	2.22	5.35
Standard deviation	0.54	4.50	0.24	0.10	0.84	3.40	4.53	191.92	156	14.76	1.09	3.82

Seawater chemistry	Ca	Sr	Ca/Sr
Units	mg/L	ug/L	
Analytical method	ICP-OES	ICP-MS	Calculated ratio
Ardrossan	459	9840	46
Balgowan	445	10,090	44

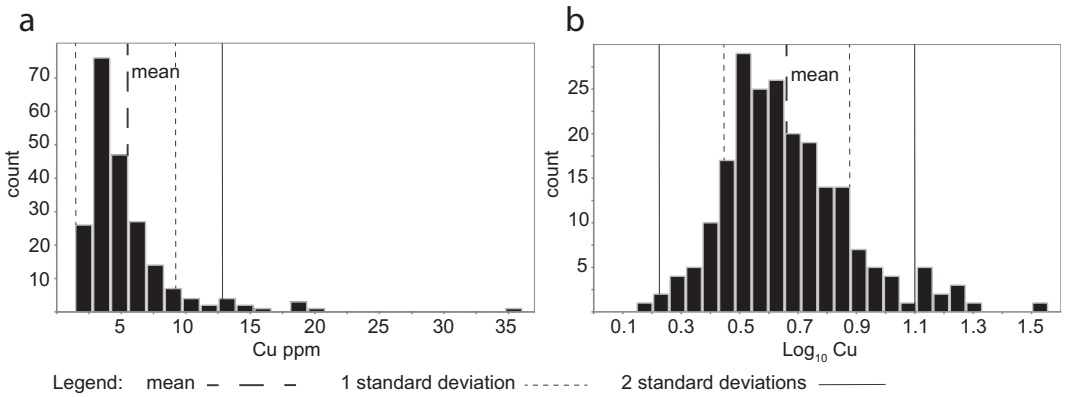

Fig. 11. Histograms for the regional Yorke Peninsula carbonate samples showing a) the concentration of Cu in all samples. The mean and 1 and 2 standard deviations above the mean are shown; b) the $\log_{10}$ Cu concentration of all samples. The mean and 1 and 2 standard deviations from the mean are shown.

Peninsula marine carbonates (Fig. 12b). Fossil-rich marine carbonates have been described in the Cobar area, and belong to the Ordovician to Devonian Girilambone Group (e.g. Burton, 2015; Glen, 1991; Iwata et al., 1995). The source of the high Ca/Sr ratio due to proximity to marine limestone can only be speculated due to having no context of the sample within the local geological stratigraphy. McQueen et al. (1999) suggested that Ca and Sr contributions to carbonate rocks in the region are primarily from aeolian dust and/or rain.

The carbonate rocks from central South Australia (Lintern and Sheard, 1999, Lintern et al., 2006) display a much tighter range in Sr concentrations, with the majority of the samples preserving Ca/Sr ratios indicative of pedogenic (Ca/Sr < 650) origin or being within the intermediate zone between pedogenic and marine origin (650 < Ca/Sr < 1260) (Fig. 12b). A small number of samples (n = 12) plot within the zone of rainwater chemistry (Fig. 12b). The closest rainwater sample point to the central South Australian carbonate samples is Woomera (Crosbie et al., 2012; Fig. 1). The Ca and Sr composition of the Woomera rainwater is in the middle of the range of rainwater chemistry determined by Crosbie et al. (2012), with Ca/Sr ratios being 177 and 219 (Fig. 12a). Some of the central South Australia carbonate samples (Lintern and Sheard, 1999, Lintern et al., 2006) also have Ca and Sr compositions in the middle of the range of the zone of rainwater chemistry, suggesting rainwater may have influenced the concentrations of these elements in some samples (Fig. 12b). However, the variation in Ca/Sr ratios between the rainwater and the central South Australian carbonates might be a function of the amount of precipitation (i.e. 4 mm for both data points) or the rainwater sample being taken from a geographically distant area to the central South Australia carbonate sampling location (Fig. 1). The majority of the central South Australian carbonate samples plot in the intermediate area between the zone of rainwater chemistry and the Yorke Peninsula marine carbonates (Fig. 12b). Lintern et al. (2006) describes three of the samples that fall within the mixed and marine carbonate zones as being limestone or preserving visible marine fossils (Fig. 12). The central South Australian carbonate sample that plots within the field of marine carbonates (Fig. 12) is also described as a limestone (Lintern et al., 2006). In general, the Ca and Sr content within the central South Australian carbonate samples shows a spread of Ca/Sr chemistry between that of rainwater chemistry and of local marine carbonates, indicating a potential mixed influence on Ca and Sr concentrations from both rainwater and the substrate.

Overall, the Ca and Sr concentrations in the Cobar and central South Australian carbonate samples shows variation similar to that observed in the Yorke Peninsula carbonate samples. It is acknowledged that other potential influences on Ca and Sr concentrations such as dust have not been considered in interpreting the potential influences on Ca and Sr concentrations in the Cobar or central South Australian carbonate samples. However, the data does indicate that a mixture of rainwater and/or marine carbonate rocks may have influenced the Ca and Sr chemistry of regolith carbonate rocks from a number of geographically disparate regions. This shows that influences on Ca and Sr concentrations within carbonates need to be considered when using these elements to discriminate between pedogenic and marine origins for carbonate rocks using criteria such as that described in Wolff et al. (2017).

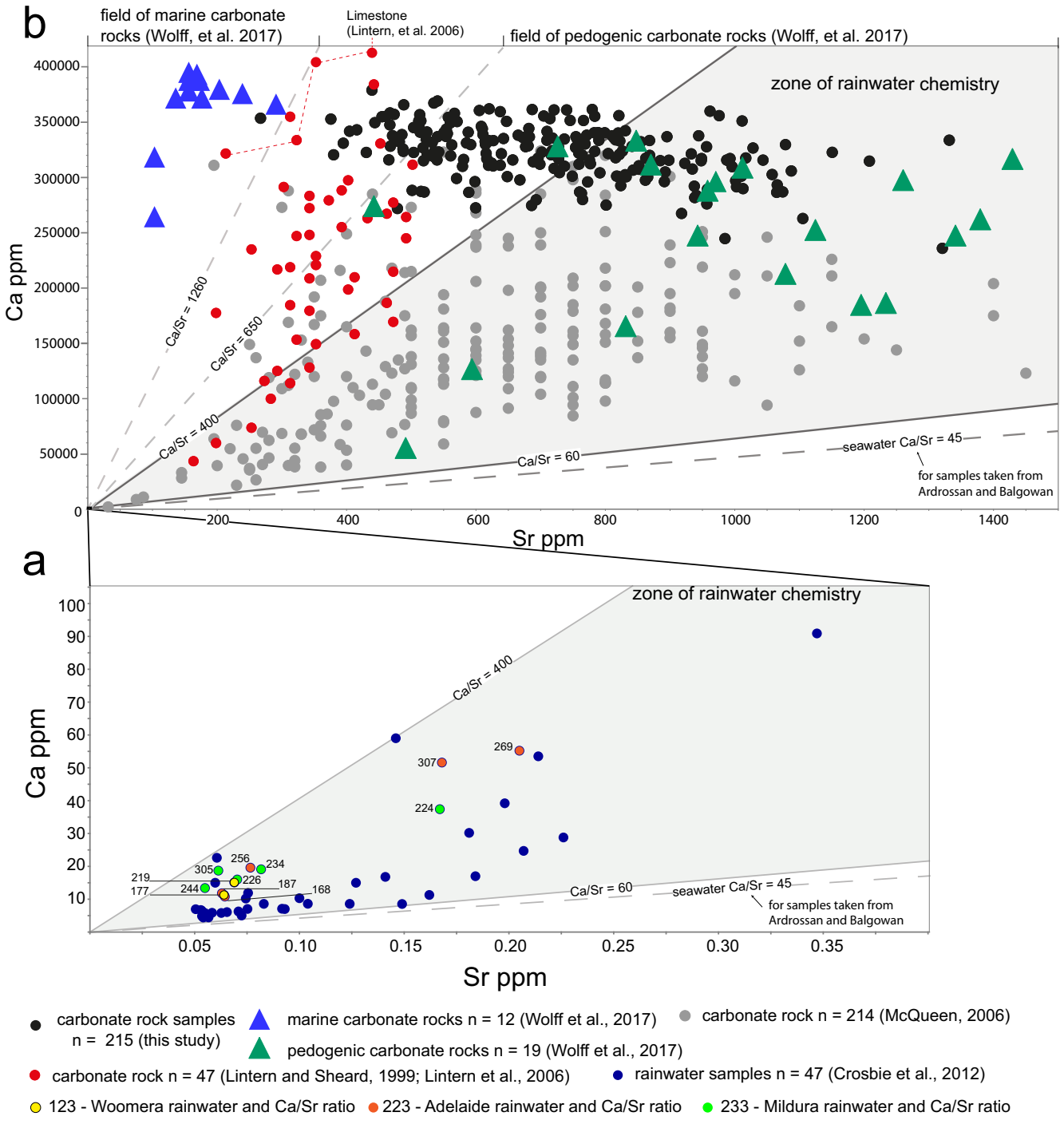

Fig. 12. Plot of Ca versus Sr. a) Ca versus Sr concentrations for rainwater chemistry taken from Crosbie et al. (2012). Note difference in scale and placement into the larger Ca versus Sr diagram shown in (b). Rainwater samples for Woomera, Adelaide and Mildura are highlighted in yellow, orange and green respectively. Ca/Sr ratios calculated from rainwater chemistry reported in Crosbie et al. (2012) are labelled for highlighted samples; b) Ca versus Sr diagram showing composition of carbonate samples from the regional Yorke Peninsula (black: this study), coastal Yorke Peninsula pedogenic carbonates (green: Wolff et al., 2017), coastal Yorke Peninsula marine carbonate rocks (blue: Wolff et al., 2017), the Cobar region (grey: McQueen, 2006) and central South Australia (red: Lintern and Sheard, 1999; Lintern et al., 2006). Samples described as limestone by Lintern et al. (2006) are also highlighted. Fields of Ca/Sr ratios defining pedogenic- and marine-derived carbonates (Wolff et al., 2017) are shown at the top of the diagram. The zone of rainwater chemistry (grey shade) is extrapolated from the seawater composition reported in Crosbie et al. (2012) and shown in (a). The seawater Ca/Sr ratio line is calculated from the average of the two Yorke Peninsula samples collected in this study (Table 1). (For interpretation of the references to color in this figure legend, the reader is referred to the web version of this article.)

5.3. Sources of Cu in pedogenic carbonate rocks on Yorke Peninsula

The potential for pedogenic carbonate rocks to preserve detectable concentrations of pathfinder elements that may be indicative of buried mineralization has been recognized by a number of authors (e.g. Poustie and Abbot, 2006; Chen et al., 2002; Lintern et al., 2012; van der Hoek et al., 2012). Of direct relevance to this study, Wolff et al. (2017) demonstrated that Cu concentrations are higher within pedogenic carbonates across the Yorke Peninsula. Comparison of Cu concentrations with Ca/Sr ratios for samples from this study (Fig. 13) shows that

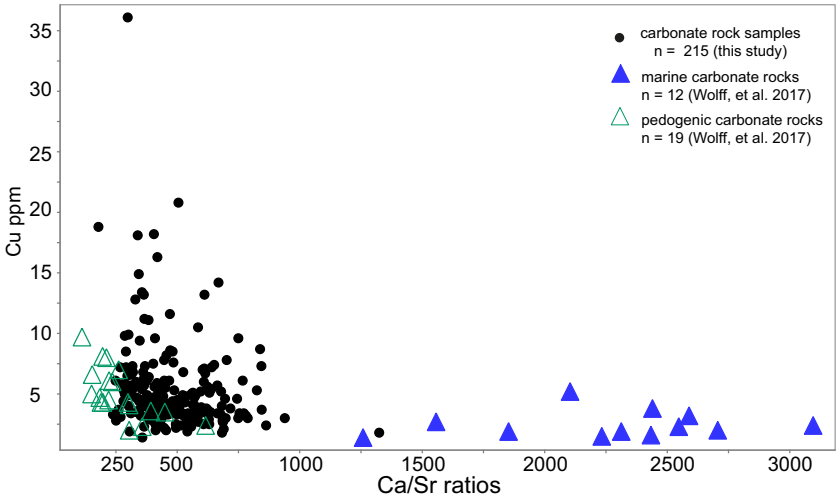

Fig. 13. Plot of Ca/Sr ratios versus Cu for carbonate rock samples from this study. Coastal marine and pedogenic carbonates sampled by Wolff et al. (2017) are also shown.

samples with higher Cu concentrations are mostly preserved in samples that have characteristically pedogenic Ca/Sr ratios (i.e. < 650). Following Wolff et al. (2017) the pedogenic carbonates should be a suitable sample medium for mineral exploration. However, the potential sources of Cu still need to be considered and include windblown contamination and contributions from underlying (potentially mineralized) rocks.

5.3.1. Windblown contamination

Dust contaminants need to be considered as airborne particles may be enriched in Cu and blown onto the carbonate rocks from nearby mining. The influences of aeolian contaminants on the geochemistry of the Yorke Peninsula carbonate rocks data has previously been assessed here as a potential for Ca and Sr contribution. Positive relationships between Al_2O_3, SiO_2 and Fe_2O_3 that may suggest clay dust contamination (Fig. 8b, c and d), and Zr versus SiO_2 and Al_2O_3 that may indicate windblown sand and soil (Fig. 8g and h) have been established. However, apart from a weak relationship of Cu to Al_2O_3, there is no relationship between Cu and any of the indicator elements of dust or other windblown contamination. Therefore, windblown contamination from clay dust, soil or sands is not considered as a source of Cu in the Yorke Peninsula carbonates.

Lead has also been suggested to be an indicator of dust contamination originating from Cu mining (e.g. Balabanova et al., 2014; Mighall et al., 2002). In this case, contamination would be manifest as a positive relationship between Pb and Cu. Comparison of Pb and Cu concentrations for the Yorke Peninsula samples shows no correlation (Fig. 10h), therefore contamination from dust originating from Cu mining is not considered to have influenced the Cu concentration within the samples used in this study.

5.3.2. Proximity to known Cu occurrence

Previous studies relating to geochemistry across the Yorke Peninsula demonstrate that Cu is mobile within the transported sediments and regolith materials overlying Cu-rich basement rocks (e.g. Dietman, 2009; Fabris, 2010; Keeling and Hartley, 2005). Dietman (2009) demonstrated that elevated Cu is preserved in carbonate rocks (e.g. 9–11 ppm) and soils (e.g. 14–20 ppm) as well as vegetation (e.g. 1.3–6.2 ppm) around the Hillside Mine site (Fig. 4). Likewise, the Moonta mining region (Fig. 4) is known to contain elevated Cu in a variety of sample media e.g. clays and transported sediments (e.g. > 80 ppm), carbonate rocks (e.g. < 25–30 ppm) and vegetation (e.g. 6–10 ppm), compared to regional background levels (e.g. Hartley, 2000; Keeling and Hartley, 2005; Wolff et al., 2017, 2018). No regional survey had been undertaken that uses carbonate rocks to test its effectiveness as an exploration sampling medium across the entire Yorke Peninsula.

The carbonate rocks from this study that contain Cu at concentrations that are 2 and 3+ standard deviations above the mean value (12.99–16.80 ppm Cu and > 16.81 ppm Cu respectively, Table 1) are spatially restricted to the Cu mining region of Moonta and Wallaroo and east of Maitland (Fig. 4). The relationship of elevated Cu and the spatial distribution with known Cu occurrences indicates that elevated Cu concentration within pedogenic carbonates can be used as an indicator towards Cu mineralization on the Yorke Peninsula, and possibly elsewhere.

The relationship between elevated Cu in carbonate rocks and proximity to known mineralization on a regional scale is illustrated by comparing the population statistics of samples within 3 km of known Cu occurrences to those that are > 3 km from known occurrences (Fig. 14). The carbonate samples within 3 km of a known Cu occurrence have a higher mean (e.g. Cu 7.02 ppm) and a standard deviation of Cu 5.4 ppm with a longer tail skewed to the right with a broader spread towards higher Cu concentrations (~13–36 ppm) compared with those that are further than 3 km away (mean 4.8 ppm indicated by black marker) and standard deviation (2.9 ppm), (Fig. 14a). The higher mean and standard deviation in the group of samples ≤ 3 km of known Cu occurrence could be influenced by two samples with higher Cu concentrations of ~20 and 36 ppm. These two samples are located < 500 m, and are the closest of any sample collected in this study, to a known Cu occurrence (Fig. 4).

It is noted that the Cu concentrations presented in this study are mostly less than those reported for carbonate Hartley (2000), which preserve > 30 ppm Cu. This is due to the samples collected by Hartley (2000) being taken from vertical profile sampling of mine pit-walls directly adjacent or overlying mineralization, at Moonta, whereas the samples in this study were taken as regional grab samples. Keeling and Hartley (2005), whom go on to further describe the regolith expression at Moonta, reported lateral dispersion of Cu within carbonate rocks approximately 100 m distance from known Cu lodes within the mine pit. This implies that the potential for pedogenic carbonate rocks to concentrate Cu is considerably greater than what is reported from the regional samples used in this study, and that higher Cu concentrations may be preserved proximal (e.g. within hundred(s) of meters) to mineralization.

The Yorke Peninsula is underlain by Cambrian and Cenozoic sediments of varying thickness (e.g. up to 70 m or more; Fabris, 2010) that may form a barrier to Cu dispersion into the overlying pedogenic

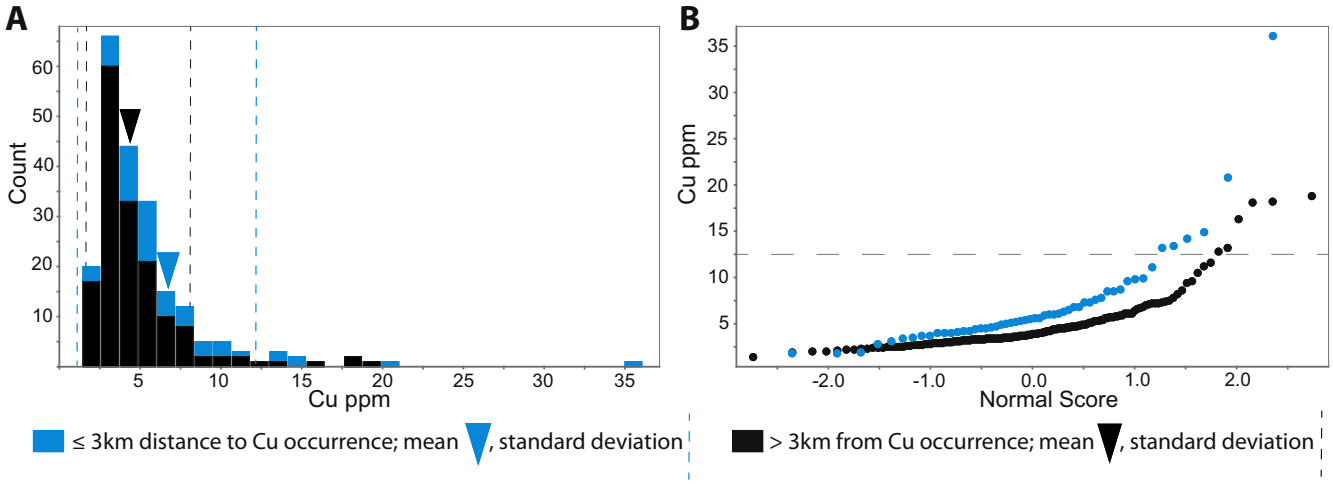

Fig. 14. a) Histogram; and b) probability plot of Cu concentrations within the regional Yorke Peninsula samples colored by proximity to known Cu occurrence. Samples within 3 km of a Cu occurrence are shown in blue, samples > 3 km from a known Cu occurrence are shown in black. The mean Cu concentrations for both groups are indicated by the triangles. The standard deviations for both groups are indicated by dashed lines of corresponding color. The grey dashed line in b) identifies a breakpoint in both populations which coincides with 2 or more standard deviations from the mean. (For interpretation of the references to color in this figure legend, the reader is referred to the web version of this article.)

carbonates (e.g. Keeling and Hartley, 2005; Wolff et al., 2017). The preservation of elevated Cu concentrations in a number of samples indicates that the dispersion barriers may be laterally discontinuous (Fig. 4), or that high Cu concentrations may have formed in more than those carbonate rocks preserved if the barriers were less extensive. Overcoming the interaction between Cu dispersion and the potential for pedogenic carbonates to preserve elevated Cu concentrations could be achieved by collecting a greater number of samples (i.e. using a < 1 km spacing or < 10 km between traverses).

5.4. Implications for exploration

The widespread occurrence of carbonate rocks and their potential to incorporate elements such as Cu from the substrate makes them an ideal sampling tool for mineral exploration. However, a number of considerations should be taken into account when identifying and sampling pedogenic carbonate rocks for mineral exploration, including:

- Identification of potential sources of Ca and Sr such as local bedrock comprising Ca-rich lithology (e.g. marine carbonates), potential for inputs from dust and rain and proximity to the coastline to ensure that Ca/Sr ratios are truly reflective of the rock origin;
- Determination of whether the carbonate rocks contain a Ca/Sr ratio consistent with pedogenic carbonate rocks i.e. < 650. Recognize also that there may be an intermediate of Ca/Sr values (650 < Ca/Sr < 1260) and investigate the geology of the region to understand the potential sample origin and whether other factors/contaminants have influenced the preserved Ca/Sr ratios;
- Identify potential sources that may contaminate the concentration of elements of interest (e.g. Cu in this study) within the carbonate rocks that occur throughout the region. This may include windblown mining dust or other dust from land use such as farming;
- Sample at a density that produces robust statistics to identify background levels versus higher concentrations, and that accounts for any potential barriers in element dispersion;
- Understand the regolith landscape processes in the region to determine whether Cu concentrations may reflect buried mineralization or are the effect of physical and/or chemical element transport.
- Usage of field-portable XRF (fpXRF) technology (e.g. Cohen et al., 2017; Wolff et al., 2017) to provide real-time data, could assist with determining both Ca/Sr ratios as well as Cu concentrations, leading to more efficient geochemical exploration.

6. Conclusion

A regional carbonate sampling survey across the Yorke Peninsula has shown that the majority of carbonate material at the surface has a pedogenic origin (Ca/Sr ratios < 650), with lesser occurrences of carbonate preserving Ca/Sr ratios intermediate between pedogenic- and marine-origin. One sample preserves a Ca/Sr ratio indicative of a marine-origin (Ca/Sr > 1260). The Ca and Sr concentration within the carbonate rocks is influenced by the chemistry of rainwater and underlying marine carbonate. These influences need to be considered when using Ca and Sr to discriminate between pedogenic and marine origins for carbonate rocks.

Pedogenic carbonate rocks throughout the Yorke Peninsula are shown to accumulate Cu in areas of known Cu mineralization. Pedogenic carbonate rocks from this study contain background Cu concentrations of ~5.3 ppm and elevated Cu concentrations above 12.99 ppm and up to 36 ppm. Pedogenic carbonate rocks preserve high Cu in concentrations coincident with areas of current or historic Cu mining. Copper found in pedogenic carbonate rocks is determined to be related to dispersion from underlying Cu-rich basement and not from windblown contamination. This study has shown that pedogenic rocks from this region can be used for exploration purpose but some consideration needs to be taken as dilution by meteoric Ca and Sr can occur and may be more apparent when Ca/Sr ratios are > 650.

Supplementary data to this article can be found online at https://doi.org/10.1016/j.gexplo.2018.08.007.

Acknowledgements

This work has been supported by the Deep Exploration Technologies Cooperative Research Centre whose activities are funded by the Australian Government's Cooperative Research Centre Program. This is DET CRC Document 2018/2002 and TRaX paper 405. The authors acknowledge Dr. Robert Ayuso and one anonymous reviewer for their review comments. The authors also gratefully acknowledge the assistance of Dr. Nathan Reid from CSIRO, Kensington, Western Australia for assistance with water sampling and analysis, and Randy Wolff and Bradley Versegi for assistance in the field and later the sorting and labelling of rock samples in the laboratory, which would otherwise have been very time-consuming.

References

Balabanova, B., Stafilov, T., Šajn, R., Bačeva, K., 2014. Comparison of response of moss, lichens and attic dust to geology and atmospheric pollution from copper mine. Int. J. Environ. Sci. Technol. 11, 517–528.

Bowen, G.J., Wilkinson, B., 2002. Spatial distribution of $\delta^{18}O$ in meteoric precipitation. Geology 30, 315–331.

Bureau of Meteorology, 2017. Wind Roses for Selected Locations in Australia. Commonwealth of Australia Bureau of Meteorology, Australia.

Bureau of Meteorology, 2018. Climate Statistics for Australian Locations; Summary Statistics Maitland SA. Commonwealth of Australia Bureau of Meteorology, Australia.

Burton, G.R., 2015. Petrological and Geochemical Evidence of Metasomatism and the Nature of the Calcic Progenitor Rock at the Doradilla Prospect, New South Wales. Report GS2015/1395. Geological Survey of New South Wales, Department Of Primary Industries.

Chen, X.Y., Lintern, M.J., Roach, I.C., 2002. Calcrete: Characteristics, Distribution and Use in Mineral Exploration. Cooperative Research Centre for Landscape Environments and Mineral Exploration.

Cheng, M.-C., You, C.-F., Lin, F.-J., Chung, C.-H., Huang, K.-F., 2010. Seasonal variation in long-range transported dust to a subtropical islet offshore northern Taiwan: chemical composition and Sr isotopic evidence in rainwater. Atmos. Environ. 44, 3386–3393.

Coggon, R.M., Teagle, D.A.H., Smith-Duque, C.E., Alt, J.C., Cooper, M.J., 2010. Reconstructing past seawater Mg/Ca and Sr/Ca from mid-ocean ridge flank calcium carbonate veins. Science 327, 1114–1117.

Cohen, D.R., Cohen, E.J., Graham, I.T., Soares, G.G., Hand, S.J., Archer, M., 2017. Geochemical exploration for vertebrate fossils using field portable XRF. J. Geochem. Explor. 181, 1–9.

Conor, C., 1995. Moonta-Wallaroo region – an interpretation of the geology of the Maitland and Wallaroo 1:100 000 sheet areas. In: Primary Industries and Resources South Australia Open File Envelope No 8886.

Conor, C., Raymond, O., Baker, T., Teale, G., Say, P., Lowe, G., 2010. Alteration and mineralisation in the Moonta-Wallaroo copper-gold mining field region, Olympic Domain, South Australia. In: Porter, T.M. (Ed.), Hydrothermal Iron Oxide Copper-gold and Related Deposits: A Global Perspective. Advances in the Understanding of IOCG Deposits. PGC Publishing, Adelaide, pp. 147–170.

Cooper, J.A., Mortimer, G.E., Rosier, C.M., Uppill, R.K., 1985. Gawler Range magmatism—further isotopic age data. Aust. J. Earth Sci. 32, 115–123.

Cowley, W.M., Conor, C., Zang, W., 2003. New and revised Proterozoic stratigraphic units on northern Yorke Peninsula. In Primary Industries and Resources, MESA Journal 29, 46–58.

Crawford, A., 1965. The Geology of Yorke Peninsula: Bulletin No. 39. Geological Society of South Australia, pp. 1–138.

Creaser, R.A., 1996. Petrogenesis of a Mesoproterozoic quartz latite-granitoid suite from the Roxby Downs area South Australia. Precambrian Res. 79, 371–394.

Creaser, R.A., Cooper, J.A., 1993. U–Pb geochronology of Middle Proterozoic felsic magmatism surrounding the Olympic Dam Cu-U-Au-Ag and Moonta Cu-Au-Ag deposits, South Australia. Econ. Geol. 88, 186–197.

Creaser, R.A., Fanning, C.M., 1993. A U–Pb zircon study of the Mesoproterozoic Charleston Granite, Gawler Craton South Australia. Aust. J. Earth Sci. 40, 519–526.

Crosbie, R., Morrow, D., Cresswell, R., Leaney, F., Lamontagne, S., Lefournour, M., 2012. New Insights to the Chemical and Isotopic Composition of Rainfall Across Australia. CSIRO Water for a Healthy Country Flagship, Australia.

Dart, R.C., Barovich, K.M., Chittleborough, D.J., Hill, S.M., 2007. Calcium in regolith carbonates of central and southern Australia: its source and implications for the global carbon cycle. Palaeogeogr. Palaeoclimatol. Palaeoecol. 249, 322–334.

Dart, R.C., Barovich, K.M., Hill, S.M., Chittleborough, D.J., 2012. Sr-isotopes as a tracer of Ca sources and mobility in profiles hosting regolith carbonates from southern Australia. Aust. J. Earth Sci. 59, 373–382.

Department of the Premier and Cabinet, 2017. South Australian Resources Information Gateway (SARIG), Map Theme- Geoscientific, Government of South Australia. https://map.sarig.sa.gov.au, Accessed date: 28 November 2017.

DEWNR, 2013. Non-prescribed Surface Water Resources Assessment - Northern and Yorke Natural Resources Management Region. Government of South Australia, through Department of Environment, Water and Natural Resources, Adelaide.

Dietman, B.J., 2009. Regolith and Associated Geochemical and Biogeochemical Expression of Buried Copper-gold Mineralisation at the Hillside Prospect, Yorke Peninsula. Honors Thesis, Unpublished. University of Adelaide, pp. 208.

Dietrich, F., Diaz, N., Deschamps, P., Ngatcha, B.N., Sebag, D., Verrecchia, E.P., 2017. Origin of calcium in pedogenic carbonate nodules from silicate watersheds in the Far North Region of Cameroon: respective contribution of in situ weathering source and dust input. Chem. Geol. 460, 54–69.

Drexel, J.F., Preiss, W.V., 1995. The geology of South Australia. In: The Phanerozoic. 2 Geological Survey of South Australia, South Australia.

Fabris, A.J., 2010. Investigation Into the Use of Radon and Soil Sampling in Exploration at the Hillside Copper-gold Deposit, South Australia. Primary Industries and Resources SA, Government of South Australia.

Fanning, C.M., Flint, R.B., Parker, A.J., Ludwig, K.R., Blisset, A.H., 1988. Refined Proterozoic evolution of the Gawler Craton, South Australia, through U–Pb zircon geochronology. Precambrian Res. 40/41, 363–386.

Fantle, M.S., Tipper, T., 2014. Calcium isotopes in the global biogeochemical Ca cycle: implications for development of a Ca isotope proxy. Earth Sci. Rev. 129, 148–177.

Ferris, G.M., Schwarz, M.P., Heithersay, P., 2002. The geological framework, distribution and controls of Fe-oxide and related alteration, and Cu-Au mineralisation in the Gawler Craton, South Australia. In: Porter, T.M. (Ed.), Hydrothermal Iron Oxide Copper-gold and Related Deposits: A Global Perspective. 2. PGC Publishing, Adelaide, pp. 1–23.

Ghavami-Riabi, R., Theart, H.F.J., De Jager, C., 2008. Detection of concealed Cu–Zn massive sulfide mineralization below eolian sand and a calcrete cover in the eastern part of the Namaqua Metamorphic Province, South Africa. J. Geochem. Explor. 97, 83–101.

Glen, R., 1991. The geology of Cobar country, Geological Survey of New South Wales. In: New South Wales Department of Minerals and Energy.

Gray, D.J., Noble, R.R.P., Reid, N., 2009. Hydrogeochemical mapping of northeast Yilgarn groundwater: Geological Survey of Western Australia. Theatr. Rec. 2009 (21), 78.

Hand, M., Reid, A., Jagodzinski, L., 2007. Tectonic framework and evolution of the Gawler Craton South Australia. Econ. Geol. 102, 1377–1395.

Hartley, K.L., 2000. Regolith Studies of the Moonta copper mines, Yorke Peninsula, South Australia. B.Sc. Honours thesis. University of Melbourne, pp. 66 (unpublished).

Hesse, P.P., McTainsh, G.H., 2003. Australian dust deposits: modern processes and the Quaternary record. Quat. Sci. Rev. 22, 2007–2035.

Hill, S.M., McQueen, K.G., Foster, K.A., 1999. Regolith carbonate accumulations in Western and Central NSW: characteristics and potential as an exploration sampling medium. In: Taylor, G.M., Pain, C.F. (Eds.), State of the Regolith, Proceedings of Regolith. 98. CRC LEME, Perth, pp. 191–208.

Hoek, J.D., Schaefer, B.F., 1998. Palaeoproterozoic Kimban mobile belt Eyre Peninsula: timing and significance of felsic and mafic magmatism and deformation. Aust. J. Earth Sci. 45, 305–313.

Iwata, K., Schmidt, B.L., Leitch, E.C., Allan, A.D., Watanabe, T., 1995. Ordovidan microfossils from the Ballast Formation (Girilambone Group) of New South Wales. Aust. J. Earth Sci. 42, 371–376.

Keeling, J.L., Hartley, K.L., 2005. Poona and Wheal Hughes Cu deposits, Moonta, South Australia. In: Butt, C.R.M., Robertson, I.D.M., Scott, K.M., Cornelius, M. (Eds.), Regolith Expression of Australian Ore Systems. Cooperative Research Centre for Landscape Environments and Mineral Exploration (CRC LEME) CSIRO Exploration and Mining Bentley Western Australia.

Khadkikar, A.S., Merh, S.S., Malik, J.N., Chamyal, L.S., 1998. Calcretes in semi-arid alluvial systems: formative pathways and sinks. Sediment. Geol. 116, 251–260.

Khadkikar, A.S., Chamyal, L.S., Ramesh, R., 2000. The character and genesis of calcrete in Late Quaternary alluvial deposits, Gujarat, western India, and its bearing on the interpretation of ancient climates. Palaeogeogr. Palaeoclimatol. Palaeoecol. 162, 239–261.

Kyser, T.K., James, N.P., Bone, Y., 1998. Alteration of Cenozoic cool-water carbonates to low-Mg calcite in marine waters, Gambier Embayment, South Australia. J. Sediment. Res. 68, 947–955.

Lintern, M.J., 1989. Study of the Distribution of Gold in Soils at Mt Hope, Western Australia. CSIRO Division of Exploration Geoscience (Restricted Report 24R, 40 pp. (Reissued as Open File Report 65, CRC LEME, Perth, 1999). Perth).

Lintern, M.J., 2015. The association of gold with calcrete. Ore Geol. Rev. 66, 132–199.

Lintern, M.J., Sheard, M., 1999. Geochemistry and Stratigraphy of the Challenger Gold Deposit Volume 1: Text, Regolith Studies Related to the Challenger Gold Deposit, Gawler Craton, South Australia. (CRC LEME open file report 78/PIRSA report book 98/10).

Lintern, M.J., Butt, C.R.M., Scott, K.M., 1997. Gold in vegetation and soil - three case studies from the goldfields of southern Western Australia. J. Geochem. Explor. 58, 1–14.

Lintern, M.J., Sheard, M., Chivas, A.R., 2006. The source of pedogenic carbonate associated with gold-calcrete anomalies in the western Gawler Craton, South Australia. Chem. Geol. 235, 299–324.

Lintern, M.J., Hough, R., Ryan, C., Watling, J., Verrall, M., 2009. Ionic gold in calcrete revealed by LA-ICP-MS, SXRF and XANES. Geochim. Cosmochim. Acta 73, 1666–1683.

Lintern, M.J., Sheard, M., Buller, N., 2011. The gold-in-calcrete anomaly at the ET gold prospect, Gawler Craton, South Australia. Appl. Geochem. 26, 2027–2043.

Lintern, M.J., Hough, R., Ryan, C., 2012. Experimental studies on the gold-in-calcrete anomaly at Edoldeh Tank Gold Prospect, Gawler Craton, South Australia. J. Geochem. Explor. 112, 189–205.

McDowell, M.C., Baynes, A., Medlin, G.C., Prideaux, G.J., 2012. The impact of European colonization on the late-Holocene non-volant mammals of Yorke Peninsula, South Australia. The Holocene 22, 1441–1450.

McQueen, K.G., 2006. Calcrete Geochemistry in the Cobar-Girilambone Region, New South Wales. CRC LEME open file report 200. CRC LEME, Bentley, Western Australia.

McQueen, K.G., Hill, S.M., Foster, K.A., 1999. The nature and distribution of regolith carbonate accumulations in southeastern Australia and their potential as a sampling medium in geochemical exploration. J. Geochem. Explor. 67, 67–82.

Mighall, T.M., Abrahams, P.W., Grattan, J.P., Hayes, D., Timberlake, S., Forsyth, S., 2002. Geochemical evidence for atmospheric pollution derived from prehistoric copper mining at Copa Hill, Cwmystwyth, mid-Wales, UK. Sci. Total Environ. 292, 69–80.

Morales-Ruano, S., Both, R.A., Golding, S.D., 2002. A fluid inclusion and stable isotope study of the Moonta copper–gold deposits, South Australia: evidence for fluid immiscibility in a magmatic hydrothermal system. Chem. Geol. 192, 211–226.

Neagle, N., 2008. A Biological Survey of the Mid North and Yorke Peninsula, South Australia, 2003–2004: Assessment of Biodiversity Assets at Risk.

Pain, C.F., Chan, R., Craig, M., Gibson, D., Kilgour, P., Wilford, J.R., 2007. RTMAP Regolith Database Field Book and Users Guide, second ed. CRC LEME, Bentley, Western Australia CRC LEME open file report 231.

Poustie, T., Abbot, P., 2006. Challenger Gold Mine — looking at a long-term future. MESA Journal 40, 4–7.

Prudencio, M.I., Dias, M.I., Waerenborgh, J.C., Ruiz, F., Trindade, M.J., Abad, M., Marques, R., Gouveia, M.A., 2011. Rare earth and other trace and major elemental

distribution in a pedogenic calcrete profile (Slimene, NE Tunisia). Catena 87, 147–156.
Quade, J., Chivas, A.R., McCulloch, M.T., 1995. Strontium and carbon isotope tracers and the origins of soil carbonate in South Australia and Victoria. Palaeogeogr. Palaeoclimatol. Palaeoecol. 113, 103–117.
Reith, F., Etschmann, B., Dart, R.C., Brewe, D.L., Vogt, S., Schmidt-Mumm, A., Brugger, J., 2011. Distribution and speciation of gold in biogenic and abiogenic calcium carbonates – implications for the formation of gold anomalous calcrete. Geochim. Cosmochim. Acta 75, 1942–1956.
Roberts, S., 2007. Northern and Yorke Natural Resources Management Region Water Monitoring Review, DWLBC Report 2006/15. Department of Water, Land and Biodiversity Conservation, Adelaide.
Salama, W., Gonzalez-Alvarez, I., Anand, R.R., 2016. Significance of weathering and regolith/landscape evolution for mineral exploration in the NE Albany-Fraser Orogen, Western Australia. Ore Geol. Rev. 73, 500–521.
Shimamura, T., Wada, T., Iwashita, M., Takaku, Y., Ohashi, H., 2006. Scavenging properties of major and trace species in rainfall collected in urban and suburban Tokyo. Atmos. Environ. 40, 4220–4227.
Skirrow, R.G., Bastrakov, E.N., Barovich, K., Fraser, G.L., Creaser, R.A., Fanning, C.M., Raymond, O.L., Davidson, G.J., 2007. Timing of iron oxide Cu-Au-(U) hydrothermal activity and Nd isotope constraints on metal sources in the Gawler Craton, South Australia. Econ. Geol. 102, 1441–1470.
van der Hoek, B.G., Hill, S.M., Dart, R.C., 2012. Calcrete and plant inter-relationships for the expression of concealed mineralization at the Tunkillia gold prospect, central Gawler Craton, Australia. Geochem.: Explor., Environ., Anal.: GEEA 12, 361–372.
Van der Hoven, S.J., Quade, J., 2002. Tracing spatial and temporal variations in the sources of calcium in pedogenic carbonates in a semiarid environment. Geoderma 108, 259–276.
Wolff, K., Tiddy, C., Giles, D., Hill, S.M., Gordon, G., 2017. Distinguishing pedogenic carbonates from weathered marine carbonates on the Yorke Peninsula, South Australia: implications for mineral exploration. J. Geochem. Explor. 181, 81–98.
Wolff, K., Hill, S.M., Tiddy, C., Giles, D., Smernik, R., 2018. Biogeochemical expression of buried iron-oxide-copper-gold (IOCG) mineral systems in mallee eucalypts on the Yorke Peninsula, southern Olympic Domain; South Australia. J. Geochem. Explor. 185, 139–152.
Zang, W.-L., Cowley, W.M., Fairclough, M., 2006. Maitland Special South Australia 1:250000 Geological Series Sheet S153-12 - Explanatory Notes. PIRSA Publishing Services, South Australia.

Appendix 5

Chapter 3:

Geochemical results for

carbonate rocks from across the Yorke Peninsula

		Duplicate ID	Transect	Location	Sample_Type	Orig_Grid_ID	Orig_East	Orig_North
Lab analytical method code	Lab analytical method code							
Unit	Unit							
Detection Limit	Detection Limit							
DataSet	SampleID							
Yorke Peninsula	YPC001		1	Cutline Rd	CaCO3 rock	GDA94_53H	754731	6135007
Yorke Peninsula	YPC002		1	Cutline Rd	CaCO3 rock	GDA94_53H	753614	6135043
Yorke Peninsula	YPC003		1	Cutline Rd	CaCO3 rock	GDA94_53H	752175	6135069
Yorke Peninsula	YPC004		1	Cutline Rd	CaCO3 rock	GDA94_53H	751432	6135086
Yorke Peninsula	YPC005		1	Cutline Rd	CaCO3 rock	GDA94_53H	750295	6135111
Yorke Peninsula	YPC006		1	Cutline Rd	CaCO3 rock	GDA94_53H	748851	6135147
Yorke Peninsula	YPC007		1	Cutline Rd	CaCO3 rock	GDA94_53H	747961	6135185
Yorke Peninsula	YPC008		1	Cutline Rd	CaCO3 rock	GDA94_53H	746877	6135193
Yorke Peninsula	YPC009		1	Cutline Rd	CaCO3 rock	GDA94_53H	745700	6135220
Yorke Peninsula	YPC010		1	Cutline Rd	CaCO3 rock	GDA94_53H	742523	6135288
Yorke Peninsula	YPC011		1	Cutline Rd	CaCO3 rock	GDA94_53H	741555	6135312
Yorke Peninsula	YPC012		1	Cutline Rd	CaCO3 rock	GDA94_53H	740596	6135332
Yorke Peninsula	YPC013		1	Cutline Rd	CaCO3 rock	GDA94_53H	739576	6135358
Yorke Peninsula	YPC014		1	Cutline Rd	CaCO3 rock	GDA94_53H	738677	6135381
Yorke Peninsula	YPC015		1	Cutline Rd	CaCO3 rock	GDA94_53H	737318	6135414
Yorke Peninsula	YPC016		1	Cutline Rd	CaCO3 rock	GDA94_53H	735745	6135454
Yorke Peninsula	YPC017		1	Cutline Rd	CaCO3 rock	GDA94_53H	732670	6135524
Yorke Peninsula	YPC018		1	Cutline Rd	CaCO3 rock	GDA94_53H	731215	6135560
Yorke Peninsula	YPC019		1	Cutline Rd	CaCO3 rock	GDA94_53H	730213	6135586
Yorke Peninsula	YPC020		1	Cutline Rd	CaCO3 rock	GDA94_53H	729196	6135606
Yorke Peninsula	YPC021		1	Cutline Rd	CaCO3 rock	GDA94_53H	728096	6135635
Yorke Peninsula	YPC022		1	Cutline Rd	CaCO3 rock	GDA94_53H	726335	6135674
Yorke Peninsula	YPC023		1	Cutline Rd	CaCO3 rock	GDA94_53H	725342	6135692
Yorke Peninsula	YPC024	YPC003	1	Cutline Rd	CaCO3 rock	GDA94_53H	752175	6135069
Yorke Peninsula	YPC025	YPC017	1	Cutline Rd	CaCO3 rock	GDA94_53H	732670	6135524
Yorke Peninsula	YPC026		2	Dump Rd	CaCO3 rock	GDA94_53H	758599	6144882
Yorke Peninsula	YPC027		2	Dump Rd	CaCO3 rock	GDA94_53H	757558	6144910
Yorke Peninsula	YPC028		2	Dump Rd	CaCO3 rock	GDA94_53H	756147	6144951
Yorke Peninsula	YPC029		2	Dump Rd	CaCO3 rock	GDA94_53H	754907	6144985
Yorke Peninsula	YPC030		2	Dump Rd	CaCO3 rock	GDA94_53H	753895	6145013
Yorke Peninsula	YPC031		2	Dump Rd	CaCO3 rock	GDA94_53H	749451	6145353
Yorke Peninsula	YPC032		2	Dump Rd	CaCO3 rock	GDA94_53H	747144	6145267
Yorke Peninsula	YPC033		2	Dump Rd	CaCO3 rock	GDA94_53H	745791	6145364
Yorke Peninsula	YPC034		2	Dump Rd	CaCO3 rock	GDA94_53H	744889	6145753
Yorke Peninsula	YPC035		2	Dump Rd	CaCO3 rock	GDA94_53H	744104	6146305
Yorke Peninsula	YPC036		2	Dump Rd	CaCO3 rock	GDA94_53H	742987	6147023
Yorke Peninsula	YPC037		2	Dump Rd	CaCO3 rock	GDA94_53H	741632	6147463
Yorke Peninsula	YPC038		2	Dump Rd	CaCO3 rock	GDA94_53H	740645	6147577
Yorke Peninsula	YPC039		2	Dump Rd	CaCO3 rock	GDA94_53H	739520	6147598
Yorke Peninsula	YPC040		2	Dump Rd	CaCO3 rock	GDA94_53H	737675	6147648
Yorke Peninsula	YPC041		2	Dump Rd	CaCO3 rock	GDA94_53H	735216	6147774
Yorke Peninsula	YPC042		2	Dump Rd	CaCO3 rock	GDA94_53H	734075	6148074
Yorke Peninsula	YPC043		2	Dump Rd	CaCO3 rock	GDA94_53H	731832	6147976
Yorke Peninsula	YPC044		2	Dump Rd	CaCO3 rock	GDA94_53H	729317	6147985
Yorke Peninsula	YPC045	YPC027	2	Dump Rd	CaCO3 rock	GDA94_53H	757558	6144910
Yorke Peninsula	YPC046	YPC037	2	Dump Rd	CaCO3 rock	GDA94_53H	741632	6147463
Yorke Peninsula	YPC047		3	Barkers Rocks Rd	CaCO3 rock	GDA94_53H	727914	6155609
Yorke Peninsula	YPC048		3	Barkers Rocks Rd	CaCO3 rock	GDA94_53H	728998	6155582
Yorke Peninsula	YPC049		3	Barkers Rocks Rd	CaCO3 rock	GDA94_53H	730190	6155560
Yorke Peninsula	YPC050		3	Barkers Rocks Rd	CaCO3 rock	GDA94_53H	731376	6155532
Yorke Peninsula	YPC051		3	Barkers Rocks Rd	CaCO3 rock	GDA94_53H	732530	6155507
Yorke Peninsula	YPC052		3	Barkers Rocks Rd	CaCO3 rock	GDA94_53H	733617	6155477
Yorke Peninsula	YPC053		3	Spicers Rd	CaCO3 rock	GDA94_53H	734800	6155449
Yorke Peninsula	YPC054		3	Spicers Rd	CaCO3 rock	GDA94_53H	736103	6155413
Yorke Peninsula	YPC055		3	Spicers Rd	CaCO3 rock	GDA94_53H	737421	6155381
Yorke Peninsula	YPC056		3	Spicers Rd	CaCO3 rock	GDA94_53H	738448	6155269
Yorke Peninsula	YPC057		3	Spicers Rd	CaCO3 rock	GDA94_53H	739661	6155104
Yorke Peninsula	YPC058		3	Spicers Rd	CaCO3 rock	GDA94_53H	740941	6154927
Yorke Peninsula	YPC059		3	Spicers Rd	CaCO3 rock	GDA94_53H	741972	6154781
Yorke Peninsula	YPC060		3	Spicers Rd	CaCO3 rock	GDA94_53H	742971	6154641
Yorke Peninsula	YPC061		3	Spicers Rd	CaCO3 rock	GDA94_53H	744985	6154552
Yorke Peninsula	YPC062		3	Spicers Rd	CaCO3 rock	GDA94_53H	747558	6154488
Yorke Peninsula	YPC063		3	Goldsworthy Rd	CaCO3 rock	GDA94_53H	750750	6154403
Yorke Peninsula	YPC064		3	Goldsworthy Rd	CaCO3 rock	GDA94_53H	751864	6154376
Yorke Peninsula	YPC065		3	Goldsworthy Rd	CaCO3 rock	GDA94_53H	752751	6154351
Yorke Peninsula	YPC066		3	Goldsworthy Rd	CaCO3 rock	GDA94_53H	757269	6154234
Yorke Peninsula	YPC067		3	Goldsworthy Rd	CaCO3 rock	GDA94_53H	758274	6154206
Yorke Peninsula	YPC068		3	Goldsworthy Rd	CaCO3 rock	GDA94_53H	759433	6154177
Yorke Peninsula	YPC069		3	Goldsworthy Rd	CaCO3 rock	GDA94_53H	760576	6154144

	RL	Orig_Survey_Method	Orig_Surve	Date	Sampled_By	Sample_Depth	Weight_kg	SiO2_pct	Al2O3_pct
Lab analytical method code								4x	4x
Unit								wt%	wt%
Detection Limit								0.1	0.01
SampleID									
YPC001	10	Garmin GPS Map60C	KWolff	2/03/2012	Hill/Stoate	ground level	2	15.4	1.97
YPC002	25	Garmin GPS Map60C	KWolff	2/03/2012	Hill/Stoate	ground level	2	9.0	1.32
YPC003	39	Garmin GPS Map60C	KWolff	2/03/2012	Hill/Stoate	ground level	2	14.5	1.89
YPC004	44	Garmin GPS Map60C	KWolff	2/03/2012	Hill/Stoate	ground level	2	6.5	1.24
YPC005	44	Garmin GPS Map60C	KWolff	2/03/2012	Hill/Stoate	ground level	2	6.0	1.08
YPC006	54	Garmin GPS Map60C	KWolff	2/03/2012	Hill/Stoate	ground level	2	14.5	1.56
YPC007	61	Garmin GPS Map60C	KWolff	2/03/2012	Hill/Stoate	ground level	2	13.4	2.32
YPC008	67	Garmin GPS Map60C	KWolff	2/03/2012	Hill/Stoate	ground level	2	9.6	1.50
YPC009	63	Garmin GPS Map60C	KWolff	2/03/2012	Hill/Stoate	ground level	2	10.0	2.71
YPC010	60	Garmin GPS Map60C	KWolff	2/03/2012	Hill/Stoate	ground level	2	11.2	1.33
YPC011	58	Garmin GPS Map60C	KWolff	2/03/2012	Hill/Stoate	ground level	2	13.3	2.60
YPC012	56	Garmin GPS Map60C	KWolff	2/03/2012	Hill/Stoate	ground level	2	13.3	1.58
YPC013	56	Garmin GPS Map60C	KWolff	2/03/2012	Hill/Stoate	ground level	2	12.4	2.03
YPC014	58	Garmin GPS Map60C	KWolff	2/03/2012	Hill/Stoate	ground level	2	16.6	1.71
YPC015	53	Garmin GPS Map60C	KWolff	2/03/2012	Hill/Stoate	ground level	2	16.3	2.63
YPC016	55	Garmin GPS Map60C	KWolff	2/03/2012	Hill/Stoate	ground level	2	10.6	1.61
YPC017	36	Garmin GPS Map60C	KWolff	2/03/2012	Hill/Stoate	ground level	2	7.7	1.36
YPC018	28	Garmin GPS Map60C	KWolff	2/03/2012	Hill/Stoate	ground level	2	9.6	1.78
YPC019	25	Garmin GPS Map60C	KWolff	2/03/2012	Hill/Stoate	ground level	2	16.9	2.25
YPC020	22	Garmin GPS Map60C	KWolff	2/03/2012	Hill/Stoate	ground level	2	6.6	1.11
YPC021	15	Garmin GPS Map60C	KWolff	2/03/2012	Hill/Stoate	ground level	2	7.7	1.68
YPC022	7	Garmin GPS Map60C	KWolff	2/03/2012	Hill/Stoate	ground level	2	5.0	1.38
YPC023	3	Garmin GPS Map60C	KWolff	2/03/2012	Hill/Stoate	ground level	2	13.8	1.76
YPC024	39	Garmin GPS Map60C	KWolff	2/03/2012	Hill/Stoate	ground level	2	9.3	1.56
YPC025	36	Garmin GPS Map60C	KWolff	2/03/2012	Hill/Stoate	ground level	2	7.9	1.27
YPC026	20	Garmin GPS Map62S	KWolff	17/03/2012	RWolff	ground level	2	5.7	0.99
YPC027	30	Garmin GPS Map62S	KWolff	17/03/2012	RWolff	ground level	2	6.9	0.89
YPC028	37	Garmin GPS Map62S	KWolff	17/03/2012	RWolff	ground level	2	7.5	0.99
YPC029	36	Garmin GPS Map62S	KWolff	17/03/2012	RWolff	ground level	2	10.6	2.01
YPC030	44	Garmin GPS Map62S	KWolff	17/03/2012	RWolff	ground level	2	18.1	3.06
YPC031	61	Garmin GPS Map62S	KWolff	17/03/2012	RWolff	ground level	2	12.2	1.48
YPC032	97	Garmin GPS Map62S	KWolff	17/03/2012	RWolff	ground level	2	10.0	1.43
YPC033	100	Garmin GPS Map62S	KWolff	17/03/2012	RWolff	ground level	2	7.0	1.16
YPC034	101	Garmin GPS Map62S	KWolff	17/03/2012	RWolff	ground level	2	7.0	1.33
YPC035	101	Garmin GPS Map62S	KWolff	17/03/2012	RWolff	ground level	2	13.6	1.59
YPC036	102	Garmin GPS Map62S	KWolff	17/03/2012	RWolff	ground level	2	21.0	3.11
YPC037	77	Garmin GPS Map62S	KWolff	17/03/2012	RWolff	ground level	2	9.0	1.19
YPC038	73	Garmin GPS Map62S	KWolff	17/03/2012	RWolff	ground level	2	11.2	2.68
YPC039	66	Garmin GPS Map62S	KWolff	17/03/2012	RWolff	ground level	2	8.4	1.35
YPC040	64	Garmin GPS Map62S	KWolff	17/03/2012	RWolff	ground level	2	14.2	1.43
YPC041	71	Garmin GPS Map62S	KWolff	17/03/2012	RWolff	ground level	2	16.9	2.37
YPC042	63	Garmin GPS Map62S	KWolff	17/03/2012	RWolff	ground level	2	14.9	2.21
YPC043	40	Garmin GPS Map62S	KWolff	17/03/2012	RWolff	ground level	2	20.8	2.42
YPC044	22	Garmin GPS Map62S	KWolff	17/03/2012	RWolff	ground level	2	6.5	1.45
YPC045	30	Garmin GPS Map62S	KWolff	17/03/2012	RWolff	ground level	2	4.7	0.79
YPC046	77	Garmin GPS Map62S	KWolff	17/03/2012	RWolff	ground level	2	13.8	1.30
YPC047	2	Garmin GPS Map62S	KWolff	18/03/2012	RWolff	ground level	2	11.8	0.70
YPC048	9	Garmin GPS Map62S	KWolff	18/03/2012	RWolff	ground level	2	15.3	1.99
YPC049	14	Garmin GPS Map62S	KWolff	18/03/2012	RWolff	ground level	2	13.9	1.92
YPC050	18	Garmin GPS Map62S	KWolff	18/03/2012	RWolff	ground level	2	10.7	1.15
YPC051	41	Garmin GPS Map62S	KWolff	18/03/2012	RWolff	ground level	2	18.6	2.71
YPC052	51	Garmin GPS Map62S	KWolff	18/03/2012	RWolff	ground level	2	12.6	1.88
YPC053	60	Garmin GPS Map62S	KWolff	18/03/2012	RWolff	ground level	2	13.0	1.90
YPC054	71	Garmin GPS Map62S	KWolff	18/03/2012	RWolff	ground level	2	10.3	1.68
YPC055	73	Garmin GPS Map62S	KWolff	18/03/2012	RWolff	ground level	2	8.0	1.86
YPC056	58	Garmin GPS Map62S	KWolff	18/03/2012	RWolff	ground level	2	4.5	0.84
YPC057	62	Garmin GPS Map62S	KWolff	18/03/2012	RWolff	ground level	2	1.9	0.50
YPC058	70	Garmin GPS Map62S	KWolff	18/03/2012	RWolff	ground level	2	4.4	0.69
YPC059	79	Garmin GPS Map62S	KWolff	18/03/2012	RWolff	ground level	2	6.1	1.29
YPC060	96	Garmin GPS Map62S	KWolff	18/03/2012	RWolff	ground level	2	8.5	1.78
YPC061	102	Garmin GPS Map62S	KWolff	18/03/2012	RWolff	ground level	2	7.3	1.38
YPC062	99	Garmin GPS Map62S	KWolff	18/03/2012	RWolff	ground level	2	7.5	1.17
YPC063	105	Garmin GPS Map62S	KWolff	18/03/2012	RWolff	ground level	2	12.0	1.70
YPC064	80	Garmin GPS Map62S	KWolff	18/03/2012	RWolff	ground level	2	10.5	1.57
YPC065	70	Garmin GPS Map62S	KWolff	18/03/2012	RWolff	ground level	2	11.5	1.85
YPC066	59	Garmin GPS Map62S	KWolff	18/03/2012	RWolff	ground level	2	9.4	1.35
YPC067	55	Garmin GPS Map62S	KWolff	18/03/2012	RWolff	ground level	2	8.3	1.20
YPC068	55	Garmin GPS Map62S	KWolff	18/03/2012	RWolff	ground level	2	6.9	0.86
YPC069	42	Garmin GPS Map62S	KWolff	18/03/2012	RWolff	ground level	2	8.0	0.92

	Fe2O3_pct	CaO_pct	Ca/Sr	MgO_pct	Na2O_pct	K2O_pct	MnO_pct	TiO2_pct	P2O5_pct	Cr2O3_pct
Lab analytical method code	4x	4x	user calculated	4x	4x	4x	4x	4x	4x	4x
Unit	wt%	wt%	ratio	wt%	wt%	wt%	wt%	wt%	wt%	wt%
Detection Limit	0.01	0.01		0.01	0.01	0.01	0.01	0.01	0.01	0.001
SampleID										
YPC001	0.83	41.85	525	1.82	0.11	0.32	0.02	0.10	0.05	0.002
YPC002	0.61	47.70	664	1.17	0.07	0.09	0.02	0.06	0.03	0.002
YPC003	0.78	44.20	679	1.20	0.09	0.25	0.02	0.09	0.03	0.005
YPC004	0.52	49.66	781	1.22	0.06	0.09	0.01	0.05	0.01	0.001
YPC005	0.46	48.91	788	1.92	0.04	0.07	0.01	0.05	0.01	0.003
YPC006	0.66	42.32	364	2.63	0.10	0.22	0.01	0.07	0.01	0.005
YPC007	1.02	43.51	502	1.52	0.14	0.27	0.02	0.10	0.02	0.003
YPC008	0.64	46.21	430	1.75	0.08	0.12	0.01	0.06	0.01	0.003
YPC009	1.04	45.28	664	1.07	0.06	0.15	0.01	0.09	0.01	0.003
YPC010	0.52	46.48	690	0.92	0.06	0.11	0.01	0.06	0.02	0.001
YPC011	1.12	43.66	411	1.37	0.14	0.26	0.01	0.10	0.02	0.003
YPC012	0.65	44.33	365	1.33	0.11	0.25	0.01	0.07	0.02	0.004
YPC013	0.80	45.06	424	1.08	0.09	0.22	0.01	0.07	0.01	0.006
YPC014	0.72	41.63	345	1.73	0.05	0.09	0.01	0.09	0.01	0.004
YPC015	1.09	39.97	374	2.51	0.10	0.21	0.01	0.11	0.01	0.004
YPC016	0.64	45.28	413	1.61	0.11	0.23	0.01	0.08	0.02	0.001
YPC017	0.53	48.63	744	1.27	0.08	0.14	0.01	0.06	0.01	0.002
YPC018	0.72	46.63	538	1.31	0.09	0.17	0.01	0.08	0.02	0.003
YPC019	0.89	42.08	464	1.28	0.10	0.32	0.01	0.09	0.01	0.009
YPC020	0.47	49.58	636	1.08	0.05	0.09	0.01	0.04	0.01	0.002
YPC021	0.74	47.73	651	1.29	0.08	0.13	0.01	0.06	0.01	0.009
YPC022	0.60	50.14	767	1.11	0.07	0.12	0.01	0.05	0.01	0.002
YPC023	0.64	44.33	435	1.09	0.13	0.28	0.02	0.08	0.04	0.002
YPC024	0.67	47.26	717	1.51	0.08	0.17	0.02	0.09	0.02	0.001
YPC025	0.51	48.09	620	1.28	0.07	0.08	0.01	0.05	0.02	0.001
YPC026	0.46	49.96	754	1.31	0.04	0.04	0.01	0.04	0.02	0.002
YPC027	0.41	49.42	494	1.19	0.05	0.04	0.01	0.03	0.01	0.001
YPC028	0.43	49.05	614	1.29	0.05	0.08	0.01	0.04	0.01	0.002
YPC029	0.82	45.73	631	1.15	0.09	0.08	0.01	0.09	0.01	0.005
YPC030	1.21	40.13	552	1.13	0.09	0.25	0.01	0.13	0.02	0.005
YPC031	0.66	43.40	421	2.81	0.07	0.09	0.01	0.06	0.03	0.007
YPC032	0.64	46.64	532	1.19	0.07	0.07	0.01	0.06	0.06	0.003
YPC033	0.65	49.47	1324	0.67	0.02	0.03	0.01	0.05	0.01	0.001
YPC034	0.54	49.12	686	0.96	0.06	0.13	0.01	0.06	0.02	0.001
YPC035	0.71	44.42	456	1.27	0.07	0.14	0.01	0.07	0.01	0.003
YPC036	1.28	38.13	455	1.19	0.14	0.19	0.01	0.13	0.01	0.003
YPC037	0.51	46.96	467	1.81	0.08	0.11	0.01	0.07	0.01	0.004
YPC038	1.11	43.79	501	1.77	0.10	0.23	0.02	0.12	0.02	0.004
YPC039	0.59	47.65	432	1.65	0.05	0.09	0.01	0.07	0.01	0.001
YPC040	0.58	44.35	514	1.05	0.04	0.09	0.01	0.08	0.01	0.003
YPC041	0.89	40.48	302	2.16	0.18	0.24	0.01	0.13	0.01	0.003
YPC042	0.82	42.56	384	1.58	0.15	0.36	0.02	0.10	0.02	0.003
YPC043	0.91	36.78	238	3.60	0.12	0.47	0.02	0.11	0.02	0.001
YPC044	0.60	49.18	459	1.33	0.07	0.13	0.02	0.05	0.02	0.004
YPC045	0.35	51.17	749	0.98	0.02	0.03	0.01	0.04	0.01	0.002
YPC046	0.56	44.25	544	1.81	0.07	0.17	0.01	0.06	0.01	0.001
YPC047	0.26	46.13	306	1.14	0.06	0.11	0.01	0.02	0.03	0.001
YPC048	0.78	43.12	428	0.92	0.14	0.36	0.03	0.10	0.03	0.003
YPC049	0.77	44.19	481	1.22	0.11	0.29	0.03	0.10	0.03	0.003
YPC050	0.45	47.13	446	0.89	0.05	0.13	0.01	0.05	0.03	0.003
YPC051	1.03	40.14	377	1.28	0.16	0.41	0.03	0.13	0.03	0.001
YPC052	0.75	44.47	390	1.18	0.08	0.17	0.02	0.11	0.03	0.002
YPC053	0.72	43.34	311	1.31	0.08	0.17	0.01	0.10	0.03	0.004
YPC054	0.68	45.91	390	1.79	0.11	0.22	0.01	0.08	0.02	0.003
YPC055	0.74	46.92	412	1.66	0.09	0.14	0.01	0.10	0.02	0.004
YPC056	0.34	50.52	501	1.69	0.01	0.02	0.01	0.04	0.01	0.002
YPC057	0.21	53.02	863	0.87	0.01	0.01	0.01	0.03	0.01	0.001
YPC058	0.29	51.39	687	1.07	0.03	0.05	0.01	0.04	0.01	0.002
YPC059	0.54	49.69	772	1.04	0.04	0.09	0.01	0.06	0.02	0.002
YPC060	0.74	47.40	698	1.22	0.06	0.12	0.01	0.07	0.01	0.003
YPC061	0.58	48.52	678	1.13	0.04	0.09	0.01	0.06	0.01	0.003
YPC062	0.49	49.36	939	0.74	0.05	0.08	0.01	0.04	0.02	0.002
YPC063	0.70	42.59	418	3.51	0.10	0.29	0.01	0.10	0.03	0.003
YPC064	0.65	45.77	434	1.78	0.07	0.16	0.01	0.08	0.01	0.004
YPC065	0.78	44.40	368	1.90	0.08	0.23	0.02	0.09	0.02	0.002
YPC066	0.56	44.37	334	3.74	0.06	0.10	0.01	0.06	0.01	0.003
YPC067	0.53	45.86	343	3.11	0.06	0.13	0.01	0.04	0.01	0.003
YPC068	0.38	49.40	629	1.11	0.04	0.07	0.01	0.03	0.01	0.001
YPC069	0.41	48.89	623	1.15	0.06	0.09	0.01	0.05	0.02	0.001

	Ba_pct	LOI_pct	SUM_pct	TOT/C_pct	TOT/S_pct	Ba_ppm	Be_ppm	Co_ppm	Cs_ppm	Ga_ppm	Hf_ppm
Lab analytical method code	4x	4x	4x	2A Leco	2A Leco	4B	4B	4B	4B	4B	4B
Unit	wt%	%	%	%	%	PPM	PPM	PPM	PPM	PPM	PPM
Detection Limit	0.01	-5.11	0.01	0.02	0.02	1	1	0.2	0.1	0.5	0.1
SampleID											
YPC001	0.01	37.66	100.11	10.87	0.05	115.00	0.50	5.50	0.60	2.40	1.40
YPC002	0.01	40.57	100.66	12.12	0.08	107.00	0.50	5.00	0.50	1.50	1.00
YPC003	0.01	37.78	100.86	10.60	0.06	114.00	0.50	5.00	0.60	2.20	1.00
YPC004	0.01	41.40	100.74	11.90	0.05	105.00	0.50	4.80	0.30	1.20	0.50
YPC005	0.01	41.97	100.56	12.59	0.06	85.00	0.50	5.30	0.30	1.00	0.50
YPC006	0.01	38.27	100.36	11.12	0.05	132.00	0.50	4.70	0.40	1.50	0.90
YPC007	0.02	37.87	100.22	10.63	0.06	189.00	0.50	4.90	0.80	2.80	1.10
YPC008	0.02	40.46	100.48	11.91	0.07	150.00	0.50	7.50	0.50	1.40	0.80
YPC009	0.01	39.87	100.28	11.66	0.05	126.00	0.50	6.00	0.80	3.00	1.00
YPC010	0.01	39.82	100.51	11.78	0.05	135.00	0.50	7.10	0.40	1.10	0.60
YPC011	0.02	38.42	101.02	11.23	0.07	147.00	0.50	5.60	1.00	2.90	1.00
YPC012	0.01	38.55	100.17	11.32	0.06	119.00	1.00	4.30	0.60	1.60	0.80
YPC013	0.01	38.71	100.52	11.33	0.06	121.00	0.50	5.30	0.70	2.10	0.90
YPC014	0.01	37.36	100.05	10.57	0.07	127.00	0.50	5.60	0.40	1.80	0.90
YPC015	0.01	36.91	99.88	10.40	0.04	148.00	0.50	6.00	0.80	3.00	1.00
YPC016	0.01	39.82	100.02	11.60	0.07	137.00	0.50	6.10	0.50	1.30	0.90
YPC017	0.01	40.88	100.65	12.02	0.07	124.00	0.50	5.90	0.40	1.30	0.50
YPC018	0.01	39.96	100.37	11.68	0.06	134.00	0.50	6.60	0.60	1.80	0.70
YPC019	0.01	36.48	100.38	10.40	0.06	144.00	0.50	5.80	0.80	2.60	0.60
YPC020	0.02	41.69	100.76	12.34	0.09	124.00	0.50	4.80	0.30	1.00	0.40
YPC021	0.01	40.83	100.24	11.63	0.07	118.00	0.50	4.60	0.50	1.80	0.50
YPC022	0.01	42.22	100.76	12.30	0.09	128.00	0.50	4.80	0.40	1.10	0.70
YPC023	0.01	38.14	100.29	11.04	0.06	106.00	0.50	5.40	0.50	1.60	1.00
YPC024	0.01	40.22	100.95	11.61	0.06	99.00	0.50	4.90	0.50	1.50	1.00
YPC025	0.01	41.05	100.30	11.97	0.08	125.00	0.50	4.40	0.30	1.00	0.60
YPC026	0.01	42.21	100.79	12.47	0.06	108.00	0.50	4.90	0.30	0.60	0.60
YPC027	0.02	41.70	100.69	12.60	0.08	127.00	0.50	5.10	0.20	0.60	0.70
YPC028	0.01	41.22	100.70	12.12	0.05	103.00	0.50	5.20	0.20	0.70	0.50
YPC029	0.02	39.80	100.45	11.08	0.05	162.00	0.50	7.70	0.70	2.00	0.50
YPC030	0.01	35.93	100.08	10.04	0.05	129.00	0.50	9.00	0.90	3.10	1.00
YPC031	0.01	39.76	100.58	11.74	0.05	133.00	0.50	5.50	0.40	1.30	0.60
YPC032	0.01	40.33	100.47	11.96	0.05	123.00	0.50	5.10	0.40	1.30	0.50
YPC033	0.01	41.53	100.56	12.43	0.05	114.00	0.50	6.80	0.40	1.00	0.30
YPC034	0.01	41.28	100.59	12.04	0.05	108.00	0.50	5.30	0.40	1.10	0.60
YPC035	0.01	38.58	100.45	11.21	0.04	124.00	0.50	5.00	0.40	1.40	0.60
YPC036	0.01	34.47	99.73	9.60	0.07	143.00	0.50	7.70	0.80	3.30	1.10
YPC037	0.01	40.73	100.44	12.14	0.04	142.00	0.50	3.70	0.40	1.30	0.40
YPC038	0.02	38.95	100.00	11.68	0.06	183.00	0.50	5.30	0.80	3.50	0.70
YPC039	0.01	41.04	100.97	12.52	0.07	145.00	0.50	6.20	0.30	1.40	0.60
YPC040	0.01	38.33	100.18	11.44	0.07	124.00	0.50	4.60	0.30	1.40	1.00
YPC041	0.02	36.60	99.96	10.51	0.08	143.00	0.50	4.90	0.70	2.20	1.10
YPC042	0.01	37.42	100.16	11.19	0.08	129.00	0.50	6.60	0.80	2.10	1.20
YPC043	0.01	34.67	99.93	10.22	0.04	98.00	0.50	5.30	0.60	2.50	1.50
YPC044	0.01	41.14	100.55	12.49	0.07	74.00	0.50	4.00	0.40	1.30	0.70
YPC045	0.01	42.52	100.59	13.03	0.08	118.00	0.50	3.80	0.20	0.25	0.70
YPC046	0.01	38.57	100.63	11.83	0.05	126.00	0.50	4.90	0.50	1.00	0.60
YPC047	0.01	39.95	100.25	12.67	0.10	52.00	0.50	2.90	0.10	0.25	0.70
YPC048	0.01	37.25	99.99	11.16	0.07	87.00	0.50	4.50	0.50	1.90	1.40
YPC049	0.01	37.98	100.52	11.67	0.08	95.00	0.50	5.10	0.50	1.90	1.30
YPC050	0.01	39.76	100.31	12.21	0.08	87.00	0.50	2.60	0.30	1.00	1.80
YPC051	0.01	35.37	99.89	10.55	0.08	107.00	0.50	6.10	0.80	2.70	1.30
YPC052	0.01	38.65	99.92	11.52	0.09	86.00	0.50	5.30	0.50	1.70	1.20
YPC053	0.01	38.91	99.57	11.50	0.11	76.00	0.50	4.90	0.50	1.80	1.10
YPC054	0.01	40.13	100.88	12.00	0.09	99.00	0.50	5.80	0.50	1.40	1.40
YPC055	0.01	40.78	100.28	12.26	0.07	90.00	0.50	3.60	0.60	1.70	0.70
YPC056	0.01	42.84	100.78	13.03	0.05	64.00	0.50	3.40	0.20	0.25	0.30
YPC057	0.01	43.96	100.49	13.76	0.11	122.00	0.50	4.70	0.05	0.25	0.20
YPC058	0.01	42.80	100.79	13.45	0.08	88.00	0.50	3.20	0.20	0.25	0.50
YPC059	0.01	41.74	100.65	12.96	0.07	104.00	0.50	5.30	0.40	1.00	0.60
YPC060	0.01	40.45	100.38	12.15	0.07	130.00	0.50	6.70	0.70	1.80	0.70
YPC061	0.01	41.30	100.42	12.60	0.06	95.00	0.50	4.80	0.30	1.30	0.50
YPC062	0.01	41.14	100.65	12.55	0.06	94.00	0.50	4.40	0.30	1.00	0.40
YPC063	0.01	39.23	100.26	11.80	0.05	124.00	0.50	4.50	0.60	1.30	1.40
YPC064	0.01	39.84	100.43	11.91	0.07	132.00	0.50	6.40	0.50	1.10	0.90
YPC065	0.02	39.33	100.20	11.85	0.08	172.00	0.50	6.10	0.60	1.80	0.80
YPC066	0.01	40.84	100.49	12.49	0.07	136.00	0.50	4.60	0.40	0.90	0.80
YPC067	0.01	41.36	100.57	12.58	0.06	112.00	0.50	4.60	0.40	0.80	0.80
YPC068	0.01	41.62	100.49	12.90	0.10	123.00	0.50	6.60	0.20	0.25	0.90
YPC069	0.01	41.16	100.72	12.53	0.08	112.00	0.50	4.70	0.30	0.25	0.60

	Nb_ppm	Rb_ppm	Sn_ppm	Sr_ppm	Ta_ppm	Th_ppm	U_ppm	V_ppm	W_ppm	Zr_ppm	Y_ppm	La_ppm	Ce_ppm
Lab analytical method code	4B	4B	4B	4B	4B	4B	4B	4B	4B	4B	4B	4B	4B
Unit	PPM	PPM	PPM	PPM	PPM	PPM	PPM	PPM	PPM	PPM	PPM	PPM	PPM
Detection Limit	0.1	0.1	1	0.5	0.1	0.2	0.1	8	0.5	0.1	0.1	0.1	0.1
SampleID													
YPC001	1.30	13.30	0.50	570.00	0.05	2.20	0.40	11.00	0.90	49.40	7.40	6.80	12.40
YPC002	1.10	9.00	0.50	513.70	0.05	1.30	0.20	11.00	0.25	35.80	7.30	6.10	9.50
YPC003	0.90	13.90	0.50	465.30	0.05	1.90	0.40	10.00	0.25	42.90	6.70	5.80	10.50
YPC004	0.70	7.50	0.50	454.70	0.05	1.20	0.20	4.00	0.25	19.40	3.70	3.60	6.20
YPC005	0.30	6.80	0.50	443.70	0.05	1.10	0.20	4.00	0.25	22.60	4.90	4.10	6.60
YPC006	0.70	11.60	0.50	830.70	0.05	1.40	0.20	9.00	0.25	34.60	5.60	4.50	9.20
YPC007	1.20	17.40	0.50	619.40	0.05	2.40	0.30	17.00	0.25	34.10	7.00	6.70	11.80
YPC008	0.40	9.90	0.50	768.70	0.05	2.40	0.05	9.00	0.25	26.80	13.90	9.70	10.70
YPC009	1.20	16.60	0.50	487.70	0.05	2.80	0.20	22.00	0.25	27.00	6.20	6.20	9.00
YPC010	0.50	9.60	0.50	481.60	0.05	1.80	0.05	4.00	0.25	22.10	6.10	5.90	8.20
YPC011	1.00	18.80	0.50	759.30	0.05	4.00	0.40	16.00	0.25	32.10	6.50	6.20	13.60
YPC012	0.70	14.00	0.50	867.90	0.05	2.20	0.30	15.00	0.25	39.80	6.20	5.10	10.40
YPC013	0.70	15.20	0.50	758.80	0.10	2.50	0.40	4.00	0.25	34.50	10.20	9.40	14.60
YPC014	1.10	13.10	0.50	861.90	0.05	2.40	0.20	11.00	0.25	49.80	7.50	7.90	11.60
YPC015	1.00	17.30	0.50	763.10	0.05	2.60	0.30	14.00	0.25	39.90	14.80	12.40	14.20
YPC016	0.70	13.10	0.50	783.60	0.05	2.60	0.20	11.00	0.25	29.30	9.20	7.00	13.10
YPC017	1.60	9.50	0.50	466.90	0.10	1.70	0.30	4.00	0.25	20.80	12.30	7.60	9.20
YPC018	0.80	12.30	0.50	619.90	0.10	2.10	0.30	12.00	0.25	27.70	8.80	9.30	12.60
YPC019	1.10	18.30	0.50	648.40	0.05	3.00	0.40	10.00	0.25	28.40	9.20	7.90	13.80
YPC020	0.30	7.90	0.50	557.30	0.05	1.20	0.20	4.00	0.25	20.90	8.10	5.70	8.50
YPC021	0.70	11.80	0.50	524.10	0.05	1.60	0.30	13.00	0.25	22.90	6.20	5.60	9.60
YPC022	0.50	9.40	0.50	467.10	0.05	0.90	0.40	8.00	0.25	23.60	5.60	4.80	7.70
YPC023	1.00	15.10	0.50	727.80	0.10	1.90	0.30	8.00	0.25	32.80	10.80	8.80	12.00
YPC024	0.80	9.80	0.50	471.00	0.10	1.40	0.30	8.00	0.25	35.00	7.60	6.10	9.90
YPC025	0.30	9.10	0.50	554.20	0.05	1.10	0.30	4.00	0.25	26.70	6.00	4.80	7.90
YPC026	0.40	6.00	0.50	473.50	0.05	1.10	0.20	4.00	0.25	27.40	6.20	4.40	7.80
YPC027	0.30	5.80	0.50	714.40	0.05	1.00	0.30	4.00	0.25	25.20	7.20	5.50	7.90
YPC028	0.40	6.40	0.50	570.80	0.05	1.10	0.20	4.00	0.25	21.80	4.50	3.70	6.50
YPC029	0.70	12.20	0.50	518.20	0.05	2.60	0.10	15.00	0.25	26.10	8.00	6.30	12.90
YPC030	1.40	18.70	0.50	520.00	0.05	3.50	0.20	17.00	0.25	37.20	11.00	10.30	15.30
YPC031	0.70	10.10	0.50	736.70	0.05	1.80	0.20	4.00	0.25	26.10	6.50	5.20	7.90
YPC032	2.30	8.80	0.50	626.80	0.05	2.10	0.10	4.00	0.25	22.30	6.50	5.70	8.30
YPC033	0.20	5.60	0.50	267.00	0.05	1.20	0.05	4.00	0.25	15.40	7.80	4.90	5.30
YPC034	0.60	8.10	0.50	511.60	0.05	1.20	0.05	4.00	0.25	22.60	8.00	6.10	10.40
YPC035	0.70	9.80	0.50	696.00	0.05	1.80	0.10	4.00	0.25	35.10	8.00	6.70	10.00
YPC036	1.30	19.40	0.50	599.50	0.10	4.50	0.20	10.00	0.25	41.30	11.60	10.30	19.10
YPC037	0.50	8.60	0.50	718.20	0.05	1.70	0.50	11.00	0.25	25.20	6.30	5.00	7.50
YPC038	1.30	18.70	0.50	624.20	0.10	2.70	0.40	20.00	0.25	33.90	5.70	5.70	12.20
YPC039	0.40	8.10	0.50	788.80	0.05	2.80	0.10	9.00	0.25	23.10	14.40	12.70	21.00
YPC040	0.60	9.40	0.50	616.70	0.05	1.40	0.10	10.00	0.25	36.10	5.70	5.00	7.30
YPC041	1.30	17.10	0.50	957.70	0.10	2.20	0.30	10.00	0.25	49.10	6.50	6.00	12.20
YPC042	1.20	17.00	0.50	791.60	0.20	3.30	0.30	13.00	0.25	42.80	9.10	7.20	14.30
YPC043	1.70	19.90	0.50	1105.20	0.10	2.20	0.90	17.00	0.25	52.30	6.70	6.20	12.70
YPC044	0.90	10.20	0.50	766.20	0.05	1.30	0.40	13.00	0.25	22.00	5.50	3.80	7.70
YPC045	0.30	5.00	0.50	488.40	0.05	0.80	0.30	4.00	0.25	26.10	4.40	3.00	5.70
YPC046	0.60	9.90	0.50	580.90	0.05	1.90	0.20	4.00	0.25	26.90	6.40	5.20	8.10
YPC047	0.30	7.20	0.50	1078.40	0.05	0.60	0.30	4.00	0.25	20.60	2.80	2.40	4.90
YPC048	1.20	15.40	0.50	720.70	0.10	2.10	0.20	14.00	0.25	59.00	8.10	7.00	13.40
YPC049	1.60	13.70	0.50	656.80	0.20	2.00	0.30	4.00	0.25	54.80	8.50	7.00	12.60
YPC050	0.30	9.80	0.50	754.50	0.05	1.10	0.30	9.00	0.25	76.60	4.40	3.60	7.90
YPC051	1.50	21.50	0.50	760.20	0.10	2.70	0.20	9.00	0.25	53.90	8.20	7.60	15.60
YPC052	1.10	14.90	0.50	815.90	0.20	2.60	0.30	10.00	0.25	44.50	7.30	7.40	13.40
YPC053	0.90	14.90	0.50	995.90	0.05	1.80	0.30	10.00	0.25	37.40	5.80	5.10	11.10
YPC054	1.00	12.40	0.50	841.20	0.10	2.00	0.05	10.00	0.25	54.30	6.60	5.60	11.30
YPC055	0.90	10.70	0.50	813.90	0.05	1.40	0.05	12.00	0.25	28.80	4.10	4.40	8.90
YPC056	0.90	5.00	0.50	720.70	0.20	0.90	0.05	4.00	0.25	14.90	2.80	2.50	4.60
YPC057	0.10	2.60	0.50	439.20	0.05	0.50	0.05	4.00	0.25	12.60	3.80	3.40	3.40
YPC058	0.30	4.20	0.50	534.90	0.05	0.50	0.05	4.00	0.25	17.00	2.90	2.50	4.00
YPC059	0.70	7.30	0.50	460.10	0.05	1.20	0.05	8.00	0.25	25.00	6.80	5.20	8.40
YPC060	0.70	10.00	0.50	485.50	0.05	2.50	0.10	11.00	0.25	24.60	13.00	12.30	13.80
YPC061	0.60	8.30	0.50	511.90	0.05	1.60	0.05	11.00	0.50	24.00	5.70	5.30	8.90
YPC062	1.00	6.20	0.50	375.70	0.20	1.00	0.05	4.00	0.25	19.20	7.90	6.90	8.10
YPC063	1.10	10.90	0.50	729.10	0.05	2.30	0.20	8.00	0.25	51.10	6.10	6.70	13.10
YPC064	0.70	10.40	0.50	753.90	0.05	2.00	0.20	12.00	0.25	38.70	7.50	6.50	11.40
YPC065	1.00	12.10	0.50	862.40	0.10	2.30	0.10	12.00	0.25	40.60	5.90	5.30	10.80
YPC066	0.50	8.10	0.50	948.70	0.05	1.50	0.40	8.00	0.25	29.60	4.40	4.00	8.10
YPC067	0.50	7.10	0.50	956.40	0.05	1.10	0.20	4.00	0.25	29.20	4.80	5.40	7.50
YPC068	0.30	5.40	0.50	561.10	0.05	1.10	0.20	4.00	0.25	25.40	5.50	4.60	6.70
YPC069	0.30	5.60	0.50	560.50	0.05	1.00	0.05	10.00	0.25	28.30	6.40	5.50	8.00

	Pr_ppm	Nd_ppm	Sm_ppm	Eu_ppm	Gd_ppm	Tb_ppm	Dy_ppm	Ho_ppm	Er_ppm	Tm_ppm	Yb_ppm	Lu_ppm	Mo_ppm
Lab analytical method code	4B	4B	4B	4B	4B	4B	4B	4B	4B	4B	4B	4B	1DX
Unit	PPM	PPM	PPM	PPM	PPM	PPM	PPM	PPM	PPM	PPM	PPM	PPM	PPM
Detection Limit	0.02	0.3	0.05	0.02	0.05	0.01	0.05	0.02	0.03	0.01	0.05	0.01	0.1
SampleID													
YPC001	1.62	6.30	1.29	0.31	1.32	0.18	1.20	0.27	0.82	0.09	0.84	0.11	0.10
YPC002	1.39	5.30	1.21	0.28	1.26	0.17	1.09	0.19	0.55	0.09	0.60	0.09	0.05
YPC003	1.42	5.60	1.21	0.28	1.27	0.17	1.03	0.27	0.63	0.09	0.55	0.11	0.05
YPC004	0.78	3.30	0.70	0.16	0.78	0.09	0.67	0.11	0.33	0.06	0.33	0.04	0.05
YPC005	0.96	4.20	0.91	0.22	0.83	0.12	0.69	0.16	0.38	0.06	0.44	0.06	0.05
YPC006	1.16	5.40	1.05	0.21	1.10	0.15	0.79	0.18	0.61	0.08	0.66	0.08	0.05
YPC007	1.55	5.60	1.34	0.27	1.26	0.18	1.11	0.25	0.73	0.11	0.79	0.11	0.05
YPC008	2.14	9.40	1.87	0.44	2.12	0.29	1.82	0.44	1.18	0.17	1.18	0.17	0.10
YPC009	1.48	5.70	1.28	0.28	1.34	0.17	1.02	0.24	0.63	0.10	0.61	0.10	0.10
YPC010	1.31	6.00	1.20	0.26	1.28	0.17	1.08	0.19	0.71	0.08	0.52	0.08	0.05
YPC011	1.65	6.50	1.39	0.28	1.25	0.18	1.10	0.23	0.78	0.09	0.72	0.10	0.05
YPC012	1.31	6.10	1.23	0.23	1.26	0.16	1.06	0.23	0.68	0.09	0.65	0.11	0.05
YPC013	2.37	9.40	1.99	0.44	1.86	0.27	1.49	0.33	0.80	0.13	0.88	0.13	0.05
YPC014	1.83	8.50	1.56	0.31	1.68	0.21	1.47	0.26	0.82	0.10	0.85	0.11	0.05
YPC015	3.10	13.00	2.57	0.54	2.85	0.37	2.04	0.45	1.29	0.18	1.08	0.17	0.05
YPC016	1.73	7.40	1.57	0.32	1.62	0.23	1.24	0.34	0.93	0.12	1.03	0.15	0.10
YPC017	1.65	8.20	1.51	0.35	1.89	0.24	1.54	0.34	0.93	0.12	0.75	0.13	0.05
YPC018	2.15	9.20	1.82	0.38	1.73	0.24	1.56	0.32	0.82	0.10	0.79	0.13	0.10
YPC019	2.01	7.60	1.61	0.38	1.84	0.23	1.41	0.28	0.94	0.12	0.82	0.14	0.05
YPC020	1.36	6.60	1.26	0.28	1.25	0.17	1.14	0.23	0.67	0.08	0.62	0.11	0.05
YPC021	1.47	7.50	1.18	0.27	1.38	0.15	1.06	0.23	0.59	0.08	0.59	0.08	0.05
YPC022	1.12	5.30	1.06	0.24	1.12	0.14	1.02	0.19	0.52	0.07	0.63	0.07	0.05
YPC023	2.10	9.90	1.84	0.40	1.92	0.24	1.64	0.35	0.99	0.12	0.87	0.12	0.05
YPC024	1.45	6.90	1.29	0.29	1.40	0.18	1.15	0.22	0.68	0.09	0.68	0.10	0.20
YPC025	1.19	5.00	1.04	0.26	1.07	0.15	1.00	0.21	0.52	0.08	0.58	0.07	0.05
YPC026	1.10	5.40	1.02	0.22	1.22	0.16	1.04	0.21	0.54	0.08	0.52	0.09	0.05
YPC027	1.40	6.60	1.28	0.30	1.44	0.17	1.02	0.21	0.64	0.09	0.67	0.10	0.05
YPC028	0.92	4.00	0.85	0.19	0.87	0.12	0.68	0.14	0.43	0.06	0.52	0.05	0.05
YPC029	1.65	7.80	1.51	0.37	1.66	0.22	1.31	0.28	0.85	0.10	0.70	0.12	0.05
YPC030	2.40	10.50	1.99	0.45	2.19	0.28	1.79	0.35	1.12	0.13	0.86	0.15	0.05
YPC031	1.14	5.30	0.99	0.26	1.12	0.16	1.08	0.19	0.59	0.09	0.65	0.10	0.05
YPC032	1.28	5.30	1.08	0.26	1.17	0.16	1.30	0.23	0.66	0.08	0.64	0.10	0.05
YPC033	1.12	5.60	0.93	0.22	1.09	0.14	0.86	0.23	0.52	0.08	0.57	0.08	0.20
YPC034	1.54	6.80	1.34	0.29	1.46	0.20	1.24	0.22	0.66	0.10	0.62	0.10	0.05
YPC035	1.55	6.70	1.28	0.27	1.46	0.19	1.43	0.26	0.75	0.09	0.76	0.11	0.05
YPC036	2.62	11.40	2.42	0.54	2.47	0.34	2.03	0.40	1.15	0.15	1.10	0.16	0.05
YPC037	1.21	5.00	0.92	0.20	0.97	0.15	1.04	0.23	0.58	0.09	0.58	0.08	0.05
YPC038	1.32	4.70	0.99	0.21	1.03	0.15	0.99	0.22	0.60	0.09	0.50	0.08	0.05
YPC039	3.29	14.00	2.91	0.62	2.87	0.38	2.22	0.46	1.23	0.18	1.11	0.17	0.05
YPC040	1.23	6.10	0.97	0.23	0.98	0.14	0.88	0.18	0.62	0.07	0.47	0.07	0.05
YPC041	1.47	6.70	1.19	0.25	1.14	0.17	1.12	0.21	0.61	0.10	0.60	0.08	0.05
YPC042	1.75	6.60	1.41	0.34	1.48	0.23	1.47	0.30	0.89	0.13	0.91	0.14	0.05
YPC043	1.50	5.00	1.31	0.27	1.26	0.19	1.39	0.29	0.70	0.10	0.62	0.09	0.10
YPC044	0.85	4.20	0.80	0.21	0.98	0.13	0.85	0.14	0.49	0.09	0.39	0.07	0.05
YPC045	0.81	3.80	0.80	0.16	0.91	0.10	0.63	0.15	0.48	0.06	0.44	0.06	0.05
YPC046	1.29	6.00	0.99	0.25	1.16	0.15	0.94	0.23	0.72	0.10	0.70	0.10	0.10
YPC047	0.50	1.90	0.47	0.10	0.45	0.07	0.49	0.07	0.25	0.04	0.27	0.04	0.05
YPC048	1.75	7.40	1.48	0.32	1.41	0.20	1.32	0.28	0.85	0.12	0.73	0.10	0.10
YPC049	1.73	7.50	1.47	0.39	1.47	0.22	1.53	0.25	0.87	0.11	0.79	0.11	0.10
YPC050	0.89	3.60	0.76	0.17	0.85	0.12	0.81	0.14	0.46	0.06	0.36	0.07	0.05
YPC051	1.86	8.40	1.59	0.36	1.48	0.21	1.29	0.28	0.85	0.11	0.79	0.11	0.10
YPC052	1.82	7.80	1.43	0.32	1.53	0.20	1.28	0.28	0.74	0.12	0.83	0.11	0.05
YPC053	1.27	5.50	1.04	0.27	1.05	0.14	1.03	0.22	0.60	0.07	0.55	0.10	0.10
YPC054	1.36	5.80	1.18	0.26	1.16	0.16	1.31	0.21	0.63	0.10	0.60	0.10	0.05
YPC055	1.07	4.00	0.84	0.19	0.90	0.12	0.94	0.14	0.44	0.06	0.43	0.06	0.05
YPC056	0.65	2.90	0.64	0.15	0.66	0.08	0.73	0.11	0.35	0.03	0.36	0.05	0.05
YPC057	0.67	2.80	0.72	0.14	0.71	0.09	0.64	0.13	0.36	0.05	0.36	0.06	0.05
YPC058	0.55	2.50	0.53	0.11	0.53	0.08	0.52	0.10	0.30	0.04	0.31	0.04	0.05
YPC059	1.31	4.90	1.10	0.24	1.25	0.17	0.88	0.20	0.68	0.08	0.47	0.08	0.05
YPC060	2.96	11.80	2.39	0.53	2.52	0.31	2.12	0.44	1.12	0.15	1.02	0.14	0.05
YPC061	1.19	5.40	1.16	0.23	1.15	0.16	1.00	0.19	0.57	0.08	0.37	0.09	0.05
YPC062	1.46	6.60	1.20	0.27	1.34	0.17	1.20	0.25	0.69	0.08	0.68	0.07	0.05
YPC063	1.62	6.80	1.21	0.23	1.31	0.16	0.94	0.19	0.56	0.08	0.55	0.07	0.10
YPC064	1.51	7.00	1.29	0.31	1.37	0.19	1.37	0.25	0.75	0.12	0.78	0.10	0.05
YPC065	1.34	5.60	1.21	0.22	1.16	0.16	1.04	0.21	0.56	0.09	0.62	0.10	0.05
YPC066	0.96	3.10	0.83	0.17	0.84	0.12	0.88	0.15	0.52	0.07	0.40	0.07	0.05
YPC067	1.10	4.30	0.97	0.21	1.07	0.14	0.79	0.17	0.50	0.06	0.48	0.06	0.05
YPC068	1.00	4.60	0.91	0.23	0.94	0.12	0.91	0.17	0.48	0.07	0.39	0.07	0.05
YPC069	1.28	5.70	1.17	0.28	1.29	0.17	0.93	0.23	0.55	0.09	0.64	0.08	0.05

	Cu_ppm	Pb_ppm	Zn_ppm	Ni_ppm	As_ppm	Cd_ppm	Sb_ppm	Bi_ppm	Ag_ppm	Au_ppb	Hg_ppm	Tl_ppm	Se_ppm
Lab analytical method code	1DX	1DX	1DX	1DX	1DX	1DX	1DX	1DX	1DX	1DX	1DX	1DX	1DX
Unit	PPM	PPM	PPM	PPM	PPM	PPM	PPM	PPM	PPM	PPB	PPM	PPM	PPM
Detection Limit	0.1	0.1	1	0.1	0.5	0.1	0.1	0.1	0.1	0.5	0.01	0.1	0.5
SampleID													
YPC001	6.80	2.10	5.00	8.40	0.25	0.05	0.05	0.30	0.05	0.25	0.03	0.05	0.25
YPC002	5.70	1.40	7.00	8.80	1.00	0.05	0.05	0.05	0.05	0.25	0.01	0.05	0.25
YPC003	5.20	2.10	6.00	10.60	1.40	0.05	0.05	0.05	0.05	0.25	0.02	0.05	0.25
YPC004	3.20	1.10	2.00	9.20	0.90	0.05	0.10	0.05	0.05	0.25	0.03	0.05	0.25
YPC005	3.00	1.30	13.00	7.40	1.10	0.05	0.05	0.05	0.05	0.25	0.03	0.05	0.25
YPC006	4.10	1.80	4.00	6.70	1.00	0.05	0.05	0.05	0.05	0.25	0.02	0.05	0.25
YPC007	4.50	2.40	4.00	5.10	1.40	0.05	0.05	0.05	0.05	0.25	0.04	0.05	0.25
YPC008	4.50	1.80	2.00	7.40	1.10	0.05	0.05	0.05	0.05	0.25	0.07	0.05	0.25
YPC009	3.40	1.70	3.00	6.30	2.70	0.05	0.05	0.05	0.05	1.70	0.05	0.10	0.25
YPC010	2.10	1.30	4.00	5.10	1.20	0.05	0.05	0.05	0.05	0.25	0.06	0.05	0.25
YPC011	2.50	2.60	4.00	5.30	1.00	0.05	0.05	0.05	0.05	0.70	0.06	0.05	0.25
YPC012	2.30	1.50	2.00	6.80	1.50	0.05	0.05	0.05	0.05	0.25	0.03	0.05	0.25
YPC013	2.70	2.20	3.00	8.10	2.00	0.05	0.05	0.05	0.05	0.25	0.03	0.05	0.25
YPC014	3.70	1.80	3.00	5.10	1.50	0.05	0.10	0.05	0.05	0.25	0.05	0.05	0.25
YPC015	4.40	2.90	4.00	7.10	2.20	0.05	0.05	0.05	0.05	0.25	0.03	0.10	0.25
YPC016	3.90	10.40	33.00	5.80	0.60	0.30	0.20	0.05	0.05	1.70	0.06	0.05	0.25
YPC017	4.60	1.50	4.00	5.90	1.20	0.05	0.05	0.05	0.05	0.25	0.06	0.05	0.25
YPC018	3.10	2.20	6.00	6.70	2.30	0.05	0.05	0.05	0.05	0.25	0.04	0.05	0.25
YPC019	3.60	3.30	12.00	7.20	1.20	0.05	0.05	0.05	0.05	0.25	0.05	0.05	0.25
YPC020	3.50	1.40	3.00	5.60	1.60	0.05	0.05	0.05	0.05	0.25	0.03	0.05	0.25
YPC021	7.40	2.00	6.00	5.60	3.30	0.05	0.10	0.05	0.05	11.80	0.04	0.05	0.25
YPC022	6.10	1.70	6.00	4.90	2.40	0.05	0.05	0.05	0.05	0.25	0.03	0.05	0.25
YPC023	4.50	2.20	6.00	8.20	1.80	0.05	0.05	0.05	0.05	0.25	0.06	0.05	0.25
YPC024	3.80	1.90	11.00	10.70	1.60	0.05	0.05	0.05	0.05	0.25	0.03	0.05	0.25
YPC025	3.40	1.50	4.00	5.40	1.80	0.05	0.05	0.05	0.05	0.25	0.05	0.10	0.25
YPC026	3.40	1.40	2.00	6.70	1.90	0.05	0.10	0.05	0.05	2.10	0.04	0.05	0.25
YPC027	2.50	1.30	3.00	6.20	2.30	0.05	0.05	0.05	0.05	0.25	0.04	0.05	0.25
YPC028	6.70	1.30	8.00	7.10	2.10	0.05	0.10	0.05	0.05	0.25	0.04	0.05	0.25
YPC029	2.50	2.90	4.00	5.30	2.90	0.05	0.05	0.05	0.05	0.25	0.05	0.05	0.50
YPC030	3.20	3.40	4.00	9.10	3.30	0.05	0.10	0.05	0.05	0.25	0.05	0.05	0.25
YPC031	3.30	1.80	9.00	5.30	1.80	0.05	0.05	0.05	0.05	0.25	0.05	0.05	0.25
YPC032	4.30	1.70	3.00	4.50	1.50	0.20	0.05	0.05	0.05	0.25	0.05	0.05	0.25
YPC033	1.80	1.50	2.00	6.00	2.00	0.05	0.05	0.05	0.05	0.25	0.11	0.10	0.25
YPC034	2.70	1.90	9.00	5.90	1.70	0.05	0.05	0.05	0.05	2.10	0.05	0.05	0.25
YPC035	4.20	2.30	7.00	6.30	1.60	0.05	0.05	0.05	0.05	0.25	0.07	0.05	0.25
YPC036	3.60	4.50	5.00	7.60	2.10	0.05	0.05	0.05	0.05	0.70	0.07	0.10	0.25
YPC037	6.10	1.30	2.00	4.20	1.70	0.05	0.05	0.05	0.05	3.00	0.03	0.05	0.25
YPC038	4.50	2.50	5.00	5.30	2.10	0.05	0.05	0.05	0.05	2.80	0.03	0.05	0.25
YPC039	3.30	2.20	2.00	3.60	2.20	0.05	0.05	0.05	0.05	1.30	0.07	0.05	0.25
YPC040	2.40	1.40	2.00	1.90	1.80	0.05	0.05	0.05	0.05	0.70	0.02	0.05	0.25
YPC041	4.90	2.70	6.00	7.90	1.70	0.05	0.05	0.05	0.05	0.80	0.06	0.05	0.25
YPC042	4.70	2.80	7.00	6.10	1.80	0.05	0.05	0.05	0.05	0.80	0.06	0.05	0.25
YPC043	3.30	2.60	5.00	7.10	2.60	0.05	0.05	0.05	0.05	0.25	0.01	0.05	0.25
YPC044	3.90	1.40	3.00	3.40	2.60	0.05	0.05	0.05	0.05	0.80	0.01	0.05	0.25
YPC045	3.00	1.00	7.00	2.60	2.50	0.05	0.05	0.05	0.05	1.00	0.02	0.05	0.25
YPC046	3.40	6.10	10.00	3.80	1.50	0.05	0.05	0.05	0.05	0.50	0.05	0.05	0.25
YPC047	1.90	0.70	2.00	1.80	1.90	0.05	0.05	0.05	0.05	0.25	0.02	0.05	0.25
YPC048	2.50	2.00	4.00	4.60	2.20	0.05	0.05	0.05	0.05	0.25	0.01	0.05	0.25
YPC049	4.40	2.20	5.00	7.10	2.40	0.05	0.05	0.05	0.05	0.25	0.02	0.05	0.50
YPC050	2.20	1.20	12.00	1.60	2.10	0.05	0.05	0.05	0.05	0.25	0.01	0.05	0.25
YPC051	4.90	3.10	6.00	8.90	1.40	0.05	0.05	0.05	0.05	0.25	0.03	0.05	0.70
YPC052	2.90	2.40	6.00	5.50	1.70	0.05	0.05	0.05	0.05	0.25	0.02	0.05	0.60
YPC053	3.40	2.00	5.00	4.40	1.60	0.05	0.05	0.05	0.05	0.25	0.01	0.05	0.80
YPC054	4.20	2.30	4.00	5.30	1.50	0.05	0.05	0.05	0.05	0.25	0.03	0.05	0.60
YPC055	2.60	1.80	3.00	3.00	1.70	0.05	0.05	0.05	0.05	0.25	0.03	0.05	0.25
YPC056	3.30	0.90	1.00	3.60	1.70	0.05	0.10	0.05	0.05	1.70	0.01	0.05	0.25
YPC057	2.40	0.60	2.00	2.50	1.10	0.05	0.05	0.05	0.05	1.50	0.02	0.05	0.25
YPC058	2.70	0.90	4.00	1.80	1.90	0.05	0.05	0.05	0.05	0.25	0.01	0.05	0.25
YPC059	3.40	1.80	8.00	2.70	1.80	0.05	0.05	0.05	0.05	0.70	0.04	0.05	0.25
YPC060	3.00	3.00	3.00	3.80	1.80	0.05	0.05	0.05	0.05	0.25	0.04	0.05	0.25
YPC061	3.30	1.90	5.00	2.70	1.90	0.05	0.05	0.05	0.05	1.00	0.02	0.05	0.25
YPC062	3.00	1.50	3.00	2.50	1.30	0.05	0.05	0.05	0.05	0.25	0.02	0.05	0.25
YPC063	5.90	2.30	4.00	4.60	1.70	0.05	0.10	0.05	0.05	0.80	0.03	0.05	0.25
YPC064	4.20	2.70	11.00	4.80	2.00	0.05	0.10	0.05	0.05	1.80	0.06	0.05	0.25
YPC065	4.50	2.40	3.00	4.20	2.30	0.05	0.05	0.05	0.05	0.25	0.03	0.05	0.25
YPC066	3.50	2.10	3.00	4.50	1.80	0.05	0.05	0.05	0.05	2.70	0.04	0.05	0.25
YPC067	3.50	1.60	5.00	5.50	2.30	0.05	0.05	0.05	0.05	1.20	0.05	0.05	0.25
YPC068	2.90	1.30	2.00	3.20	1.40	0.05	0.10	0.10	0.05	0.60	0.02	0.10	0.25
YPC069	3.70	1.40	2.00	3.50	2.20	0.05	0.05	0.05	0.05	0.25	0.04	0.05	0.25

		Duplicate ID	Transect	Location	Sample_Type	Orig_Grid_ID	Orig_East	Orig_North
Yorke Peninsula	YPC070	YPC044	2	Dump Rd	CaCO3 rock	GDA94_53H	729317	6147985
Yorke Peninsula	YPC071	YPC055	3	Spicers Rd	CaCO3 rock	GDA94_53H	737421	6155381
Yorke Peninsula	YPC072	YPC056	3	Spicers Rd	CaCO3 rock	GDA94_53H	738448	6155269
Yorke Peninsula	YPC073	YPC066	3	Goldsworthy Rd	CaCO3 rock	GDA94_53H	757269	6154234
Yorke Peninsula	YPC074		4	Black Bobs Rd	CaCO3 rock	GDA94_53H	763310	6169311
Yorke Peninsula	YPC075		4	Black Bobs Rd	CaCO3 rock	GDA94_53H	762309	6169336
Yorke Peninsula	YPC076		4	Black Bobs Rd	CaCO3 rock	GDA94_53H	760171	6169390
Yorke Peninsula	YPC077		4	Black Bobs Rd	CaCO3 rock	GDA94_53H	756818	6169472
Yorke Peninsula	YPC078		4	Black Bobs Rd	CaCO3 rock	GDA94_53H	755572	6169503
Yorke Peninsula	YPC079		4	Black Bobs Rd	CaCO3 rock	GDA94_53H	754541	6169528
Yorke Peninsula	YPC080		4	Black Bobs Rd	CaCO3 rock	GDA94_53H	753519	6169555
Yorke Peninsula	YPC081		4	Black Bobs Rd	CaCO3 rock	GDA94_53H	752533	6169581
Yorke Peninsula	YPC082		4	Black Bobs Rd	CaCO3 rock	GDA94_53H	751167	6169617
Yorke Peninsula	YPC083		4	Black Bobs Rd	CaCO3 rock	GDA94_53H	749114	6169663
Yorke Peninsula	YPC084		4	Black Bobs Rd	CaCO3 rock	GDA94_53H	748017	6169687
Yorke Peninsula	YPC085		4	Black Bobs Rd	CaCO3 rock	GDA94_53H	747008	6169684
Yorke Peninsula	YPC086		4	Black Bobs Rd	CaCO3 rock	GDA94_53H	744652	6169658
Yorke Peninsula	YPC087		4	Black Bobs Rd	CaCO3 rock	GDA94_53H	743524	6169679
Yorke Peninsula	YPC088		4	Black Bobs Rd	CaCO3 rock	GDA94_53H	740775	6169703
Yorke Peninsula	YPC089		4	Black Bobs Rd	CaCO3 rock	GDA94_53H	739655	6169734
Yorke Peninsula	YPC090		4	Black Bobs Rd	CaCO3 rock	GDA94_53H	738248	6169771
Yorke Peninsula	YPC091		4	Black Bobs Rd	CaCO3 rock	GDA94_53H	737270	6169797
Yorke Peninsula	YPC092		4	Black Bobs Rd	CaCO3 rock	GDA94_53H	736252	6169822
Yorke Peninsula	YPC093		4	Black Bobs Rd	CaCO3 rock	GDA94_53H	734953	6169856
Yorke Peninsula	YPC094		4	Black Bobs Rd	CaCO3 rock	GDA94_53H	733666	6169889
Yorke Peninsula	YPC095		4	Black Bobs Rd	CaCO3 rock	GDA94_53H	732533	6169916
Yorke Peninsula	YPC096		4	Black Bobs Rd	CaCO3 rock	GDA94_53H	731449	6169946
Yorke Peninsula	YPC097	YPC082	4	Black Bobs Rd	CaCO3 rock	GDA94_53H	751167	6169617
Yorke Peninsula	YPC098	YPC088	4	Black Bobs Rd	CaCO3 rock	GDA94_53H	740775	6169703
Yorke Peninsula	YPC099	YPC094	4	Black Bobs Rd	CaCO3 rock	GDA94_53H	733666	6169889
Yorke Peninsula	YPC100		5	James Well Rd	CaCO3 rock	GDA94_53H	764541	6180799
Yorke Peninsula	YPC101		5	James Well Rd	CaCO3 rock	GDA94_53H	763854	6180816
Yorke Peninsula	YPC102		5	James Well Rd	CaCO3 rock	GDA94_53H	762915	6180840
Yorke Peninsula	YPC103		5	James Well Rd	CaCO3 rock	GDA94_53H	761775	6180866
Yorke Peninsula	YPC104		5	James Well Rd	CaCO3 rock	GDA94_53H	760688	6180896
Yorke Peninsula	YPC105		5	James Well Rd	CaCO3 rock	GDA94_53H	759693	6180921
Yorke Peninsula	YPC106		5	James Well Rd	CaCO3 rock	GDA94_53H	758685	6180946
Yorke Peninsula	YPC107		5	Yarrum Rd	CaCO3 rock	GDA94_53H	750002	6181168
Yorke Peninsula	YPC108		5	Yarrum Rd	CaCO3 rock	GDA94_53H	748162	6181215
Yorke Peninsula	YPC109		5	Yarrum Rd	CaCO3 rock	GDA94_53H	746942	6181249
Yorke Peninsula	YPC110		5	Yarrum Rd	CaCO3 rock	GDA94_53H	743315	6181335
Yorke Peninsula	YPC111		5	Barley Stacks Rd	CaCO3 rock	GDA94_53H	741448	6181386
Yorke Peninsula	YPC112		5	Barley Stacks Rd	CaCO3 rock	GDA94_53H	739514	6181436
Yorke Peninsula	YPC113		5	Barley Stacks Rd	CaCO3 rock	GDA94_53H	738396	6181464
Yorke Peninsula	YPC114		5	Barley Stacks Rd	CaCO3 rock	GDA94_53H	737182	6181489
Yorke Peninsula	YPC115		5	Barley Stacks Rd	CaCO3 rock	GDA94_53H	735780	6181525
Yorke Peninsula	YPC116		5	Barley Stacks Rd	CaCO3 rock	GDA94_53H	734256	6181564
Yorke Peninsula	YPC117		5	Barley Stacks Rd	CaCO3 rock	GDA94_53H	733162	6181590
Yorke Peninsula	YPC118	YPC108	5	Yarrum Rd	CaCO3 rock	GDA94_53H	748162	6181215
Yorke Peninsula	YPC119		6	Moody Rd	CaCO3 rock	GDA94_53H	729447	6191277
Yorke Peninsula	YPC120		6	Moody Rd	CaCO3 rock	GDA94_53H	731229	6191744
Yorke Peninsula	YPC121		6	Moody Rd	CaCO3 rock	GDA94_53H	732605	6192099
Yorke Peninsula	YPC122		6	Moody Rd	CaCO3 rock	GDA94_53H	735774	6192445
Yorke Peninsula	YPC123		6	Moody Rd	CaCO3 rock	GDA94_53H	736836	6192476
Yorke Peninsula	YPC124		6	Moody Rd	CaCO3 rock	GDA94_53H	737981	6192500
Yorke Peninsula	YPC125		6	Moody Rd	CaCO3 rock	GDA94_53H	740760	6192582
Yorke Peninsula	YPC126		6	Pistol Club Rd	CaCO3 rock	GDA94_53H	751263	6194344
Yorke Peninsula	YPC127		6	Pistol Club Rd	CaCO3 rock	GDA94_53H	752310	6194324
Yorke Peninsula	YPC128		6	Pistol Club Rd	CaCO3 rock	GDA94_53H	753462	6194063
Yorke Peninsula	YPC129		6	Johnson Rd	CaCO3 rock	GDA94_53H	756786	6193679
Yorke Peninsula	YPC130		6	Johnson Rd	CaCO3 rock	GDA94_53H	757887	6193648
Yorke Peninsula	YPC131		6	Johnson Rd	CaCO3 rock	GDA94_53H	760083	6193593
Yorke Peninsula	YPC132		6	Peterson Rd	CaCO3 rock	GDA94_53H	762039	6193540
Yorke Peninsula	YPC133		6	Peterson Rd	CaCO3 rock	GDA94_53H	763060	6193481
Yorke Peninsula	YPC134		6	Peterson Rd	CaCO3 rock	GDA94_53H	764175	6193279
Yorke Peninsula	YPC135		6	Cane Rd	CaCO3 rock	GDA94_53H	766193	6192915
Yorke Peninsula	YPC136		6	Cane Rd	CaCO3 rock	GDA94_53H	767489	6192686
Yorke Peninsula	YPC137	YPC124	6	Moody Rd	CaCO3 rock	GDA94_53H	737981	6192500
Yorke Peninsula	YPC138	YPC130	6	Johnson Rd	CaCO3 rock	GDA94_53H	757887	6193648
Yorke Peninsula	YPC139		7	Coleman Rd	CaCO3 rock	GDA94_53H	775125	6208523
Yorke Peninsula	YPC140		7	Coleman Rd	CaCO3 rock	GDA94_53H	774210	6208448
Yorke Peninsula	YPC141		7	Coleman Rd	CaCO3 rock	GDA94_53H	772954	6208344
Yorke Peninsula	YPC142		7	Coleman Rd	CaCO3 rock	GDA94_53H	771811	6208248
Yorke Peninsula	YPC143		7	Coleman Rd	CaCO3 rock	GDA94_53H	770531	6208150

	RL	Orig_Survey_Method	Orig_Surve	Date	Sampled_By	Sample_Depth	Weight_kg	SiO2_pct	Al2O3_pct
YPC070	22	Garmin GPS Map62S	KWolff	17/03/2012	RWolff	ground level	2	6.8	1.34
YPC071	73	Garmin GPS Map62S	KWolff	18/03/2012	RWolff	ground level	2	6.7	1.68
YPC072	58	Garmin GPS Map62S	KWolff	18/03/2012	RWolff	ground level	2	4.2	0.84
YPC073	59	Garmin GPS Map62S	KWolff	18/03/2012	RWolff	ground level	2	7.9	1.33
YPC074	20	Garmin GPS Map62S	KWolff	24/03/2012	RWolff	ground level	2	9.6	1.89
YPC075	32	Garmin GPS Map62S	KWolff	24/03/2012	RWolff	ground level	2	11.3	1.49
YPC076	77	Garmin GPS Map62S	KWolff	24/03/2012	RWolff	ground level	2	9.9	2.13
YPC077	76	Garmin GPS Map62S	KWolff	24/03/2012	RWolff	ground level	2	3.9	0.95
YPC078	74	Garmin GPS Map62S	KWolff	24/03/2012	RWolff	ground level	2	12.9	2.17
YPC079	78	Garmin GPS Map62S	KWolff	24/03/2012	RWolff	ground level	2	9.7	1.68
YPC080	88	Garmin GPS Map62S	KWolff	24/03/2012	RWolff	ground level	2	13.1	1.39
YPC081	97	Garmin GPS Map62S	KWolff	24/03/2012	RWolff	ground level	2	16.3	1.57
YPC082	103	Garmin GPS Map62S	KWolff	24/03/2012	RWolff	ground level	2	9.2	1.56
YPC083	112	Garmin GPS Map62S	KWolff	24/03/2012	RWolff	ground level	2	10.8	1.52
YPC084	112	Garmin GPS Map62S	KWolff	24/03/2012	RWolff	ground level	2	22.7	2.44
YPC085	105	Garmin GPS Map62S	KWolff	24/03/2012	RWolff	ground level	2	17.8	2.11
YPC086	84	Garmin GPS Map62S	KWolff	24/03/2012	RWolff	ground level	2	9.7	1.12
YPC087	86	Garmin GPS Map62S	KWolff	24/03/2012	RWolff	ground level	2	11.0	1.55
YPC088	117	Garmin GPS Map62S	KWolff	24/03/2012	RWolff	ground level	2	14.5	1.65
YPC089	90	Garmin GPS Map62S	KWolff	24/03/2012	RWolff	ground level	2	19.4	3.02
YPC090	61	Garmin GPS Map62S	KWolff	24/03/2012	RWolff	ground level	2	19.3	2.13
YPC091	49	Garmin GPS Map62S	KWolff	24/03/2012	RWolff	ground level	2	20.6	2.45
YPC092	39	Garmin GPS Map62S	KWolff	24/03/2012	RWolff	ground level	2	14.4	1.81
YPC093	26	Garmin GPS Map62S	KWolff	24/03/2012	RWolff	ground level	2	12.5	1.97
YPC094	17	Garmin GPS Map62S	KWolff	24/03/2012	RWolff	ground level	2	9.2	2.14
YPC095	14	Garmin GPS Map62S	KWolff	24/03/2012	RWolff	ground level	2	10.4	0.95
YPC096	7	Garmin GPS Map62S	KWolff	24/03/2012	RWolff	ground level	2	10.1	1.81
YPC097	103	Garmin GPS Map62S	KWolff	24/03/2012	RWolff	ground level	2	8.9	1.71
YPC098	117	Garmin GPS Map62S	KWolff	24/03/2012	RWolff	ground level	2	19.9	1.99
YPC099	17	Garmin GPS Map62S	KWolff	24/03/2012	RWolff	ground level	2	9.1	2.16
YPC100	55	Garmin GPS Map62S	KWolff	25/03/2012	RWolff	ground level	2	17.6	1.72
YPC101	55	Garmin GPS Map62S	KWolff	25/03/2012	RWolff	ground level	2	13.0	1.62
YPC102	83	Garmin GPS Map62S	KWolff	25/03/2012	RWolff	ground level	2	5.2	0.82
YPC103	94	Garmin GPS Map62S	KWolff	25/03/2012	RWolff	ground level	2	1.9	0.30
YPC104	93	Garmin GPS Map62S	KWolff	25/03/2012	RWolff	ground level	2	5.0	0.85
YPC105	99	Garmin GPS Map62S	KWolff	25/03/2012	RWolff	ground level	2	10.4	1.19
YPC106	107	Garmin GPS Map62S	KWolff	25/03/2012	RWolff	ground level	2	15.0	2.00
YPC107	126	Garmin GPS Map62S	KWolff	25/03/2012	RWolff	ground level	2	11.0	2.51
YPC108	107	Garmin GPS Map62S	KWolff	25/03/2012	RWolff	ground level	2	11.4	2.36
YPC109	100	Garmin GPS Map62S	KWolff	25/03/2012	RWolff	ground level	2	12.2	1.94
YPC110	78	Garmin GPS Map62S	KWolff	25/03/2012	RWolff	ground level	2	8.3	1.80
YPC111	94	Garmin GPS Map62S	KWolff	31/03/2012	RWolff	ground level	2	8.6	1.31
YPC112	106	Garmin GPS Map62S	KWolff	31/03/2012	RWolff	ground level	2	9.0	1.50
YPC113	87	Garmin GPS Map62S	KWolff	31/03/2012	RWolff	ground level	2	10.3	2.06
YPC114	80	Garmin GPS Map62S	KWolff	31/03/2012	RWolff	ground level	2	11.7	1.87
YPC115	58	Garmin GPS Map62S	KWolff	31/03/2012	RWolff	ground level	2	6.7	1.33
YPC116	50	Garmin GPS Map62S	KWolff	31/03/2012	RWolff	ground level	2	8.6	1.78
YPC117	48	Garmin GPS Map62S	KWolff	31/03/2012	RWolff	ground level	2	12.0	2.24
YPC118	107	Garmin GPS Map62S	KWolff	31/03/2012	RWolff	ground level	2	7.9	1.71
YPC119	6	Garmin GPS Map62S	KWolff	31/03/2012	RWolff	ground level	2	11.0	0.40
YPC120	11	Garmin GPS Map62S	KWolff	31/03/2012	RWolff	ground level	2	20.2	1.93
YPC121	37	Garmin GPS Map62S	KWolff	31/03/2012	RWolff	ground level	2	20.3	1.92
YPC122	69	Garmin GPS Map62S	KWolff	31/03/2012	RWolff	ground level	2	13.3	2.21
YPC123	77	Garmin GPS Map62S	KWolff	31/03/2012	RWolff	ground level	2	13.3	2.54
YPC124	86	Garmin GPS Map62S	KWolff	31/03/2012	RWolff	ground level	2	8.7	1.82
YPC125	129	Garmin GPS Map62S	KWolff	31/03/2012	RWolff	ground level	2	11.6	1.64
YPC126	221	Garmin GPS Map62S	KWolff	31/03/2012	RWolff	ground level	2	4.7	1.01
YPC127	211	Garmin GPS Map62S	KWolff	31/03/2012	RWolff	ground level	2	5.2	1.02
YPC128	186	Garmin GPS Map62S	KWolff	31/03/2012	RWolff	ground level	2	7.6	1.41
YPC129	139	Garmin GPS Map62S	KWolff	31/03/2012	RWolff	ground level	2	6.3	1.28
YPC130	131	Garmin GPS Map62S	KWolff	31/03/2012	RWolff	ground level	2	9.6	1.64
YPC131	106	Garmin GPS Map62S	KWolff	31/03/2012	RWolff	ground level	2	7.8	1.49
YPC132	90	Garmin GPS Map62S	KWolff	31/03/2012	RWolff	ground level	2	7.7	1.71
YPC133	96	Garmin GPS Map62S	KWolff	31/03/2012	RWolff	ground level	2	11.7	1.92
YPC134	99	Garmin GPS Map62S	KWolff	31/03/2012	RWolff	ground level	2	9.9	1.49
YPC135	86	Garmin GPS Map62S	KWolff	31/03/2012	RWolff	ground level	2	13.3	2.08
YPC136	64	Garmin GPS Map62S	KWolff	31/03/2012	RWolff	ground level	2	21.6	1.67
YPC137	86	Garmin GPS Map62S	KWolff	31/03/2012	RWolff	ground level	2	8.8	1.81
YPC138	131	Garmin GPS Map62S	KWolff	31/03/2012	RWolff	ground level	2	12.2	1.95
YPC139	81	Garmin GPS Map62S	KWolff	1/04/2012	RWolff	ground level	2	14.7	1.51
YPC140	95	Garmin GPS Map62S	KWolff	1/04/2012	RWolff	ground level	2	18.7	1.72
YPC141	108	Garmin GPS Map62S	KWolff	1/04/2012	RWolff	ground level	2	13.8	1.44
YPC142	116	Garmin GPS Map62S	KWolff	1/04/2012	RWolff	ground level	2	10.6	1.40
YPC143	118	Garmin GPS Map62S	KWolff	1/04/2012	RWolff	ground level	2	9.8	1.11

	Fe2O3_pct	CaO_pct	Ca/Sr	MgO_pct	Na2O_pct	K2O_pct	MnO_pct	TiO2_pct	P2O5_pct	Cr2O3_pct
YPC070	0.54	49.14	682	1.01	0.05	0.06	0.01	0.07	0.01	0.004
YPC071	0.66	47.63	435	1.72	0.06	0.08	0.01	0.12	0.01	0.001
YPC072	0.35	50.57	526	1.67	0.04	0.04	0.01	0.05	0.02	0.001
YPC073	0.56	44.04	261	4.57	0.06	0.07	0.01	0.06	0.01	0.001
YPC074	0.78	46.20	387	1.43	0.10	0.12	0.01	0.08	0.01	0.004
YPC075	0.71	44.44	312	2.30	0.08	0.13	0.01	0.06	0.02	0.001
YPC076	1.25	45.80	450	1.22	0.05	0.09	0.01	0.10	0.01	0.002
YPC077	0.45	51.65	683	1.08	0.01	0.01	0.01	0.04	0.01	0.002
YPC078	0.92	44.09	607	1.05	0.07	0.21	0.02	0.12	0.02	0.005
YPC079	0.72	46.65	384	1.26	0.20	0.35	0.01	0.07	0.01	0.003
YPC080	0.68	44.15	351	1.86	0.08	0.15	0.01	0.08	0.01	0.001
YPC081	0.68	40.87	312	2.69	0.07	0.21	0.01	0.07	0.02	0.004
YPC082	0.67	47.40	555	1.08	0.04	0.08	0.01	0.07	0.02	0.002
YPC083	0.66	46.34	566	1.21	0.02	0.04	0.01	0.08	0.01	0.001
YPC084	1.06	38.05	568	1.15	0.08	0.17	0.01	0.10	0.05	0.003
YPC085	0.89	41.45	495	1.28	0.04	0.13	0.01	0.10	0.01	0.006
YPC086	0.48	45.00	400	3.11	0.04	0.07	0.01	0.04	0.01	0.001
YPC087	0.63	46.09	586	1.16	0.02	0.06	0.01	0.07	0.03	0.003
YPC088	0.68	43.45	365	1.60	0.07	0.20	0.01	0.08	0.02	0.004
YPC089	1.28	39.15	404	1.28	0.08	0.25	0.01	0.11	0.01	0.003
YPC090	0.83	40.09	269	2.13	0.11	0.32	0.01	0.10	0.01	0.001
YPC091	0.98	38.43	400	2.54	0.09	0.33	0.02	0.12	0.02	0.004
YPC092	0.73	43.43	496	1.48	0.11	0.28	0.02	0.09	0.02	0.001
YPC093	0.78	45.02	523	1.22	0.08	0.23	0.01	0.10	0.02	0.001
YPC094	0.87	47.13	623	1.12	0.09	0.19	0.02	0.12	0.02	0.001
YPC095	0.37	46.69	251	1.42	0.04	0.10	0.01	0.04	0.03	0.002
YPC096	0.78	45.70	318	2.03	0.09	0.09	0.01	0.09	0.01	0.002
YPC097	0.74	47.70	580	1.00	0.05	0.08	0.01	0.07	0.01	0.005
YPC098	0.81	39.43	300	2.01	0.12	0.32	0.01	0.10	0.02	0.004
YPC099	0.88	47.16	609	1.13	0.09	0.20	0.03	0.11	0.03	0.003
YPC100	0.78	40.15	267	2.64	0.11	0.25	0.01	0.08	0.02	0.001
YPC101	0.75	44.04	318	2.36	0.11	0.12	0.01	0.09	0.02	0.002
YPC102	0.37	50.66	584	1.39	0.01	0.03	0.01	0.04	0.01	0.003
YPC103	0.16	49.07	542	4.96	0.01	0.01	0.01	0.01	0.01	0.003
YPC104	0.38	50.58	464	1.19	0.02	0.03	0.01	0.04	0.01	0.003
YPC105	0.52	46.86	443	1.35	0.02	0.05	0.01	0.06	0.01	0.003
YPC106	0.97	43.52	488	1.08	0.02	0.13	0.01	0.08	0.05	0.002
YPC107	1.28	44.98	503	1.06	0.04	0.11	0.01	0.10	0.03	0.003
YPC108	1.09	45.20	596	0.96	0.07	0.14	0.01	0.09	0.03	0.001
YPC109	0.82	44.88	390	1.43	0.13	0.21	0.01	0.09	0.03	0.004
YPC110	0.75	47.63	426	1.44	0.06	0.07	0.01	0.09	0.03	0.002
YPC111	0.55	45.15	280	3.84	0.10	0.09	0.01	0.07	0.01	0.002
YPC112	0.62	42.80	281	5.14	0.08	0.08	0.01	0.07	0.02	0.003
YPC113	0.85	45.97	483	1.40	0.03	0.05	0.02	0.10	0.02	0.004
YPC114	0.76	45.17	460	1.48	0.04	0.06	0.01	0.09	0.02	0.004
YPC115	0.55	47.13	376	2.44	0.07	0.08	0.01	0.07	0.02	0.003
YPC116	0.72	48.00	825	0.76	0.07	0.07	0.01	0.08	0.03	0.003
YPC117	0.90	44.71	570	1.21	0.11	0.28	0.03	0.12	0.02	0.002
YPC118	0.80	48.29	685	0.95	0.04	0.08	0.01	0.07	0.03	0.002
YPC119	0.16	47.25	358	1.32	0.10	0.11	0.01	0.01	0.03	0.001
YPC120	0.69	40.34	575	0.98	0.11	0.34	0.02	0.09	0.04	0.002
YPC121	0.71	40.21	558	0.97	0.09	0.35	0.01	0.09	0.03	0.002
YPC122	0.87	43.01	361	2.12	0.11	0.24	0.02	0.11	0.02	0.003
YPC123	1.02	43.65	446	1.59	0.14	0.29	0.02	0.12	0.03	0.003
YPC124	0.76	46.68	422	1.51	0.08	0.11	0.01	0.09	0.02	0.002
YPC125	0.69	43.38	535	3.43	0.07	0.23	0.03	0.08	0.02	0.003
YPC126	0.38	49.75	505	1.71	0.06	0.06	0.01	0.04	0.02	0.001
YPC127	0.35	49.80	434	1.29	0.07	0.12	0.01	0.03	0.01	0.002
YPC128	0.56	48.17	505	1.34	0.13	0.15	0.01	0.05	0.01	0.002
YPC129	0.45	49.19	472	1.17	0.09	0.24	0.01	0.04	0.03	0.001
YPC130	0.83	46.59	405	1.92	0.18	0.19	0.01	0.09	0.01	0.003
YPC131	0.56	47.60	415	1.86	0.10	0.18	0.01	0.07	0.01	0.002
YPC132	1.12	48.13	564	0.97	0.04	0.08	0.01	0.07	0.01	0.005
YPC133	0.98	45.32	392	1.31	0.08	0.13	0.01	0.09	0.01	0.003
YPC134	1.26	47.04	500	1.04	0.10	0.20	0.01	0.08	0.02	0.005
YPC135	1.74	42.67	342	1.98	0.07	0.14	0.02	0.10	0.03	0.004
YPC136	0.73	33.01	179	7.20	0.13	0.40	0.01	0.09	0.01	0.003
YPC137	0.77	47.32	439	1.54	0.10	0.15	0.01	0.09	0.01	0.001
YPC138	0.88	44.81	419	1.57	0.25	0.30	0.01	0.10	0.01	0.004
YPC139	0.68	42.06	361	2.99	0.12	0.22	0.01	0.10	0.02	0.002
YPC140	0.78	39.68	301	2.55	0.10	0.27	0.01	0.11	0.02	0.002
YPC141	0.58	44.18	407	1.47	0.05	0.08	0.01	0.08	0.03	0.003
YPC142	0.55	46.90	522	1.06	0.06	0.11	0.02	0.09	0.02	0.002
YPC143	0.52	47.32	508	1.11	0.04	0.08	0.01	0.06	0.02	0.004

	Ba_pct	LOI_pct	SUM_pct	TOT/C_pct	TOT/S_pct	Ba_ppm	Be_ppm	Co_ppm	Cs_ppm	Ga_ppm	Hf_ppm
YPC070	0.01	41.37	100.38	12.60	0.07	108.00	0.50	3.50	0.40	0.90	0.40
YPC071	0.01	41.32	100.02	12.38	0.06	87.00	0.50	3.00	0.50	1.40	0.50
YPC072	0.01	42.83	100.59	13.14	0.06	67.00	0.50	3.60	0.20	0.25	0.30
YPC073	0.02	41.67	100.26	11.39	0.01	135.00	0.50	5.00	0.40	0.25	0.60
YPC074	0.01	40.06	100.27	11.07	0.01	129.00	0.50	4.80	0.50	0.25	0.70
YPC075	0.02	39.74	100.35	11.24	0.01	174.00	0.50	8.10	0.40	0.25	1.10
YPC076	0.01	39.76	100.33	10.86	0.22	144.00	2.00	5.50	0.50	0.25	0.90
YPC077	0.01	42.97	101.02	12.18	0.04	125.00	0.50	7.90	0.30	0.25	0.30
YPC078	0.01	38.53	100.13	10.60	0.06	117.00	3.00	7.50	0.60	0.25	1.00
YPC079	0.02	39.80	100.44	11.26	0.01	196.00	2.00	5.50	0.50	0.25	0.90
YPC080	0.01	38.79	100.36	10.88	0.05	150.00	2.00	5.90	0.40	0.25	1.50
YPC081	0.01	37.60	100.10	10.63	0.10	125.00	4.00	5.70	0.50	0.25	1.40
YPC082	0.01	40.22	100.36	11.15	0.03	110.00	0.50	5.60	0.40	0.25	0.70
YPC083	0.01	39.73	100.45	10.98	0.10	116.00	3.00	4.20	0.40	0.25	0.80
YPC084	0.01	34.34	100.12	9.41	0.05	126.00	0.50	5.20	0.60	0.90	1.10
YPC085	0.01	36.27	100.15	10.16	0.02	116.00	0.50	5.50	0.60	0.60	1.20
YPC086	0.01	40.83	100.47	11.54	0.01	85.00	0.50	4.50	0.40	0.25	0.60
YPC087	0.01	39.75	100.35	11.29	0.03	120.00	2.00	5.30	0.40	0.25	0.50
YPC088	0.01	38.02	100.29	10.76	0.01	120.00	0.50	4.90	0.30	0.25	1.10
YPC089	0.02	35.49	100.05	9.76	0.01	154.00	0.50	7.80	0.80	1.50	1.30
YPC090	0.01	35.35	100.40	9.67	0.03	95.00	0.50	4.50	0.70	0.25	1.30
YPC091	0.01	34.63	100.23	9.47	0.08	111.00	2.00	6.70	0.70	1.00	1.70
YPC092	0.01	37.58	100.01	10.56	0.09	105.00	0.50	7.60	0.60	0.25	1.90
YPC093	0.01	38.41	100.36	10.83	0.04	109.00	2.00	5.20	0.60	0.25	1.60
YPC094	0.01	39.53	100.41	11.04	0.07	107.00	0.50	6.00	0.60	0.25	1.10
YPC095	0.01	40.17	100.23	11.52	0.08	59.00	4.00	3.10	0.20	0.25	0.70
YPC096	0.01	39.62	100.30	10.87	0.03	149.00	0.50	4.40	0.50	0.25	1.30
YPC097	0.01	40.25	100.57	11.15	0.03	104.00	0.50	5.20	0.40	0.25	0.70
YPC098	0.01	35.37	100.10	9.80	0.08	112.00	0.50	4.90	0.70	0.25	1.80
YPC099	0.01	39.55	100.44	11.08	0.01	120.00	0.50	6.80	0.50	0.70	1.10
YPC100	0.02	36.76	100.15	10.19	0.05	166.00	1.00	5.50	0.60	0.25	1.90
YPC101	0.02	38.53	100.69	10.57	0.10	153.00	3.00	4.30	0.40	0.25	1.50
YPC102	0.01	42.28	100.84	11.97	0.06	92.00	1.00	5.00	0.20	0.25	0.70
YPC103	0.01	44.50	100.98	12.72	0.01	70.00	0.50	3.00	0.10	0.25	0.10
YPC104	0.01	42.41	100.47	12.12	0.01	117.00	0.50	3.80	0.20	0.25	0.60
YPC105	0.01	39.96	100.39	11.28	0.12	156.00	0.50	2.80	0.30	0.25	1.70
YPC106	0.01	37.31	100.19	10.41	0.04	157.00	1.00	3.70	0.60	0.70	1.20
YPC107	0.01	39.12	100.21	10.69	0.12	147.00	2.00	4.40	0.70	1.00	1.50
YPC108	0.02	38.97	100.38	10.99	0.10	147.00	1.00	5.90	0.70	1.30	1.70
YPC109	0.02	39.03	100.80	10.70	0.01	144.00	0.50	4.50	0.70	2.40	1.30
YPC110	0.01	40.84	101.01	11.00	0.04	132.00	1.00	3.80	0.50	3.70	0.80
YPC111	0.01	40.93	100.68	11.09	0.08	96.00	2.00	2.10	0.30	2.70	1.80
YPC112	0.01	41.21	100.56	11.29	0.01	102.00	2.00	6.00	0.30	2.40	0.80
YPC113	0.01	39.66	100.51	10.68	0.04	94.00	0.50	5.70	0.40	3.10	1.60
YPC114	0.01	39.30	100.55	10.63	0.08	96.00	0.50	4.70	0.50	2.40	1.70
YPC115	0.01	41.88	100.31	11.67	0.10	102.00	0.50	4.30	0.30	1.50	0.80
YPC116	0.01	40.72	100.81	11.31	0.07	94.00	0.50	5.20	0.60	1.80	0.80
YPC117	0.01	38.67	100.33	10.57	0.01	110.00	0.50	8.30	0.70	2.40	1.80
YPC118	0.01	40.76	100.61	11.28	0.02	141.00	0.50	3.80	0.60	1.70	0.70
YPC119	0.01	40.00	100.42	11.21	0.09	54.00	0.50	2.00	0.10	0.25	0.60
YPC120	0.01	35.39	100.18	9.85	0.01	104.00	0.50	6.60	0.60	1.90	1.10
YPC121	0.01	35.38	100.03	9.74	0.01	108.00	0.50	5.50	0.60	2.00	1.50
YPC122	0.01	38.38	100.40	10.76	0.03	115.00	0.50	6.50	0.60	2.00	1.30
YPC123	0.01	38.15	100.88	10.48	0.04	119.00	0.50	5.60	0.70	2.50	1.10
YPC124	0.02	40.37	100.18	11.07	0.01	121.00	0.50	4.60	0.40	2.00	1.10
YPC125	0.01	39.44	100.63	10.83	0.01	97.00	0.50	4.70	0.40	1.50	1.30
YPC126	0.02	43.01	100.75	12.09	0.05	164.00	0.50	3.10	0.30	0.70	0.50
YPC127	0.02	42.60	100.53	12.01	0.03	172.00	0.50	3.70	0.20	0.80	0.70
YPC128	0.02	40.89	100.38	11.21	0.05	167.00	0.50	4.70	0.40	1.20	0.90
YPC129	0.01	41.75	100.58	11.81	0.01	105.00	0.50	5.30	0.30	1.00	0.40
YPC130	0.02	39.90	101.01	11.11	0.03	142.00	0.50	5.30	0.40	1.40	1.10
YPC131	0.01	40.90	100.62	11.24	0.14	123.00	0.50	5.10	0.40	1.30	0.80
YPC132	0.01	40.72	100.57	11.15	0.04	147.00	0.50	7.90	0.50	1.60	1.40
YPC133	0.02	38.86	100.42	10.61	0.04	157.00	0.50	5.50	0.60	2.00	0.70
YPC134	0.01	39.78	100.95	11.14	0.01	134.00	0.50	5.20	0.60	1.30	0.90
YPC135	0.02	38.17	100.25	10.28	0.06	158.00	0.50	6.70	0.60	2.40	1.30
YPC136	0.01	35.12	99.98	9.11	0.01	150.00	0.50	3.50	0.50	1.70	1.40
YPC137	0.01	40.45	101.10	11.07	0.11	112.00	0.50	4.50	0.50	1.90	0.90
YPC138	0.01	38.37	100.48	10.57	0.01	151.00	0.50	5.70	0.50	1.80	1.40
YPC139	0.02	37.95	100.33	10.43	0.02	158.00	0.50	5.00	0.50	1.40	1.40
YPC140	0.02	36.23	100.16	9.91	0.05	157.00	0.50	5.60	0.60	1.60	1.40
YPC141	0.02	38.62	100.41	10.85	0.06	169.00	0.50	4.80	0.50	1.30	1.60
YPC142	0.01	39.49	100.33	10.96	0.01	93.00	0.50	3.80	0.50	1.20	1.20
YPC143	0.02	40.28	100.39	11.28	0.06	179.00	0.50	5.50	0.50	0.90	0.80

	Nb_ppm	Rb_ppm	Sn_ppm	Sr_ppm	Ta_ppm	Th_ppm	U_ppm	V_ppm	W_ppm	Zr_ppm	Y_ppm	La_ppm	Ce_ppm
YPC070	0.40	9.50	0.50	514.80	0.05	0.90	0.10	8.00	0.25	25.40	4.90	4.50	6.60
YPC071	0.90	9.20	0.50	782.80	0.05	1.30	0.05	13.00	0.25	28.80	2.80	3.40	6.60
YPC072	0.30	5.00	0.50	686.90	0.05	0.90	0.05	4.00	0.25	15.20	4.20	4.00	5.10
YPC073	0.40	7.80	0.50	1208.10	0.05	1.70	0.60	9.00	0.25	25.20	4.70	5.20	9.10
YPC074	0.80	12.00	0.50	852.40	0.05	1.90	0.30	15.00	0.25	30.40	3.90	3.90	7.50
YPC075	1.10	11.70	0.50	1017.10	0.05	3.60	0.40	11.00	0.25	43.60	10.00	8.20	14.00
YPC076	1.20	12.80	0.50	727.70	0.05	2.70	0.30	26.00	0.25	36.40	6.30	5.40	8.90
YPC077	0.40	5.60	0.50	540.60	0.05	1.20	0.40	4.00	0.25	14.90	5.20	4.30	6.30
YPC078	1.30	16.30	0.50	518.90	0.05	2.30	0.20	15.00	0.25	43.80	7.80	6.90	12.10
YPC079	1.00	24.40	0.50	868.30	0.10	1.90	0.20	9.00	0.25	37.90	13.60	15.00	11.80
YPC080	1.10	12.20	0.50	898.20	0.05	2.10	0.30	11.00	0.25	49.30	4.10	5.00	9.10
YPC081	1.10	12.00	0.50	937.50	0.05	2.40	0.20	4.00	0.25	61.40	6.80	5.10	9.90
YPC082	0.70	9.60	0.50	610.80	0.05	2.10	0.30	9.00	0.25	24.50	10.20	9.60	13.30
YPC083	0.80	8.10	0.50	585.30	0.05	1.60	0.20	4.00	0.25	32.20	4.80	4.50	8.30
YPC084	1.40	12.80	0.50	478.60	0.05	3.20	0.20	9.00	0.25	49.80	10.70	8.90	15.30
YPC085	1.20	11.60	0.50	598.40	0.05	2.20	0.20	12.00	0.25	47.60	4.80	4.20	9.30
YPC086	0.40	6.60	0.50	804.40	0.05	1.50	0.30	4.00	0.25	36.20	3.70	3.00	5.50
YPC087	0.70	8.40	0.50	562.60	0.05	1.70	0.30	10.00	0.25	24.40	7.10	6.80	10.70
YPC088	1.10	11.30	0.50	851.90	0.10	2.10	0.40	9.00	0.25	40.10	5.60	5.40	10.20
YPC089	1.30	19.70	0.50	693.10	0.10	3.60	0.30	12.00	0.25	41.20	14.00	10.70	19.70
YPC090	1.30	14.90	0.50	1064.80	0.05	2.60	1.00	13.00	0.25	53.40	6.70	7.60	13.20
YPC091	1.80	16.00	0.50	686.00	0.10	3.00	0.60	16.00	0.25	72.10	8.60	8.40	16.10
YPC092	1.30	11.90	0.50	626.50	0.05	2.50	0.30	4.00	0.25	59.40	6.80	6.60	12.40
YPC093	1.20	12.70	0.50	615.70	0.70	2.10	0.30	10.00	0.25	59.50	7.00	6.70	12.70
YPC094	1.30	12.10	0.50	540.50	0.05	2.30	0.40	11.00	0.25	43.20	8.60	8.50	16.00
YPC095	0.30	7.30	0.50	1331.60	0.05	1.20	0.40	4.00	0.25	30.10	4.30	3.80	8.20
YPC096	1.60	11.40	0.50	1028.20	0.10	1.90	0.60	18.00	0.25	47.70	5.70	6.30	11.40
YPC097	0.40	9.90	0.50	588.00	0.05	2.10	0.30	10.00	0.25	22.60	7.20	7.20	10.50
YPC098	1.10	14.30	0.50	938.10	0.10	2.00	0.40	11.00	0.25	63.20	5.20	5.40	10.40
YPC099	1.50	11.90	0.50	553.80	0.05	2.20	0.40	11.00	0.25	48.70	8.90	8.60	16.00
YPC100	1.20	12.60	0.50	1074.10	0.05	2.30	0.30	9.00	0.25	78.50	5.00	5.50	11.80
YPC101	1.20	11.80	0.50	991.00	0.10	2.90	0.30	9.00	0.25	69.90	9.20	7.60	15.10
YPC102	0.50	4.70	0.50	620.40	0.05	0.90	0.30	4.00	0.25	23.20	4.90	5.40	7.50
YPC103	0.10	1.80	0.50	647.20	0.05	0.40	0.50	4.00	0.25	7.40	2.40	1.50	2.80
YPC104	0.40	4.60	0.50	779.70	0.05	1.10	0.20	4.00	0.25	25.30	3.30	3.50	5.30
YPC105	1.10	6.00	0.50	756.20	0.05	1.40	0.40	8.00	0.25	78.00	4.00	3.70	5.30
YPC106	1.20	12.10	0.50	637.50	0.10	2.40	0.30	12.00	0.25	43.30	6.60	7.20	9.50
YPC107	1.60	11.20	0.50	639.20	0.05	4.10	0.30	20.00	0.25	50.30	8.30	7.50	12.30
YPC108	1.60	13.00	0.50	542.40	0.10	2.40	0.30	16.00	0.25	44.30	7.20	6.70	11.70
YPC109	1.00	12.90	0.50	821.60	0.05	3.20	0.40	14.00	0.25	52.10	8.40	7.20	12.30
YPC110	2.30	11.40	0.50	799.00	0.20	2.70	0.10	28.00	0.25	37.80	6.70	6.80	12.50
YPC111	1.50	8.40	0.50	1150.70	0.05	1.30	0.05	19.00	0.25	43.00	3.60	4.30	7.90
YPC112	0.90	9.80	0.50	1087.40	0.05	1.40	0.05	20.00	0.25	31.90	4.60	5.00	9.40
YPC113	1.20	12.80	0.50	680.60	0.05	2.20	0.05	13.00	0.25	48.00	8.20	8.10	13.70
YPC114	1.10	12.00	0.50	701.80	0.05	1.90	0.05	15.00	0.25	51.30	6.10	6.40	12.30
YPC115	0.60	8.20	0.50	895.20	0.05	0.90	0.30	8.00	0.25	25.20	4.50	3.30	7.00
YPC116	0.90	9.40	0.50	415.80	0.05	1.50	0.20	11.00	0.25	31.40	4.90	4.10	10.10
YPC117	1.30	14.00	0.50	560.90	0.05	2.90	0.20	4.00	0.25	64.80	11.50	8.90	17.60
YPC118	1.00	9.30	0.50	503.60	0.05	1.80	0.20	10.00	0.25	28.10	6.70	5.50	8.50
YPC119	0.05	5.00	0.50	944.20	0.05	0.90	0.40	4.00	0.25	17.70	3.00	2.30	5.20
YPC120	1.10	15.40	0.50	501.30	0.05	2.20	0.20	10.00	0.25	42.60	6.40	5.70	12.60
YPC121	1.10	15.00	0.50	515.10	0.10	2.00	0.10	4.00	0.25	55.60	6.20	5.60	10.80
YPC122	1.40	13.50	0.50	852.10	0.10	2.90	0.30	10.00	0.25	57.20	9.00	7.70	16.00
YPC123	1.50	14.80	0.50	698.80	0.20	2.50	0.10	4.00	0.25	45.90	8.30	6.80	15.10
YPC124	0.90	10.30	0.50	789.90	0.05	1.50	0.05	13.00	0.25	34.40	6.00	4.90	10.50
YPC125	0.80	11.40	0.50	579.20	0.05	1.80	0.20	4.00	0.25	51.60	6.70	5.50	10.80
YPC126	0.40	6.10	0.50	704.80	0.05	1.10	0.05	4.00	0.25	22.50	3.00	2.80	5.40
YPC127	0.20	6.50	0.50	820.90	0.05	1.20	0.05	4.00	0.25	23.90	3.90	2.80	5.50
YPC128	1.30	10.70	0.50	681.70	0.10	3.20	0.20	4.00	0.25	35.20	22.20	21.20	23.70
YPC129	0.30	12.60	0.50	745.60	0.05	1.30	0.20	4.00	0.25	18.30	4.50	3.30	6.70
YPC130	0.90	13.10	0.50	822.30	0.05	1.50	0.20	13.00	0.25	40.90	5.50	4.70	9.60
YPC131	0.90	11.80	0.50	819.90	0.20	1.30	0.20	4.00	0.25	35.00	5.20	4.50	9.20
YPC132	0.70	9.50	0.50	609.90	0.05	2.20	0.20	28.00	0.25	42.20	7.90	7.70	10.90
YPC133	0.80	11.80	0.50	826.40	0.10	2.30	0.20	18.00	0.25	35.20	5.20	4.20	7.50
YPC134	1.00	10.00	0.50	672.40	0.10	2.40	0.20	36.00	0.25	33.70	4.90	4.00	9.00
YPC135	1.50	13.10	0.50	892.50	0.10	3.50	0.20	32.00	0.25	54.50	5.60	4.90	10.90
YPC136	1.10	15.70	0.50	1320.90	0.10	1.70	0.20	11.00	0.25	53.40	4.60	4.40	9.90
YPC137	1.00	10.20	0.50	771.20	0.05	2.10	0.10	9.00	0.25	35.40	5.70	5.10	10.30
YPC138	0.70	16.20	0.50	764.10	0.05	1.80	0.20	15.00	0.25	48.60	6.20	5.50	11.10
YPC139	0.90	9.00	0.50	832.10	0.05	1.80	0.30	10.00	0.25	52.80	5.50	4.40	9.30
YPC140	1.10	11.20	0.50	941.00	0.05	2.10	0.20	9.00	0.25	68.20	6.60	4.90	9.90
YPC141	0.70	8.00	0.50	775.40	0.10	1.90	0.20	4.00	0.25	53.70	5.30	5.20	9.90
YPC142	1.00	8.40	0.50	642.60	0.20	1.20	0.05	4.00	0.25	48.30	3.40	3.50	7.60
YPC143	0.60	6.80	0.50	665.20	0.05	1.60	0.10	4.00	0.25	36.90	5.00	3.80	7.80

	Pr_ppm	Nd_ppm	Sm_ppm	Eu_ppm	Gd_ppm	Tb_ppm	Dy_ppm	Ho_ppm	Er_ppm	Tm_ppm	Yb_ppm	Lu_ppm	Mo_ppm
YPC070	1.12	4.60	0.91	0.19	0.88	0.12	0.80	0.15	0.47	0.06	0.34	0.06	0.05
YPC071	0.77	3.10	0.70	0.14	0.61	0.09	0.63	0.13	0.31	0.06	0.35	0.04	0.05
YPC072	0.96	4.40	0.91	0.22	0.93	0.10	0.68	0.15	0.40	0.05	0.30	0.05	0.05
YPC073	1.16	4.40	0.97	0.18	0.98	0.12	0.61	0.12	0.50	0.07	0.57	0.06	0.05
YPC074	0.89	4.00	0.61	0.14	0.74	0.10	0.64	0.12	0.37	0.05	0.44	0.07	0.05
YPC075	1.79	6.70	1.44	0.38	1.59	0.24	1.52	0.38	0.85	0.14	0.95	0.15	0.10
YPC076	1.18	5.10	0.95	0.20	0.94	0.14	0.95	0.19	0.75	0.08	0.59	0.09	0.20
YPC077	0.93	4.20	0.83	0.15	0.80	0.10	0.64	0.11	0.40	0.04	0.51	0.06	0.05
YPC078	1.53	6.00	1.18	0.24	1.24	0.18	1.40	0.24	0.77	0.11	0.74	0.11	0.05
YPC079	2.85	13.10	2.13	0.49	2.35	0.30	1.82	0.34	1.12	0.14	1.05	0.15	0.05
YPC080	1.06	4.80	0.72	0.17	0.80	0.11	0.83	0.16	0.35	0.05	0.41	0.05	0.05
YPC081	1.29	4.70	1.14	0.22	1.21	0.16	0.91	0.21	0.67	0.09	0.72	0.09	0.05
YPC082	2.17	8.40	1.67	0.42	1.74	0.25	1.66	0.28	0.85	0.14	0.86	0.11	0.05
YPC083	1.14	4.10	0.78	0.17	0.94	0.13	0.82	0.16	0.63	0.07	0.42	0.06	0.05
YPC084	1.99	8.40	1.62	0.34	1.74	0.25	1.39	0.27	0.95	0.14	0.74	0.13	0.10
YPC085	1.11	4.10	0.83	0.19	0.92	0.11	0.84	0.12	0.48	0.09	0.37	0.06	0.05
YPC086	0.73	2.90	0.63	0.12	0.62	0.08	0.56	0.09	0.40	0.05	0.32	0.05	0.05
YPC087	1.58	6.40	1.28	0.26	1.34	0.18	1.13	0.25	0.66	0.10	0.48	0.08	0.05
YPC088	1.32	7.00	1.05	0.23	1.11	0.13	0.99	0.15	0.59	0.08	0.45	0.08	0.05
YPC089	2.82	13.00	2.46	0.58	2.47	0.36	1.78	0.40	1.29	0.18	1.10	0.17	0.10
YPC090	1.77	7.10	1.32	0.27	1.38	0.19	0.99	0.23	0.71	0.10	0.59	0.08	0.05
YPC091	1.92	9.50	1.49	0.32	1.66	0.23	1.18	0.27	0.83	0.13	0.63	0.10	0.05
YPC092	1.53	6.10	1.18	0.25	1.34	0.18	1.23	0.19	0.65	0.10	0.53	0.09	0.10
YPC093	1.50	6.20	1.21	0.30	1.27	0.18	1.19	0.25	0.71	0.09	0.69	0.09	0.05
YPC094	1.97	6.90	1.49	0.30	1.50	0.21	1.33	0.26	0.84	0.12	0.85	0.12	0.05
YPC095	1.00	3.60	0.78	0.16	0.78	0.10	0.66	0.15	0.55	0.05	0.44	0.06	0.05
YPC096	1.44	5.50	1.14	0.22	1.12	0.16	0.98	0.19	0.59	0.08	0.59	0.08	0.05
YPC097	1.65	5.90	1.24	0.28	1.30	0.18	1.07	0.21	0.87	0.09	0.65	0.08	0.05
YPC098	1.28	4.80	0.97	0.19	0.95	0.13	0.87	0.14	0.56	0.07	0.49	0.08	0.05
YPC099	2.00	6.80	1.63	0.36	1.56	0.22	1.37	0.31	0.94	0.12	0.71	0.12	0.05
YPC100	1.26	4.80	0.97	0.19	1.00	0.14	0.73	0.19	0.56	0.08	0.51	0.07	0.05
YPC101	1.84	7.60	1.58	0.31	1.65	0.25	1.59	0.30	0.94	0.12	0.75	0.13	0.05
YPC102	1.22	5.00	0.92	0.20	0.90	0.13	0.75	0.20	0.48	0.07	0.39	0.04	0.05
YPC103	0.34	1.40	0.24	0.06	0.32	0.04	0.40	0.06	0.26	0.02	0.15	0.02	0.05
YPC104	0.75	3.30	0.63	0.12	0.76	0.08	0.51	0.11	0.31	0.04	0.21	0.04	0.05
YPC105	0.81	3.20	0.53	0.12	0.62	0.08	0.67	0.11	0.46	0.05	0.40	0.07	0.05
YPC106	1.31	6.50	1.09	0.19	1.09	0.15	0.93	0.23	0.60	0.09	0.61	0.07	0.10
YPC107	1.65	6.70	1.09	0.28	1.29	0.19	1.19	0.24	0.72	0.11	0.73	0.10	0.10
YPC108	1.45	6.70	1.21	0.25	1.22	0.17	1.03	0.18	0.73	0.10	0.58	0.09	0.05
YPC109	1.78	7.50	1.37	0.31	1.60	0.21	1.49	0.27	0.76	0.12	0.81	0.11	0.05
YPC110	1.54	6.10	1.23	0.25	1.26	0.18	1.16	0.24	0.71	0.08	0.52	0.10	0.05
YPC111	0.88	3.70	0.52	0.15	0.76	0.10	0.51	0.14	0.41	0.06	0.39	0.04	0.05
YPC112	1.14	4.20	0.92	0.20	0.99	0.13	0.70	0.19	0.44	0.06	0.30	0.05	0.10
YPC113	1.75	7.80	1.38	0.32	1.37	0.21	1.43	0.26	0.80	0.12	0.75	0.13	0.05
YPC114	1.45	6.20	1.08	0.27	1.23	0.15	1.10	0.25	0.59	0.08	0.57	0.10	0.05
YPC115	0.82	3.80	0.79	0.17	0.79	0.10	0.82	0.13	0.37	0.05	0.34	0.06	0.05
YPC116	1.14	4.80	1.09	0.22	1.13	0.14	0.85	0.19	0.45	0.07	0.44	0.08	0.10
YPC117	2.27	8.90	2.00	0.44	2.17	0.27	1.93	0.34	1.01	0.16	1.07	0.15	0.05
YPC118	1.29	5.20	1.03	0.25	1.10	0.15	0.96	0.19	0.50	0.09	0.49	0.09	0.05
YPC119	0.61	2.40	0.58	0.13	0.64	0.07	0.57	0.08	0.31	0.04	0.28	0.04	0.05
YPC120	1.44	6.20	1.28	0.30	1.30	0.17	1.28	0.22	0.72	0.10	0.67	0.09	0.05
YPC121	1.40	5.70	1.22	0.30	1.27	0.17	1.06	0.23	0.65	0.10	0.50	0.10	0.05
YPC122	1.94	8.60	1.68	0.38	1.81	0.23	1.48	0.27	0.80	0.13	0.71	0.12	0.05
YPC123	1.76	7.30	1.48	0.34	1.61	0.20	1.38	0.28	0.68	0.11	0.63	0.10	0.05
YPC124	1.32	5.10	1.23	0.25	1.14	0.14	1.02	0.20	0.56	0.09	0.48	0.07	0.05
YPC125	1.32	6.00	1.21	0.28	1.19	0.16	1.10	0.22	0.62	0.09	0.51	0.08	0.05
YPC126	0.72	3.50	0.61	0.15	0.58	0.07	0.58	0.09	0.29	0.05	0.32	0.06	0.05
YPC127	0.71	3.20	0.65	0.14	0.72	0.09	0.64	0.08	0.34	0.05	0.32	0.05	0.05
YPC128	4.74	20.60	3.93	0.82	4.34	0.52	3.40	0.62	1.80	0.28	1.63	0.22	0.30
YPC129	0.83	2.60	0.84	0.21	1.02	0.12	0.95	0.14	0.53	0.07	0.39	0.06	0.05
YPC130	1.15	6.10	1.03	0.24	1.19	0.14	1.04	0.17	0.51	0.08	0.55	0.08	0.05
YPC131	1.13	4.20	0.95	0.21	0.97	0.12	1.01	0.18	0.46	0.07	0.55	0.07	0.05
YPC132	1.80	6.80	1.53	0.35	1.53	0.17	1.22	0.23	0.66	0.10	0.54	0.09	0.05
YPC133	1.03	3.40	0.92	0.17	0.88	0.12	0.94	0.16	0.48	0.08	0.65	0.08	0.05
YPC134	1.04	4.80	0.86	0.21	0.88	0.11	0.60	0.17	0.44	0.07	0.38	0.07	0.10
YPC135	1.28	5.20	1.12	0.26	1.22	0.14	0.97	0.18	0.60	0.10	0.64	0.10	0.30
YPC136	1.11	4.50	0.86	0.18	0.95	0.12	0.79	0.16	0.53	0.08	0.47	0.06	0.10
YPC137	1.31	4.80	1.23	0.28	1.11	0.15	0.99	0.19	0.57	0.09	0.54	0.09	0.05
YPC138	1.36	5.70	1.19	0.28	1.21	0.17	1.13	0.20	0.52	0.10	0.56	0.09	0.05
YPC139	1.12	5.00	1.00	0.20	1.04	0.13	0.93	0.14	0.46	0.07	0.44	0.09	0.05
YPC140	1.20	5.40	1.20	0.26	1.15	0.15	1.22	0.21	0.70	0.09	0.58	0.10	0.05
YPC141	1.21	5.20	0.96	0.23	1.15	0.13	0.97	0.17	0.56	0.08	0.44	0.08	0.05
YPC142	0.83	4.30	0.76	0.17	0.79	0.09	0.68	0.12	0.30	0.05	0.37	0.05	0.10
YPC143	0.97	3.90	0.82	0.23	1.03	0.11	0.81	0.15	0.43	0.07	0.45	0.06	0.05

	Cu_ppm	Pb_ppm	Zn_ppm	Ni_ppm	As_ppm	Cd_ppm	Sb_ppm	Bi_ppm	Ag_ppm	Au_ppb	Hg_ppm	Tl_ppm	Se_ppm
YPC070	4.00	1.20	3.00	4.00	1.80	0.05	0.05	0.05	0.05	1.80	0.03	0.05	0.25
YPC071	2.90	1.70	3.00	3.50	1.70	0.05	0.10	0.05	0.05	1.40	0.04	0.05	0.25
YPC072	3.20	1.00	1.00	3.20	1.60	0.05	0.10	0.05	0.05	1.60	0.02	0.05	0.25
YPC073	3.70	2.10	5.00	5.70	0.90	0.05	0.05	0.10	0.05	3.60	0.04	0.05	0.25
YPC074	3.60	2.00	3.00	6.60	1.90	0.05	0.10	0.05	0.05	0.25	0.04	0.05	0.25
YPC075	6.60	2.70	6.00	7.70	2.40	0.05	0.10	0.05	0.05	1.80	0.07	0.05	1.00
YPC076	3.40	3.50	7.00	8.90	7.90	0.05	0.30	0.05	0.05	1.20	0.11	0.10	0.25
YPC077	1.80	1.30	2.00	6.30	1.90	0.05	0.20	0.05	0.05	4.80	0.06	0.10	0.25
YPC078	2.50	2.50	10.00	7.80	1.70	0.05	0.05	0.05	0.05	0.25	0.05	0.05	0.25
YPC079	6.40	1.00	2.00	4.80	2.20	0.05	0.05	0.05	0.05	0.50	0.07	0.05	0.25
YPC080	3.20	1.20	2.00	6.10	1.30	0.05	0.05	0.05	0.05	0.25	0.07	0.05	0.25
YPC081	5.70	1.60	119.00	7.30	1.50	0.05	0.05	0.05	0.05	1.70	0.07	0.05	0.25
YPC082	3.10	2.10	3.00	5.90	1.80	0.05	0.05	0.05	0.05	0.25	0.07	0.05	0.25
YPC083	3.50	1.50	2.00	4.80	1.60	0.05	0.05	0.05	0.05	2.80	0.08	0.05	0.25
YPC084	2.90	2.40	6.00	7.70	1.10	0.05	0.05	0.05	0.05	0.80	0.06	0.05	0.25
YPC085	2.20	1.90	2.00	5.00	1.50	0.05	0.05	0.05	0.05	3.40	0.05	0.05	0.60
YPC086	2.80	1.30	3.00	6.40	1.00	0.05	0.05	0.05	0.05	2.40	0.04	0.05	0.25
YPC087	2.70	1.80	3.00	5.90	1.20	0.05	0.05	0.05	0.05	1.20	0.04	0.05	0.25
YPC088	5.70	1.80	4.00	5.60	1.50	0.05	0.05	0.05	0.05	0.70	0.05	0.05	0.25
YPC089	2.90	3.40	4.00	7.70	1.80	0.05	0.05	0.05	0.05	0.90	0.08	0.10	0.90
YPC090	3.10	2.20	3.00	7.50	1.50	0.05	0.05	0.05	0.05	2.20	0.04	0.05	0.25
YPC091	4.50	2.90	4.00	10.40	1.00	0.05	0.05	0.05	0.05	1.60	0.03	0.10	1.00
YPC092	4.20	2.30	4.00	6.20	1.00	0.05	0.05	0.05	0.05	0.60	0.07	0.05	0.25
YPC093	4.90	2.40	4.00	6.70	1.00	0.05	0.05	0.05	0.05	0.25	0.08	0.05	0.60
YPC094	5.60	2.90	4.00	7.20	1.20	0.05	0.05	0.05	0.05	0.60	0.05	0.05	0.25
YPC095	2.80	1.00	3.00	4.10	0.25	0.05	0.05	0.05	0.05	0.25	0.01	0.05	0.50
YPC096	7.30	2.10	4.00	6.30	2.60	0.05	0.20	0.05	0.05	3.60	0.03	0.05	0.50
YPC097	2.80	1.90	2.00	4.90	1.30	0.05	0.10	0.05	0.05	0.50	0.06	0.05	0.25
YPC098	5.30	2.00	5.00	6.70	1.20	0.05	0.05	0.05	0.05	0.90	0.05	0.05	0.70
YPC099	6.00	3.00	5.00	8.80	1.10	0.05	0.05	0.05	0.05	0.25	0.05	0.05	0.50
YPC100	7.20	2.10	5.00	6.10	1.20	0.05	0.10	0.05	0.05	3.00	0.07	0.05	0.25
YPC101	5.40	3.30	5.00	10.10	2.70	0.05	0.10	0.05	0.05	1.40	0.10	0.05	0.25
YPC102	3.10	1.00	5.00	4.10	1.10	0.05	0.10	0.05	0.05	1.80	0.04	0.05	0.60
YPC103	2.40	0.50	7.00	3.30	1.20	0.05	0.05	0.05	0.05	3.00	0.01	0.05	0.25
YPC104	3.30	0.90	12.00	4.10	1.30	0.05	0.05	0.05	0.05	1.80	0.04	0.05	0.25
YPC105	4.80	1.00	4.00	3.10	2.00	0.05	0.10	0.05	0.05	1.20	0.06	0.05	0.25
YPC106	3.80	2.40	7.00	4.80	1.80	0.05	0.10	0.05	0.05	0.25	0.04	0.05	0.25
YPC107	3.70	2.70	5.00	4.70	2.90	0.05	0.05	0.05	0.05	1.20	0.06	0.05	0.25
YPC108	3.50	2.60	4.00	4.40	2.10	0.05	0.05	0.05	0.05	0.25	0.05	0.05	0.25
YPC109	4.00	2.90	5.00	4.20	2.50	0.05	0.10	0.10	0.05	1.20	0.05	0.05	0.25
YPC110	3.40	2.70	4.00	4.50	1.50	0.05	0.05	0.05	0.05	0.60	0.04	0.05	0.25
YPC111	4.40	1.40	3.00	4.80	2.20	0.05	0.10	0.05	0.05	1.80	0.05	0.05	0.25
YPC112	5.30	1.90	3.00	6.50	1.50	0.05	0.10	0.05	0.05	2.40	0.05	0.05	0.25
YPC113	3.60	3.30	6.00	8.10	1.60	0.05	0.05	0.05	0.05	1.60	0.04	0.05	0.25
YPC114	3.50	2.60	6.00	7.80	1.60	0.05	0.05	0.05	0.05	0.25	0.05	0.05	0.25
YPC115	6.10	1.20	3.00	5.20	1.80	0.05	0.05	0.20	0.05	1.90	0.03	0.05	0.25
YPC116	5.30	2.00	4.00	6.80	2.30	0.05	0.05	0.05	0.05	1.40	0.05	0.05	0.25
YPC117	4.70	3.00	7.00	7.60	1.70	0.05	0.05	0.05	0.05	0.80	0.04	0.05	0.25
YPC118	2.80	2.00	4.00	3.30	2.30	0.05	0.05	0.05	0.05	0.25	0.05	0.05	0.25
YPC119	1.40	0.80	1.00	2.00	1.40	0.05	0.05	0.05	0.05	0.25	0.02	0.05	0.25
YPC120	4.90	2.20	4.00	6.40	1.90	0.05	0.05	0.05	0.05	2.30	0.03	0.05	0.25
YPC121	5.00	2.00	9.00	7.60	1.50	0.05	0.05	0.05	0.05	0.25	0.04	0.05	0.25
YPC122	5.90	3.40	5.00	8.40	1.60	0.05	0.05	0.05	0.05	2.00	0.06	0.05	0.25
YPC123	7.80	2.90	6.00	6.30	1.00	0.05	0.05	0.05	0.05	1.90	0.04	0.05	0.25
YPC124	5.10	2.30	4.00	4.50	2.10	0.05	0.05	0.05	0.05	4.80	0.04	0.05	0.25
YPC125	4.80	2.00	3.00	6.00	1.50	0.05	0.05	0.05	0.05	0.25	0.03	0.05	0.25
YPC126	3.70	0.80	2.00	4.70	1.50	0.05	0.05	0.05	0.05	0.25	0.05	0.05	0.25
YPC127	4.70	0.90	3.00	4.80	0.60	0.05	0.10	0.05	0.05	1.00	0.07	0.05	0.25
YPC128	20.80	1.80	3.00	4.30	1.00	0.05	0.05	0.05	0.05	1.50	0.04	0.05	0.25
YPC129	8.60	1.20	3.00	6.30	1.20	0.05	0.05	0.05	0.05	0.90	0.02	0.05	0.25
YPC130	18.20	1.40	3.00	7.80	2.00	0.05	0.05	0.05	0.05	0.25	0.01	0.05	0.25
YPC131	4.20	1.60	3.00	6.40	1.00	0.05	0.10	0.05	0.05	0.25	0.04	0.05	0.25
YPC132	4.10	1.60	2.00	5.70	11.60	0.05	0.30	0.05	0.05	0.50	0.05	0.05	0.25
YPC133	3.20	1.60	3.00	6.30	4.40	0.05	0.30	0.05	0.05	1.50	0.04	0.05	0.25
YPC134	3.70	1.30	5.00	4.70	10.40	0.05	0.30	0.05	0.05	0.25	0.03	0.05	0.25
YPC135	4.60	2.90	5.00	7.60	10.70	0.05	0.30	0.05	0.05	0.80	0.03	0.05	0.25
YPC136	18.80	2.40	4.00	16.10	3.90	0.05	0.40	0.05	0.05	5.90	0.03	0.05	0.25
YPC137	5.60	2.30	4.00	4.80	1.00	0.05	0.05	0.05	0.05	2.70	0.04	0.05	0.25
YPC138	16.30	1.60	4.00	6.20	1.60	0.05	0.05	0.05	0.05	0.25	0.02	0.05	0.25
YPC139	6.80	2.40	4.00	7.20	2.10	0.05	0.20	0.05	0.05	1.90	0.03	0.05	0.25
YPC140	9.90	2.50	4.00	10.20	1.50	0.05	0.05	0.05	0.05	1.10	0.07	0.05	0.25
YPC141	5.60	1.80	3.00	6.90	1.80	0.05	0.10	0.05	0.05	1.50	0.08	0.05	0.25
YPC142	3.40	2.00	3.00	5.10	1.60	0.05	0.20	0.05	0.05	1.10	0.02	0.05	0.25
YPC143	3.90	1.30	3.00	4.70	3.00	0.05	0.20	0.05	0.05	3.00	0.05	0.05	0.25

		Duplicate ID	Transect	Location	Sample_Type	Orig_Grid_ID	Orig_East	Orig_North
Yorke Peninsula	YPC144		7	Coleman Rd	CaCO3 rock	GDA94_53H	768779	6208010
Yorke Peninsula	YPC145		7	Coleman Rd	CaCO3 rock	GDA94_53H	765913	6208598
Yorke Peninsula	YPC146		7	Coleman Rd	CaCO3 rock	GDA94_53H	764683	6208680
Yorke Peninsula	YPC147		7	Honner Rd	CaCO3 rock	GDA94_53H	763528	6208676
Yorke Peninsula	YPC148		7	Honner Rd	CaCO3 rock	GDA94_53H	758942	6208208
Yorke Peninsula	YPC149		7	Honner Rd	CaCO3 rock	GDA94_53H	757727	6208082
Yorke Peninsula	YPC150		7	Pipeline Rd	CaCO3 rock	GDA94_53H	755400	6208103
Yorke Peninsula	YPC151		7	Pipeline Rd	CaCO3 rock	GDA94_53H	751022	6208414
Yorke Peninsula	YPC152		7	Pipeline Rd	CaCO3 rock	GDA94_53H	749123	6209142
Yorke Peninsula	YPC153		7	Pipeline Rd	CaCO3 rock	GDA94_53H	748470	6209278
Yorke Peninsula	YPC154		7	Pipeline Rd	CaCO3 rock	GDA94_53H	747070	6209678
Yorke Peninsula	YPC155		7	Pipeline Rd	CaCO3 rock	GDA94_53H	744901	6210312
Yorke Peninsula	YPC156		7	Ferguson Rd	CaCO3 rock	GDA94_53H	743145	6210359
Yorke Peninsula	YPC157		7	Ferguson Rd	CaCO3 rock	GDA94_53H	741997	6210389
Yorke Peninsula	YPC158		7	Ferguson Rd	CaCO3 rock	GDA94_53H	740024	6211086
Yorke Peninsula	YPC159		7	Ferguson Rd	CaCO3 rock	GDA94_53H	737674	6212139
Yorke Peninsula	YPC160		7	Tipara Springs Rd	CaCO3 rock	GDA94_53H	735704	6212860
Yorke Peninsula	YPC161		7	Tipara Springs Rd	CaCO3 rock	GDA94_53H	734040	6213231
Yorke Peninsula	YPC162	YPC140	7	Coleman Rd	CaCO3 rock	GDA94_53H	774210	6208448
Yorke Peninsula	YPC163	YPC150	7	Pipeline Rd	CaCO3 rock	GDA94_53H	755400	6208103
Yorke Peninsula	YPC164	YPC158	7	Ferguson Rd	CaCO3 rock	GDA94_53H	740024	6211086
Yorke Peninsula	YPC165	YPC166	8	Kulpara Maitland Rd	CaCO3 rock	GDA94_53H	773708	6223564
Yorke Peninsula	YPC166		8	Kulpara Maitland Rd	CaCO3 rock	GDA94_53H	773708	6223564
Yorke Peninsula	YPC167		8	Holman Rd	CaCO3 rock	GDA94_53H	769068	6223705
Yorke Peninsula	YPC168		8	Holman Rd	CaCO3 rock	GDA94_53H	767779	6223743
Yorke Peninsula	YPC169		8	Holman Rd	CaCO3 rock	GDA94_53H	766173	6223795
Yorke Peninsula	YPC170		8	Holman Rd	CaCO3 rock	GDA94_53H	764731	6223819
Yorke Peninsula	YPC171		8	Holman Rd	CaCO3 rock	GDA94_53H	763352	6223810
Yorke Peninsula	YPC172		8	Holman Rd	CaCO3 rock	GDA94_53H	761879	6223795
Yorke Peninsula	YPC173		8	Holman Rd	CaCO3 rock	GDA94_53H	760637	6223789
Yorke Peninsula	YPC174		8	Peddlar Rd	CaCO3 rock	GDA94_53H	759588	6223784
Yorke Peninsula	YPC175		8	Peddlar Rd	CaCO3 rock	GDA94_53H	758320	6223769
Yorke Peninsula	YPC176		8	Peddlar Rd	CaCO3 rock	GDA94_53H	757175	6223759
Yorke Peninsula	YPC177		8	Peddlar Rd	CaCO3 rock	GDA94_53H	755954	6223748
Yorke Peninsula	YPC178		8	Peddlar Rd	CaCO3 rock	GDA94_53H	753600	6223730
Yorke Peninsula	YPC179		8	Peddlar Rd	CaCO3 rock	GDA94_53H	752444	6223718
Yorke Peninsula	YPC180		8	Peddlar Rd	CaCO3 rock	GDA94_53H	750027	6223743
Yorke Peninsula	YPC181		8	Peddlar Rd	CaCO3 rock	GDA94_53H	748556	6223789
Yorke Peninsula	YPC182		8	Peddlar Rd	CaCO3 rock	GDA94_53H	746972	6223828
Yorke Peninsula	YPC183		8	Peddlar Rd	CaCO3 rock	GDA94_53H	745978	6223854
Yorke Peninsula	YPC184		8	Peddlar Rd	CaCO3 rock	GDA94_53H	740253	6224016
Yorke Peninsula	YPC185	YPC167	8	Holman Rd	CaCO3 rock	GDA94_53H	769068	6223705
Yorke Peninsula	YPC186	YPC174	8	Peddlar Rd	CaCO3 rock	GDA94_53H	759588	6223784
Yorke Peninsula	YPC187		9	Bird Island Rd	CaCO3 rock	GDA94_53H	737692	6237829
Yorke Peninsula	YPC188		9	Bird Island Rd	CaCO3 rock	GDA94_53H	738732	6237803
Yorke Peninsula	YPC189		9	Bird Island Rd	CaCO3 rock	GDA94_53H	740390	6237760
Yorke Peninsula	YPC190		9	Bird Island Rd	CaCO3 rock	GDA94_53H	741714	6237731
Yorke Peninsula	YPC191		9	Shooting Club Rd	CaCO3 rock	GDA94_53H	743291	6237689
Yorke Peninsula	YPC192		9	Shooting Club Rd	CaCO3 rock	GDA94_53H	744433	6237660
Yorke Peninsula	YPC193		9	Shooting Club Rd	CaCO3 rock	GDA94_53H	745843	6237627
Yorke Peninsula	YPC194		9	Thomas Plains Rd	CaCO3 rock	GDA94_53H	753190	6238307
Yorke Peninsula	YPC195		9	Thomas Plains Rd	CaCO3 rock	GDA94_53H	754200	6238280
Yorke Peninsula	YPC196		9	Thomas Plains Rd	CaCO3 rock	GDA94_53H	755470	6238245
Yorke Peninsula	YPC197		9	Thomas Plains Rd	CaCO3 rock	GDA94_53H	756785	6238207
Yorke Peninsula	YPC198		9	Thomas Plains Rd	CaCO3 rock	GDA94_53H	758129	6238171
Yorke Peninsula	YPC199		9	Thomas Plains Rd	CaCO3 rock	GDA94_53H	760136	6238121
Yorke Peninsula	YPC200		9	Thomas Plains Rd	CaCO3 rock	GDA94_53H	761372	6238085
Yorke Peninsula	YPC201		9	Thomas Plains Rd	CaCO3 rock	GDA94_53H	762445	6238059
Yorke Peninsula	YPC202		9	Thomas Plains Rd	CaCO3 rock	GDA94_53H	763543	6238031
Yorke Peninsula	YPC203		9	Thomas Plains Rd	CaCO3 rock	GDA94_53H	764784	6237995
Yorke Peninsula	YPC204		9	Sand Pit Rd	CaCO3 rock	GDA94_53H	771966	6231507
Yorke Peninsula	YPC205		9	Sand Pit Rd	CaCO3 rock	GDA94_53H	773232	6231400
Yorke Peninsula	YPC206		9	Sand Pit Rd	CaCO3 rock	GDA94_53H	774288	6231316
Yorke Peninsula	YPC207		9	Sand Pit Rd	CaCO3 rock	GDA94_53H	775567	6231206
Yorke Peninsula	YPC208		9	Sand Pit Rd	CaCO3 rock	GDA94_53H	776935	6231094
Yorke Peninsula	YPC209	YPC195	9	Thomas Plains Rd	CaCO3 rock	GDA94_53H	754200	6238280
Yorke Peninsula	YPC210	YPC201	9	Thomas Plains Rd	CaCO3 rock	GDA94_53H	762445	6238059
Yorke Peninsula	TIP001c	Rock01		Nth of Arthurton Waylands Rd	CaCO3 rock	GDA94_53H	753802	6215153
Yorke Peninsula	TIP001g	Rock05		Nth of Arthurton Waylands Rd	CaCO3 rock	GDA94_53H	753802	6215153
Yorke Peninsula	WAR001	Rock02		Kadina	CaCO3 rock	GDA94_53H	751433	6240759
Yorke Peninsula	MNL024	Rock03		Minlaton	CaCO3 rock	GDA94_53H	740690	6143940
Yorke Peninsula	MNL044	Rock04		Walking Trail Gum Flat Minlaton	CaCO3 rock	GDA94_53H	738452	6148975

	RL	Orig_Survey_Method	Orig_Surve	Date	Sampled_By	Sample_Depth	Weight_kg	SiO2_pct	Al2O3_pct
YPC144	118	Garmin GPS Map62S	KWolff	1/04/2012	RWolff	ground level	2	12.1	1.35
YPC145	138	Garmin GPS Map62S	KWolff	1/04/2012	RWolff	ground level	2	20.9	2.09
YPC146	161	Garmin GPS Map62S	KWolff	1/04/2012	RWolff	ground level	2	8.4	1.53
YPC147	160	Garmin GPS Map62S	KWolff	1/04/2012	RWolff	ground level	2	15.0	2.74
YPC148	175	Garmin GPS Map62S	KWolff	1/04/2012	RWolff	ground level	2	6.3	1.38
YPC149	179	Garmin GPS Map62S	KWolff	1/04/2012	RWolff	ground level	2	21.1	3.32
YPC150	203	Garmin GPS Map62S	KWolff	1/04/2012	RWolff	ground level	2	17.0	1.91
YPC151	136	Garmin GPS Map62S	KWolff	1/04/2012	RWolff	ground level	2	5.8	1.19
YPC152	124	Garmin GPS Map62S	KWolff	1/04/2012	RWolff	ground level	2	8.4	2.64
YPC153	104	Garmin GPS Map62S	KWolff	1/04/2012	RWolff	ground level	2	10.4	1.70
YPC154	127	Garmin GPS Map62S	KWolff	1/04/2012	RWolff	ground level	2	4.9	1.02
YPC155	130	Garmin GPS Map62S	KWolff	1/04/2012	RWolff	ground level	2	13.1	1.31
YPC156	120	Garmin GPS Map62S	KWolff	1/04/2012	RWolff	ground level	2	29.6	2.37
YPC157	103	Garmin GPS Map62S	KWolff	1/04/2012	RWolff	ground level	2	12.7	1.50
YPC158	75	Garmin GPS Map62S	KWolff	1/04/2012	RWolff	ground level	2	19.7	1.36
YPC159	51	Garmin GPS Map62S	KWolff	1/04/2012	RWolff	ground level	2	18.9	1.50
YPC160	31	Garmin GPS Map62S	KWolff	1/04/2012	RWolff	ground level	2	13.4	1.65
YPC161	22	Garmin GPS Map62S	KWolff	1/04/2012	RWolff	ground level	2	19.1	1.82
YPC162	95	Garmin GPS Map62S	KWolff	1/04/2012	RWolff	ground level	2	16.9	1.64
YPC163	203	Garmin GPS Map62S	KWolff	1/04/2012	RWolff	ground level	2	14.9	1.61
YPC164	75	Garmin GPS Map62S	KWolff	1/04/2012	RWolff	ground level	2	18.4	1.29
YPC165	104	Garmin GPS Map62S	KWolff	14/04/2012	RWolff	ground level	2	6.2	0.94
YPC166	104	Garmin GPS Map62S	KWolff	14/04/2012	RWolff	ground level	2	6.1	0.87
YPC167	146	Garmin GPS Map62S	KWolff	14/04/2012	RWolff	ground level	2	10.0	1.48
YPC168	141	Garmin GPS Map62S	KWolff	14/04/2012	RWolff	ground level	2	12.3	1.91
YPC169	131	Garmin GPS Map62S	KWolff	14/04/2012	RWolff	ground level	2	12.7	1.83
YPC170	123	Garmin GPS Map62S	KWolff	14/04/2012	RWolff	ground level	2	8.9	1.56
YPC171	117	Garmin GPS Map62S	KWolff	14/04/2012	RWolff	ground level	2	9.5	1.54
YPC172	114	Garmin GPS Map62S	KWolff	14/04/2012	RWolff	ground level	2	5.6	0.99
YPC173	114	Garmin GPS Map62S	KWolff	14/04/2012	RWolff	ground level	2	9.9	1.54
YPC174	113	Garmin GPS Map62S	KWolff	14/04/2012	RWolff	ground level	2	13.0	1.45
YPC175	99	Garmin GPS Map62S	KWolff	14/04/2012	RWolff	ground level	2	11.2	1.56
YPC176	95	Garmin GPS Map62S	KWolff	14/04/2012	RWolff	ground level	2	5.3	0.95
YPC177	86	Garmin GPS Map62S	KWolff	14/04/2012	RWolff	ground level	2	3.4	0.61
YPC178	80	Garmin GPS Map62S	KWolff	14/04/2012	RWolff	ground level	2	9.2	1.33
YPC179	79	Garmin GPS Map62S	KWolff	14/04/2012	RWolff	ground level	2	9.4	1.41
YPC180	98	Garmin GPS Map62S	KWolff	14/04/2012	RWolff	ground level	2	12.2	2.07
YPC181	81	Garmin GPS Map62S	KWolff	14/04/2012	RWolff	ground level	2	7.9	1.82
YPC182	77	Garmin GPS Map62S	KWolff	14/04/2012	RWolff	ground level	2	14.7	2.49
YPC183	65	Garmin GPS Map62S	KWolff	14/04/2012	RWolff	ground level	2	14.4	2.28
YPC184	42	Garmin GPS Map62S	KWolff	14/04/2012	RWolff	ground level	2	10.3	1.21
YPC185	146	Garmin GPS Map62S	KWolff	14/04/2012	RWolff	ground level	2	10.5	1.51
YPC186	113	Garmin GPS Map62S	KWolff	14/04/2012	RWolff	ground level	2	12.2	1.47
YPC187	4	Garmin GPS Map62S	KWolff	14/04/2012	RWolff	ground level	2	17.5	1.05
YPC188	8	Garmin GPS Map62S	KWolff	14/04/2012	RWolff	ground level	2	14.1	1.90
YPC189	16	Garmin GPS Map62S	KWolff	14/04/2012	RWolff	ground level	2	16.0	2.29
YPC190	20	Garmin GPS Map62S	KWolff	14/04/2012	RWolff	ground level	2	12.4	2.25
YPC191	27	Garmin GPS Map62S	KWolff	14/04/2012	RWolff	ground level	2	13.6	2.65
YPC192	29	Garmin GPS Map62S	KWolff	14/04/2012	RWolff	ground level	2	21.2	3.02
YPC193	37	Garmin GPS Map62S	KWolff	14/04/2012	RWolff	ground level	2	13.5	2.16
YPC194	41	Garmin GPS Map62S	KWolff	14/04/2012	RWolff	ground level	2	17.4	2.40
YPC195	41	Garmin GPS Map62S	KWolff	14/04/2012	RWolff	ground level	2	14.5	1.84
YPC196	41	Garmin GPS Map62S	KWolff	14/04/2012	RWolff	ground level	2	12.9	2.10
YPC197	44	Garmin GPS Map62S	KWolff	15/04/2012	RWolff	ground level	2	12.2	1.94
YPC198	44	Garmin GPS Map62S	KWolff	15/04/2012	RWolff	ground level	2	12.8	2.17
YPC199	49	Garmin GPS Map62S	KWolff	15/04/2012	RWolff	ground level	2	12.1	2.20
YPC200	55	Garmin GPS Map62S	KWolff	15/04/2012	RWolff	ground level	2	12.9	2.44
YPC201	61	Garmin GPS Map62S	KWolff	15/04/2012	RWolff	ground level	2	12.2	2.28
YPC202	69	Garmin GPS Map62S	KWolff	15/04/2012	RWolff	ground level	2	20.5	2.38
YPC203	76	Garmin GPS Map62S	KWolff	15/04/2012	RWolff	ground level	2	15.4	1.99
YPC204	109	Garmin GPS Map62S	KWolff	15/04/2012	RWolff	ground level	2	11.7	1.68
YPC205	115	Garmin GPS Map62S	KWolff	15/04/2012	RWolff	ground level	2	11.1	1.79
YPC206	119	Garmin GPS Map62S	KWolff	15/04/2012	RWolff	ground level	2	11.8	1.39
YPC207	100	Garmin GPS Map62S	KWolff	15/04/2012	RWolff	ground level	2	13.9	1.61
YPC208	118	Garmin GPS Map62S	KWolff	15/04/2012	RWolff	ground level	2	10.0	1.21
YPC209	41	Garmin GPS Map62S	KWolff	14/04/2012	RWolff	ground level	2	12.4	1.72
YPC210	61	Garmin GPS Map62S	KWolff	15/04/2012	RWolff	ground level	2	12.3	2.38
TIP001c	115	Garmin GPS Map62S	KWolff		KWolff	ground level	2	8.2	1.2
TIP001g	115	Garmin GPS Map62S	KWolff		KWolff	ground level	2	6.4	0.91
WAR001	29	Garmin GPS Map62S	KWolff		KWolff	ground level	2	12.21	1.72
MNL024	81	Garmin GPS Map62S	KWolff		KWolff	ground level	2	19.1	2.46
MNL044	60	Garmin GPS Map62S	KWolff		KWolff	ground level	2	11.46	1.01

	Fe2O3_pct	CaO_pct	Ca/Sr	MgO_pct	Na2O_pct	K2O_pct	MnO_pct	TiO2_pct	P2O5_pct	Cr2O3_pct
YPC144	0.59	46.13	557	1.23	0.09	0.17	0.01	0.08	0.01	0.004
YPC145	0.89	38.63	289	2.05	0.12	0.36	0.01	0.12	0.02	0.001
YPC146	0.55	47.89	412	1.30	0.15	0.24	0.01	0.05	0.03	0.001
YPC147	0.93	42.02	347	1.35	0.19	0.58	0.01	0.10	0.02	0.001
YPC148	0.50	49.12	347	1.46	0.05	0.07	0.01	0.06	0.01	0.001
YPC149	1.15	37.42	291	2.12	0.05	0.12	0.01	0.24	0.01	0.003
YPC150	0.73	42.11	367	1.40	0.11	0.27	0.01	0.10	0.03	0.002
YPC151	0.55	49.72	454	1.18	0.06	0.08	0.01	0.07	0.01	0.001
YPC152	1.66	46.45	537	1.15	0.06	0.10	0.01	0.08	0.01	0.004
YPC153	0.71	46.52	541	1.15	0.09	0.14	0.01	0.08	0.01	0.002
YPC154	0.46	50.36	374	1.14	0.04	0.04	0.01	0.03	0.01	0.001
YPC155	0.53	44.17	303	2.02	0.08	0.12	0.01	0.07	0.01	0.001
YPC156	0.95	34.24	248	1.56	0.12	0.27	0.01	0.11	0.01	0.003
YPC157	0.63	44.96	345	1.22	0.06	0.13	0.01	0.07	0.01	0.001
YPC158	0.52	40.56	286	1.76	0.06	0.11	0.01	0.06	0.01	0.003
YPC159	0.66	41.45	332	1.52	0.07	0.15	0.01	0.07	0.01	0.001
YPC160	0.65	44.77	368	1.05	0.07	0.18	0.03	0.08	0.02	0.001
YPC161	0.72	41.66	446	0.89	0.09	0.24	0.01	0.09	0.02	0.002
YPC162	0.76	40.79	291	2.58	0.11	0.26	0.01	0.09	0.02	0.004
YPC163	0.62	43.71	402	1.27	0.10	0.23	0.01	0.07	0.02	0.005
YPC164	0.52	41.56	297	1.63	0.06	0.09	0.01	0.06	0.01	0.001
YPC165	0.47	49.92	695	0.83	0.05	0.05	0.01	0.04	0.02	0.003
YPC166	0.41	50.09	632	0.89	0.03	0.04	0.01	0.04	0.02	0.001
YPC167	0.68	46.73	409	1.58	0.10	0.15	0.02	0.08	0.02	0.004
YPC168	0.92	44.09	332	2.23	0.12	0.21	0.01	0.09	0.02	0.006
YPC169	0.84	41.03	275	4.58	0.14	0.25	0.01	0.09	0.03	0.003
YPC170	0.70	47.25	417	1.37	0.09	0.18	0.01	0.07	0.02	0.003
YPC171	0.69	47.11	493	1.08	0.07	0.18	0.01	0.08	0.03	0.003
YPC172	0.38	50.30	564	0.91	0.04	0.08	0.01	0.05	0.02	0.003
YPC173	0.62	46.49	389	1.46	0.08	0.21	0.01	0.08	0.02	0.001
YPC174	0.77	45.37	452	1.00	0.06	0.13	0.01	0.07	0.02	0.001
YPC175	0.65	44.18	320	2.96	0.09	0.13	0.02	0.08	0.01	0.002
YPC176	0.41	50.52	488	1.12	0.03	0.03	0.01	0.04	0.01	0.002
YPC177	0.25	49.79	365	3.03	0.03	0.02	0.01	0.02	0.01	0.001
YPC178	0.56	46.79	639	1.92	0.07	0.13	0.02	0.07	0.06	0.002
YPC179	0.59	47.82	845	1.09	0.06	0.10	0.03	0.08	0.04	0.001
YPC180	0.86	44.37	319	1.63	0.11	0.29	0.01	0.10	0.04	0.003
YPC181	0.75	47.80	481	1.06	0.05	0.06	0.01	0.09	0.04	0.002
YPC182	1.10	42.13	298	1.94	0.20	0.34	0.01	0.11	0.04	0.002
YPC183	0.93	42.35	286	2.35	0.13	0.26	0.02	0.12	0.03	0.002
YPC184	0.56	47.53	611	0.73	0.04	0.09	0.01	0.07	0.02	0.002
YPC185	0.74	46.68	470	1.46	0.08	0.11	0.02	0.08	0.02	0.004
YPC186	0.81	45.87	485	1.03	0.06	0.11	0.01	0.09	0.02	0.001
YPC187	0.55	40.94	355	2.79	0.09	0.18	0.02	0.06	0.03	0.002
YPC188	0.82	42.90	364	2.01	0.13	0.28	0.02	0.10	0.04	0.001
YPC189	0.97	42.13	402	1.79	0.10	0.24	0.02	0.12	0.03	0.001
YPC190	0.94	43.76	339	1.79	0.13	0.26	0.01	0.12	0.05	0.002
YPC191	1.03	43.04	329	1.50	0.15	0.31	0.02	0.13	0.06	0.002
YPC192	1.21	38.48	343	1.22	0.20	0.50	0.02	0.14	0.06	0.003
YPC193	0.88	44.10	356	1.30	0.14	0.33	0.01	0.12	0.03	0.001
YPC194	0.99	41.41	383	1.53	0.14	0.34	0.02	0.14	0.02	0.005
YPC195	0.79	45.14	749	0.80	0.10	0.19	0.03	0.11	0.04	0.002
YPC196	0.90	44.84	843	1.02	0.08	0.22	0.07	0.12	0.02	0.001
YPC197	0.81	45.57	669	1.14	0.08	0.23	0.04	0.11	0.03	0.005
YPC198	0.92	44.19	585	1.52	0.11	0.34	0.03	0.12	0.05	0.001
YPC199	0.88	45.25	604	0.95	0.12	0.19	0.06	0.12	0.04	0.003
YPC200	0.95	43.96	456	1.34	0.14	0.22	0.02	0.12	0.03	0.003
YPC201	0.94	45.14	641	1.09	0.12	0.23	0.04	0.12	0.03	0.002
YPC202	0.97	39.18	366	1.75	0.12	0.30	0.03	0.12	0.02	0.003
YPC203	0.80	42.14	369	1.88	0.11	0.21	0.02	0.10	0.02	0.003
YPC204	0.74	44.84	447	1.84	0.08	0.19	0.03	0.09	0.02	0.003
YPC205	0.67	46.16	537	1.03	0.05	0.08	0.02	0.11	0.02	0.002
YPC206	0.57	46.41	623	0.99	0.05	0.14	0.09	0.09	0.04	0.002
YPC207	0.68	44.65	598	1.15	0.06	0.15	0.03	0.08	0.03	0.002
YPC208	0.60	47.66	619	0.93	0.04	0.09	0.02	0.06	0.02	0.004
YPC209	0.72	46.31	838	0.74	0.07	0.16	0.02	0.09	0.03	0.005
YPC210	0.98	44.79	611	1.14	0.12	0.25	0.04	0.12	0.03	0.003
TIP001c	0.53	48.44	569	1.14	0.03	0.1	0.01	0.05	0.02	0.0005
TIP001g	0.39	50.45	596	1.08	0.05	0.07	0.005	0.05	0.03	0.0005
WAR001	0.67	45.93	702	0.77	0.08	0.28	0.02	0.09	0.04	0.0005
MNL024	0.9	40.09	487	1.41	0.11	0.33	0.01	0.09	0.05	0.0005
MNL044	0.38	46.84	455	1.19	0.05	0.15	0.005	0.03	0.01	0.0005

	Ba_pct	LOI_pct	SUM_pct	TOT/C_pct	TOT/S_pct	Ba_ppm	Be_ppm	Co_ppm	Cs_ppm	Ga_ppm	Hf_ppm
YPC144	0.01	38.78	100.51	10.72	0.08	115.00	0.50	3.00	0.40	1.30	0.90
YPC145	0.01	34.72	99.97	9.51	0.06	143.00	0.50	5.40	0.80	5.60	1.60
YPC146	0.01	40.81	100.97	11.77	0.05	161.00	2.00	3.50	0.70	4.60	0.60
YPC147	0.02	37.06	99.99	10.47	0.07	208.00	0.50	3.30	1.20	6.20	0.90
YPC148	0.02	41.82	100.79	11.71	0.04	178.00	0.50	2.20	0.40	5.10	0.80
YPC149	0.01	34.47	100.00	9.09	0.05	164.00	0.50	5.70	0.40	7.90	2.40
YPC150	0.01	36.76	100.47	10.25	0.05	149.00	0.50	5.00	0.60	6.60	1.40
YPC151	0.01	42.06	100.69	11.95	0.06	145.00	0.50	3.10	0.30	3.80	0.80
YPC152	0.01	39.99	100.58	10.91	0.05	139.00	0.50	5.50	0.60	5.70	0.90
YPC153	0.01	39.82	100.63	11.27	0.05	90.00	0.50	4.50	0.60	4.40	1.00
YPC154	0.01	42.65	100.64	12.29	0.05	138.00	0.50	3.90	0.40	3.00	0.60
YPC155	0.01	39.13	100.59	11.20	0.08	135.00	0.50	7.50	0.40	2.90	0.90
YPC156	0.01	30.65	99.84	8.29	0.05	130.00	0.50	4.10	0.70	5.00	1.80
YPC157	0.01	38.94	100.21	10.99	0.06	117.00	0.50	8.10	0.50	3.80	0.70
YPC158	0.01	35.90	100.10	10.11	0.06	99.00	0.50	5.50	0.40	1.80	1.20
YPC159	0.01	36.03	100.36	9.90	0.04	124.00	2.00	5.80	0.40	2.70	1.10
YPC160	0.01	38.21	100.15	10.69	0.05	81.00	1.00	7.70	0.40	2.50	1.30
YPC161	0.01	35.74	100.41	10.13	0.06	66.00	0.50	4.60	0.50	2.30	1.50
YPC162	0.02	37.27	100.42	10.53	0.07	163.00	0.50	5.00	0.50	2.10	2.10
YPC163	0.01	37.89	100.40	10.71	0.04	148.00	0.50	4.40	0.50	2.30	0.90
YPC164	0.01	36.59	100.19	10.24	0.06	110.00	0.50	5.50	0.40	1.20	1.10
YPC165	0.02	42.03	100.59	12.24	0.09	152.00	0.50	4.60	0.30	0.80	0.40
YPC166	0.02	42.08	100.58	12.25	0.08	155.00	0.50	5.50	0.30	0.80	0.40
YPC167	0.02	39.75	100.61	11.26	0.05	140.00	0.50	5.50	0.70	1.80	1.30
YPC168	0.01	38.60	100.55	10.79	0.05	167.00	0.50	4.30	0.70	1.50	1.30
YPC169	0.02	39.06	100.58	11.08	0.05	153.00	0.50	4.10	0.50	1.70	1.20
YPC170	0.02	40.27	100.46	11.71	0.06	141.00	0.50	4.50	0.70	1.20	1.30
YPC171	0.02	40.11	100.46	11.64	0.06	164.00	0.50	4.60	0.70	1.90	0.60
YPC172	0.02	42.11	100.50	12.42	0.06	138.00	0.50	4.80	0.30	0.80	0.80
YPC173	0.01	40.01	100.46	11.61	0.06	131.00	1.00	3.80	0.40	1.30	0.60
YPC174	0.02	38.27	100.16	10.92	0.05	150.00	0.50	5.40	0.50	1.40	1.50
YPC175	0.01	39.50	100.37	11.29	0.05	123.00	0.50	4.10	0.50	1.10	1.00
YPC176	0.01	42.16	100.63	12.15	0.07	140.00	0.50	2.90	0.30	0.25	0.60
YPC177	0.01	43.43	100.63	12.54	0.06	114.00	0.50	2.00	0.20	0.60	0.70
YPC178	0.01	40.47	100.62	11.71	0.05	114.00	2.00	4.00	0.40	0.25	1.10
YPC179	0.01	39.89	100.51	11.29	0.04	103.00	0.50	3.00	0.40	0.90	1.20
YPC180	0.02	38.78	100.45	10.83	0.05	176.00	0.50	4.30	0.50	1.90	1.70
YPC181	0.02	40.76	100.38	11.24	0.07	178.00	0.50	3.90	0.50	1.80	0.80
YPC182	0.02	37.35	100.40	9.93	0.07	163.00	0.50	5.40	0.90	3.00	1.30
YPC183	0.02	37.58	100.42	9.44	0.06	152.00	0.50	3.80	0.60	2.40	1.40
YPC184	0.01	39.87	100.46	11.09	0.08	110.00	0.50	5.20	0.30	1.10	0.70
YPC185	0.02	39.50	100.75	10.78	0.06	141.00	0.50	5.20	0.50	1.30	0.80
YPC186	0.01	38.80	100.44	10.72	0.07	165.00	0.50	5.60	0.50	1.30	1.70
YPC187	0.01	37.04	100.23	10.60	0.08	83.00	0.50	4.00	0.30	1.00	0.60
YPC188	0.01	37.98	100.29	10.44	0.08	130.00	0.50	5.00	0.50	1.90	1.10
YPC189	0.01	36.53	100.19	9.62	0.05	119.00	0.50	5.00	0.60	2.30	1.60
YPC190	0.01	38.55	100.23	10.05	0.07	143.00	0.50	5.80	0.50	2.30	1.40
YPC191	0.01	37.94	100.41	10.46	0.07	134.00	0.50	6.20	0.70	2.60	0.90
YPC192	0.01	33.99	100.06	8.98	0.08	129.00	0.50	6.20	0.80	3.00	1.20
YPC193	0.02	37.85	100.38	10.44	0.07	150.00	0.50	4.60	0.70	1.90	1.50
YPC194	0.02	35.75	100.16	9.70	0.06	192.00	0.50	5.60	0.90	2.10	2.20
YPC195	0.01	37.46	101.01	10.33	0.07	142.00	0.50	5.60	0.70	1.70	1.20
YPC196	0.01	37.90	100.18	10.00	0.05	115.00	0.50	6.60	0.70	1.90	1.20
YPC197	0.01	38.44	100.57	10.50	0.05	121.00	0.50	6.70	0.60	1.80	1.00
YPC198	0.02	38.17	100.47	10.54	0.05	131.00	0.50	8.70	0.60	2.00	2.00
YPC199	0.01	38.33	100.28	9.55	0.04	123.00	0.50	7.00	0.90	2.00	1.40
YPC200	0.02	38.12	100.20	10.38	0.06	140.00	0.50	6.20	0.70	2.20	1.20
YPC201	0.01	38.30	100.53	9.71	0.06	122.00	0.50	8.30	0.70	2.20	1.80
YPC202	0.02	34.57	99.95	9.40	0.05	150.00	0.50	7.00	0.90	2.60	1.60
YPC203	0.01	37.28	99.94	10.05	0.04	142.00	0.50	6.20	0.70	1.80	1.50
YPC204	0.02	39.10	100.30	10.74	0.05	139.00	0.50	6.40	0.60	1.20	1.10
YPC205	0.01	39.31	100.38	10.90	0.05	113.00	0.50	6.10	0.50	1.70	1.20
YPC206	0.01	38.81	100.37	11.01	0.05	112.00	0.50	5.50	0.50	1.30	0.80
YPC207	0.01	38.25	100.63	10.76	0.04	139.00	0.50	7.50	0.50	1.30	1.00
YPC208	0.02	39.77	100.41	11.27	0.06	148.00	0.50	4.90	0.40	0.90	1.00
YPC209	0.01	38.37	100.64	10.54	0.06	115.00	0.50	5.50	0.50	1.50	1.30
YPC210	0.01	38.26	100.41	10.68	0.07	122.00	0.50	8.70	0.70	2.20	1.60
TIP001c	0.02	40.87	100.62	11.3	0.05	108.00	0.50	5.20	0.30	1.00	0.40
TIP001g	0.02	41.36	100.82	11.7	0.07	113.00	0.50	4.60	0.30	0.03	0.50
WAR001	0.02	38.58	100.42	10.5	0.07	114.00	0.50	4.70	0.40	1.60	1.20
MNL024	0.02	35.67	100.24	9.48	0.06	147.00	0.50	6.80	0.90	2.20	1.10
MNL044	0.02	39.37	100.53	10.9	0.08	117.00	0.50	1.50	0.20	0.03	0.40

	Nb_ppm	Rb_ppm	Sn_ppm	Sr_ppm	Ta_ppm	Th_ppm	U_ppm	V_ppm	W_ppm	Zr_ppm	Y_ppm	La_ppm	Ce_ppm
YPC144	0.90	9.70	0.50	591.90	0.05	1.10	0.30	11.00	0.25	41.30	4.90	3.50	7.00
YPC145	1.80	15.90	0.50	956.80	0.20	2.40	1.10	39.00	0.25	73.70	8.20	8.10	15.80
YPC146	0.60	16.10	0.50	830.90	0.05	1.40	0.20	26.00	0.25	23.30	4.50	5.90	10.60
YPC147	2.00	38.20	0.50	865.40	0.20	2.40	0.40	28.00	0.25	34.40	5.30	6.70	13.40
YPC148	1.60	9.40	0.50	1011.40	0.05	1.60	0.30	26.00	0.25	35.30	4.30	3.30	5.20
YPC149	7.90	10.10	0.50	917.80	1.50	2.90	0.50	48.00	0.25	82.40	5.30	4.90	8.10
YPC150	2.40	15.50	0.50	819.30	0.20	2.60	0.10	20.00	0.70	69.20	9.20	9.70	16.50
YPC151	0.60	7.90	0.50	783.60	0.05	1.70	0.05	17.00	0.25	33.10	4.70	3.30	7.10
YPC152	1.10	8.90	0.50	617.80	0.10	3.90	0.20	35.00	0.25	32.90	4.60	3.70	8.00
YPC153	1.20	10.60	0.50	614.20	0.05	1.60	0.10	22.00	0.25	43.00	5.90	6.70	8.70
YPC154	0.30	4.50	0.50	961.80	0.05	1.70	0.05	16.00	0.25	22.40	2.80	2.40	4.70
YPC155	1.40	8.70	0.50	1043.70	0.05	2.20	0.10	15.00	0.25	39.20	8.50	7.20	15.40
YPC156	2.40	15.60	0.50	984.90	0.20	2.00	0.30	21.00	0.25	57.60	5.70	6.10	12.20
YPC157	0.90	9.00	0.50	932.80	0.05	2.90	0.30	17.00	0.25	38.60	11.00	10.60	20.80
YPC158	0.70	9.00	0.50	1012.80	0.05	1.80	0.30	9.00	0.25	38.30	6.30	5.90	11.80
YPC159	0.70	9.30	1.00	891.20	0.10	1.90	0.30	11.00	0.25	42.20	7.80	6.40	13.20
YPC160	0.90	11.10	0.50	868.50	0.05	2.20	0.40	14.00	0.25	59.10	7.60	7.60	14.90
YPC161	0.40	11.50	0.50	667.90	0.05	1.60	0.30	14.00	0.25	48.90	5.40	5.60	10.80
YPC162	1.20	10.30	0.50	1002.80	0.10	2.90	0.20	11.00	0.25	51.80	5.20	5.50	12.00
YPC163	0.70	12.60	0.50	776.90	0.05	2.70	0.20	9.00	0.25	48.60	8.60	9.30	15.00
YPC164	0.20	9.10	0.50	1001.40	0.05	1.80	0.40	10.00	0.25	37.50	5.60	5.90	12.20
YPC165	0.80	5.30	0.50	513.10	0.20	1.00	0.05	11.00	0.25	19.80	5.00	4.50	7.50
YPC166	0.20	4.90	0.50	566.80	0.05	0.70	0.05	10.00	0.25	21.70	3.80	3.40	6.50
YPC167	1.00	11.50	0.50	816.00	0.05	1.90	0.50	15.00	0.25	36.10	8.10	8.20	13.20
YPC168	1.30	15.80	0.50	948.10	0.20	2.10	0.20	17.00	0.25	43.20	6.40	8.50	14.10
YPC169	0.90	15.50	0.50	1065.70	0.20	2.10	0.30	14.00	0.25	44.40	7.60	9.20	16.00
YPC170	0.90	11.90	0.50	810.50	0.05	2.30	0.20	15.00	0.25	48.70	6.20	6.70	13.10
YPC171	1.10	13.10	0.50	682.60	0.05	1.80	0.20	16.00	0.25	30.10	7.20	7.70	11.50
YPC172	0.80	7.10	0.50	637.50	0.10	1.60	0.05	11.00	0.25	30.00	12.00	15.50	15.50
YPC173	0.90	11.10	0.50	854.90	0.05	2.10	0.30	16.00	0.25	34.80	6.90	6.50	12.30
YPC174	0.70	10.70	0.50	717.70	0.05	1.50	0.30	17.00	0.25	42.50	5.00	5.60	9.60
YPC175	1.20	9.40	0.50	987.60	0.05	1.40	0.30	14.00	0.25	56.30	6.90	8.20	12.90
YPC176	0.05	4.60	0.50	740.20	0.05	1.00	0.20	12.00	0.25	22.00	3.00	3.30	5.90
YPC177	0.70	3.30	0.50	975.90	0.05	0.50	0.10	10.00	0.25	17.90	2.00	2.70	4.50
YPC178	0.60	8.00	0.50	523.30	0.05	1.30	0.20	15.00	0.25	43.60	8.80	7.20	12.20
YPC179	1.00	7.90	0.50	404.60	0.05	1.40	0.20	17.00	0.25	38.10	5.80	5.30	10.00
YPC180	1.00	14.30	0.50	992.70	0.10	2.20	0.30	18.00	0.25	53.10	7.90	8.10	14.70
YPC181	1.30	9.60	0.50	709.80	0.05	2.10	0.20	13.00	0.25	30.50	6.60	6.90	11.60
YPC182	3.00	21.60	0.50	1010.20	0.50	2.80	0.90	16.00	0.25	57.90	8.20	8.80	16.40
YPC183	1.80	17.10	0.50	1057.80	0.05	2.90	0.40	15.00	0.25	49.20	9.40	9.10	17.50
YPC184	0.70	7.50	0.50	555.80	0.05	1.10	0.20	10.00	0.25	26.00	6.20	5.20	9.50
YPC185	2.00	12.60	0.50	709.60	0.20	1.50	0.30	12.00	0.25	36.20	6.20	5.60	9.90
YPC186	1.50	11.30	0.50	676.70	0.20	1.90	0.20	10.00	0.25	55.80	5.60	5.30	10.10
YPC187	0.50	7.70	0.50	823.80	0.05	1.20	0.05	4.00	0.25	25.80	5.10	4.90	9.10
YPC188	1.20	12.30	0.50	842.90	0.05	2.00	0.20	11.00	0.25	41.80	6.10	6.10	13.00
YPC189	1.50	13.70	0.50	748.90	0.10	2.50	0.70	20.00	0.25	52.40	8.00	7.70	16.00
YPC190	1.20	14.20	0.50	922.80	0.10	2.00	0.30	15.00	0.25	46.70	6.00	5.70	12.20
YPC191	1.20	16.60	0.50	934.40	0.05	2.10	0.40	14.00	0.25	40.20	9.10	7.00	14.60
YPC192	2.00	21.20	0.50	801.20	0.10	2.60	0.30	15.00	0.25	51.00	14.30	10.40	19.80
YPC193	2.00	18.20	0.50	884.90	0.20	2.30	0.30	15.00	0.25	57.90	7.50	8.00	15.10
YPC194	1.40	18.00	0.50	772.60	0.10	2.40	0.90	18.00	0.25	63.30	7.00	6.70	14.90
YPC195	1.40	13.90	0.50	430.50	0.10	1.70	0.50	13.00	0.25	52.60	7.60	6.80	12.70
YPC196	1.30	15.50	0.50	380.00	0.10	2.00	0.40	18.00	0.60	52.60	11.50	10.90	18.40
YPC197	1.40	12.80	0.50	487.20	0.20	2.10	0.50	9.00	0.25	46.90	9.40	9.00	16.00
YPC198	1.50	14.90	0.50	539.80	0.10	2.10	0.20	14.00	0.25	67.60	10.40	10.00	19.30
YPC199	1.60	16.00	0.50	535.60	0.20	2.50	0.30	14.00	0.25	60.90	13.00	14.60	28.30
YPC200	1.40	16.40	0.50	688.50	0.20	2.80	0.50	13.00	0.25	55.80	12.30	10.90	20.50
YPC201	1.20	15.60	0.50	503.60	0.05	2.30	0.30	12.00	0.25	58.30	15.70	12.40	23.20
YPC202	1.70	18.20	0.50	764.80	0.10	2.90	0.90	15.00	0.25	67.00	8.90	8.50	17.10
YPC203	1.60	14.90	0.50	817.40	0.05	2.10	0.60	10.00	0.25	59.40	6.30	5.90	13.30
YPC204	1.10	12.90	0.50	716.30	0.05	2.10	0.40	9.00	0.25	43.60	9.10	6.70	13.80
YPC205	1.60	8.10	0.50	614.60	0.10	2.00	0.20	11.00	0.25	44.80	5.40	4.70	8.90
YPC206	4.00	8.60	0.50	532.40	0.50	1.40	0.20	9.00	0.25	39.40	8.30	6.90	9.90
YPC207	1.00	11.20	0.50	533.60	0.05	2.00	0.20	4.00	0.25	42.00	10.50	8.60	14.00
YPC208	0.60	7.60	0.50	550.50	0.10	1.40	0.20	10.00	0.25	39.20	5.30	4.80	8.90
YPC209	1.10	12.10	0.50	394.90	0.10	1.70	0.40	4.00	0.25	46.70	7.50	7.20	11.90
YPC210	1.60	16.30	0.50	524.40	0.20	2.70	0.60	16.00	0.25	57.00	16.10	13.20	25.20
TIP001c	0.90	6.70	0.50	608.20	0.05	1.80	0.20	11.00	0.03	20.10	18.20	14.10	15.40
TIP001g	0.60	5.10	0.50	605.20	0.05	1.80	0.30	4.00	0.03	17.40	16.20	12.70	17.70
WAR001	1.50	12.00	0.50	467.70	0.10	1.60	0.30	15.00	0.03	43.50	7.40	7.60	12.10
MNL024	1.70	17.70	0.50	588.90	0.10	2.70	0.40	17.00	0.03	38.60	8.60	7.70	13.00
MNL044	0.60	7.60	0.50	736.60	0.05	0.90	0.50	4.00	0.03	18.40	2.40	2.50	4.60

	Pr_ppm	Nd_ppm	Sm_ppm	Eu_ppm	Gd_ppm	Tb_ppm	Dy_ppm	Ho_ppm	Er_ppm	Tm_ppm	Yb_ppm	Lu_ppm	Mo_ppm
YPC144	0.79	3.60	0.70	0.17	0.75	0.11	0.79	0.14	0.37	0.07	0.42	0.05	0.05
YPC145	1.75	8.70	1.48	0.33	1.38	0.22	1.49	0.32	0.70	0.11	0.73	0.12	0.10
YPC146	1.30	4.20	0.94	0.24	0.99	0.14	0.73	0.16	0.53	0.06	0.43	0.06	0.05
YPC147	1.49	5.60	1.13	0.27	1.04	0.17	1.02	0.16	0.54	0.11	0.60	0.09	0.05
YPC148	0.71	2.00	0.49	0.10	0.65	0.11	0.82	0.20	0.48	0.08	0.50	0.08	0.05
YPC149	0.99	3.30	0.81	0.16	0.96	0.13	0.89	0.18	0.53	0.08	0.60	0.09	0.20
YPC150	2.18	8.80	1.57	0.38	1.66	0.25	1.64	0.34	0.89	0.12	0.89	0.16	0.05
YPC151	0.78	3.50	0.65	0.18	0.74	0.11	0.74	0.17	0.43	0.08	0.55	0.07	0.05
YPC152	0.90	2.30	0.76	0.21	0.80	0.13	0.56	0.16	0.36	0.06	0.47	0.07	0.20
YPC153	1.47	5.20	1.20	0.23	1.17	0.15	0.79	0.21	0.62	0.09	0.40	0.07	0.05
YPC154	0.55	2.40	0.54	0.14	0.68	0.07	0.51	0.09	0.37	0.05	0.46	0.06	0.05
YPC155	1.77	7.10	1.52	0.38	1.60	0.23	1.44	0.26	0.84	0.12	0.86	0.13	0.05
YPC156	1.44	4.00	1.03	0.28	1.22	0.18	1.25	0.22	0.59	0.09	0.44	0.09	0.05
YPC157	2.49	6.90	2.15	0.48	1.87	0.33	1.98	0.38	1.18	0.17	1.31	0.16	0.05
YPC158	1.32	5.50	1.14	0.30	1.16	0.16	1.11	0.21	0.64	0.10	0.62	0.08	0.05
YPC159	1.66	7.60	1.39	0.32	1.67	0.19	1.23	0.27	0.70	0.10	0.62	0.11	0.05
YPC160	1.67	7.00	1.30	0.29	1.30	0.22	1.32	0.27	0.66	0.10	0.69	0.12	0.05
YPC161	1.28	4.10	1.04	0.26	1.00	0.15	0.93	0.25	0.33	0.08	0.43	0.06	0.05
YPC162	1.35	5.20	1.07	0.22	1.19	0.16	1.34	0.20	0.71	0.10	0.64	0.10	0.10
YPC163	2.20	9.20	1.70	0.39	1.75	0.26	1.42	0.36	0.97	0.11	0.64	0.11	0.10
YPC164	1.40	5.30	1.01	0.25	1.22	0.16	0.96	0.20	0.60	0.09	0.78	0.10	0.05
YPC165	0.97	3.40	0.69	0.19	0.83	0.12	0.52	0.19	0.39	0.07	0.33	0.08	0.05
YPC166	0.87	3.00	0.74	0.14	0.68	0.10	0.45	0.11	0.29	0.04	0.38	0.05	0.05
YPC167	1.58	7.00	1.28	0.28	1.31	0.19	1.02	0.25	0.66	0.10	0.66	0.08	0.05
YPC168	1.83	7.90	1.41	0.35	1.39	0.17	1.12	0.19	0.70	0.08	0.58	0.08	0.05
YPC169	2.16	5.30	1.37	0.29	1.35	0.20	1.24	0.23	0.74	0.11	0.62	0.10	0.05
YPC170	1.61	7.20	1.16	0.26	1.17	0.20	0.86	0.20	0.51	0.09	0.53	0.09	0.05
YPC171	1.48	4.70	1.24	0.25	1.23	0.18	1.14	0.21	0.59	0.08	0.67	0.09	0.05
YPC172	3.45	12.40	2.18	0.52	2.44	0.35	2.18	0.41	1.25	0.13	0.87	0.13	0.05
YPC173	1.49	7.00	1.40	0.30	1.48	0.22	0.98	0.21	0.76	0.12	0.54	0.07	0.05
YPC174	1.23	5.50	0.97	0.21	0.77	0.13	0.61	0.16	0.49	0.06	0.55	0.06	0.05
YPC175	1.66	6.40	1.13	0.26	1.33	0.17	0.93	0.17	0.64	0.08	0.64	0.07	0.05
YPC176	0.77	3.40	0.60	0.13	0.55	0.08	0.69	0.12	0.38	0.04	0.35	0.04	0.10
YPC177	0.52	2.60	0.30	0.08	0.34	0.05	0.26	0.07	0.17	0.01	0.17	0.02	0.05
YPC178	1.57	6.20	1.38	0.26	1.58	0.20	1.21	0.28	0.73	0.14	0.78	0.13	0.10
YPC179	1.29	4.30	0.94	0.21	0.89	0.14	0.72	0.17	0.53	0.07	0.39	0.05	0.10
YPC180	1.81	5.90	1.26	0.33	1.36	0.21	1.31	0.26	0.66	0.12	0.75	0.12	0.05
YPC181	1.63	6.90	1.21	0.28	1.35	0.17	1.00	0.20	0.55	0.09	0.56	0.09	0.10
YPC182	2.06	8.30	1.67	0.33	1.48	0.21	1.35	0.26	0.74	0.11	0.84	0.12	0.30
YPC183	2.18	9.00	1.90	0.42	1.93	0.26	1.49	0.33	1.01	0.14	0.84	0.16	0.05
YPC184	1.33	6.00	1.26	0.27	1.30	0.17	1.04	0.21	0.55	0.09	0.62	0.09	0.05
YPC185	1.36	5.50	1.02	0.25	1.13	0.16	1.04	0.23	0.61	0.09	0.52	0.09	0.05
YPC186	1.36	5.70	1.05	0.23	1.15	0.15	1.09	0.21	0.47	0.09	0.60	0.10	0.05
YPC187	1.22	5.20	1.07	0.23	1.10	0.15	1.02	0.21	0.50	0.06	0.58	0.07	0.20
YPC188	1.52	6.20	1.25	0.29	1.27	0.18	1.24	0.24	0.61	0.08	0.56	0.08	0.10
YPC189	2.07	8.50	1.67	0.38	1.80	0.24	1.61	0.29	0.81	0.10	0.75	0.11	0.20
YPC190	1.41	5.70	1.18	0.26	1.22	0.16	1.22	0.26	0.69	0.09	0.62	0.11	0.10
YPC191	1.76	7.30	1.54	0.35	1.54	0.23	1.51	0.30	0.92	0.12	0.78	0.12	0.05
YPC192	2.72	11.00	2.42	0.52	2.47	0.35	2.30	0.51	1.49	0.21	1.05	0.19	0.10
YPC193	1.88	8.00	1.58	0.32	1.53	0.21	1.26	0.27	0.73	0.11	0.75	0.12	0.05
YPC194	1.78	6.50	1.39	0.31	1.42	0.19	1.09	0.25	0.62	0.09	0.68	0.10	0.05
YPC195	1.69	6.80	1.28	0.32	1.41	0.19	1.37	0.28	0.73	0.10	0.66	0.10	0.05
YPC196	2.55	10.00	1.97	0.49	2.10	0.29	2.09	0.38	1.05	0.13	1.03	0.15	0.10
YPC197	2.15	8.90	1.87	0.37	1.78	0.24	1.60	0.30	0.90	0.13	0.85	0.12	0.05
YPC198	2.53	10.00	1.91	0.44	1.96	0.27	1.76	0.34	1.02	0.15	1.09	0.14	0.05
YPC199	4.03	16.00	2.93	0.65	2.78	0.37	2.27	0.41	1.16	0.17	1.05	0.15	0.05
YPC200	2.67	10.20	2.28	0.53	2.36	0.32	1.87	0.40	1.09	0.16	1.15	0.18	0.05
YPC201	3.31	13.60	2.73	0.62	3.14	0.41	2.58	0.51	1.48	0.21	1.18	0.19	0.05
YPC202	2.10	9.20	1.64	0.39	1.86	0.25	1.74	0.30	0.98	0.14	0.85	0.11	0.10
YPC203	1.52	7.60	1.29	0.32	1.32	0.17	1.05	0.18	0.66	0.10	0.55	0.09	0.05
YPC204	1.81	7.80	1.54	0.35	1.68	0.23	1.45	0.29	0.75	0.13	0.83	0.12	0.05
YPC205	1.15	4.90	1.02	0.20	1.05	0.14	0.90	0.19	0.50	0.09	0.52	0.07	0.05
YPC206	1.67	7.00	1.39	0.31	1.46	0.20	1.25	0.24	0.70	0.09	0.76	0.10	0.10
YPC207	2.18	8.80	1.96	0.43	2.18	0.26	1.50	0.34	0.83	0.12	0.89	0.14	0.05
YPC208	1.22	4.60	0.92	0.21	0.97	0.14	1.10	0.17	0.53	0.07	0.50	0.07	0.30
YPC209	1.80	6.70	1.53	0.34	1.52	0.20	1.30	0.28	0.76	0.11	0.76	0.11	0.10
YPC210	3.43	14.70	2.94	0.68	3.00	0.40	2.33	0.44	1.39	0.20	1.32	0.19	0.05
TIP001c	3.52	15.40	3.38	0.67	3.35	0.51	2.95	0.61	1.72	0.24	1.44	0.22	0.05
TIP001g	3.27	13.40	3.20	0.61	3.10	0.46	2.97	0.57	1.59	0.23	1.40	0.23	0.05
WAR001	1.62	7.00	1.49	0.28	1.36	0.19	1.20	0.25	0.69	0.10	0.66	0.10	0.05
MNL024	1.65	6.70	1.31	0.29	1.21	0.18	1.19	0.24	0.71	0.12	0.65	0.11	0.05
MNL044	0.52	2.20	0.41	0.11	0.42	0.07	0.34	0.07	0.26	0.03	0.22	0.03	0.05

	Cu_ppm	Pb_ppm	Zn_ppm	Ni_ppm	As_ppm	Cd_ppm	Sb_ppm	Bi_ppm	Ag_ppm	Au_ppb	Hg_ppm	Tl_ppm	Se_ppm
YPC144	2.30	1.50	4.00	3.50	1.00	0.05	0.10	0.05	0.05	2.00	0.03	0.05	0.25
YPC145	5.80	3.20	5.00	8.10	1.80	0.05	0.10	0.20	0.05	0.90	0.10	0.05	0.25
YPC146	2.00	1.00	3.00	4.10	0.70	0.05	0.10	0.05	0.05	0.25	0.04	0.05	0.25
YPC147	9.40	1.80	4.00	5.10	0.80	0.05	0.10	0.05	0.05	0.25	0.07	0.05	0.25
YPC148	5.90	0.90	2.00	3.20	0.25	0.05	0.10	0.05	0.05	0.25	0.06	0.05	0.25
YPC149	7.20	1.50	2.00	7.00	2.70	0.05	0.20	0.05	0.05	0.25	0.03	0.05	0.25
YPC150	4.00	2.90	9.00	3.40	0.80	0.05	0.05	0.05	0.05	0.25	0.06	0.05	0.25
YPC151	3.30	1.10	2.00	2.80	0.60	0.05	0.05	0.05	0.05	0.90	0.08	0.05	0.25
YPC152	2.60	1.90	3.00	5.30	4.20	0.05	0.10	0.05	0.05	0.25	0.07	0.05	0.25
YPC153	1.90	1.70	5.00	5.20	1.40	0.05	0.05	0.05	0.05	1.30	0.04	0.05	0.25
YPC154	3.10	0.80	1.00	3.40	1.80	0.05	0.05	0.05	0.05	0.60	0.06	0.05	0.25
YPC155	4.00	2.30	2.00	6.60	1.00	0.05	0.05	0.05	0.05	0.25	0.06	0.05	0.25
YPC156	6.10	2.70	2.00	9.00	1.50	0.05	0.05	0.20	0.05	0.25	0.03	0.05	0.25
YPC157	4.40	3.20	3.00	6.90	1.40	0.05	0.05	0.05	0.05	0.25	0.05	0.05	0.25
YPC158	5.00	2.20	3.00	5.80	1.10	0.05	0.05	0.05	0.05	0.25	0.07	0.05	0.60
YPC159	4.70	2.40	3.00	6.40	1.80	0.05	0.05	0.05	0.05	0.25	0.10	0.05	0.25
YPC160	4.60	2.50	3.00	6.50	1.90	0.05	0.05	0.05	0.05	0.25	0.06	0.05	0.25
YPC161	4.00	1.90	4.00	6.20	1.70	0.05	0.05	0.05	0.05	0.25	0.04	0.05	0.25
YPC162	8.50	2.70	4.00	8.40	1.60	0.05	0.10	0.05	0.05	0.25	0.08	0.05	0.25
YPC163	4.70	2.20	11.00	3.30	1.10	0.05	0.05	0.05	0.05	0.25	0.08	0.05	0.25
YPC164	6.50	2.30	2.00	6.80	1.90	0.05	0.05	0.05	0.05	0.25	0.06	0.05	0.25
YPC165	4.60	1.10	3.00	3.00	1.20	0.05	0.05	0.05	0.05	0.25	0.06	0.05	0.25
YPC166	5.10	1.20	2.00	2.50	1.50	0.05	0.10	0.05	0.05	0.90	0.05	0.05	0.60
YPC167	9.60	2.30	5.00	4.70	1.50	0.05	0.10	0.05	0.05	0.50	0.04	0.05	0.25
YPC168	6.00	2.50	7.00	5.00	0.60	0.05	0.20	0.05	0.05	0.25	0.04	0.05	0.25
YPC169	5.80	2.00	5.00	5.30	1.00	0.05	0.10	0.05	0.05	0.60	0.04	0.05	0.25
YPC170	4.00	1.80	3.00	4.40	0.90	0.05	0.05	0.05	0.05	0.25	0.04	0.05	0.50
YPC171	3.50	1.40	8.00	3.60	1.30	0.05	0.05	0.05	0.05	0.25	0.04	0.05	0.25
YPC172	5.10	1.30	2.00	3.20	1.70	0.05	0.05	0.05	0.05	0.80	0.05	0.05	0.25
YPC173	4.50	1.70	4.00	3.80	1.70	0.05	0.20	0.05	0.05	0.25	0.04	0.05	0.25
YPC174	5.50	2.00	3.00	5.50	2.40	0.05	0.20	0.05	0.05	0.25	0.06	0.05	0.25
YPC175	5.60	2.70	3.00	3.00	1.60	0.05	0.20	0.05	0.05	0.25	0.04	0.05	0.25
YPC176	5.30	1.20	2.00	1.70	2.40	0.05	0.05	0.05	0.05	0.70	0.05	0.05	0.25
YPC177	6.30	0.80	3.00	1.50	1.60	0.05	0.10	0.05	0.05	1.00	0.03	0.05	0.25
YPC178	5.40	2.00	9.00	3.10	2.10	0.05	0.10	0.05	0.05	0.25	0.03	0.05	0.25
YPC179	3.70	1.90	5.00	3.80	2.30	0.05	0.10	0.05	0.05	0.25	0.04	0.05	0.25
YPC180	6.80	2.50	5.00	4.70	1.70	0.20	0.10	0.05	0.05	0.25	0.07	0.05	0.25
YPC181	8.50	2.20	8.00	1.00	2.00	0.05	0.10	0.05	0.05	0.80	0.03	0.05	0.50
YPC182	36.10	3.00	10.00	4.00	2.10	0.05	0.10	0.05	0.05	1.20	0.02	0.05	1.10
YPC183	9.80	4.40	24.00	4.70	1.60	0.20	0.05	0.05	0.05	0.90	0.05	0.05	0.70
YPC184	13.20	1.50	4.00	3.60	2.50	0.05	0.05	0.05	0.05	2.20	0.01	0.05	0.50
YPC185	11.60	2.60	5.00	4.00	2.00	0.05	0.10	0.05	0.05	2.60	0.02	0.05	0.25
YPC186	7.60	2.20	3.00	3.30	2.70	0.05	0.20	0.05	0.05	1.70	0.02	0.05	0.70
YPC187	5.40	1.70	3.00	4.60	4.10	0.10	0.05	0.05	0.05	1.60	0.01	0.05	0.80
YPC188	13.20	3.00	8.00	4.90	2.70	0.10	0.05	0.05	0.05	2.10	0.01	0.05	0.60
YPC189	7.50	3.30	7.00	5.80	3.00	0.05	0.05	0.05	0.05	1.30	0.02	0.05	0.70
YPC190	18.10	2.80	10.00	4.40	1.40	0.10	0.05	0.05	0.05	1.60	0.02	0.05	1.30
YPC191	12.80	3.00	9.00	5.20	1.60	0.10	0.05	0.05	0.05	2.80	0.02	0.05	1.10
YPC192	14.90	3.80	10.00	5.40	0.80	0.10	0.05	0.05	0.05	1.80	0.02	0.05	0.70
YPC193	13.40	3.40	7.00	3.60	2.40	0.05	0.05	0.05	0.05	1.40	0.03	0.05	1.10
YPC194	11.10	3.30	5.00	6.10	2.80	0.05	0.05	0.05	0.05	0.70	0.03	0.05	0.50
YPC195	9.60	3.80	6.00	4.70	2.40	0.05	0.10	0.05	0.05	0.25	0.01	0.05	0.60
YPC196	7.30	4.40	6.00	6.60	2.90	0.10	0.10	0.05	0.05	0.25	0.02	0.05	0.25
YPC197	14.20	4.20	7.00	8.60	2.90	0.10	0.05	0.05	0.05	0.80	0.01	0.20	0.25
YPC198	10.50	4.30	7.00	6.90	3.30	0.10	0.10	0.05	0.05	0.25	0.01	0.05	0.60
YPC199	7.00	4.20	5.00	7.60	2.40	0.10	0.10	0.05	0.05	0.25	0.03	0.05	0.60
YPC200	8.20	5.00	6.00	4.80	2.20	0.05	0.05	0.05	0.05	0.25	0.04	0.10	0.60
YPC201	7.20	4.70	5.00	8.40	2.70	0.10	0.05	0.05	0.05	0.25	0.02	0.05	0.25
YPC202	11.20	4.00	7.00	11.10	2.40	0.05	0.10	0.05	0.05	1.70	0.03	0.05	0.50
YPC203	7.30	3.60	5.00	7.20	2.80	0.05	0.20	0.05	0.05	1.70	0.03	0.10	0.25
YPC204	6.10	3.70	9.00	7.80	2.20	0.10	0.10	0.05	0.05	0.25	0.03	0.05	0.25
YPC205	3.30	3.10	6.00	4.80	2.10	0.05	0.10	0.05	0.05	0.25	0.01	0.05	0.60
YPC206	3.40	2.90	4.00	7.90	1.70	0.10	0.10	0.05	0.05	0.25	0.02	0.05	0.50
YPC207	3.90	3.80	5.00	6.40	2.10	0.05	0.10	0.05	0.05	0.25	0.03	0.05	0.50
YPC208	3.80	2.40	4.00	4.40	3.50	0.05	0.20	0.05	0.05	0.25	0.01	0.05	0.50
YPC209	8.70	3.90	5.00	6.30	1.90	0.05	0.10	0.05	0.05	1.60	0.01	0.05	0.25
YPC210	7.10	5.00	6.00	9.50	2.80	0.10	0.10	0.05	0.05	0.60	0.01	0.05	0.25
TIP001c	4.10	1.80	2.00	5.90	2.20	0.05	0.05	0.05	0.05	1.50	0.04	0.05	0.03
TIP001g	5.20	1.80	4.00	5.00	1.60	0.05	0.05	0.05	0.05	1.10	0.01	0.05	0.70
WAR001	7.80	2.00	4.00	6.70	2.50	0.10	0.05	0.05	0.05	0.90	0.02	0.05	0.03
MNL024	3.40	2.40	6.00	6.10	2.40	0.10	0.05	0.05	0.05	3.50	0.04	0.10	0.03
MNL044	2.00	1.20	3.00	4.40	1.40	0.05	0.05	0.05	0.05	1.40	0.01	0.05	0.03

Appendix 6

Chapter 3:

Seawater chemistry

From

Balgowan and Ardrossan

Seawater Analysis

ICP-OES:

Data Set	*Number*	*Location*	*UTM_Grid_ID*	*Easting*	*Northing*	*m_A_S_L*	*Temp*	*Cond*	*Time*	*pH*	*Eh*	*Notes*
Seawater	ARD	Ardrossan	GDA94_53H	768561	6187062	0	15.2	56000	7.52am	8.29	227	Ardrossan Jetty
Seawater	BAL	Balgowan	GDA94_53H	729320	6199207	0	17.4	54900	10.59am	8.07	190	taken off the groin

Data Set	*Number*	*Location*	*Si*	*Ca*	*K*	*Mg*	*Na*	*S*	*Al*	*As*	*B*	*Cd*	*Co*
			mg/L	*mg/L*	*mg/L*	*mg/L*	*mg/L*	*mg/L*	*mg/L*	*mg/L*	*mg/L*	*mg/L*	*mg/L*
Seawater	ARD	Ardrossan	0.182	459	457	1430	12200	1020	< 1.0	< 1.0	5.71	< 1.0	< 1.0
Seawater	BAL	Balgowan	0.157	445	439	1380	12200	993	< 1.0	< 1.0	5.75	< 1.0	< 1.0

Data Set	*Number*	*Location*	*Cr*	*Cu*	*Fe*	*Mn*	*Mo*	*Ni*	*P*	*Pb*	*Se*	*Zn*
			mg/L	*mg/L*	*mg/L*	*mg/L*	*mg/L*	*mg/L*	*mg/L*	*mg/L*	*mg/L*	*mg/L*
Seawater	ARD	Ardrossan	< 1.0	< 1.0	< 1.0	< 1.0	< 1.0	< 1.0	< 2.0	< 1.0	< 1.0	< 1.0
Seawater	BAL	Balgowan	< 1.0	< 1.0	< 1.0	< 1.0	< 1.0	< 1.0	< 2.0	< 1.0	< 1.0	< 1.0

Seawater Analysis

ICP-MS:

Data Set	Number	Location	UTM_Grid_IL	Easting	Northing	m_A_S_L	Temp	Cond	Time	pH	Eh	Notes
Seawater	ARD	Ardrossan	GDA94_53H	768561	6187062	0	15.2	56000	7.52am	8.29	227	Ardrossan Jetty
Seawater	BAL	Balgowan	GDA94_53H	729320	6199207	0	17.4	54900	10.59am	8.07	190	taken off the groin

Data Set	Number	Location	Li	Sc	V	Cr	Mn	Co	Ni	Cu	Zn	Ga	Ge
			ug/L	ug/L	ug/L	ug/L	ug/L	ug/L	ug/L	ug/L	ug/L	ug/L	ug/L
Seawater	ARD	Ardrossan	274.6	0.5	13.8	1.8	3.2	<2	9	3	18	<0.2	<0.2
Seawater	BAL	Balgowan	245.1	0.5	12	1	1.8	<2	5	2	22	<0.2	<0.2

Data Set	Number	Location	As	Se	Rb	Sr	Y	Zr	Nb	Mo	Ag	Cd	In
			ug/L	ug/L	ug/L	ug/L	ug/L	ug/L	ug/L	ug/L	ug/L	ug/L	ug/L
Seawater	ARD	Ardrossan	1	5.9	148.9	9840	<0.2	<0.2	<0.2	13.1	<0.2	<0.2	<0.2
Seawater	BAL	Balgowan	1	6.2	146.5	10090	<0.2	<0.2	<0.2	13.5	<0.2	<0.2	<0.2

Data Set	Number	Location	Sn	Sb	Te	Ba	La	Ce	Pr	Nd	Sm	Eu	Gd
			ug/L	ug/L	ug/L	ug/L	ug/L	ug/L	ug/L	ug/L	ug/L	ug/L	ug/L
Seawater	ARD	Ardrossan	0.4	0.4	2.5	12	<0.2	<0.2	<0.2	<0.2	<0.2	<0.2	<0.2
Seawater	BAL	Balgowan	0.3	0.3	1.2	22	<0.2	<0.2	<0.2	<0.2	<0.2	<0.2	<0.2

Data Set	Number	Location	Tb	Dy	Ho	Er	Tm	Yb	Lu	Hf	Ta	W	Tl
			ug/L	ug/L	ug/L	ug/L	ug/L	ug/L	ug/L	ug/L	ug/L	ug/L	ug/L
Seawater	ARD	Ardrossan	<0.2	<0.2	<0.2	<0.2	<0.2	<0.2	<0.2	<0.2	<0.2	<0.2	<0.4
Seawater	BAL	Balgowan	<0.2	<0.2	<0.2	<0.2	<0.2	<0.2	<0.2	<0.2	<0.2	<0.2	<0.4

Data Set	Number	Location	Pb	Bi	Th	U
			ug/L	ug/L	ug/L	ug/L
Seawater	ARD	Ardrossan	<0.4	<0.6	<0.2	3.6
Seawater	BAL	Balgowan	<0.4	<0.6	<0.2	3.9

Appendix 7

Published Article

Chapter 4:

Biogeochemical expression of buried iron-oxide-copper-gold (IOCG) mineral systems in mallee eucalypts on the Yorke Peninsula, southern Olympic Domain; South Australia.

Journal of Geochemical Exploration 185 (2018) 139–152

Journal of Geochemical Exploration 185 (2018) 139–152

Contents lists available at ScienceDirect

Journal of Geochemical Exploration

journal homepage: www.elsevier.com/locate/gexplo

Biogeochemical expression of buried iron-oxide-copper-gold (IOCG) mineral systems in mallee eucalypts on the Yorke Peninsula, southern Olympic Domain; South Australia

Keryn Wolff[a,*], Steven M. Hill[b], Caroline Tiddy[a,1], David Giles[a,1], Ronald J. Smernik[c]

[a] Deep Exploration Technologies Cooperative Research Centre (DET CRC), Department of Earth Sciences, University of Adelaide, Australia
[b] Geological Survey of South Australia, Department of the Premier and Cabinet, Government of South Australia, Australia
[c] School of Agriculture, Food and Wine, Waite Campus, University of Adelaide, Australia

ARTICLE INFO

Keywords:
Biogeochemistry
Eucalyptus
Exploration
Copper
Mallee
Yorke Peninsula

ABSTRACT

We report on the results of a regional scale biogeochemical sampling program conducted on the Yorke Peninsula, South Australia, utilising four locally occurring *Eucalyptus* species with mallee-form. Our purpose is to determine if there is an empirical relationship between Cu accumulation in the mallee leaves and elevated Cu in the underlying basement rocks – such that the mallee species might be a useful biogeochemical exploration tool in this area. The basement rocks of the Yorke Peninsula are prospective for iron oxide-copper-gold (IOCG) mineralisation but are mantled by Cambrian to Quaternary sedimentary rocks of variable thickness that inhibit traditional surface geochemical exploration techniques. There is no evidence to link Cu concentrations to dust contamination or fertiliser usage. Leaves of the four mallee species have comparable log normal population distributions of Cu, with a range between 1.6 ppm and 10 ppm. Higher concentrations of Cu (> 6 ppm) occur more commonly within 3 km of known Cu occurrences. These results suggest that all four mallee species have the ability to concentrate higher amounts of Cu in their leaves when the underlying/local geology also contains elevated Cu. The results suggest that biogeochemical sampling of multiple mallee species over large regions could be a useful exploration technique in covered areas of southern Australia where mallee species are widespread and densely populated.

1. Introduction

Australia has vast areas of cover sediments ranging in depth from a few metres to a few hundred metres (Anand, 2005), which are an impediment to mineral exploration (e.g. Fabris, 2010; Hillis et al., 2014; Noble, 2012; Reid et al., 2008). Exploring these areas can be costly and time consuming when using traditional methods such as drilling (e.g. Hillis et al., 2014; Hulme and Hill, 2003; Reid and Hill, 2010). The use of biogeochemistry for identifying mineralisation through variable depths of cover is becoming well established and is a non-invasive, efficient and cost effective exploration method (e.g. Hulme and Hill, 2003; Lintern et al., 2013b; Reid and Hill, 2010).

Globally, biogeochemistry has been used for detection of a wide range of mineral commodities including Au, Pt, Pd, base metals and rare earth elements (e.g. Cohen et al., 1987; Dunn, 1986, 2007; Kovalevsky, 1987; Lintern et al., 2013b; Närhi et al., 2014; Rencz and Watson, 1989). In Australia, studies have also shown that various plant species have the ability to concentrate elements of interest (e.g. Au, Cu, Zn, As, Cr and Pb). These species include pine and native cypress (*Pinus radiata* and *Callitris* sp.: Arne et al., 1999; Ashley and Wolfenden, 2005; Cohen et al., 2005), gum trees (*Eucalyptus* including *camaldulensis*, *brevifolia*, *pruinosa* and *concinna*: Hulme and Hill, 2003; Lintern et al., 2013b; Reid and Hill, 2010; van der Hoek et al., 2012), 'mulga' wattle (*Acacia aneura*: Lintern et al., 2013a), saltbush (*Atriplex*: Brown and Hill, 2005), spinifex (*Triodia pungens*: Reid and Hill, 2010; Reid and Hill, 2013) and bluebush (*Maireana*: Lintern et al., 1997). Thus far, biogeochemistry in the Australian context has most commonly been restricted to local-scale 'orientation' sampling across areas of known mineralisation or less often, laboratory experimentation (e.g. Lintern et al., 2013a). Sampling programs of regional-scale are less common (although see Brown and Hill, 2005; Mitchell et al., 2015) but are an important component of the research agenda as they provide an unbiased, empirical measure of the entire sample population, which in turn provides the opportunity to differentiate 'anomalous' results from

* Corresponding author at: Department of Earth Sciences, Mawson Building, University of Adelaide, North Terrace Campus, Adelaide, SA 5005, Australia.
E-mail address: keryn.wolff@adelaide.edu.au (K. Wolff).
[1] Now at Future Industries Institute, University of South Australia.

https://doi.org/10.1016/j.gexplo.2017.11.017
Received 20 April 2017; Received in revised form 30 October 2017; Accepted 21 November 2017
Available online 27 November 2017
0375-6742/

Fig. 1. Photo image of *Eucalyptus* that grow throughout the Yorke Peninsula. This photo shows the deep rooted nature of these genera. This species is an *E. gracilis* which also clearly displays the mallee-form with a visible lignotuber at the base of the trunk. Person pictured for scale is approximately 1.5 m tall.

'background'.

The success of biogeochemistry as an indicator of mineralisation relies on the ability of the plant to transfer ore or pathfinder elements from depth through the roots upwards to the bark, twigs, fruit and leaves, which can then be sampled and analysed using similar methods as for rock or soils (e.g. Närhi et al., 2014; Reid and Hill, 2010). In order to penetrate thick cover and interact with a large volume of regolith and basement materials it is desirable that the target species for biogeochemical sampling have deep and/or laterally extensive root systems. Eucalypts are particularly suitable as they typically form extensive root systems that penetrate deeply into the cover sediments (e.g. Fensham and Fairfax, 2007; Handreck, 1997; Hulme and Hill, 2003; Lintern et al., 2013b; Lintern et al., 1997; Wrigley and Fagg, 2010), (Fig. 1). Hulme and Hill (2003) reported that *Eucalyptus camaldulensis* has root systems that can occupy soil volumes > 4000 m^3. Other eucalypts such as *Eucalyptus marginata* have roots that may penetrate as deeply as 40 m (Wrigley and Fagg, 2010).

Eucalyptus is the most widespread native genus throughout Australia (Brooker et al., 2002; Hulme and Hill, 2003). There are at least 783 *Eucalyptus* species of which 60% may have a 'mallee' growth habit under appropriate conditions (e.g. Slee et al., 2006). Mallee describes a growth habit where multiple trunks emerge from a lignotuber at, or just below ground level and serve the purpose to re-sprout from dormant buds following fire or other disturbance (e.g. Brooker et al., 2002; Butt, 2005; Slee et al., 2006). Eucalypts tend to adopt the mallee form in drier climates and are common across arid southern Australia (e.g. Australian Native Vegetation Assessment, 2001, Fig. 2). Approximately 96 species of *Eucalyptus* are found in South Australia and 75 of those are considered mallee (Slee et al., 2006). Hybridisation can be characteristic of mallee species and this complicates identification (Brooker et al., 2002).

The ability of eucalypts to concentrate trace metals within their organs (e.g. leaves, twigs, bark and fruit) has been established in several studies (e.g. Dunn, 2007; Butt et al., 2005a and references therein). Consequently *Eucalyptus* biogeochemistry has the potential to identify areas of anomalous trace metal concentrations within the regolith or underlying basement (e.g. Butt et al., 2005a; Dunn, 2007; Hulme and Hill, 2003; Reid and Hill, 2010; van der Hoek et al., 2012). There are no published studies investigating the ability of mallee-eucalypts to incorporate Cu for the purpose of mineral exploration.

The basement rocks of the Yorke Peninsula region of South Australia are considered highly prospective for iron oxide-copper-gold mineralisation (IOCG) (e.g. Conor et al., 2010). The region has < 5% exposed basement rocks, the remainder being covered by a diverse range of sediments (e.g. Cowley et al., 2003; Wolff et al., 2017; Zang et al., 2006). These cover sediments form a barrier to geochemical exploration (e.g. Fabris, 2010; Mokhtari et al., 2009; Salama et al., 2016). Thirteen mallee *Eucalyptus* species are distributed throughout this region (Brooker et al., 2002), and some trees are proximal to known Cu mineralisation (Fig. 3).

In this paper we present the results of a regional-scale sampling program (218 samples over an area of 4000 km^2), focussing on Cu concentration in the leaves of mallee-eucalypt species across the Yorke Peninsula. Our purpose is to characterise the sample population and determine if there is an empirical relationship between elevated Cu concentration in the mallee leaves and elevated Cu in the underlying basement rocks – such that the mallee leaves might be a useful biogeochemical exploration tool in this area. In order to achieve this purpose we first seek to rule out potential sources of contamination in the leaf chemistry (wind-blown dust and fertiliser), assess variations in the population statistics that might indicate inter-species differences in Cu accumulation and then apply some simple tests to determine if higher concentrations of Cu in the mallee leaves correlate with known Cu accumulations in the basement rock.

2. Study area

2.1. Geological setting and mineralisation

The Yorke Peninsula is within the Olympic Domain on the south-eastern margin of the Gawler Craton (Fig. 2). Iron-oxide-copper-gold (IOCG) mineralisation hosted within the broader Olympic Domain includes the supergiant Olympic Dam as well as the Prominent Hill and Carrapateena deposits (Fig. 2) (Conor et al., 2010). IOCG mineralisation in the Olympic Domain is hosted within variable rock types including the Proterozoic Wallaroo Group and Hiltaba Suite granites (Conor et al., 2010; Cowley et al., 2003). The Wallaroo Group in the central and northern Yorke Peninsula hosts IOCG mineralisation of varying concentration and depth, including the historic Moonta-Wallaroo district and the Hillside deposit (Conor et al., 2010; Zang et al., 2006), (Fig. 2).

The Moonta-Wallaroo Cu mining district on the western Yorke Peninsula (Fig. 3) hosts vein style Cu mineralisation in shear zones that cross cut Paleo- to Mesoproterozoic rocks (Conor et al., 2010). The depth of Cu mineralisation, in the Moonta-Wallaroo district, ranges from 100 m to 300 m in mined locations and around 15 m or less at some prospects (Department of the Premier and Cabinet, 2017). Historically, the average grade of Cu mined throughout the district was around 5% (Conor et al., 2010). At Hillside on the eastern Yorke Peninsula (Fig. 3), Cu mineralisation is hosted by Proterozoic basement rocks within a shear zone beneath 5 to 10 m of cover and sub-cropping in the vicinity of the historic Hillside mine shaft (Fabris, 2010). As at Moonta-Wallaroo, historic mining activity included a significant component of shallow, oxidised material (native Cu and Cu-carbonates) with grades up to 44% Cu, whereas current identified resources are dominated by sulphide material with typical concentrations of 0.5 to

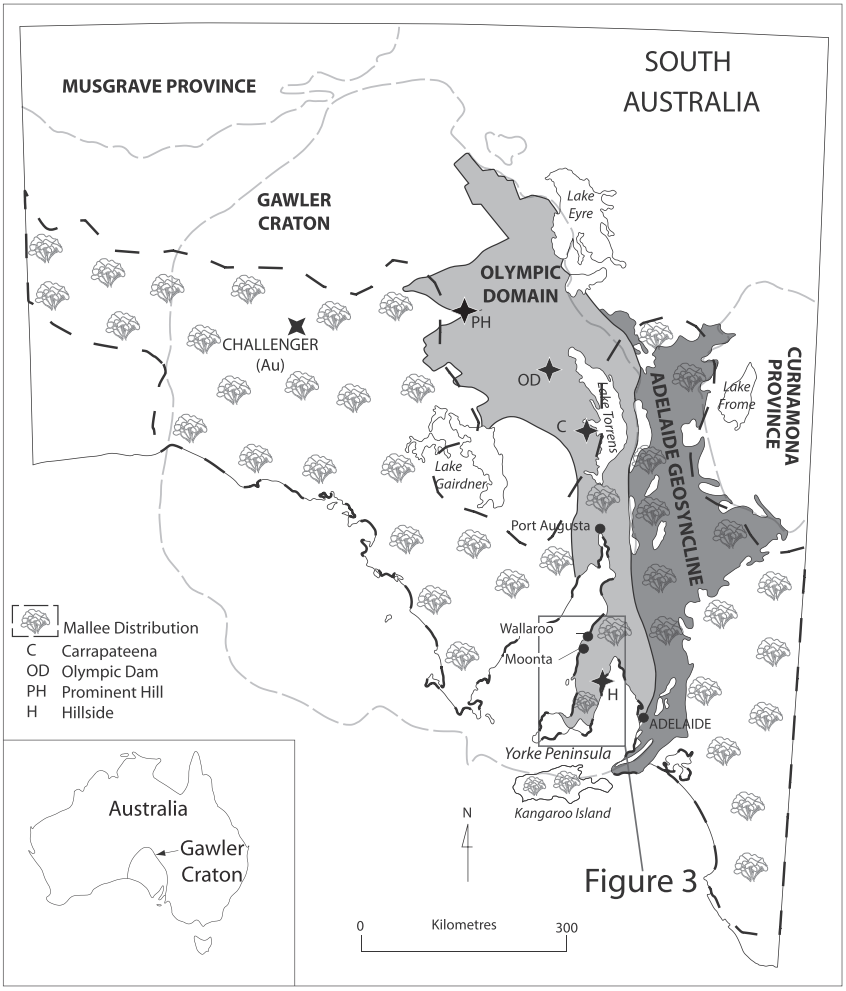

Fig. 2. Simplified geological map of South Australia showing study location within the Olympic Domain of the Gawler Craton (modified after Conor et al., 2010). Also shown is mallee distribution across South Australia (modified after Australian Native Vegetation Assessment, 2001). Inset: Australia showing location of the Gawler Craton.

2% Cu (Department of the Premier and Cabinet, 2017).

Copper has also historically been mined around Maitland and at scattered locations along the east-coast (Fig. 3). Maitland Copper Mine (Fig. 3) hosts high-grade Cu in surface carbonates (up to 25% Cu) whilst the primary Cu lodes (typically 0.3–11% Cu) are in quartz vein fractures within schist from the Wallaroo Group between 10 m and 70 m deep (Department of the Premier and Cabinet, 2017). Harts Mine (Fig. 3), contained up to 40% Cu sulphides in quartz vein fractures, with lesser concentrations as Cu carbonate found in weathered Wallaroo Group rocks exposed at the surface (e.g. Conor, 1995; Department of the Premier and Cabinet, 2017). Parara Mine (Fig. 3) was mined for Cu sulphides to a depth of 60 m (Zang et al., 2006) and produced 23.4 t at 25% Cu (Department of the Premier and Cabinet, 2017). Copper, as azurite and malachite also occurs in Cambrian carbonate rocks at Curramulka (Zang et al., 2006) and Kurra Murka, albeit in only minor concentrations (e.g. deposit no. 5122, Department of the Premier and Cabinet, 2017). Other Cu occurrences, prospects and abandoned mines are shown in Fig. 3.

The Wallaroo Group forms the basement in the central and northern Yorke Peninsula and is unconformably overlain by younger Cambrian to Quaternary sediments of < 1 m and up to at least 1500 m thickness (Crawford, 1965; Drexel and Preiss, 1995; Zang et al., 2006; Zang and Hore, 2001) (Fig. 3). Cambrian sediments include alternating limestone, sandstone and mudstone of up to 1400 m (Drexel and Preiss, 1995; Zang et al., 2006). Carboniferous to Permian sedimentation is dominated by glaciogenic sedimentary rocks including glacial diamictite, till, and shallow marine sedimentary rocks containing glacial erratics (Drexel and Preiss, 1995; Zang et al., 2006). Cenozoic sediments include fossiliferous and sandy limestone of the St Vincent Basin and Pirie Basin, clays and sands as well as aeolian dunes, beach and tidal sediments and soil (Zang et al., 2006). There has been extensive development of indurated pedogenic materials, particularly pedogenic carbonates which are typically located at, or within meters of, the current erosion surface within the sedimentary cover rocks (e.g. Cowley et al., 2003; Wolff et al., 2017; Zang et al., 2006).

2.2. Landscape

The Yorke Peninsula is mostly of low relief and comprises gentle undulating slopes and plains with an average height of 150 m above sea level (ASL) (DEWNR, 2013; Roberts, 2007). The highest elevations across the Yorke Peninsula occur in the central region surrounding Arthurton (250 m ASL) (Crawford, 1965; DEWNR, 2013; Zang et al., 2006). The coastline varies from sandy or rocky beaches to cliffs and steeply eroded hills (Roberts, 2007). Large areas of sand dunes and swales dominate portions of the north-west and central to south-east areas of the Yorke Peninsula, whilst playa salt lakes and clay pans dominate the landscape to the south. The water table generally occurs at 2 m or greater below the surface (DEWNR, 2017). There is a NNE-SSW trending escarpment extending along the eastern coastline northwards from Ardrossan (Crawford, 1965) forming rugged, eroded cliffs and steep-sloped hills.

2.3. Climate

The climate across the Yorke Peninsula is typically ‘Mediterranean’

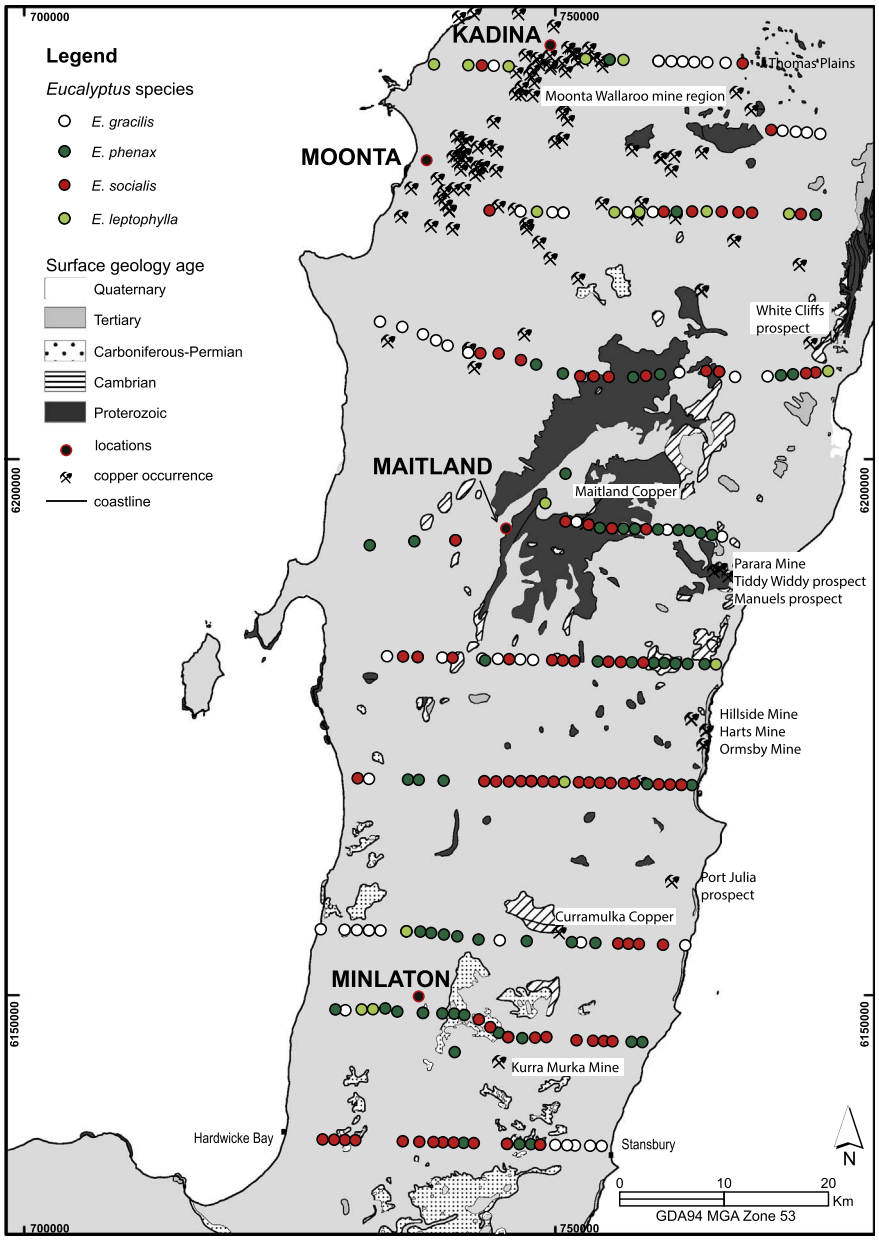

Fig. 3. Simplified surface geology map of Yorke Peninsula (downloadable GIS data extracted from SARIG: https://map.sarig.sa.gov.au Last accessed 04/04/2017). The location of the various *Eucalyptus* species sampled is shown. The location of this map, within South Australia, is shown in Fig. 2.

with hot dry summers and mild and wetter winters (Neagle, 2008). The maximum average temperature ranges from 27 °C to 30 °C during summer and 15 °C to 16 °C during winter. Rainfall across the Yorke Peninsula typically averages around 500 mm per year with June recording the greatest rainfalls (~70 mm) (Bureau of Meteorology, 2017). Annual evaporation rate of rainfall is high. The general direction of the prevailing wind is from the west, being more from the north-west during the warmer months and the south-west during the cooler months.

2.4. Vegetation

Most of the natural vegetation, i.e. that which occurred prior to European settlement across the Yorke Peninsula, has been cleared for grazing and cropping (DEWNR, 2013; McDowell et al., 2012; Neagle, 2008; Zang et al., 2006). Widespread cropping includes cereal grains, oil grains and legumes as the majority of the region contains moderately fertile soils (DEWNR, 2017). Much of the remaining native vegetation is restricted to corridors along roadside verges and fence lines, which act as windbreaks. Patches of woodland typically remains on ground that is the least suitable for agriculture (Neagle, 2008).

The majority of the native vegetation can be broadly characterized as open mallee woodland and shrubland (Neagle, 2008). The woodlands contain *Eucalyptus*, *Melaleuca* (Tea tree), *Acacia* (wattle), *Allocasaurina* (sheoak) and *Callitris* (cypress) with an understory of grasses or sedges such as *Triodia* (spinifex), *Gahnia* (sedge), *Lomandra* (a perennial herb), *Atriplex* (saltbush) and *Lepidosperma* (sedge). Coastal shrublands and lowlands contain *Eucalyptus*, *Avicennia marina* (mangrove), *Atriplex* (saltbush), *Maireana* (bluebush) and *Halosarcia* (samphire), while watercourse communities contain *Eucalyptus*, *Acacias* and various understory grasses (Neagle, 2008; Zang et al., 2006).

There are fourteen species of *Eucalyptus* (*E.*) that occur across the Yorke Peninsula of which thirteen are considered mallee (Brooker et al., 2002). With the exception of *E. diversifolia* (*Eucalyptus sub genera Eucalyptus*) all other eucalypts fall into various sections of the sub genera *Symphyomyrtus* as follows: *E. angulosa*, *E. rugosa*, *E. incrassata*, *E. dumosa*, *E. percostata*, *E. brachycalyx* and *E. phenax* subsp. *phenax*, *E. calycogona* subsp. *calycogona*, *E. gracilis*, *E. leptophylla*, *E. socialis* subsp.

socialis, *E. socialis* subsp. *glossy leaves* and *E. oleosa* subsp. *oleosa*. *Eucalyptus* sub genera *Exsertaria*; *E. camaldulensis* subsp. *camaldulensis* (River Red Gum) is the only native occurring eucalypt-tree (single trunk, tree form) found on the Yorke Peninsula. Hybridisation of species from sub genera can occur which makes identification difficult (Brooker et al., 2002). Natural integration between more closely related species found throughout the region such as *E.incrassata* and *E. angulosa* can also occur (Brooker et al., 2002).

3. Materials and methods

3.1. Sampling strategy

This study differs from typical 'orientation' style biogeochemical surveys in that there are not specific positive or negative control points. Although there are areas of known mineralisation within the survey area we have not sought to establish key locations where it is possible to compare known Cu concentrations in the subsurface with Cu concentrations in the sampled leaves. Nor do we have access to data from which we can independently determine the bioavailability of key elements in the subsurface. Rather, our strategy has been to collect regional samples in a program that is subject to the same practical considerations as experienced by exploration companies operating in covered terrains – where there may be little or no prior knowledge of the subsurface metal distribution or speciation *but* where biogeochemistry offers the potential for cheap, rapid and environmentally sensitive first pass reconnaissance sampling. The most relevant question in this survey is; can the biogeochemistry be used as an empirical tool to highlight sub regions within the survey area where there is a greater likelihood of discovering economic Cu mineralisation and where further exploration should be focussed?

In order to answer this question we first need to characterise the entire sample population (by systematic sampling avoiding the temptation to focus on known mineralisation) and then determine if there is a spatial relationship between elevated concentrations of ore and pathfinder elements and areas of known mineralisation.

The framework of our sampling program was provided by the grid-like distribution of remnant mallee forest along road corridors throughout the Yorke Peninsula. Samples of leaves from mallee-eucalypts were collected approximately every 1 km along ten, east-west road corridors with a north-south spacing of roughly 10 km (Fig. 3). Samples from four different mallee-form sub-species of *Eucalyptus* were collected and include *E. gracilis*, *E. phenax*, *E. socialis* and *E. leptophylla* (Fig. 3). Individual eucalypts were identified using EUCLID (Brooker et al., 2002). A variety of species were sampled as individual sub-species of *Eucalyptus* have preferred habitats e.g. inland, dunes and swales, or coastal cliff-tops (Neagle, 2008). Where no eucalypts were present at designated sample locations, the spacing was extended slightly until a suitable tree could be located. Overall, a grid pattern was formed that extended from Stansbury and Hardwicke Bay in the south to Kadina and Thomas Plains in the north (Fig. 3).

Samples were collected at the end of summer (March through to April 2012) prior to winter rainfall. In other studies from arid Australia (e.g. Hulme and Hill, 2003; Reid and Hill, 2010) this timing has been associated with maximum biogeochemical expression, with the inference that water and metal are sourced from the deeper parts of root systems during times of scarce surface water. This timing is also prior to application of fertilisers used during and following crop sowing (Department of State Development, 2014), which may be a potential source of contamination.

3.2. Sampling methods

A total of 218 leaf samples were collected from trees that appeared healthy and mature (i.e. not a sapling). Hands were cleaned and dried between samples in order to minimise potential contamination transferred by hand. Approximately 200 g of leaves were collected at each site and where possible, were sampled from trees on the southern side of the road and at the farthest side of the tree from the road. This method was chosen to reduce contamination from road dust. All samples were placed in calico bags to allow air circulation and delay the onset of rotting as per Dunn (2007). Samples were later dried in their original calico bags in an oven at 60 °C for 36–48 h. Dried samples were sorted by separating the leaves from any twigs which may have remained attached and discarding any leaves that did not appear to be healthy. Approximately 60–80 g of the best leaves were reserved for analysis.

Dust contamination may result in analytical data that reflect the composition of the dust rather than the concentration of metals accumulated in the tissues of the plant (Lintern et al., 2013b; Mitchell et al., 2015). Such contamination may be minimized by sampling methodology, for example by ensuring hands are cleaned and dried between samples and choice of sample location (as above) and by post sampling treatment, for example washing with water prior to drying (e.g. Arne et al., 1999; Hulme, 2008; Mitchell et al., 2015). Some studies (e.g. Dunn, 2007; Hulme and Hill, 2003) have shown that dust contamination on Eucalyptus leaves is negligible and not greatly improved by washing. This led Hulme and Hill (2003) and Dunn (2007) to infer that dust particles shed easily from the waxy surfaces of eucalyptus leaves and that washing is not a critical component of the sampling protocol for eucalypt species. Following this advice we did not wash the samples collected in this study. However we have analysed for a range of elements typically enriched in wind-born dust (Al, Fe, Zr) as a means of quantifying potential dust contamination.

As the application of fertiliser is widespread across the entire sampling area, and also represents a potential wind-born contaminant, the chemistry of a locally used fertiliser (urea and diammonium phosphate (DAP), Fabris, 2010) was used to determine any contamination and/or influence on the leaf chemistry.

Samples were sent to ACME Analytical Laboratories in Vancouver, Canada for analysis. Samples were first macerated to 100-mesh prior to aqua regia digestion of 5 g aliquots. Inductively-coupled plasma-mass spectrometry (ICP-MS) was used to determine element concentrations. Included with these analyses were ACME Laboratories standards as well as additional duplicates. One in every 10 samples were replicated in the laboratory. Laboratory standards were included in the analytical batches at a rate of 1 standard for every ten unknowns. The standards included; STD CDV-1 (n = 8), STD V14 (n = 2) and STD V16 (n = 10). Laboratory blanks were also included at a rate of one in every ten unknowns. All analyses of standards and blanks fell within acceptable range of the expected values, with expected and mean ± standard deviation of the measured Cu concentrations (ppm) as follows: CDV-1 (8.61, 8.49 ± 0.84), V14 (4.8, 4.85 ± 0.23), V16 (6.69, 6.65 ± 0.67), and blank (< 0.01, 0.003 ± 0.01).

3.3. Data treatment and statistics

The biogeochemical data were imported into ioGAS™ software in order to characterise population statistics, determine the extent of dust and fertiliser contamination, compare between mallee species and assess spatial relationships with areas of known mineralisation.

Standard data treatment included constructing histograms and probability plots of both the raw concentration data and $\log_{10}$ concentration data of the mallee leaf analyses. As a general rule the trace metal concentrations, including Cu, tend to have log normal population distributions and as such it is appropriate to report key population statistics (mean, standard deviations, range) of the $\log_{10}$ data. We used such statistics as a means of comparing the concentrations of numerous elements in the leaves of the four main mallee species analysed in this study, in order to test if there were systematic, species-dependent differences in element uptake. X-Y plots were used to assess the potential for dust and fertiliser contamination, in particular seeking to identify

linear trends in suspected contaminants (Al, Fe and Zr in dust; K, P and Zn in fertiliser) and determine any correlation between these elements and Cu.

Lastly, we have applied a simple test to determine if elevated concentrations of Cu in mallee leaves are likely to be spatially correlated with Cu mineralisation in the subsurface. Our options for geostatistical correlation are limited in this survey area because the distribution of Cu concentration in the subsurface is largely unknown. We do not have access to a regional Cu-in-basement dataset of comparable spatial resolution to the mallee data and instead have used the distribution of historic Cu prospects as an imperfect first pass approximation. Our approach is to apply a 3 km search radius around known Cu prospects and compare the populations of Cu in mallee leaves from inside and outside the search radius.

4. Results

4.1. Distribution of mallee

The distribution of mallee-eucalypt species sampled is shown in Fig. 3. 218 samples were taken from four species as follows; *E. gracilis* (53), *E. phenax* (60), *E. socialis* (87), and *E. leptophylla* (18). *E. gracilis* was found to be concentrated in the north and south of the study area. *E. phenax* was found to be broadly distributed across the central and southern regions of the study area, with only a few sampled in the northern area. *E. socialis* was the most commonly sampled and most widespread species. The northern-most transect had the least amount of *E. socialis* sampled. *E. leptophylla* was found to be concentrated in the northern portion of the study area, with only sparse distribution in the central and southern areas.

4.2. Chemistry

Of the 53 elements analysed, 28 were above analytical detection limits in the leaf samples. Results for these are included in Supplementary data Appendix 1. Representative data for selected elements are given in Table 1. The focus of this paper is on Cu as there is not enough Au above detection limits to be useful (Appendix 1). There are no particularly useful patterns in the other 21 elements.

Leaves from all mallee species contain Cu ranging from 1.59 ppm to 10.04 ppm (Table 1). The distribution of Cu in all species is shown in Fig. 4. The average Cu for all species sampled is 3.80 ppm (Table 1). Both the lowest and highest concentrations occur in *E. phenax*. *E. phenax, E. socialis* and *E. gracilis* contain similar average Cu concentrations while *E. leptophylla* contains the highest average Cu ppm concentration (Table 1; Fig. 4). The widest range in Cu concentration is found in *E. phenax* (Table 1; Fig. 4).

Aluminium, Fe and Zr results are included as measures of dust contamination. Aluminium was measured at or slightly above analytical detection limit in 92 samples (Table 1, Appendix 1). Concentration of Al ranged from 0.01% to 0.03% which is barely above detection limit (Al, 0.01%). Up to half of each species sampled contained Al concentrations above detection limits. Of these only half again were above detection limits by only 0.01% or 0.02%. Iron was measured in all leaf samples

Table 1
Biogeochemistry summary statistics of *Eucalyptus* leaves representative of the Yorke Peninsula.

Eucalyptus species	*n*	Element	Method	Detection	Min	Max	Mean	Median	Std deviation
E. gracilis	53	Cu			1.95	8.35	4.09	3.89	1.41
E. phenax	60				1.59	10.04	3.86	3.46	1.53
E. socialis	87		ppm	0.01	1.67	7.77	3.29	3.01	1.16
E. leptophylla	18				2.15	8.83	5.21	5.02	1.75
All species	218				1.59	10.04	3.8	3.44	1.48
E. gracilis	53	Cu	$\log_{10}$		0.29	0.92	0.59	0.59	0.15
E. phenax	60				0.20	1.00	0.56	0.54	0.16
E. socialis	87			n/a	0.22	0.89	0.49	0.48	0.14
E. leptophylla	18				0.33	0.95	0.69	0.70	0.16
All species	218				0.20	1.00	0.55	0.54	0.16
E. gracilis	53	P	%		0.05	0.13	0.08	0.07	0.02
E. phenax	60				0.04	0.16	0.07	0.06	0.03
E. socialis	87			0.001	0.04	0.13	0.07	0.06	0.02
E. leptophylla	18				0.06	0.11	0.08	0.08	0.02
All species	218				0.04	0.16	0.07	0.07	0.02
E. gracilis	53	K	%		0.31	0.87	0.46	0.45	0.10
E. phenax	60				0.29	0.87	0.55	0.54	0.13
E. socialis	87			0.01	0.30	0.83	0.52	0.51	0.10
E. leptophylla	18				0.36	0.90	0.56	0.52	0.14
All species	218				0.29	0.90	0.52	0.50	0.12
E. gracilis	22	Al	%		0.01	0.03	0.01	0.01	0.01
E. phenax	19				0.01	0.02	0.01	0.01	0.00
E. socialis	44			0.01	0.01	0.03	0.02	0.02	0.01
E. leptophylla	7				0.01	0.02	0.02	0.02	0.00
All species	92				0.01	0.03	0.01	0.01	0.01
E. gracilis	53	Fe	%		0.01	0.03	0.01	0.01	0.00
E. phenax	60				0.01	0.02	0.01	0.01	0.00
E. socialis	87			0.001	0.01	0.03	0.01	0.01	0.00
E. leptophylla	18				0.01	0.02	0.01	0.01	0.00
All species	218				0.01	0.03	0.01	0.01	0.00
E. gracilis	53	Zn	ppm		4.7	22	12.35	12.10	3.28
E. phenax	60				5.4	24	12.22	11.45	4.46
E. socialis	87			0.1	7	26.7	13.65	13.40	3.37
E. leptophylla	18				7.5	23.4	14.57	14.95	4.24
All species	218				4.7	26.7	13.01	12.75	3.81
E. gracilis	53	Zr	ppm		0.02	0.18	0.06	0.06	0.03
E. phenax	60				0.03	0.14	0.06	0.06	0.02
E. socialis	87			0.01	0.02	0.21	0.08	0.07	0.04
E. leptophylla	18				0.03	0.13	0.07	0.06	0.03
All species	218				0.02	0.21	0.07	0.06	0.03

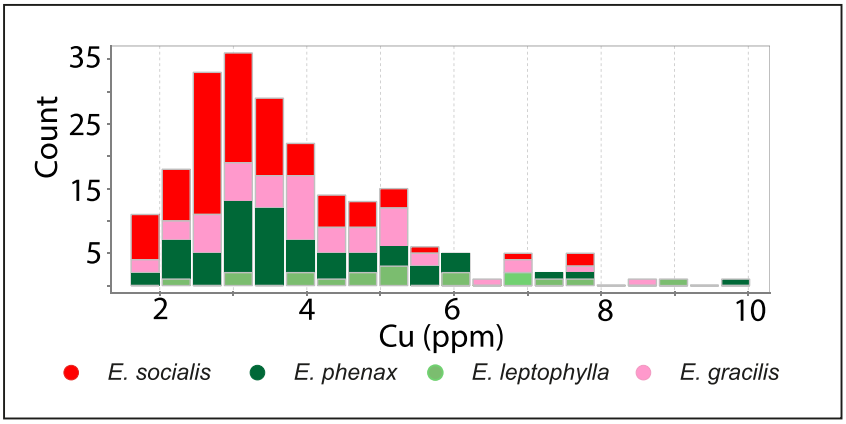

Fig. 4. Stacked histogram plot showing distribution of Cu in each species of mallee-eucalypt.

and concentrations ranged from 0.006% to 0.028% (Table 1). The range in Fe concentration was similar for all four species. Zirconium was measured in all samples and concentration ranged from 0.02 ppm to 0.21 ppm. There were minimal differences in Zr concentration among eucalypt species with *E. socialis* containing the highest average concentration (Table 1). Aluminium and Zr display a mutual linear relationship although the low detection values and fewer results affect how these appear (Fig. 5a). Iron and Zr share a very close positive linear relationship (Fig. 5a). Copper has a poorly correlated relationship with Zr (Fig. 5a).

Potassium, P, and Zn results are included as potential measures of fertiliser contamination and to measure any potential preference for

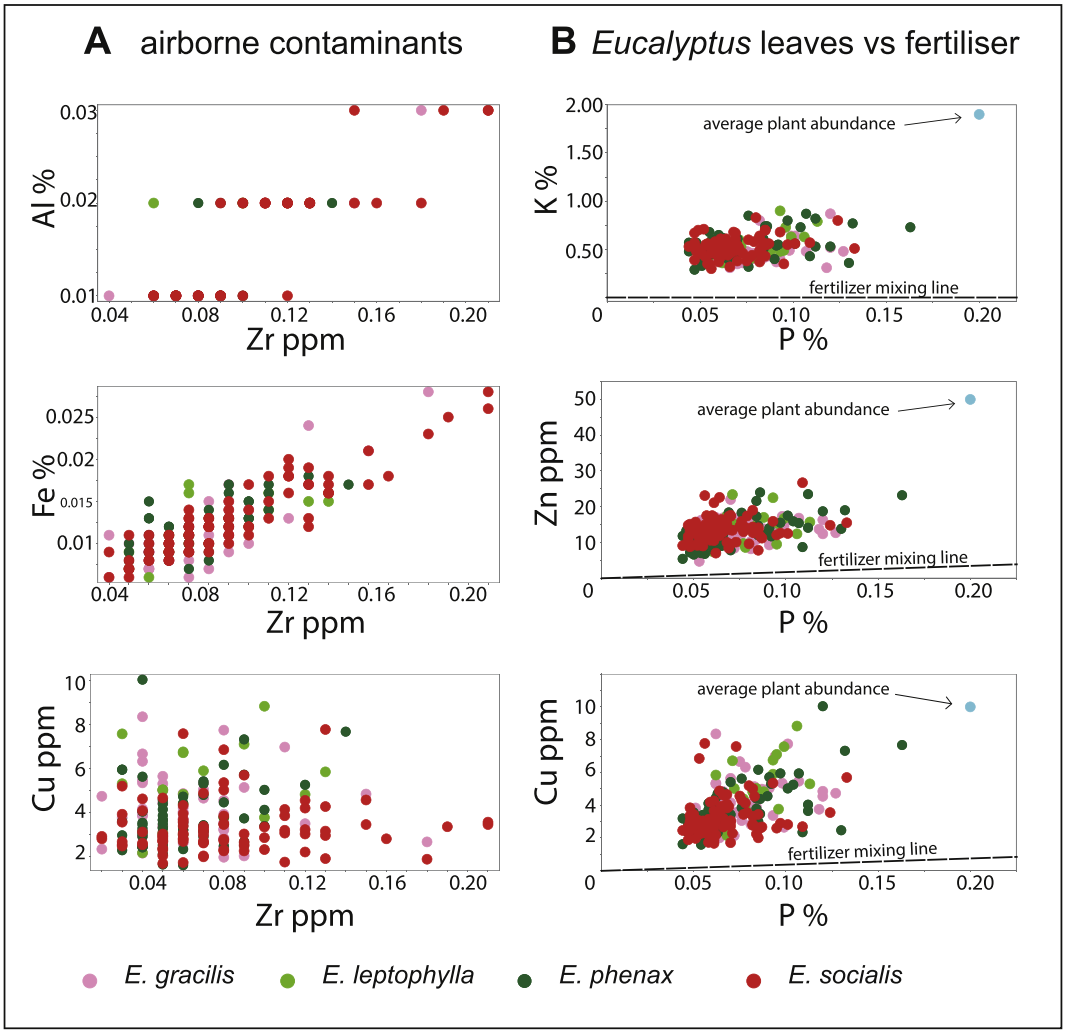

Fig. 5. XY plots of various element concentrations found in mallee-eucalypt leaves from the Yorke Peninsula; A: concentrations of dust contaminants (Al, Fe and Zr) plotted against Cu; B: elements found in fertiliser (P, K and Zn) plotted against Cu concentration. A fertiliser mixing line based on di-ammonium phosphate (DAP) data from Fabris (2010) shows the expected trend in concentration based on fertiliser uptake. The blue dots indicate the average abundance of respective elements in all plants based on Dunn (2007). (For interpretation of the references to colour in this figure legend, the reader is referred to the web version of this article.)

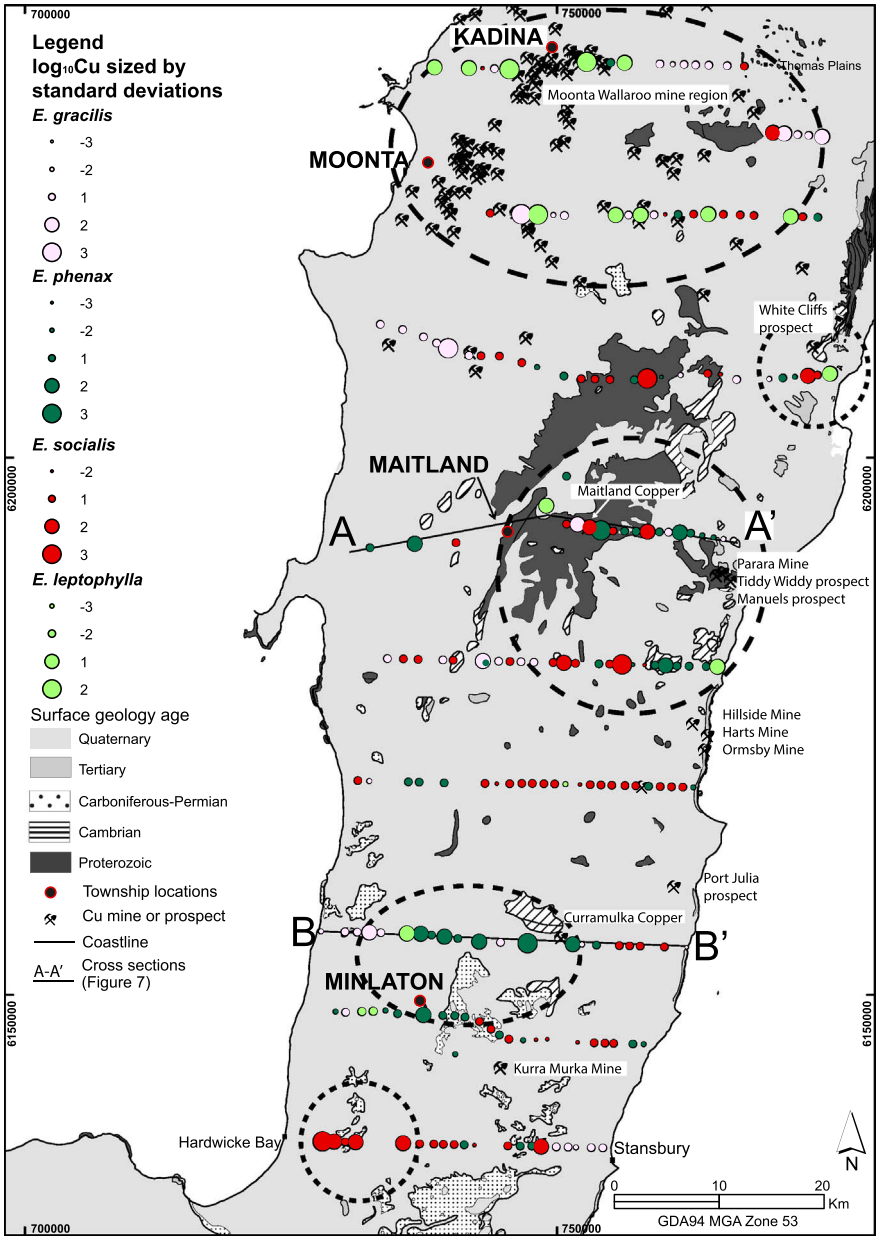

Fig. 6. Distribution of $\log_{10}$Cu in mallee across Yorke Peninsula. The overall pattern of the various species of Eucalyptus display a trend for concentrating higher levels of Cu into their leaves nearby to regions where Cu is known to occur as indicated. Regions of elevated Cu concentration are indicated by dashed lines. Cross sections A-A′ and B- B′ are presented in Fig. 9.

trace element uptake related to plant physiology and growth (Table 1, Fig. 5b). Phosphorus was measured in all samples and concentrations ranged from 0.04% to 1.63% (Table 1). There were minimal differences in average P concentrations across all four species with *E. phenax* containing the highest average concentration (Table 1, Fig. 5b). Potassium was measured in all samples and concentrations ranged from 0.29% to 0.90% (Fig. 5b). The range of K concentration was similar in all four species (Table 1). Zinc was detected in all samples and concentrations ranged from 4.7 ppm to 26.7 ppm (Table 1). Similar Zn average concentrations were found within all four species. There is no clear relationship between K and P. Potassium and P concentrations are clustered, with little scatter, above the fertiliser mixing line and below the average plant composition (Fig. 5b). Zinc and P appear to have a very weak positive relationship with a slight clustering of data points and some scatter but also well above the fertiliser mixing line (Fig. 5b). Copper and P do not show strong correlation of results (Fig. 5b).

5. Discussion

5.1. Potential sources of contamination

Dust and fertilisers are considered the two largest sources of potential contamination of the mallee leaves throughout the study area. Dust contamination needs to be considered as airborne particles may be enriched in Cu from nearby mining. Fertilisers used in cropping can contain Cu and therefore may influence the apparent Cu content of the mallee leaves. The influences of these contaminants on the geochemical data have been assessed by comparing the concentrations and associations of typical aeolian contaminants and various elements found in fertiliser samples.

5.1.1. Dust contamination

Airborne and/or roadside dust contamination can be assessed by comparing relationships between Al, Fe, Zr and Cu (e.g. Kabata-Pendias and Pendias, 2001). Within dust, Al and Fe are mostly found in fine grained clay (i.e. aluminosilicates) and iron-oxide particles. Both Al and

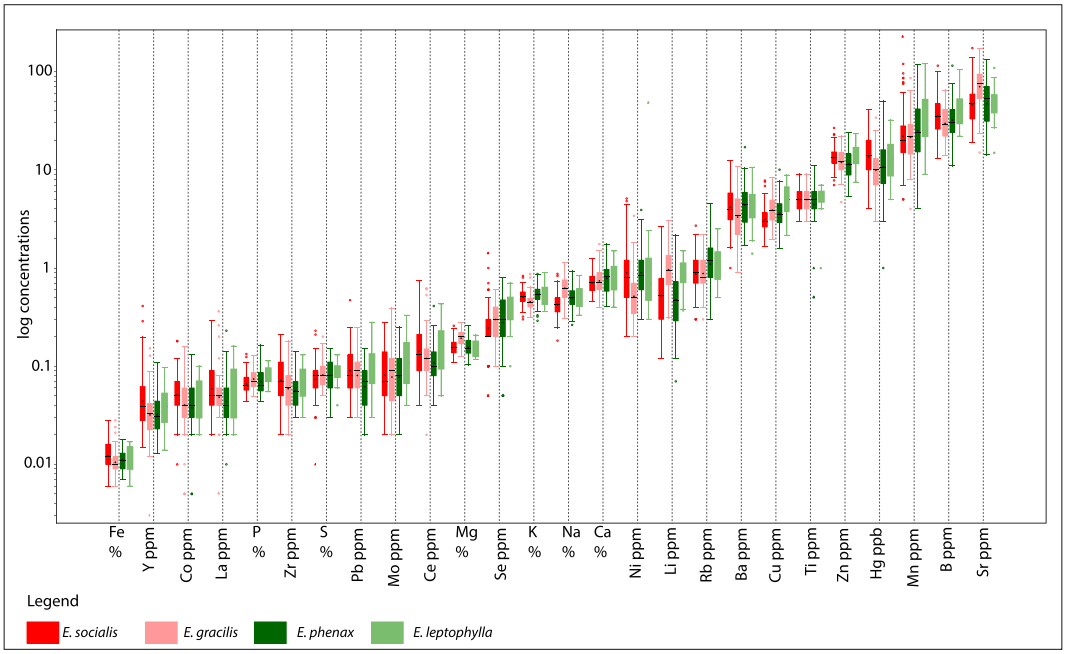

Fig. 7. Tukey box plots for all elements on a common Y axis and logged. Elements with > 90% of their results above detection were used. Solid rectangles represent data that is within 1 standard deviation of the mean. Lines represent 2 standard deviations from the mean and outliers are represented by dots. Within the solid rectangles the black dash is the mean and the black dot is the median.

Fe are major constituents in soils (Kabata-Pendias and Pendias, 2001). Zirconium is mostly found in sand (Fitzpatrick and Chittleborough, 2002), which occurs extensively throughout the region. Within plants, Al and Zr are not essential elements for growth and Fe is only required in trace amounts (e.g. Dunn, 2007) therefore small amounts of dust contamination would be expected to have a strong influence on the Al, Fe and Zr concentrations in the leaves.

Relationships between Al, Fe, Zr and Cu are shown in Fig. 5a. A strong positive linear relationship is shown between Fe and Zr. A similar relationship is observed between Al and Zr, albeit not as distinctly linear due to Al concentrations being so close to detection levels (Fig. 5a). Although these elements are at very low concentrations, the linear relationships are consistent with dust contamination (e.g. from soil components, Kabata-Pendias and Pendias, 2001; Fitzpatrick and Chittleborough, 2002). There is no relationship between Cu and Zr (Fig. 5a) as would be expected if dust contamination contributed substantially to the total Cu detected in leaf samples. This suggests that Cu is being incorporated into the eucalypts independently from the elements that comprise windblown dust and is sourced from elsewhere. The very low concentration levels of these elements (Al, Fe and Zr) also indicate that dust contamination has not impacted the overall chemical content of the leaves and that the improvement to data quality, by having pre-washed the samples, would be negligible.

5.1.2. Fertiliser contamination

Fertiliser application during the cropping season is widespread throughout the Yorke Peninsula (Department of State Development, 2014). Use of phosphate fertilisers have been shown to significantly increase the foliar content of P (e.g. Bennett et al., 1996; Crous et al., 2015) and could conceivably result in increased uptake of other essential nutrients or trace elements, either directly from the fertiliser or from the substrate as a result of more vigorous plant growth. Therefore, it is important to determine the impact, if any, of fertilisers on the Cu concentration in the eucalypt leaves. Whilst it is unknown exactly how much fertiliser the eucalypts have access to and are taking up, the concentrations of P, K, Zn and Cu in the leaves can be directly compared to actual fertiliser that is used throughout the region (Fig. 5b).

Di-ammonium phosphate (DAP) fertiliser is commonly used throughout Yorke Peninsula (Fabris, 2010). This fertiliser contains relatively high concentrations of Cu (75 ppm) which may be taken up by eucalypts dependant on root access, quantity applied and proximity to fertiliser application. This would therefore suggest that Cu concentrations in the eucalypts may merely be reflecting the fertiliser usage.

A fertiliser mixing line based on P, K, Zn and Cu concentrations in the DAP is shown in Fig. 5b. Both K and Zn versus P concentrations sit well above the fertiliser mixing line (Fig. 5b). Copper and P concentrations are also observed well above the fertiliser mixing line (Fig. 5b).

The broad scatter of data points for Cu concentration versus P is different to the narrower range in concentrations for K and Zn versus P (Fig. 5b) suggesting that there is no relationship of Cu to K, Zn or P and that these concentration patterns do not reflect contamination from fertiliser.

5.2. Natural uptake of elements

Essential elements for healthy plant growth such as P, K, Zn and Cu were not only included for fertiliser analysis but also used to assess whether the four species of mallee-eucalypts in this study are taking up elements in a similar manner. Phosphorus and K are considered major essential elements for plant growth while Zn and Cu are only required in trace amounts (Dunn, 2007). These elements were compared with ranges of plant concentrations reported by other authors (e.g. Attiwill and Adams, 1996; Barrow, 1977; Dunn, 2007; Gazola et al., 2015).

Phosphorus and K are both major essential elements that are taken up by eucalypts for growth but tend to have narrow concentration ranges in all species (e.g. Gazola et al., 2015; Grove and Thomson, 1986; Judd et al., 1996). Similar narrow ranges in concentration of P and K are also observed in the eucalypts of this study (Fig. 5b).

Zinc is required in trace amounts and tends to have an uptake synergistic with P (Kabata-Pendias and Pendias, 2001), implying that Zn, where available, will also be incorporated into the eucalypt along with P. A weak positive relationship between P and Zn was observed in the Yorke Peninsula data, (Fig. 5b) suggesting the uptake of Zn reflects the natural uptake by the eucalypts in this region.

Copper is also required in trace amounts by eucalypts and similarly

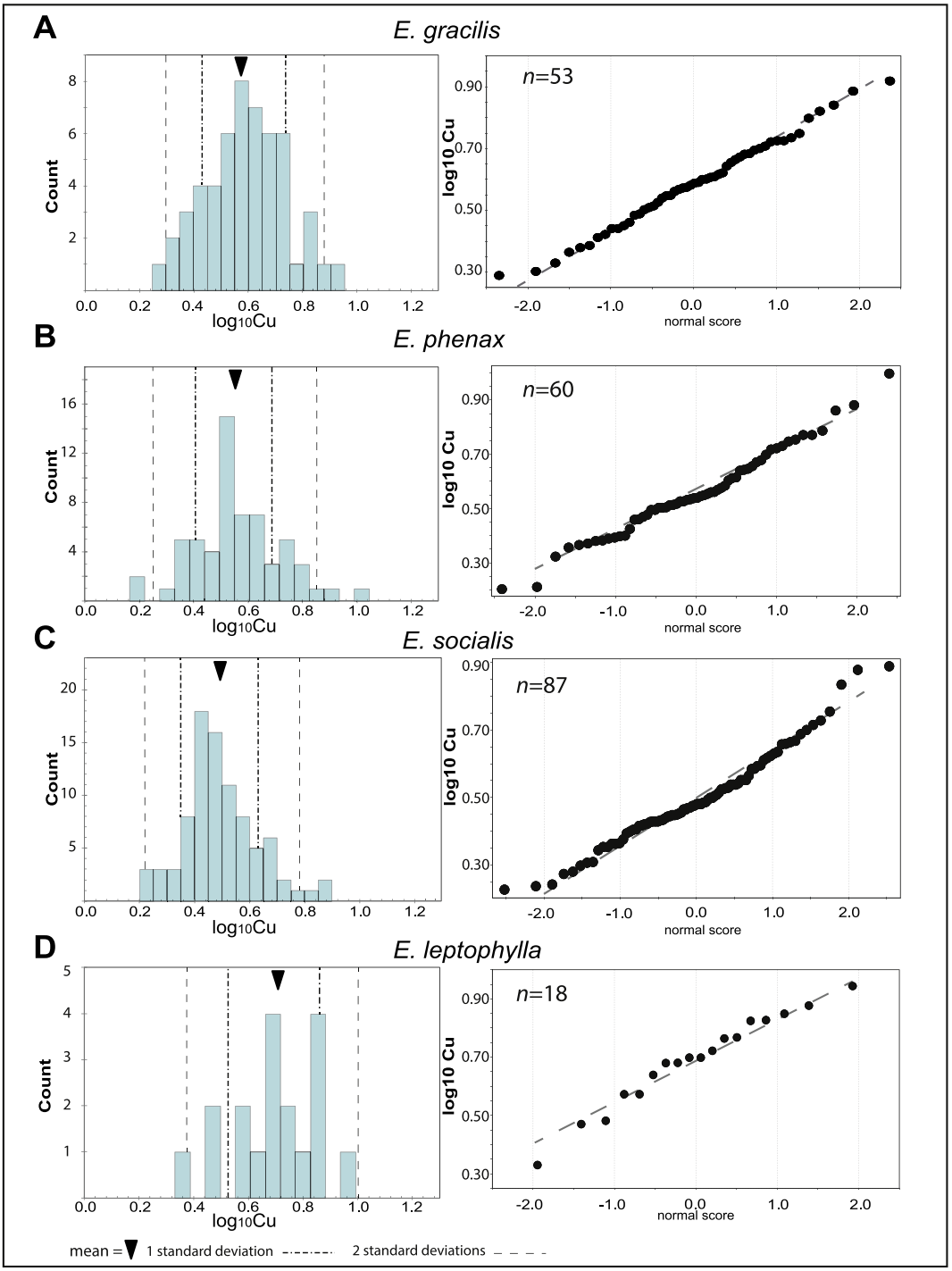

Fig. 8. Histograms (left) and normal probability plots (right) for A. *E. gracilis*; B. *E. phenax*; C. *E. socialis*; and D. *E. leptophylla*. Although *E. leptophylla* (D) has a higher overall concentration of Cu, the values remain within the ranges observed for the other species (A, B and C). Black arrow: (arithmetic) mean; dark dashed lines: 1 standard deviation; light dashed lines: 2 standard deviations.

shares a synergistic partnership with P (Kabata-Pendias and Pendias, 2001). This also implies a natural uptake of Cu where P is available. The Yorke Peninsula data does not show any obvious relationship between Cu and P (Fig. 5b); however, the broader range of Cu concentrations may mask any subtle relationships that may be present. The natural background levels of Cu taken up by the mallee in this region is suggested to be reflected by the dominant (average) population of Cu values (Fig. 4; i.e. an average of Cu 3.8 ppm). The Cu data also shows a population of samples with above average Cu concentrations (Fig. 4), suggesting an active enrichment process other than natural uptake of elements.

Plants growing in a Cu-rich substrate will naturally take up higher concentrations of Cu (Dunn, 2007; Kabata-Pendias and Pendias, 2001). Kabata-Pendias and Pendias (2001) also suggest that when there are higher concentrations of trace elements in soils, plants will take up more of that element even though it may not necessarily be a hyper-accumulator by definition (e.g. Kabata-Pendias and Pendias, 2001). The broad range of Cu concentrations within the Yorke Peninsula data and the observation of a population of samples with above average Cu concentrations (Fig. 5b) suggests there are mallee-eucalypts that are

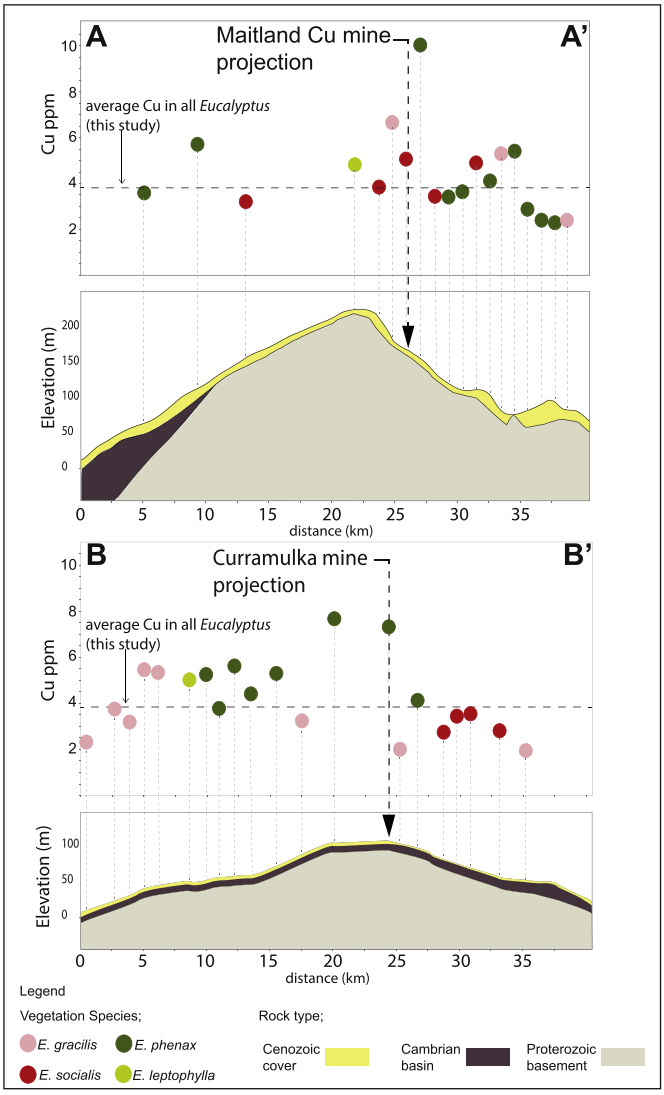

Fig. 9. Biogeochemical cross sections through transects containing Maitland Copper Mine (A to A′ Fig. 6) and Curramulka Copper Mine (B to B′ Fig. 6). The position of each mine is indicated within the respective transect. Both sections demonstrate a trend of decreasing Cu concentration in leaves of various *Eucalyptus* species with increasing distance from the mine.

taking up Cu in excess of biological requirements. Samples with higher Cu concentration are located in the north, east and southwest of the study area, and in most cases are coincident with regions of known Cu mineralisation (Fig. 6). The spatial relationship between the higher Cu concentrations in the leaves to Cu occurrences suggests that there is elevated Cu in the substrate that the trees have access to.

5.3. Statistical considerations for Cu in eucalypts

Previous authors (e.g. Butt et al., 2005b; Dunn, 2007) suggest that complications may arise if sampling a variety of different vegetation or by mixing species from the same genus, therefore there is a need to address any differences in the uptake of trace elements between *E. gracilis*, *E. phenax*, *E. socialis* and *E. leptophylla*. In this study, we are particularly interested in whether or not each species is taking up Cu in the same way. As there is limited existing data regarding trace element uptake in mallee eucalypts, we are limited in this study to comparing population statistics from each species (Table 1) in order to identify any systematic variations between them.

Comparison of data for all elements in the four species (Fig. 7) shows they have very similar means and standard deviations, with each species overlapping in range within the first and third quartiles. We infer from these data that the four species have a very similar uptake of a wide range of nutrients and other trace elements which suggests that their biogeochemical response is comparable. Thus, we consider it reasonable to pool the data from the four species without performing any further normalisation.

E. leptophylla has slightly more Cu than the other three species, although still with overlapping populations at the first and third quartiles (Fig. 7). Cu concentrations for *E. gracilis* (n = 53), *E. phenax* (n = 60) and *E. socialis* (n = 87) have similar mean $\log_{10}$ Cu concentrations of between 0.49 and 0.59 ppm. *E. leptophylla* (n = 18) has a higher average $\log_{10}$ Cu concentration of 0.69 ppm (Fig. 8). The probability plots for *E. gracilis*, *E. phenax* and *E. socialis* are comparable, with relatively straight lines between − 2 and + 2 standard deviations (Fig. 8). *E. leptophylla* also forms a straight line on the probability plot, although displaced to higher values than the other species and with a higher mean (Fig. 8). Although the Cu concentrations are slightly higher for *E. leptophylla*, the uptake of Cu displays a similar pattern for all four species (Fig. 8) with the higher concentrations coinciding with nearby Cu occurrence (Fig. 6).

E. leptophylla samples are more common in the Cu mining regions of Kadina and Moonta (Figs. 3 and 6). As the biogeochemical uptake of trace elements (including Cu) is comparable for all four species, the possibility that higher concentrations of Cu in the plants are related to

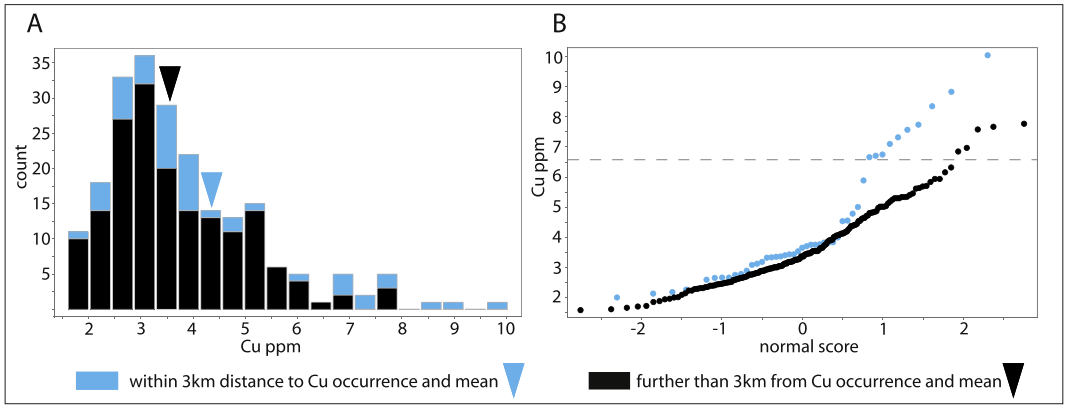

Fig. 10. A; histogram and B; probability plot showing relationship of Cu concentration in trees that are within 3 km (blue) to known Cu occurrence compared to trees > 3 km away from Cu occurrence (black). Trees within 3 km to known Cu occurrence have a higher mean Cu concentration (4.3 ppm indicated by blue marker) and standard deviation (2 ppm) with a longer tail skewed to the right with a broader spread towards higher Cu concentrations (2–10 ppm) compared with those that are further than 3 km away (mean 3.6 ppm indicated by black marker) and standard deviation (1.2 ppm). The dashed line in B identifies a breakpoint in both populations which we interpret as a threshold value of interest for this region. (For interpretation of the references to colour in this figure legend, the reader is referred to the web version of this article.)

higher Cu concentration in the substrate and potentially proximity to buried Cu mineralisation needs to be considered.

5.4. Eucalypt expression of Cu nearby to Cu occurrence

Dietman (2009) demonstrated that the soils surrounding the Hillside Cu mine (Figs. 3 and 6), are elevated in Cu. Likewise, clays, transported sediments and carbonate rocks that make up the soils surrounding the Moonta mining region contain elevated Cu compared to regional background levels (e.g. Keeling et al., 2005; Wolff et al., 2017). These studies suggest that Cu is mobile within the transported sediments and regolith materials overlying basement rocks enriched in Cu, and thus has the potential to be biologically available.

The tendency for the mallee eucalypt leaves to be slightly elevated in Cu in the vicinity of known mineral occurrences is supported by the results of this study (Figs. 6 and 9). Mallee-eucalypts occurring nearby the Maitland and Curramulka Cu mines show elevated Cu in the leaves compared to the more distal eucalypts (Fig. 9). Additionally, in the northern Yorke Peninsula, there is a complex pattern of elevated Cu concentration in *Eucalyptus* leaves throughout the Moonta-Wallaroo mine region and in the vicinity of White Cliffs prospect (Fig. 9). This trend of Cu in *Eucalyptus* adjacent known Cu occurrence is observed independent of the species. This further supports the proposition that all four mallee-eucalypt species are taking up Cu similarly, and that they can collectively be used to identify regions of elevated Cu in soil and in the underlying basement.

The relationship between elevated Cu in mallee leaves and proximity to known mineralisation on a regional scale is illustrated by comparing the population statistics of trees within 3 km of known Cu occurrences to those that are > 3 km from known occurrences (Fig. 10). The trees closest to known Cu occurrences have a higher mean, greater standard deviation and are more skewed to higher values (Fig. 10a). The elevated concentrations in trees within 3 km of a known Cu occurrence are also highlighted as being a separate data population with Cu concentrations > 4 ppm and again at 6 ppm (Fig. 10b). This implies that trees within a relatively short distance of a Cu occurrence have a greater probability of taking up Cu in higher concentrations compared with those that are further away.

It is acknowledged that there are some trees that grow nearby to Cu occurrence that do not contain elevated Cu concentrations. There are various factors that may impact the trees ability to transfer Cu from the substrate to the leaves. For example, the depth of Cu-rich substrate may be beyond the depth of root penetration, the particular soil horizon that the roots reside in may not be elevated in Cu, or individual trees may have differing abilities to collect and store trace elements in their leaves (e.g. Dunn, 2007). As the trees were sampled 1 km apart, subtle variations in depth of cover or the lithology of underlying basement rocks may hamper root access, which could also affect the ability for a tree to take in more Cu. Higher density sampling may resolve these issues.

5.5. Elevated Cu concentrations in trees that are not nearby to Cu occurrences

In comparing these two populations (i.e. trees within 3 km from a Cu occurrence and trees > 3 km, Fig. 10), the population within 3 km of known Cu occurrences, has a higher proportion of samples above 4 ppm Cu and a distinct sub population above 6 ppm Cu. This Cu concentration (> 6 ppm) also corresponds to an apparent break on the Cu probability plot (Fig. 10b) for the remaining samples that are not within 3 km. This serves as a useful threshold for identifying interesting results worthy of follow up.

The Hardwicke Bay area has mallee-eucalypts that contain elevated concentrations of Cu yet are not directly adjacent to known Cu occurrences (Fig. 6). The group of mallee-eucalypts at Hardwicke Bay (Fig. 6) occur as a cluster of 3 samples that are spaced 1 km apart. It is possible that this cluster of trees with elevated Cu represents the surface expression of buried mineralisation. This area is underlain by thick Carboniferous-Permian sedimentary rocks (up to 500 m e.g. Drexel and Preiss, 1995; Zang and Hore, 2001) that have not been reported to host mineralisation on Yorke Peninsula or elsewhere across South Australia (Drexel and Preiss, 1995). A possibility that cannot be ruled out is that the elevated Cu in mallee leaves at Hardwicke Bay is a transported signal, either via physical transport of Cu in Quaternary sediments or via groundwater.

5.6. Implications for biogeochemical exploration for Cu

The widespread occurrence of mallee-eucalypts and their ability to transfer elemental signals from deep in the substrate they grow in makes them a potential tool for exploration. There are limitations that should be considered in designing a mallee biogeochemical survey:

- Identify the species of vegetation and the extent of its occurrence within the region of interest.
- Identify potential sources of contamination that occur throughout the region. This may include land use such as farming or mining.
- Sample at a density that produces robust statistics to identify background levels versus concentrations that are above background.
- Understand the regolith landscape processes in the region to determine whether biogeochemical signatures may reflect buried mineralisation or are the effect of physical and/or chemical element transport.

6. Conclusions

A variety of mallee-eucalypt species are shown to accumulate Cu in their leaves in areas of known Cu mineralisation across the Yorke Peninsula. The mallee-eucalypts contain background Cu concentrations of ~3.8 ppm with higher Cu concentrations above 6 ppm and up to 10.04 ppm. The higher concentrations of Cu are located nearby to Cu mines or prospects. The widespread distribution of mallee-eucalypt across southern Australia and their ability to access and transfer geochemical signals from deep within the substrate implies they are a readily available biogeochemical sample medium. This implies that sampling mallee-eucalypts in an environment such as Yorke Peninsula may be an effective, rapid, cheap and non-invasive exploration method that can be applied at large scales.

Supplementary data to this article can be found online at https://doi.org/10.1016/j.gexplo.2017.11.017.

Acknowledgements

This work has been supported by the Deep Exploration Technologies Cooperative Research Centre whose activities are funded by the Australian Government's Cooperative Research Centre Programme. This is DET CRC Document 2017/984 and TRaX paper 388. The authors acknowledge the two anonymous reviewers who provided constructive comments which improved this manuscript. The authors also gratefully acknowledge the assistance of Randy Wolff and Bradley Versegi for assistance in the field and later the sorting and labelling of samples in the laboratory, which would otherwise have been very time-consuming.

References

Anand, R.R., 2005. Weathering history, landscape evolution and implications for exploration. In: Anand, R.R., Butt, C.R.M., Robertson, I.D.M., Scott, K.M., Cornelius, M. (Eds.), Cooperative Research Centre for Landscape Environments and Mineral Exploration (CRC LEME) CSIRO Exploration and Mining Bentley West. Aust, Australia.

Arne, D.C., Stott, J.E., Waldron, H.M., 1999. Biogeochemistry of the Ballarat east goldfield, Victoria, Australia. J. Geochem. Explor. 67, 1–14.

Ashley, P.M., Wolfenden, B.J., 2005. Halls peak massive sulphide deposits, New England, NSW. In: Butt, C.R.M., Robertson, I.D.M., Scott, K.M., Cornelius, M. (Eds.), Regolith Expression of Australian Ore Systems; A Compilation of Exploration Case Histories

With Conceptual Dispersion, Process and Exploration Models. Cooperative Research Centre for Landscape Environments and Mineral Exploration (CRC LEME) CSIRO Exploration and Mining, Bentley, Western Australia.
Attiwill, P.M., Adams, M.A., 1996. Nutrition of Eucalypts. CSIRO Publishing, Australia.
Australian Native Vegetation Assessment, 2001. Australian Natural Resources Atlas. National Land and Water Resources Audit. Land and Water Australia, Canberra.
Barrow, N.J., 1977. Phosphorus uptake and utilization by tree seedlings. Aust. J. Bot. 25, 571–584.
Bennett, L.T., Weston, C.J., Judd, T.S., Attiwill, P.M., Whiteman, P.H., 1996. The effects of fertilizers on early growth and foliar nutrient concentrations of three plantation eucalypts on high quality sites in Gippsland, southeastern Australia. For. Ecol. Manag. 89, 213–226.
Brooker, M.I.H., Slee, A.V., Connors, J.R., Duffy, S.M., 2002. Eucalypts of Southern Australia; EUCLID Software CD, Second Edition. CSIRO Publishing, Australia.
Brown, A.D., Hill, S.M., 2005. White Dam Au-Cu prospect, Curnamona Province, South Australia. In: Butt, C.R.M., Robertson, I.D.M., Scott, K.M., Cornelius, M. (Eds.), Regolith expression of Australian ore systems; a compilation of exploration case histories with conceptual dispersion, process and exploration models. Cooperative Research Centre for Landscape Environments and Mineral Exploration (CRC LEME) CSIRO Exploration and Mining, Western Australia.
Bureau of Meteorology, 2017. Climate Statistics for Australian Locations; Summary Statistics Maitland SA. Commonwealth of Australia Bureau of Meteorology, Australia.
Butt, C.R.M., 2005. Vegetation communities. In: Butt, C.R.M., Robertson, I.D.M., Scott, K.M., Cornelius, M. (Eds.), Regolith Expression of Australian Ore Systems; A Compilation of Exploration Case Histories With Conceptual Dispersion, Process and Exploration Models. Cooperative Research Centre for Landscape Environments and Mineral Exploration (CRC LEME) CSIRO Exploration and Mining, Bentley West. Aust. Australia, pp. 49–51.
Butt, C.R.M., Robertson, I.D.M., Scott, K.M., Cornelius, M. (Eds.), 2005. Regolith Expression of Australian Ore Systems; a Compilation of Exploration Case Histories with Conceptual Dispersion, Process and Exploration Models. CRC LEME, Perth WA.
Butt, C.R.M., Scott, K.M., Cornelius, M., Robertson, I.D.M., 2005b. Sample media. In: Butt, C.R.M., Robertson, I.D.M., Scott, K.M., Cornelius, M. (Eds.), Regolith Expression of Australian Ore Systems; A Compilation of Exploration Case Histories with Conceptual Dispersion, Process and Exploration Models. Cooperative Research Centre for Landscape Environments and Mineral Exploration (CRC LEME) CSIRO Exploration and Mining, Bentley West. Aust. Australia, pp. 53–79.
Cohen, D.R., Hoffman, E.L., Nichol, I., 1987. Biogeochemistry: a geochemical method for gold exploration in the Canadian shield. J. Geochem. Explor. 29, 49–73.
Cohen, D.R., Dunlop, A.C., Shen, X.C., Alipour, S., 2005. Mrangelli Pb-Zn-As prospect, Cobar District, New South Wales. In: Butt, C.R.M., Robertson, I.D.M., Scott, K.M., Cornelius, M. (Eds.), Regolith expression of Australian ore systems; a compilation of exploration case histories with conceptual dispersion, process and exploration models. Cooperative Research Centre for Landscape Environments and Mineral Exploration (CRC LEME) CSIRO Exploration and Mining, Bentley, Western Australia.
Conor, C., 1995. Moonta-Wallaroo Region — An Interpretation of the Geology of the Maitland and Wallaroo 1:100 000 Sheet Areas. Primary Industries and Resources South Australia Open File Envelope No 8886.
Conor, C., Raymond, O., Baker, T., Teale, G., Say, P., Lowe, G., 2010. Alteration and mineralisation in the Moonta-Wallaroo copper-gold mining field region, Olympic Domain, South Australia. In: Porter, T.M. (Ed.), Hydrothermal Iron Oxide Copper-Gold and Related Deposits: A Global Perspective. Advances in the Understanding of IOCG Deposits. PGC Publishing, Adelaide, pp. 147–170.
Cowley, W.M., Conor, C., Zang, W., 2003. New and revised Proterozoic stratigraphic units on northern Yorke Peninsula. Primary Industries and Resources, MESA Journal 29, 46–58.
Crawford, A., 1965. The Geology of Yorke Peninsula: Bulletin No. 39. Geological Society of South Australia, pp. 1–138.
Crous, K.Y., Osvaldsson, A., Ellsworth, D.S., 2015. Is phosphorus limiting in a mature eucalyptus woodland? Phosphorus fertilisation stimulates stem growth. Plant Soil 391, 293–305.
Department of State Development, 2014. Understanding dryland farming: information for mineral explorers in South Australia. Report Book 2013/00017, Resources and Energy Group., V2.0. Department of State Development, Adelaide, South Australia.
Department of the Premier and Cabinet, 2017. South Australian Resources Information Gateway (SARIG), map layers (mines and mineral deposits), Government of South Australia. https://map.sarig.sa.gov.au, Accessed date: 4 April 2017.
DEWNR, 2013. Non-prescribed Surface Water Resources Assessment - Northern and Yorke Natural Resources Management Region, Government of South Australia, through Department of Environment. Water and Natural Resources, Adelaide.
DEWNR, 2017. Nature maps. Department of Environment, Water and Natural Resources, Government of South Australia. http://naturemaps.sa.gov.au/index.html, Accessed date: 4 April 2017.
Dietman, B.J., 2009. Regolith and Associated Geochemical and Biogeochemical Expression of Buried Copper-Gold Mineralisation at the Hillside Prospect, Yorke Peninsula (Honors Thesis, Unpublished). University of Adelaide, pp. 208.
Drexel, J.F., Preiss, W.V., 1995. The Geology of South Australia, Volume 2; The Phanerozoic. Geological Survey of South Australia, South Australia.
Dunn, C., 1986. Biogeochemistry as an aid to exploration for gold, platinum and palladium in the northern forests of Saskatchewan, Canada. J. Geochem. Explor. 25, 21–40.
Dunn, C., 2007. Biogeochemistry in Mineral Exploration, 2 ed. Elsevier, Amsterdam, The Netherlands.
Fabris, A.J., 2010. Investigation Into the Use of Radon and Soil Sampling in Exploration at the Hillside Copper-Gold Deposit, South Australia. Primary Indusries and Resources SA, Government of South Australia.
Fensham, R.J., Fairfax, R.J., 2007. Drought-related tree death of savanna eucalypts: species susceptibility, soil conditions and root architecture. J. Veg. Sci. 18, 71–80.
Fitzpatrick, R.W., Chittleborough, D.J., 2002. Titanium and zirconium minerals. In: Dixon, J.B., Schulze, D.G. (Eds.), Soil Mineralogy with Environmental Applications (Soil Science Society of America Book Series, No. 7). Soil Science Society of America, Wisconsin, USA.
Gazola, R.d.N., Buzetti, S., Filho, M.C.M.T., Dinalli, R.P., de Moraes, M.L.T., Celestrino, T.d.S., da Silva, P.H.M., Dupas, E., 2015. Doses of N, P and K in the cultivation of eucalyptus in soil originally under Cerrado vegetation. Semina: Ciências Agrárias 36, 1895–1912.
Grove, T.S., Thomson, B.D., N., M., 1986. Nutritional physiology of eucalypts: uptake, distribution and utilization. In: Attiwill, P.M., Adams, M.A. (Eds.), Nutrition of Eucalypts. CSIRO Publishing, Australia, pp. 448.
Handreck, K.A., 1997. Phosphorus requirements of Australian native plants. Aust. J. Soil Res. 35, 241–289.
Hillis, R., Giles, D., Van Der Wielen, S., Baensch, A., Cleverley, J., Fabris, A.J., Halley, S., Harris, M., Hill, S.M., Kanck, P.A., Kepic, A., Soe, S., Stewart, G., Uvarova, Y., 2014. Coiled tubing drilling and real-time sensing-enabling prospecting drilling in the 21st century. In: Kelley, K.D., Golden, H.C. (Eds.), SEG Conference on Keystone- Building Exploration Capability for the 21st Century. Society of Economic Geologists Special Publications Series, Issue 18 Keystone, Colorado, pp. 243–259.
van der Hoek, B.G., Hill, S.M., Dart, R.C., 2012. Calcrete and plant inter-relationships for the expression of concealed mineralization at the Tunkillia gold prospect, central Gawler craton, Australia. Geochemistry: Exploration, Environment, Analysis: GEEA 12, 361–372.
Hulme, K.A., 2008. *Eucalyptus camaldulensis* (River Red Gum) Biogeochemistry; An Innovative Tool for Mineral Exploration in the Curnamona Province and Adjacent Regions (PhD thesis). University of Adelaide, South Australia.
Hulme, K.A., Hill, S.M., 2003. River red gums as a biogeochemical sampling medium in mineral exploration and environmental chemistry programs in the Curnamona Craton and adjacent regions of NSW and SA. In: Roach, I.C. (Ed.), Advances in Regolith. CRC LEME.
Judd, T.S., Attiwill, P.M., Adams, M.A., 1996. Nutrient concentration in eucalyptus: a synthesis in relation to differences between taxa, sites and components. In: Attiwill, P.M., Adams, M.A. (Eds.), Nutrition of Eucalypts. CSIRO Publishing, Australia, pp. 448.
Kabata-Pendias, A., Pendias, H., 2001. Trace Elements in Soils and Plants. CRC Press LLC, Boca Raton, Florida.
Keeling, J.L., Hartley, K.L., Butt, C.R.M., Robertson, I.D.M., Scott, K.M., Cornelius, M., 2005. Poona and Wheal Hughes Cu Deposits, Moonta, South Australia. Cooperative Research Centre for Landscape Environments and Mineral Exploration (CRC LEME) CSIRO Exploration and Mining, Bentley West. Aust. Australia.
Kovalevsky, A.L., 1987. Biogeochemical Exploration for Mineral Deposits. VNU Science Press, The Netherlands.
Lintern, M.J., Butt, C.R.M., Scott, K.M., 1997. Gold in vegetation and soils — three case studies from the goldfields of southern Western Australia. J. Geochem. Explor. 58, 1–14.
Lintern, M., Anand, R., Ryan, C., Paterson, D., 2013a. Natural gold particles in eucalyptus leaves and their relevance to exploration for buried gold deposits. Nat. Commun. 4.
Lintern, M.J., Anand, R.R., Ryan, C., Paterson, D., 2013b. Natural gold particles in *Eucalyptus* leaves and their relevance to exploration for buried gold deposits. Nat. Commun. 4, 1.
McDowell, M.C., Baynes, A., Medlin, G.C., Prideaux, G.J., 2012. The impact of European colonization on the late-Holocene non-volant mammals of Yorke Peninsula, South Australia. The Holocene 22, 1441–1450.
Mitchell, C., Hill, S.M., Giles, D., Hulme, K.A., 2015. El Niño–La Niña cycles and bio-geochemical sampling: variability of element concentrations within *E. camaldulensis* leaves in semi-arid Australia. Geochemistry: Exploration, Environment, Analysis: GEEA 15, 350–360.
Mokhtari, A.R., Cohen, D.R., Gatehouse, S.G., 2009. Geochemical effects of deeply buried Cu–Au mineralization on transported regolith in an arid terrain. Geochemistry: Exploration, Environment, Analysis: GEEA 9, 227–236.
Närhi, P., Middleton, M., Sutinen, R., 2014. Biogeochemical multi-element signatures in common juniper at Mäkärärova, Finnish Lapland: implications for Au and REE exploration. J. Geochem. Explor. 138, 50–58.
Neagle, N., 2008. A Biological Survey of the Mid North and Yorke Peninsula, South Australia, 2003–2004: Assessment of Biodiversity Assets at Risk.
Noble, R.R.P., 2012. Transported cover in northwestern Victoria, Australia — an impediment to geochemical exploration for gold. J. Geochem. Explor. 112, 139–151.
Reid, N., Hill, S.M., 2010. Biogeochemical sampling for mineral exploration in arid terrains: Tanami Gold Province, Australia. J. Geochem. Explor. 104, 105–117.
Reid, N., Hill, S.M., 2013. Spinifex biogeochemistry across arid Australia: mineral exploration potential and chromium accumulation. Appl. Geochem. 29, 92–101.
Reid, N., Hill, S.M., Lewis, D.M., 2008. Spinifex biogeochemical expressions of buried gold mineralisation: the great mineral exploration penetrator of transported regolith. Appl. Geochem. 23, 76–84.
Rencz, A.N., Watson, G.P., 1989. Biogeochemistry and LANDSAT TM data: application to gold exploration in northern New Brunswick. J. Geochem. Explor. 34, 271–284.
Roberts, S., 2007. Northern and Yorke Natural Resources Management Region Water Monitoring Review, DWLBC Report 2006/15. Department of Water, Land and Biodiversity Conservation, Adelaide.
Salama, W., Gonzalez-Alvarez, I., Anand, R.R., 2016. Significance of weathering and regolith/landscape evolution for mineral exploration in the NE Albany-Fraser Orogen, Western Australia. Ore Geol. Rev. 73, 500–521.
Slee, A.V., Brooker, M.I.H., Duffy, S.M., West, J.G., 2006. Eucalypts of Australia; EUCLID Software CD, Third Edition. CSIRO Publishing, Melbourne.

Wolff, K., Tiddy, C., Giles, D., Hill, S.M., Gordon, G., 2017. Distinguishing pedogenic carbonates from weathered marine carbonates on the Yorke Peninsula, South Australia: implications for mineral exploration. J. Geochem. Explor. 181, 81–98.
Wrigley, J., Fagg, M., 2010. Eucalypts: A Celebration/John Wrigley and Murray Fagg. Allen & Unwin, Crows Nest NSW.
Zang, W., Hore, S., 2001. TER 1 Yorke Peninsula: Well Completion Report. Department of Primary Industry and Resources, South Australia.
Zang, W.-l., Cowley, W.M., Fairclough, M., 2006. Maitland Special South Australia 1:250000 Geological Series Sheet S153-12. Explanatory Notes PIRSA Publishing Services, South Australia.

Appendix 8

Chapter 4:

Biogeochemistry results

for

Mallee-eucalypt foliage

from the

Yorke Peninsula

	*NOTE values below detection have been halved	Duplicate ID	Sample_Type	Transect	Location	Orig_Grid_ID	Orig_East	Orig_North	GA_RL
Lab analytical method code	Lab analytical method code								
Unit	Unit								
Detection Limit	Detection Limit								
DataSet	SampleID								
Yorke Peninsula	YPM001		VEG	1	Cutline Rd	GDA94_53H	754731	6135007	10
Yorke Peninsula	YPM002		VEG	1	Cutline Rd	GDA94_53H	753614	6135043	25
Yorke Peninsula	YPM003		VEG	1	Cutline Rd	GDA94_53H	752175	6135069	39
Yorke Peninsula	YPM004		VEG	1	Cutline Rd	GDA94_53H	751432	6135086	44
Yorke Peninsula	YPM005		VEG	1	Cutline Rd	GDA94_53H	750295	6135111	44
Yorke Peninsula	YPM006	YPM023	VEG	1	Cutline Rd	GDA94_53H	748851	6135147	54
Yorke Peninsula	YPM007		VEG	1	Cutline Rd	GDA94_53H	747961	6135185	61
Yorke Peninsula	YPM008		VEG	1	Cutline Rd	GDA94_53H	746877	6135193	67
Yorke Peninsula	YPM009	YPM024	VEG	1	Cutline Rd	GDA94_53H	745700	6135220	63
Yorke Peninsula	YPM012		VEG	1	Cutline Rd	GDA94_53H	742523	6135288	60
Yorke Peninsula	YPM013		VEG	1	Cutline Rd	GDA94_53H	741555	6135312	58
Yorke Peninsula	YPM014		VEG	1	Cutline Rd	GDA94_53H	740596	6135332	56
Yorke Peninsula	YPM015		VEG	1	Cutline Rd	GDA94_53H	739576	6135358	56
Yorke Peninsula	YPM016		VEG	1	Cutline Rd	GDA94_53H	738677	6135381	58
Yorke Peninsula	YPM017		VEG	1	Cutline Rd	GDA94_53H	737318	6135414	53
Yorke Peninsula	YPM018		VEG	1	Cutline Rd	GDA94_53H	735745	6135454	55
Yorke Peninsula	YPM019		VEG	1	Cutline Rd	GDA94_53H	731215	6135560	28
Yorke Peninsula	YPM020		VEG	1	Cutline Rd	GDA94_53H	730213	6135586	25
Yorke Peninsula	YPM021		VEG	1	Cutline Rd	GDA94_53H	729196	6135606	22
Yorke Peninsula	YPM022		VEG	1	Cutline Rd	GDA94_53H	728096	6135635	15
Yorke Peninsula	YPM023	YPM006	VEG	1	Cutline Rd	GDA94_53H	748851	6135147	54
Yorke Peninsula	YPM024	YPM009	VEG	1	Cutline Rd	GDA94_53H	745700	6135220	63
Yorke Peninsula	YPM025		VEG	2	Dump Rd	GDA94_53H	758599	6144882	20
Yorke Peninsula	YPM026		VEG	2	Dump Rd	GDA94_53H	757558	6144910	30
Yorke Peninsula	YPM027		VEG	2	Dump Rd	GDA94_53H	755740	6144963	37
Yorke Peninsula	YPM028		VEG	2	Dump Rd	GDA94_53H	754907	6144985	36
Yorke Peninsula	YPM029		VEG	2	Dump Rd	GDA94_53H	753895	6145013	44
Yorke Peninsula	YPM030		VEG	2	Dump Rd	GDA94_53H	752327	6145057	47
Yorke Peninsula	YPM031		VEG	2	Dump Rd	GDA94_53H	749451	6145353	61
Yorke Peninsula	YPM032		VEG	2	Dump Rd	GDA94_53H	748376	6145305	68
Yorke Peninsula	YPM033		VEG	2	Dump Rd	GDA94_53H	747144	6145267	97
Yorke Peninsula	YPM034	YPM048	VEG	2	Dump Rd	GDA94_53H	745791	6145364	100
Yorke Peninsula	YPM035		VEG	2	Dump Rd	GDA94_53H	744889	6145753	101
Yorke Peninsula	YPM036		VEG	2	Dump Rd	GDA94_53H	744104	6146305	101
Yorke Peninsula	YPM037		VEG	2	Dump Rd	GDA94_53H	742987	6147023	102
Yorke Peninsula	YPM038		VEG	2	Dump Rd	GDA94_53H	741632	6147463	77
Yorke Peninsula	YPM039		VEG	2	Dump Rd	GDA94_53H	740645	6147577	73
Yorke Peninsula	YPM040		VEG	2	Dump Rd	GDA94_53H	739520	6147598	66
Yorke Peninsula	YPM041	YPM049	VEG	2	Dump Rd	GDA94_53H	737675	6147648	64
Yorke Peninsula	YPM042		VEG	2	Dump Rd	GDA94_53H	735216	6147774	71
Yorke Peninsula	YPM043		VEG	2	Dump Rd	GDA94_53H	734075	6148074	63
Yorke Peninsula	YPM044		VEG	2	Dump Rd	GDA94_53H	732896	6148009	51
Yorke Peninsula	YPM045		VEG	2	Dump Rd	GDA94_53H	731832	6147976	40
Yorke Peninsula	YPM046		VEG	2	Dump Rd	GDA94_53H	730266	6147918	26
Yorke Peninsula	YPM047		VEG	2	Dump Rd	GDA94_53H	729317	6147985	22
Yorke Peninsula	YPM048	YPM034	VEG	2	Dump Rd	GDA94_53H	745791	6145364	100
Yorke Peninsula	YPM049	YPM041	VEG	2	Dump Rd	GDA94_53H	737675	6147648	64
Yorke Peninsula	YPM050		VEG	3	Barkers Rocks Rd	GDA94_53H	727914	6155609	2
Yorke Peninsula	YPM051		VEG	3	Barkers Rocks Rd	GDA94_53H	730190	6155560	14
Yorke Peninsula	YPM052		VEG	3	Barkers Rocks Rd	GDA94_53H	731376	6155532	18
Yorke Peninsula	YPM053	YPM071	VEG	3	Barkers Rocks Rd	GDA94_53H	732530	6155507	41
Yorke Peninsula	YPM054		VEG	3	Barkers Rocks Rd	GDA94_53H	733617	6155477	51
Yorke Peninsula	YPM055	YPM072	VEG	3	Barkers Rocks Rd	GDA94_53H	736103	6155413	71
Yorke Peninsula	YPM056		VEG	3	Barkers Rocks Rd	GDA94_53H	737421	6155381	73
Yorke Peninsula	YPM057		VEG	3	Spicers Rd	GDA94_53H	738448	6155269	58
Yorke Peninsula	YPM058		VEG	3	Spicers Rd	GDA94_53H	739661	6155104	62
Yorke Peninsula	YPM059		VEG	3	Spicers Rd	GDA94_53H	740941	6154927	70
Yorke Peninsula	YPM060		VEG	3	Spicers Rd	GDA94_53H	742971	6154641	96
Yorke Peninsula	YPM061		VEG	3	Spicers Rd	GDA94_53H	744985	6154552	102
Yorke Peninsula	YPM062		VEG	3	Spicers Rd	GDA94_53H	747558	6154488	99
Yorke Peninsula	YPM063		VEG	3	Spicers Rd	GDA94_53H	751864	6154376	80
Yorke Peninsula	YPM064		VEG	3	Spicers Rd	GDA94_53H	752751	6154351	70
Yorke Peninsula	YPM065		VEG	3	Goldsworthy Rd	GDA94_53H	754120	6154313	69
Yorke Peninsula	YPM066		VEG	3	Goldsworthy Rd	GDA94_53H	756294	6154258	55
Yorke Peninsula	YPM067		VEG	3	Goldsworthy Rd	GDA94_53H	757269	6154234	59
Yorke Peninsula	YPM068		VEG	3	Goldsworthy Rd	GDA94_53H	758274	6154206	55
Yorke Peninsula	YPM069		VEG	3	Goldsworthy Rd	GDA94_53H	760576	6154144	42

*NOTE values below detection have been halved	Orig_Survey_Method	Orig_Survey_By	Orig_Survey_Date	Sampled_By	Treatment	Species
Lab analytical method code						
Unit						
Detection Limit						
SampleID						
YPM001	Garmin GPS Map60CSX	KWolff	2/03/2012	Hill/Stoate	dried for 48hrs at 60'C	E. gracilis
YPM002	Garmin GPS Map60CSX	KWolff	2/03/2012	Hill/Stoate	dried for 48hrs at 60'C	E. gracilis
YPM003	Garmin GPS Map60CSX	KWolff	2/03/2012	Hill/Stoate	dried for 48hrs at 60'C	E. gracilis
YPM004	Garmin GPS Map60CSX	KWolff	2/03/2012	Hill/Stoate	dried for 48hrs at 60'C	E. gracilis
YPM005	Garmin GPS Map60CSX	KWolff	2/03/2012	Hill/Stoate	dried for 48hrs at 60'C	E. gracilis
YPM006	Garmin GPS Map60CSX	KWolff	2/03/2012	Hill/Stoate	dried for 48hrs at 60'C	E. socialis
YPM007	Garmin GPS Map60CSX	KWolff	2/03/2012	Hill/Stoate	dried for 48hrs at 60'C	E. phenax
YPM008	Garmin GPS Map60CSX	KWolff	2/03/2012	Hill/Stoate	dried for 48hrs at 60'C	E. phenax
YPM009	Garmin GPS Map60CSX	KWolff	2/03/2012	Hill/Stoate	dried for 48hrs at 60'C	E. socialis
YPM012	Garmin GPS Map60CSX	KWolff	2/03/2012	Hill/Stoate	dried for 48hrs at 60'C	E. socialis
YPM013	Garmin GPS Map60CSX	KWolff	2/03/2012	Hill/Stoate	dried for 48hrs at 60'C	E. phenax
YPM014	Garmin GPS Map60CSX	KWolff	2/03/2012	Hill/Stoate	dried for 48hrs at 60'C	E. socialis
YPM015	Garmin GPS Map60CSX	KWolff	2/03/2012	Hill/Stoate	dried for 48hrs at 60'C	E. socialis
YPM016	Garmin GPS Map60CSX	KWolff	2/03/2012	Hill/Stoate	dried for 48hrs at 60'C	E. socialis
YPM017	Garmin GPS Map60CSX	KWolff	2/03/2012	Hill/Stoate	dried for 48hrs at 60'C	E. socialis
YPM018	Garmin GPS Map60CSX	KWolff	2/03/2012	Hill/Stoate	dried for 48hrs at 60'C	E. socialis
YPM019	Garmin GPS Map60CSX	KWolff	2/03/2012	Hill/Stoate	dried for 48hrs at 60'C	E. socialis
YPM020	Garmin GPS Map60CSX	KWolff	2/03/2012	Hill/Stoate	dried for 48hrs at 60'C	E. socialis
YPM021	Garmin GPS Map60CSX	KWolff	2/03/2012	Hill/Stoate	dried for 48hrs at 60'C	E. socialis
YPM022	Garmin GPS Map60CSX	KWolff	2/03/2012	Hill/Stoate	dried for 48hrs at 60'C	E. socialis
YPM023	Garmin GPS Map60CSX	KWolff	2/03/2012	Hill/Stoate	dried for 48hrs at 60'C	E. socialis
YPM024	Garmin GPS Map60CSX	KWolff	2/03/2012	Hill/Stoate	dried for 48hrs at 60'C	E. socialis
YPM025	Garmin GPS Map62S	KWolff	17/03/2012	KWolff	dried for 48hrs at 60'C	E. phenax
YPM026	Garmin GPS Map62S	KWolff	17/03/2012	KWolff	dried for 48hrs at 60'C	E. phenax
YPM027	Garmin GPS Map62S	KWolff	17/03/2012	KWolff	dried for 48hrs at 60'C	E. socialis
YPM028	Garmin GPS Map62S	KWolff	17/03/2012	KWolff	dried for 48hrs at 60'C	E. socialis
YPM029	Garmin GPS Map62S	KWolff	17/03/2012	KWolff	dried for 48hrs at 60'C	E. socialis
YPM030	Garmin GPS Map62S	KWolff	17/03/2012	KWolff	dried for 48hrs at 60'C	E. socialis
YPM031	Garmin GPS Map62S	KWolff	17/03/2012	KWolff	dried for 48hrs at 60'C	E. socialis
YPM032	Garmin GPS Map62S	KWolff	17/03/2012	KWolff	dried for 48hrs at 60'C	E. socialis
YPM033	Garmin GPS Map62S	KWolff	17/03/2012	KWolff	dried for 48hrs at 60'C	E. phenax
YPM034	Garmin GPS Map62S	KWolff	17/03/2012	KWolff	dried for 48hrs at 60'C	E. socialis
YPM035	Garmin GPS Map62S	KWolff	17/03/2012	KWolff	dried for 48hrs at 60'C	E. phenax
YPM036	Garmin GPS Map62S	KWolff	17/03/2012	KWolff	dried for 48hrs at 60'C	E. socialis
YPM037	Garmin GPS Map62S	KWolff	17/03/2012	KWolff	dried for 48hrs at 60'C	E. socialis
YPM038	Garmin GPS Map62S	KWolff	17/03/2012	KWolff	dried for 48hrs at 60'C	E. phenax
YPM039	Garmin GPS Map62S	KWolff	17/03/2012	KWolff	dried for 48hrs at 60'C	E. phenax
YPM040	Garmin GPS Map62S	KWolff	17/03/2012	KWolff	dried for 48hrs at 60'C	E. phenax
YPM041	Garmin GPS Map62S	KWolff	17/03/2012	KWolff	dried for 48hrs at 60'C	E. phenax
YPM042	Garmin GPS Map62S	KWolff	17/03/2012	KWolff	dried for 48hrs at 60'C	E. phenax
YPM043	Garmin GPS Map62S	KWolff	17/03/2012	KWolff	dried for 48hrs at 60'C	E. phenax
YPM044	Garmin GPS Map62S	KWolff	17/03/2012	KWolff	dried for 48hrs at 60'C	E. leptophylla
YPM045	Garmin GPS Map62S	KWolff	17/03/2012	KWolff	dried for 48hrs at 60'C	E. leptophylla
YPM046	Garmin GPS Map62S	KWolff	17/03/2012	KWolff	dried for 48hrs at 60'C	E. gracilis
YPM047	Garmin GPS Map62S	KWolff	17/03/2012	KWolff	dried for 48hrs at 60'C	E. phenax
YPM048	Garmin GPS Map62S	KWolff	17/03/2012	KWolff	dried for 48hrs at 60'C	E. socialis
YPM049	Garmin GPS Map62S	KWolff	17/03/2012	KWolff	dried for 48hrs at 60'C	E. phenax
YPM050	Garmin GPS Map62S	KWolff	18/03/2012	KWolff	dried for 48hrs at 60'C	E. gracilis
YPM051	Garmin GPS Map62S	KWolff	18/03/2012	KWolff	dried for 48hrs at 60'C	E. gracilis
YPM052	Garmin GPS Map62S	KWolff	18/03/2012	KWolff	dried for 48hrs at 60'C	E. gracilis
YPM053	Garmin GPS Map62S	KWolff	18/03/2012	KWolff	dried for 48hrs at 60'C	E. gracilis
YPM054	Garmin GPS Map62S	KWolff	18/03/2012	KWolff	dried for 48hrs at 60'C	E. gracilis
YPM055	Garmin GPS Map62S	KWolff	18/03/2012	KWolff	dried for 48hrs at 60'C	E. leptophylla
YPM056	Garmin GPS Map62S	KWolff	18/03/2012	KWolff	dried for 48hrs at 60'C	E. phenax
YPM057	Garmin GPS Map62S	KWolff	18/03/2012	KWolff	dried for 48hrs at 60'C	E. phenax
YPM058	Garmin GPS Map62S	KWolff	18/03/2012	KWolff	dried for 48hrs at 60'C	E. phenax
YPM059	Garmin GPS Map62S	KWolff	18/03/2012	KWolff	dried for 48hrs at 60'C	E. phenax
YPM060	Garmin GPS Map62S	KWolff	18/03/2012	KWolff	dried for 48hrs at 60'C	E. phenax
YPM061	Garmin GPS Map62S	KWolff	18/03/2012	KWolff	dried for 48hrs at 60'C	E. gracilis
YPM062	Garmin GPS Map62S	KWolff	18/03/2012	KWolff	dried for 48hrs at 60'C	E. phenax
YPM063	Garmin GPS Map62S	KWolff	18/03/2012	KWolff	dried for 48hrs at 60'C	E. phenax
YPM064	Garmin GPS Map62S	KWolff	18/03/2012	KWolff	dried for 48hrs at 60'C	E. gracilis
YPM065	Garmin GPS Map62S	KWolff	18/03/2012	KWolff	dried for 48hrs at 60'C	E. phenax
YPM066	Garmin GPS Map62S	KWolff	18/03/2012	KWolff	dried for 48hrs at 60'C	E. socialis
YPM067	Garmin GPS Map62S	KWolff	18/03/2012	KWolff	dried for 48hrs at 60'C	E. socialis
YPM068	Garmin GPS Map62S	KWolff	18/03/2012	KWolff	dried for 48hrs at 60'C	E. socialis
YPM069	Garmin GPS Map62S	KWolff	18/03/2012	KWolff	dried for 48hrs at 60'C	E. socialis

*NOTE values below detection have been halved	Sample_Description	Date_Sampled	Mo_ppm	Cu_ppm	Pb_ppm	Zn_ppm	Ag_ppm	Ni_ppm	Co_ppm	Mn_ppm
Lab analytical method code	*phyllodes are leaves		1VE	1VE	1VE	1VE	1VE	1VE	1VE	1VE
Unit			PPM	PPM	PPM	PPM	PPB	PPM	PPM	PPM
Detection Limit			0.01	0.01	0.01	0.1	2	0.1	0.01	1
SampleID										
YPM001	phyllodes	2/03/2012	0.04	3.06	0.15	12.4	1	1	0.04	26
YPM002	phyllodes	2/03/2012	0.13	4.54	0.09	12.4	1	1.1	0.04	45
YPM003	phyllodes	2/03/2012	0.06	2.65	0.09	14.7	1	0.7	0.07	64
YPM004	phyllodes	2/03/2012	0.07	3.48	0.11	10.5	1	1.2	0.1	54
YPM005	phyllodes	2/03/2012	0.03	3.91	0.06	13.7	1	0.7	0.03	22
YPM006	phyllodes	2/03/2012	0.16	4.61	0.1	14.5	1	0.8	0.04	78
YPM007	phyllodes	2/03/2012	0.08	3.13	0.11	13.1	1	2.4	0.03	20
YPM008	phyllodes	2/03/2012	0.1	4.45	0.15	9	1	1.4	0.07	27
YPM009	phyllodes	2/03/2012	0.03	2.36	0.09	14.8	1	4.3	0.03	42
YPM012	phyllodes	2/03/2012	0.18	2.01	0.08	14.1	1	1.6	0.08	31
YPM013	phyllodes	2/03/2012	0.02	2.66	0.08	9	1	0.5	0.02	7
YPM014	phyllodes	2/03/2012	0.13	2.8	0.09	13.6	1	1	0.08	12
YPM015	phyllodes	2/03/2012	0.03	2.62	0.06	7.8	1	1	0.04	16
YPM016	phyllodes	2/03/2012	0.07	3.01	0.06	15.1	1	0.7	0.03	10
YPM017	phyllodes	2/03/2012	0.19	3.55	0.15	14.8	1	0.6	0.08	15
YPM018	phyllodes	2/03/2012	0.05	5.69	0.07	15.5	1	0.7	0.04	27
YPM019	phyllodes	2/03/2012	0.09	5.35	0.16	15.9	1	1.1	0.07	29
YPM020	phyllodes	2/03/2012	0.03	2.79	0.07	8.4	1	0.8	0.08	86
YPM021	phyllodes	2/03/2012	0.07	5.19	0.05	9.6	1	1.6	0.08	75
YPM022	phyllodes	2/03/2012	0.03	7.58	0.09	10.1	1	1.2	0.02	11
YPM023	phyllodes	2/03/2012	0.18	4.65	0.08	15.1	1	1	0.04	77
YPM024	phyllodes	2/03/2012	0.02	2.52	0.05	13.4	1	4.4	0.04	38
YPM025	phyllodes	17/03/2012	0.07	2.47	0.12	13.8	1	0.7	0.03	14
YPM026	phyllodes	17/03/2012	0.05	5.02	0.15	17.5	1	1.5	0.07	12
YPM027	phyllodes	17/03/2012	0.1	3.93	0.07	16.4	1	1.9	0.04	18
YPM028	phyllodes	17/03/2012	0.11	3.91	0.07	17.3	1	0.5	0.09	19
YPM029	phyllodes	17/03/2012	0.03	3.01	0.07	11.7	1	0.6	0.04	24
YPM030	phyllodes	17/03/2012	0.02	1.67	0.07	11.1	1	0.4	0.01	25
YPM031	phyllodes	17/03/2012	0.04	2.02	0.06	10.6	1	0.2	0.05	15
YPM032	phyllodes	17/03/2012	0.03	1.71	0.07	17.3	1	0.5	0.03	20
YPM033	phyllodes	17/03/2012	0.1	2.35	0.1	8.7	1	0.6	0.05	14
YPM034	phyllodes	17/03/2012	0.05	2.9	0.03	17.5	1	0.3	0.03	24
YPM035	phyllodes	17/03/2012	0.06	3.26	0.05	8.8	1	0.9	0.02	10
YPM036	phyllodes	17/03/2012	0.04	2.69	0.06	26.7	1	0.6	0.04	5
YPM037	phyllodes	17/03/2012	0.12	3.26	0.08	21.1	1	1.5	0.05	22
YPM038	phyllodes	17/03/2012	0.08	3.65	0.03	14.1	1	1	0.05	31
YPM039	phyllodes	17/03/2012	0.19	3.47	0.04	12.4	1	1.7	0.08	26
YPM040	phyllodes	17/03/2012	0.07	4.03	0.05	23.5	1	1.1	0.07	77
YPM041	phyllodes	17/03/2012	0.07	5.94	0.04	15.4	1	1	0.03	24
YPM042	phyllodes	17/03/2012	0.04	3.27	0.03	9.5	1	0.8	0.03	57
YPM043	phyllodes	17/03/2012	0.03	2.41	0.03	13.3	1	0.7	0.06	61
YPM044	phyllodes	17/03/2012	0.07	3.05	0.08	12.9	1	1.2	0.1	41
YPM045	phyllodes	17/03/2012	0.1	2.97	0.08	7.5	1	0.7	0.03	40
YPM046	phyllodes	17/03/2012	0.03	4.73	0.04	12.7	1	1	0.06	23
YPM047	phyllodes	17/03/2012	0.03	2.45	0.02	8.4	1	0.8	0.03	35
YPM048	phyllodes	17/03/2012	0.05	2.66	0.04	17.5	1	0.3	0.02	22
YPM049	phyllodes	17/03/2012	0.05	5.94	0.04	15.5	1	1.2	0.005	24
YPM050	phyllodes	18/03/2012	0.1	2.32	0.03	10.6	1	0.3	0.02	29
YPM051	phyllodes	18/03/2012	0.09	3.75	0.04	13.7	1	0.9	0.05	59
YPM052	phyllodes	18/03/2012	0.09	3.19	0.06	7.9	1	0.4	0.04	17
YPM053	phyllodes	18/03/2012	0.12	5.46	0.03	16.8	1	0.4	0.04	18
YPM054	phyllodes	18/03/2012	0.05	5.34	0.04	10.1	1	0.6	0.08	27
YPM055	phyllodes	18/03/2012	0.16	5.02	0.05	14.8	1	0.4	0.07	51
YPM056	phyllodes	18/03/2012	0.19	5.25	0.06	15.9	1	0.6	0.06	37
YPM057	phyllodes	18/03/2012	0.08	3.78	0.08	21.6	1	1.1	0.13	117
YPM058	phyllodes	18/03/2012	0.09	5.62	0.03	18.3	1	0.7	0.02	82
YPM059	phyllodes	18/03/2012	0.05	4.41	0.07	17.3	1	0.8	0.06	60
YPM060	phyllodes	18/03/2012	0.06	5.3	0.06	11.7	1	0.6	0.05	38
YPM061	phyllodes	18/03/2012	0.03	3.24	0.06	10.9	1	0.4	0.05	11
YPM062	phyllodes	18/03/2012	0.25	7.67	0.12	23.2	1	0.8	0.07	37
YPM063	phyllodes	18/03/2012	0.21	7.32	0.09	19	1	1.1	0.05	17
YPM064	phyllodes	18/03/2012	0.05	2.01	0.08	9.9	1	0.4	0.04	13
YPM065	phyllodes	18/03/2012	0.15	4.13	0.04	11.1	1	0.5	0.03	7
YPM066	phyllodes	18/03/2012	0.12	2.73	0.05	13.5	1	0.6	0.02	16
YPM067	phyllodes	18/03/2012	0.04	3.44	0.06	12.5	1	2.3	0.06	13
YPM068	phyllodes	18/03/2012	0.16	3.55	0.04	17.4	1	0.9	0.05	19
YPM069	phyllodes	18/03/2012	0.1	2.84	0.18	14.3	1	0.7	0.05	28

*NOTE values below detection have been halved	Fe_pct	As_ppm	U_ppm	Au_ppb	Th_ppm	Sr_ppm	Cd_ppm	Sb_ppm	Bi_ppm	V_ppm	Ca_pct	P_pct
Lab analytical method code	1VE	1VE	1VE	1VE	1VE	1VE	1VE	1VE	1VE	1VE	1VE	1VE
Unit	wt%	PPM	PPM	PPB	PPM	PPM	PPM	PPM	PPM	PPM	wt%	wt%
Detection Limit	0.001	0.1	0.01	0.2	0.01	0.5	0.01	0.02	0.02	2	0.01	0.001
SampleID												
YPM001	0.015	0.05	0.005	2.2	0.01	27.1	0.01	0.01	0.01	1	1.03	0.076
YPM002	0.017	0.05	0.005	0.7	0.02	33.6	0.005	0.01	0.01	1	1.09	0.12
YPM003	0.028	0.05	0.005	0.3	0.04	28.2	0.01	0.01	0.01	1	1.19	0.099
YPM004	0.024	0.05	0.005	0.1	0.03	45.6	0.02	0.01	0.01	1	1.75	0.083
YPM005	0.013	0.05	0.005	0.1	0.01	15	0.005	0.01	0.01	1	0.57	0.082
YPM006	0.011	0.05	0.005	0.1	0.005	39.8	0.005	0.01	0.01	1	1.07	0.066
YPM007	0.011	0.05	0.005	0.2	0.01	45	0.02	0.01	0.01	1	0.88	0.055
YPM008	0.013	0.05	0.005	0.1	0.02	64.6	0.005	0.02	0.01	1	0.8	0.062
YPM009	0.01	0.05	0.005	0.1	0.005	29.6	0.005	0.01	0.01	1	0.61	0.047
YPM012	0.012	0.05	0.005	0.1	0.01	36.2	0.05	0.01	0.01	1	0.8	0.085
YPM013	0.015	0.05	0.02	0.1	0.02	86.9	0.005	0.01	0.01	1	0.88	0.065
YPM014	0.009	0.05	0.005	0.1	0.01	47.2	0.01	0.01	0.01	1	0.58	0.061
YPM015	0.01	0.05	0.01	0.1	0.01	65.8	0.03	0.01	0.01	1	0.8	0.085
YPM016	0.014	0.05	0.005	0.1	0.02	107.5	0.02	0.01	0.01	1	0.83	0.048
YPM017	0.012	0.05	0.005	0.1	0.01	26.5	0.01	0.01	0.01	1	0.72	0.124
YPM018	0.012	0.05	0.005	0.1	0.01	19.1	0.005	0.01	0.01	1	0.52	0.133
YPM019	0.015	0.05	0.005	0.1	0.02	21.7	0.005	0.01	0.01	1	1.04	0.093
YPM020	0.009	0.05	0.005	0.1	0.005	27.5	0.005	0.01	0.01	1	1.02	0.069
YPM021	0.011	0.05	0.005	0.1	0.005	30.3	0.005	0.01	0.01	1	1.2	0.08
YPM022	0.013	0.05	0.005	0.1	0.02	23	0.005	0.01	0.01	1	0.85	0.073
YPM023	0.011	0.05	0.005	0.1	0.005	39.2	0.005	0.01	0.01	1	1.1	0.068
YPM024	0.008	0.05	0.005	0.1	0.005	30.9	0.01	0.01	0.01	1	0.64	0.049
YPM025	0.017	0.05	0.005	0.5	0.02	25.9	0.005	0.01	0.01	1	1.12	0.13
YPM026	0.017	0.05	0.005	0.1	0.01	21	0.005	0.01	0.01	1	0.94	0.101
YPM027	0.011	0.05	0.005	0.1	0.005	44.2	0.02	0.01	0.01	1	0.8	0.065
YPM028	0.008	0.05	0.005	0.1	0.005	46.9	0.03	0.01	0.01	1	0.69	0.069
YPM029	0.008	0.05	0.005	0.1	0.01	33	0.03	0.01	0.01	1	0.49	0.057
YPM030	0.009	0.05	0.005	0.1	0.01	26.5	0.05	0.01	0.01	1	0.54	0.061
YPM031	0.009	0.05	0.005	0.1	0.005	79.6	0.05	0.01	0.01	1	0.73	0.059
YPM032	0.011	0.05	0.005	0.1	0.01	56.2	0.03	0.01	0.01	1	0.79	0.07
YPM033	0.012	0.05	0.005	0.1	0.01	75.9	0.04	0.01	0.01	1	1.17	0.109
YPM034	0.006	0.05	0.005	0.3	0.005	21.8	0.04	0.01	0.07	1	0.47	0.06
YPM035	0.009	0.05	0.005	0.1	0.005	89.1	0.005	0.01	0.02	1	0.88	0.056
YPM036	0.013	0.05	0.005	0.1	0.01	115	0.03	0.01	0.01	1	1.01	0.109
YPM037	0.012	0.05	0.005	0.1	0.02	40.9	0.03	0.01	0.01	1	0.67	0.061
YPM038	0.01	0.05	0.005	0.4	0.005	30.9	0.05	0.01	0.01	1	0.8	0.112
YPM039	0.011	0.05	0.01	0.1	0.01	20.5	0.005	0.01	0.01	1	0.79	0.086
YPM040	0.013	0.05	0.005	0.1	0.005	52.8	0.08	0.01	0.01	1	1.75	0.112
YPM041	0.008	0.05	0.005	0.1	0.005	14.9	0.01	0.01	0.01	1	0.54	0.107
YPM042	0.012	0.05	0.005	0.1	0.005	72.5	0.005	0.01	0.01	1	1.16	0.05
YPM043	0.009	0.05	0.005	0.1	0.01	29.4	0.01	0.01	0.01	1	0.58	0.046
YPM044	0.009	0.05	0.005	0.1	0.005	46.9	0.005	0.01	0.01	1	0.57	0.055
YPM045	0.011	0.05	0.005	0.1	0.02	109.1	0.005	0.01	0.01	1	0.97	0.06
YPM046	0.011	0.05	0.005	0.4	0.005	156.5	0.01	0.01	0.01	1	1.5	0.127
YPM047	0.009	0.05	0.005	0.1	0.005	108.9	0.005	0.01	0.01	1	1.01	0.051
YPM048	0.006	0.1	0.005	0.1	0.005	22.4	0.04	0.01	0.01	1	0.47	0.057
YPM049	0.008	0.05	0.005	0.1	0.005	16.4	0.01	0.01	0.01	1	0.57	0.097
YPM050	0.006	0.05	0.005	0.1	0.005	71.7	0.01	0.01	0.01	1	0.66	0.066
YPM051	0.01	0.05	0.005	0.4	0.005	112	0.01	0.01	0.01	1	1.41	0.118
YPM052	0.012	0.05	0.005	0.1	0.02	76.3	0.02	0.01	0.01	1	0.89	0.054
YPM053	0.011	0.05	0.005	0.1	0.02	71.9	0.005	0.01	0.01	1	0.61	0.107
YPM054	0.009	0.05	0.005	0.1	0.01	73.1	0.005	0.01	0.01	1	0.65	0.062
YPM055	0.011	0.1	0.005	0.1	0.01	40	0.005	0.01	0.01	1	0.63	0.084
YPM056	0.018	0.05	0.005	0.1	0.03	15.3	0.005	0.01	0.01	1	0.54	0.104
YPM057	0.016	0.05	0.005	0.1	0.02	51.4	0.005	0.01	0.01	1	1.29	0.084
YPM058	0.009	0.05	0.005	0.1	0.005	14.2	0.01	0.01	0.01	1	0.84	0.076
YPM059	0.012	0.05	0.005	0.1	0.005	20.2	0.005	0.01	0.01	1	1	0.084
YPM060	0.013	0.05	0.005	0.1	0.01	38.4	0.005	0.01	0.01	1	0.73	0.092
YPM061	0.014	0.05	0.005	0.1	0.02	46.7	0.005	0.01	0.01	1	0.75	0.07
YPM062	0.017	0.05	0.005	0.1	0.02	20.2	0.005	0.01	0.01	1	0.58	0.163
YPM063	0.015	0.05	0.005	0.1	0.02	25.5	0.005	0.01	0.01	1	0.63	0.132
YPM064	0.014	0.05	0.005	0.1	0.02	79	0.005	0.01	0.01	1	0.92	0.064
YPM065	0.011	0.05	0.005	0.1	0.005	60.2	0.005	0.01	0.01	1	0.75	0.06
YPM066	0.009	0.05	0.005	0.1	0.005	54.3	0.04	0.01	0.01	1	0.8	0.07
YPM067	0.011	0.05	0.02	0.1	0.01	81.8	0.02	0.01	0.01	1	0.72	0.05
YPM068	0.007	0.05	0.005	0.1	0.005	24	0.04	0.01	0.01	1	0.6	0.079
YPM069	0.013	0.05	0.005	0.1	0.02	47.2	0.16	0.01	0.01	1	1.25	0.082

*NOTE values below detection have been halved	La_ppm	Cr_ppm	Mg_pct	Ba_ppm	Ti_ppm	B_ppm	Al_pct	Na_pct	K_pct	W_ppm	Sc_ppm	Tl_ppm
Lab analytical method code	1VE	1VE	1VE	1VE	1VE	1VE	1VE	1VE	1VE	1VE	1VE	1VE
Unit	PPM	PPM	wt%	PPM	PPM	PPM	wt%	wt%	wt%	PPM	PPM	PPM
Detection Limit	0.01	0.1	0.001	0.1	1	1	0.01	0.001	0.01	0.1	0.1	0.02
SampleID												
YPM001	0.04	1.2	0.201	3.7	6	54	0.01	0.818	0.47	0.05	0.2	0.01
YPM002	0.06	1.2	0.162	3.4	9	14	0.01	0.607	0.87	0.05	0.2	0.01
YPM003	0.12	1.3	0.221	6.6	9	48	0.03	1.136	0.64	0.05	0.2	0.01
YPM004	0.07	1.2	0.173	7.2	7	40	0.02	0.644	0.46	0.05	0.2	0.01
YPM005	0.05	1.1	0.139	4.5	6	17	0.01	0.492	0.8	0.05	0.2	0.01
YPM006	0.04	1.1	0.192	4.2	5	100	0.005	0.369	0.46	0.05	0.3	0.01
YPM007	0.04	1.2	0.124	4.4	4	37	0.005	0.5	0.56	0.05	0.3	0.01
YPM008	0.05	1.1	0.139	5.3	5	27	0.005	0.576	0.62	0.05	0.3	0.01
YPM009	0.03	1.3	0.175	3.3	4	26	0.005	0.33	0.67	0.05	0.3	0.01
YPM012	0.05	1.2	0.165	5.7	6	23	0.01	0.732	0.7	0.05	0.2	0.01
YPM013	0.1	1.2	0.165	4.3	5	30	0.01	0.544	0.4	0.05	0.4	0.01
YPM014	0.1	1.2	0.156	2.6	5	26	0.005	0.558	0.61	0.05	0.3	0.01
YPM015	0.07	1.1	0.137	3	6	40	0.005	0.379	0.43	0.05	0.3	0.01
YPM016	0.08	1.2	0.168	3.4	4	41	0.01	0.375	0.5	0.05	0.2	0.01
YPM017	0.04	1.1	0.125	3.5	8	26	0.005	0.831	0.8	0.05	0.3	0.01
YPM018	0.06	1.1	0.118	1.6	9	29	0.01	0.638	0.51	0.05	0.2	0.01
YPM019	0.06	1.2	0.178	4.2	7	33	0.01	0.872	0.68	0.05	0.3	0.01
YPM020	0.02	1	0.148	3.7	5	25	0.005	0.352	0.61	0.05	0.2	0.01
YPM021	0.02	0.9	0.164	5.4	5	28	0.005	0.466	0.83	0.05	0.2	0.01
YPM022	0.05	1.1	0.164	3	5	61	0.005	0.454	0.46	0.05	0.3	0.01
YPM023	0.03	1.1	0.2	4.1	5	96	0.005	0.388	0.48	0.05	0.2	0.01
YPM024	0.02	1.2	0.185	3.6	4	24	0.005	0.328	0.7	0.05	0.3	0.01
YPM025	0.06	1.3	0.134	5.6	9	54	0.01	0.481	0.36	0.05	0.2	0.01
YPM026	0.05	1.2	0.156	4.3	7	48	0.01	0.557	0.56	0.05	0.3	0.01
YPM027	0.04	1.2	0.155	2.9	5	23	0.005	0.504	0.44	0.05	0.2	0.01
YPM028	0.03	1.1	0.161	3.5	5	13	0.005	0.379	0.67	0.05	0.2	0.01
YPM029	0.03	1.1	0.181	3.1	4	35	0.005	0.323	0.47	0.05	0.2	0.01
YPM030	0.04	1.2	0.168	4.2	4	41	0.005	0.649	0.55	0.05	0.2	0.01
YPM031	0.04	1.2	0.204	7.6	4	42	0.005	0.182	0.44	0.05	0.2	0.01
YPM032	0.07	1.1	0.168	6	5	43	0.005	0.392	0.54	0.05	0.2	0.01
YPM033	0.04	0.05	0.172	8.2	8	42	0.005	0.434	0.43	0.05	0.2	0.01
YPM034	0.03	1.2	0.112	3.1	4	24	0.005	0.364	0.56	0.05	0.3	0.01
YPM035	0.02	1.1	0.135	5.3	4	30	0.005	0.371	0.59	0.05	0.3	0.01
YPM036	0.04	1.1	0.198	5	6	65	0.01	0.254	0.57	0.05	0.3	0.01
YPM037	0.05	1.2	0.169	4.2	4	32	0.01	0.406	0.52	0.05	0.3	0.01
YPM038	0.04	1.1	0.148	4.6	7	27	0.005	0.433	0.82	0.05	0.2	0.01
YPM039	0.03	1	0.213	3.4	5	48	0.005	0.591	0.74	0.05	0.2	0.01
YPM040	0.04	1.1	0.256	10.4	7	65	0.005	0.42	0.53	0.05	0.3	0.01
YPM041	0.02	1.2	0.15	2.7	6	22	0.005	0.311	0.87	0.05	0.3	0.01
YPM042	0.02	1.3	0.161	3.1	4	42	0.005	0.468	0.46	0.05	0.3	0.01
YPM043	0.04	0.1	0.141	2.9	3	30	0.005	0.626	0.53	0.05	0.2	0.01
YPM044	0.03	1	0.125	1.4	4	29	0.005	0.62	0.43	0.05	0.3	0.01
YPM045	0.05	1.1	0.159	1.9	4	27	0.005	0.554	0.43	0.05	0.2	0.01
YPM046	0.02	1.1	0.2	2.3	7	57	0.005	0.455	0.48	0.05	0.2	0.01
YPM047	0.03	1.2	0.259	2.1	3	31	0.005	0.527	0.33	0.05	0.3	0.01
YPM048	0.02	1.1	0.109	2.9	3	24	0.005	0.345	0.53	0.05	0.2	0.01
YPM049	0.01	1	0.143	2.8	6	21	0.005	0.302	0.8	0.05	0.2	0.01
YPM050	0.005	1.1	0.167	0.9	4	21	0.005	0.47	0.42	0.05	0.3	0.01
YPM051	0.03	1	0.256	1.6	7	60	0.005	0.411	0.31	0.05	0.2	0.01
YPM052	0.05	1.1	0.22	1.6	4	31	0.01	0.715	0.47	0.05	0.2	0.01
YPM053	0.05	1.2	0.206	1.4	7	22	0.01	0.643	0.48	0.05	0.2	0.01
YPM054	0.03	1.2	0.215	1	4	16	0.005	0.957	0.46	0.05	0.1	0.01
YPM055	0.03	1.2	0.127	2.6	5	42	0.005	0.695	0.59	0.05	0.2	0.01
YPM056	0.07	1.2	0.172	2.1	7	24	0.02	0.789	0.73	0.05	0.2	0.01
YPM057	0.04	1.2	0.142	4.1	6	52	0.01	0.481	0.5	0.05	0.2	0.01
YPM058	0.02	1.1	0.174	6.1	5	26	0.005	0.263	0.85	0.05	0.2	0.01
YPM059	0.03	1.2	0.148	5.5	5	37	0.005	0.457	0.61	0.05	0.3	0.01
YPM060	0.05	1.3	0.182	3.6	6	28	0.01	0.542	0.55	0.05	0.2	0.01
YPM061	0.06	1.3	0.178	2.2	6	33	0.01	0.764	0.43	0.05	0.3	0.01
YPM062	0.08	1.3	0.166	5.9	11	37	0.02	0.928	0.73	0.05	0.3	0.01
YPM063	0.06	1.3	0.181	5.9	9	33	0.02	0.651	0.77	0.05	0.3	0.01
YPM064	0.07	1.2	0.224	6.5	5	45	0.01	0.761	0.36	0.05	0.05	0.01
YPM065	0.03	1.2	0.145	8.6	4	37	0.005	0.484	0.65	0.05	0.3	0.01
YPM066	0.03	1.3	0.135	4.8	4	40	0.005	0.384	0.54	0.05	0.3	0.01
YPM067	0.04	1.3	0.143	3.6	4	52	0.005	0.343	0.49	0.05	0.2	0.01
YPM068	0.03	1.2	0.113	3.8	5	22	0.005	0.443	0.58	0.05	0.2	0.01
YPM069	0.06	2.1	0.213	8.6	5	41	0.02	0.631	0.37	0.05	0.05	0.01

*NOTE values below detection have been halved	S_pct	Hg_ppb	Se_ppm	Te_ppm	Ga_ppm	Cs_ppm	Ge_ppm	Hf_ppm	Nb_ppm	Rb_ppm	Sn_ppm	Ta_ppm
Lab analytical method code	1VE	1VE	1VE	1VE	1VE	1VE	1VE	1VE	1VE	1VE	1VE	1VE
Unit	wt%	PPB	PPM	PPM	PPM	PPM	PPM	PPM	PPM	PPM	PPM	PPM
Detection Limit	0.01	1	0.1	0.02	0.1	0.005	0.01	0.001	0.01	0.1	0.02	0.001
SampleID												
YPM001	0.17	17	0.6	0.01	0.05	0.008	0.005	0.004	0.005	0.9	0.02	0.0005
YPM002	0.09	3	0.4	0.01	0.05	0.009	0.02	0.003	0.005	1.9	0.01	0.0005
YPM003	0.1	11	0.5	0.01	0.05	0.023	0.005	0.007	0.005	2.2	0.01	0.0005
YPM004	0.12	34	0.6	0.01	0.05	0.013	0.005	0.007	0.005	0.7	0.02	0.0005
YPM005	0.07	7	0.1	0.01	0.05	0.007	0.03	0.001	0.005	1.7	0.01	0.0005
YPM006	0.12	21	0.2	0.01	0.05	0.0025	0.005	0.004	0.005	0.4	0.01	0.0005
YPM007	0.08	12	0.3	0.01	0.05	0.005	0.005	0.003	0.005	0.8	0.02	0.0005
YPM008	0.09	9	0.2	0.01	0.05	0.008	0.03	0.0005	0.005	1.6	0.01	0.0005
YPM009	0.07	16	0.3	0.01	0.05	0.0025	0.005	0.0005	0.005	0.8	0.01	0.0005
YPM012	0.09	12	0.3	0.01	0.05	0.008	0.005	0.003	0.005	1.5	0.01	0.0005
YPM013	0.06	28	0.4	0.01	0.05	0.012	0.01	0.005	0.005	0.7	0.01	0.0005
YPM014	0.07	10	0.1	0.01	0.05	0.006	0.02	0.002	0.005	0.9	0.01	0.0005
YPM015	0.09	26	0.3	0.01	0.05	0.005	0.005	0.0005	0.005	0.6	0.01	0.0005
YPM016	0.05	17	0.3	0.01	0.05	0.009	0.005	0.003	0.005	0.6	0.01	0.0005
YPM017	0.15	14	1.4	0.01	0.05	0.007	0.005	0.0005	0.005	1.8	0.01	0.0005
YPM018	0.11	8	0.3	0.01	0.05	0.01	0.005	0.003	0.005	1.1	0.01	0.0005
YPM019	0.15	17	0.7	0.01	0.05	0.012	0.005	0.003	0.01	2.2	0.01	0.0005
YPM020	0.13	17	1	0.01	0.05	0.0025	0.005	0.0005	0.005	0.8	0.01	0.0005
YPM021	0.1	21	0.5	0.01	0.05	0.0025	0.005	0.002	0.005	2.7	0.01	0.0005
YPM022	0.12	41	0.4	0.01	0.05	0.007	0.005	0.002	0.005	0.6	0.01	0.0005
YPM023	0.13	27	0.2	0.01	0.05	0.0025	0.005	0.001	0.005	0.3	0.01	0.0005
YPM024	0.08	15	0.2	0.01	0.05	0.0025	0.005	0.001	0.005	1	0.01	0.0005
YPM025	0.09	27	0.3	0.01	0.05	0.01	0.005	0.002	0.005	0.7	0.01	0.0005
YPM026	0.11	15	0.7	0.01	0.05	0.01	0.005	0.004	0.005	1.4	0.01	0.0005
YPM027	0.09	8	0.2	0.01	0.05	0.005	0.005	0.003	0.005	0.7	0.01	0.0005
YPM028	0.06	4	0.2	0.01	0.05	0.0025	0.005	0.002	0.005	1.2	0.01	0.0005
YPM029	0.05	18	0.2	0.01	0.05	0.005	0.005	0.002	0.005	0.9	0.01	0.0005
YPM030	0.05	14	0.1	0.01	0.05	0.0025	0.005	0.001	0.005	0.6	0.01	0.0005
YPM031	0.05	23	0.1	0.01	0.05	0.0025	0.005	0.0005	0.005	0.6	0.01	0.0005
YPM032	0.07	26	0.2	0.01	0.05	0.006	0.005	0.001	0.005	0.9	0.01	0.0005
YPM033	0.04	31	0.3	0.01	0.05	0.007	0.005	0.003	0.005	0.8	0.01	0.0005
YPM034	0.08	5	0.1	0.01	0.05	0.005	0.005	0.002	0.005	1.6	0.01	0.0005
YPM035	0.08	13	0.05	0.01	0.05	0.0025	0.005	0.0005	0.005	0.7	0.01	0.0005
YPM036	0.08	29	0.2	0.03	0.05	0.006	0.005	0.0005	0.005	0.6	0.01	0.0005
YPM037	0.09	6	0.2	0.01	0.05	0.01	0.02	0.004	0.005	0.5	0.01	0.0005
YPM038	0.12	8	0.4	0.01	0.05	0.006	0.03	0.002	0.005	2	0.01	0.0005
YPM039	0.14	12	0.2	0.01	0.05	0.008	0.01	0.001	0.005	1.2	0.01	0.0005
YPM040	0.14	25	0.5	0.01	0.05	0.0025	0.02	0.003	0.005	0.8	0.01	0.0005
YPM041	0.1	1	0.2	0.01	0.05	0.0025	0.03	0.0005	0.005	2	0.01	0.0005
YPM042	0.08	14	0.4	0.01	0.05	0.0025	0.005	0.005	0.005	0.8	0.01	0.001
YPM043	0.08	10	0.8	0.01	0.05	0.005	0.02	0.002	0.005	0.8	0.01	0.0005
YPM044	0.07	15	0.1	0.01	0.05	0.006	0.03	0.002	0.005	0.8	0.01	0.0005
YPM045	0.06	13	0.3	0.01	0.05	0.008	0.02	0.002	0.005	1	0.01	0.0005
YPM046	0.08	23	0.2	0.02	0.05	0.0025	0.01	0.0005	0.005	0.8	0.01	0.0005
YPM047	0.08	21	0.3	0.03	0.05	0.0025	0.005	0.0005	0.005	0.5	0.01	0.0005
YPM048	0.08	7	0.1	0.01	0.05	0.005	0.005	0.0005	0.005	1.5	0.01	0.0005
YPM049	0.08	6	0.2	0.01	0.05	0.0025	0.02	0.0005	0.005	1.8	0.01	0.0005
YPM050	0.08	6	0.4	0.01	0.05	0.0025	0.005	0.0005	0.005	1.5	0.01	0.0005
YPM051	0.11	22	0.3	0.01	0.05	0.0025	0.03	0.0005	0.005	0.3	0.01	0.0005
YPM052	0.07	14	0.4	0.01	0.05	0.009	0.005	0.0005	0.005	1.1	0.01	0.0005
YPM053	0.1	13	0.3	0.01	0.05	0.009	0.01	0.0005	0.005	1.3	0.01	0.0005
YPM054	0.1	7	0.6	0.01	0.05	0.006	0.02	0.0005	0.005	1.2	0.01	0.0005
YPM055	0.12	16	0.4	0.01	0.05	0.007	0.005	0.002	0.005	0.9	0.01	0.0005
YPM056	0.13	8	0.2	0.01	0.05	0.015	0.01	0.008	0.005	1.6	0.01	0.0005
YPM057	0.11	18	0.3	0.01	0.05	0.01	0.01	0.003	0.005	0.7	0.01	0.0005
YPM058	0.1	6	0.05	0.01	0.05	0.0025	0.04	0.0005	0.005	2.1	0.01	0.0005
YPM059	0.14	15	0.5	0.01	0.05	0.006	0.02	0.002	0.005	1.5	0.01	0.0005
YPM060	0.13	7	0.5	0.01	0.05	0.009	0.02	0.003	0.005	1.3	0.01	0.0005
YPM061	0.09	16	0.3	0.01	0.05	0.01	0.005	0.002	0.005	1	0.01	0.0005
YPM062	0.14	9	0.4	0.01	0.05	0.014	0.04	0.0005	0.005	1.5	0.01	0.0005
YPM063	0.15	7	0.5	0.01	0.05	0.012	0.03	0.003	0.005	2.2	0.01	0.0005
YPM064	0.08	15	0.2	0.01	0.05	0.012	0.005	0.003	0.005	0.6	0.01	0.0005
YPM065	0.09	17	0.5	0.01	0.05	0.006	0.02	0.0005	0.005	1.3	0.01	0.0005
YPM066	0.09	21	0.2	0.01	0.05	0.005	0.005	0.0005	0.005	1.1	0.01	0.0005
YPM067	0.08	20	0.3	0.01	0.05	0.006	0.02	0.001	0.005	0.7	0.01	0.0005
YPM068	0.09	7	0.2	0.01	0.05	0.0025	0.01	0.0005	0.005	1.2	0.01	0.0005
YPM069	0.13	20	0.2	0.01	0.05	0.011	0.005	0.006	0.005	0.5	0.01	0.0005

*NOTE values below detection have been halved	Zr_ppm	Y_ppm	Ce_ppm	In_ppm	Re_ppb	Be_ppm	Li_ppm	Pd_ppb	Pt_ppb
Lab analytical method code	1VE	1VE	1VE	1VE	1VE	1VE	1VE	1VE	1VE
Unit	PPM	PPM	PPM	PPM	PPB	PPM	PPM	PPB	PPB
Detection Limit	0.01	0.001	0.01	0.02	1	0.1	0.01	2	1
SampleID									
YPM001	0.07	0.039	0.11	0.01	0.5	0.05	0.66	1	1
YPM002	0.08	0.05	0.13	0.01	0.5	0.05	0.31	1	0.5
YPM003	0.18	0.088	0.29	0.01	0.5	0.05	0.65	1	0.5
YPM004	0.12	0.074	0.17	0.01	0.5	0.05	0.75	1	0.5
YPM005	0.08	0.029	0.1	0.01	0.5	0.05	0.43	1	0.5
YPM006	0.04	0.032	0.08	0.01	0.5	0.05	1.95	1	0.5
YPM007	0.04	0.032	0.08	0.01	0.5	0.05	0.54	1	0.5
YPM008	0.08	0.036	0.1	0.01	0.5	0.05	0.43	1	0.5
YPM009	0.05	0.027	0.05	0.01	0.5	0.05	0.72	1	0.5
YPM012	0.07	0.039	0.14	0.01	0.5	0.05	0.18	1	0.5
YPM013	0.09	0.054	0.23	0.01	0.5	0.05	1.23	1	0.5
YPM014	0.06	0.062	0.23	0.01	0.5	0.05	0.78	1	0.5
YPM015	0.07	0.038	0.16	0.01	0.5	0.05	0.71	1	0.5
YPM016	0.09	0.059	0.22	0.01	0.5	0.05	0.62	1	0.5
YPM017	0.06	0.041	0.11	0.01	0.5	0.05	0.24	1	0.5
YPM018	0.09	0.043	0.13	0.01	0.5	0.05	0.48	1	0.5
YPM019	0.08	0.051	0.15	0.01	0.5	0.05	0.51	1	0.5
YPM020	0.02	0.02	0.06	0.01	0.5	0.05	0.68	1	0.5
YPM021	0.03	0.016	0.04	0.01	12	0.05	0.47	1	0.5
YPM022	0.06	0.032	0.1	0.01	0.5	0.05	0.68	1	0.5
YPM023	0.05	0.029	0.08	0.01	0.5	0.05	1.95	1	0.5
YPM024	0.04	0.024	0.06	0.01	0.5	0.05	0.69	1	0.5
YPM025	0.08	0.037	0.12	0.01	0.5	0.05	0.29	1	0.5
YPM026	0.1	0.04	0.12	0.01	0.5	0.05	0.28	1	0.5
YPM027	0.06	0.028	0.1	0.01	0.5	0.05	0.14	1	0.5
YPM028	0.03	0.02	0.06	0.01	0.5	0.05	0.18	1	0.5
YPM029	0.05	0.027	0.08	0.01	0.5	0.05	0.67	1	0.5
YPM030	0.05	0.026	0.1	0.01	0.5	0.05	0.65	1	0.5
YPM031	0.05	0.027	0.07	0.01	0.5	0.05	0.73	1	0.5
YPM032	0.06	0.029	0.16	0.01	0.5	0.05	0.23	1	0.5
YPM033	0.05	0.027	0.08	0.01	0.5	0.05	0.38	1	0.5
YPM034	0.02	0.018	0.06	0.01	0.5	0.05	0.16	1	0.5
YPM035	0.04	0.02	0.05	0.01	0.5	0.05	0.61	1	0.5
YPM036	0.07	0.035	0.11	0.01	1	0.05	1.19	1	0.5
YPM037	0.07	0.029	0.12	0.01	0.5	0.05	0.91	1	1
YPM038	0.05	0.02	0.1	0.01	0.5	0.05	0.31	1	0.5
YPM039	0.05	0.029	0.09	0.01	0.5	0.05	0.68	1	0.5
YPM040	0.04	0.027	0.1	0.01	0.5	0.05	0.59	1	0.5
YPM041	0.03	0.014	0.04	0.01	0.5	0.05	0.17	1	0.5
YPM042	0.05	0.026	0.08	0.01	0.5	0.05	1.85	1	0.5
YPM043	0.04	0.044	0.11	0.01	0.5	0.05	0.74	1	0.5
YPM044	0.05	0.027	0.07	0.01	0.5	0.05	0.81	1	0.5
YPM045	0.06	0.036	0.12	0.01	0.5	0.05	0.99	1	0.5
YPM046	0.02	0.019	0.05	0.01	0.5	0.05	0.9	1	0.5
YPM047	0.04	0.023	0.08	0.01	1	0.05	0.95	1	0.5
YPM048	0.03	0.015	0.07	0.01	0.5	0.05	0.2	1	0.5
YPM049	0.03	0.016	0.05	0.01	0.5	0.05	0.19	1	0.5
YPM050	0.02	0.003	0.02	0.01	0.5	0.05	0.61	1	0.5
YPM051	0.03	0.016	0.07	0.01	0.5	0.05	2.12	1	0.5
YPM052	0.08	0.035	0.15	0.01	0.5	0.05	0.4	1	0.5
YPM053	0.04	0.033	0.13	0.01	0.5	0.05	1.33	1	0.5
YPM054	0.04	0.028	0.08	0.01	0.5	0.05	0.64	1	0.5
YPM055	0.05	0.03	0.1	0.01	0.5	0.05	1.26	1	0.5
YPM056	0.12	0.07	0.21	0.01	0.5	0.05	0.54	1	0.5
YPM057	0.08	0.044	0.14	0.01	0.5	0.05	1.74	1	0.5
YPM058	0.04	0.013	0.06	0.01	0.5	0.05	0.17	1	0.5
YPM059	0.06	0.032	0.1	0.01	0.5	0.05	0.24	1	0.5
YPM060	0.07	0.038	0.12	0.01	0.5	0.05	0.69	1	0.5
YPM061	0.08	0.05	0.15	0.01	0.5	0.05	1.37	1	0.5
YPM062	0.14	0.069	0.2	0.01	0.5	0.05	0.34	1	0.5
YPM063	0.09	0.048	0.15	0.01	0.5	0.05	0.54	1	0.5
YPM064	0.09	0.048	0.15	0.01	0.5	0.05	1.05	1	0.5
YPM065	0.05	0.025	0.1	0.01	0.5	0.05	0.29	1	0.5
YPM066	0.05	0.028	0.07	0.01	0.5	0.05	0.48	1	0.5
YPM067	0.08	0.029	0.09	0.01	0.5	0.05	0.49	1	0.5
YPM068	0.03	0.021	0.07	0.01	0.5	0.05	0.12	1	0.5
YPM069	0.1	0.047	0.14	0.01	0.5	0.05	0.47	1	0.5

	*NOTE values below detection have been halved	Duplicate ID	Sample_Type	Transect	Location	Orig_Grid_ID	Orig_East	Orig_North	GA_RL
Yorke Peninsula	YPM070		VEG	3	Goldsworthy Rd	GDA94_53H	762695	6154072	39
Yorke Peninsula	YPM071	YPM053	VEG	3	Barkers Rocks Rd	GDA94_53H	732530	6155507	41
Yorke Peninsula	YPM072	YPM055	VEG	3	Barkers Rocks Rd	GDA94_53H	736103	6155413	71
Yorke Peninsula	YPM075		VEG	4	Black Bobs Rd	GDA94_53H	763310	6169311	20
Yorke Peninsula	YPM076	YPM 099	VEG	4	Black Bobs Rd	GDA94_53H	762309	6169336	32
Yorke Peninsula	YPM077		VEG	4	Black Bobs Rd	GDA94_53H	761247	6169363	52
Yorke Peninsula	YPM078		VEG	4	Black Bobs Rd	GDA94_53H	760171	6169390	77
Yorke Peninsula	YPM079		VEG	4	Black Bobs Rd	GDA94_53H	759059	6169418	73
Yorke Peninsula	YPM080		VEG	4	Black Bobs Rd	GDA94_53H	757833	6169449	72
Yorke Peninsula	YPM081		VEG	4	Black Bobs Rd	GDA94_53H	756818	6169472	76
Yorke Peninsula	YPM082		VEG	4	Black Bobs Rd	GDA94_53H	755572	6169503	74
Yorke Peninsula	YPM083		VEG	4	Black Bobs Rd	GDA94_53H	754541	6169528	78
Yorke Peninsula	YPM084		VEG	4	Black Bobs Rd	GDA94_53H	753519	6169555	88
Yorke Peninsula	YPM085		VEG	4	Black Bobs Rd	GDA94_53H	752533	6169581	97
Yorke Peninsula	YPM086		VEG	4	Black Bobs Rd	GDA94_53H	751167	6169617	103
Yorke Peninsula	YPM087		VEG	4	Black Bobs Rd	GDA94_53H	750135	6169635	107
Yorke Peninsula	YPM088		VEG	4	Black Bobs Rd	GDA94_53H	749114	6169663	112
Yorke Peninsula	YPM089	YPM 100	VEG	4	Black Bobs Rd	GDA94_53H	748017	6169687	112
Yorke Peninsula	YPM090		VEG	4	Black Bobs Rd	GDA94_53H	747008	6169684	105
Yorke Peninsula	YPM091		VEG	4	Black Bobs Rd	GDA94_53H	745882	6169651	101
Yorke Peninsula	YPM092		VEG	4	Black Bobs Rd	GDA94_53H	744652	6169658	84
Yorke Peninsula	YPM093		VEG	4	Black Bobs Rd	GDA94_53H	743524	6169679	86
Yorke Peninsula	YPM094		VEG	4	Black Bobs Rd	GDA94_53H	739655	6169734	90
Yorke Peninsula	YPM095		VEG	4	Black Bobs Rd	GDA94_53H	737270	6169797	49
Yorke Peninsula	YPM096		VEG	4	Black Bobs Rd	GDA94_53H	736252	6169822	39
Yorke Peninsula	YPM097		VEG	4	Black Bobs Rd	GDA94_53H	732533	6169916	14
Yorke Peninsula	YPM098		VEG	4	Black Bobs Rd	GDA94_53H	731449	6169946	7
Yorke Peninsula	YPM099	YPM076	VEG	4	Black Bobs Rd	GDA94_53H	762309	6169336	32
Yorke Peninsula	YPM100	YPM089	VEG	4	Black Bobs Rd	GDA94_53H	748017	6169687	112
Yorke Peninsula	YPM102		VEG	5	James Well Rd	GDA94_53H	765629	6180781	27
Yorke Peninsula	YPM103		VEG	5	James Well Rd	GDA94_53H	764541	6180799	55
Yorke Peninsula	YPM104		VEG	5	James Well Rd	GDA94_53H	762915	6180840	83
Yorke Peninsula	YPM105		VEG	5	James Well Rd	GDA94_53H	761775	6180866	94
Yorke Peninsula	YPM106		VEG	5	James Well Rd	GDA94_53H	760688	6180896	93
Yorke Peninsula	YPM107		VEG	5	James Well Rd	GDA94_53H	759693	6180921	99
Yorke Peninsula	YPM108		VEG	5	James Well Rd	GDA94_53H	758685	6180946	107
Yorke Peninsula	YPM109		VEG	5	James Well Rd	GDA94_53H	757583	6180975	120
Yorke Peninsula	YPM110		VEG	5	James Well Rd	GDA94_53H	756553	6181001	125
Yorke Peninsula	YPM111		VEG	5	James Well Rd	GDA94_53H	755361	6181032	134
Yorke Peninsula	YPM112		VEG	5	James Well Rd	GDA94_53H	754336	6181055	138
Yorke Peninsula	YPM113	YPM 126	VEG	5	Yarrum Rd	GDA94_53H	752112	6181116	150
Yorke Peninsula	YPM114		VEG	5	Yarrum Rd	GDA94_53H	751011	6181142	137
Yorke Peninsula	YPM115		VEG	5	Yarrum Rd	GDA94_53H	750002	6181168	126
Yorke Peninsula	YPM116		VEG	5	Yarrum Rd	GDA94_53H	748162	6181215	107
Yorke Peninsula	YPM117		VEG	5	Yarrum Rd	GDA94_53H	746942	6181249	100
Yorke Peninsula	YPM118		VEG	5	Yarrum Rd	GDA94_53H	745887	6181272	97
Yorke Peninsula	YPM119		VEG	5	Yarrum Rd	GDA94_53H	744831	6181299	90
Yorke Peninsula	YPM120		VEG	5	Yarrum Rd	GDA94_53H	743315	6181335	78
Yorke Peninsula	YPM121		VEG	5	Barley Stacks Rd	GDA94_53H	740508	6181409	108
Yorke Peninsula	YPM122		VEG	5	Barley Stacks Rd	GDA94_53H	739514	6181436	106
Yorke Peninsula	YPM123	YPM127	VEG	5	Barley Stacks Rd	GDA94_53H	737182	6181489	80
Yorke Peninsula	YPM124		VEG	5	Barley Stacks Rd	GDA94_53H	735780	6181525	58
Yorke Peninsula	YPM125		VEG	5	Barley Stacks Rd	GDA94_53H	734256	6181564	50
Yorke Peninsula	YPM126	YPM113	VEG	5	Yarrum Rd	GDA94_53H	752112	6181116	150
Yorke Peninsula	YPM127	YPM123	VEG	5	Barley Stacks Rd	GDA94_53H	737182	6181489	80
Yorke Peninsula	YPM128		VEG	6	Moody Rd	GDA94_53H	732605	6192099	37
Yorke Peninsula	YPM129		VEG	6	Moody Rd	GDA94_53H	736836	6192476	77
Yorke Peninsula	YPM130	YPM146	VEG	6	Moody Rd	GDA94_53H	740760	6192582	129
Yorke Peninsula	YPM131		VEG	6	Pistol Club Rd	GDA94_53H	751263	6194344	221
Yorke Peninsula	YPM132		VEG	6	Pistol Club Rd	GDA94_53H	752310	6194324	211
Yorke Peninsula	YPM133		VEG	6	Pistol Club Rd	GDA94_53H	753462	6194063	186
Yorke Peninsula	YPM134		VEG	6	Pistol Club Rd	GDA94_53H	754541	6193761	170
Yorke Peninsula	YPM135		VEG	6	Pistol Club Rd	GDA94_53H	755699	6193695	151
Yorke Peninsula	YPM136		VEG	6	Johnson Rd	GDA94_53H	756786	6193679	139
Yorke Peninsula	YPM137	YPM147	VEG	6	Johnson Rd	GDA94_53H	757887	6193648	131
Yorke Peninsula	YPM138		VEG	6	Johnson Rd	GDA94_53H	758978	6193621	108
Yorke Peninsula	YPM139		VEG	6	Johnson Rd	GDA94_53H	760083	6193593	106
Yorke Peninsula	YPM140		VEG	6	Peterson Rd	GDA94_53H	760961	6193569	94
Yorke Peninsula	YPM141		VEG	6	Peterson Rd	GDA94_53H	762039	6193540	90
Yorke Peninsula	YPM142		VEG	6	Peterson Rd	GDA94_53H	763060	6193481	96
Yorke Peninsula	YPM143		VEG	6	Peterson Rd	GDA94_53H	764175	6193279	99
Yorke Peninsula	YPM144		VEG	6	Peterson Rd	GDA94_53H	765239	6193088	93

*NOTE values below detection have been halved	Orig_Survey_Method	Orig_Survey_By	Orig_Survey_Date	Sampled_By	Treatment	Species
YPM070	Garmin GPS Map62S	KWolff	18/03/2012	KWolff	dried for 48hrs at 60'C	E. gracilis
YPM071	Garmin GPS Map62S	KWolff	18/03/2012	KWolff	dried for 48hrs at 60'C	E. gracilis
YPM072	Garmin GPS Map62S	KWolff	18/03/2012	KWolff	dried for 48hrs at 60'C	E. leptophylla
YPM075	Garmin GPS Map62S	KWolff	24/03/2012	KWolff	dried for 48hrs at 60'C	E. phenax
YPM076	Garmin GPS Map62S	KWolff	24/03/2012	KWolff	dried for 48hrs at 60'C	E. socialis
YPM077	Garmin GPS Map62S	KWolff	24/03/2012	KWolff	dried for 48hrs at 60'C	E. socialis
YPM078	Garmin GPS Map62S	KWolff	24/03/2012	KWolff	dried for 48hrs at 60'C	E. socialis
YPM079	Garmin GPS Map62S	KWolff	24/03/2012	KWolff	dried for 48hrs at 60'C	E. phenax
YPM080	Garmin GPS Map62S	KWolff	24/03/2012	KWolff	dried for 48hrs at 60'C	E. socialis
YPM081	Garmin GPS Map62S	KWolff	24/03/2012	KWolff	dried for 48hrs at 60'C	E. socialis
YPM082	Garmin GPS Map62S	KWolff	24/03/2012	KWolff	dried for 48hrs at 60'C	E. socialis
YPM083	Garmin GPS Map62S	KWolff	24/03/2012	KWolff	dried for 48hrs at 60'C	E. socialis
YPM084	Garmin GPS Map62S	KWolff	24/03/2012	KWolff	dried for 48hrs at 60'C	E. socialis
YPM085	Garmin GPS Map62S	KWolff	24/03/2012	KWolff	dried for 48hrs at 60'C	E. socialis
YPM086	Garmin GPS Map62S	KWolff	24/03/2012	KWolff	dried for 48hrs at 60'C	E. leptophylla
YPM087	Garmin GPS Map62S	KWolff	24/03/2012	KWolff	dried for 48hrs at 60'C	E. socialis
YPM088	Garmin GPS Map62S	KWolff	24/03/2012	KWolff	dried for 48hrs at 60'C	E. socialis
YPM089	Garmin GPS Map62S	KWolff	24/03/2012	KWolff	dried for 48hrs at 60'C	E. socialis
YPM090	Garmin GPS Map62S	KWolff	24/03/2012	KWolff	dried for 48hrs at 60'C	E. socialis
YPM091	Garmin GPS Map62S	KWolff	24/03/2012	KWolff	dried for 48hrs at 60'C	E. socialis
YPM092	Garmin GPS Map62S	KWolff	24/03/2012	KWolff	dried for 48hrs at 60'C	E. socialis
YPM093	Garmin GPS Map62S	KWolff	24/03/2012	KWolff	dried for 48hrs at 60'C	E. socialis
YPM094	Garmin GPS Map62S	KWolff	24/03/2012	KWolff	dried for 48hrs at 60'C	E. phenax
YPM095	Garmin GPS Map62S	KWolff	24/03/2012	KWolff	dried for 48hrs at 60'C	E. phenax
YPM096	Garmin GPS Map62S	KWolff	24/03/2012	KWolff	dried for 48hrs at 60'C	E. phenax
YPM097	Garmin GPS Map62S	KWolff	24/03/2012	KWolff	dried for 48hrs at 60'C	E. gracilis
YPM098	Garmin GPS Map62S	KWolff	24/03/2012	KWolff	dried for 48hrs at 60'C	E. socialis
YPM099	Garmin GPS Map62S	KWolff	24/03/2012	KWolff	dried for 48hrs at 60'C	E. socialis
YPM100	Garmin GPS Map62S	KWolff	24/03/2012	KWolff	dried for 48hrs at 60'C	E. socialis
YPM102	Garmin GPS Map62S	KWolff	25/03/2012	KWolff	dried for 48hrs at 60'C	E. leptophylla
YPM103	Garmin GPS Map62S	KWolff	25/03/2012	KWolff	dried for 48hrs at 60'C	E. phenax
YPM104	Garmin GPS Map62S	KWolff	25/03/2012	KWolff	dried for 48hrs at 60'C	E. phenax
YPM105	Garmin GPS Map62S	KWolff	25/03/2012	KWolff	dried for 48hrs at 60'C	E. phenax
YPM106	Garmin GPS Map62S	KWolff	25/03/2012	KWolff	dried for 48hrs at 60'C	E. phenax
YPM107	Garmin GPS Map62S	KWolff	25/03/2012	KWolff	dried for 48hrs at 60'C	E. phenax
YPM108	Garmin GPS Map62S	KWolff	25/03/2012	KWolff	dried for 48hrs at 60'C	E. socialis
YPM109	Garmin GPS Map62S	KWolff	25/03/2012	KWolff	dried for 48hrs at 60'C	E. phenax
YPM110	Garmin GPS Map62S	KWolff	25/03/2012	KWolff	dried for 48hrs at 60'C	E. socialis
YPM111	Garmin GPS Map62S	KWolff	25/03/2012	KWolff	dried for 48hrs at 60'C	E. socialis
YPM112	Garmin GPS Map62S	KWolff	25/03/2012	KWolff	dried for 48hrs at 60'C	E. phenax
YPM113	Garmin GPS Map62S	KWolff	25/03/2012	KWolff	dried for 48hrs at 60'C	E. socialis
YPM114	Garmin GPS Map62S	KWolff	25/03/2012	KWolff	dried for 48hrs at 60'C	E. socialis
YPM115	Garmin GPS Map62S	KWolff	25/03/2012	KWolff	dried for 48hrs at 60'C	E. socialis
YPM116	Garmin GPS Map62S	KWolff	25/03/2012	KWolff	dried for 48hrs at 60'C	E. gracilis
YPM117	Garmin GPS Map62S	KWolff	25/03/2012	KWolff	dried for 48hrs at 60'C	E. gracilis
YPM118	Garmin GPS Map62S	KWolff	25/03/2012	KWolff	dried for 48hrs at 60'C	E. socialis
YPM119	Garmin GPS Map62S	KWolff	25/03/2012	KWolff	dried for 48hrs at 60'C	E. gracilis
YPM120	Garmin GPS Map62S	KWolff	25/03/2012	KWolff	dried for 48hrs at 60'C	E. gracilis
YPM121	Garmin GPS Map62S	KWolff	31/03/2012	KWolff	dried for 48hrs at 60'C	E. socialis
YPM122	Garmin GPS Map62S	KWolff	31/03/2012	KWolff	dried for 48hrs at 60'C	E. gracilis
YPM123	Garmin GPS Map62S	KWolff	31/03/2012	KWolff	dried for 48hrs at 60'C	E. socialis
YPM124	Garmin GPS Map62S	KWolff	31/03/2012	KWolff	dried for 48hrs at 60'C	E. socialis
YPM125	Garmin GPS Map62S	KWolff	31/03/2012	KWolff	dried for 48hrs at 60'C	E. gracilis
YPM126	Garmin GPS Map62S	KWolff	31/03/2012	KWolff	dried for 48hrs at 60'C	E. socialis
YPM127	Garmin GPS Map62S	KWolff	31/03/2012	KWolff	dried for 48hrs at 60'C	E. socialis
YPM128	Garmin GPS Map62S	KWolff	31/03/2012	KWolff	dried for 48hrs at 60'C	E. phenax
YPM129	Garmin GPS Map62S	KWolff	31/03/2012	KWolff	dried for 48hrs at 60'C	E. phenax
YPM130	Garmin GPS Map62S	KWolff	31/03/2012	KWolff	dried for 48hrs at 60'C	E. socialis
YPM131	Garmin GPS Map62S	KWolff	31/03/2012	KWolff	dried for 48hrs at 60'C	E. socialis
YPM132	Garmin GPS Map62S	KWolff	31/03/2012	KWolff	dried for 48hrs at 60'C	E. gracilis
YPM133	Garmin GPS Map62S	KWolff	31/03/2012	KWolff	dried for 48hrs at 60'C	E. socialis
YPM134	Garmin GPS Map62S	KWolff	31/03/2012	KWolff	dried for 48hrs at 60'C	E. phenax
YPM135	Garmin GPS Map62S	KWolff	31/03/2012	KWolff	dried for 48hrs at 60'C	E. socialis
YPM136	Garmin GPS Map62S	KWolff	31/03/2012	KWolff	dried for 48hrs at 60'C	E. phenax
YPM137	Garmin GPS Map62S	KWolff	31/03/2012	KWolff	dried for 48hrs at 60'C	E. phenax
YPM138	Garmin GPS Map62S	KWolff	31/03/2012	KWolff	dried for 48hrs at 60'C	E. socialis
YPM139	Garmin GPS Map62S	KWolff	31/03/2012	KWolff	dried for 48hrs at 60'C	E. phenax
YPM140	Garmin GPS Map62S	KWolff	31/03/2012	KWolff	dried for 48hrs at 60'C	E. gracilis
YPM141	Garmin GPS Map62S	KWolff	31/03/2012	KWolff	dried for 48hrs at 60'C	E. phenax
YPM142	Garmin GPS Map62S	KWolff	31/03/2012	KWolff	dried for 48hrs at 60'C	E. phenax
YPM143	Garmin GPS Map62S	KWolff	31/03/2012	KWolff	dried for 48hrs at 60'C	E. phenax
YPM144	Garmin GPS Map62S	KWolff	31/03/2012	KWolff	dried for 48hrs at 60'C	E. phenax

*NOTE values below detection have been halved	Sample_Description	Date_Sampled	Mo_ppm	Cu_ppm	Pb_ppm	Zn_ppm	Ag_ppm	Ni_ppm	Co_ppm	Mn_ppm
YPM070	phyllodes	18/03/2012	0.02	1.95	0.09	4.7	1	0.8	0.07	14
YPM071	phyllodes	18/03/2012	0.15	5.34	0.1	17.3	1	0.5	0.06	18
YPM072	phyllodes	18/03/2012	0.18	5.02	0.12	15.1	1	0.4	0.04	47
YPM075	phyllodes	24/03/2012	0.08	2.1	0.04	6.8	1	0.4	0.04	7
YPM076	phyllodes	24/03/2012	0.07	2.67	0.04	11.2	1	0.3	0.03	15
YPM077	phyllodes	24/03/2012	0.1	2.76	0.06	9.3	1	0.6	0.07	20
YPM078	phyllodes	24/03/2012	0.06	2.6	0.06	12.1	1	0.4	0.05	9
YPM079	phyllodes	24/03/2012	0.11	3.13	0.08	9.6	1	0.9	0.04	7
YPM080	phyllodes	24/03/2012	0.06	2.29	0.06	13.5	1	0.5	0.04	14
YPM081	phyllodes	24/03/2012	0.11	2.67	0.04	13.4	1	1.1	0.07	23
YPM082	phyllodes	24/03/2012	0.15	2.93	0.04	13	1	1.5	0.04	12
YPM083	phyllodes	24/03/2012	0.06	2.7	0.03	10.7	1	0.7	0.05	49
YPM084	phyllodes	24/03/2012	0.07	2.49	0.05	9	1	1.1	0.07	14
YPM085	phyllodes	24/03/2012	0.11	2.24	0.08	13.1	1	1	0.05	15
YPM086	phyllodes	24/03/2012	0.05	2.15	0.03	17.4	1	2.4	0.07	11
YPM087	phyllodes	24/03/2012	0.06	2.29	0.08	13.4	1	0.8	0.04	26
YPM088	phyllodes	24/03/2012	0.06	3.14	0.05	14.9	1	1.3	0.03	17
YPM089	phyllodes	24/03/2012	0.22	2.9	0.09	12.6	1	1.1	0.03	16
YPM090	phyllodes	24/03/2012	0.14	2.53	0.07	12.6	1	0.4	0.04	13
YPM091	phyllodes	24/03/2012	0.22	2.46	0.08	9.1	1	2.7	0.05	12
YPM092	phyllodes	24/03/2012	0.13	1.97	0.07	15.7	1	1.1	0.02	10
YPM093	phyllodes	24/03/2012	0.09	2.77	0.1	19	1	0.9	0.05	21
YPM094	phyllodes	24/03/2012	0.09	2.95	0.04	11.9	1	0.8	0.03	11
YPM095	phyllodes	24/03/2012	0.1	4.55	0.04	12.6	1	1.2	0.09	101
YPM096	phyllodes	24/03/2012	0.2	4.38	0.05	24	1	1.1	0.08	67
YPM097	phyllodes	24/03/2012	0.03	2.44	0.06	10.6	1	0.4	0.04	33
YPM098	phyllodes	24/03/2012	0.06	3.1	0.04	9.2	1	1	0.05	32
YPM099	phyllodes	24/03/2012	0.06	2.59	0.06	11.8	1	0.4	0.05	15
YPM100	phyllodes	24/03/2012	0.22	2.82	0.06	12.5	1	1	0.05	16
YPM102	phyllodes	25/03/2012	0.12	4.38	0.07	9.7	1	0.8	0.05	40
YPM103	phyllodes	25/03/2012	0.13	3.37	0.04	18.4	1	0.9	0.03	107
YPM104	phyllodes	25/03/2012	0.12	3	0.03	12	1	0.5	0.04	36
YPM105	phyllodes	25/03/2012	0.16	4.71	0.02	14.3	3	0.5	0.04	37
YPM106	phyllodes	25/03/2012	0.09	6.16	0.06	14.7	1	0.4	0.03	23
YPM107	phyllodes	25/03/2012	0.02	3.2	0.07	7.7	1	0.3	0.02	10
YPM108	phyllodes	25/03/2012	0.07	2.24	0.08	14.1	1	0.5	0.03	10
YPM109	phyllodes	25/03/2012	0.06	1.59	0.03	7	1	0.5	0.02	8
YPM110	phyllodes	25/03/2012	0.16	7.77	0.22	23.1	1	4.3	0.06	16
YPM111	phyllodes	25/03/2012	0.16	2.63	0.06	12.8	1	0.6	0.05	12
YPM112	phyllodes	25/03/2012	0.2	3.55	0.02	10	1	1.6	0.02	24
YPM113	phyllodes	25/03/2012	0.09	4.19	0.09	16.1	1	0.6	0.05	30
YPM114	phyllodes	25/03/2012	0.26	4.31	0.04	15.9	1	3.1	0.06	24
YPM115	phyllodes	25/03/2012	0.11	3.01	0.14	12.1	1	0.5	0.05	11
YPM116	phyllodes	25/03/2012	0.09	4.42	0.05	11.8	1	0.5	0.04	8
YPM117	phyllodes	25/03/2012	0.09	4.98	0.08	13.1	1	0.5	0.05	12
YPM118	phyllodes	25/03/2012	0.05	3.47	0.11	14.3	1	1.1	0.05	19
YPM119	phyllodes	25/03/2012	0.19	4.06	0.04	9.9	1	0.3	0.06	17
YPM120	phyllodes	25/03/2012	0.08	5.64	0.12	15.4	1	1	0.01	22
YPM121	phyllodes	31/03/2012	0.08	2.98	0.08	9.5	1	0.5	0.03	22
YPM122	phyllodes	31/03/2012	0.39	3.37	0.05	14.2	1	0.6	0.06	42
YPM123	phyllodes	31/03/2012	0.09	2.97	0.11	9.2	1	4.8	0.07	27
YPM124	phyllodes	31/03/2012	0.04	3.66	0.17	10.5	1	2.8	0.04	120
YPM125	phyllodes	31/03/2012	0.13	4.08	0.06	10.3	1	0.4	0.03	16
YPM126	phyllodes	31/03/2012	0.09	4.26	0.13	17	1	0.5	0.05	25
YPM127	phyllodes	31/03/2012	0.1	3.04	0.11	10.7	1	5.1	0.07	27
YPM128	phyllodes	31/03/2012	0.12	3.59	0.14	10	1	1.1	0.005	16
YPM129	phyllodes	31/03/2012	0.17	5.71	0.09	14	1	1.1	0.08	107
YPM130	phyllodes	31/03/2012	0.2	3.21	0.12	12.9	1	0.7	0.04	14
YPM131	phyllodes	31/03/2012	0.07	3.83	0.11	16.6	1	0.7	0.06	25
YPM132	phyllodes	31/03/2012	0.09	6.66	0.08	17.1	1	1.2	0.05	24
YPM133	phyllodes	31/03/2012	0.19	5.01	0.15	12.8	1	1.9	0.06	24
YPM134	phyllodes	31/03/2012	0.1	10.04	0.07	18.7	1	2.1	0.06	32
YPM135	phyllodes	31/03/2012	0.14	3.33	0.1	14.1	1	1.3	0.03	22
YPM136	phyllodes	31/03/2012	0.13	3.43	0.04	9.4	1	1.6	0.06	18
YPM137	phyllodes	31/03/2012	0.05	3.64	0.08	7.8	1	2	0.08	23
YPM138	phyllodes	31/03/2012	0.03	4.87	0.13	11.9	1	0.8	0.08	17
YPM139	phyllodes	31/03/2012	0.06	4.11	0.12	9.2	1	1.1	0.06	15
YPM140	phyllodes	31/03/2012	0.06	5.3	0.09	14.2	1	0.5	0.12	22
YPM141	phyllodes	31/03/2012	0.05	5.41	0.09	7.8	1	0.5	0.03	17
YPM142	phyllodes	31/03/2012	0.04	2.88	0.08	10.2	1	0.5	0.02	23
YPM143	phyllodes	31/03/2012	0.05	2.4	0.07	7.2	1	0.4	0.11	21
YPM144	phyllodes	31/03/2012	0.03	2.32	0.06	8.8	1	0.4	0.03	4

*NOTE values below detection have been halved	Fe_pct	As_ppm	U_ppm	Au_ppb	Th_ppm	Sr_ppm	Cd_ppm	Sb_ppm	Bi_ppm	V_ppm	Ca_pct	P_pct
YPM070	0.009	0.1	0.005	0.1	0.01	33.2	0.005	0.01	0.01	1	0.7	0.053
YPM071	0.012	0.05	0.005	0.1	0.01	74.4	0.005	0.01	0.05	1	0.62	0.098
YPM072	0.009	0.05	0.005	0.1	0.005	42.2	0.005	0.01	0.01	1	0.65	0.072
YPM075	0.008	0.05	0.005	0.1	0.005	86.9	0.01	0.01	0.03	1	0.69	0.056
YPM076	0.008	0.05	0.005	0.1	0.005	50.8	0.07	0.01	0.01	1	0.61	0.087
YPM077	0.013	0.2	0.005	0.1	0.02	48.2	0.02	0.01	0.01	1	0.6	0.051
YPM078	0.013	0.05	0.005	0.1	0.02	59	0.05	0.01	0.01	1	0.92	0.095
YPM079	0.013	0.1	0.005	0.1	0.01	64.9	0.02	0.01	0.01	1	0.85	0.065
YPM080	0.009	0.05	0.005	0.4	0.01	59	0.05	0.01	0.01	1	0.73	0.054
YPM081	0.01	0.05	0.005	0.1	0.005	26.1	0.02	0.01	0.01	1	0.68	0.06
YPM082	0.01	0.05	0.005	0.3	0.01	41.3	0.02	0.01	0.01	1	0.73	0.06
YPM083	0.014	0.05	0.005	0.1	0.03	56.7	0.03	0.01	0.01	1	0.77	0.047
YPM084	0.011	0.05	0.005	0.1	0.02	49.3	0.005	0.01	0.01	1	0.56	0.055
YPM085	0.017	0.05	0.005	0.1	0.02	45	0.02	0.01	0.01	1	0.73	0.084
YPM086	0.006	0.1	0.005	0.3	0.005	34	0.005	0.01	0.1	1	0.78	0.068
YPM087	0.01	0.05	0.005	0.1	0.01	23.3	0.06	0.01	0.03	1	0.56	0.071
YPM088	0.01	0.05	0.005	0.1	0.01	21	0.04	0.01	0.01	1	0.52	0.058
YPM089	0.011	0.2	0.005	0.1	0.005	26.2	0.03	0.01	0.01	1	0.61	0.097
YPM090	0.007	0.05	0.005	0.1	0.005	32	0.01	0.01	0.01	1	0.52	0.058
YPM091	0.007	0.05	0.005	0.1	0.005	38.6	0.03	0.01	0.01	1	0.61	0.044
YPM092	0.009	0.1	0.005	0.1	0.005	42.6	0.02	0.01	0.01	1	0.59	0.051
YPM093	0.013	0.05	0.005	0.2	0.02	50.8	0.02	0.01	0.01	1	0.96	0.082
YPM094	0.01	0.05	0.005	0.1	0.005	77.4	0.01	0.01	0.01	1	1.04	0.06
YPM095	0.009	0.05	0.005	0.1	0.01	65	0.005	0.01	0.01	1	0.91	0.09
YPM096	0.011	0.05	0.005	0.1	0.005	64.9	0.005	0.02	0.01	1	0.9	0.086
YPM097	0.007	0.05	0.005	0.1	0.005	78.3	0.005	0.01	0.01	1	0.62	0.052
YPM098	0.008	0.05	0.005	0.4	0.005	50.4	0.01	0.01	0.01	1	0.57	0.052
YPM099	0.01	0.05	0.005	0.1	0.005	50.3	0.05	0.01	0.01	1	0.59	0.086
YPM100	0.01	0.05	0.005	0.2	0.02	26.7	0.04	0.01	0.06	1	0.61	0.101
YPM102	0.017	0.05	0.005	0.9	0.01	87	0.005	0.01	0.01	1	0.61	0.077
YPM103	0.012	0.2	0.005	0.1	0.01	132.5	0.005	0.01	0.01	1	1.02	0.069
YPM104	0.01	0.05	0.005	0.3	0.01	36.7	0.005	0.01	0.01	1	0.75	0.085
YPM105	0.009	0.05	0.005	0.3	0.005	39.9	0.005	0.01	0.01	1	0.47	0.063
YPM106	0.012	0.05	0.005	0.9	0.02	19.5	0.005	0.03	0.01	1	0.67	0.085
YPM107	0.01	0.05	0.005	0.1	0.01	82.1	0.005	0.01	0.08	1	1.13	0.051
YPM108	0.013	0.05	0.005	0.1	0.02	49.2	0.02	0.01	0.03	1	0.59	0.053
YPM109	0.01	0.05	0.005	0.1	0.02	59.9	0.02	0.01	0.01	1	0.85	0.054
YPM110	0.016	0.1	0.005	0.4	0.02	35.5	0.02	0.01	0.01	1	0.67	0.056
YPM111	0.012	0.05	0.005	0.1	0.02	44.9	0.02	0.01	0.01	1	0.79	0.061
YPM112	0.007	0.05	0.005	0.1	0.01	29.7	0.005	0.01	0.01	1	0.58	0.05
YPM113	0.017	0.05	0.03	0.2	0.03	70.9	0.02	0.01	0.01	1	0.74	0.059
YPM114	0.011	0.05	0.005	0.1	0.02	26.8	0.01	0.01	0.01	1	0.54	0.076
YPM115	0.012	0.05	0.005	0.3	0.02	44.2	0.04	0.01	0.01	1	0.82	0.055
YPM116	0.008	0.05	0.005	0.3	0.005	71.4	0.005	0.01	0.01	1	0.69	0.066
YPM117	0.009	0.05	0.005	0.1	0.01	87.5	0.005	0.01	0.01	1	0.76	0.087
YPM118	0.011	0.05	0.01	0.4	0.01	47.5	0.02	0.01	0.01	1	0.72	0.064
YPM119	0.007	0.05	0.005	0.1	0.005	58.5	0.005	0.01	0.01	1	0.51	0.069
YPM120	0.008	0.05	0.005	0.4	0.01	40.4	0.005	0.01	0.01	1	0.47	0.07
YPM121	0.009	0.05	0.005	0.2	0.005	55.6	0.005	0.01	0.01	1	0.75	0.07
YPM122	0.009	0.05	0.005	0.4	0.005	86.9	0.005	0.01	0.01	1	0.9	0.093
YPM123	0.01	0.3	0.005	0.1	0.01	60.9	0.005	0.01	0.01	1	0.72	0.054
YPM124	0.014	0.05	0.005	0.1	0.005	43.5	0.01	0.01	0.01	1	1.1	0.061
YPM125	0.008	0.05	0.005	0.2	0.005	23.4	0.005	0.01	0.01	1	0.41	0.081
YPM126	0.016	0.05	0.03	0.1	0.03	72.5	0.02	0.01	0.01	1	0.83	0.061
YPM127	0.009	0.05	0.005	0.5	0.01	63	0.005	0.01	0.01	1	0.74	0.055
YPM128	0.007	0.05	0.005	0.1	0.005	34.4	0.005	0.01	0.01	1	0.52	0.059
YPM129	0.013	0.05	0.005	0.3	0.02	60.2	0.005	0.01	0.01	1	1.19	0.091
YPM130	0.017	0.05	0.01	0.4	0.03	47	0.005	0.01	0.01	1	0.54	0.066
YPM131	0.013	0.05	0.005	0.5	0.02	55.9	0.04	0.01	0.01	1	0.66	0.068
YPM132	0.01	0.05	0.005	0.4	0.005	85.7	0.005	0.01	0.01	1	0.63	0.075
YPM133	0.012	0.05	0.005	0.3	0.02	37.6	0.03	0.01	0.01	1	0.6	0.082
YPM134	0.015	0.05	0.005	0.3	0.02	57.4	0.005	0.01	0.01	1	1.16	0.12
YPM135	0.015	0.05	0.005	0.4	0.02	50.2	0.04	0.01	0.01	1	0.81	0.082
YPM136	0.009	0.05	0.005	0.1	0.005	65.6	0.005	0.01	0.01	1	0.84	0.07
YPM137	0.01	0.05	0.005	0.1	0.01	69.2	0.005	0.01	0.01	1	0.97	0.062
YPM138	0.012	0.05	0.005	0.1	0.01	97.2	0.01	0.01	0.01	1	0.57	0.064
YPM139	0.016	0.05	0.005	0.1	0.03	47.9	0.005	0.01	0.01	1	0.53	0.058
YPM140	0.008	0.05	0.005	0.1	0.005	76.5	0.01	0.01	0.01	1	0.72	0.062
YPM141	0.014	0.1	0.005	0.1	0.02	70.9	0.005	0.01	0.01	1	0.56	0.07
YPM142	0.009	0.05	0.005	0.2	0.01	120.9	0.005	0.01	0.01	1	0.91	0.067
YPM143	0.008	0.05	0.08	0.1	0.005	44.5	0.01	0.01	0.03	1	0.46	0.048
YPM144	0.012	0.05	0.005	0.1	0.01	85.1	0.005	0.01	0.01	1	0.72	0.063

*NOTE values below detection have been halved	La_ppm	Cr_ppm	Mg_pct	Ba_ppm	Ti_ppm	B_ppm	Al_pct	Na_pct	K_pct	W_ppm	Sc_ppm	Tl_ppm
YPM070	0.2	1.7	0.213	1.4	3	62	0.01	0.306	0.47	0.05	0.05	0.01
YPM071	0.06	1	0.211	1.4	6	22	0.01	0.611	0.49	0.05	0.2	0.01
YPM072	0.03	1.1	0.119	2.7	5	45	0.005	0.608	0.53	0.05	0.2	0.01
YPM075	0.03	1	0.183	17	4	29	0.005	0.316	0.45	0.05	0.2	0.01
YPM076	0.04	0.9	0.143	3.7	5	39	0.005	0.304	0.56	0.05	0.3	0.01
YPM077	0.09	1	0.157	3.6	4	34	0.01	0.499	0.46	0.05	0.2	0.01
YPM078	0.05	1.2	0.15	3.1	7	37	0.01	0.358	0.35	0.05	0.3	0.01
YPM079	0.06	1.1	0.207	4.4	5	31	0.01	0.507	0.43	0.05	0.2	0.01
YPM080	0.03	0.9	0.183	7.5	4	20	0.005	0.383	0.56	0.05	0.2	0.01
YPM081	0.04	1.1	0.132	3.7	4	20	0.005	0.347	0.49	0.05	0.2	0.01
YPM082	0.03	1	0.174	2.2	4	20	0.005	0.492	0.45	0.05	0.3	0.01
YPM083	0.13	1.1	0.156	5	4	36	0.005	0.249	0.39	0.05	0.3	0.01
YPM084	0.13	1	0.167	4	4	39	0.01	0.341	0.54	0.05	0.3	0.01
YPM085	0.06	1.2	0.118	4.8	7	39	0.02	0.469	0.57	0.05	0.3	0.01
YPM086	0.02	1.1	0.178	4.8	4	22	0.005	0.331	0.5	0.05	0.2	0.01
YPM087	0.05	1	0.148	2.4	5	23	0.005	0.443	0.51	0.05	0.2	0.01
YPM088	0.05	1	0.123	3.1	4	35	0.005	0.432	0.46	0.05	0.3	0.01
YPM089	0.05	1	0.138	3.9	6	18	0.005	0.279	0.55	0.05	0.2	0.01
YPM090	0.03	0.9	0.125	2.1	4	17	0.005	0.37	0.58	0.05	0.2	0.01
YPM091	0.05	1	0.141	2.8	3	30	0.005	0.337	0.53	0.05	0.2	0.01
YPM092	0.04	0.9	0.146	3.2	4	22	0.005	0.385	0.45	0.05	0.2	0.01
YPM093	0.06	1.1	0.154	4.9	6	22	0.01	0.287	0.46	0.05	0.3	0.01
YPM094	0.03	1	0.175	3.7	4	21	0.005	0.407	0.48	0.05	0.2	0.01
YPM095	0.04	0.8	0.196	2.2	6	32	0.005	0.589	0.4	0.05	0.3	0.01
YPM096	0.03	0.9	0.193	3.2	6	29	0.005	0.551	0.56	0.05	0.1	0.01
YPM097	0.02	1	0.143	1.3	4	24	0.005	0.451	0.45	0.05	0.3	0.01
YPM098	0.03	1	0.2	1	4	26	0.005	0.488	0.71	0.05	0.2	0.01
YPM099	0.05	1	0.144	3.5	6	35	0.005	0.307	0.55	0.05	0.3	0.01
YPM100	0.05	1	0.142	4	6	19	0.005	0.29	0.56	0.05	0.3	0.01
YPM102	0.03	1.1	0.194	3.8	5	85	0.005	0.583	0.42	0.05	0.2	0.01
YPM103	0.03	1	0.185	7.2	5	75	0.005	0.435	0.45	0.05	0.2	0.01
YPM104	0.03	1	0.166	3.3	5	33	0.005	0.515	0.56	0.05	0.2	0.01
YPM105	0.03	0.05	0.184	2.7	4	11	0.005	0.287	0.6	0.05	0.3	0.01
YPM106	0.07	1.9	0.112	2.6	5	35	0.02	0.63	0.74	0.05	0.05	0.01
YPM107	0.05	1	0.203	5.2	4	33	0.005	0.433	0.36	0.05	0.2	0.01
YPM108	0.07	1.2	0.134	4.6	4	24	0.01	0.406	0.42	0.05	0.3	0.01
YPM109	0.04	1.2	0.105	3.8	4	21	0.005	0.518	0.44	0.05	0.2	0.01
YPM110	0.08	1.1	0.137	3.6	5	32	0.02	0.5	0.46	0.05	0.3	0.01
YPM111	0.05	1.3	0.146	6.6	5	25	0.01	0.364	0.47	0.05	0.2	0.01
YPM112	0.03	1.1	0.119	5.5	4	28	0.005	0.431	0.5	0.05	0.2	0.01
YPM113	0.15	1.1	0.21	7.6	5	43	0.02	0.521	0.47	0.05	0.3	0.01
YPM114	0.05	1.2	0.131	2.2	5	40	0.005	0.461	0.6	0.05	0.4	0.01
YPM115	0.09	1.1	0.149	4.6	4	33	0.01	0.443	0.53	0.05	0.3	0.01
YPM116	0.03	1.1	0.164	3.2	4	21	0.005	0.599	0.43	0.05	0.2	0.01
YPM117	0.05	1	0.146	5.2	6	23	0.005	0.618	0.51	0.05	0.2	0.01
YPM118	0.04	1.2	0.145	3.9	5	41	0.005	0.413	0.45	0.05	0.2	0.01
YPM119	0.03	1	0.188	2.7	5	25	0.005	0.678	0.42	0.05	0.2	0.01
YPM120	0.04	1.1	0.159	3.2	5	51	0.005	0.421	0.35	0.05	0.2	0.01
YPM121	0.03	1.1	0.16	5.1	5	32	0.005	0.431	0.49	0.05	0.2	0.01
YPM122	0.03	1	0.221	3.3	6	44	0.005	0.761	0.4	0.05	0.2	0.01
YPM123	0.04	1	0.184	2.8	4	47	0.005	0.494	0.35	0.05	0.3	0.01
YPM124	0.05	1.1	0.243	4.6	5	68	0.01	0.432	0.57	0.05	0.2	0.01
YPM125	0.03	1.1	0.148	1.1	5	40	0.005	0.614	0.46	0.05	0.2	0.01
YPM126	0.13	1.2	0.216	8.2	5	41	0.02	0.531	0.46	0.05	0.2	0.01
YPM127	0.04	1.1	0.183	2.8	4	49	0.005	0.457	0.35	0.05	0.3	0.01
YPM128	0.02	1.1	0.138	1.7	4	23	0.005	0.675	0.48	0.05	0.2	0.01
YPM129	0.05	1	0.203	4.2	6	64	0.01	0.719	0.54	0.05	0.3	0.01
YPM130	0.08	1.3	0.141	3.4	5	53	0.02	0.481	0.54	0.05	0.3	0.01
YPM131	0.07	1.2	0.147	5.7	5	28	0.01	0.37	0.53	0.05	0.4	0.01
YPM132	0.06	1.1	0.224	4.5	5	25	0.005	0.989	0.48	0.05	0.3	0.01
YPM133	0.06	1	0.125	3.6	6	21	0.01	0.612	0.49	0.05	0.2	0.01
YPM134	0.07	1.2	0.196	3.9	8	48	0.005	0.561	0.53	0.05	0.3	0.01
YPM135	0.07	1	0.147	9.3	6	30	0.01	0.493	0.64	0.05	0.3	0.01
YPM136	0.1	1	0.141	4.6	4	21	0.005	0.381	0.61	0.05	0.2	0.01
YPM137	0.14	1.1	0.167	6	4	24	0.005	0.413	0.56	0.05	0.3	0.01
YPM138	0.18	1.2	0.132	2.6	5	41	0.01	0.424	0.61	0.05	0.3	0.01
YPM139	0.09	1.2	0.135	2.4	5	24	0.02	0.693	0.58	0.05	0.5	0.01
YPM140	0.04	1	0.169	4.1	4	18	0.005	0.49	0.54	0.05	0.1	0.01
YPM141	0.23	0.7	0.176	2.9	5	20	0.01	0.649	0.61	0.05	0.3	0.01
YPM142	0.05	1.8	0.192	2.9	4	28	0.005	0.581	0.52	0.05	0.05	0.01
YPM143	0.12	1.1	0.143	2.1	4	27	0.005	0.459	0.57	0.05	0.3	0.01
YPM144	0.04	1.2	0.146	5.5	5	39	0.005	0.433	0.58	0.05	0.2	0.01

*NOTE values below detection have been halved	S_pct	Hg_ppb	Se_ppm	Te_ppm	Ga_ppm	Cs_ppm	Ge_ppm	Hf_ppm	Nb_ppm	Rb_ppm	Sn_ppm	Ta_ppm
YPM070	0.11	25	0.2	0.01	0.05	0.007	0.005	0.003	0.005	0.4	0.02	0.0005
YPM071	0.09	5	0.3	0.01	0.05	0.01	0.03	0.004	0.005	1.3	0.02	0.0005
YPM072	0.09	10	0.4	0.01	0.05	0.0025	0.02	0.006	0.005	0.6	0.01	0.0005
YPM075	0.06	13	0.3	0.01	0.05	0.0025	0.01	0.002	0.005	0.5	0.01	0.0005
YPM076	0.05	15	0.1	0.01	0.05	0.008	0.02	0.0005	0.005	0.8	0.01	0.0005
YPM077	0.05	8	0.2	0.01	0.05	0.008	0.02	0.002	0.005	0.8	0.01	0.0005
YPM078	0.06	20	0.3	0.01	0.05	0.009	0.005	0.003	0.005	1	0.01	0.0005
YPM079	0.04	12	0.2	0.01	0.05	0.007	0.005	0.001	0.005	0.5	0.01	0.0005
YPM080	0.05	9	0.1	0.01	0.05	0.009	0.03	0.0005	0.005	1.2	0.01	0.0005
YPM081	0.05	11	0.2	0.01	0.05	0.006	0.01	0.003	0.005	1.4	0.01	0.0005
YPM082	0.05	9	0.2	0.01	0.05	0.005	0.01	0.005	0.005	1.1	0.01	0.0005
YPM083	0.04	7	0.05	0.01	0.05	0.006	0.005	0.004	0.005	0.6	0.01	0.0005
YPM084	0.06	10	0.2	0.03	0.05	0.006	0.005	0.001	0.005	0.9	0.01	0.0005
YPM085	0.06	20	0.2	0.01	0.05	0.012	0.01	0.002	0.005	0.6	0.01	0.0005
YPM086	0.04	8	0.2	0.01	0.05	0.0025	0.005	0.001	0.005	1.1	0.01	0.0005
YPM087	0.05	7	0.3	0.01	0.05	0.007	0.005	0.002	0.005	0.6	0.01	0.0005
YPM088	0.03	15	0.2	0.01	0.05	0.0025	0.02	0.0005	0.005	0.5	0.01	0.0005
YPM089	0.06	7	0.2	0.01	0.05	0.006	0.005	0.005	0.005	0.8	0.01	0.0005
YPM090	0.04	10	0.2	0.01	0.05	0.0025	0.02	0.005	0.005	0.8	0.01	0.0005
YPM091	0.01	7	0.2	0.01	0.05	0.0025	0.02	0.003	0.005	0.7	0.01	0.0005
YPM092	0.03	10	0.4	0.01	0.05	0.006	0.03	0.0005	0.005	0.5	0.01	0.0005
YPM093	0.06	18	0.2	0.01	0.05	0.007	0.01	0.004	0.005	0.7	0.01	0.0005
YPM094	0.05	8	0.4	0.01	0.05	0.006	0.02	0.005	0.005	1.3	0.01	0.0005
YPM095	0.08	14	0.4	0.01	0.05	0.005	0.005	0.003	0.005	0.5	0.01	0.0005
YPM096	0.08	8	0.4	0.01	0.05	0.006	0.005	0.003	0.005	1	0.01	0.0005
YPM097	0.06	9	0.2	0.01	0.05	0.0025	0.005	0.0005	0.005	0.7	0.01	0.0005
YPM098	0.06	9	0.3	0.01	0.05	0.0025	0.02	0.0005	0.005	0.8	0.01	0.0005
YPM099	0.05	16	0.1	0.01	0.05	0.008	0.03	0.002	0.005	0.8	0.01	0.0005
YPM100	0.09	11	0.2	0.01	0.05	0.006	0.005	0.003	0.005	0.9	0.01	0.0005
YPM102	0.08	17	0.7	0.01	0.05	0.006	0.03	0.0005	0.005	0.5	0.01	0.0005
YPM103	0.08	16	0.8	0.01	0.05	0.007	0.005	0.002	0.005	0.4	0.01	0.0005
YPM104	0.1	8	0.2	0.01	0.05	0.008	0.005	0.001	0.005	1.1	0.01	0.0005
YPM105	0.05	7	0.3	0.01	0.05	0.007	0.05	0.003	0.005	1.2	0.01	0.0005
YPM106	0.12	7	0.5	0.01	0.05	0.012	0.005	0.004	0.005	1.9	0.03	0.0005
YPM107	0.08	20	0.2	0.01	0.05	0.008	0.005	0.003	0.005	0.7	0.06	0.0005
YPM108	0.09	14	0.4	0.01	0.05	0.012	0.005	0.006	0.005	0.9	0.05	0.0005
YPM109	0.07	8	0.3	0.01	0.05	0.007	0.005	0.002	0.005	0.8	0.01	0.0005
YPM110	0.08	11	0.3	0.01	0.05	0.013	0.005	0.004	0.005	1.5	0.02	0.0005
YPM111	0.08	6	0.3	0.01	0.05	0.009	0.02	0.002	0.005	1.5	0.01	0.0005
YPM112	0.07	9	0.3	0.01	0.05	0.005	0.005	0.0005	0.005	2.2	0.03	0.0005
YPM113	0.08	13	0.2	0.01	0.05	0.017	0.005	0.002	0.005	0.9	0.01	0.0005
YPM114	0.1	13	0.5	0.01	0.05	0.007	0.005	0.004	0.005	0.8	0.01	0.0005
YPM115	0.1	13	0.2	0.01	0.05	0.01	0.005	0.004	0.005	1.4	0.01	0.001
YPM116	0.08	6	0.3	0.02	0.05	0.0025	0.01	0.003	0.005	0.7	0.01	0.0005
YPM117	0.1	8	0.2	0.01	0.05	0.006	0.005	0.002	0.005	1.3	0.01	0.0005
YPM118	0.09	21	0.2	0.01	0.05	0.008	0.005	0.003	0.005	0.8	0.01	0.0005
YPM119	0.09	10	0.2	0.01	0.05	0.0025	0.005	0.0005	0.005	1	0.01	0.0005
YPM120	0.05	6	0.4	0.01	0.05	0.006	0.02	0.002	0.005	0.8	0.01	0.0005
YPM121	0.09	12	0.2	0.01	0.05	0.006	0.005	0.0005	0.005	0.7	0.01	0.0005
YPM122	0.1	13	0.5	0.01	0.05	0.0025	0.005	0.0005	0.005	0.5	0.01	0.0005
YPM123	0.07	27	0.6	0.01	0.05	0.005	0.005	0.0005	0.005	0.3	0.01	0.0005
YPM124	0.12	21	0.6	0.01	0.05	0.007	0.005	0.0005	0.005	0.6	0.01	0.0005
YPM125	0.11	7	0.2	0.01	0.05	0.0025	0.01	0.0005	0.005	0.7	0.01	0.0005
YPM126	0.08	17	0.3	0.01	0.05	0.017	0.005	0.007	0.005	0.9	0.01	0.0005
YPM127	0.08	27	0.6	0.01	0.05	0.006	0.005	0.002	0.005	0.3	0.01	0.0005
YPM128	0.08	3	0.3	0.01	0.05	0.0025	0.005	0.002	0.005	0.9	0.01	0.0005
YPM129	0.1	9	0.5	0.01	0.05	0.008	0.005	0.005	0.005	0.9	0.01	0.0005
YPM130	0.09	11	0.3	0.02	0.05	0.012	0.005	0.003	0.005	0.6	0.01	0.0005
YPM131	0.07	11	0.3	0.01	0.05	0.011	0.02	0.003	0.005	1.3	0.01	0.0005
YPM132	0.08	12	0.3	0.01	0.05	0.006	0.005	0.003	0.005	1.1	0.01	0.0005
YPM133	0.09	12	0.3	0.01	0.05	0.009	0.005	0.002	0.005	1.1	0.01	0.0005
YPM134	0.12	12	0.6	0.01	0.05	0.008	0.01	0.0005	0.005	1.4	0.01	0.0005
YPM135	0.08	11	0.3	0.01	0.05	0.009	0.005	0.002	0.005	1.3	0.01	0.001
YPM136	0.06	11	0.2	0.01	0.05	0.0025	0.005	0.0005	0.005	1.6	0.01	0.0005
YPM137	0.06	9	0.5	0.01	0.05	0.007	0.005	0.003	0.005	1.3	0.01	0.0005
YPM138	0.07	12	0.2	0.01	0.05	0.008	0.005	0.002	0.005	1.2	0.01	0.001
YPM139	0.06	6	0.4	0.01	0.05	0.013	0.02	0.005	0.005	1.5	0.01	0.0005
YPM140	0.08	6	0.1	0.01	0.05	0.0025	0.005	0.002	0.005	1.4	0.01	0.0005
YPM141	0.07	4	0.3	0.01	0.05	0.017	0.02	0.004	0.005	1.8	0.01	0.0005
YPM142	0.12	11	0.2	0.01	0.05	0.011	0.005	0.002	0.005	1.5	0.03	0.0005
YPM143	0.05	13	0.05	0.01	0.05	0.008	0.005	0.001	0.005	1.6	0.04	0.0005
YPM144	0.08	7	0.2	0.01	0.05	0.009	0.005	0.004	0.005	0.8	0.02	0.0005

*NOTE values below detection have been halved	Zr_ppm	Y_ppm	Ce_ppm	In_ppm	Re_ppb	Be_ppm	Li_ppm	Pd_ppb	Pt_ppb
YPM070	0.08	0.152	0.62	0.01	2	0.05	1.79	1	0.5
YPM071	0.07	0.052	0.12	0.01	0.5	0.05	1.41	1	0.5
YPM072	0.05	0.032	0.1	0.01	0.5	0.05	1.11	1	0.5
YPM075	0.05	0.027	0.06	0.01	0.5	0.05	0.18	1	0.5
YPM076	0.05	0.037	0.1	0.01	0.5	0.05	0.37	1	0.5
YPM077	0.06	0.079	0.17	0.01	0.5	0.05	0.47	1	0.5
YPM078	0.07	0.034	0.1	0.01	0.5	0.05	0.15	1	0.5
YPM079	0.07	0.043	0.12	0.01	0.5	0.05	0.34	1	0.5
YPM080	0.05	0.024	0.07	0.01	0.5	0.05	0.13	1	0.5
YPM081	0.05	0.056	0.09	0.01	0.5	0.05	0.13	1	0.5
YPM082	0.05	0.027	0.09	0.01	0.5	0.05	0.65	1	0.5
YPM083	0.08	0.111	0.29	0.01	0.5	0.05	0.22	1	0.5
YPM084	0.09	0.095	0.35	0.01	0.5	0.05	0.61	1	0.5
YPM085	0.09	0.061	0.17	0.01	0.5	0.05	0.55	1	0.5
YPM086	0.04	0.025	0.05	0.01	0.5	0.05	0.37	1	0.5
YPM087	0.08	0.034	0.12	0.01	0.5	0.05	0.22	1	0.5
YPM088	0.07	0.034	0.09	0.01	0.5	0.05	0.47	1	0.5
YPM089	0.05	0.028	0.1	0.01	0.5	0.05	0.21	1	0.5
YPM090	0.03	0.02	0.06	0.01	0.5	0.05	0.43	1	0.5
YPM091	0.03	0.027	0.11	0.01	0.5	0.05	0.33	1	0.5
YPM092	0.07	0.024	0.1	0.01	0.5	0.05	0.33	1	0.5
YPM093	0.08	0.052	0.14	0.01	0.5	0.05	0.46	1	0.5
YPM094	0.03	0.018	0.07	0.01	0.5	0.05	0.52	1	0.5
YPM095	0.05	0.021	0.09	0.01	0.5	0.05	1.21	1	0.5
YPM096	0.05	0.026	0.08	0.01	0.5	0.05	0.81	1	0.5
YPM097	0.04	0.012	0.07	0.01	0.5	0.05	0.94	1	0.5
YPM098	0.04	0.017	0.06	0.01	0.5	0.05	1.19	1	0.5
YPM099	0.04	0.029	0.1	0.01	1	0.05	0.35	1	0.5
YPM100	0.05	0.035	0.1	0.01	0.5	0.05	0.18	1	0.5
YPM102	0.06	0.021	0.1	0.01	0.5	0.05	1.49	1	0.5
YPM103	0.06	0.032	0.09	0.01	0.5	0.05	1.88	1	0.5
YPM104	0.04	0.028	0.1	0.01	0.5	0.05	0.29	1	0.5
YPM105	0.06	0.024	0.07	0.01	0.5	0.05	0.32	1	0.5
YPM106	0.08	0.052	0.14	0.01	0.5	0.05	0.26	1	0.5
YPM107	0.06	0.025	0.1	0.01	0.5	0.05	1.18	1	0.5
YPM108	0.08	0.049	0.19	0.01	0.5	0.05	0.16	1	0.5
YPM109	0.06	0.021	0.09	0.01	0.5	0.05	0.12	1	0.5
YPM110	0.13	0.062	0.18	0.01	1	0.05	0.12	1	0.5
YPM111	0.09	0.04	0.1	0.01	0.5	0.05	0.13	1	0.5
YPM112	0.06	0.018	0.06	0.01	0.5	0.05	0.07	1	0.5
YPM113	0.12	0.096	0.36	0.01	0.5	0.05	0.96	1	0.5
YPM114	0.06	0.032	0.12	0.01	0.5	0.05	0.27	1	0.5
YPM115	0.12	0.05	0.22	0.01	0.5	0.05	0.3	1	0.5
YPM116	0.05	0.02	0.07	0.01	0.5	0.05	0.39	1	0.5
YPM117	0.05	0.022	0.1	0.01	0.5	0.05	0.72	1	0.5
YPM118	0.08	0.033	0.13	0.01	0.5	0.05	0.7	1	0.5
YPM119	0.04	0.015	0.07	0.01	0.5	0.05	0.41	1	0.5
YPM120	0.05	0.023	0.07	0.01	0.5	0.05	1.14	1	0.5
YPM121	0.06	0.018	0.09	0.01	0.5	0.05	1.54	1	0.5
YPM122	0.05	0.017	0.06	0.01	0.5	0.05	1.88	1	0.5
YPM123	0.07	0.032	0.1	0.01	0.5	0.05	1.9	1	0.5
YPM124	0.06	0.031	0.12	0.01	0.5	0.05	2.29	1	0.5
YPM125	0.04	0.016	0.08	0.01	0.5	0.05	1.08	1	0.5
YPM126	0.13	0.076	0.34	0.01	0.5	0.05	0.73	1	0.5
YPM127	0.06	0.026	0.09	0.01	0.5	0.05	1.9	1	0.5
YPM128	0.03	0.018	0.05	0.01	0.5	0.05	0.54	1	0.5
YPM129	0.09	0.036	0.13	0.01	0.5	0.05	1.83	1	0.5
YPM130	0.12	0.067	0.19	0.01	0.5	0.05	0.43	1	0.5
YPM131	0.08	0.046	0.19	0.01	0.5	0.05	0.42	1	0.5
YPM132	0.04	0.036	0.12	0.01	0.5	0.05	1.86	1	0.5
YPM133	0.08	0.043	0.14	0.01	0.5	0.05	0.66	1	0.5
YPM134	0.04	0.036	0.15	0.01	0.5	0.05	0.46	1	0.5
YPM135	0.1	0.052	0.17	0.01	0.5	0.05	0.48	1	0.5
YPM136	0.04	0.062	0.21	0.01	0.5	0.05	0.49	1	0.5
YPM137	0.05	0.076	0.26	0.01	0.5	0.05	0.51	1	0.5
YPM138	0.07	0.095	0.43	0.01	0.5	0.05	1.66	1	0.5
YPM139	0.1	0.061	0.24	0.01	0.5	0.05	0.47	1	0.5
YPM140	0.05	0.021	0.09	0.01	0.5	0.05	0.87	1	0.5
YPM141	0.07	0.037	0.41	0.01	0.5	0.05	0.48	1	0.5
YPM142	0.07	0.023	0.09	0.01	0.5	0.05	0.34	1	0.5
YPM143	0.04	0.109	0.26	0.01	0.5	0.05	0.93	1	0.5
YPM144	0.06	0.029	0.1	0.01	0.5	0.05	0.48	1	0.5

	*NOTE values below detection have been halved	Duplicate ID	Sample_Type	Transect	Location	Orig_Grid_ID	Orig_East	Orig_North	GA_RL
Yorke Peninsula	YPM145		VEG	6	Cane Rd	GDA94_53H	766193	6192915	86
Yorke Peninsula	YPM146	YPM130	VEG	6	Moody Rd	GDA94_53H	740760	6192582	129
Yorke Peninsula	YPM147	YPM137	VEG	6	Johnson Rd	GDA94_53H	757887	6193648	131
Yorke Peninsula	YPM148		VEG	7	Coleman Rd	GDA94_53H	776309	6208641	18
Yorke Peninsula	YPM149		VEG	7	Coleman Rd	GDA94_53H	775125	6208523	81
Yorke Peninsula	YPM150		VEG	7	Coleman Rd	GDA94_53H	774210	6208448	95
Yorke Peninsula	YPM151		VEG	7	Coleman Rd	GDA94_53H	772954	6208344	108
Yorke Peninsula	YPM152		VEG	7	Coleman Rd	GDA94_53H	771811	6208248	116
Yorke Peninsula	YPM153		VEG	7	Coleman Rd	GDA94_53H	770531	6208150	118
Yorke Peninsula	YPM154		VEG	7	Coleman Rd	GDA94_53H	767453	6208088	118
Yorke Peninsula	YPM155	YPM175	VEG	7	Coleman Rd	GDA94_53H	765913	6208598	138
Yorke Peninsula	YPM156		VEG	7	Coleman Rd	GDA94_53H	764683	6208680	161
Yorke Peninsula	YPM157		VEG	7	Honner Rd	GDA94_53H	762125	6208529	160
Yorke Peninsula	YPM158		VEG	7	Honner Rd	GDA94_53H	760289	6208345	172
Yorke Peninsula	YPM159		VEG	7	Honner Rd	GDA94_53H	758942	6208208	175
Yorke Peninsula	YPM160		VEG	7	Honner Rd	GDA94_53H	757727	6208082	179
Yorke Peninsula	YPM161		VEG	7	Pipeline Rd	GDA94_53H	755400	6208103	203
Yorke Peninsula	YPM162		VEG	7	Pipeline Rd	GDA94_53H	753977	6208144	173
Yorke Peninsula	YPM163		VEG	7	Pipeline Rd	GDA94_53H	752680	6208181	164
Yorke Peninsula	YPM164		VEG	7	Pipeline Rd	GDA94_53H	751022	6208414	136
Yorke Peninsula	YPM165		VEG	7	Pipeline Rd	GDA94_53H	748470	6209278	104
Yorke Peninsula	YPM166		VEG	7	Pipeline Rd	GDA94_53H	747025	6209694	127
Yorke Peninsula	YPM167		VEG	7	Pipeline Rd	GDA94_53H	744901	6210312	130
Yorke Peninsula	YPM168		VEG	7	Ferguson Rd	GDA94_53H	743145	6210359	120
Yorke Peninsula	YPM169	YPM176	VEG	7	Ferguson Rd	GDA94_53H	741997	6210389	103
Yorke Peninsula	YPM170		VEG	7	Ferguson Rd	GDA94_53H	740024	6211086	75
Yorke Peninsula	YPM171		VEG	7	Ferguson Rd	GDA94_53H	738921	6211577	64
Yorke Peninsula	YPM172		VEG	7	Ferguson Rd	GDA94_53H	737674	6212139	51
Yorke Peninsula	YPM173		VEG	7	Ferguson Rd	GDA94_53H	735704	6212860	31
Yorke Peninsula	YPM174		VEG	7	Tipara Springs Rd	GDA94_53H	733578	6213340	22
Yorke Peninsula	YPM175	YPM155	VEG	7	Coleman Rd	GDA94_53H	765913	6208598	138
Yorke Peninsula	YPM176	YPM169	VEG	7	Ferguson Rd	GDA94_53H	741997	6210389	103
Yorke Peninsula	YPM178	YPM198	VEG	8	Kulpara Maitland Rd	GDA94_53H	775130	6223525	107
Yorke Peninsula	YPM179		VEG	8	Kulpara Maitland Rd	GDA94_53H	773708	6223564	104
Yorke Peninsula	YPM180		VEG	8	Kulpara Maitland Rd	GDA94_53H	772589	6223597	108
Yorke Peninsula	YPM181		VEG	8	Holman Rd	GDA94_53H	769068	6223705	146
Yorke Peninsula	YPM182		VEG	8	Holman Rd	GDA94_53H	767779	6223743	141
Yorke Peninsula	YPM183		VEG	8	Holman Rd	GDA94_53H	766173	6223795	131
Yorke Peninsula	YPM184		VEG	8	Holman Rd	GDA94_53H	764731	6223819	123
Yorke Peninsula	YPM185		VEG	8	Holman Rd	GDA94_53H	763352	6223810	117
Yorke Peninsula	YPM186		VEG	8	Holman Rd	GDA94_53H	761879	6223795	114
Yorke Peninsula	YPM187		VEG	8	Holman Rd	GDA94_53H	760637	6223789	114
Yorke Peninsula	YPM188		VEG	8	Peddlar Rd	GDA94_53H	759588	6223784	113
Yorke Peninsula	YPM189		VEG	8	Peddlar Rd	GDA94_53H	758320	6223769	99
Yorke Peninsula	YPM190		VEG	8	Peddlar Rd	GDA94_53H	757175	6223759	95
Yorke Peninsula	YPM191		VEG	8	Peddlar Rd	GDA94_53H	755954	6223748	86
Yorke Peninsula	YPM193	YPM199	VEG	8	Peddlar Rd	GDA94_53H	751066	6223704	90
Yorke Peninsula	YPM194		VEG	8	Peddlar Rd	GDA94_53H	750027	6223743	98
Yorke Peninsula	YPM195		VEG	8	Peddlar Rd	GDA94_53H	748556	6223789	81
Yorke Peninsula	YPM196		VEG	8	Peddlar Rd	GDA94_53H	746972	6223828	77
Yorke Peninsula	YPM197		VEG	8	Peddlar Rd	GDA94_53H	744033	6223914	46
Yorke Peninsula	YPM198	YPM178	VEG	8	Kulpara Maitland Rd	GDA94_53H	775130	6223525	107
Yorke Peninsula	YPM199	YPM193	VEG	8	Peddlar Rd	GDA94_53H	751066	6223704	90
Yorke Peninsula	YPM200		VEG	9	Bird Island Rd	GDA94_53H	738732	6237803	8
Yorke Peninsula	YPM201		VEG	9	Shooting Club Rd	GDA94_53H	741984	6237720	20
Yorke Peninsula	YPM202		VEG	9	Shooting Club Rd	GDA94_53H	743291	6237689	27
Yorke Peninsula	YPM203		VEG	9	Shooting Club Rd	GDA94_53H	744433	6237660	29
Yorke Peninsula	YPM204		VEG	9	Shooting Club Rd	GDA94_53H	745843	6237627	37
Yorke Peninsula	YPM205		VEG	9	Thomas Plains Rd	GDA94_53H	753190	6238307	41
Yorke Peninsula	YPM206	YPM220	VEG	9	Thomas Plains Rd	GDA94_53H	755470	6238245	41
Yorke Peninsula	YPM207		VEG	9	Thomas Plains Rd	GDA94_53H	756785	6238207	44
Yorke Peninsula	YPM208	YPM221	VEG	9	Thomas Plains Rd	GDA94_53H	760136	6238121	49
Yorke Peninsula	YPM209		VEG	9	Thomas Plains Rd	GDA94_53H	761372	6238085	55
Yorke Peninsula	YPM210		VEG	9	Thomas Plains Rd	GDA94_53H	762445	6238059	61
Yorke Peninsula	YPM211		VEG	9	Thomas Plains Rd	GDA94_53H	763543	6238031	69
Yorke Peninsula	YPM212		VEG	9	Thomas Plains Rd	GDA94_53H	764784	6237995	76
Yorke Peninsula	YPM213		VEG	9	Thomas Plains Rd	GDA94_53H	766548	6237945	89
Yorke Peninsula	YPM214		VEG	9	Thomas Plains Rd	GDA94_53H	768175	6237903	99
Yorke Peninsula	YPM215		VEG	9	Sand Pit Rd	GDA94_53H	770894	6231581	104
Yorke Peninsula	YPM216		VEG	9	Sand Pit Rd	GDA94_53H	771966	6231507	109
Yorke Peninsula	YPM217		VEG	9	Sand Pit Rd	GDA94_53H	773232	6231400	115
Yorke Peninsula	YPM218		VEG	9	Sand Pit Rd	GDA94_53H	774288	6231316	119

*NOTE values below detection have been halved	Orig_Survey_Method	Orig_Survey_By	Orig_Survey_Date	Sampled_By	Treatment	Species
YPM145	Garmin GPS Map62S	KWolff	31/03/2012	KWolff	dried for 48hrs at 60'C	E. gracilis
YPM146	Garmin GPS Map62S	KWolff	31/03/2012	KWolff	dried for 48hrs at 60'C	E. socialis
YPM147	Garmin GPS Map62S	KWolff	31/03/2012	KWolff	dried for 48hrs at 60'C	E. phenax
YPM148	Garmin GPS Map62S	KWolff	1/04/2012	KWolff	dried for 48hrs at 60'C	E. leptophylla
YPM149	Garmin GPS Map62S	KWolff	1/04/2012	KWolff	dried for 48hrs at 60'C	E. socialis
YPM150	Garmin GPS Map62S	KWolff	1/04/2012	KWolff	dried for 48hrs at 60'C	E. socialis
YPM151	Garmin GPS Map62S	KWolff	1/04/2012	KWolff	dried for 48hrs at 60'C	E. phenax
YPM152	Garmin GPS Map62S	KWolff	1/04/2012	KWolff	dried for 48hrs at 60'C	E. phenax
YPM153	Garmin GPS Map62S	KWolff	1/04/2012	KWolff	dried for 48hrs at 60'C	E. gracilis
YPM154	Garmin GPS Map62S	KWolff	1/04/2012	KWolff	dried for 48hrs at 60'C	E. gracilis
YPM155	Garmin GPS Map62S	KWolff	1/04/2012	KWolff	dried for 48hrs at 60'C	E. socialis
YPM156	Garmin GPS Map62S	KWolff	1/04/2012	KWolff	dried for 48hrs at 60'C	E. socialis
YPM157	Garmin GPS Map62S	KWolff	1/04/2012	KWolff	dried for 48hrs at 60'C	E. gracilis
YPM158	Garmin GPS Map62S	KWolff	1/04/2012	KWolff	dried for 48hrs at 60'C	E. phenax
YPM159	Garmin GPS Map62S	KWolff	1/04/2012	KWolff	dried for 48hrs at 60'C	E. socialis
YPM160	Garmin GPS Map62S	KWolff	1/04/2012	KWolff	dried for 48hrs at 60'C	E. phenax
YPM161	Garmin GPS Map62S	KWolff	1/04/2012	KWolff	dried for 48hrs at 60'C	E. socialis
YPM162	Garmin GPS Map62S	KWolff	1/04/2012	KWolff	dried for 48hrs at 60'C	E. socialis
YPM163	Garmin GPS Map62S	KWolff	1/04/2012	KWolff	dried for 48hrs at 60'C	E. socialis
YPM164	Garmin GPS Map62S	KWolff	1/04/2012	KWolff	dried for 48hrs at 60'C	E. phenax
YPM165	Garmin GPS Map62S	KWolff	1/04/2012	KWolff	dried for 48hrs at 60'C	E. phenax
YPM166	Garmin GPS Map62S	KWolff	1/04/2012	KWolff	dried for 48hrs at 60'C	E. socialis
YPM167	Garmin GPS Map62S	KWolff	1/04/2012	KWolff	dried for 48hrs at 60'C	E. socialis
YPM168	Garmin GPS Map62S	KWolff	1/04/2012	KWolff	dried for 48hrs at 60'C	E. socialis
YPM169	Garmin GPS Map62S	KWolff	1/04/2012	KWolff	dried for 48hrs at 60'C	E. gracilis
YPM170	Garmin GPS Map62S	KWolff	1/04/2012	KWolff	dried for 48hrs at 60'C	E. gracilis
YPM171	Garmin GPS Map62S	KWolff	1/04/2012	KWolff	dried for 48hrs at 60'C	E. gracilis
YPM172	Garmin GPS Map62S	KWolff	1/04/2012	KWolff	dried for 48hrs at 60'C	E. gracilis
YPM173	Garmin GPS Map62S	KWolff	1/04/2012	KWolff	dried for 48hrs at 60'C	E. gracilis
YPM174	Garmin GPS Map62S	KWolff	1/04/2012	KWolff	dried for 48hrs at 60'C	E. gracilis
YPM175	Garmin GPS Map62S	KWolff	1/04/2012	KWolff	dried for 48hrs at 60'C	E. socialis
YPM176	Garmin GPS Map62S	KWolff	1/04/2012	KWolff	dried for 48hrs at 60'C	E. gracilis
YPM178	Garmin GPS Map62S	KWolff	14/04/2012	KWolff	dried for 48hrs at 60'C	E. phenax
YPM179	Garmin GPS Map62S	KWolff	14/04/2012	KWolff	dried for 48hrs at 60'C	E. socialis
YPM180	Garmin GPS Map62S	KWolff	14/04/2012	KWolff	dried for 48hrs at 60'C	E. leptophylla
YPM181	Garmin GPS Map62S	KWolff	14/04/2012	KWolff	dried for 48hrs at 60'C	E. socialis
YPM182	Garmin GPS Map62S	KWolff	14/04/2012	KWolff	dried for 48hrs at 60'C	E. socialis
YPM183	Garmin GPS Map62S	KWolff	14/04/2012	KWolff	dried for 48hrs at 60'C	E. socialis
YPM184	Garmin GPS Map62S	KWolff	14/04/2012	KWolff	dried for 48hrs at 60'C	E. leptophylla
YPM185	Garmin GPS Map62S	KWolff	14/04/2012	KWolff	dried for 48hrs at 60'C	E. socialis
YPM186	Garmin GPS Map62S	KWolff	14/04/2012	KWolff	dried for 48hrs at 60'C	E. phenax
YPM187	Garmin GPS Map62S	KWolff	14/04/2012	KWolff	dried for 48hrs at 60'C	E. socialis
YPM188	Garmin GPS Map62S	KWolff	14/04/2012	KWolff	dried for 48hrs at 60'C	E. gracilis
YPM189	Garmin GPS Map62S	KWolff	14/04/2012	KWolff	dried for 48hrs at 60'C	E. leptophylla
YPM190	Garmin GPS Map62S	KWolff	14/04/2012	KWolff	dried for 48hrs at 60'C	E. gracilis
YPM191	Garmin GPS Map62S	KWolff	14/04/2012	KWolff	dried for 48hrs at 60'C	E. leptophylla
YPM193	Garmin GPS Map62S	KWolff	14/04/2012	KWolff	dried for 48hrs at 60'C	E. gracilis
YPM194	Garmin GPS Map62S	KWolff	14/04/2012	KWolff	dried for 48hrs at 60'C	E. gracilis
YPM195	Garmin GPS Map62S	KWolff	14/04/2012	KWolff	dried for 48hrs at 60'C	E. leptophylla
YPM196	Garmin GPS Map62S	KWolff	14/04/2012	KWolff	dried for 48hrs at 60'C	E. gracilis
YPM197	Garmin GPS Map62S	KWolff	14/04/2012	KWolff	dried for 48hrs at 60'C	E. socialis
YPM198	Garmin GPS Map62S	KWolff	14/04/2012	KWolff	dried for 48hrs at 60'C	E. phenax
YPM199	Garmin GPS Map62S	KWolff	14/04/2012	KWolff	dried for 48hrs at 60'C	E. gracilis
YPM200	Garmin GPS Map62S	KWolff	14/04/2012	KWolff	dried for 48hrs at 60'C	E. leptophylla
YPM201	Garmin GPS Map62S	KWolff	14/04/2012	KWolff	dried for 48hrs at 60'C	E. leptophylla
YPM202	Garmin GPS Map62S	KWolff	14/04/2012	KWolff	dried for 48hrs at 60'C	E. socialis
YPM203	Garmin GPS Map62S	KWolff	14/04/2012	KWolff	dried for 48hrs at 60'C	E. gracilis
YPM204	Garmin GPS Map62S	KWolff	14/04/2012	KWolff	dried for 48hrs at 60'C	E. leptophylla
YPM205	Garmin GPS Map62S	KWolff	14/04/2012	KWolff	dried for 48hrs at 60'C	E. leptophylla
YPM206	Garmin GPS Map62S	KWolff	14/04/2012	KWolff	dried for 48hrs at 60'C	E. phenax
YPM207	Garmin GPS Map62S	KWolff	15/04/2012	KWolff	dried for 48hrs at 60'C	E. leptophylla
YPM208	Garmin GPS Map62S	KWolff	15/04/2012	KWolff	dried for 48hrs at 60'C	E. gracilis
YPM209	Garmin GPS Map62S	KWolff	15/04/2012	KWolff	dried for 48hrs at 60'C	E. gracilis
YPM210	Garmin GPS Map62S	KWolff	15/04/2012	KWolff	dried for 48hrs at 60'C	E. gracilis
YPM211	Garmin GPS Map62S	KWolff	15/04/2012	KWolff	dried for 48hrs at 60'C	E. gracilis
YPM212	Garmin GPS Map62S	KWolff	15/04/2012	KWolff	dried for 48hrs at 60'C	E. gracilis
YPM213	Garmin GPS Map62S	KWolff	15/04/2012	KWolff	dried for 48hrs at 60'C	E. gracilis
YPM214	Garmin GPS Map62S	KWolff	15/04/2012	KWolff	dried for 48hrs at 60'C	E. socialis
YPM215	Garmin GPS Map62S	KWolff	15/04/2012	KWolff	dried for 48hrs at 60'C	E. socialis
YPM216	Garmin GPS Map62S	KWolff	15/04/2012	KWolff	dried for 48hrs at 60'C	E. gracilis
YPM217	Garmin GPS Map62S	KWolff	15/04/2012	KWolff	dried for 48hrs at 60'C	E. gracilis
YPM218	Garmin GPS Map62S	KWolff	15/04/2012	KWolff	dried for 48hrs at 60'C	E. gracilis

*NOTE values below detection have been halved	Sample_Description	Date_Sampled	Mo_ppm	Cu_ppm	Pb_ppm	Zn_ppm	Ag_ppm	Ni_ppm	Co_ppm	Mn_ppm
YPM145	phyllodes	31/03/2012	0.04	2.4	0.06	9.1	1	0.4	0.03	4
YPM146	phyllodes	31/03/2012	0.17	2.94	0.25	11.7	1	0.7	0.06	13
YPM147	phyllodes	31/03/2012	0.03	3.46	0.05	7.7	1	1.7	0.08	21
YPM148	phyllodes	1/04/2012	0.05	3.76	0.07	8.6	1	0.6	0.08	24
YPM149	phyllodes	1/04/2012	0.06	2.79	0.13	14.4	1	0.6	0.07	5
YPM150	phyllodes	1/04/2012	0.05	4.54	0.14	12.7	1	0.9	0.11	37
YPM151	phyllodes	1/04/2012	0.05	2.51	0.1	6.6	1	0.5	0.05	20
YPM152	phyllodes	1/04/2012	0.05	3.85	0.05	14.1	1	0.4	0.06	6
YPM153	phyllodes	1/04/2012	0.06	2.77	0.07	16.2	1	0.2	0.03	10
YPM154	phyllodes	1/04/2012	0.07	4.83	0.11	9.8	1	0.6	0.16	29
YPM155	phyllodes	1/04/2012	0.07	1.86	0.12	12.3	1	0.6	0.08	20
YPM156	phyllodes	1/04/2012	0.07	2.3	0.08	14.9	1	3.8	0.18	57
YPM157	phyllodes	1/04/2012	0.1	2.59	0.04	7.1	1	0.3	0.04	12
YPM158	phyllodes	1/04/2012	0.05	1.62	0.05	5.4	1	0.7	0.03	11
YPM159	phyllodes	1/04/2012	0.05	6.85	0.05	10.9	1	0.5	0.08	11
YPM160	phyllodes	1/04/2012	0.19	3.19	0.08	9.2	1	0.8	0.05	19
YPM161	phyllodes	1/04/2012	0.18	4.07	0.11	10	1	0.7	0.05	21
YPM162	phyllodes	1/04/2012	0.28	3.05	0.17	17.6	1	1	0.09	24
YPM163	phyllodes	1/04/2012	0.19	4.13	0.11	14.2	1	0.7	0.05	16
YPM164	phyllodes	1/04/2012	0.15	3.52	0.07	8.4	1	0.8	0.06	35
YPM165	phyllodes	1/04/2012	0.09	2.27	0.08	11.2	1	1.4	0.03	24
YPM166	phyllodes	1/04/2012	0.07	2.67	0.11	14	1	0.5	0.05	22
YPM167	phyllodes	1/04/2012	0.03	3.36	0.15	8.8	1	0.5	0.05	7
YPM168	phyllodes	1/04/2012	0.07	3.37	0.1	15.2	1	0.4	0.04	13
YPM169	phyllodes	1/04/2012	0.06	4	0.1	16.9	1	0.5	0.06	25
YPM170	phyllodes	1/04/2012	0.24	7.74	0.14	16.3	1	0.5	0.07	8
YPM171	phyllodes	1/04/2012	0.1	4.15	0.08	22	1	0.7	0.05	55
YPM172	phyllodes	1/04/2012	0.16	4.2	0.09	11.5	1	3.4	0.03	20
YPM173	phyllodes	1/04/2012	0.16	3.54	0.1	11.3	1	0.3	0.03	29
YPM174	phyllodes	1/04/2012	0.04	3.83	0.08	9.7	1	0.4	0.07	43
YPM175	phyllodes	1/04/2012	0.07	1.73	0.13	12.1	1	0.6	0.06	19
YPM176	phyllodes	1/04/2012	0.06	3.66	0.09	13.4	1	0.9	0.07	24
YPM178	phyllodes	14/04/2012	0.12	3.72	0.1	14.6	1	1.4	0.005	64
YPM179	phyllodes	14/04/2012	0.15	3.14	0.25	17.2	1	0.9	0.03	86
YPM180	phyllodes	14/04/2012	0.13	5.3	0.06	15.7	1	1	0.05	44
YPM181	phyllodes	14/04/2012	0.05	3.55	0.47	22.6	1	2.4	0.06	59
YPM182	phyllodes	14/04/2012	0.05	3.44	0.24	13	1	1	0.07	96
YPM183	phyllodes	14/04/2012	0.16	3.18	0.1	12.6	1	0.4	0.05	16
YPM184	phyllodes	14/04/2012	0.06	5.89	0.04	15.7	1	0.6	0.03	17
YPM185	phyllodes	14/04/2012	0.06	3.44	0.15	13.6	1	1.4	0.12	34
YPM186	phyllodes	14/04/2012	0.03	3.41	0.08	8.7	1	0.8	0.02	25
YPM187	phyllodes	14/04/2012	0.04	2.19	0.16	7	1	0.4	0.05	61
YPM188	phyllodes	14/04/2012	0.05	3.71	0.13	12.1	1	0.3	0.03	19
YPM189	phyllodes	14/04/2012	0.21	3.76	0.14	15.2	1	0.3	0.04	54
YPM190	phyllodes	14/04/2012	0.11	3.77	0.25	10.3	1	0.3	0.05	27
YPM191	phyllodes	14/04/2012	0.04	6.71	0.28	23.4	1	0.7	0.02	83
YPM193	phyllodes	14/04/2012	0.11	3.89	0.11	10.8	1	0.4	0.005	15
YPM194	phyllodes	14/04/2012	0.14	2.14	0.09	8.4	1	1.8	0.02	11
YPM195	phyllodes	14/04/2012	0.12	8.83	0.11	12.4	1	48.3	0.06	9
YPM196	phyllodes	14/04/2012	0.04	8.35	0.1	17	1	0.4	0.005	25
YPM197	phyllodes	14/04/2012	0.11	3.84	0.23	13.3	1	0.5	0.07	15
YPM198	phyllodes	14/04/2012	0.13	3.37	0.12	9.6	1	0.8	0.02	67
YPM199	phyllodes	14/04/2012	0.06	2.9	0.07	12.1	1	0.3	0.03	18
YPM200	phyllodes	14/04/2012	0.17	5.84	0.13	14.5	1	1.4	0.08	121
YPM201	phyllodes	14/04/2012	0.3	4.81	0.19	13.7	1	0.4	0.04	87
YPM202	phyllodes	14/04/2012	0.04	1.89	0.22	11.7	1	0.7	0.12	17
YPM203	phyllodes	14/04/2012	0.12	3.09	0.11	10.2	1	0.6	0.005	22
YPM204	phyllodes	14/04/2012	0.09	7.1	0.12	9.5	1	0.5	0.02	14
YPM205	phyllodes	14/04/2012	0.1	7.57	0.09	16.7	1	0.5	0.03	24
YPM206	phyllodes	14/04/2012	0.05	3.19	0.12	11.8	1	1	0.03	48
YPM207	phyllodes	15/04/2012	0.33	6.75	0.07	22.5	1	1	0.04	41
YPM208	phyllodes	15/04/2012	0.09	3.55	0.09	13.1	1	0.3	0.04	28
YPM209	phyllodes	15/04/2012	0.04	2.77	0.09	7.3	1	0.7	0.06	10
YPM210	phyllodes	15/04/2012	0.04	3.28	0.07	9.5	1	0.3	0.04	28
YPM211	phyllodes	15/04/2012	0.04	5.04	0.12	9.3	1	0.4	0.04	20
YPM212	phyllodes	15/04/2012	0.07	2.83	0.13	8.2	1	0.5	0.02	13
YPM213	phyllodes	15/04/2012	0.1	4.85	0.08	16.3	1	0.4	0.04	8
YPM214	phyllodes	15/04/2012	0.1	3.34	0.22	15.9	1	0.8	0.12	40
YPM215	phyllodes	15/04/2012	0.12	4.56	0.22	14.5	1	2.3	0.18	226
YPM216	phyllodes	15/04/2012	0.17	6.32	0.11	15.3	1	1.7	0.12	86
YPM217	phyllodes	15/04/2012	0.22	5.13	0.12	15.4	1	0.4	0.09	30
YPM218	phyllodes	15/04/2012	0.03	4.01	0.14	15.4	1	0.2	0.04	32

*NOTE values below detection have been halved	Fe_pct	As_ppm	U_ppm	Au_ppb	Th_ppm	Sr_ppm	Cd_ppm	Sb_ppm	Bi_ppm	V_ppm	Ca_pct	P_pct
YPM145	0.013	0.05	0.005	0.1	0.02	82.5	0.005	0.01	0.01	1	0.69	0.063
YPM146	0.018	0.05	0.005	0.1	0.03	41.6	0.01	0.01	0.01	1	0.53	0.062
YPM147	0.011	0.05	0.005	0.1	0.01	56.7	0.005	0.01	0.01	1	0.84	0.061
YPM148	0.013	0.05	0.005	0.6	0.01	57.5	0.005	0.01	0.01	1	0.96	0.078
YPM149	0.018	0.05	0.005	0.4	0.03	97.9	0.03	0.01	0.01	1	0.87	0.067
YPM150	0.019	0.05	0.005	0.1	0.04	53.7	0.05	0.01	0.01	1	0.74	0.083
YPM151	0.013	0.1	0.005	0.1	0.01	98.6	0.01	0.01	0.01	1	0.77	0.05
YPM152	0.009	0.05	0.02	0.1	0.005	50.6	0.02	0.01	0.01	1	0.48	0.076
YPM153	0.012	0.1	0.005	0.1	0.01	130.6	0.005	0.01	0.01	1	1.13	0.054
YPM154	0.021	0.05	0.005	0.4	0.03	67.1	0.005	0.01	0.01	1	0.62	0.066
YPM155	0.023	0.05	0.005	0.1	0.04	87.8	0.01	0.01	0.01	1	0.93	0.061
YPM156	0.018	0.1	0.005	0.1	0.02	173.8	0.01	0.01	0.01	1	0.99	0.056
YPM157	0.009	0.05	0.005	0.1	0.005	49.4	0.005	0.01	0.01	1	0.4	0.056
YPM158	0.011	0.05	0.005	0.1	0.02	76.3	0.005	0.01	0.01	1	0.53	0.044
YPM159	0.012	0.05	0.005	0.1	0.01	90.1	0.005	0.01	0.01	1	0.87	0.053
YPM160	0.012	0.05	0.005	0.1	0.01	60.4	0.005	0.01	0.01	1	0.69	0.058
YPM161	0.009	0.05	0.005	0.1	0.005	47	0.02	0.01	0.01	1	0.46	0.068
YPM162	0.018	0.05	0.01	0.1	0.02	47.5	0.02	0.01	0.01	1	0.8	0.07
YPM163	0.019	0.05	0.01	0.2	0.02	80.1	0.005	0.01	0.01	1	0.65	0.078
YPM164	0.009	0.05	0.005	0.1	0.005	45.3	0.005	0.01	0.01	1	0.41	0.062
YPM165	0.009	0.05	0.005	0.1	0.005	32.3	0.005	0.01	0.01	1	0.58	0.062
YPM166	0.012	0.05	0.005	0.1	0.02	41.4	0.04	0.01	0.01	1	0.52	0.066
YPM167	0.012	0.05	0.005	0.1	0.02	31	0.005	0.01	0.01	1	0.54	0.048
YPM168	0.01	0.05	0.005	0.1	0.01	35.9	0.02	0.01	0.01	1	0.53	0.063
YPM169	0.011	0.05	0.005	0.1	0.01	93.6	0.005	0.01	0.01	1	0.77	0.066
YPM170	0.015	0.05	0.005	0.1	0.02	63.6	0.005	0.01	0.01	1	0.59	0.101
YPM171	0.01	0.05	0.005	0.1	0.005	91.8	0.01	0.01	0.01	1	1.06	0.07
YPM172	0.011	0.05	0.005	0.1	0.01	95.1	0.005	0.01	0.01	1	0.87	0.066
YPM173	0.011	0.05	0.005	0.1	0.01	92.6	0.005	0.01	0.01	1	0.64	0.068
YPM174	0.007	0.05	0.04	0.1	0.005	41.8	0.02	0.01	0.01	1	0.54	0.051
YPM175	0.02	0.05	0.005	0.1	0.03	85.1	0.02	0.01	0.01	1	0.89	0.058
YPM176	0.011	0.05	0.005	0.1	0.01	84.4	0.005	0.01	0.01	1	0.71	0.067
YPM178	0.013	0.1	0.005	0.1	0.02	52.8	0.02	0.01	0.06	1	0.87	0.058
YPM179	0.017	0.3	0.005	0.4	0.03	45.9	0.03	0.01	0.01	1	0.66	0.06
YPM180	0.007	0.05	0.005	0.1	0.005	14.9	0.005	0.01	0.01	1	0.4	0.113
YPM181	0.028	0.2	0.01	0.1	0.04	59.7	0.04	0.01	0.01	1	1.07	0.064
YPM182	0.026	0.2	0.02	0.1	0.04	66.5	0.02	0.01	0.01	1	0.7	0.077
YPM183	0.016	0.05	0.01	0.3	0.03	50.9	0.01	0.01	0.01	1	0.87	0.061
YPM184	0.01	0.05	0.01	0.1	0.02	26.9	0.005	0.01	0.01	1	0.43	0.093
YPM185	0.017	0.05	0.02	0.1	0.03	66.8	0.04	0.01	0.01	1	0.68	0.085
YPM186	0.01	0.1	0.005	0.1	0.02	57.5	0.005	0.01	0.01	1	0.68	0.055
YPM187	0.013	0.05	0.04	0.1	0.04	31.8	0.005	0.01	0.01	1	0.49	0.062
YPM188	0.012	0.1	0.005	0.3	0.02	97.5	0.005	0.01	0.01	1	0.67	0.062
YPM189	0.014	0.1	0.005	0.3	0.02	32	0.005	0.01	0.01	1	0.59	0.096
YPM190	0.013	0.05	0.005	0.3	0.02	173.9	0.005	0.01	0.01	1	1.1	0.06
YPM191	0.011	0.1	0.005	0.6	0.01	58.4	0.01	0.03	0.01	1	1.49	0.071
YPM193	0.009	0.05	0.02	0.1	0.005	97.7	0.01	0.01	0.01	1	0.75	0.084
YPM194	0.009	0.2	0.005	0.1	0.01	120.8	0.005	0.01	0.01	1	0.52	0.072
YPM195	0.016	0.05	0.06	0.1	0.02	47.4	0.005	0.01	0.01	1	0.61	0.106
YPM196	0.009	0.05	0.005	0.1	0.005	145.9	0.005	0.01	0.01	1	0.89	0.062
YPM197	0.018	0.1	0.01	0.2	0.03	53.3	0.01	0.01	0.01	1	0.82	0.048
YPM198	0.014	0.05	0.005	0.3	0.02	54	0.01	0.01	0.01	1	0.9	0.06
YPM199	0.009	0.05	0.02	0.1	0.005	153.6	0.01	0.01	0.01	1	1.19	0.085
YPM200	0.015	0.05	0.005	0.1	0.02	52.3	0.05	0.01	0.01	1	1.02	0.062
YPM201	0.015	0.1	0.09	0.1	0.02	52.4	0.005	0.01	0.01	1	1.22	0.082
YPM202	0.016	0.05	0.005	0.3	0.03	45.7	0.01	0.01	0.01	1	0.57	0.047
YPM203	0.01	0.05	0.005	0.1	0.01	43.8	0.01	0.01	0.01	1	0.48	0.056
YPM204	0.012	0.05	0.005	0.1	0.02	50.1	0.005	0.01	0.01	1	0.84	0.095
YPM205	0.009	0.05	0.005	0.1	0.005	56.1	0.005	0.01	0.01	1	1.05	0.099
YPM206	0.012	0.05	0.04	0.4	0.02	49	0.005	0.01	0.01	1	1.17	0.044
YPM207	0.01	0.05	0.06	0.3	0.005	49.5	0.005	0.01	0.01	1	0.86	0.093
YPM208	0.01	0.05	0.005	0.1	0.01	66.4	0.005	0.01	0.01	1	0.75	0.073
YPM209	0.01	0.05	0.01	0.1	0.02	76	0.005	0.01	0.01	1	0.48	0.049
YPM210	0.01	0.05	0.005	0.1	0.005	24.5	0.005	0.01	0.01	1	0.47	0.056
YPM211	0.011	0.05	0.01	0.1	0.01	116	0.005	0.01	0.01	1	0.79	0.091
YPM212	0.011	0.05	0.005	0.1	0.01	92.3	0.005	0.01	0.01	1	0.62	0.081
YPM213	0.008	0.05	0.005	0.1	0.005	168.1	0.005	0.01	0.01	1	1.29	0.12
YPM214	0.025	0.05	0.07	0.1	0.04	138.6	0.04	0.01	0.01	2	1.13	0.062
YPM215	0.021	0.05	0.005	0.1	0.04	35.1	0.03	0.01	0.01	1	0.61	0.075
YPM216	0.008	0.05	0.005	0.1	0.005	88.1	0.005	0.01	0.01	1	0.87	0.078
YPM217	0.01	0.05	0.005	0.1	0.005	57.7	0.005	0.01	0.01	1	0.52	0.083
YPM218	0.006	0.05	0.005	0.1	0.005	98.4	0.005	0.01	0.01	1	0.75	0.079

*NOTE values below detection have been halved	La_ppm	Cr_ppm	Mg_pct	Ba_ppm	Ti_ppm	B_ppm	Al_pct	Na_pct	K_pct	W_ppm	Sc_ppm	Tl_ppm
YPM145	0.04	1.1	0.15	5.5	5	38	0.005	0.444	0.59	0.05	0.3	0.01
YPM146	0.08	1.3	0.135	3.2	5	44	0.02	0.391	0.51	0.05	0.3	0.01
YPM147	0.12	1.2	0.157	5.4	4	21	0.005	0.397	0.54	0.05	0.3	0.01
YPM148	0.05	1	0.14	7.5	6	50	0.01	0.357	0.41	0.05	0.2	0.01
YPM149	0.07	1.2	0.175	8.5	6	57	0.02	0.388	0.48	0.05	0.3	0.01
YPM150	0.09	1.1	0.132	8.4	7	50	0.02	0.556	0.51	0.05	0.2	0.01
YPM151	0.05	1	0.15	3.9	4	20	0.01	0.347	0.47	0.05	0.2	0.01
YPM152	0.03	1.1	0.133	5.1	5	32	0.005	0.429	0.32	0.05	0.4	0.01
YPM153	0.04	1.1	0.204	10.4	4	63	0.005	0.478	0.41	0.05	0.3	0.01
YPM154	0.26	1.2	0.176	4.7	6	30	0.02	0.752	0.5	0.05	0.2	0.01
YPM155	0.12	1.2	0.155	7.2	6	57	0.02	0.471	0.51	0.05	0.3	0.01
YPM156	0.09	1.1	0.258	7	5	61	0.02	0.287	0.3	0.05	0.3	0.01
YPM157	0.04	1	0.125	1.8	4	14	0.005	0.588	0.49	0.05	0.4	0.01
YPM158	0.05	1.5	0.107	7	4	16	0.005	0.376	0.57	0.05	0.3	0.01
YPM159	0.09	1.1	0.183	5.8	4	31	0.005	0.245	0.55	0.05	0.2	0.01
YPM160	0.04	1.1	0.14	6.5	5	34	0.005	0.567	0.6	0.05	0.3	0.01
YPM161	0.04	1	0.124	2.9	5	13	0.005	0.445	0.68	0.05	0.3	0.01
YPM162	0.15	1.1	0.183	7.1	6	49	0.02	0.638	0.38	0.05	0.3	0.01
YPM163	0.08	1.1	0.162	6.4	6	54	0.02	0.519	0.44	0.05	0.2	0.01
YPM164	0.03	1.1	0.121	2.4	5	22	0.005	0.628	0.52	0.05	0.2	0.01
YPM165	0.03	0.9	0.123	3	4	24	0.005	0.569	0.51	0.05	0.3	0.01
YPM166	0.06	1.1	0.118	2.8	5	26	0.01	0.415	0.32	0.05	0.2	0.01
YPM167	0.06	1	0.142	3.3	4	41	0.01	0.367	0.52	0.05	0.3	0.01
YPM168	0.04	0.2	0.16	3.6	4	27	0.005	0.353	0.49	0.05	0.2	0.01
YPM169	0.04	1.1	0.22	4.3	5	25	0.005	0.583	0.39	0.05	0.2	0.01
YPM170	0.07	1	0.177	3.7	7	26	0.01	0.948	0.64	0.05	0.3	0.01
YPM171	0.05	0.9	0.209	5	5	27	0.005	0.449	0.37	0.05	0.2	0.01
YPM172	0.06	1	0.22	2.6	5	39	0.005	0.607	0.31	0.05	0.2	0.01
YPM173	0.05	1	0.16	2.1	5	25	0.01	0.803	0.42	0.05	0.3	0.01
YPM174	0.04	1	0.182	1.1	4	33	0.005	0.568	0.38	0.05	0.2	0.01
YPM175	0.1	1.1	0.148	7	5	50	0.02	0.439	0.48	0.05	0.3	0.01
YPM176	0.05	0.9	0.213	4	5	22	0.005	0.635	0.41	0.05	0.2	0.01
YPM178	0.07	1.3	0.145	9.3	5	46	0.01	0.495	0.52	0.05	0.3	0.01
YPM179	0.09	1.2	0.188	2.7	5	28	0.02	0.526	0.37	0.05	0.3	0.01
YPM180	0.03	1.1	0.121	3.9	7	87	0.005	0.573	0.79	0.05	0.4	0.01
YPM181	0.13	1.3	0.181	6.6	6	63	0.03	0.354	0.58	0.05	0.4	0.01
YPM182	0.29	1.5	0.169	7	7	43	0.03	0.591	0.42	0.05	0.3	0.01
YPM183	0.14	1.3	0.146	7.6	5	47	0.02	0.604	0.42	0.05	0.3	0.01
YPM184	0.1	1.2	0.117	4	6	36	0.005	0.395	0.9	0.05	0.2	0.01
YPM185	0.14	1.2	0.137	7.1	6	43	0.02	0.432	0.7	0.05	0.3	0.01
YPM186	0.05	1.2	0.135	4.8	4	31	0.01	0.647	0.68	0.05	0.3	0.01
YPM187	0.23	1.2	0.145	2	5	35	0.02	0.592	0.5	0.05	0.3	0.01
YPM188	0.06	1.1	0.16	10.8	4	31	0.01	0.515	0.58	0.05	0.3	0.01
YPM189	0.07	1.2	0.149	5.4	7	31	0.02	0.628	0.73	0.05	0.3	0.01
YPM190	0.06	1.1	0.21	4.3	5	20	0.01	0.611	0.47	0.05	0.3	0.01
YPM191	0.04	1	0.207	6.4	5	29	0.005	0.492	0.6	0.05	0.3	0.01
YPM193	0.05	1.1	0.188	4.3	5	44	0.005	0.612	0.52	0.05	0.3	0.01
YPM194	0.03	1.1	0.182	2.6	5	36	0.005	0.539	0.44	0.05	0.3	0.01
YPM195	0.16	1.1	0.157	6.1	7	42	0.02	0.839	0.63	0.05	0.4	0.01
YPM196	0.04	1.2	0.229	7.2	4	39	0.005	0.403	0.41	0.05	0.3	0.01
YPM197	0.12	1.1	0.146	5.7	5	57	0.02	0.387	0.48	0.05	0.3	0.01
YPM198	0.08	1	0.154	10.2	5	48	0.01	0.507	0.51	0.05	0.3	0.01
YPM199	0.05	1.2	0.219	6.2	5	65	0.005	0.447	0.42	0.05	0.2	0.01
YPM200	0.06	1.1	0.163	3.5	5	35	0.02	0.584	0.36	0.05	0.3	0.01
YPM201	0.11	1.1	0.141	10.6	6	105	0.02	0.465	0.63	0.05	0.3	0.01
YPM202	0.09	1.4	0.156	2.5	5	54	0.02	0.679	0.57	0.05	0.3	0.01
YPM203	0.06	1.1	0.177	2.8	4	29	0.005	0.675	0.38	0.05	0.3	0.01
YPM204	0.09	1.2	0.132	5.4	6	53	0.01	0.414	0.49	0.05	0.3	0.01
YPM205	0.11	1.1	0.18	5.4	6	30	0.005	0.365	0.63	0.05	0.2	0.01
YPM206	0.04	1.2	0.103	7.7	3	69	0.01	0.45	0.48	0.05	0.2	0.01
YPM207	0.07	1.1	0.159	3.9	6	34	0.005	0.578	0.48	0.05	0.2	0.01
YPM208	0.05	1	0.217	5.1	5	16	0.005	0.728	0.36	0.05	0.3	0.01
YPM209	0.05	1.1	0.169	3.2	4	29	0.01	0.665	0.33	0.05	0.2	0.01
YPM210	0.08	1.1	0.181	2.2	4	24	0.01	0.716	0.55	0.05	0.3	0.01
YPM211	0.36	1.1	0.253	4	6	42	0.01	0.532	0.37	0.05	0.3	0.01
YPM212	0.05	0.4	0.203	3.4	5	33	0.005	0.73	0.43	0.05	0.2	0.01
YPM213	0.03	1.7	0.276	7.8	4	43	0.01	0.859	0.52	0.05	0.05	0.01
YPM214	0.14	2	0.191	12.5	7	115	0.03	0.426	0.5	0.05	0.3	0.01
YPM215	0.13	1.8	0.133	7.1	7	66	0.03	0.555	0.38	0.05	0.2	0.01
YPM216	0.04	1.4	0.174	8.2	5	31	0.005	0.525	0.4	0.05	0.1	0.01
YPM217	0.05	1.6	0.187	3.4	5	22	0.01	0.984	0.4	0.05	0.1	0.01
YPM218	0.03	1.7	0.259	3.3	3	23	0.005	0.65	0.46	0.05	0.05	0.01

*NOTE values below detection have been halved	S_pct	Hg_ppb	Se_ppm	Te_ppm	Ga_ppm	Cs_ppm	Ge_ppm	Hf_ppm	Nb_ppm	Rb_ppm	Sn_ppm	Ta_ppm
YPM145	0.07	8	0.2	0.01	0.05	0.007	0.005	0.0005	0.005	0.9	0.01	0.0005
YPM146	0.08	12	0.2	0.01	0.05	0.014	0.005	0.007	0.005	0.7	0.02	0.0005
YPM147	0.05	8	0.2	0.01	0.05	0.0025	0.005	0.003	0.005	1.5	0.01	0.0005
YPM148	0.1	18	0.3	0.01	0.05	0.011	0.01	0.006	0.005	1.1	0.02	0.0005
YPM149	0.11	21	0.4	0.01	0.05	0.017	0.005	0.004	0.005	0.8	0.01	0.0005
YPM150	0.09	21	0.3	0.01	0.05	0.018	0.02	0.008	0.005	0.8	0.01	0.0005
YPM151	0.07	15	0.2	0.01	0.05	0.016	0.02	0.002	0.005	1.7	0.02	0.0005
YPM152	0.07	18	0.5	0.01	0.05	0.01	0.005	0.0005	0.005	0.8	0.01	0.0005
YPM153	0.07	19	0.3	0.01	0.05	0.009	0.005	0.001	0.005	0.8	0.01	0.0005
YPM154	0.09	11	0.2	0.01	0.05	0.018	0.04	0.002	0.005	1.2	0.01	0.0005
YPM155	0.1	25	0.2	0.01	0.05	0.02	0.02	0.005	0.005	1.2	0.01	0.0005
YPM156	0.07	30	0.05	0.01	0.05	0.016	0.005	0.002	0.005	0.9	0.01	0.001
YPM157	0.06	12	0.2	0.01	0.05	0.008	0.005	0.001	0.005	2.1	0.01	0.0005
YPM158	0.03	6	0.2	0.01	0.05	0.013	0.02	0.0005	0.005	4.5	0.01	0.0005
YPM159	0.1	6	0.2	0.01	0.05	0.01	0.005	0.005	0.005	1.2	0.01	0.0005
YPM160	0.05	8	0.4	0.01	0.05	0.008	0.02	0.001	0.005	2	0.01	0.0005
YPM161	0.05	5	0.3	0.01	0.05	0.008	0.005	0.004	0.005	1.5	0.01	0.0005
YPM162	0.08	19	0.4	0.01	0.05	0.012	0.005	0.003	0.005	0.6	0.01	0.0005
YPM163	0.07	12	0.3	0.01	0.05	0.015	0.005	0.005	0.005	0.8	0.01	0.0005
YPM164	0.06	6	0.2	0.01	0.05	0.006	0.005	0.004	0.005	1.5	0.01	0.0005
YPM165	0.05	6	0.1	0.01	0.05	0.006	0.005	0.002	0.005	0.9	0.01	0.0005
YPM166	0.05	11	0.1	0.01	0.05	0.008	0.005	0.005	0.005	0.7	0.01	0.0005
YPM167	0.06	11	0.1	0.01	0.05	0.009	0.02	0.003	0.005	0.7	0.01	0.0005
YPM168	0.03	9	0.1	0.01	0.05	0.007	0.005	0.004	0.005	1	0.01	0.0005
YPM169	0.05	14	0.4	0.03	0.05	0.007	0.005	0.0005	0.005	0.6	0.01	0.0005
YPM170	0.07	10	0.1	0.01	0.05	0.014	0.005	0.005	0.005	1.5	0.01	0.0005
YPM171	0.05	8	0.3	0.01	0.05	0.006	0.005	0.004	0.005	0.6	0.01	0.0005
YPM172	0.07	12	0.4	0.01	0.05	0.008	0.005	0.003	0.005	0.7	0.01	0.0005
YPM173	0.05	11	0.3	0.01	0.05	0.008	0.02	0.0005	0.005	1	0.01	0.0005
YPM174	0.06	9	0.4	0.01	0.05	0.0025	0.005	0.0005	0.005	0.6	0.01	0.0005
YPM175	0.08	15	0.4	0.01	0.05	0.015	0.005	0.007	0.005	1.1	0.01	0.0005
YPM176	0.06	11	0.2	0.01	0.05	0.006	0.005	0.007	0.005	0.6	0.01	0.0005
YPM178	0.06	18	0.5	0.01	0.05	0.012	0.005	0.0005	0.005	0.8	0.05	0.0005
YPM179	0.09	14	0.4	0.01	0.05	0.018	0.005	0.007	0.005	1.1	0.01	0.001
YPM180	0.09	5	0.3	0.01	0.05	0.0025	0.04	0.0005	0.005	2.2	0.01	0.0005
YPM181	0.09	40	0.4	0.01	0.1	0.023	0.01	0.007	0.005	1.2	0.03	0.0005
YPM182	0.08	14	0.4	0.01	0.05	0.027	0.005	0.004	0.005	1	0.02	0.0005
YPM183	0.05	15	0.4	0.01	0.05	0.015	0.005	0.005	0.005	0.7	0.01	0.0005
YPM184	0.08	8	0.3	0.01	0.05	0.017	0.005	0.0005	0.005	2.5	0.01	0.0005
YPM185	0.08	12	0.3	0.01	0.05	0.017	0.005	0.003	0.005	1.2	0.01	0.001
YPM186	0.05	8	0.4	0.01	0.05	0.014	0.005	0.0005	0.005	1.8	0.01	0.0005
YPM187	0.07	24	0.3	0.01	0.05	0.011	0.005	0.0005	0.005	0.7	0.01	0.0005
YPM188	0.05	6	0.3	0.01	0.05	0.012	0.005	0.004	0.005	1.2	0.01	0.0005
YPM189	0.08	9	0.4	0.01	0.05	0.014	0.005	0.001	0.005	0.9	0.03	0.0005
YPM190	0.07	10	0.2	0.01	0.05	0.009	0.005	0.002	0.005	1.1	0.05	0.0005
YPM191	0.07	23	0.3	0.01	0.05	0.005	0.02	0.0005	0.005	0.7	0.05	0.0005
YPM193	0.07	9	0.6	0.01	0.05	0.01	0.005	0.0005	0.005	1.3	0.01	0.0005
YPM194	0.05	6	0.3	0.01	0.05	0.005	0.005	0.0005	0.005	1.2	0.01	0.0005
YPM195	0.11	13	0.5	0.01	0.05	0.013	0.03	0.0005	0.005	2.1	0.01	0.0005
YPM196	0.07	13	0.4	0.01	0.05	0.006	0.005	0.0005	0.005	0.5	0.01	0.0005
YPM197	0.06	22	0.5	0.01	0.05	0.016	0.005	0.006	0.005	1.2	0.01	0.0005
YPM198	0.06	7	0.5	0.01	0.05	0.012	0.005	0.007	0.005	0.8	0.01	0.0005
YPM199	0.07	19	0.5	0.01	0.05	0.007	0.005	0.002	0.005	0.7	0.01	0.0005
YPM200	0.09	10	0.3	0.01	0.05	0.011	0.005	0.002	0.005	0.5	0.01	0.0005
YPM201	0.09	19	0.6	0.01	0.05	0.013	0.005	0.004	0.005	1.4	0.01	0.0005
YPM202	0.08	7	0.4	0.01	0.05	0.014	0.02	0.006	0.005	1.1	0.01	0.0005
YPM203	0.06	6	0.3	0.01	0.05	0.006	0.005	0.0005	0.005	0.6	0.01	0.0005
YPM204	0.08	18	0.5	0.02	0.05	0.008	0.005	0.004	0.005	1	0.01	0.0005
YPM205	0.08	5	0.6	0.01	0.05	0.0025	0.005	0.0005	0.005	1.6	0.01	0.0005
YPM206	0.08	33	0.4	0.01	0.05	0.008	0.02	0.002	0.005	0.6	0.01	0.0005
YPM207	0.1	9	0.5	0.01	0.05	0.008	0.005	0.002	0.005	0.8	0.01	0.0005
YPM208	0.07	7	0.6	0.01	0.05	0.007	0.005	0.0005	0.005	0.8	0.01	0.001
YPM209	0.05	6	0.3	0.01	0.05	0.009	0.005	0.002	0.005	0.7	0.01	0.0005
YPM210	0.07	12	0.2	0.01	0.05	0.01	0.005	0.006	0.005	0.8	0.01	0.0005
YPM211	0.09	11	0.4	0.01	0.05	0.009	0.005	0.0005	0.005	0.7	0.01	0.0005
YPM212	0.06	5	0.4	0.01	0.05	0.007	0.02	0.002	0.005	0.7	0.01	0.0005
YPM213	0.13	10	0.3	0.01	0.05	0.01	0.005	0.008	0.005	0.8	0.01	0.0005
YPM214	0.23	23	0.5	0.01	0.1	0.025	0.01	0.008	0.005	0.9	0.04	0.0005
YPM215	0.21	15	0.3	0.01	0.05	0.03	0.005	0.005	0.005	1	0.03	0.0005
YPM216	0.2	7	0.4	0.01	0.05	0.008	0.005	0.002	0.005	0.9	0.01	0.0005
YPM217	0.15	10	0.4	0.01	0.05	0.013	0.005	0.004	0.005	0.7	0.01	0.0005
YPM218	0.12	10	0.3	0.01	0.05	0.008	0.02	0.0005	0.005	0.5	0.01	0.0005

*NOTE values below detection have been halved	Zr_ppm	Y_ppm	Ce_ppm	In_ppm	Re_ppb	Be_ppm	Li_ppm	Pd_ppb	Pt_ppb
YPM145	0.08	0.022	0.09	0.01	0.5	0.05	0.49	1	0.5
YPM146	0.13	0.057	0.2	0.01	0.5	0.05	0.36	1	0.5
YPM147	0.06	0.068	0.24	0.01	0.5	0.05	0.44	1	0.5
YPM148	0.08	0.041	0.15	0.01	0.5	0.05	0.69	1	0.5
YPM149	0.16	0.05	0.21	0.01	0.5	0.05	0.53	1	1
YPM150	0.12	0.077	0.22	0.01	0.5	0.05	0.69	1	0.5
YPM151	0.09	0.052	0.14	0.01	0.5	0.05	0.24	1	0.5
YPM152	0.05	0.025	0.08	0.01	0.5	0.05	0.52	1	1
YPM153	0.08	0.03	0.1	0.01	0.5	0.05	0.61	1	0.5
YPM154	0.15	0.128	0.61	0.01	0.5	0.05	3.06	1	0.5
YPM155	0.18	0.071	0.27	0.01	0.5	0.05	1.32	1	0.5
YPM156	0.1	0.091	0.24	0.01	0.5	0.05	2.2	1	0.5
YPM157	0.06	0.022	0.09	0.01	0.5	0.05	0.5	1	0.5
YPM158	0.05	0.034	0.11	0.01	0.5	0.05	0.16	1	0.5
YPM159	0.08	0.048	0.17	0.01	0.5	0.05	0.49	1	0.5
YPM160	0.06	0.033	0.13	0.01	0.5	0.05	0.27	1	1
YPM161	0.04	0.03	0.09	0.01	0.5	0.05	0.24	1	0.5
YPM162	0.11	0.053	0.33	0.01	0.5	0.05	0.92	1	0.5
YPM163	0.11	0.054	0.2	0.01	0.5	0.05	0.44	1	0.5
YPM164	0.04	0.018	0.07	0.01	0.5	0.05	0.2	1	0.5
YPM165	0.03	0.026	0.06	0.01	0.5	0.05	0.32	1	0.5
YPM166	0.06	0.036	0.14	0.01	0.5	0.05	0.17	1	0.5
YPM167	0.07	0.052	0.19	0.01	0.5	0.05	0.78	1	0.5
YPM168	0.06	0.023	0.11	0.01	0.5	0.05	0.62	1	0.5
YPM169	0.06	0.029	0.1	0.01	2	0.05	1.21	1	0.5
YPM170	0.08	0.051	0.18	0.01	0.5	0.05	0.91	1	0.5
YPM171	0.04	0.036	0.09	0.01	0.5	0.05	1.1	1	0.5
YPM172	0.06	0.04	0.18	0.01	0.5	0.05	2.26	1	0.5
YPM173	0.08	0.039	0.13	0.01	0.5	0.05	0.81	1	0.5
YPM174	0.04	0.028	0.11	0.01	0.5	0.05	0.7	1	0.5
YPM175	0.11	0.066	0.26	0.01	0.5	0.05	1.1	1	0.5
YPM176	0.06	0.038	0.11	0.01	0.5	0.05	1.23	1	0.5
YPM178	0.09	0.046	0.17	0.01	0.5	0.05	0.46	1	0.5
YPM179	0.13	0.042	0.21	0.01	0.5	0.05	0.4	1	0.5
YPM180	0.03	0.014	0.08	0.01	0.5	0.05	0.38	1	0.5
YPM181	0.21	0.287	0.42	0.01	0.5	0.05	2.65	1	0.5
YPM182	0.21	0.197	0.69	0.01	0.5	0.05	0.75	1	0.5
YPM183	0.11	0.076	0.32	0.01	1	0.05	1.08	1	0.5
YPM184	0.07	0.071	0.22	0.01	1	0.05	0.77	1	0.5
YPM185	0.15	0.127	0.37	0.01	0.5	0.05	1.21	1	0.5
YPM186	0.07	0.027	0.14	0.01	0.5	0.05	0.42	1	0.5
YPM187	0.12	0.41	0.74	0.01	0.5	0.05	0.64	1	0.5
YPM188	0.06	0.04	0.15	0.01	0.5	0.05	1.22	1	0.5
YPM189	0.1	0.042	0.16	0.01	0.5	0.05	0.85	1	0.5
YPM190	0.08	0.042	0.14	0.01	0.5	0.05	1.05	1	0.5
YPM191	0.06	0.027	0.07	0.01	0.5	0.05	1.13	1	0.5
YPM193	0.04	0.019	0.12	0.01	0.5	0.05	1.43	1	0.5
YPM194	0.04	0.028	0.1	0.01	0.5	0.05	0.8	3	0.5
YPM195	0.1	0.066	0.43	0.01	0.5	0.05	0.51	1	0.5
YPM196	0.04	0.024	0.1	0.01	0.5	0.05	1.81	1	0.5
YPM197	0.11	0.07	0.32	0.01	0.5	0.05	0.85	1	0.5
YPM198	0.1	0.048	0.18	0.01	0.5	0.05	0.46	1	0.5
YPM199	0.04	0.039	0.1	0.01	0.5	0.05	2.04	1	0.5
YPM200	0.13	0.058	0.18	0.01	1	0.05	0.74	1	0.5
YPM201	0.12	0.097	0.29	0.01	0.5	0.05	1.03	1	0.5
YPM202	0.13	0.159	0.21	0.01	0.5	0.05	0.78	1	0.5
YPM203	0.05	0.04	0.13	0.01	1	0.05	0.7	1	0.5
YPM204	0.09	0.049	0.21	0.01	0.5	0.05	0.73	1	0.5
YPM205	0.03	0.042	0.25	0.01	0.5	0.05	0.75	1	0.5
YPM206	0.06	0.054	0.12	0.01	3	0.05	1.9	1	0.5
YPM207	0.06	0.051	0.26	0.01	4	0.05	1.31	1	0.5
YPM208	0.06	0.025	0.12	0.01	0.5	0.05	0.9	1	0.5
YPM209	0.08	0.034	0.13	0.01	0.5	0.05	0.97	1	0.5
YPM210	0.07	0.056	0.2	0.01	0.5	0.05	0.83	1	0.5
YPM211	0.07	0.057	0.53	0.01	2	0.05	1.92	1	0.5
YPM212	0.08	0.031	0.12	0.01	0.5	0.05	0.91	1	0.5
YPM213	0.06	0.035	0.12	0.01	0.5	0.05	1.13	1	0.5
YPM214	0.19	0.103	0.37	0.01	0.5	0.05	0.78	1	0.5
YPM215	0.15	0.169	0.33	0.01	0.5	0.05	2.57	1	0.5
YPM216	0.04	0.026	0.12	0.01	0.5	0.05	1.36	1	0.5
YPM217	0.09	0.041	0.21	0.01	0.5	0.05	0.64	1	0.5
YPM218	0.06	0.026	0.09	0.01	0.5	0.05	0.89	1	0.5

	*NOTE values below detection have been halved	Duplicate ID	Sample_Type	Transect	Location	Orig_Grid_ID	Orig_East	Orig_North	GA_RL
Yorke Peninsula	YPM219		VEG	9	Sand Pit Rd	GDA94_53H	775567	6231206	100
Yorke Peninsula	YPM220	YPM206	VEG	9	Thomas Plains Rd	GDA94_53H	755470	6238245	41
Yorke Peninsula	YPM221	YPM208	VEG	9	Thomas Plains Rd	GDA94_53H	760136	6238121	49
Yorke Peninsula	MNL024	Veg03	VEG		NR	GDA94_53H	740691	6143941	79
Yorke Peninsula	MAT003	Veg05	VEG		NR	GDA94_53H	751261	6198898	160
Yorke Peninsula	MAT004	Veg06	VEG		NR	GDA94_53H	749339	6196108	169
Yorke Peninsula	WAU001	Veg07	VEG		NR	GDA94_53H	743600	6181152	78

fertiliser* fertiliser* Fabris (2010)

fertiliser* fertiliser* Fabris (2010)

fertiliser* fertiliser* Fabris (2010)

fertiliser* fertiliser* Fabris (2010)

plant average # plant average # Dunn (2007)

*NOTE values below detection have been halved	Orig_Survey_Method	Orig_Survey_By	Orig_Survey_Date	Sampled_By	Treatment	Species
YPM219	Garmin GPS Map62S	KWolff	15/04/2012	KWolff	dried for 48hrs at 60'C	E. gracilis
YPM220	Garmin GPS Map62S	KWolff	15/04/2012	KWolff	dried for 48hrs at 60'C	E. phenax
YPM221	Garmin GPS Map62S	KWolff	15/04/2012	KWolff	dried for 48hrs at 60'C	E. gracilis
MNL024	Garmin GPS Map62S	KWolff		KWolff	dried for 48hrs at 60'C	E. phenax
MAT003	Garmin GPS Map62S	KWolff		KWolff	dried for 48hrs at 60'C	E. phenax
MAT004	Garmin GPS Map62S	KWolff		KWolff	dried for 48hrs at 60'C	E. leptophylla
WAU001	Garmin GPS Map62S	KWolff		KWolff	dried for 48hrs at 60'C	E. phenax

fertiliser* Fabris (2010)

fertiliser* Fabris (2010)

fertiliser* Fabris (2010)

fertiliser* Fabris (2010)
plant average # Dunn (2007)

*NOTE values below detection have been halved	Sample_Description	Date_Sampled	Mo_ppm	Cu_ppm	Pb_ppm	Zn_ppm	Ag_ppm	Ni_ppm	Co_ppm	Mn_ppm
YPM219	phyllodes	15/04/2012	0.19	6.97	0.09	11.7	1	0.2	0.06	25
YPM220	phyllodes	15/04/2012	0.06	4.79	0.09	12.3	1	1.2	0.04	43
YPM221	phyllodes	15/04/2012	0.1	4.64	0.08	13.8	1	0.2	0.02	30
MNL024	phyllodes		0.07	2.5	0.06	9.9	1	1.8	0.02	17
MAT003	phyllodes		0.06	3.3	0.08	12.1	1	3.1	0.06	21
MAT004	phyllodes		0.07	4.82	0.15	17	1	2.4	0.06	34
WAU001	phyllodes		0.11	2.89	0.11	9.2	1	3.9	0.03	77
fertiliser* Fabris (2010)			4.5	70	0.25	330		50	18	1100
fertiliser* Fabris (2010)			4.8	75	0.25	345		50	18.5	1100
fertiliser* Fabris (2010)			0.05	0.25	0.25	0.25		0.5	0.1	5
fertiliser* Fabris (2010)			0.05	0.25	0.25	0.25		0.5	0.1	5
plant average # Dunn (2007)				10						

*NOTE values below detection have been halved	Fe_pct	As_ppm	U_ppm	Au_ppb	Th_ppm	Sr_ppm	Cd_ppm	Sb_ppm	Bi_ppm	V_ppm	Ca_pct	P_pct
YPM219	0.013	0.1	0.005	0.1	0.02	59.3	0.005	0.01	0.01	1	0.46	0.094
YPM220	0.008	0.05	0.03	0.1	0.005	38.2	0.005	0.01	0.01	1	0.96	0.066
YPM221	0.007	0.05	0.005	0.1	0.005	78.5	0.005	0.01	0.01	1	0.87	0.088
MNL024	0.008	0.05	0.005	0.4	0.005	23.1	0.03	0.01	0.01	3	0.53	0.052
MAT003	0.009	0.05	0.005	0.2	0.005	44.4	0.005	0.01	0.01	5	0.54	0.058
MAT004	0.016	0.1	0.005	0.3	0.01	60.7	0.005	0.01	0.01	1	1.44	0.088
WAU001	0.013	0.05	0.02	0.8	0.005	99.2	0.005	0.01	0.01	1	1.6	0.047
fertiliser* Fabris (2010)	1.93			2							0.19	19.26
fertiliser* Fabris (2010)	1.88			1							0.19	19.35
fertiliser* Fabris (2010)	0.005			0.5							0.005	0.0075
fertiliser* Fabris (2010)	0.005			0.5							0.005	0.003
plant average # Dunn (2007)	50											0.2

*NOTE values below detection have been halved	La_ppm	Cr_ppm	Mg_pct	Ba_ppm	Ti_ppm	B_ppm	Al_pct	Na_pct	K_pct	W_ppm	Sc_ppm	Tl_ppm
YPM219	0.08	1.8	0.272	3.9	5	17	0.02	0.965	0.49	0.05	0.1	0.01
YPM220	0.04	1.8	0.123	5.6	3	43	0.01	0.598	0.54	0.05	0.05	0.01
YPM221	0.05	1.7	0.239	5.5	4	17	0.005	0.833	0.43	0.05	0.05	0.01
MNL024	0.03	1.7	0.113	2.2	0.5	22	0.005	0.425	0.49	0.05	0.2	0.01
MAT003	0.04	1.9	0.149	6.2	1	29	0.005	0.612	0.55	0.05	0.3	0.01
MAT004	0.07	1.7	0.199	4.1	1	52	0.02	0.59	0.49	0.05	0.2	0.01
WAU001	0.03	1.8	0.197	9.1	0.5	115	0.005	0.306	0.29	0.05	0.2	0.01
fertiliser* Fabris (2010)			0.18						0.12			
fertiliser* Fabris (2010)			0.19						0.122			
fertiliser* Fabris (2010)			0.005						0.005			
fertiliser* Fabris (2010)			0.005						0.005			
plant average # Dunn (2007)							0.008		1.9			

*NOTE values below detection have been halved	S_pct	Hg_ppb	Se_ppm	Te_ppm	Ga_ppm	Cs_ppm	Ge_ppm	Hf_ppm	Nb_ppm	Rb_ppm	Sn_ppm	Ta_ppm
YPM219	0.13	9	0.2	0.01	0.05	0.011	0.04	0.006	0.005	1	0.02	0.0005
YPM220	0.14	18	0.2	0.01	0.05	0.007	0.005	0.004	0.005	0.6	0.01	0.0005
YPM221	0.15	10	0.4	0.01	0.05	0.008	0.005	0.0005	0.005	0.8	0.01	0.0005
MNL024	0.11	18	0.05	0.01	0.05	0.0025	0.02	0.0005	0.005	0.8	0.01	0.0005
MAT003	0.14	16	0.05	0.01	0.05	0.006	0.02	0.002	0.005	1.7	0.01	0.0005
MAT004	0.13	32	0.2	0.01	0.05	0.01	0.01	0.001	0.005	1	0.01	0.0005
WAU001	0.13	50	0.2	0.01	0.05	0.006	0.005	0.0005	0.005	0.3	0.01	0.0005
fertiliser* Fabris (2010)			<0.5							9.5		
fertiliser* Fabris (2010)			<0.5							10		
fertiliser* Fabris (2010)			<0.5							0.05		
fertiliser* Fabris (2010)			<0.5							0.05		
plant average # Dunn (2007)												

*NOTE values below detection have been halved	Zr_ppm	Y_ppm	Ce_ppm	In_ppm	Re_ppb	Be_ppm	Li_ppm	Pd_ppb	Pt_ppb
YPM219	0.11	0.048	0.18	0.01	0.5	0.05	1.32	1	0.5
YPM220	0.07	0.039	0.1	0.01	3	0.05	1.22	1	0.5
YPM221	0.07	0.031	0.13	0.01	2	0.05	0.95	1	0.5
MNL024	0.05	0.021	0.08	0.01	0.5	0.05	0.44	1	0.5
MAT003	0.05	0.023	0.09	0.01	0.5	0.05	0.78	1	0.5
MAT004	0.06	0.035	0.14	0.01	0.5	0.05	1.05	1	0.5
WAU001	0.04	0.021	0.09	0.01	0.5	0.05	2.16	1	0.5
fertiliser* Fabris (2010)			0.5						
fertiliser* Fabris (2010)			0.65						
fertiliser* Fabris (2010)			0.025						
fertiliser* Fabris (2010) plant average # Dunn (2007)			0.025						